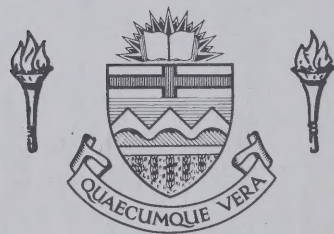


# **For Reference**

---

**NOT TO BE TAKEN FROM THIS ROOM**

Ex LIBRIS  
UNIVERSITATIS  
ALBERTAENSIS







THE UNIVERSITY OF ALBERTA

GEOTECHNICAL BEHAVIOUR OF OIL SANDS AT ELEVATED  
TEMPERATURES AND PRESSURES

VOLUME II

APPENDICES

Thermal Conductivity Tests

One Dimensional Diffusion Tests

Permeability Tests

by



JOHN GORDON AGAR

A THESIS

SUBMITTED TO THE FACULTY OF GRADUATE STUDIES AND RESEARCH  
IN PARTIAL FULFILLMENT OF THE REQUIREMENTS FOR THE DEGREE

DOCTOR OF PHILOSOPHY

IN

GEOTECHNIQUE

DEPARTMENT OF CIVIL ENGINEERING

EDMONTON, ALBERTA

SPRING, 1984



VOLUME II

Appendices	Page
A. Apparatus Compliance Testing and Calibrations	502
B. Thermal Expansion Tests	528
C. One Dimensional Compression Tests	591
D. Permeability Tests	602
E. Triaxial Tests	648
F. Grain Size Analyses	766
G. Scanning Electron Microphotographs	787
H. X-Ray Diffraction Analyses	802
I. Viscosity of Athabasca Bitumen After Unsaturated Heating	812
J. Computer Codes for One Dimensional Heat Consolidation Analyses	816
K. One Dimensional Heat Consolidation in Oil Sands: Numerical Solutions	842
L. Results of Thermoelastic Consolidation Analyses	860



LIST OF FIGURES IN APPENDIX A

<u>FIGURE</u>		<u>Page</u>
A1	Thermal Expansion of Water	507
A2	Compressibility of Water at Elevated Temperatures	508
A3	Pressure Increase During Constant Volume Heating	509
A4	Thermal Expansion of Quartz	510
A5	Consolidometer: Correction for Apparatus Thermal Expansion	511
A6	Consolidometer: Correction for Stress Induced Apparatus Expansion	512
A7	Consolidometer: Correction for Back Pressure Induced Apparatus Expansion	513
A8	Consolidometer: LVDT Correction for Vertical Thermal Expansion of the Apparatus	514
A9	Consolidometer: LVDT Correction for Vertical Apparatus Compression	515
A10	Consolidometer: Volume Change Correction for Thermal Expansion of Extraneous Water	516
A11	Consolidometer: Piston Friction at Elevated Temperatures and Back Pressures	517
A12	Triaxial Apparatus: Piston Friction at Elevated Confining Stresses and Temperatures Using a Non-Lubricated Piston	518
A13	Triaxial Apparatus: Influence of Lubrication on Measured Piston Friction	519
A14	Triaxial Apparatus: Correction for Piston Friction with Applied Vertical Load	520
A15	Triaxial Rubber Membrane Compliance at Elevated Temperatures	521
A16	Triaxial Apparatus: Accuracy of Internal and External Axial Strain Measuring Devices During Compression of an Aluminium Sample at 20°C	522



<u>FIGURE</u>		<u>Page</u>
A17	Triaxial Apparatus: Accuracy of an Internal Lateral Strain Measuring Device During Compression of an Aluminium Sample at 20°C	523
A18	Triaxial Apparatus: Accuracy of Internal and External Axial Strain Measuring Devices During Compression of an Aluminium Sample at 250°C	524
A19	Triaxial Apparatus: Accuracy of an Internal Lateral Strain Measuring Device During Compression of an Aluminium Sample at 250°C	525
A20	Triaxial Apparatus: Compliance of Volume Change Measurements During Thermal Expansion of an Aluminium Sample	526
A21	Schematic Cross Section of a Membrane Extension Testing Apparatus Used at Elevated Temperatures in an Oven	527



LIST OF TABLES IN APPENDIX A

<u>Table</u>		<u>Page</u>
A-1	Properties of System Fluids	503
A-2	Thermal Expansion and Compression Properties of Apparatus Materials	504
A-3	Volume Change Properties of Some Minerals	505
A-4	Summary of Calibrations for Electronic Measuring Devices	506



## LIST OF FIGURES IN APPENDIX B

<u>FIGURE</u>		<u>Page</u>
B1	Temperature Versus Time: Test COS1	532
B2	Back Pressure Versus Time: Test COS1	533
B3	Sample Height Versus Time: Test COS1	534
B4	Undrained Volumetric Thermal Expansion: Test COS1	535
B5	Temperature Versus Time: Test COS2	537
B6	Back Pressure Versus Time: Test COS2	538
B7	Sample Height Versus Time: Test COS2	539
B8	Undrained Volumetric Thermal Expansion: Test COS2	540
B9	Temperature Versus Time: Test COS3	543
B10	Back Pressure Versus Time: Test COS3	544
B11	Sample Height Versus Time: Test COS3	545
B12	Undrained Volumetric Thermal Expansion: Test COS3	546
B13	Temperature Versus Time: Test COS4	548
B14	Back Pressure Versus Time: Test COS4	549
B15	Sample Height Versus Time: Test COS4	550
B16	Undrained Volumetric Thermal Expansion: Test COS4	551
B17	Temperature Versus Time: Test COS5	554
B18	Back Pressure Versus Time: Test COS5	555
B19	Confining Pressure Versus Time: Test COS5	556
B20	Sample Height Versus Time: Test COS5	557
B21	Undrained Volumetric Thermal Expansion: Test COS5	558



<u>FIGURE</u>		<u>Page</u>
B22	Undrained Volumetric Thermal Expansion: Test COS5	559
B23	Pore Pressure Response to Undrained Heating: Test COS5	560
B24	Pore Pressure Response to Undrained Heating: Test COS5	561
B25	Pore Pressure Response to Undrained Heating: Test COS5	562
B26	Temperature Versus Time: Test COS6	565
B27	Back Pressure Versus Time: Test COS6	566
B28	Sample Height Versus Time: Test COS6	567
B29	Drained Volumetric Thermal Expansion: Test COS6	568
B30	Volume of Pore Fluid Drained During Heating: Test COS6	569
B31	Equivalent Undrained Thermal Expansion: Test COS6	570
B32	Temperature Versus Time: Test COS7	572
B33	Back Pressure Versus Time: Test COS7	573
B34	Sample Height Versus Time: Test COS7	574
B35	Drained Thermal Expansion: Test COS7	575
B36	Volume of Pore Fluid Drained During Heating: Test COS7	576
B37	Equivalent Undrained Thermal Expansion: Test COS7	577
B38	Temperature Versus Time: TEST COS8	580
B39	Back Pressure Versus Time: Test COS8	581
B40	Sample Height Versus Time: Test COS8	582



<u>FIGURE</u>		<u>Page</u>
B41	Undrained Volumetric Thermal Expansion: Test COS8	583
B42	Undrained Thermal Expansion at Initiation of Gas Exsolution: Test COS8	584
B43	Temperature Versus Time: Test COS9	586
B44	Back Pressure Versus Time: Test COS9	587
B45	Confining Stress Versus Time: Test COS9	588
B46	Sample Height Versus Time: Test COS9	589
B47	Undrained Volumetric Thermal Expansion: Test COS9	590



## LIST OF FIGURES IN APPENDIX C

<u>FIGURE</u>		<u>Page</u>
C1	One Dimensional Compression at 20°C: Test CPERM5	593
C2	One Dimensional Compression at 22°C: Test CPERM7	594
C3	One Dimensional Compression at 22°C: Test COS9	595
C4	One Dimensional Compression at 22°C: Test CPERM4	596
C5	One Dimensional Compression at 100°C: Test CPERM4	597
C6	One Dimensional Compression at 150°C: Test CPERM7	598
C7	One Dimensional Compression at 200°C: Test CPERM5	599
C8	One Dimensional Compression at 250°C: Test CPERM6	600
C9	One Dimensional Compression at 300°C: Test COS9	601



LIST OF FIGURES IN APPENDIX D

<u>FIGURE</u>		<u>Page</u>
D1	Flow Rate: Test CPERM1 (20°C)	605
D2	Pressure Variation With Time: Test CPERM1	606
D3	Flow Rate: Test CPERM2 (48°C)	608
D4	Pressure Variation With Time: Test CPERM2	609
D5	Flow Velocity Vs. Pressure Difference: Test CPERM3	612
D6	Drained Thermal Expansion: Test CPERM4	616
D7	Undrained Thermal Expansion: Test CPERM4	617
D8	Flow Velocity Vs. Pressure Difference: Test CPERM4	618
D9	Fluid Mobility Vs. Normalized Flow Volume: Test CPERM4	619
D10	Drained Thermal Expansion: Test CPERM5	623
D11	Flow Velocity Vs. Pressure Difference: Test CPERM5	624
D12	Fluid Mobility Vs. Normalized Flow Volume: Test CPERM5	625
D13	Drained Thermal Expansion: Test CPERM6	628
D14	Flow Velocity Vs. Pressure Difference: Test CPERM6	629
D15	Fluid Mobility Vs. Normalized Flow Volume: Test CPERM6	630
D16	Flow Velocity Vs. Pressure Difference: Test CPERM7	634
D17	Drained Thermal Expansion: Test CPERM7	635
D18	Volume of Fluid Drained During Heating: Test CPERM7	636



<u>FIGURE</u>		<u>Page</u>
D19	Flow Velocity Vs. Pressure Difference: Test CPERM8	639
D20	Drained Thermal Expansion: Test CPERM8	640
D21	Fluid Mobility Vs. Normalized Flow Volume: Test CPERM8	641
D22	Flow Velocity Vs. Pressure Difference: Test CPERM9	645
D23	Drained Thermal Expansion: Test CPERM9	646
D24	Fluid Mobility Vs. Normalized Flow Volume: Test CPERM9	647



LIST OF FIGURES IN APPENDIX E

<u>FIGURE</u>		<u>Page</u>
E1.1	Triaxial Test TOS1: B Test	653
E1.2	Triaxial Test TOS1: Undrained Compressibility	654
E.13	Triaxial Test TOS1: Drained Isotropic Compressibility	655
E1.4	Triaxial Test TOS1: Stress Path	656
E1.5	Triaxial Test TOS1: Deviator Stress Vs. Strain	657
E2.1	Triaxial Test TOS2: B Test	660
E2.2	Triaxial Test TOS2: Stress Path	661
E2.3	Triaxial Test TOS2: Deviator Stress Vs. Strain	662
E3.1	Triaxial Test TOS3: B Test	665
E3.2	Triaxial Test TOS3: Stress Path	666
E3.3	Triaxial Test TOS3: Deviator Stress Vs. Strain	667
E4.1	Triaxial Test TOS4: B Test	670
E4.2	Triaxial Test TOS4: Stress Path	671
E4.3	Triaxial Test TOS4: Deviator Stress Vs. Strain	672
E5.1	Triaxial Test TOS5: Stress Path	675
E5.2	Triaxial Test TOS5: Deviator Stress Vs. Strain	676
E6.1	Triaxial Test TOS6: Drained Thermal Expansion	679
E6.2	Triaxial Test TOS6: Stress Path	680
E6.3	Triaxial Test TOS6: Deviator Stress Vs. Strain	681



<u>FIGURE</u>		<u>Page</u>
E7.1	Triaxial Test TOS7: Drained Thermal Expansion	684
E7.2	Triaxial Test TOS7: Stress Path	685
E7.3	Triaxial Test TOS7: Deviator Stress Vs. Strain	686
E8.1	Triaxial Test TOS8: Volume of Pore Fluid Drained During Heating	689
E8.2	Triaxial Test TOS8: B Test	690
E8.3	Triaxial Test TOS8: Undrained Compressibility	691
E8.4	Triaxial Test TOS8: Drained Isotropic Compressibility	692
E9.1	Triaxial Test TOS9: Confining Stress/Pore Pressure Vs. Temperature	695
E9.2	Triaxial Test TOS9: Thermal Expansion of Pore Fluids	696
E9.3	Triaxial Test TOS9: Vertical Thermal Expansion	697
E10.1	Triaxial Test TOS10: Modified B Test	702
E10.2	Triaxial Test TOS10: Effective Stress Path	703
E10.3	Triaxial Test TOS10: Pore Pressure and Confining Stress Changes With Temperature	704
E10.4	Triaxial Test TOS10: Pore Pressure Response to Undrained Heating	705
E10.5	Triaxial Test TOS10: Vertical Strain During Heating	706
E10.6	Triaxial Test TOS10: Volume of Fluid Expelled During Heating	707
E10.7	Triaxial Test TOS10: Deviator Stress and Undrained Pore Pressure Changes With Vertical Strain	708



<u>FIGURE</u>		<u>Page</u>
E11.1	Triaxial Test TOS11: Modified B Test	711
E11.2	Triaxial Test TOS11: Stress Path	712
E11.3	Triaxial Test TOS11: Pore Pressure and Effective Stress Changes During Undrained Heating	713
E11.4	Triaxial Test TOS11: Deviator Stress Vs. Axial Strain	714
E11.5	Triaxial Test TOS11: Pore Pressure Changes and Axial Strain During Undrained Heating	715
E12.1	Triaxial Test TOS12: Axial Thermal Expansion	718
E12.2	Triaxial Test TOS12: Drained Isotropic Compression	719
E12.3	Triaxial Test TOS12: Stress Path	720
E12.4	Triaxial Test TOS12: Deviator Stress Vs. Strain	721
E13.1	Triaxial Test TOS13: Pore Pressure and Confining Stress Vs. Temperature	724
E13.2	Triaxial Test TOS13: Axial Thermal Expansion	725
E13.3	Triaxial Test TOS13: Volume of Pore Fluid Expelled During Heating	726
E.14.1	Triaxial Test TOS14: Three Stage Stress Path	730
E.14.2	Triaxial Test TOS14: Deviator Stress Vs. Strain	731
E15.1	Triaxial Test TOS15: Volume of Pore Fluid Expelled During Heating	734
E15.2	Triaxial Test TOS15: Drained Isotropic Compression	735
E15.3	Triaxial Test TOS15: Stress Path	736



<u>FIGURE</u>		<u>Page</u>
E15.4	Triaxial Test TOS15: Deviator Stress Vs. Strain	737
E15.5	Triaxial Test TOS15: Pore Pressure Response to Undrained Heating	738
E16.1	Triaxial Test TOS16: Volume of Pore Fluid Drained During Heating	741
E16.2	Triaxial Test TOS16: Vertical Thermal Expansion	742
E17.1	Triaxial Test TOS17: Volume of Pore Fluid Drained During Heating	745
E17.2	Triaxial Test TOS17: Stress Path	746
E17.3	Triaxial Test TOS17: Deviator Stress Vs. Strain	747
E18.1	Triaxial Test TOS18: Volume of Pore Fluid Expelled During Heating	750
E18.2	Triaxial Test TOS18: Stress Path	751
E18.3	Triaxial Test TOS18: Deviator Stress Vs. Strain	752
E19.1	Triaxial Test TOS19: Volume of Pore Fluid Expelled During Heating	755
E19.2	Triaxial Test TOS19: Drained Isotropic Compression	756
E19.3	Triaxial Test TOS19: Stress Path	757
E19.4	Triaxial Test TOS19: Deviator Stress Vs. Strain	758
E20.1	Unconfined Compression Test TOS20: Vertical Stress Vs. Strain	760
E20.2	Unconfined Compression Test TOS20: Vertical Strain Rate	761



LIST OF FIGURES IN APPENDIX F

<u>FIGURE</u>		<u>Page</u>
F1	Sample #41: Test COS9	763
F2	Sample #36A (top): CPERM4	764
F3	Sample #36A (bottom): CPERM4	765
F4	Sample #31A (top): CPERM5	766
F5	Sample #31A (bottom): CPERM5	767
F6	Sample #31A (bottom centre): Test CPERM5	768
F7	Sample #31B: Test CPERM6	769
F8	Sample #36B: Test CPERM9	770
F9	Sample #25: Test TOS1	771
F10	Sample #33: Test TOS2	772
F11	Sample #43: Test TOS3	773
F12	Sample #44: Test TOS4	774
F13	Sample #17: Test TOS5	775
F14	Sample #16: Test TOS6	776
F15	Sample #45: Test TOS7	777
F16	Sample #20: Test TOS10	778
F17	Sample #22: Test TOS11	779
F18	Sample #29: Test TOS12	780
F19	Samples #5, 7, 8: Test TOS14	781
F20	Sample #23: Test TOS17	782
F21	Sample #24: Test TOS18	783
F22	Sample #19: Test TOS19	784
F23	Sample #12B: Test TOS15	785



LIST OF PHOTOGRAPHIC PLATES IN APPENDIX G

<u>Plate</u>		<u>Page</u>
G-1	Oven-dried McMurray Formation oil sand from the Suncor minesite.	788
G-2	Crystal overgrowth in McMurray Formation oil sand from the Suncor minesite.	788
G-3	Tension crack in "case-hardened" Athabasca bitumen between two sand grains (in oven-dried oil sand).	789
G-4	"Case-hardening" of bitumen due to unsaturated heating of Athabasca oil sand.	789
G-5	Oil-free McMurray Formation sand grains (loosely packed).	790
G-6	Oil-free McMurray Formation sand grains.	790
G-7	Oil-free Saline Creek sand grains (closely packed).	791
G-8	Intact oil-rich Saline Creek oil sand fabric.	791
G-9	Bitumen-coated Saline Creek sand grains.	792
G-10	Rugose pore channel in Saline Creek oil sand.	792
G-11	Crystal overgrowth features in Saline Creek oil sand.	793
G-12	Saline Creek oil sand fabric following 100°C permeability test in which 10 percent of the bitumen was removed.	793
G-13	Saline Creek sand grain after 100°C permeability experiment.	794
G-14	Saline Creek oil sand fabric after 100°C permeability experiment.	794
G-15	Bitumen-coated Saline Creek sand grains after 100°C permeability experiment.	795



<u>Plate</u>		<u>Page</u>
G-16	Saline Creek oil sand fabric following a 250°C permeability experiment.	795
G-17	Clay particles in Saline Creek oil sand after a 250°C permeability experiment.	796
G-18	Clay particles in Saline Creek oil sand fabric (note the platy shape of clay particles).	796
G-19	Saline Creek oil sand fabric after compression under 6 MPa confining stress and 300°C.	797
G-20	Bitumen-coated Saline Creek sand grains following 300°C compression test.	797
G-21	Remoulded Saline Creek oil sand fabric (note the clusters of "oil-bonded" grains).	798
G-22	Saline Creek oil sand fabric after triaxial compression under 8 MPa effective confining stress at 200°C.	798
G-23	Saline Creek oil sand fabric along the shear plane following triaxial compression at 200°C.	799
G-24	Saline Creek oil sand fabric after triaxial compression at 200°C (J1 constant stress path).	799
G-25	Saline Creek oil sand - shear plane fabric after 200°C triaxial compression test.	800
G-26	Oil-rich fabric of Saline Creek oil sand after 125°C triaxial compression test.	800
G-27	Cold Lake oil sand fabric after triaxial compression under 4 MPa effective confining stress at 200°C.	801



LIST OF FIGURES IN APPENDIX H

<u>FIGURE</u>		<u>Page</u>
H1	Sample #20: Test TOS10 (before)	804
H2	Sample #20: Test TOS10 (after)	804
H3	Sample #31: Tests CPERM5 & CPERM6 (before)	805
H4	Sample #31A: Test CPERM5 (after)	805
H5	Sample 31B: Test CPERM6 (after)	806
H6	Sample #41: Test COS9 (before)	807
H7	Sample #41: Test COS9 (after)	807
H8	Sample #20 (fines < 2 $\mu$ m): Test TOS10 (before)	808
H9	Sample #20 (fines < 2 $\mu$ m): Test TOS10 (after)	808
H10	Sample #31 (fines < 2 $\mu$ m): Tests CPERM5 & CPERM6 (before)	809
H11	Sample #31A (fines < 2 $\mu$ m): Test CPERM6 (after)	809
H12	Sample #31 (fines < 2 $\mu$ m): Test CPERM6 (after)	810
H13	Sample #41 (fines < 2 $\mu$ m): Test COS9 (before)	811
H14	Sample #41 (fines < 2 $\mu$ m): Test COS9 (after)	811



## LIST OF FIGURES IN APPENDIX K

<u>FIGURE</u>		<u>Page</u>
K1.1	Transient Temperatures - One-Way Drainage (1 Hour Time Step)	844
K1.2	Transient Temperatures - One-Way Drainage (1 Hour Time Step)	845
K1.3	Transient Vertical Expansion - One- Way Drainage (1 Hour Time Step)	845
K2.1	Transient Temperatures - One-Way Drainage (10 Minute Time Step)	846
K2.2	Transient Excess Pore Pressures-One- Way Drainage (10 Minute Time Step)	847
K2.3	Transient Vertical Expansion - One- Way Drainage (10 Minute Time Step)	847
K3.1	Transient Temperatures - One-Way Drainage (1 Minute Time Step)	848
K3.2	Transient Excess Pore Pressures-One- Way Drainage (1 Minute Time Step)	849
K3.3	Transient Vertical Expansion - One- Way Drainage (1 Minute Time Step)	849
K4.1	Transient Temperatures - One-Way Drainage (30 Second Time Step)	850
K4.2	Transient Excess Pore Pressures-One- Way Drainage (30 Second Time Step)	851
K4.3	Transient Vertical Expansion - One- Way Drainage (30 Second Time Step)	851
K5.1	Transient Temperatures - One-Way Drainage (15 Second Time Step)	852
K5.2	Transient Excess Pore Pressures-One- Way Drainage (15 Second Time Step)	853



<u>FIGURE</u>		<u>Page</u>
K5.3	Transient Vertical Expansion - One-Way Drainage (15 Second Time Step)	853
K5.6	Transient Temperatures for One-Way Drainage (1 Minute Time Step)	855
K7.1	Transient Excess Pore Pressures ( $R_T = 1800$ )	856
K7.2	Transient Vertical Expansion ( $R_T = 1800$ )	856
K8.1	Transient Excess Pore Pressures ( $R_T = 180$ )	857
K8.2	Transient Vertical Expansion ( $R_T = 180$ )	857
K9.1	Transient Excess Pore Pressures ( $R_T = 18$ )	858
K9.2	Transient Vertical Expansion ( $R_T = 18$ )	858
K10.1	Transient Excess Pore Pressures ( $R_T = 5$ )	859
K10.2	Transient Vertical Expansion ( $R_T = 5$ )	859



LIST OF FIGURES IN APPENDIX L

<u>FIGURE</u>		<u>Page</u>
L1.1	Stress Changes Around the Shaft After 6 Months of Steam Injection	862
L1.2	Deformations Around the Shaft After 6 Months of Steam Injection	862
L1.3	Effective Stresses Around the Shaft After 6 Months of Steam Injection	863
L2.1	Stress Changes Around the Shaft After 2 Years of Steam Injection	864
L2.2	Deformations Around the Shaft After 2 Years of Steam Injection	864
L2.3	Effective Stresses Around the Shaft After 2 Years of Steam Injection	865
L3.1	Stress Changes Around the Shaft After 1 Month of Steam Injection	867
L3.2	Deformations Around the Shaft After 1 Month of Steam Injection	867
L3.3	Effective Stresses Around the Shaft After 1 Month of Steam Injection	868
L3.4	Stress Changes Around the Shaft After 1 Year of Steam Injection	869
L3.5	Deformations Around the Shaft After 1 Year of Steam Injection	869
L3.6	Effective Stresses Around the Shaft After 1 Year of Steam Injection	870
L3.7	Stress Changes Around the Shaft After 4 Years of Steam Injection	871
L3.8	Deformations Around the Shaft After 4 Years of Steam Injection	871
L3.9	Effective Stresses Around the Shaft After 4 Years of Steam Injection	872



<u>FIGURE</u>		<u>Page</u>
L4.1	Stress Changes Around the Shaft After 1 Month of Steam Injection	874
L4.2	Deformations Around the Shaft After 1 Month of Steam Injection	874
L4.3	Effective Stresses Around the Shaft After 1 Month of Steam Injection	875
L4.4	Stress Changes Around the Shaft After 6 Months of Steam Injection	876
L4.5	Deformations Around the Shaft After 6 Months of Steam Injection	876
L4.6	Effective Stresses Around the Shaft After 6 Months of Steam Injection	877
L4.7	Stress Changes Around the Shaft After 1 Year of Steam Injection	878
L4.8	Deformations Around the Shaft After 1 Year of Steam Injection	878
L4.9	Effective Stresses Around the Shaft After 1 Year of Steam Injection	879
L4.10	Stress Changes Around the Shaft After 4 Years of Steam Injection	880
L4.11	Deformations Around the Shaft After 4 Years of Steam Injection	880
L4.12	Effective Stresses Around the Shaft After 4 Years of Steam Injection	881
L5.1	Stress Changes Around the Shaft After 1 Month of Drained Heating	883
L5.2	Deformations Around the Shaft After 1 Month of Drained Heating	883
L5.3	Effective Stresses Around the Shaft After 1 Month of Drained Heating	884



<u>FIGURE</u>	<u>Page</u>
L5.4 Stress Changes Around the Shaft After 1 Year of Drained Heating	885
L5.5 Deformations Around the Shaft After 1 Year of Drained Heating	885
L5.6 Effective Stresses Around the Shaft After 1 Year of Drained Heating	886
L5.7 Stress Changes Around the Shaft After 4 Years of Drained Heating	887
L5.8 Deformations Around the Shaft After 4 Years of Drained Heating	887
L5.9 Effective Stresses Around the Shaft After 4 Years of Drained Heating	888
L6.1 Stress Changes Around the Shaft After 1 Month of Undrained Heating (constant thermoelastic coefficients)	890
L6.2 Deformations Around the Shaft After 1 Month of Undrained Heating (constant thermoelastic coefficients)	890
L6.3 Stress Changes Around the Shaft After 1 Year of Undrained Heating (constant thermoelastic coefficients)	891
L6.4 Deformations Around the Shaft After 1 Year of Undrained Heating (constant thermoelastic coefficients)	891
L6.5 Stress Changes Around the Shaft After 4 Years of Undrained Heating (constant thermoelastic coefficients)	892
L6.6 Deformations Around the Shaft After 4 Years of Undrained Heating (constant thermoelastic coefficients)	892
L7.1 Stress Changes Around the Shaft After 1 Month of Transient Undrained Heating	894



<u>FIGURE</u>		<u>Page</u>
L7.2	Deformations Around the Shaft After 1 Month of Transient Undrained Heating	894
L7.3	Effective Stresses Around the Shaft After 1 Month of Transient Undrained Heating	895
L7.4	Stress Changes Around the Shaft After 1 Year of Transient Undrained Heating	896
L7.5	Deformations Around the Shaft After 1 Year of Transient Undrained Heating	896
L7.6	Effective Stress Around the Shaft After 1 Year of Transient Undrained Heating	897
L7.7	Stress Changes Around the Shaft After 4 Years of Transient Undrained Heating	898
L7.8	Deformations Around the Shaft After 4 Years of Transient Undrained Heating	898
L7.9	Effective Stresses Around the Shaft After 4 Years of Transient Undrained Heating	899
L8.1	Stress Changes Around the Shaft After 1 Month of Steam Injection in Shale	901
L8.2	Deformations Around the Shaft After 1 Month of Steam Injection in Shale	901
L8.3	Effective Stresses Around the Shaft After 1 Month of Steam Injection in Shale	902
L8.4	Stress Changes Around the Shaft After 1 Year of Steam Injection in Shale	903
L8.5	Deformations Around the Shaft After 1 Year of Steam Injection in Shale	903



<u>FIGURE</u>		<u>Page</u>
L8.6	Effective Stresses Around the Shaft After 1 Year of Steam Injection in Shale	904
L8.7	Stress Changes Around the Shaft After 4 Years of Steam Injection in Shale	905
L8.8	Stress Changes Around the Shaft After 4 Years of Steam Injection in Shale	905
L8.9	Stress Changes Around the Shaft After 4 Years of Steam Injection in Shale	906



## APPENDIX A

### APPARATUS COMPLIANCE TESTING AND CALIBRATIONS



TABLE A-1  
PROPERTIES OF SYSTEM FLUIDS

FLUID	DENSITY AT 25°C AND ATMOSPHERIC PRESSURE ( $\text{kg}/\text{m}^3$ )	FREEZE POINT (°C)	BOILING POINT (°C)	FLASH POINT (°C)	DYNAMIC VISCOSITY AT 25°C AND ATMOSPHERIC PRESSURE (mPa•s)
Distilled Water	1.000	0°C	100°C	10°C	1.0
Athabasca Bitumen	1.03 - 1.05	-	-	-	$2 - 3 \times 10^6$
Silicone Oil Cell Fluid (Dow Corning 710G)	1.10 - 1.12	-22°C	230°C	301°C	550.0



TABLE A-2  
THERMAL EXPANSION AND COMPRESSION PROPERTIES  
OF APPARATUS MATERIALS

MATERIAL	LINEAR COEFFICIENT OF THERMAL EXPANSION ( $^{\circ}\text{C}^{-1}$ )	VOLUME COEFFICIENT OF THERMAL EXPANSION ( $^{\circ}\text{C}^{-1}$ )	YOUNG'S MODULUS (kPa)	POISSON'S RATIO
Aluminum	$23.0 * 10^{-6}$	$69.0 * 10^{-6}$	$67 * 10^6$ @ $25^{\circ}\text{C}$ $44 * 10^6$ @ $250^{\circ}\text{C}$	0.25
Stainless Steel	$17.8 * 10^{-6}$	$53.4 * 10^{-6}$	$193 * 10^6$ @ $25^{\circ}\text{C}$ $130 * 10^6$ @ $250^{\circ}\text{C}$	0.25
Copper	$16.7 * 10^{-6}$	$50.1 * 10^{-6}$	—	—
Brass	$18.7 * 10^{-6}$	$56.1 * 10^{-6}$	—	—
Silicone Rubber	$1.7 * 10^{-4}$	$5.2 * 10^{-4}$	36 kPa (extension @ $25^{\circ}\text{C}$ )	0.50



TABLE A-3  
VOLUME CHANGE PROPERTIES OF SOME MINERALS

MINERAL SOLID	TEMPERATURE RANGE (°C)	COEFFICIENT OF VOLUME THERMAL EXPANSION (°C <sup>-1</sup> )	ISOTROPIC COMPRESSIBILITY (MPa <sup>-1</sup> )	MELTING POINT TEMPERATURE (°C)
Alpha Quartz Crystal	20	3.4 * 10 <sup>-6</sup>	27 * 10 <sup>-6</sup>	Inversion @ 573°C
Alpha Quartz Crystal	400	69.0 * 10 <sup>-6</sup>	-	1050°C
Beta Quartz Crystals	575 - 1000	-3.0 * 10 <sup>-6</sup>	18 * 10 <sup>-6</sup>	-
Barite (BaSO <sub>4</sub> )	20 - 200	57.0 * 10 <sup>-6</sup>	17 * 10 <sup>-6</sup>	-
Halite (NaCl)	-80 - 20	107.0 * 10 <sup>-6</sup>	43 * 10 <sup>-6</sup>	804°C
Gypsum (CaSO <sub>4</sub> •2H <sub>2</sub> O)	20 - 100	73.0 * 10 <sup>-6</sup>	25 * 10 <sup>-6</sup>	-
Diamond (C)	20 - 1200	10.0 * 10 <sup>-6</sup>	2 * 10 <sup>-6</sup>	-



TABLE A-4

## SUMMARY OF CALIBRATIONS FOR ELECTRONIC MEASURING DEVICES

<u>Electronic Measuring Device</u>	<u>Calibration</u>	<u>Precision</u>
1. Consolidometer LVDT (1000 HR)	1.965 mm/V	$\pm .001$ mm/V
2. Volume change LVDT (500 HR)	10.0 ml/V	$\pm .10$ ml to $\pm .001$ ml
3. Triaxial External LVDT (1000 HR)	1.559 mm/V	$\pm .005$ mm
4. 7 MPa Strain Gauge Back Pressure Transducer	190.50 kPa/mV	$\pm .10$ kPa
5. 7 MPa S.G. Confining Pressure Transducer	185.36 kPa/mV	$\pm .10$ kPa
6. 35 MPa S.G. (Air Cooled) Back Pressure Transducer	1262.80 kPa/mV	$\pm .50$ kPa
7. 35 MPa Strain Gauge Confining Pressure Transducer	1145.60 kPa/mV	$\pm .50$ kPa
8. 35 MPa S.G. Upstream Back Pressure Transducer	1167.40 kPa/mV	$\pm .50$ kPa
9. 35 MPa S.G. Downstream Back Pressure Transducer	1080.00 kPa/mV	$\pm .50$ kPa
10. 500 kPa Validyne Differential Pressure Transducer	37.10 kPa/mV	$\pm .10$ kPa
11. 140 kPa Validyne Differential Pressure Transducer	10.748 kPa/mV	$\pm .01$ kPa
12. 220 kN Strain Gauge Load Cell	31.207 kN/mV	$\pm .01$ kN
13. 440 kN Strain Gauge Load Cell	35.063 kN/mV	$\pm .01$ kN
14. Internal Axial Strain Gauge Yoke a) Axial Arm #1 b) Axial Arm #2	4.610 mm/V 4.075 mm/V	$\pm .01$ mm $\pm .01$ mm
15. Lateral Strain Gauge Clamp Device	0.500 mm/V	$\pm .01$ mm
16. J Type Thermocouples (Iron/Constantin)	$^{\circ}$ C (Linearized Circuit)	$\pm .5$ $^{\circ}$ C



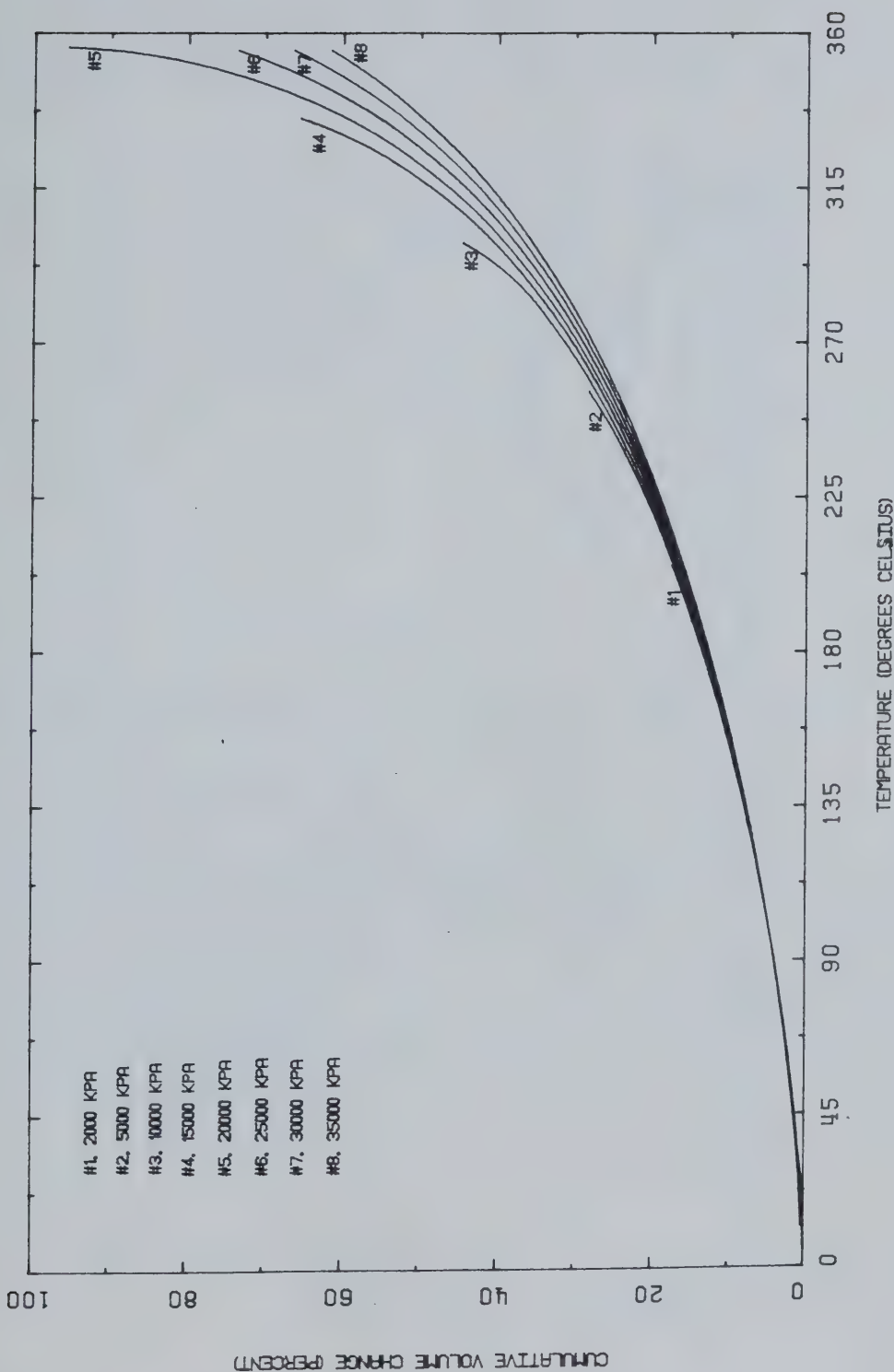


FIGURE A1 Thermal Expansion of Water



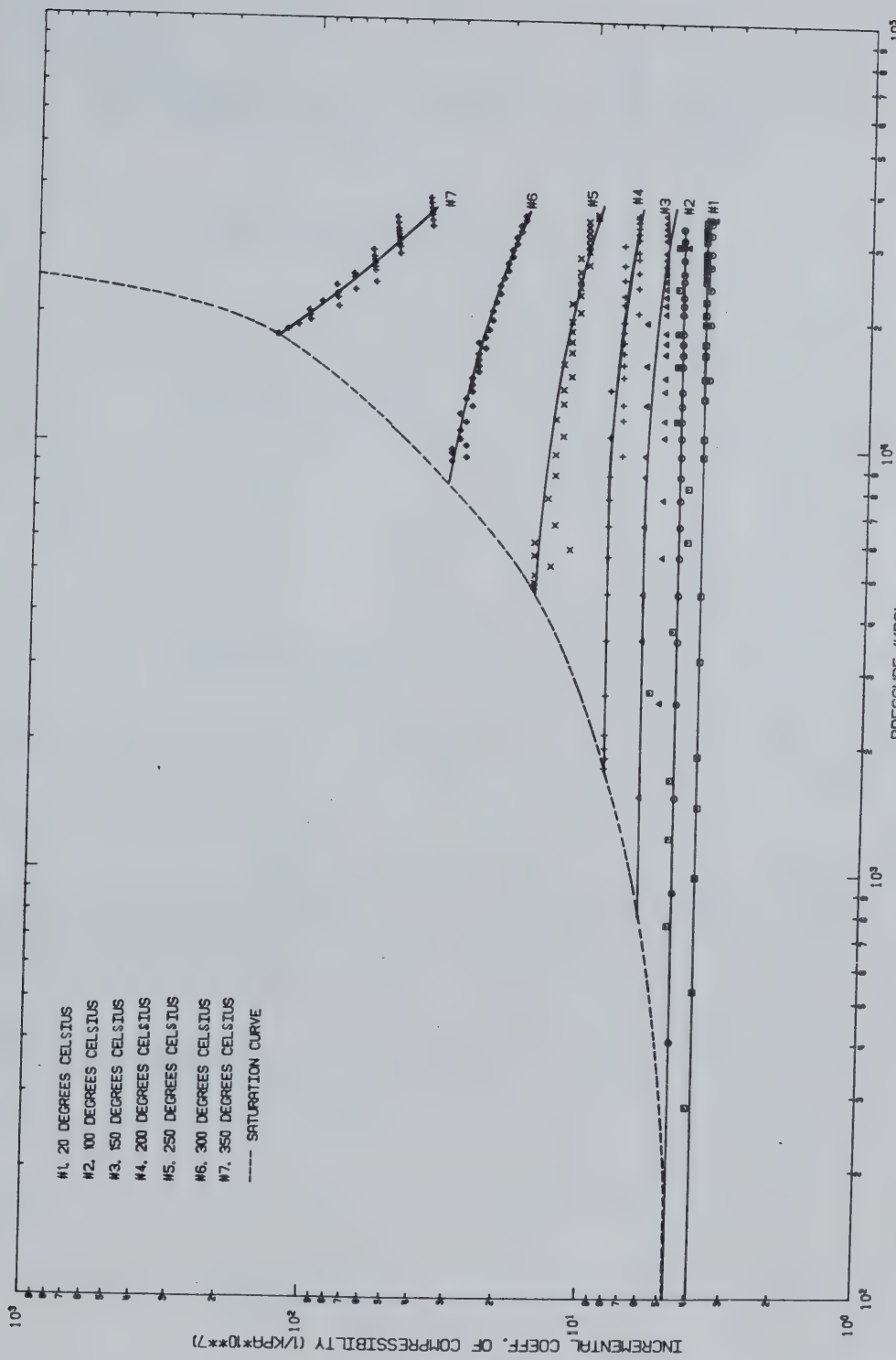


FIGURE A2 Compressibility of Water at Elevated Temperatures



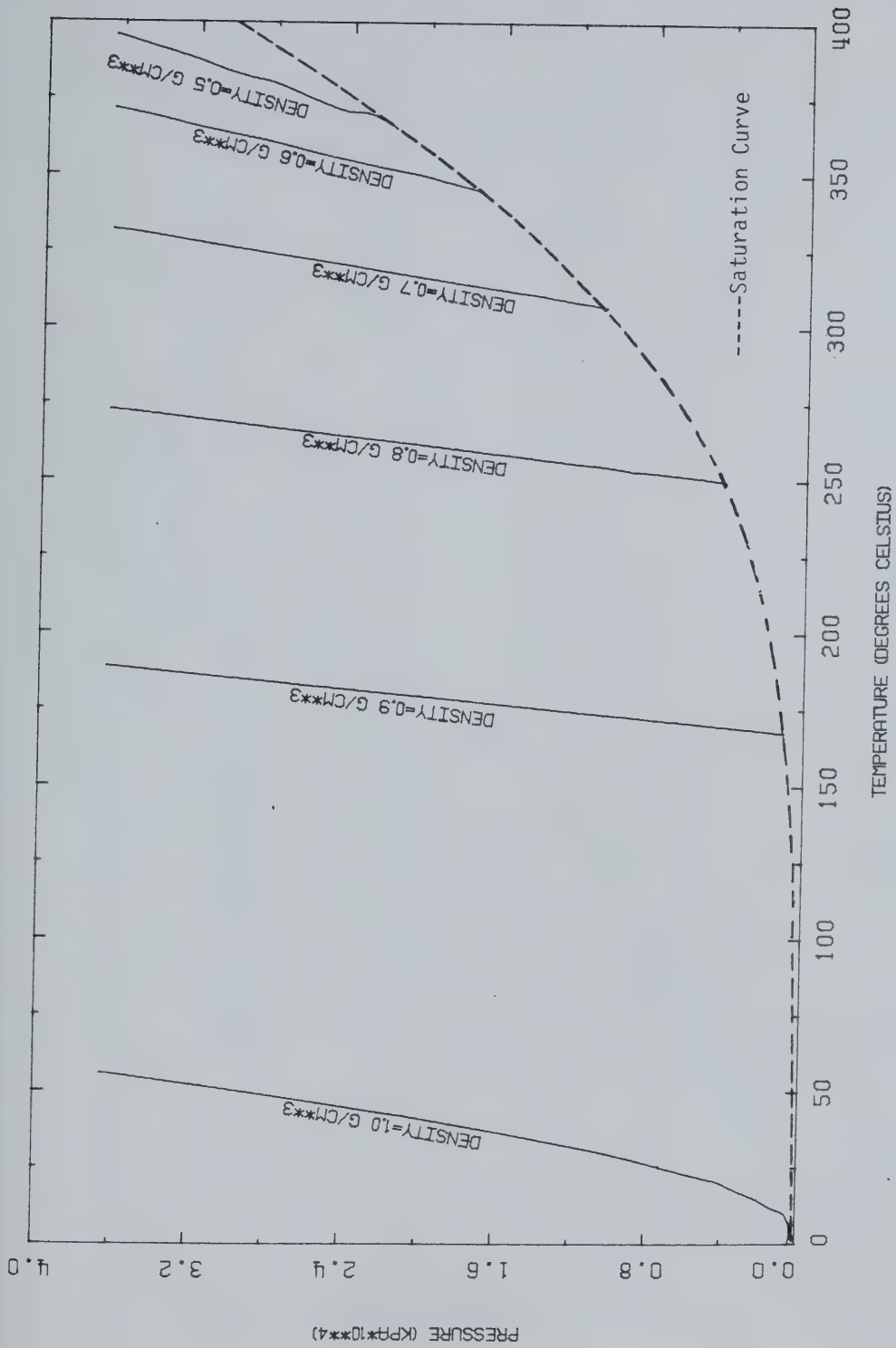


FIGURE A3 Pressure Increase During Constant Volume Heating



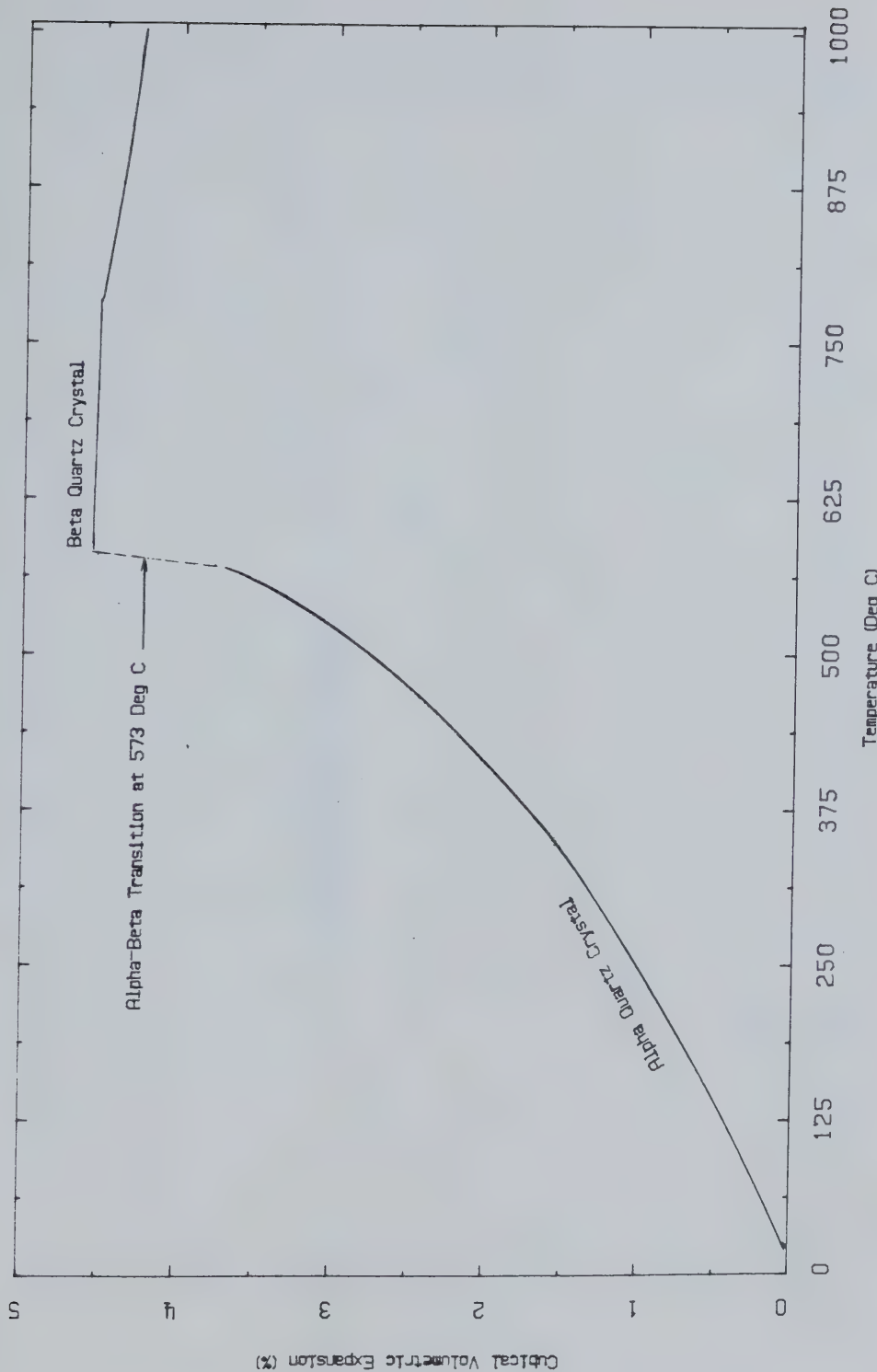


FIGURE A4 Thermal Expansion of Quartz



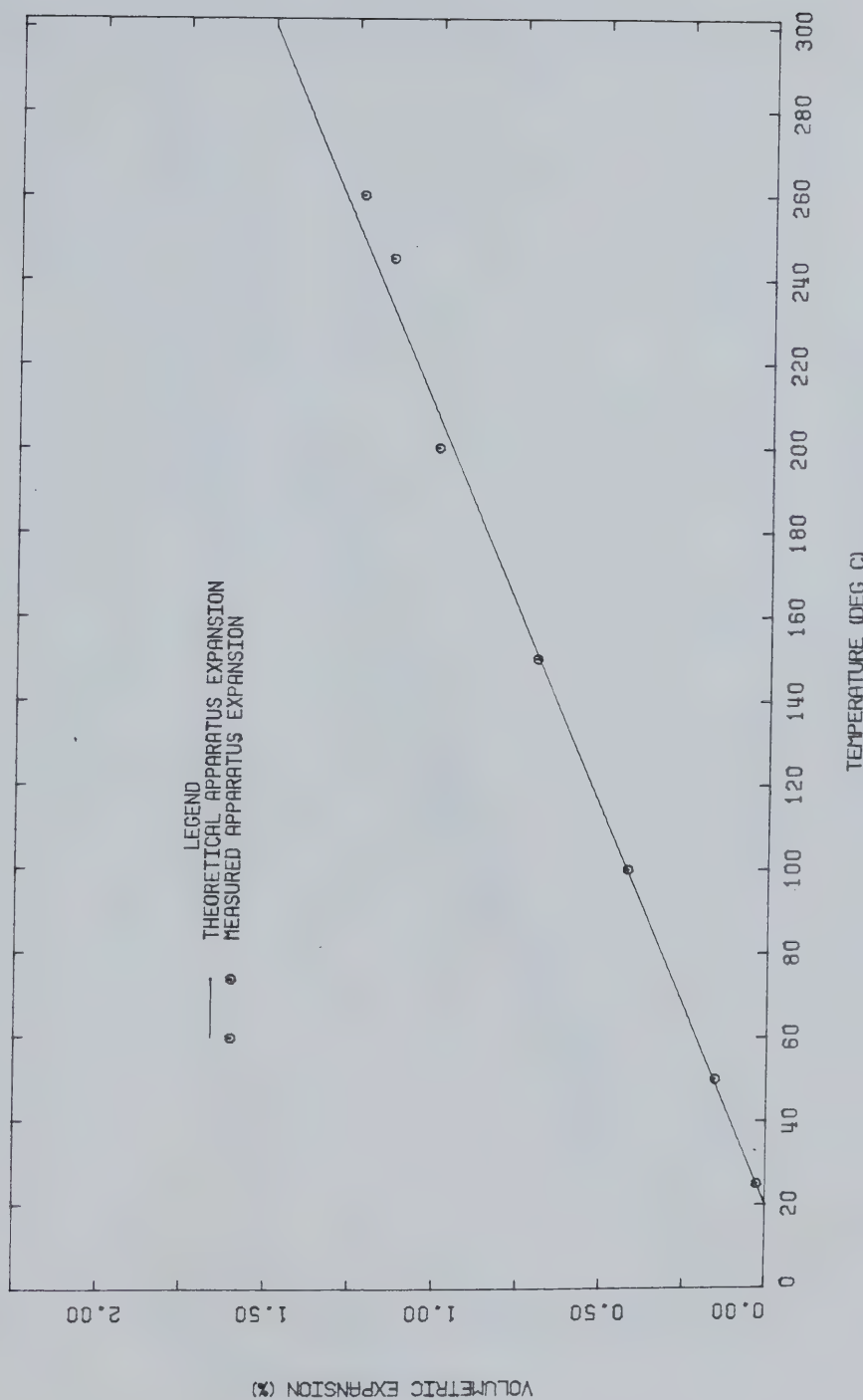


FIGURE A5 Consilidometer: Correction for Apparatus Thermal Expansion



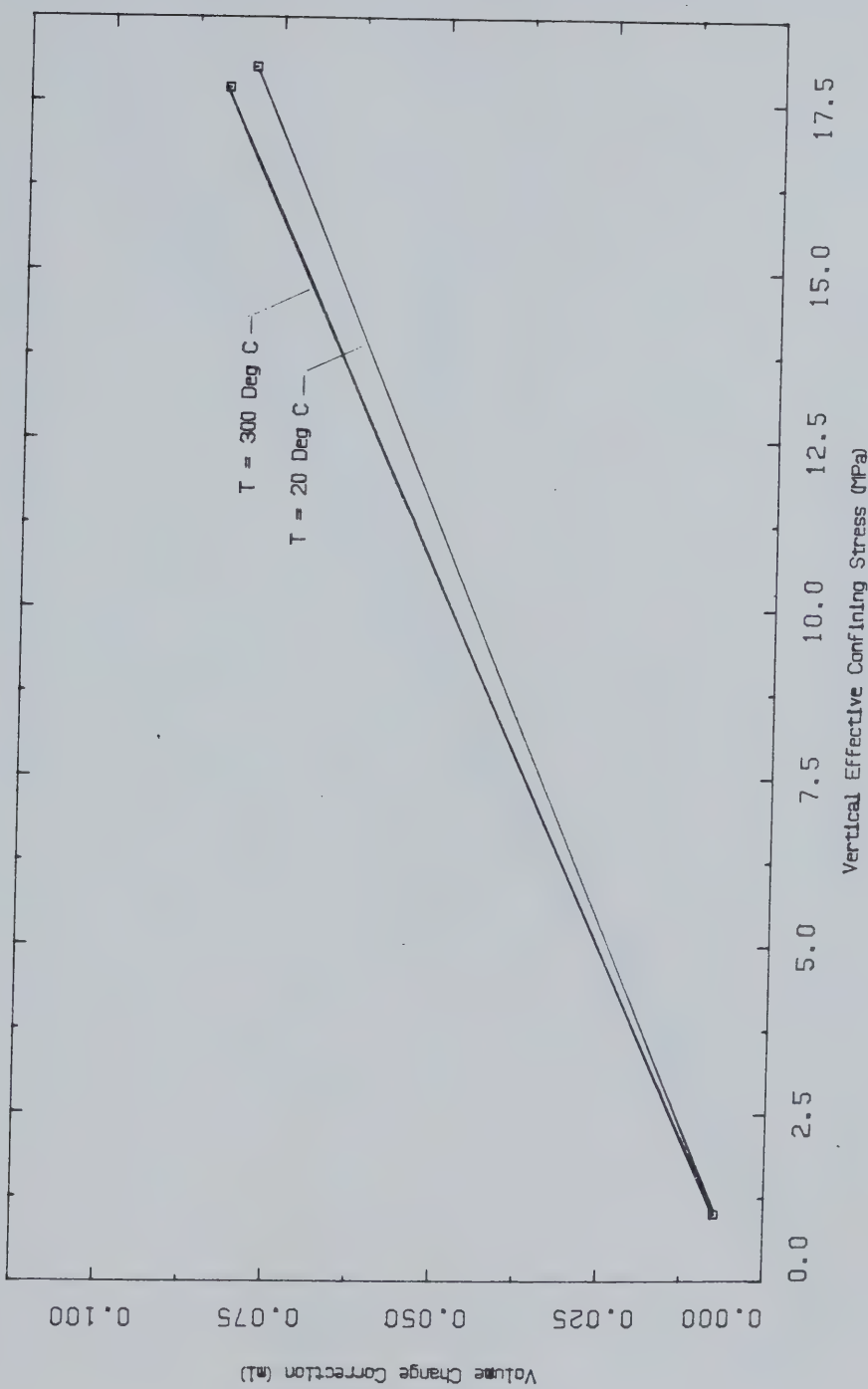


FIGURE A6 Consolidometer: Correction for Stress Induced Apparatus Expansion



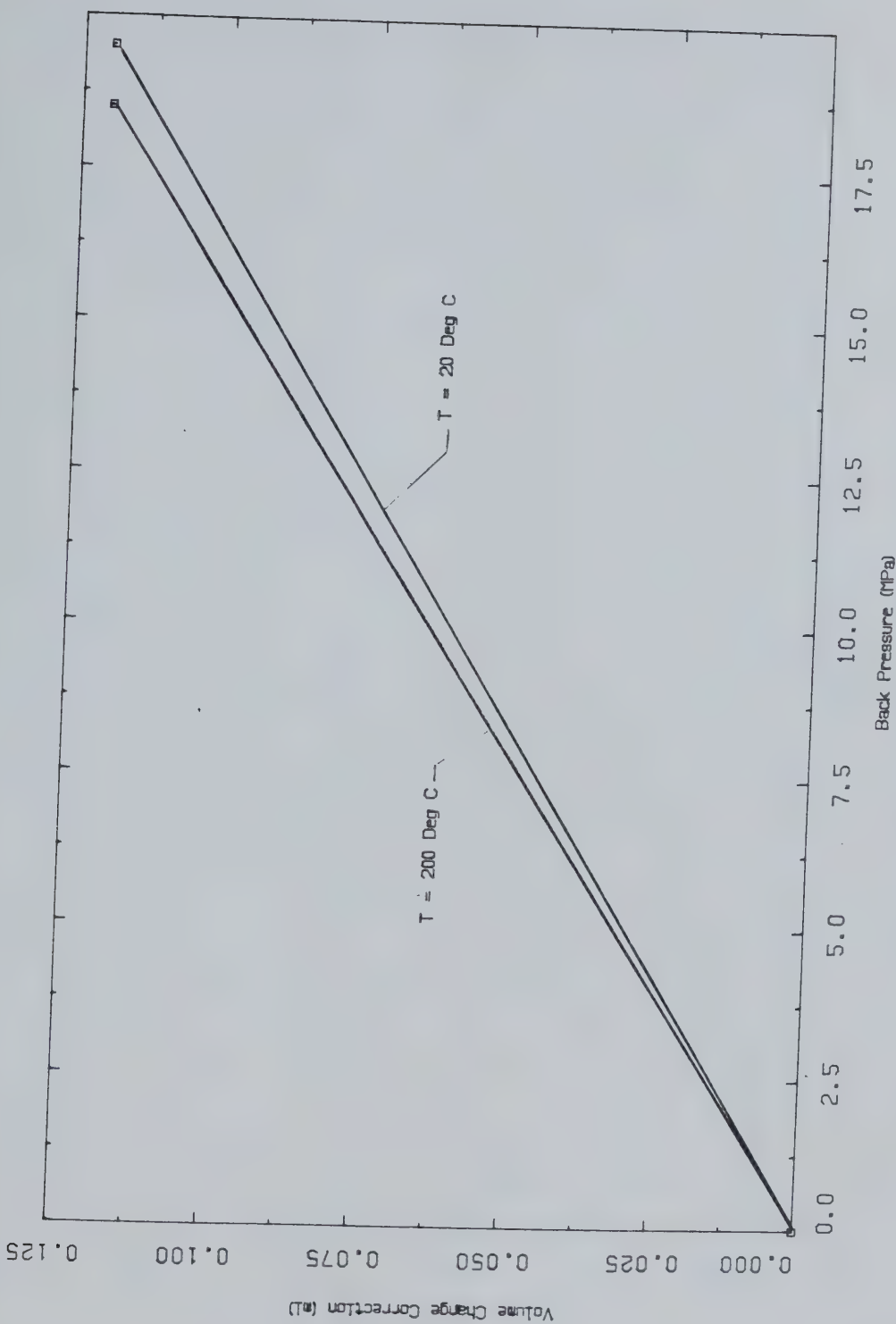


FIGURE A7 Consol idometer: Correction for Back Pressure Induced Apparatus Expansion



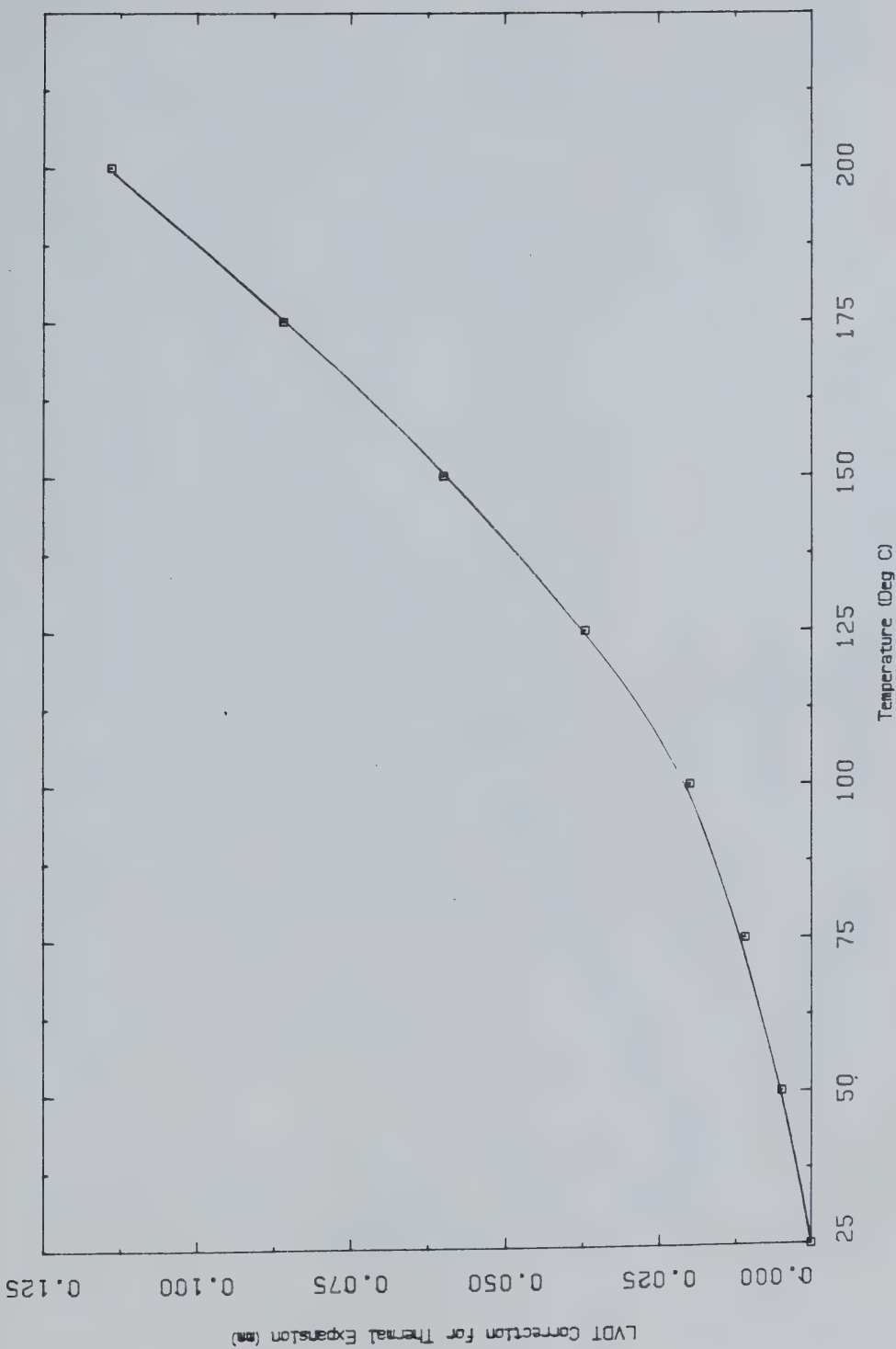


FIGURE A8 Consolidometer: LVDT Correction for Vertical Thermal Expansion of the Apparatus



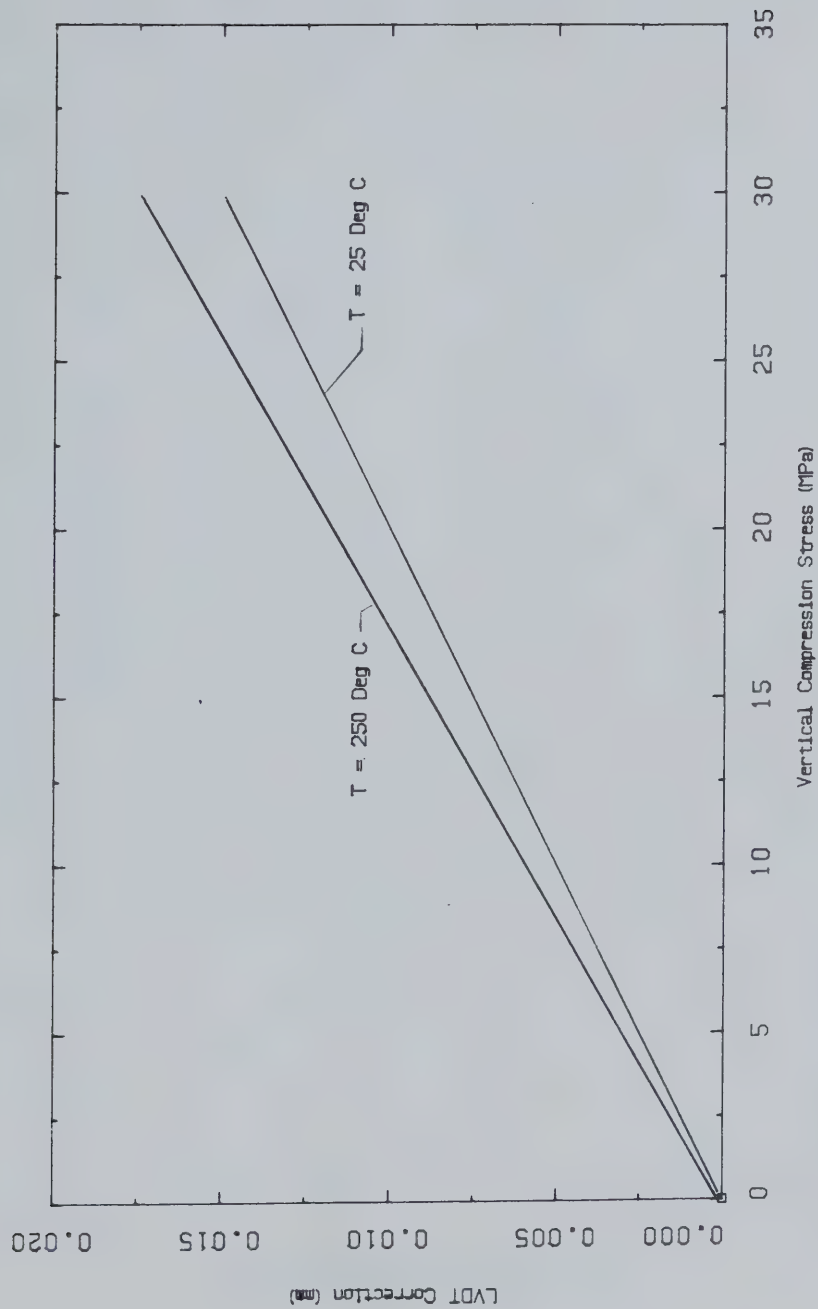


FIGURE A9 Consolidometer: LVDT Correction for Vertical Apparatus Compression



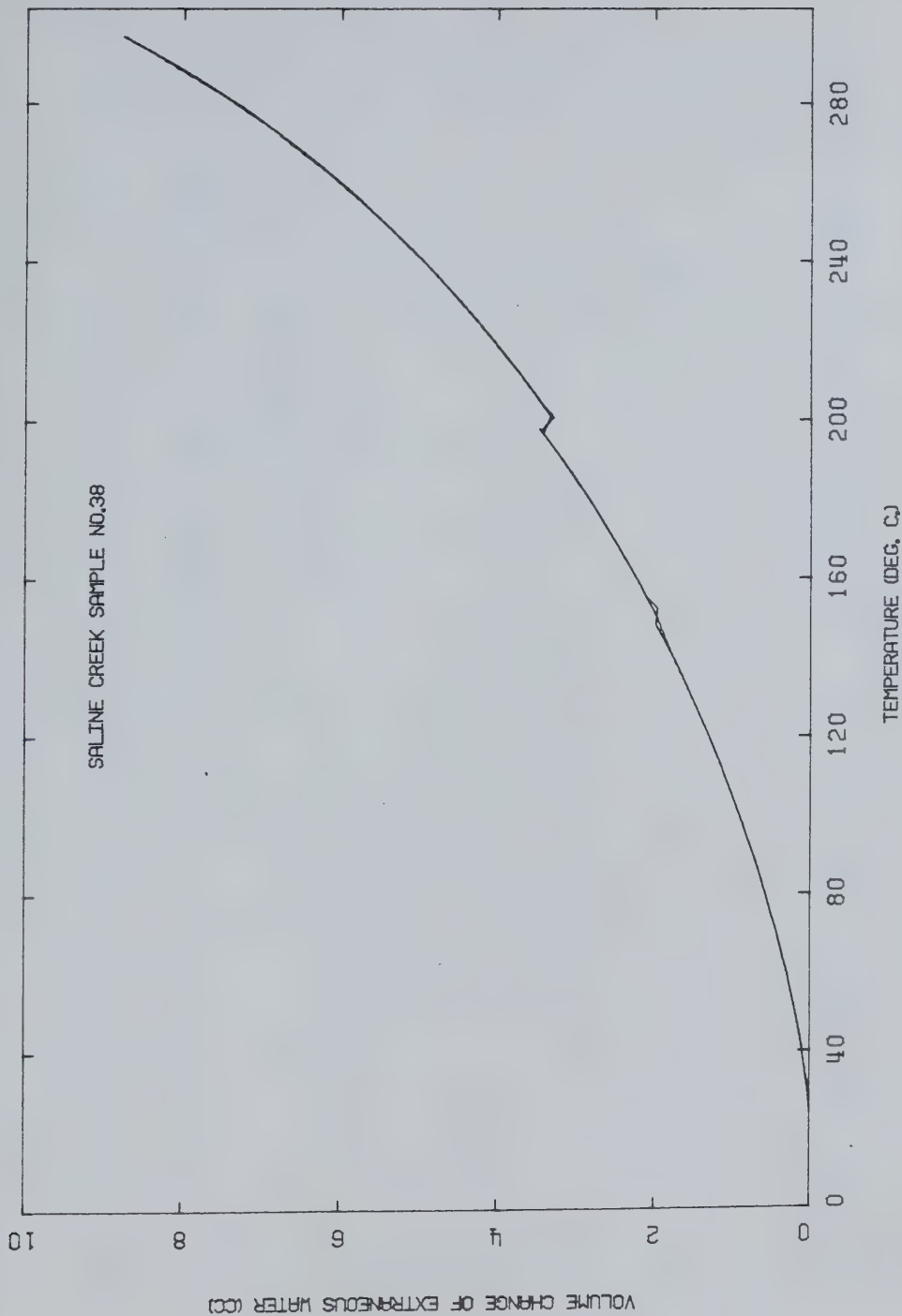


FIGURE A10 Consoliodometer: Volume Change Correction for Thermal Expansion of Extraneous Water



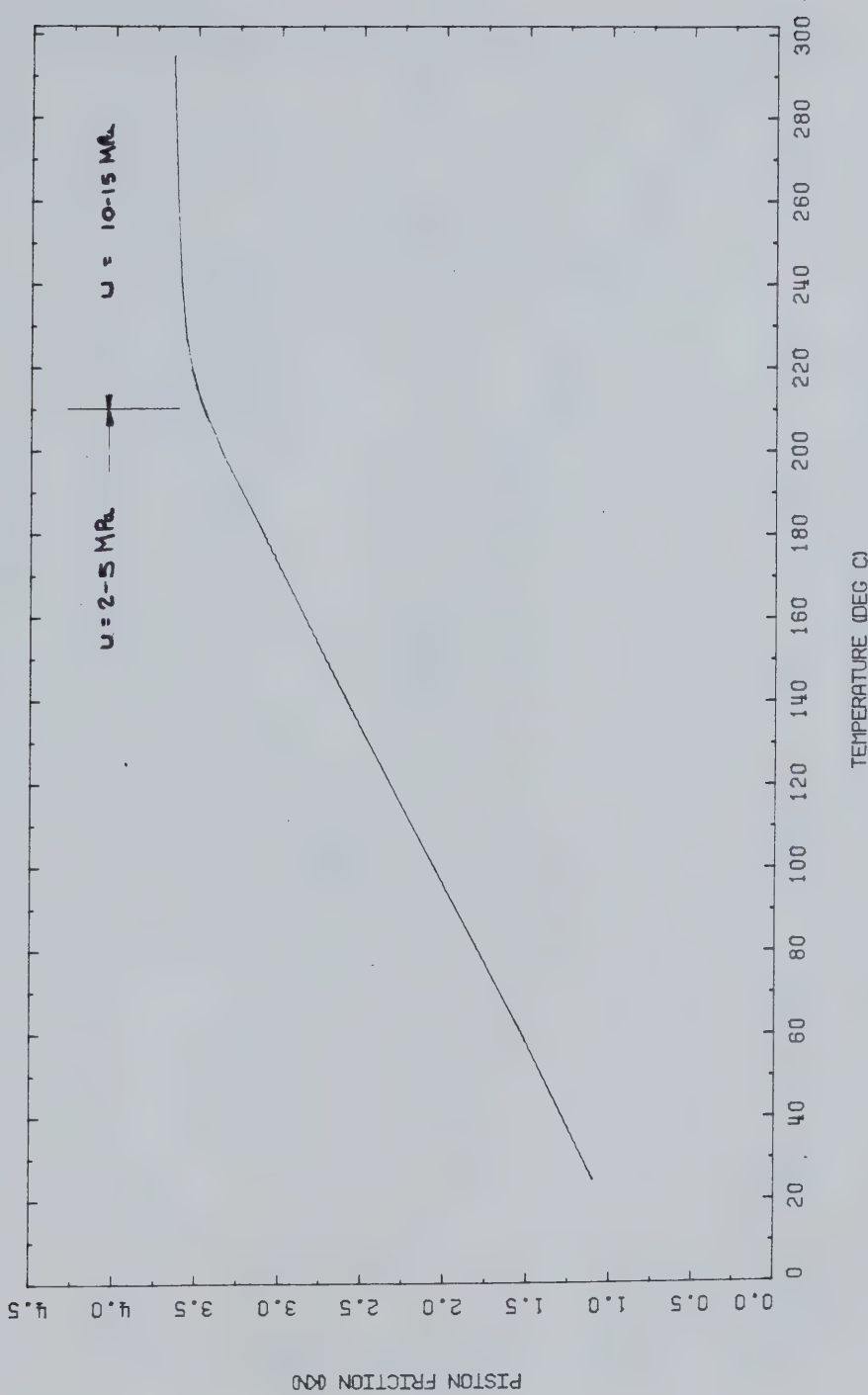


FIGURE A11 Consolidometer: Piston Friction at Elevated Temperatures and Back Pressures



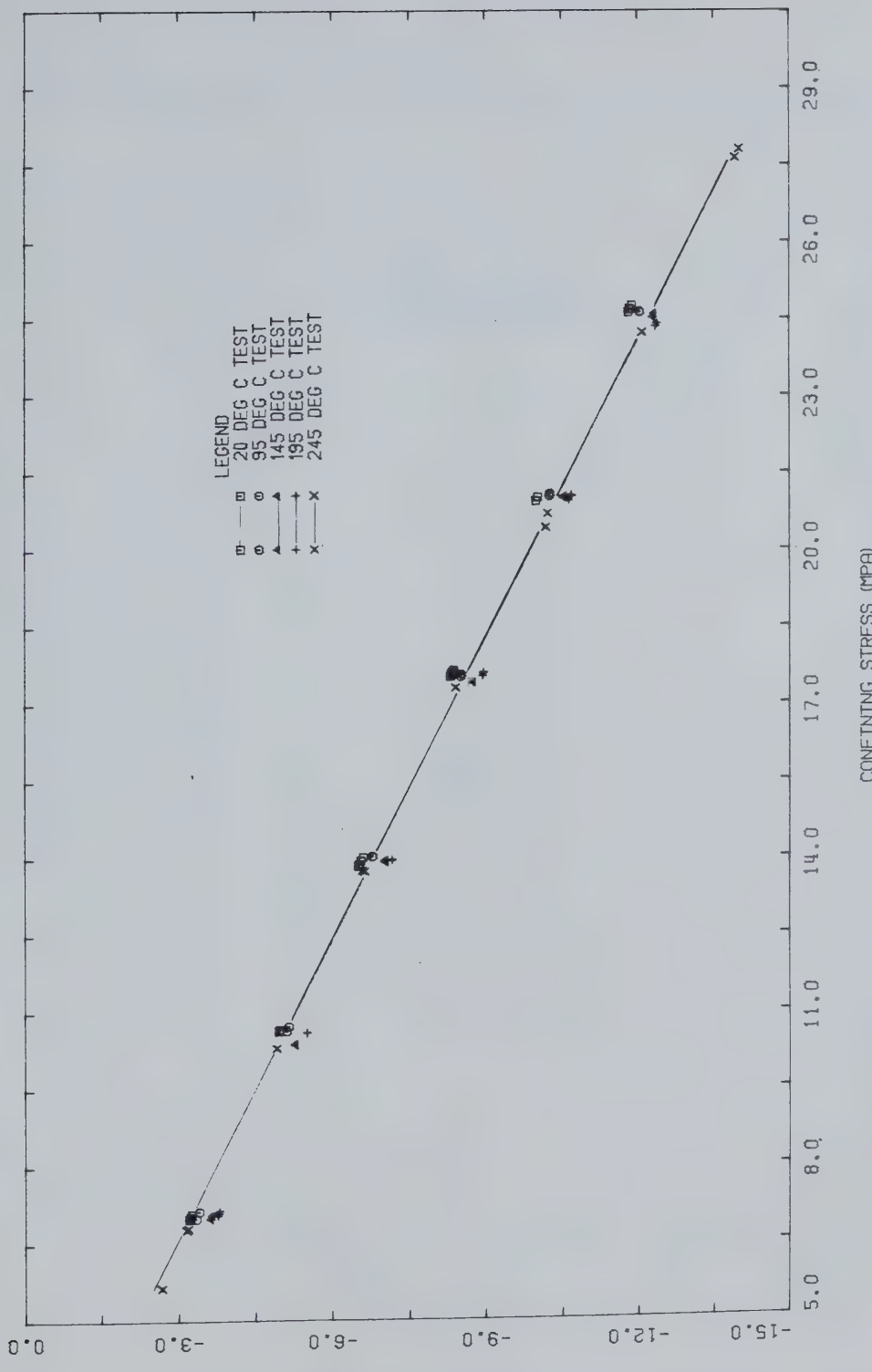


FIGURE A12 Triaxial Apparatus: Piston Friction at Elevated Confining Stresses and Temperatures Using a Non-Lubricated Piston



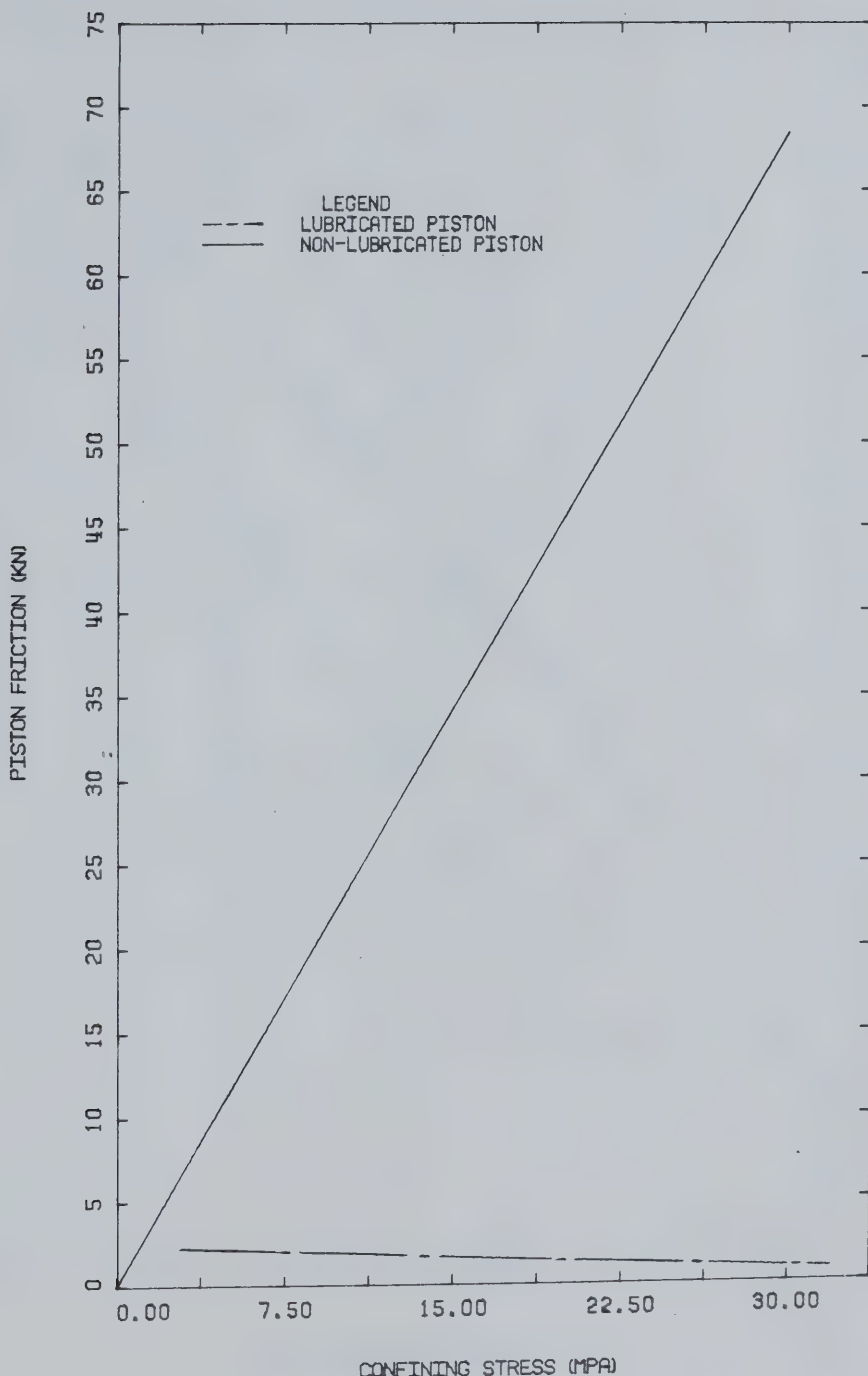


FIGURE A13 Triaxial Apparatus: Influence of Lubrication on Measured Piston Friction



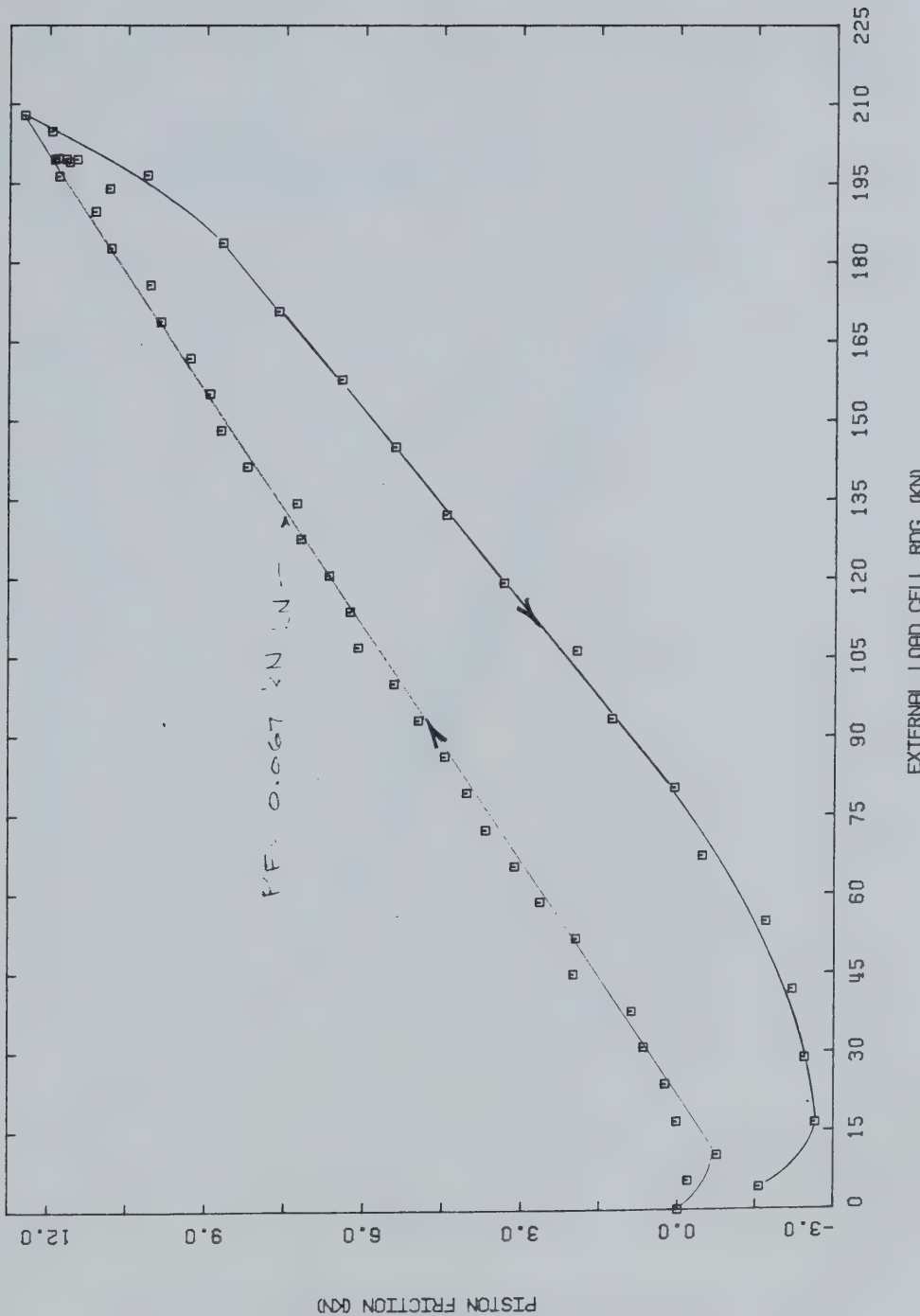


FIGURE A14 Triaxial Apparatus: Correction for Piston Friction with Applied Vertical Load



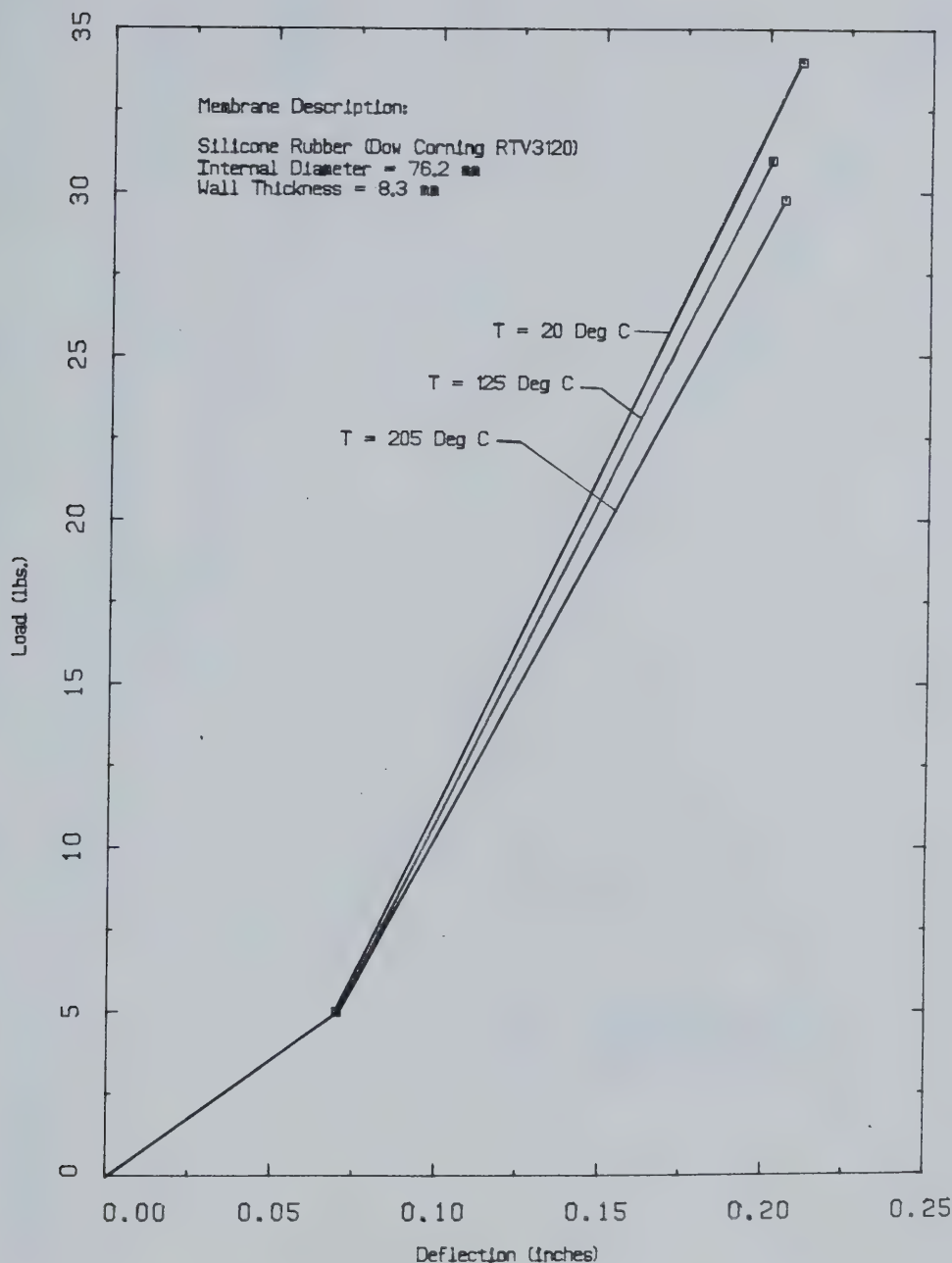


FIGURE A15 Triaxial Rubber Membrane Compliance at Elevated Temperatures



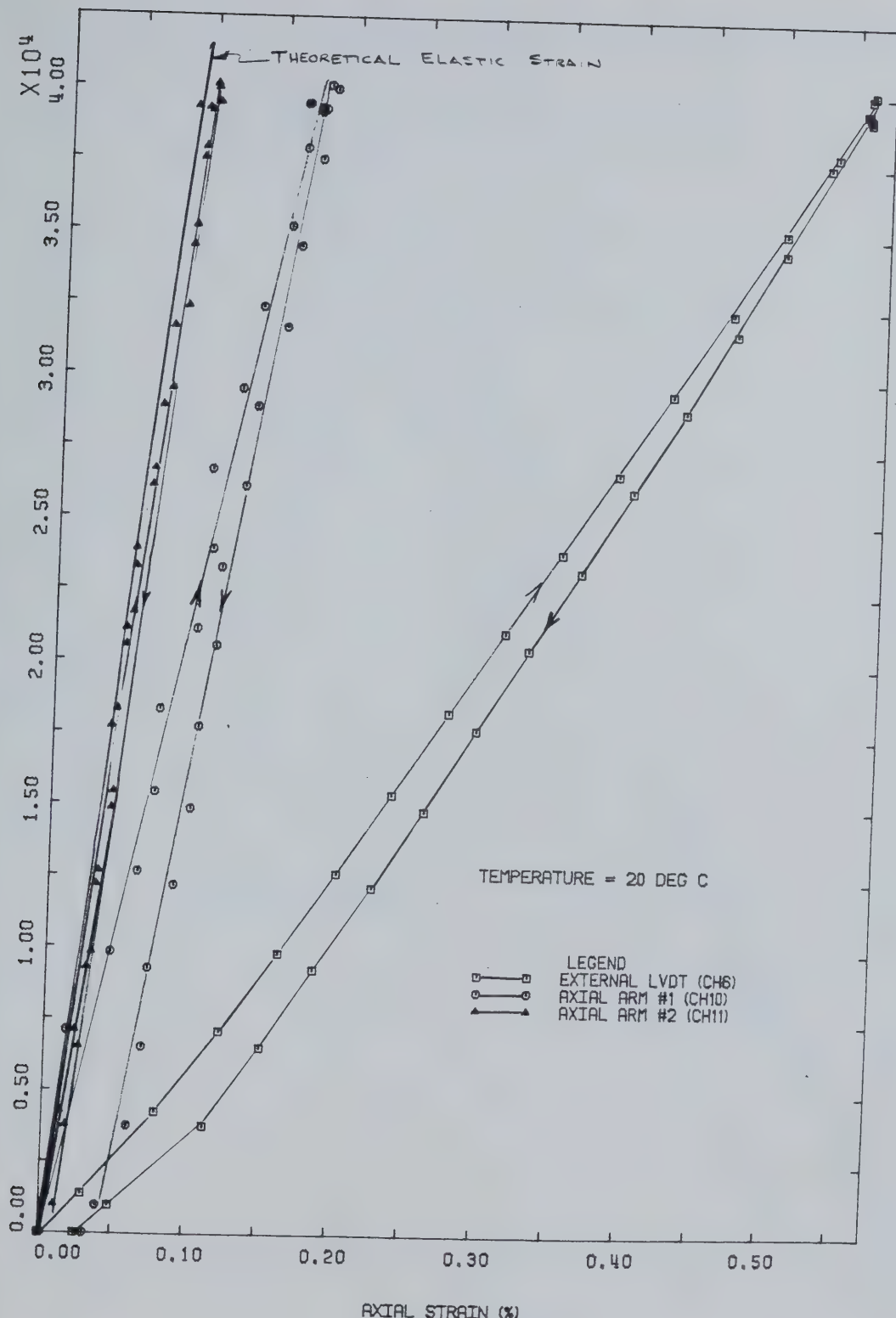


FIGURE A16 Triaxial Apparatus: Accuracy of Internal and External Axial Strain Measuring Devices During Compression of an Aluminium Sample at 20°C



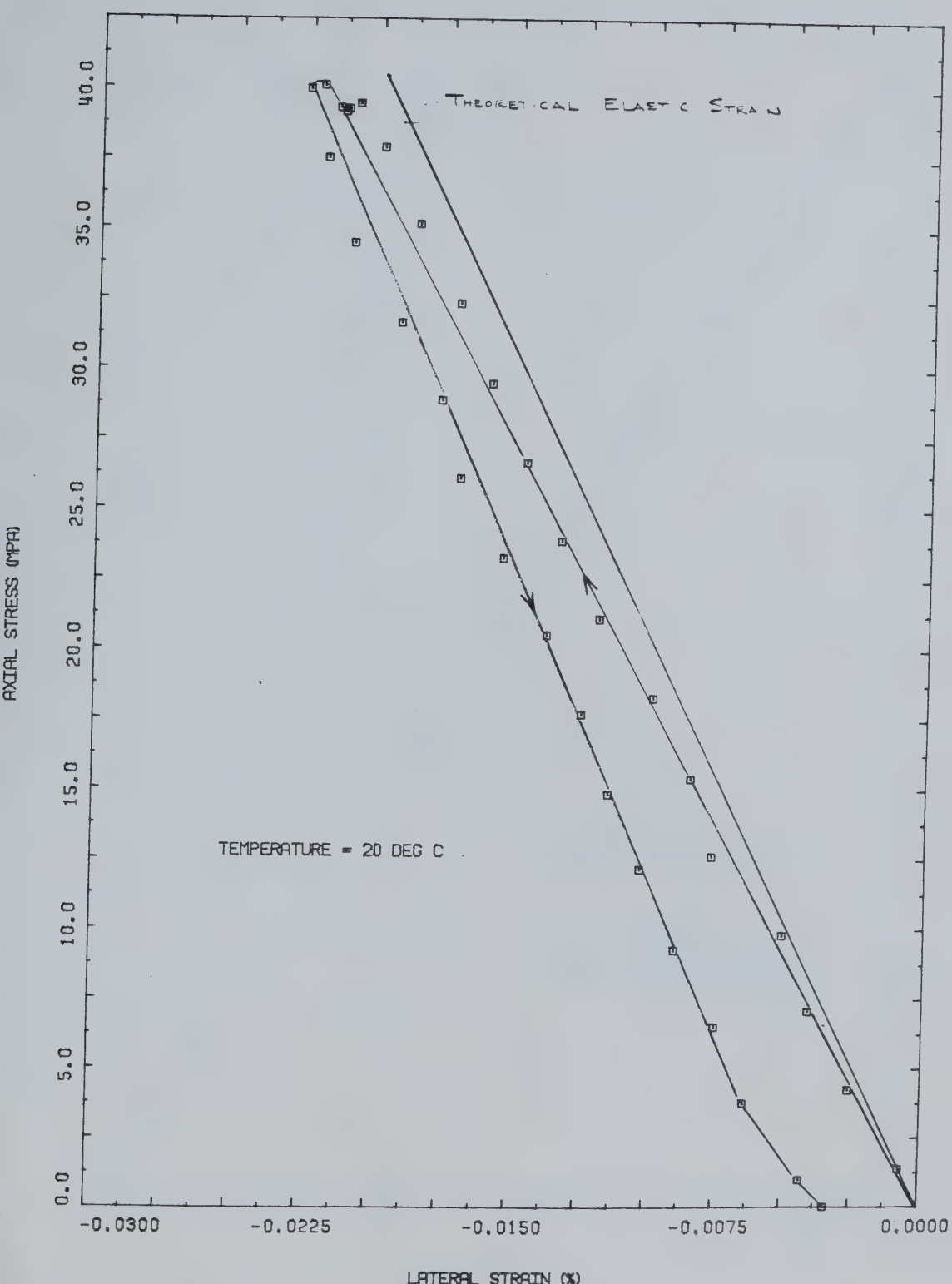


FIGURE A17 Triaxial Apparatus: Accuracy of an Internal Lateral Strain Measuring Device During Compression of an Aluminium Sample at 20°C



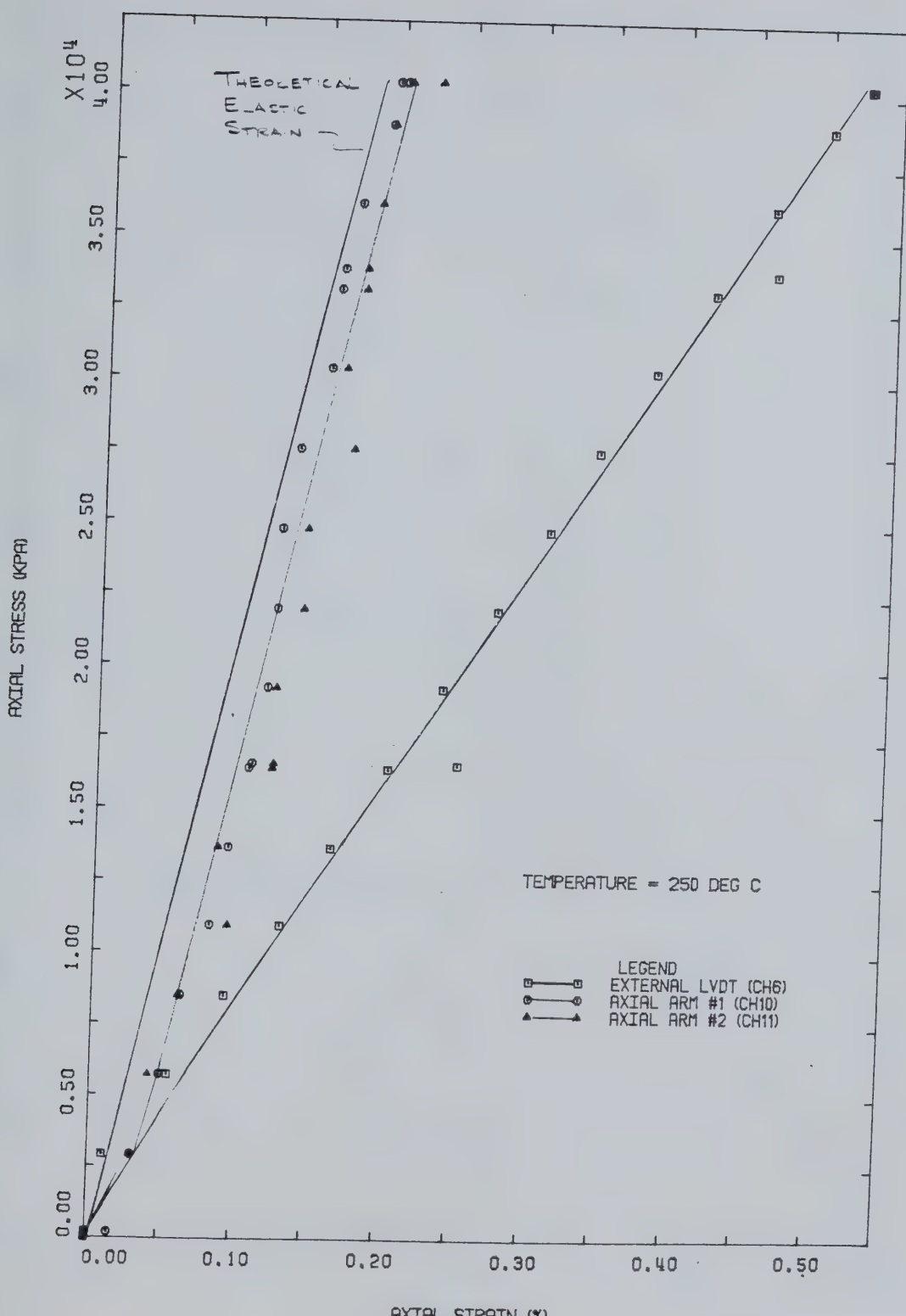


FIGURE A18 Triaxial Apparatus: Accuracy of Internal and External Axial Strain Measuring Devices During Compression of an Aluminium Sample at 250°C



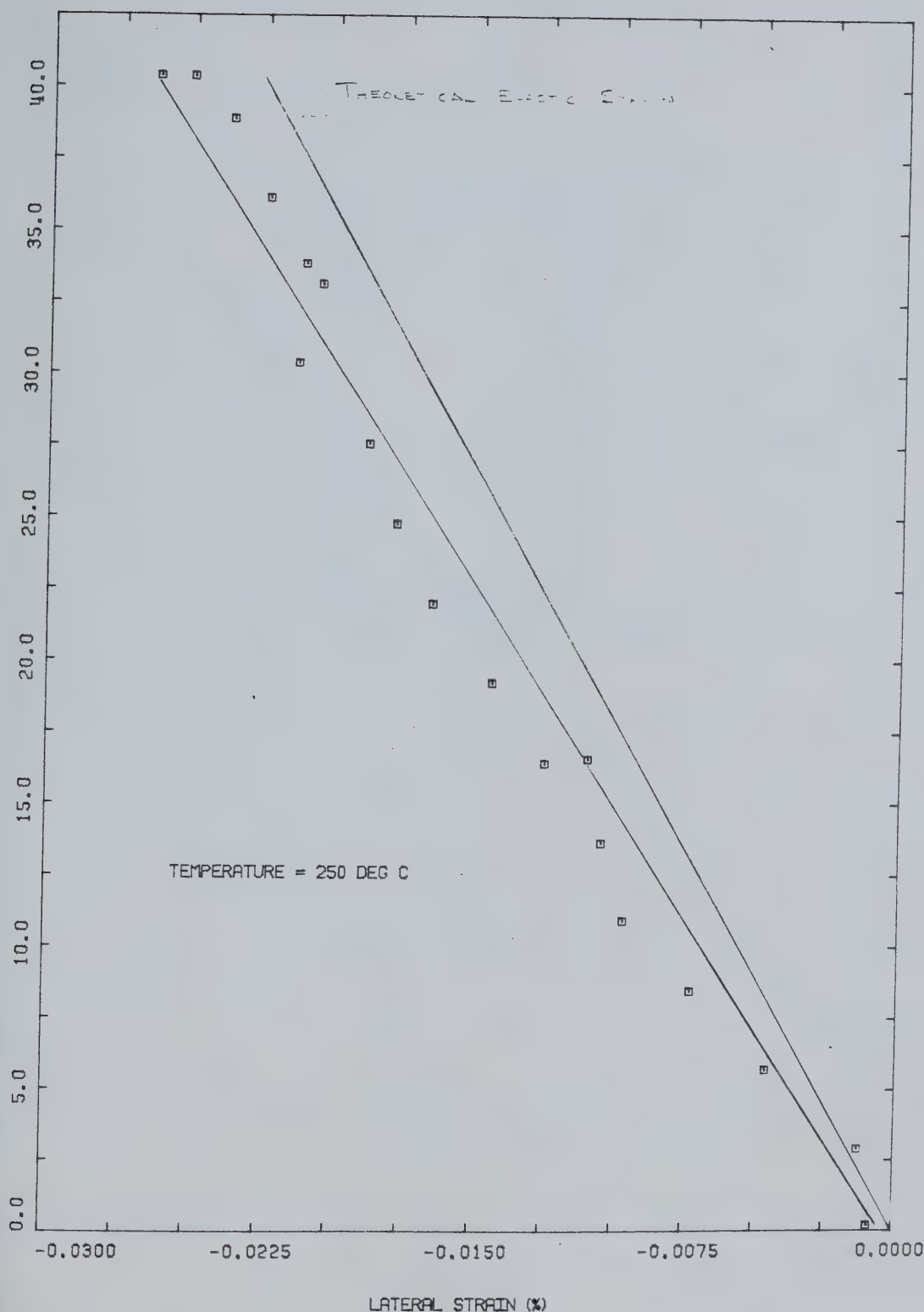
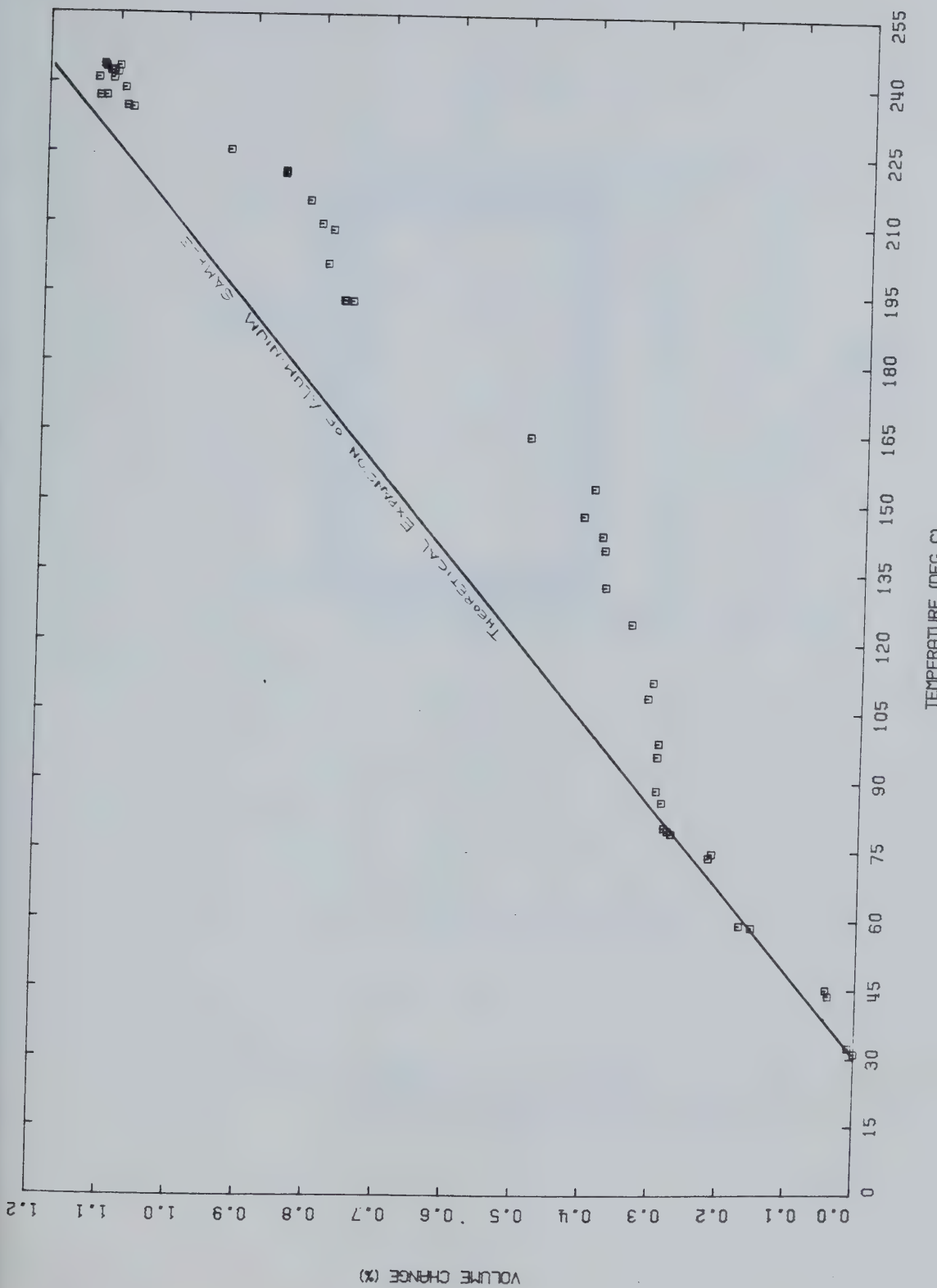


FIGURE A19 Triaxial Apparatus: Accuracy of an Internal Lateral Strain Measuring Device During Compression of an Aluminium Sample at 250°C



FIGURE A20 Triaxial Apparatus: Compliance of Volume Change Measurements During Thermal Expansion of an Aluminium Sample





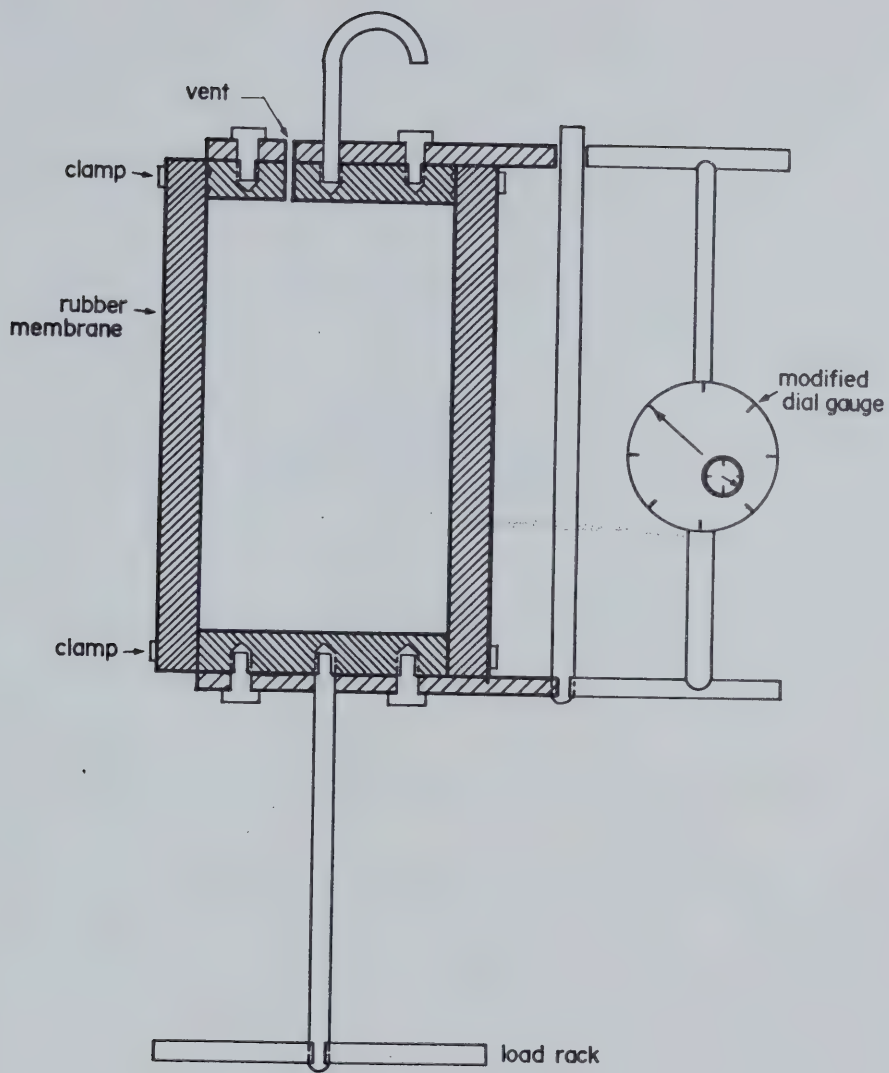


FIGURE A21 Schematic Cross Section of a Membrane Extension Testing Apparatus Used at Elevated Temperatures in an Oven



APPENDIX B  
THERMAL EXPANSION TESTS



TABLE B-1  
SUMMARY OF TEST DATA FOR THERMAL EXPANSION TESTS

Test Number	Sample Number	Type of Test	Maximum Temperature (°C)	Maximum Back Pressure (MPa)	Effective Confining Stress (MPa)	Total Sample Expansion (%)	Volume of Pore Fluid Expelled (%)
COS 1	5	Undrained	200	2.4	0.05	73.0	-
COS 2	32	Undrained	200	2.5	0.05	10.0	-
COS 3	30	Gas Exsolution	242	4.0	0.05	9.5	-
COS 4	38	Undrained	300	15.0	0.05	11.3	-
COS 5	18	Undrained	292	17.0	0.05-6.0	9.2	-
COS 6	10A	Drained	300	15.0	6.0	0.9	6.6
COS 7	10B	Drained	300	15.0	0.05	0.8	8.1
COS 8	42	Gas Exsolution	300	10.0	0.05	24.0	-
COS 9	41	Undrained	300	10.0	0.05	15.2	-



## TEST COS1

Undrained Thermal Expansion of Saline Creek  
Oil Sand Sample No. 5 Under Nominal  
Effective Confining Stress from 24 - 200°C

Procedural Details: Test COS 1

1. Saline Creek sample no. 5 was warmed to room temperature (approximately 24°C) under a nominal vertical confining stress of sufficient magnitude to prevent expansion of the sample.
2. The vertical stress and back pressure were increased simultaneously to approximately 2000 kPa (290 psi) in 200 kPa increments. The sample was left to saturate under this 2000 kpa back pressure for a period exceeding 24 hours.
3. The back pressure valve was closed isolating the 2000 kPa back pressure in the cell.
4. Cell temperatures were elevated in stages as follows: 24°C, 60°C, 100°C, 150°C, 200°C.
5. The applied vertical stress was adjusted continuously to maintain approximately zero effective vertical stress in the sample as temperature increased.
6. The sample height (i.e. piston position) was monitored throughout the test.
7. A significant volume change in the order of 60 percent was observed when the temperature was raised from 150°C to 200°C. This volume change is believed to have been due to



gas exsolution and/or phase change of pore fluids adjacent to heating rods in the test cell. It is believed that local overheating may have occurred when such a large temperature increment (50°C) was applied.



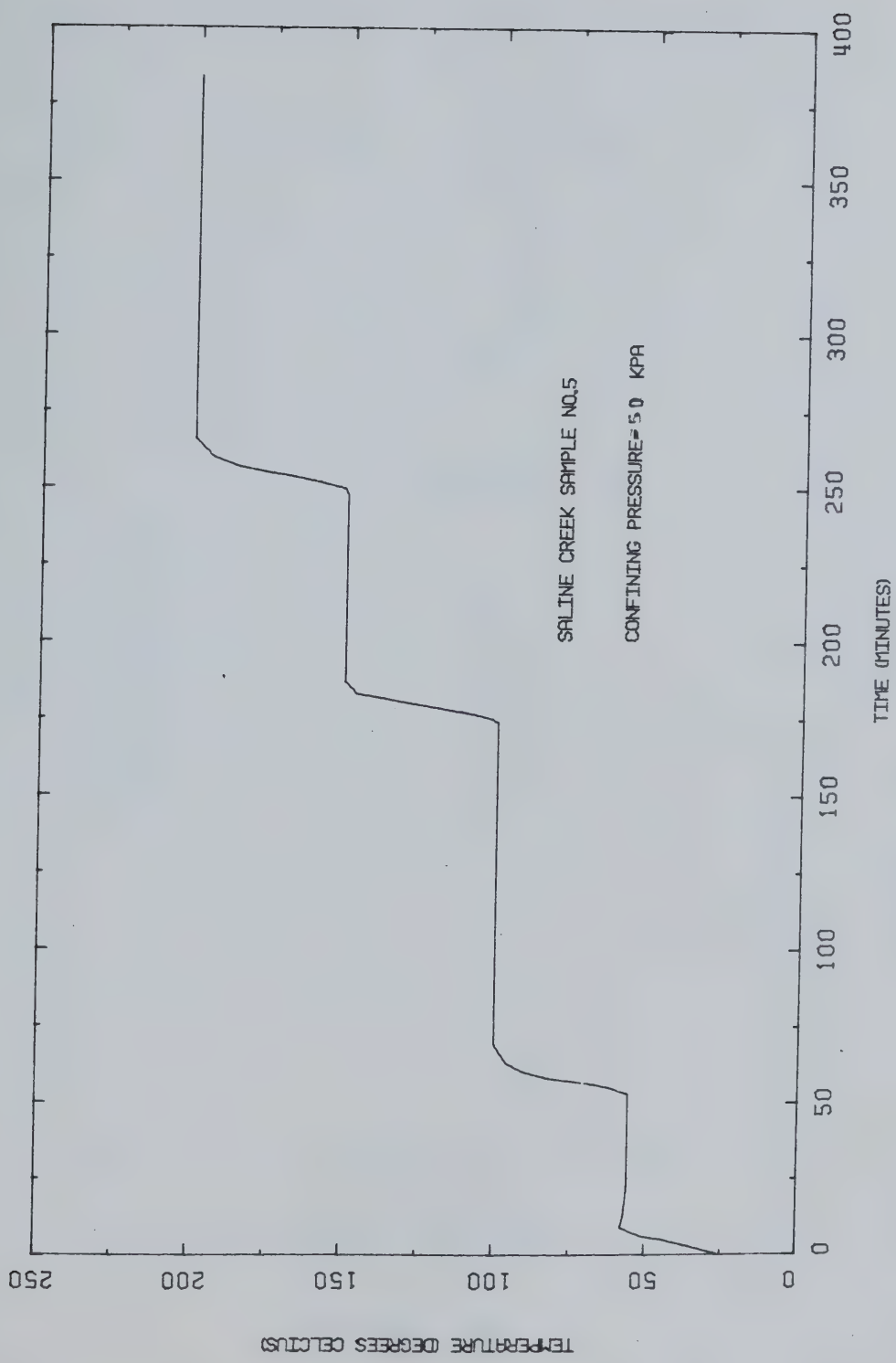


FIGURE B1 Temperature Versus Time: Test COS1



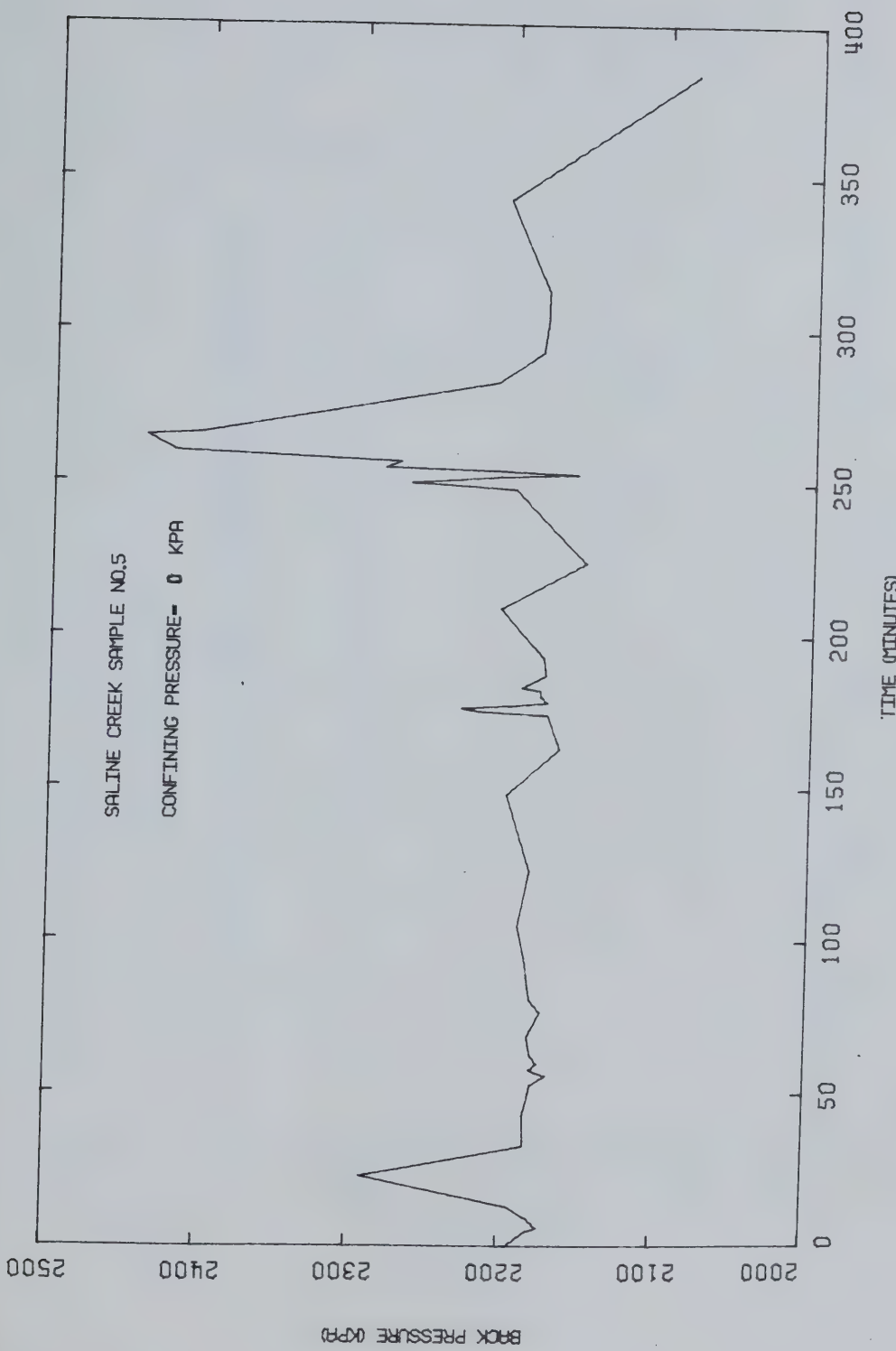


FIGURE B2 Back Pressure Versus Time: Test C051



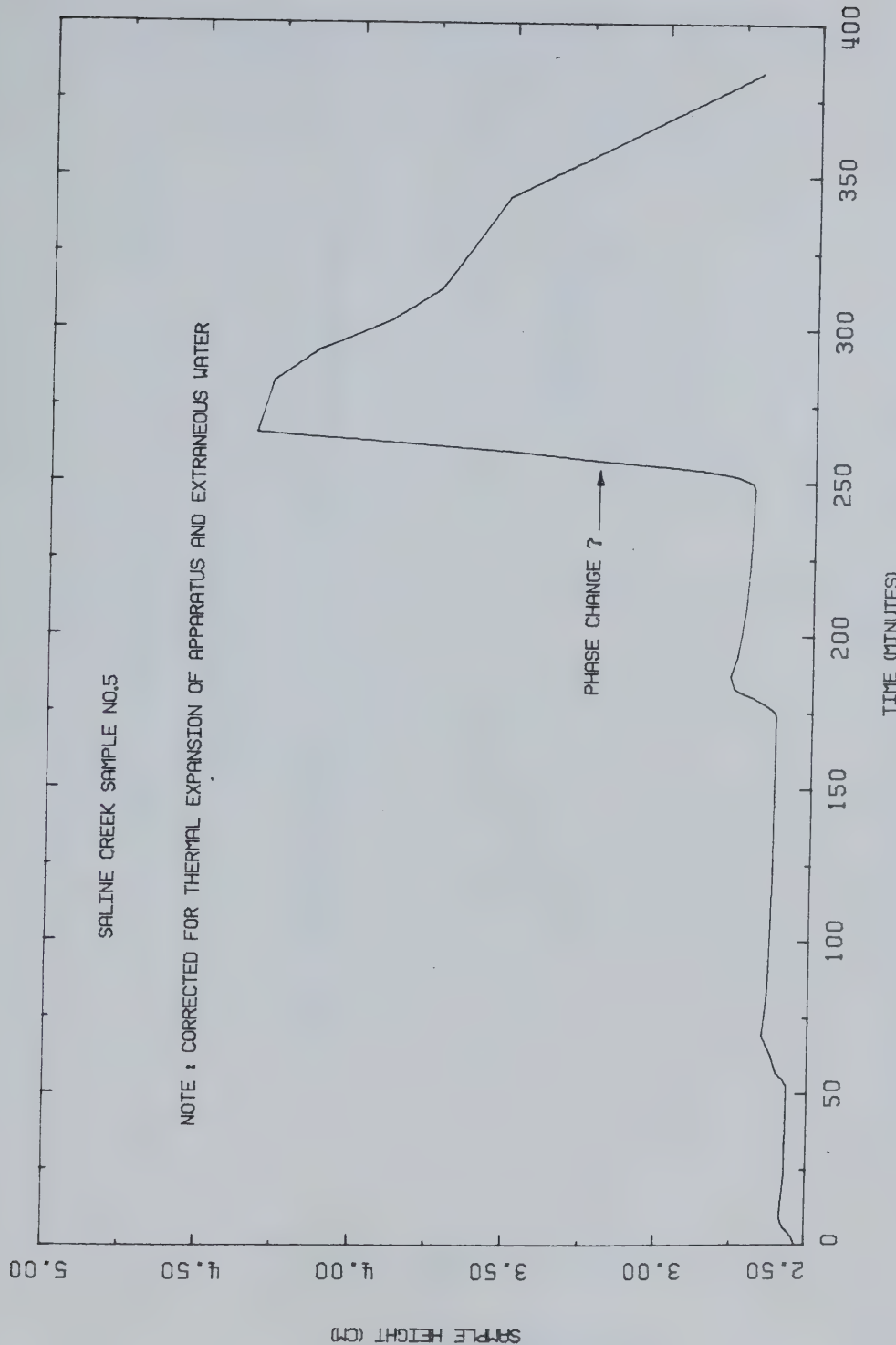


FIGURE B3 Sample Height Versus Time: Test COS1



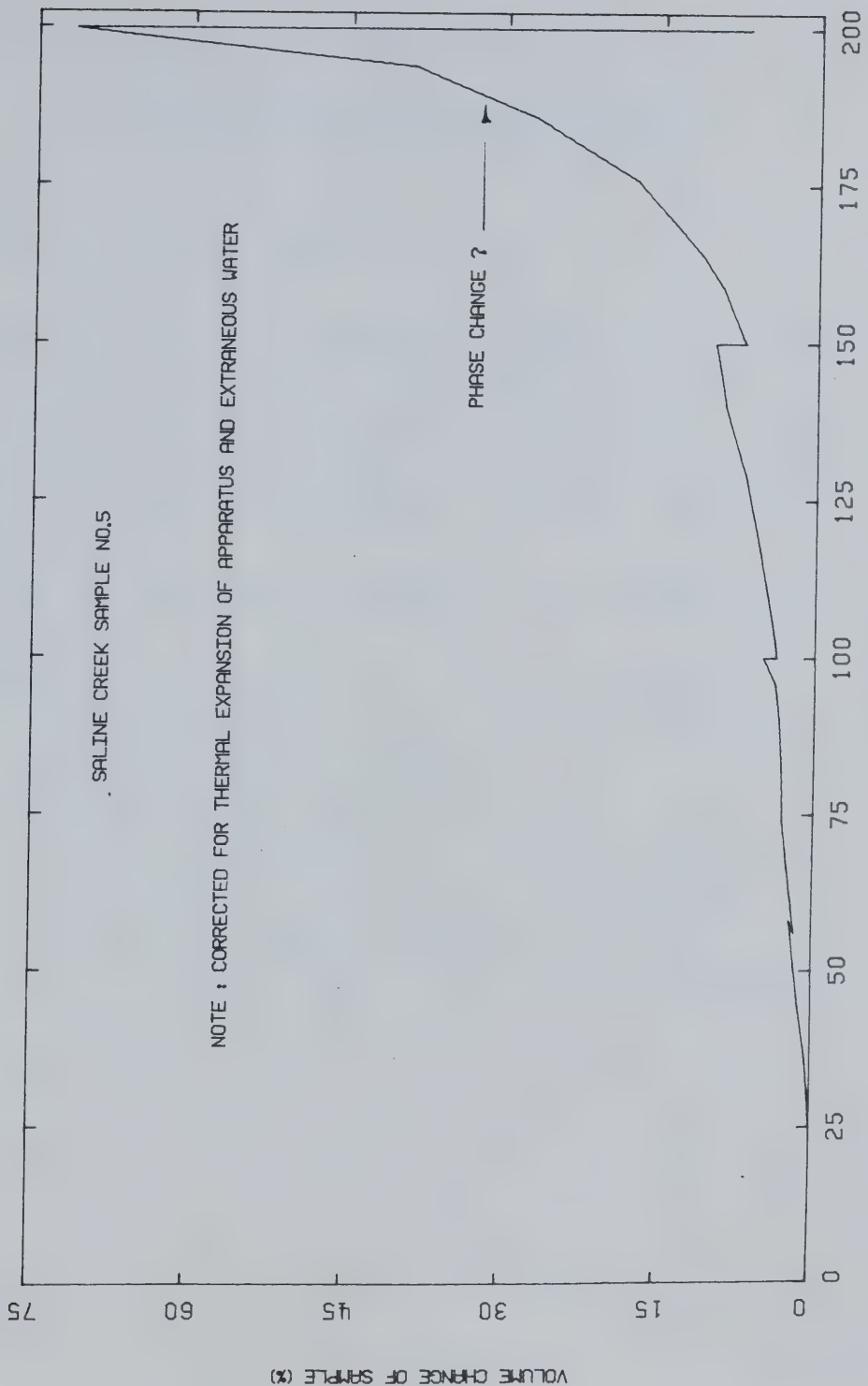


FIGURE B4 Undrained Volumetric Thermal Expansion: Test COS1



## TEST COS2

Undrained Thermal Expansion of Saline Creek  
Oil Sand Sample No. 32 under Nominal Effective  
Confining Stress (50 kPa) from 20-200°C

Procedural Details: Test COS 2

1. Sample No. 32 was warmed to room temperature under confined conditions to prevent thermal expansion of the sample.
2. The sample was saturated under confining and back pressures of approximately 2000 kPa for a period exceeding 24 hours. The 2000 kPa back pressure was then shut in and drainage prevented.
3. Cell temperatures were increased in 10°C increments up to 200°C.
4. The confining pressure was adjusted continuously to maintain approximately 50 kPa effective vertical stress in the sample as heating proceeded.
5. At 180°C the back pressure and confining pressure were increased to 2500 kPa to prevent large volume changes associated with phase change and/or gas exsolution.
6. The test was terminated at 200°C after the development of a leak in the back pressure system.



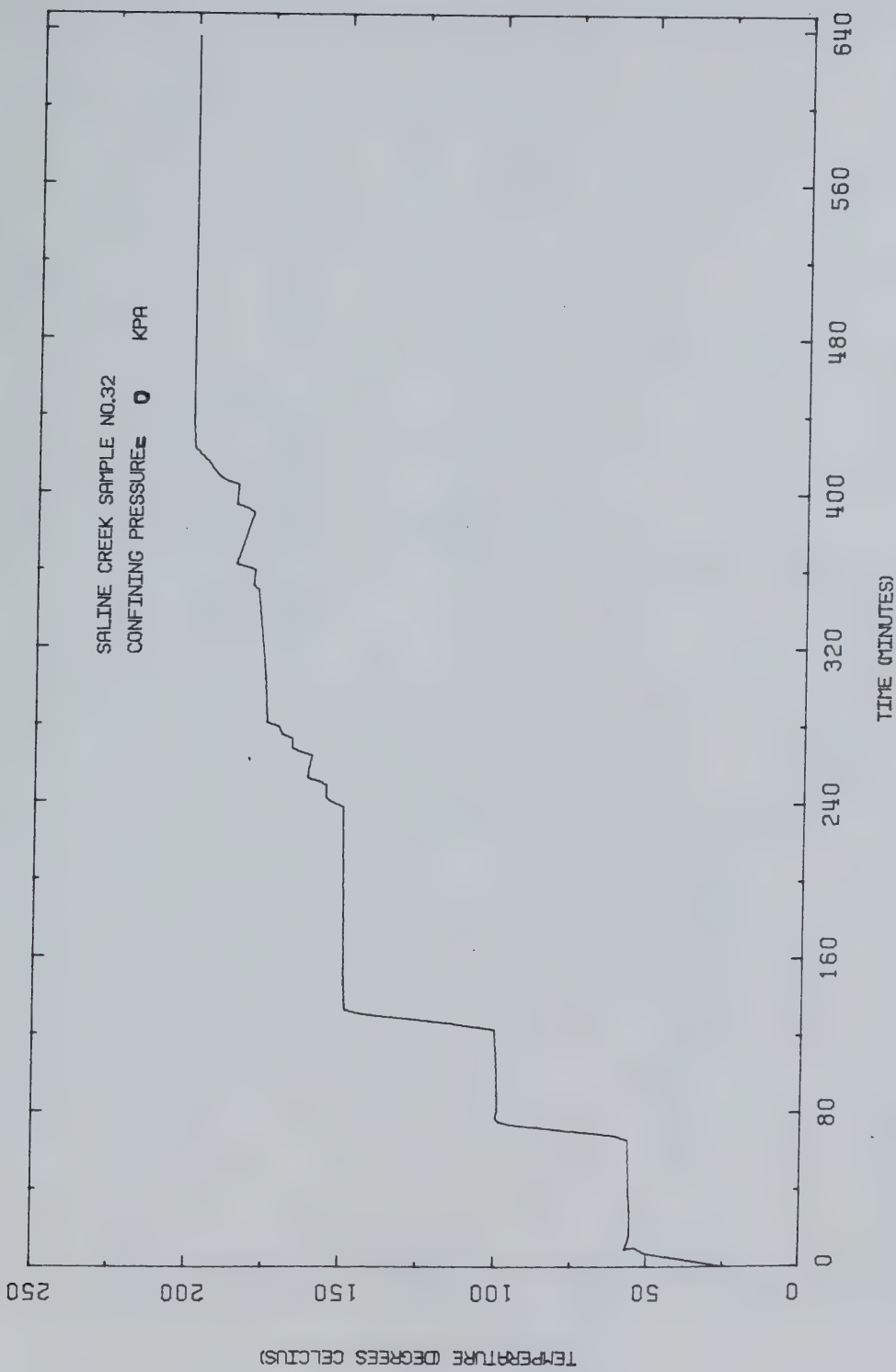


FIGURE B5 Temperature Versus Time: Test COS2



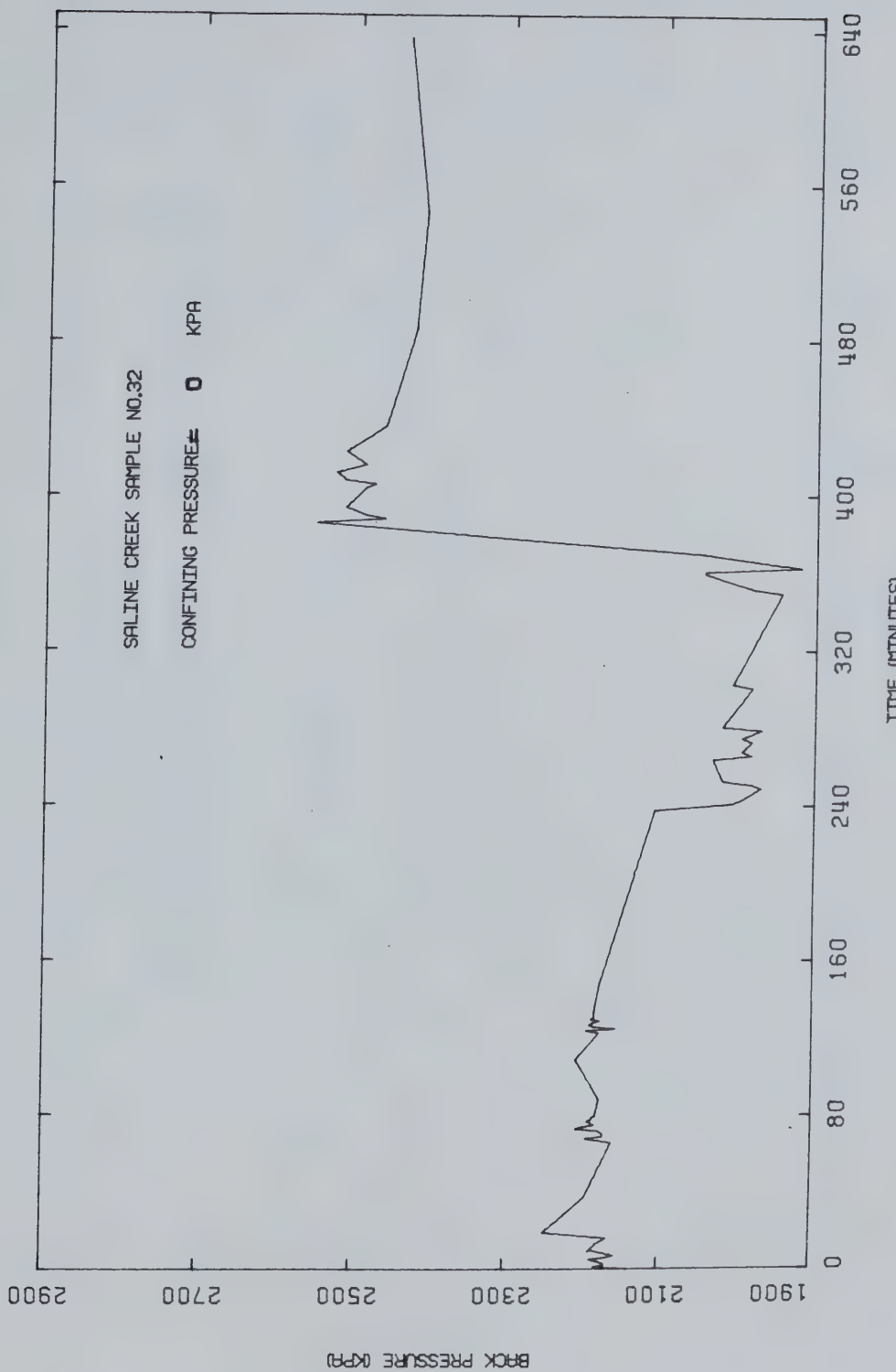


FIGURE B6 Back Pressure Versus Time: Test COS2



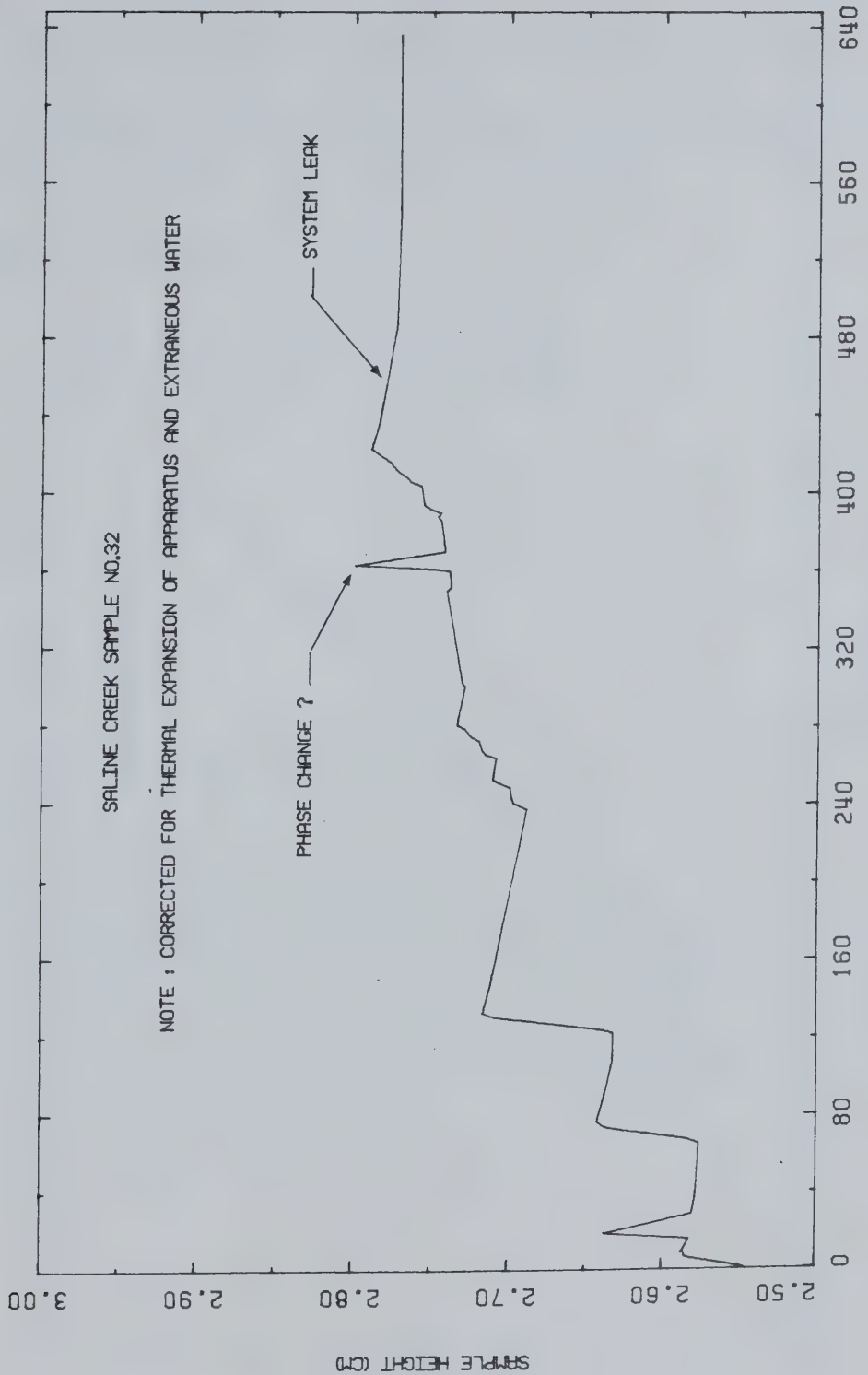


FIGURE B7 Sample Height Versus Time: Test COS2



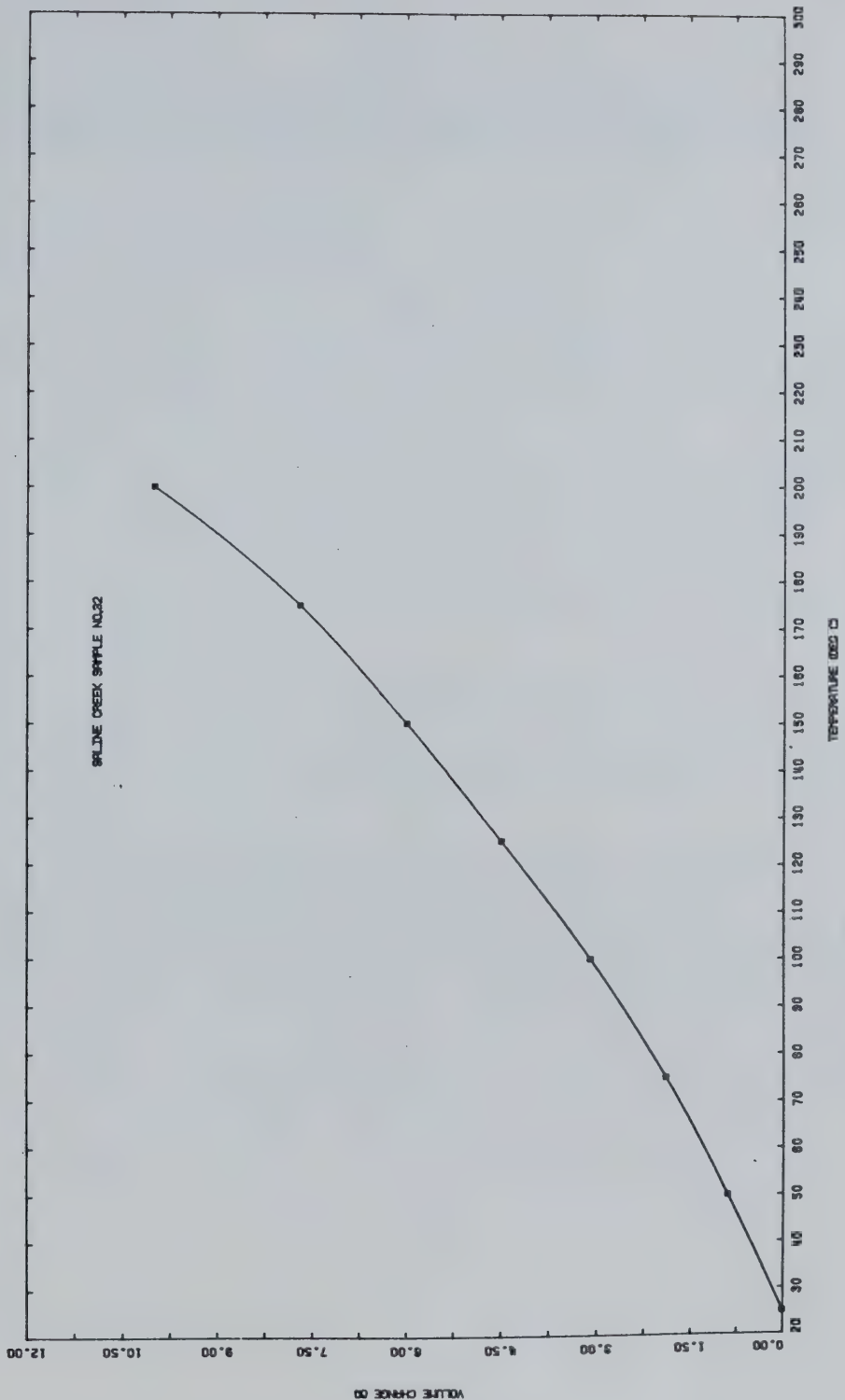


FIGURE B8 Undrained Volumetric Thermal Expansion:  
Test COS2



## TEST COS3

Undrained Thermal Expansion under Nominal Effective Confining Stress (50 kPa) and Gas Exsolution Test For Saline Creek Oil Sample No. 32 at Temperatures from 25-242°C

Procedural Details: Test COS 3

1. Saline Creek Sample No. 32 was confined under a nominal confining pressure to prevent thermal expansion as it warmed to room temperature.
2. The sample was saturated under confining and back pressures of approximately 2000 kPa for a period exceeding 24 hours.
3. The vertical confining pressure and back pressure were initially reduced to 200 kPa. The back pressure valves were then shut in.
4. The cell temperature was raised in 5°C increments.
5. Confining and back pressure were increased only when required to prevent phase change/or gas exsolution of the pore fluids.
6. Each time that large volumetric expansion was observed which was believed to be due to phase change/gas exsolution, the cell temperature was immediately decreased to the previous temperature increment. The confining pressure was increased gradually during these mini cool-down phases to maintain near-constant back pressure and to re-establish the previous sample volume.
7. The confining and back pressures were then increased



simultaneously prior to applying the next temperature increment.

8. The purpose of the above procedure was to attempt to define a pressure-temperature relationship corresponding to gas exsolution and/or phase change of the pore fluids.
9. The test was terminated at 242°C due to an electrical power shut-down at the University of Alberta.



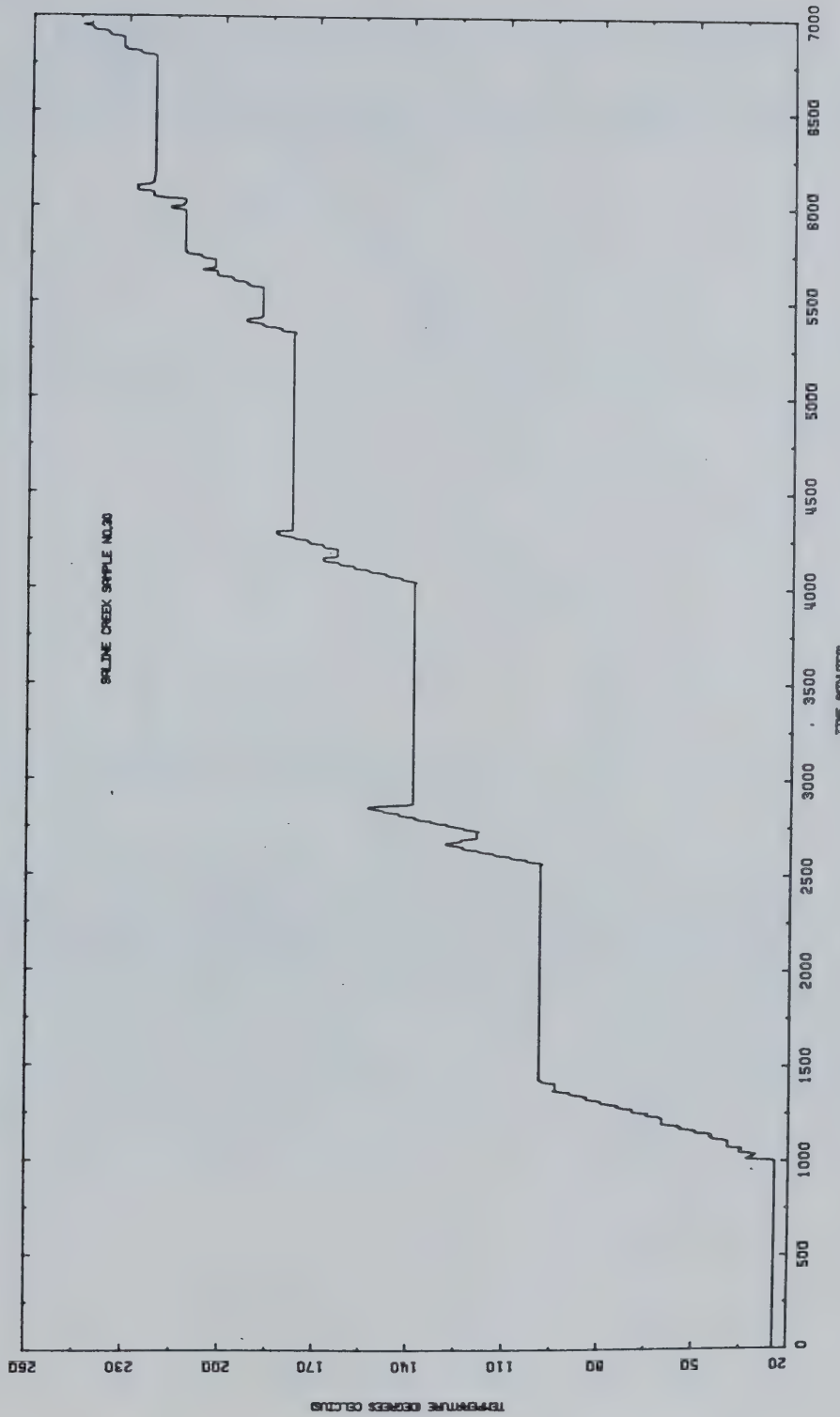


FIGURE B9 Temperature Versus Time: Test COS3



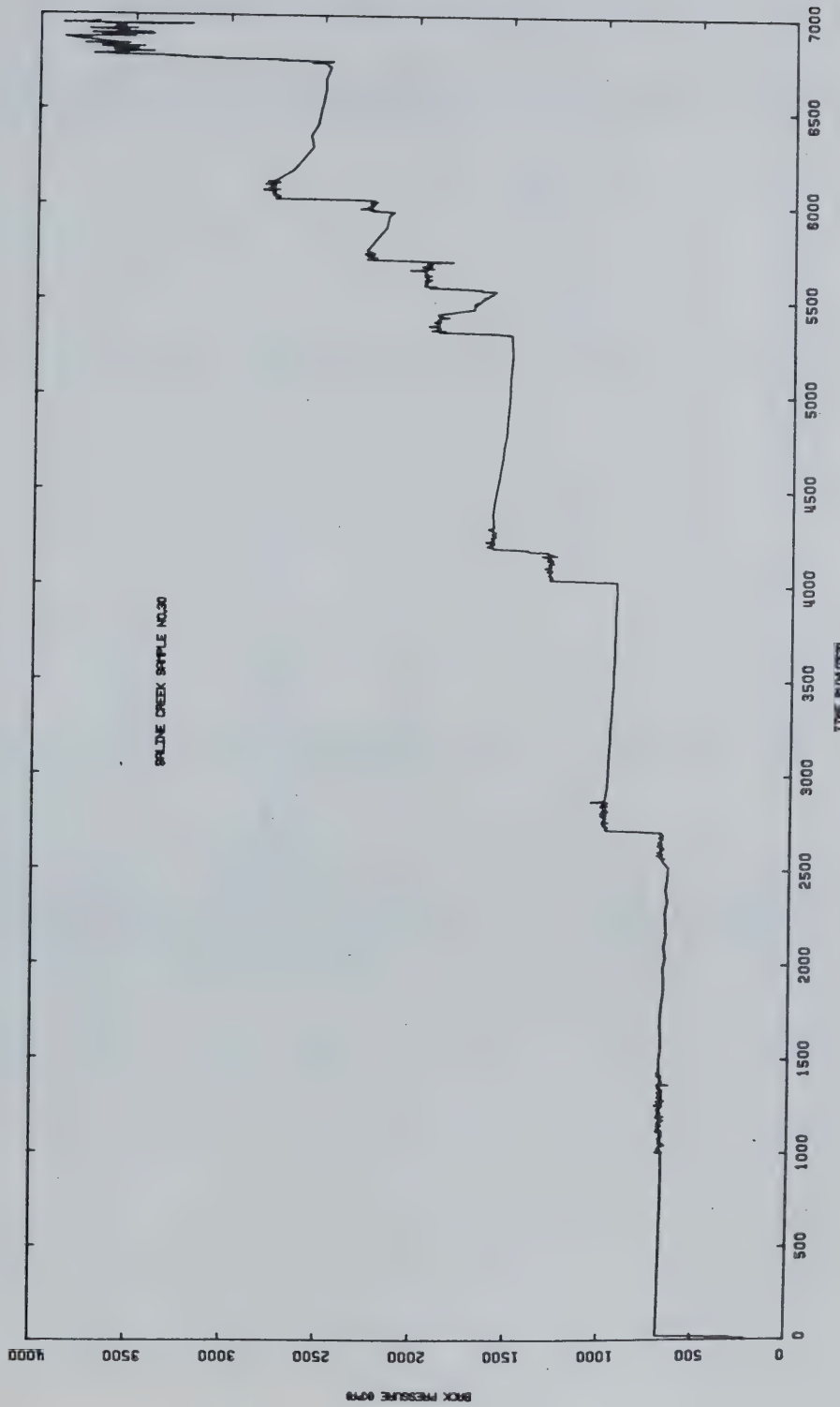


FIGURE B10 Back Pressure Versus Time: Test C03



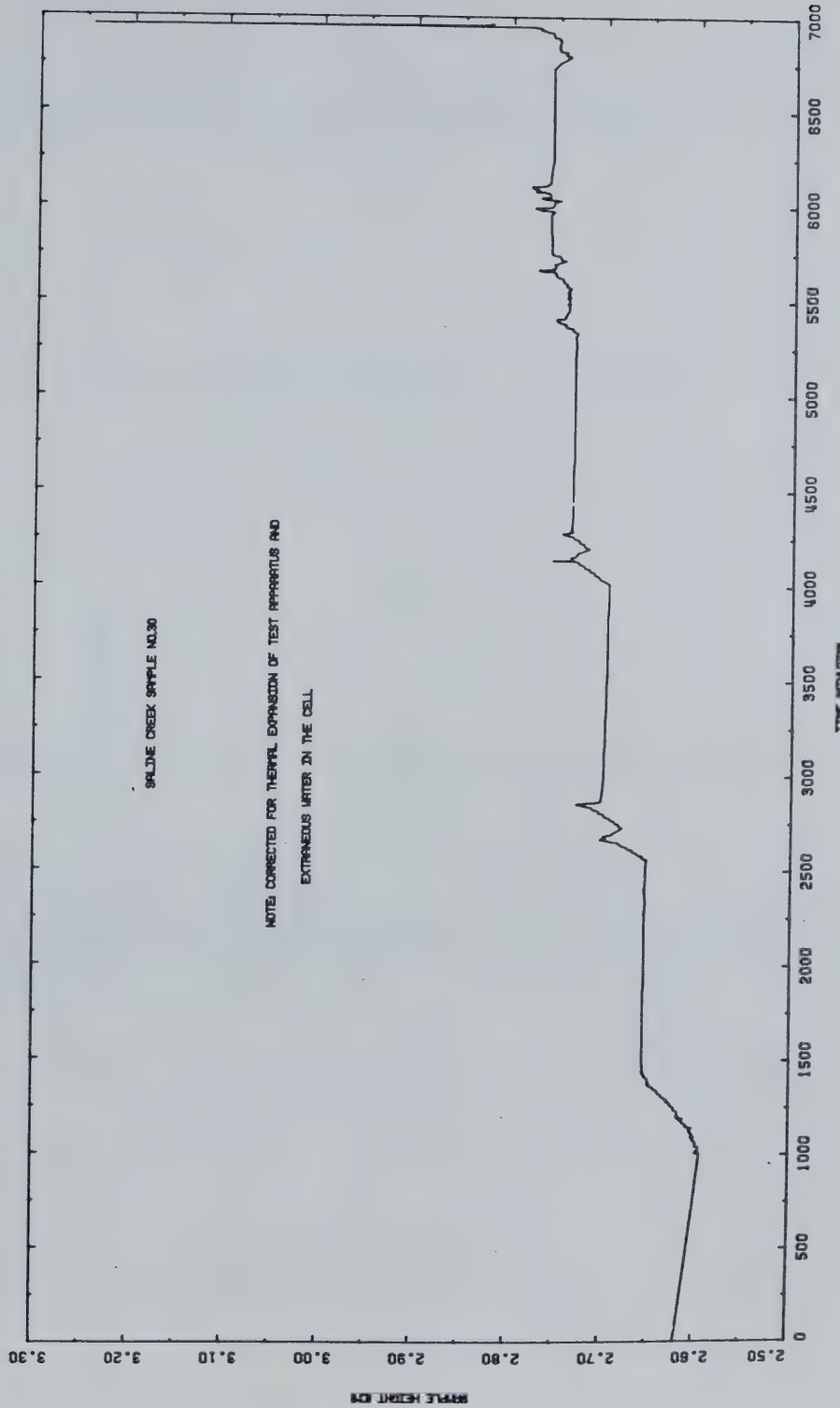


FIGURE B11 Sample Height Versus Time: Test COS3



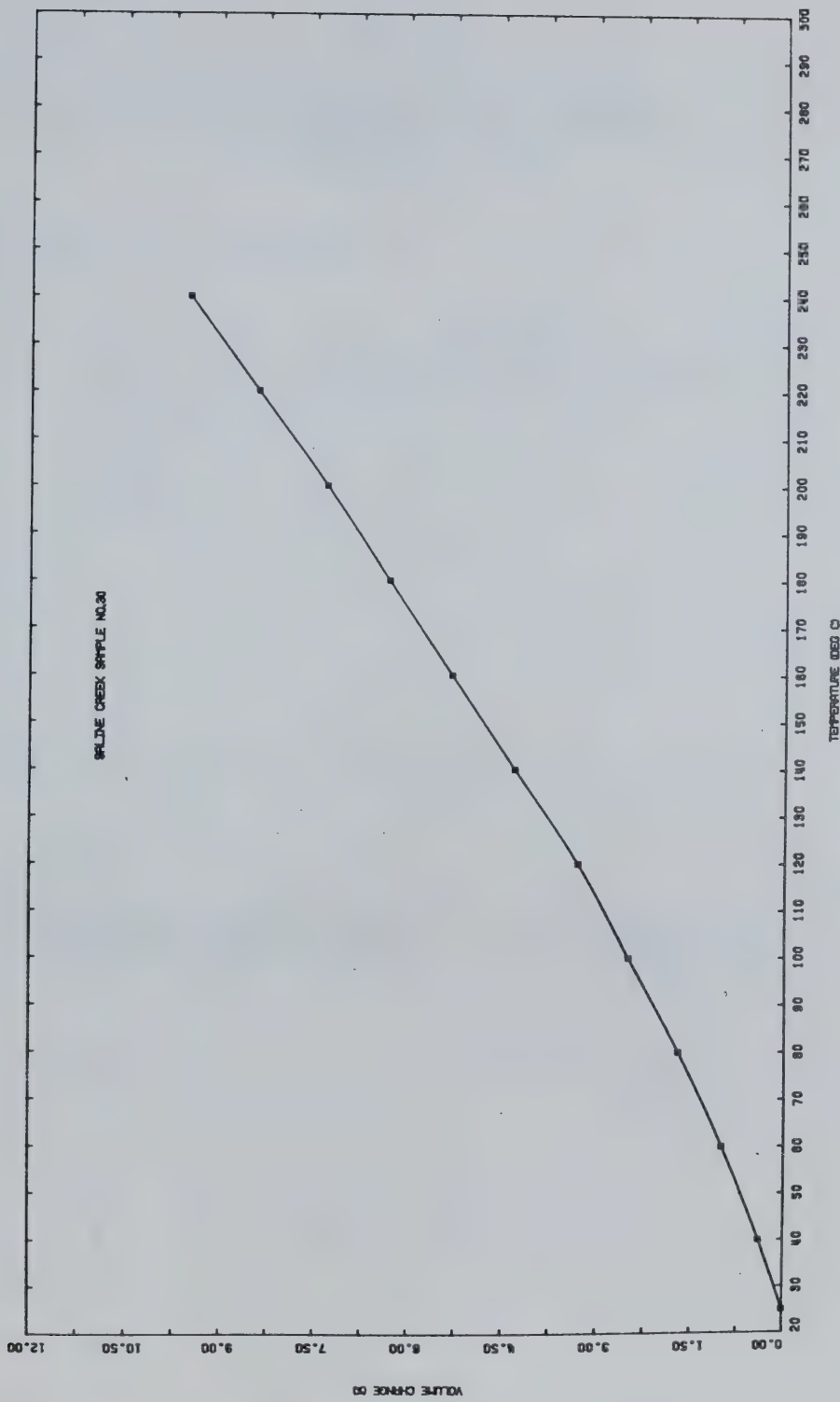


FIGURE B12 Undrained Volumetric Thermal Expansion:  
Test CO33



## TEST COS4

Undrained Thermal Expansion of Saline Creek  
Oil Sand Sample No. 38 under Nominal  
Effective Confining Stress (50 kPa) and over the  
Temperature Range 25-300°C

Procedural Details: Test COS4

1. Sample no. 38 was warmed to room temperature under nominal confining pressure to prevent thermal expansion.
2. The sample was saturated under back and confining pressures of 2000 kPa for a period exceeding 24 hours. The 2000 kPa back pressure was then shut in.
3. The cell temperature was raised in 5°C increments.
4. The confining pressure was adjusted continuously during heating to maintain approximately zero effective vertical stress on the sample.
5. Back pressures and confining pressures of sufficient magnitude to prevent phase change and/or gas exsolution were applied as follows:

<u>Temperature Range</u>	<u>Back Pressure</u>
25 - 150°C	2000 kPa
151 - 200°C	5000 kPa
201 - 300°C	15000 kPa
300 - 25°C (cool down)	15000 kPa

6. Sample height was monitored during the test.



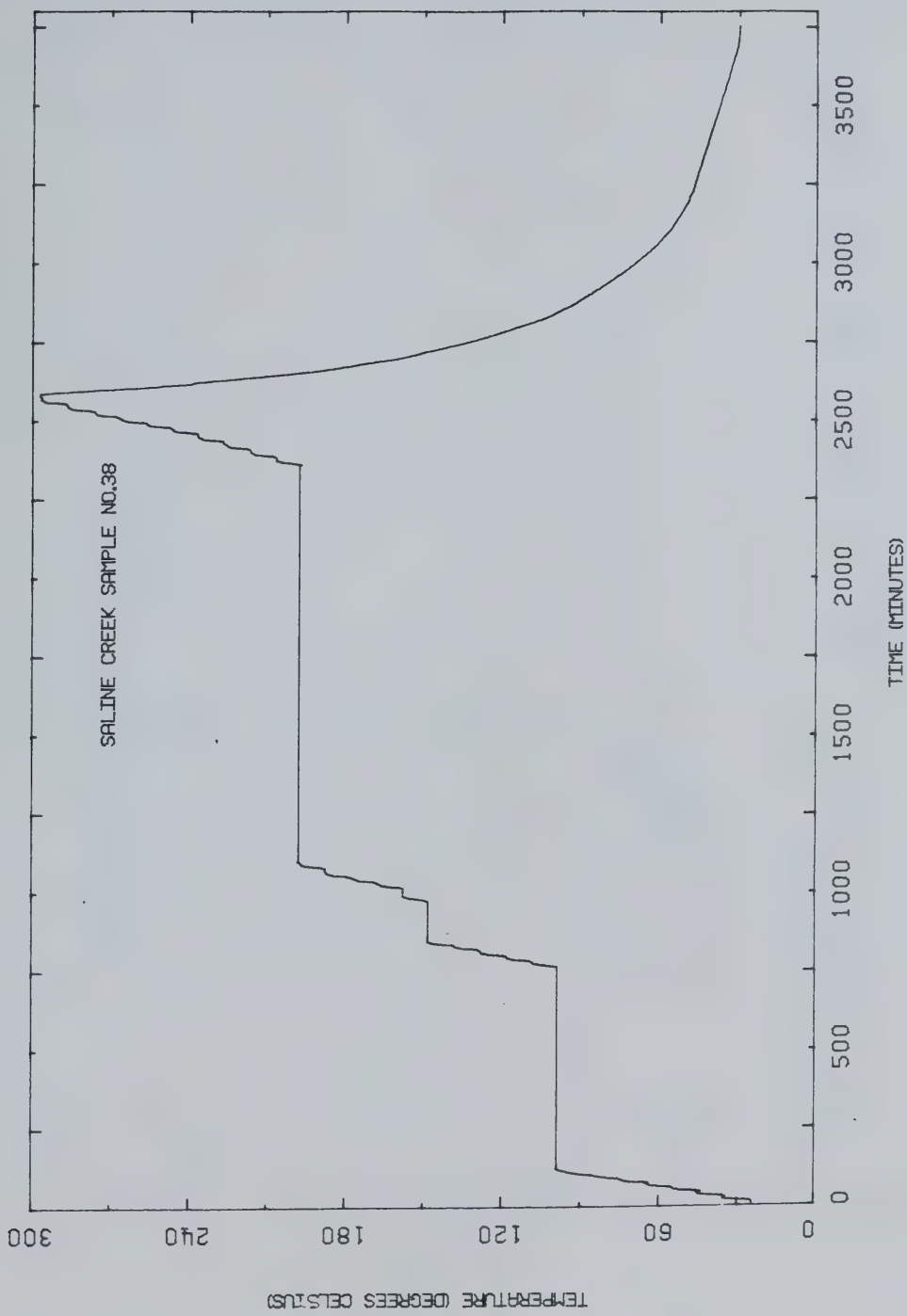


FIGURE B13 Temperature Versus Time: Test  $\dagger$  COS4



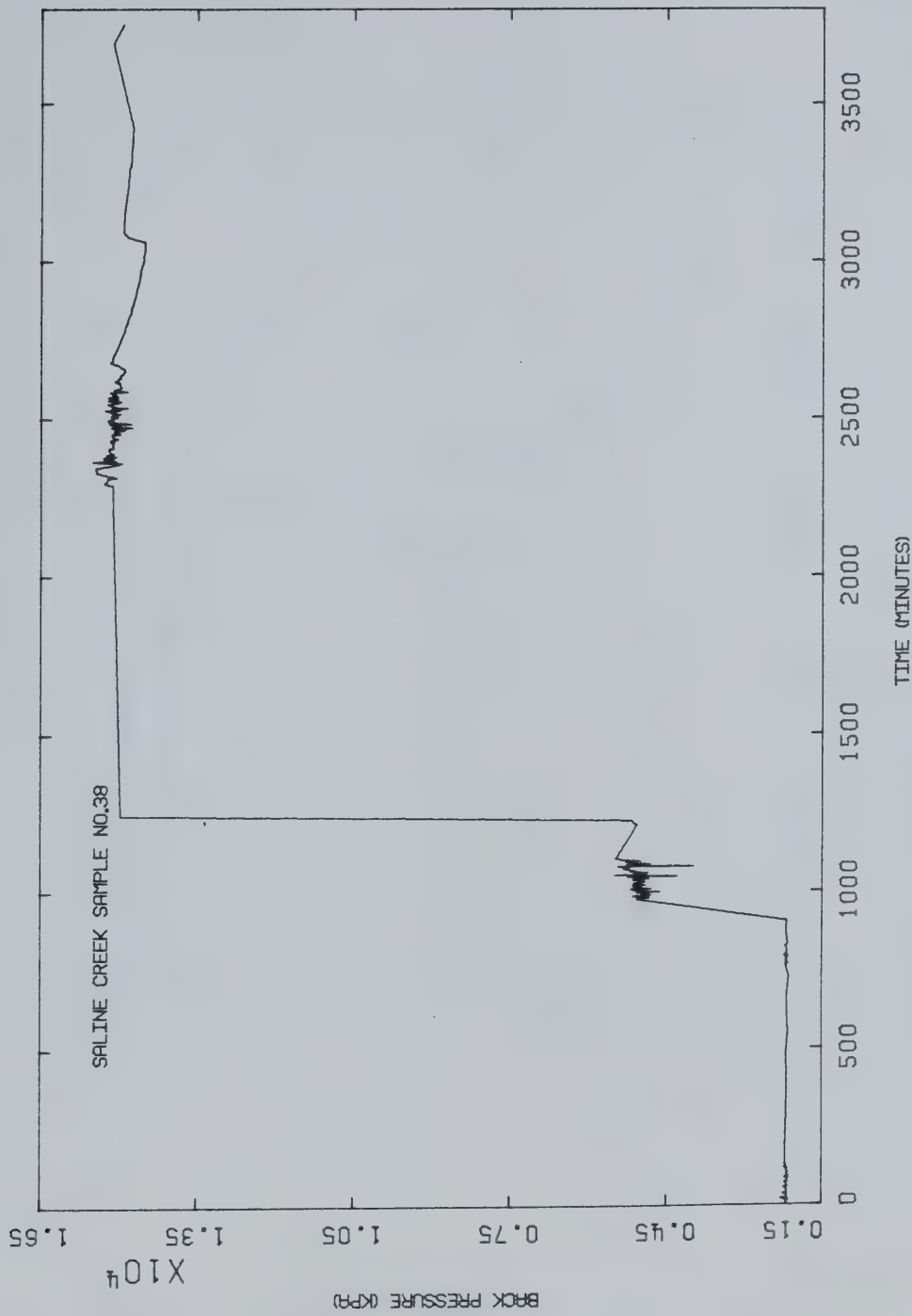


FIGURE B14 Back Pressure Versus Time: Test C054



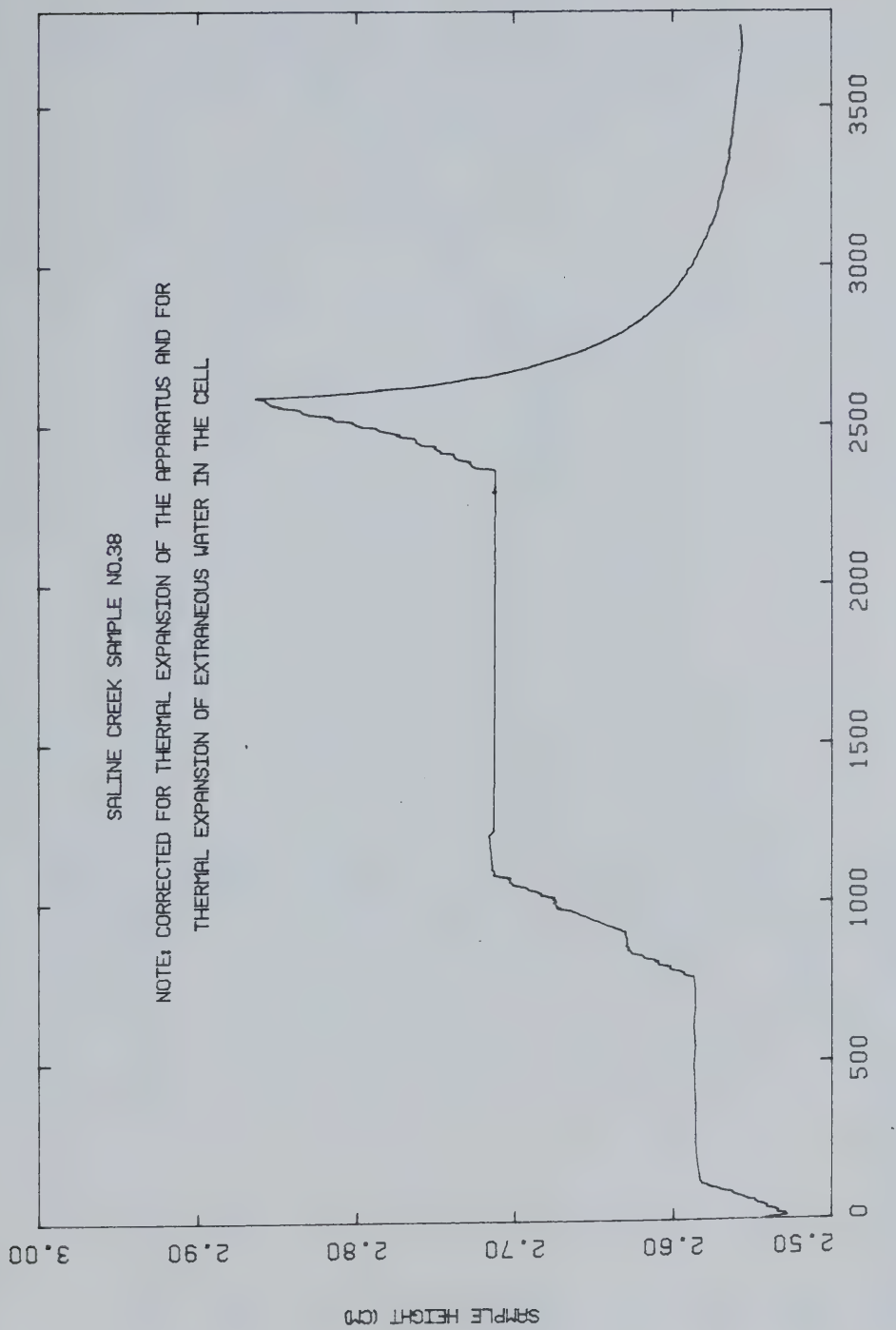


FIGURE B15 Sample Height Versus Time: Test COS4



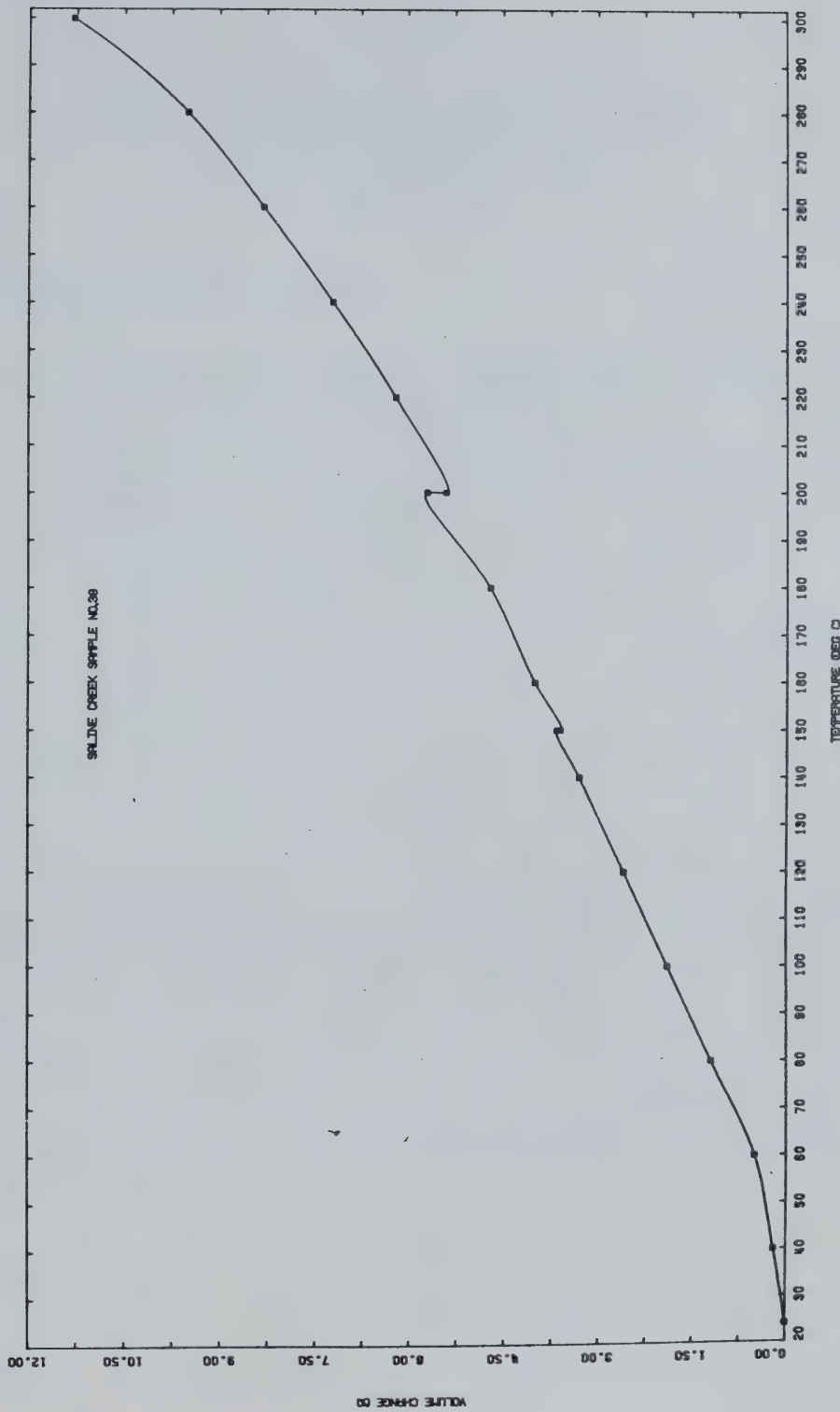


FIGURE B16 Undrained Volumetric Thermal Expansion:  
Test COS4



## TEST COS5

Undrained Thermal Expansion and Pore Pressure Response to the Undrained Heating of Saline Creek Oil Sand Sample No. 18 at Effective Confining Stresses 0.05 - 6.0 MPa and Over the Temperature Range 20 - 292°C

Procedural Details: Test COS5

1. Sample No. 18 was saturated at approximately 2000 kPa (290 psi) back pressure for 24 hours +.
2. Confining pressure and back pressure were increased simultaneously to approximately 5000 kPa (725 psi).
3. Confining pressure was then increased to approximately 11,000 kPa (1600 psi) in 200 kPa increments.
4. The sample drainage valves were closed and a back pressure of 5000 kPa (725 psi) was shut in.
5. The sample was heated incrementally with the confining pressure held constant and the increase in pore fluid pressure (back pressure) was monitored during undrained heating. After the back pressure had increased to equal the confining pressure (ram pressure + piston friction), heating was continued up to 150°C with approximately zero vertical effective stress on the sample.
6. The confining pressure was then increased to approximately 17,000 kPa while the back pressure was maintained at approximately 11,000 kPa. Drainage of pore fluid from the



sample was permitted under this effective stress level (approximately 6000 kPa).

7. The back pressure of approximately 11,000 kPa was shut in and further drainage prevented.
8. Heating of the sample above 150°C was continued and the undrained pore pressure increase was monitored until it equalized with the confining pressure. This pore pressure build-up occurred very rapidly, as anticipated.
9. Heating of the sample under approximately zero effective vertical stress was continued up to 292°C when leakage past the O-ring seal occurred causing a sudden drop in the back pressure and allowing sudden uncontrolled pore fluid drainage. The test was terminated at this point.



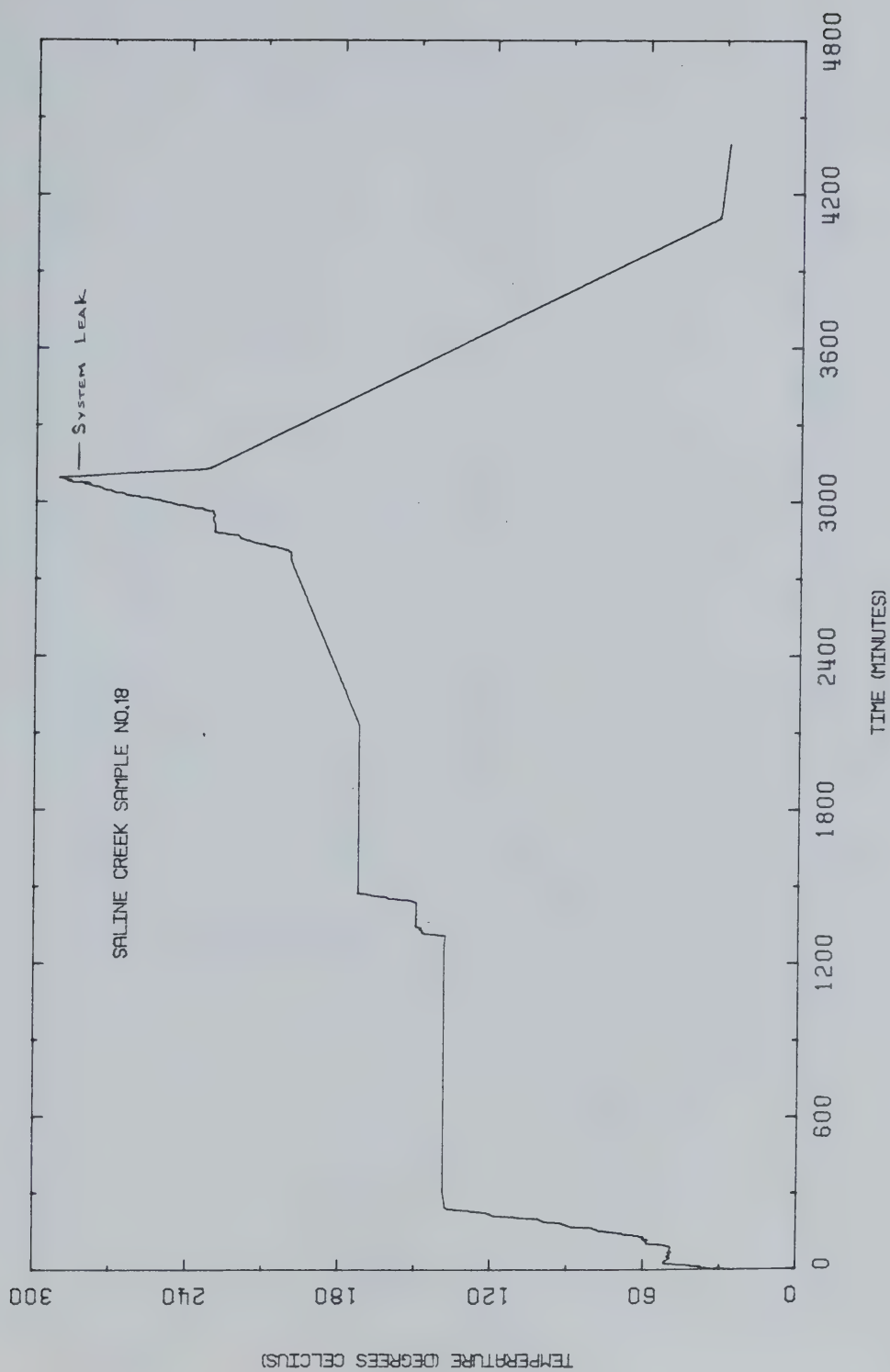


FIGURE B17 Temperature Versus Time: Test COSS



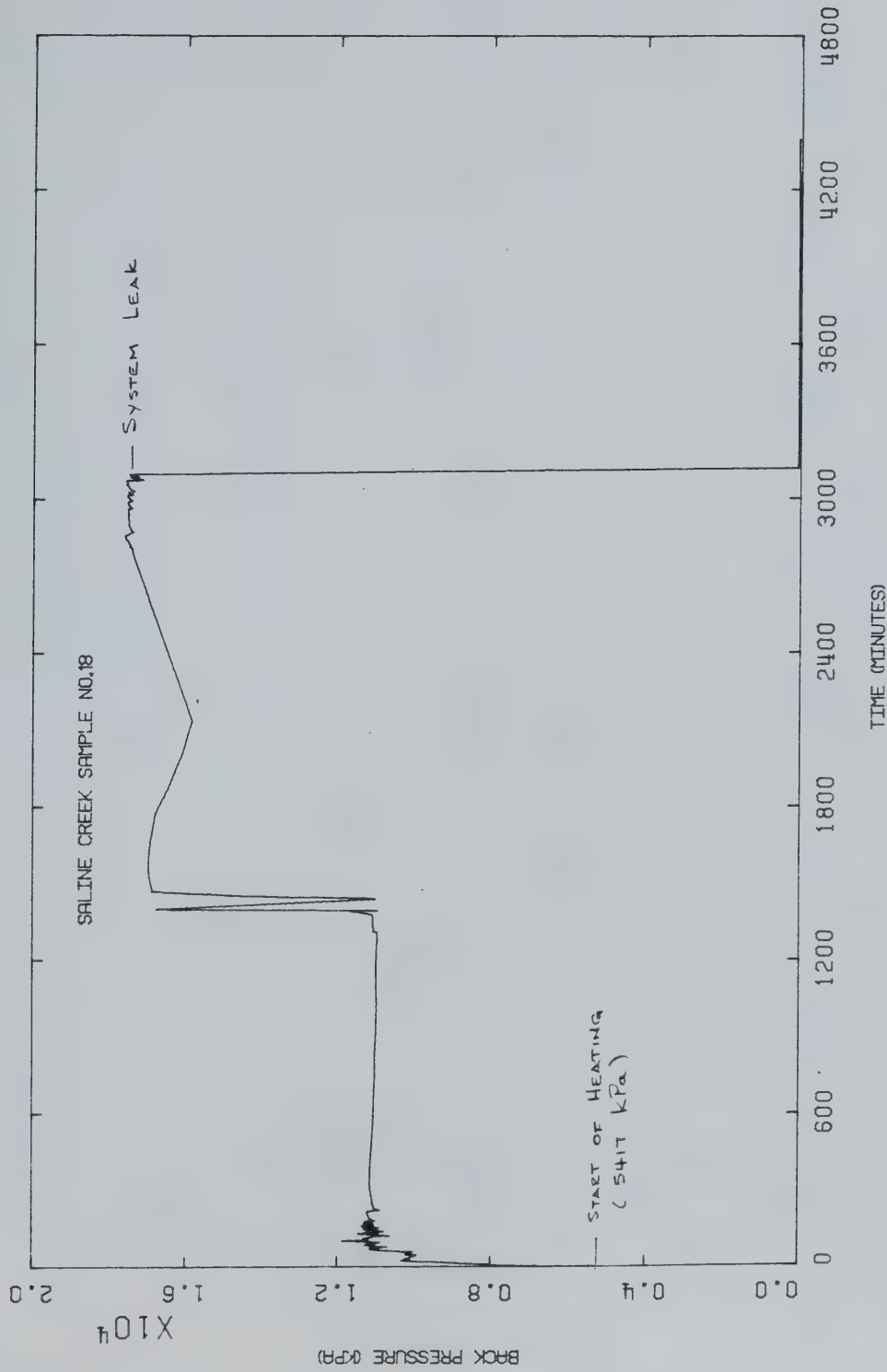


FIGURE B18 Back Pressure Versus Time: Test COSS



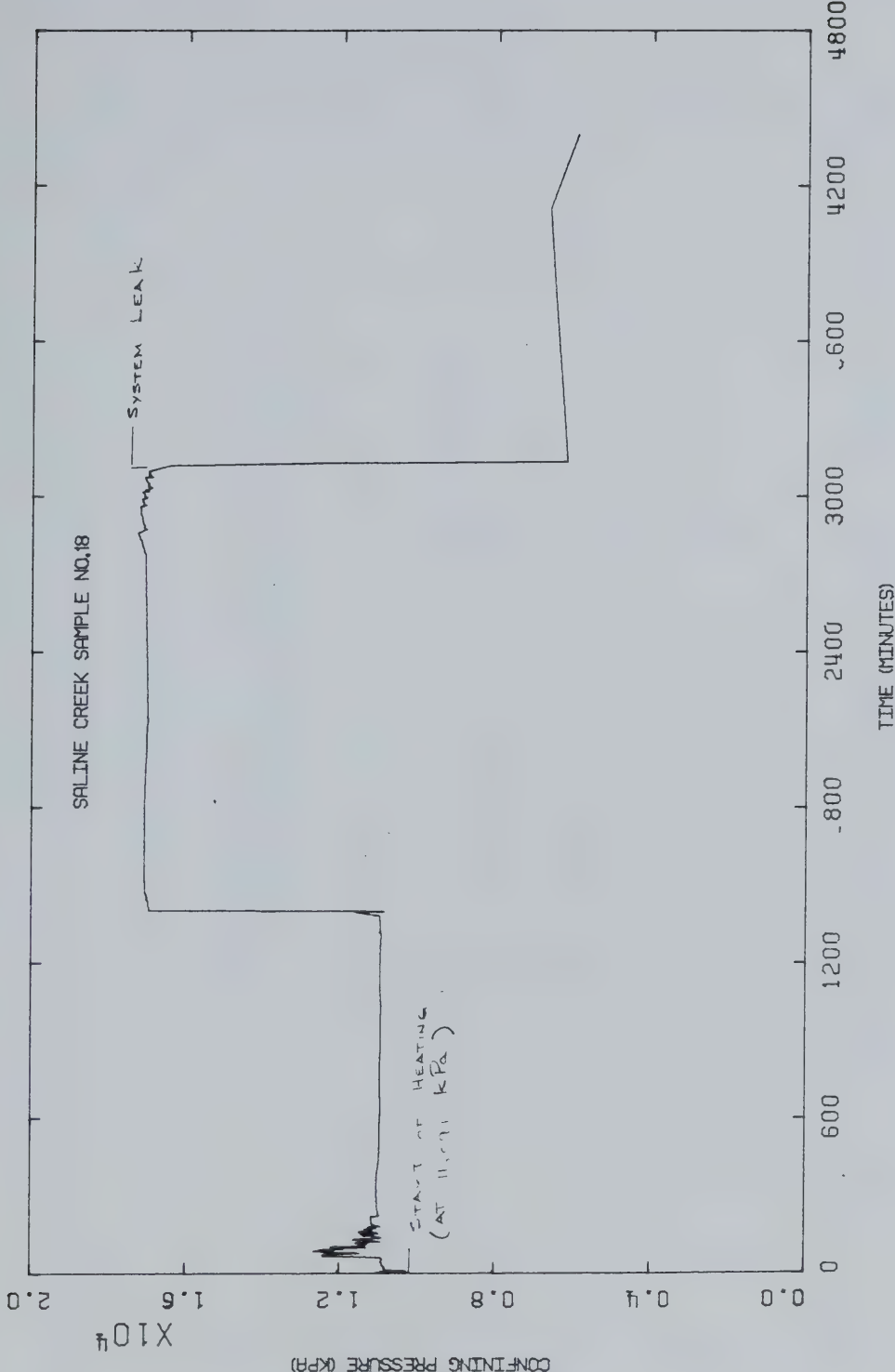


FIGURE B19 Confining Pressure Versus Time: Test C055



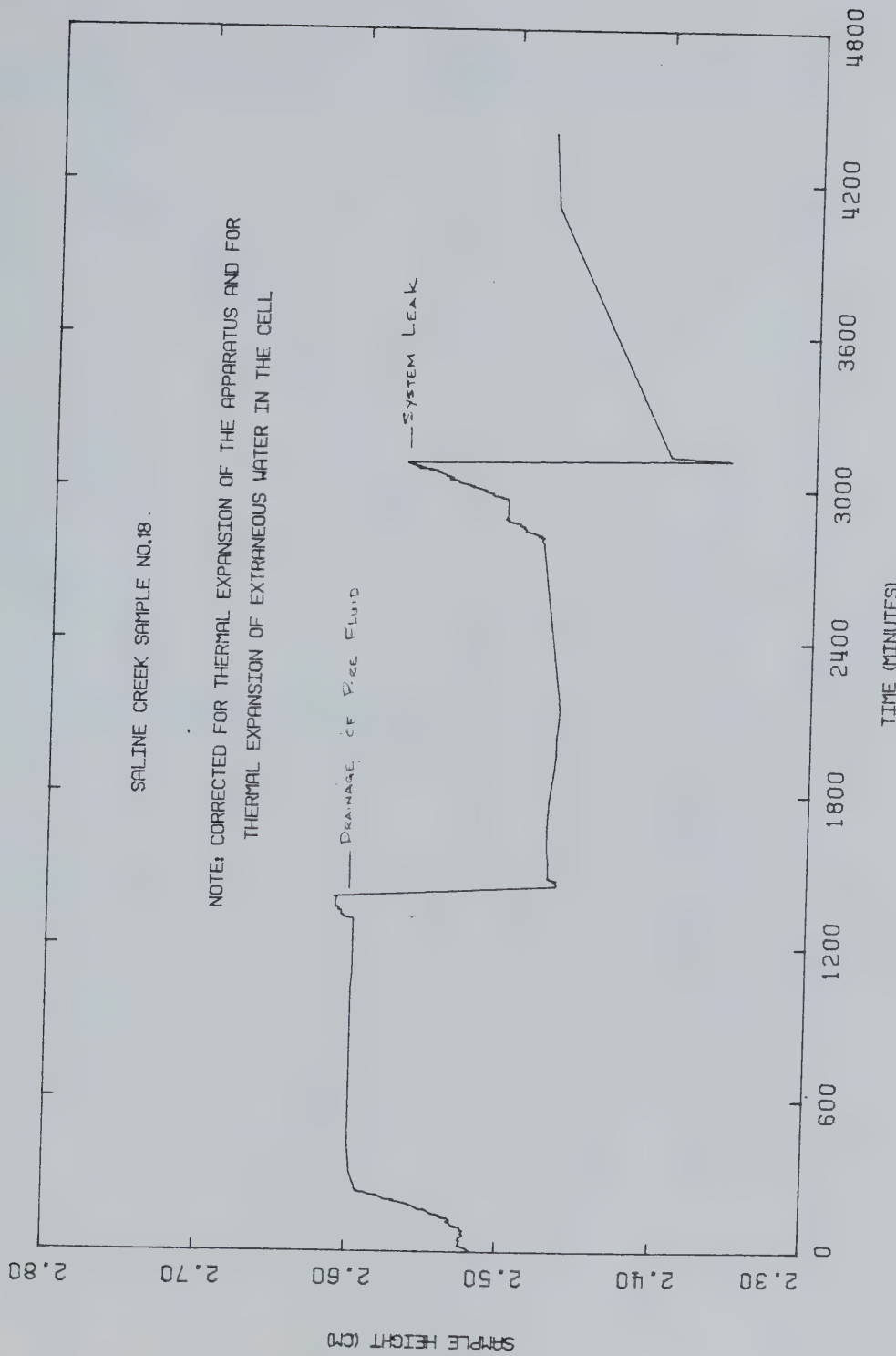


FIGURE B20 Sample Height Versus Time: Test C055



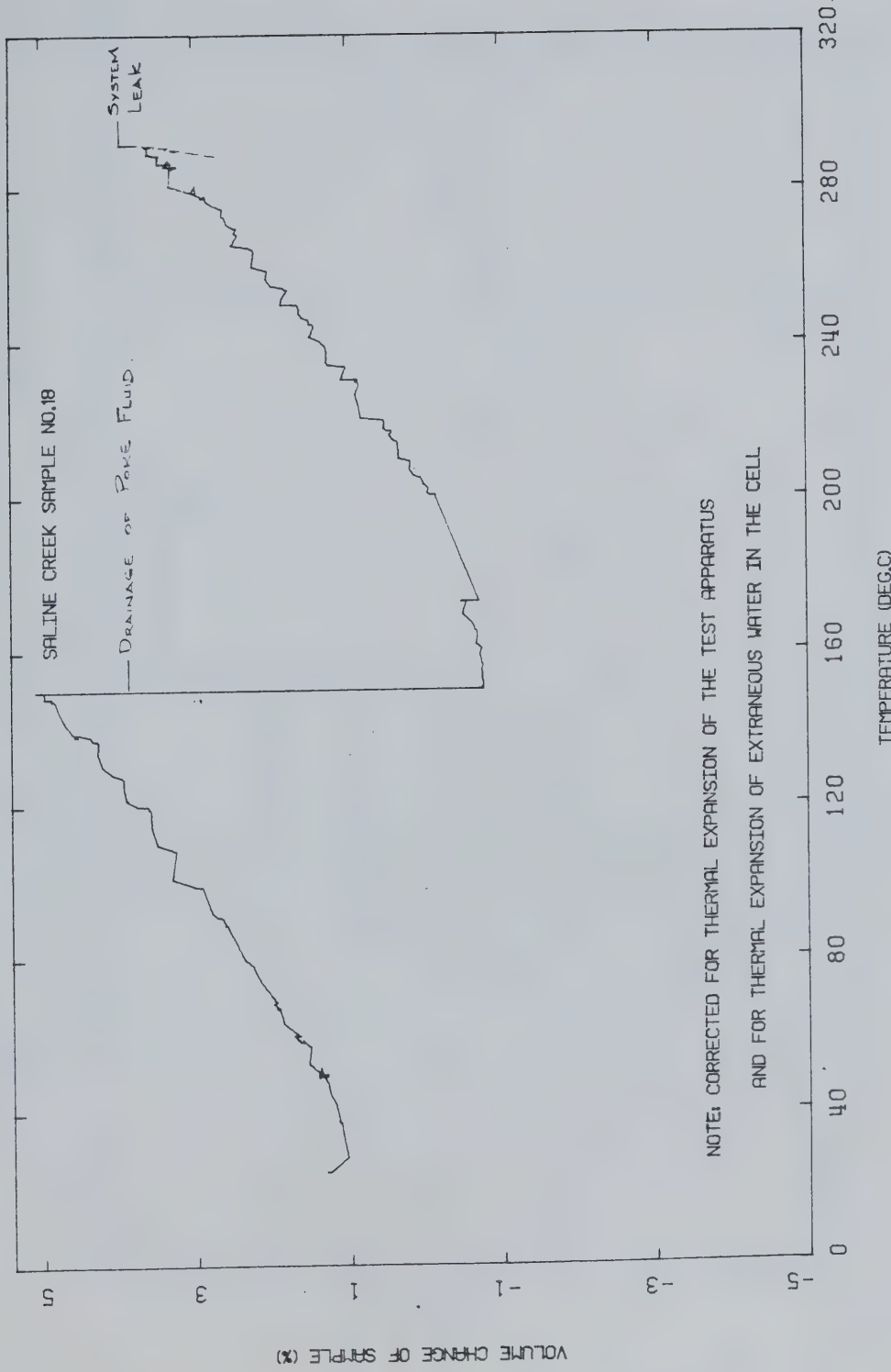


FIGURE B21 Undrained Volumetric Thermal Expansion:  
Test C055



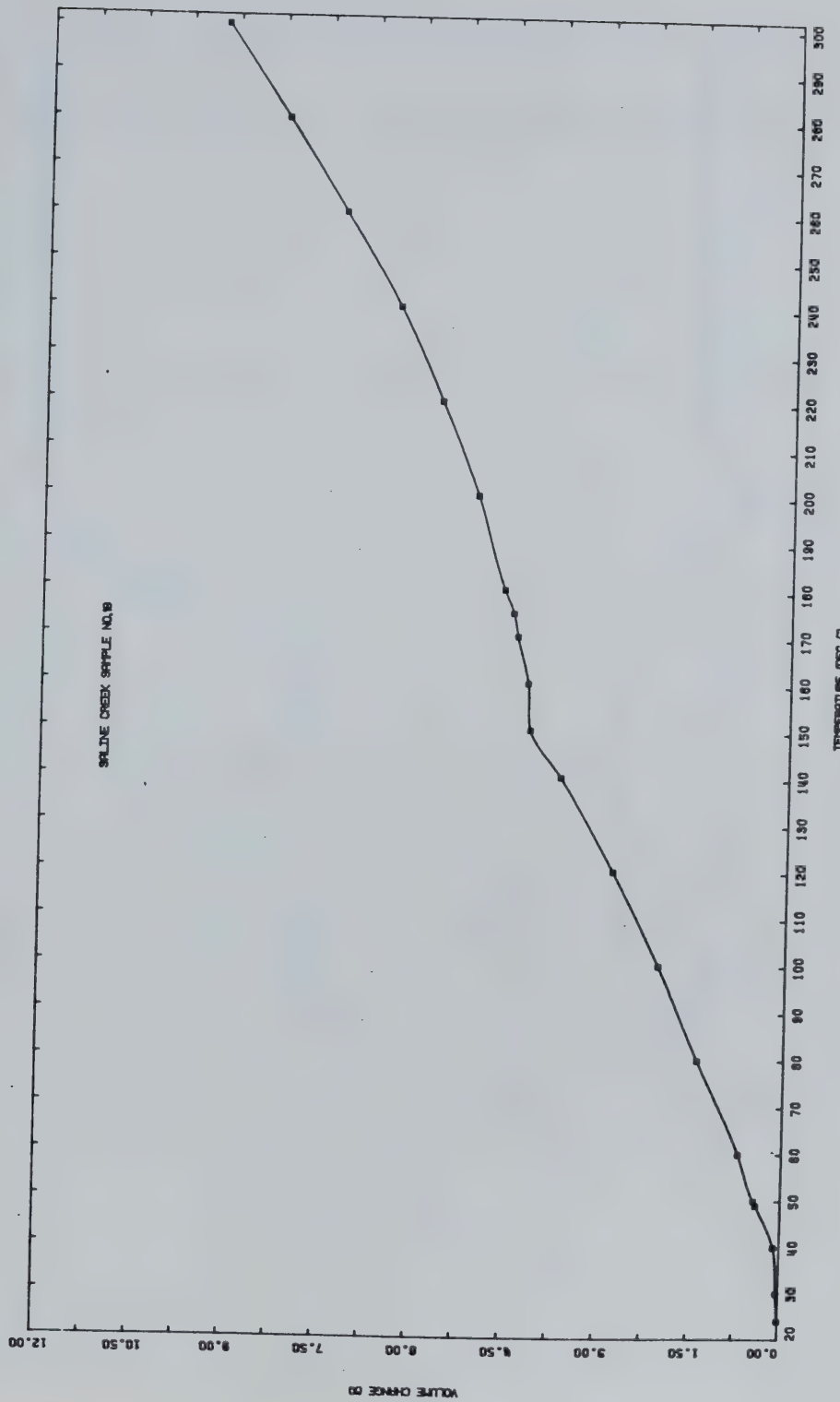


FIGURE B22 Undrained Volumetric Thermal Expansion:  
Test C055



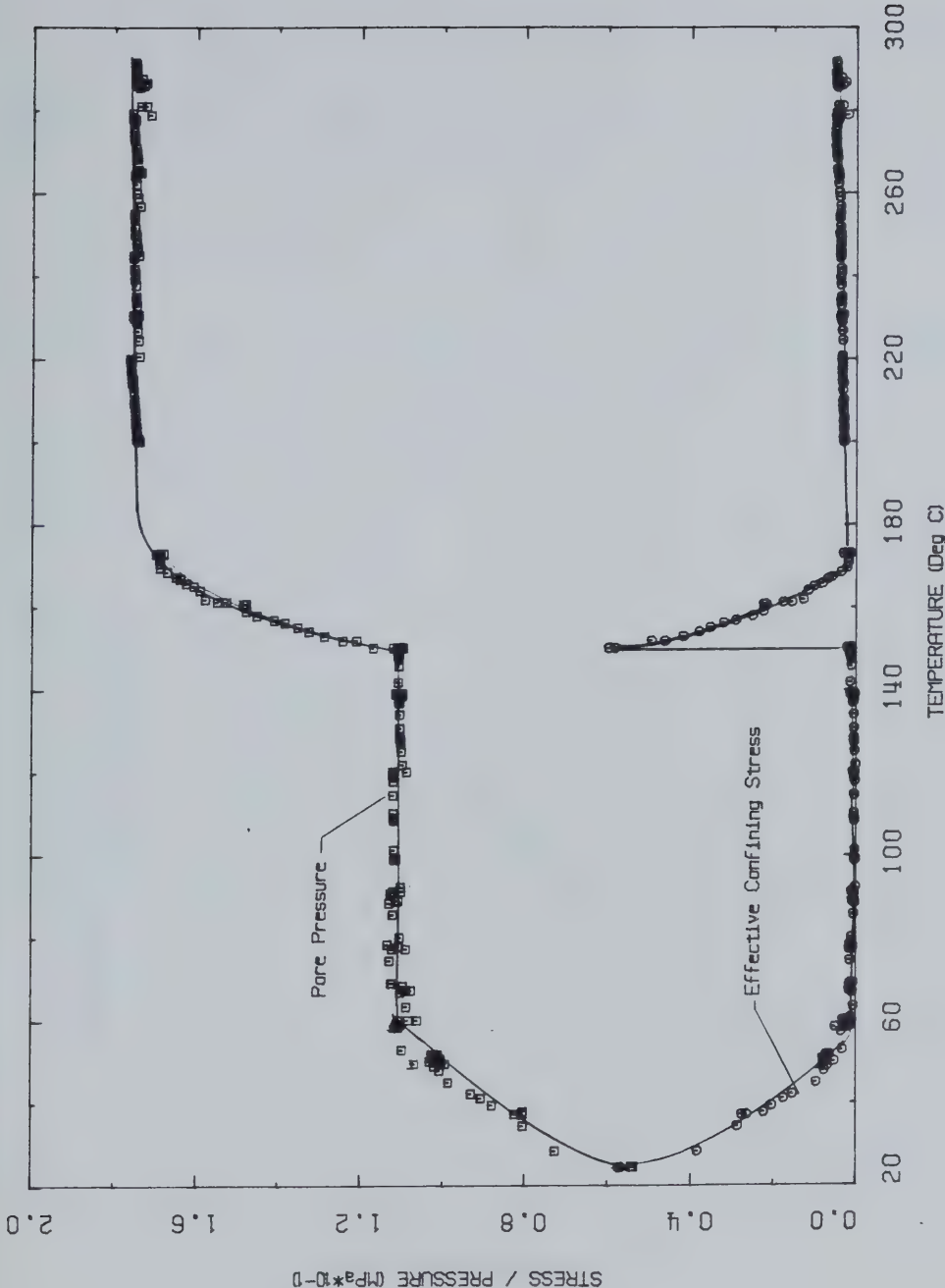


FIGURE B23 Pore Pressure Response to Undrained Heating: Test C055



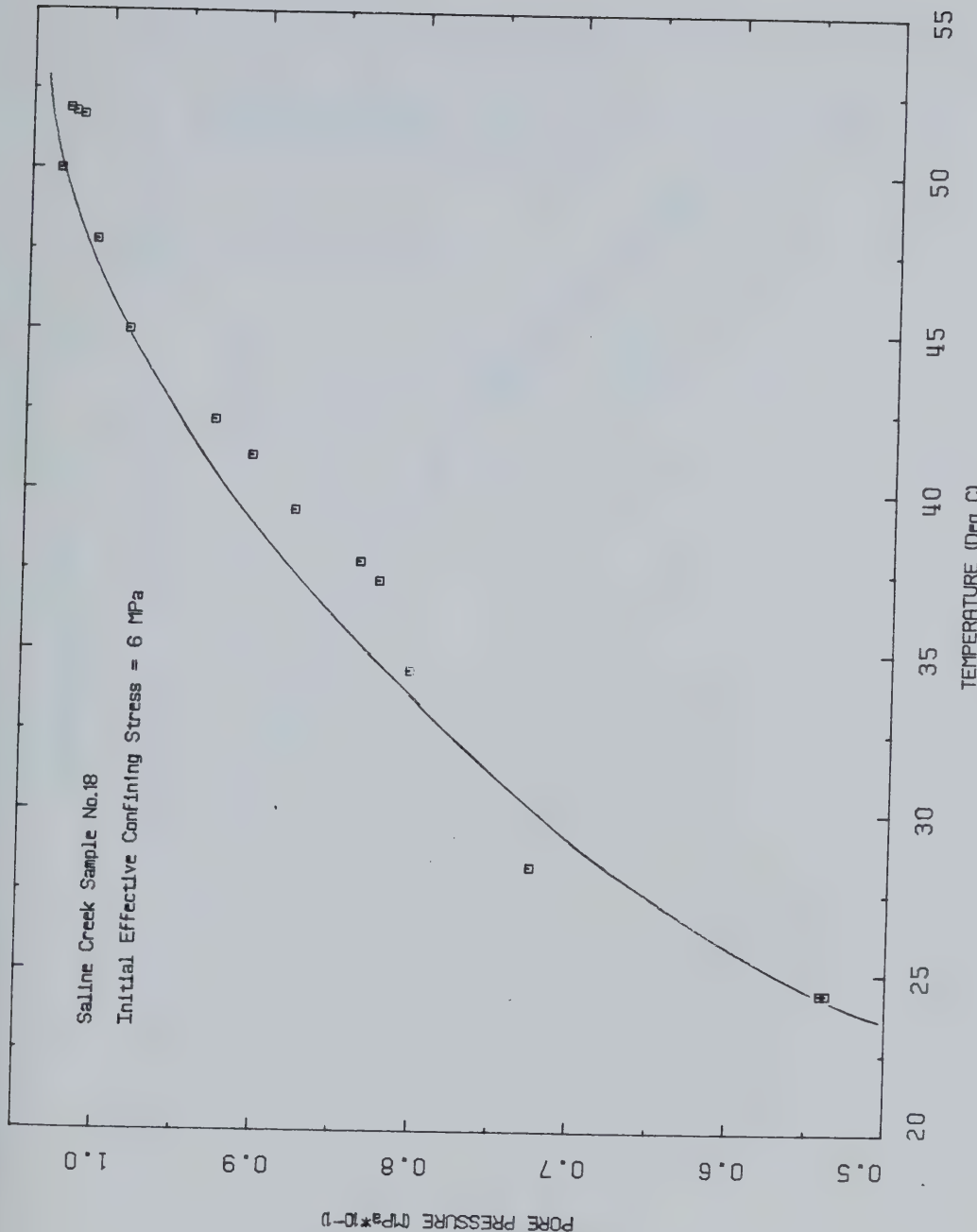


FIGURE B24 Pore Pressure Response to Undrained Heating: Test C055



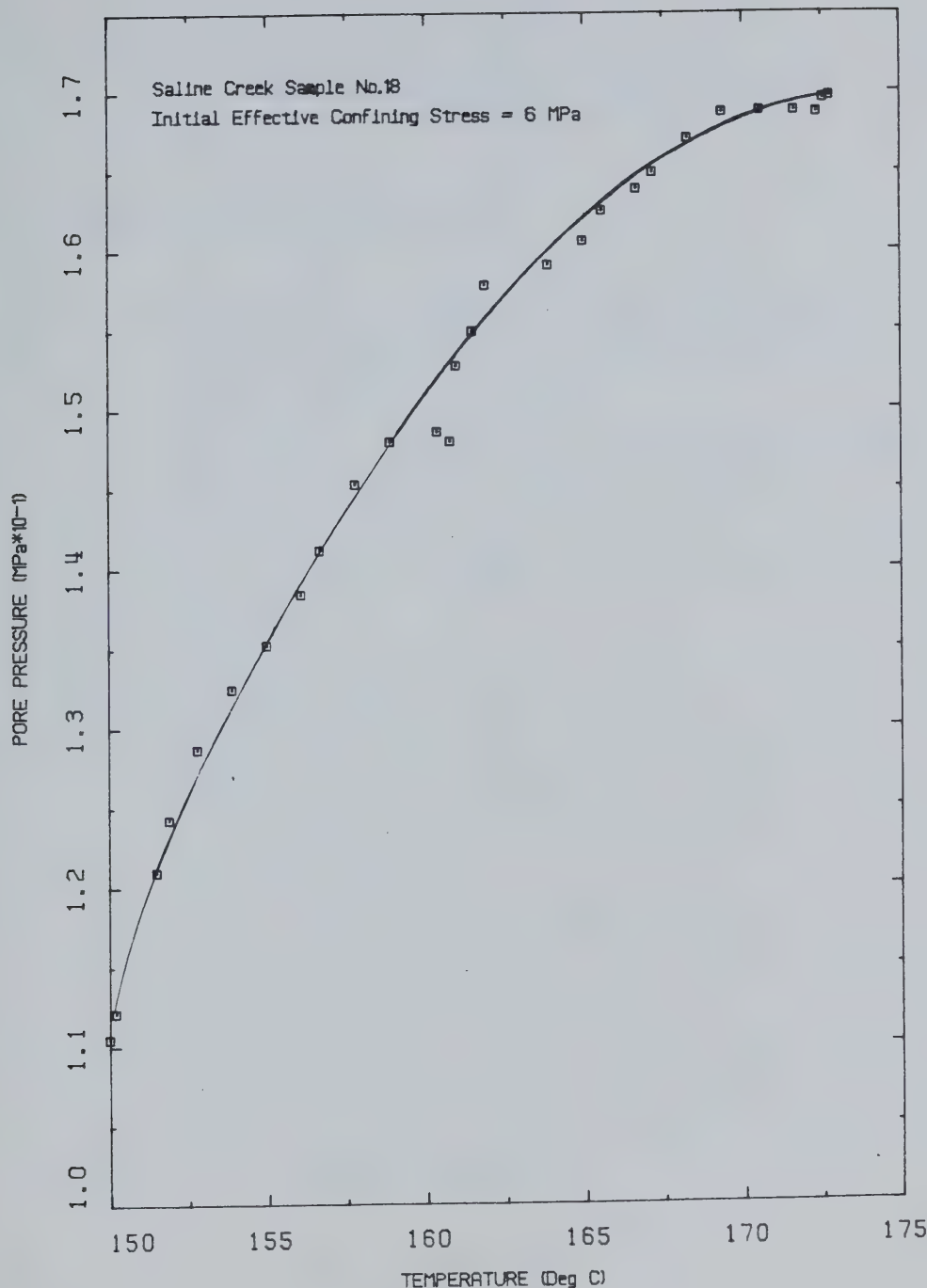


FIGURE B25 Pore Pressure Response to Undrained Heating: Test COS5



## TEST COS6

Drained Thermal Expansion of Saline Creek Oil  
Sand Sample No. 10A at 6 MPa Effective  
Confining Stress and Temperatures from 20 - 300°C

Procedural Details: Test COS6

1. Sample no. 10A was warmed to room temperature under confining pressure of sufficient magnitude to prevent thermal expansion of the sample.
2. The sample was saturated over a period exceeding 24 hours under confining and back pressures of 2000 kPa.
3. The back pressure and confining pressures were increased simultaneously in increments of 200 kPa to approximately 5000 kPa.
4. The confining pressure was then increased to 11,000 kPa and the 5000 kPa back pressure was maintained. The back pressure line was left open to permit drainage of fluid from the sample and communication of fluid pressure with the volume change cell.
5. The cell temperature was increased in 5°C to 10°C increments to 200°C and sample height was monitored along with the volume change of the pore fluids.
6. The confining pressure was then increased step-wise to 21,000 kPa while the back pressure was increased to 15,000 kPa maintaining a constant 6000 kPa difference between the confining and back pressures.



7. The cell temperature was then raised in 10°C increments from 200°C to 300°C. The sample height and volume of pore fluid drained from the sample were monitored continuously.
8. It should be noted that a small system leak developed between temperatures 108°C and 140°C. It is estimated that approximately 1 to 2 ml of pore fluid escaped from the cell prior to repairing this leak. Accordingly, the volume change data presented may be in error by as much as 2 percent for this test.



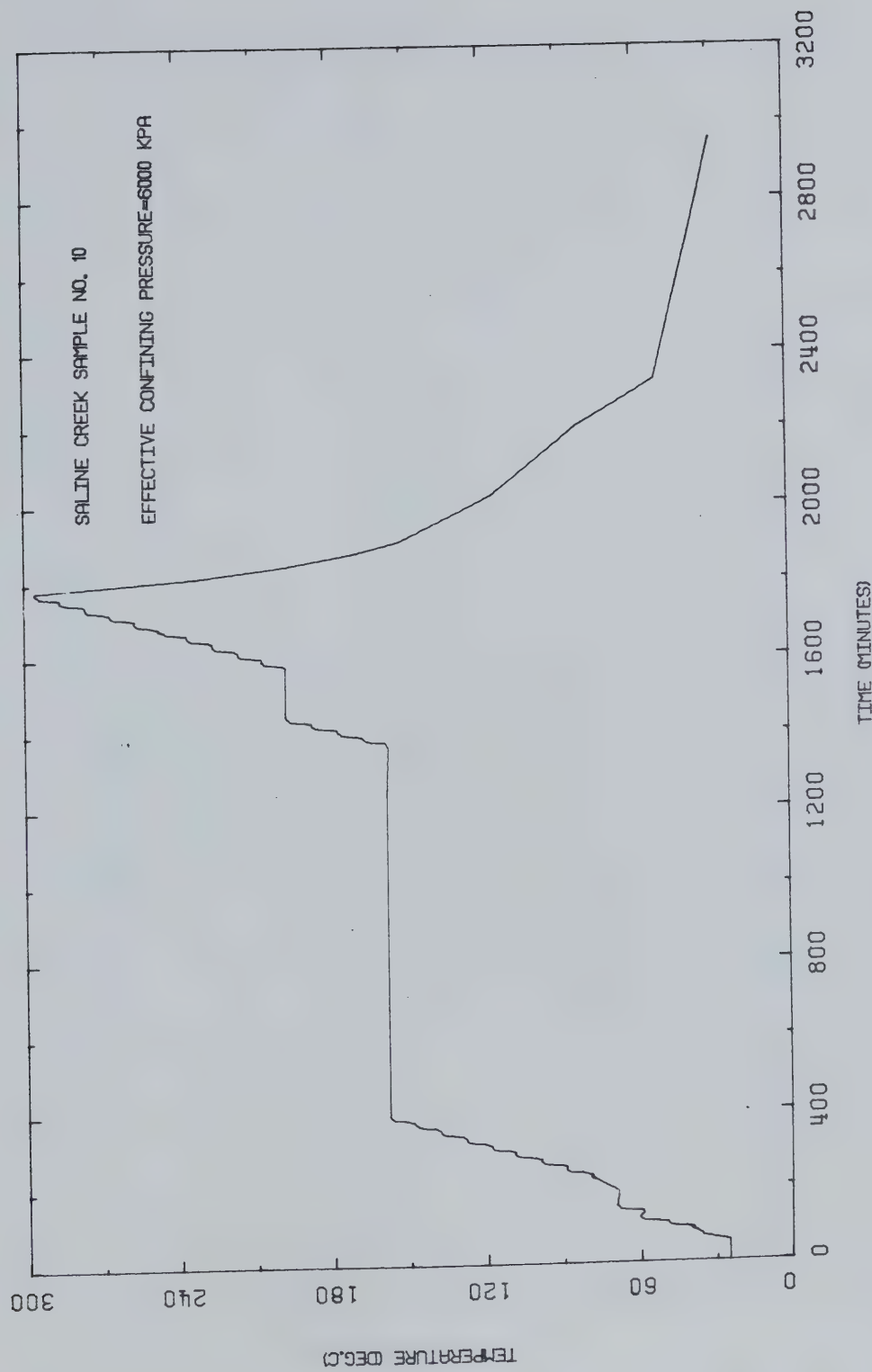


FIGURE B26 Temperature Versus Time: Test C056



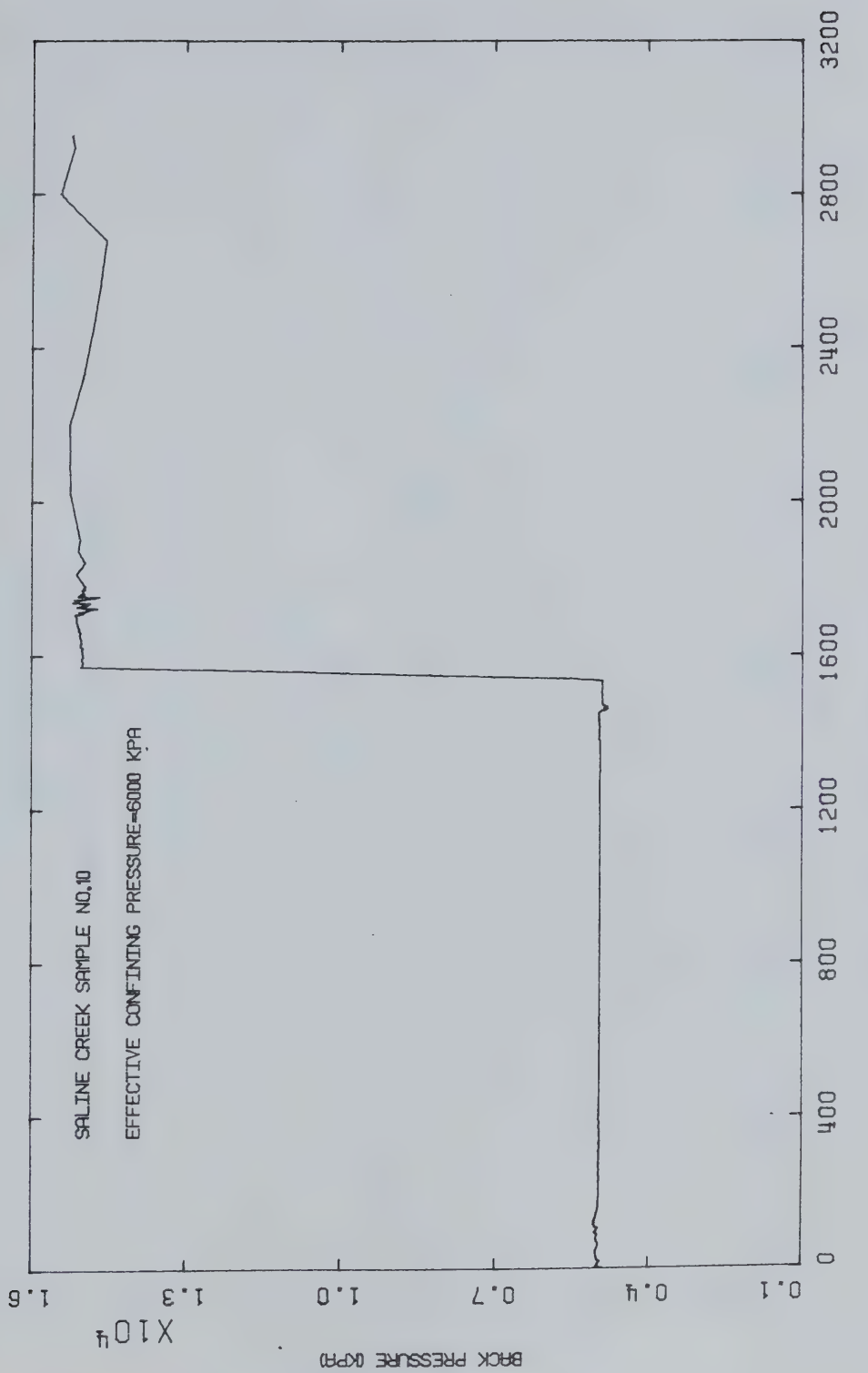


FIGURE B27 Back Pressure Versus Time: Test C056



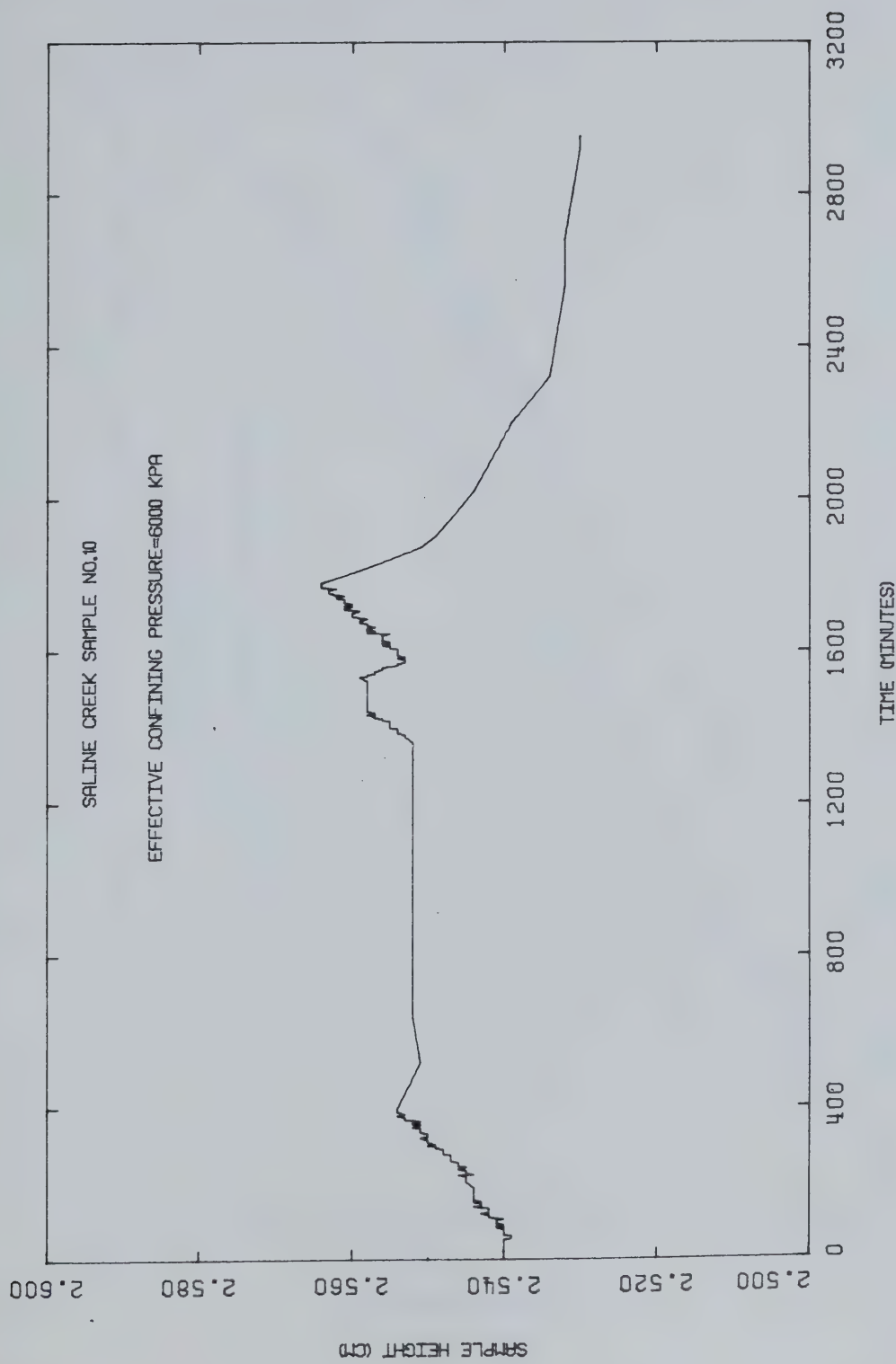


FIGURE B28 Sample Height Versus Time: Test COSS6



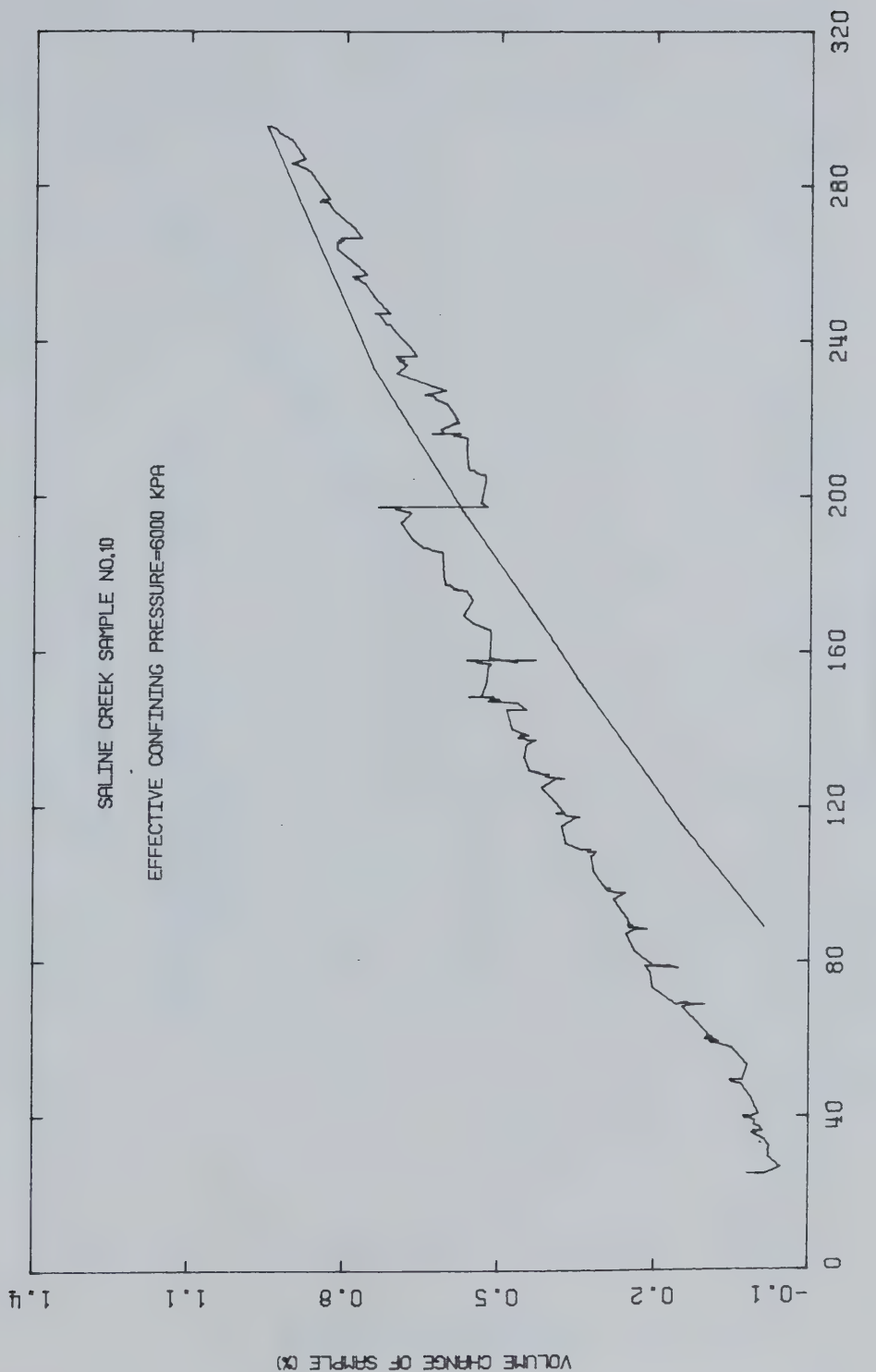


FIGURE B29  
Drained Volumetric Thermal Expansion: Test  
CO56



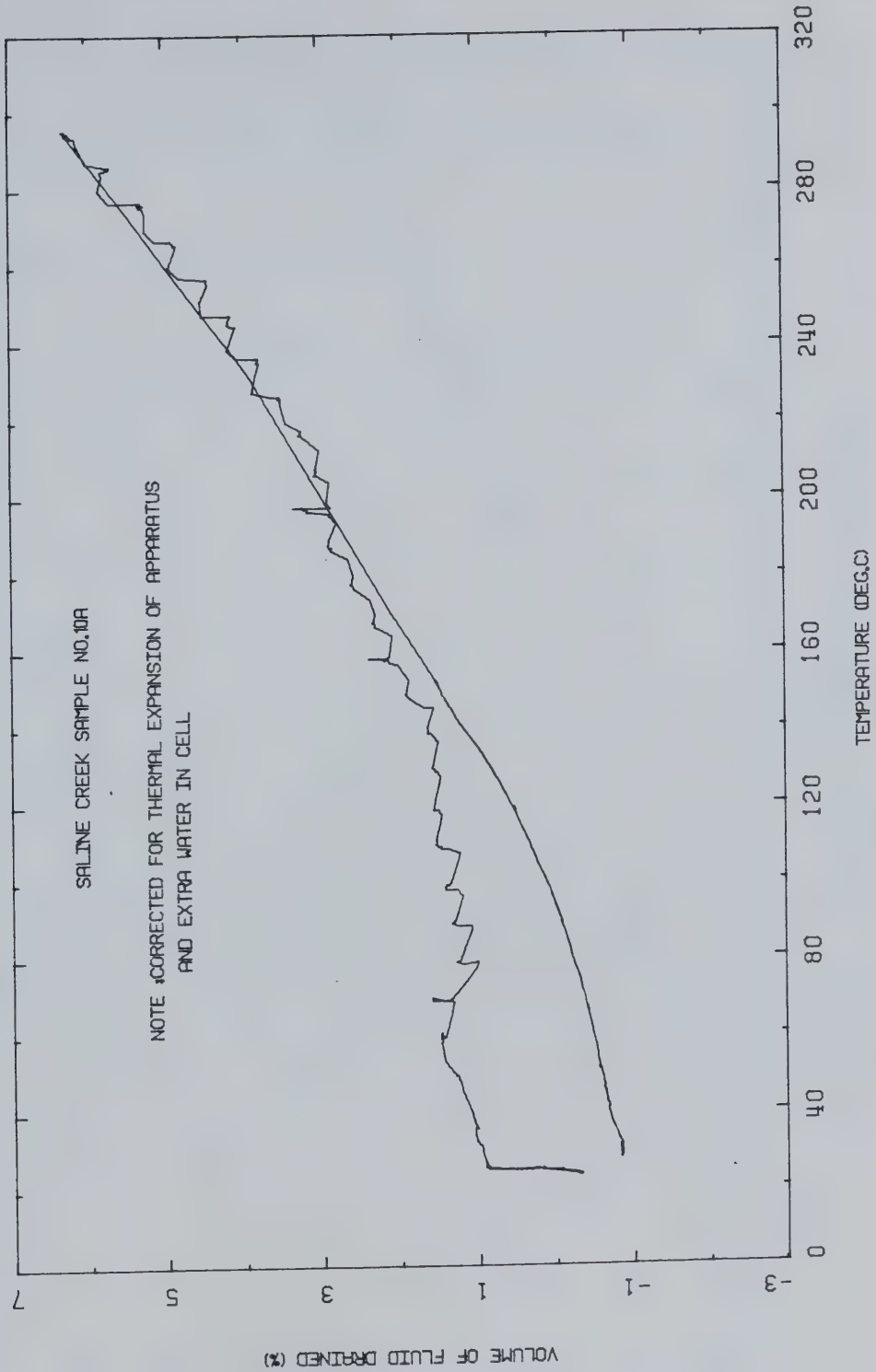


FIGURE B30      Volume of Pore Fluid Drained During  
Heating: Test C056



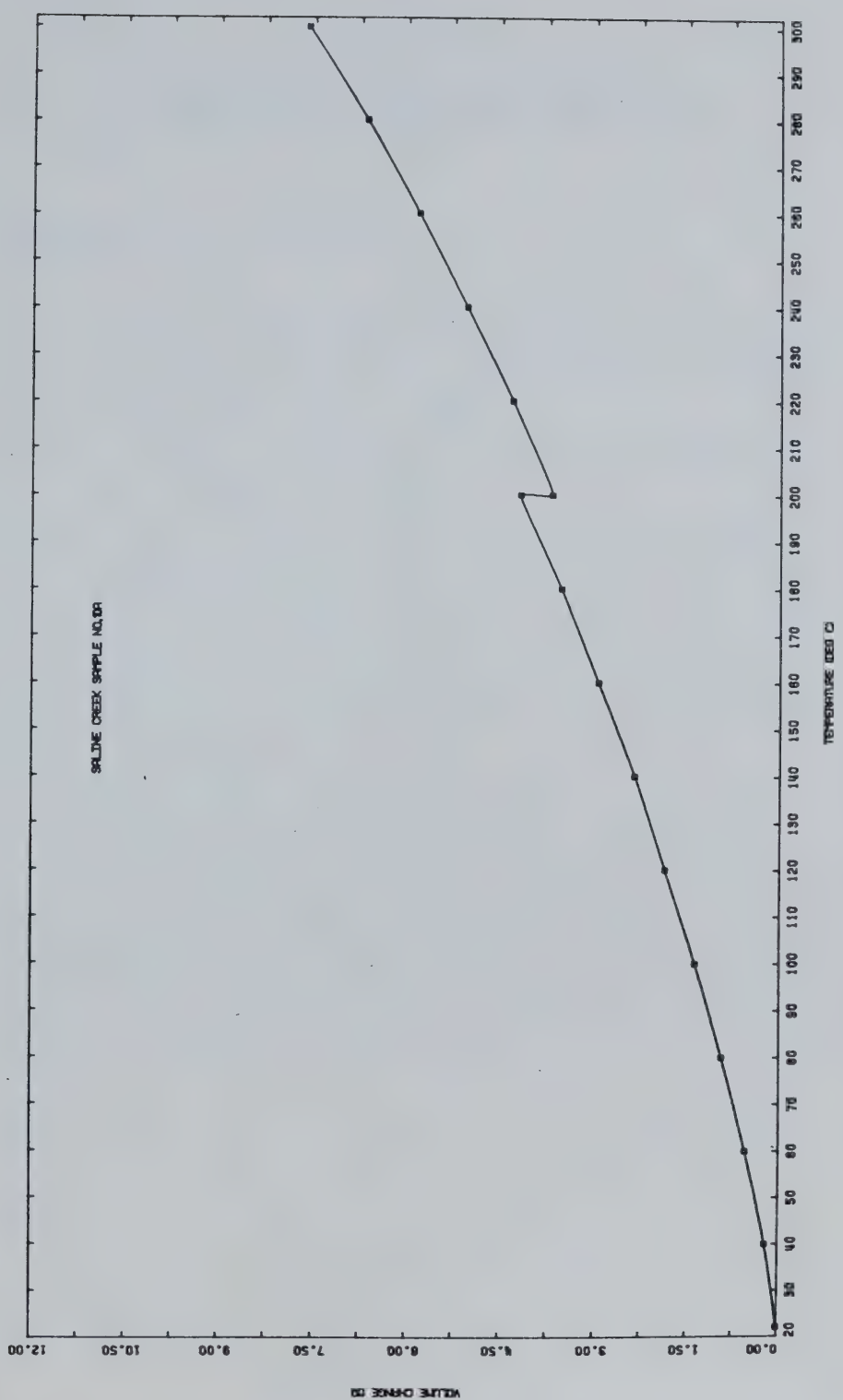


FIGURE B31      Equivalent Undrained Thermal Expansion:  
Test COS6



## TEST COS7

Drained Thermal Expansion of Saline Creek Oil  
Sand Sample No. 10B at Nominal Effective  
Confining Stress and Temperatures from 20 - 300°C

Procedural Details: Test COS7

1. Sample 10B was warmed to room temperature under a nominal confining pressure of sufficient magnitude to prevent thermal expansion of the sample.
2. The sample was saturated for a period of 24 hours under a back pressure of 2000 kPa.
3. Confining pressure and back pressure were increased simultaneously, step-wise to 5000 kPa. The back pressure line was left open to permit communication of pore fluid drainage with the volume change measuring apparatus.
4. Cell temperatures were increased in 5°C to 10°C increments up to 200°C.
5. Confining pressure and back pressure were increased simultaneously, step-wise from 5000 kPa to 15,000 kPa.
6. Cell temperatures were then increased in 5°C to 10°C increments from 200°C to 300°C.
7. Sample height and pore fluid drainage volume were monitored continuously throughout the test.



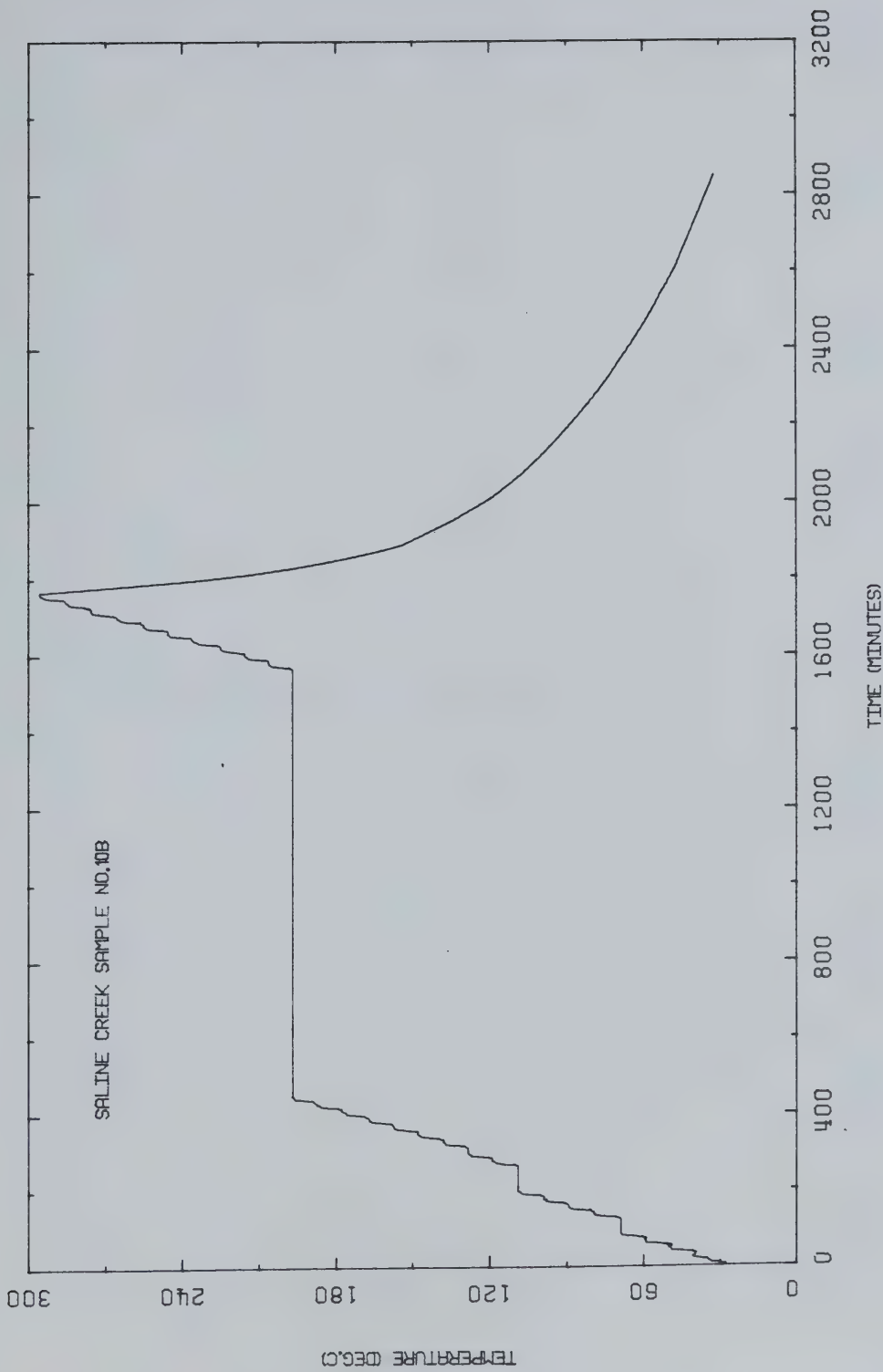


FIGURE B32 Temperature Versus Time: Test COS7



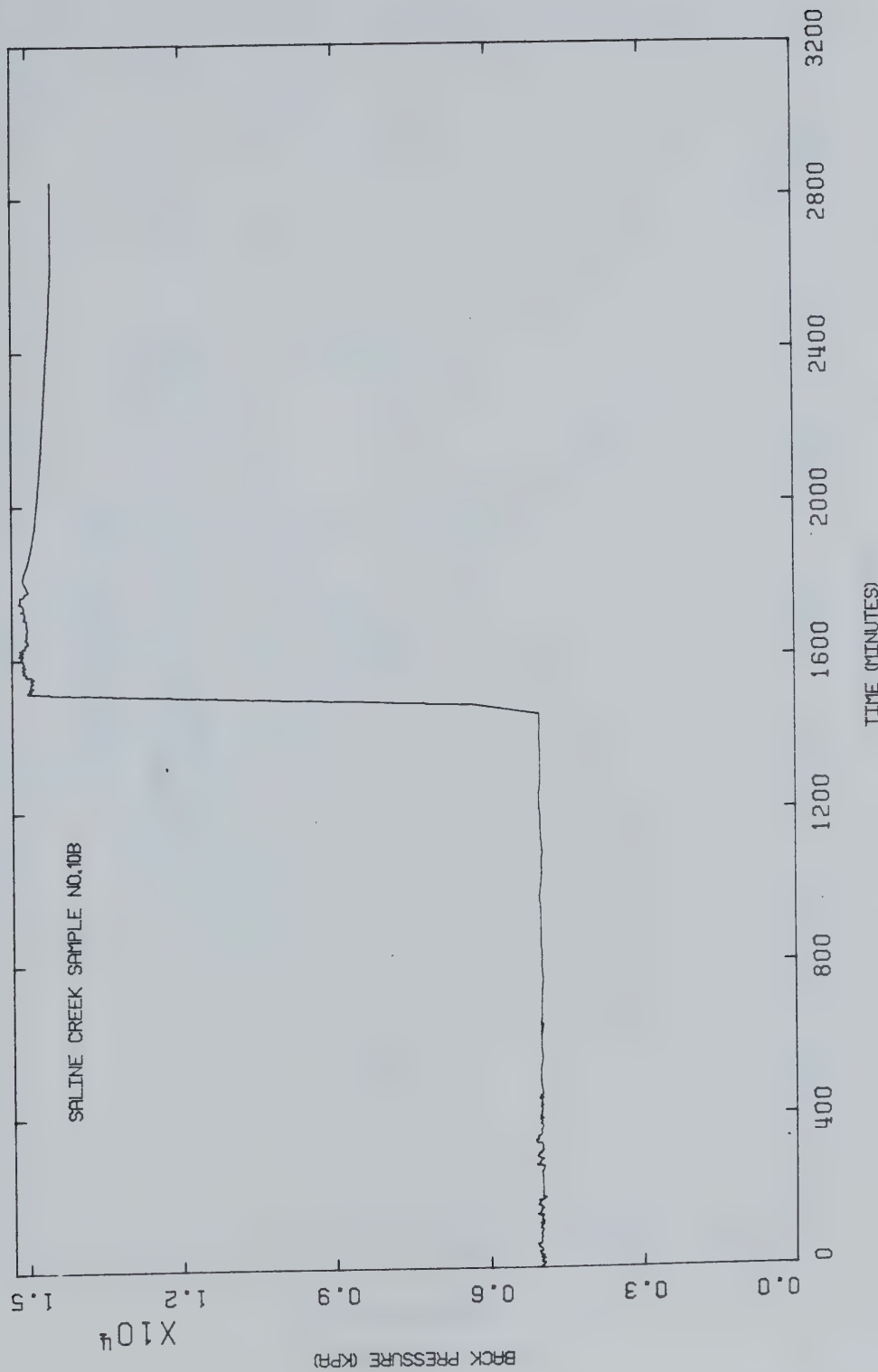


FIGURE B33 Back Pressure Versus Time: Test C057



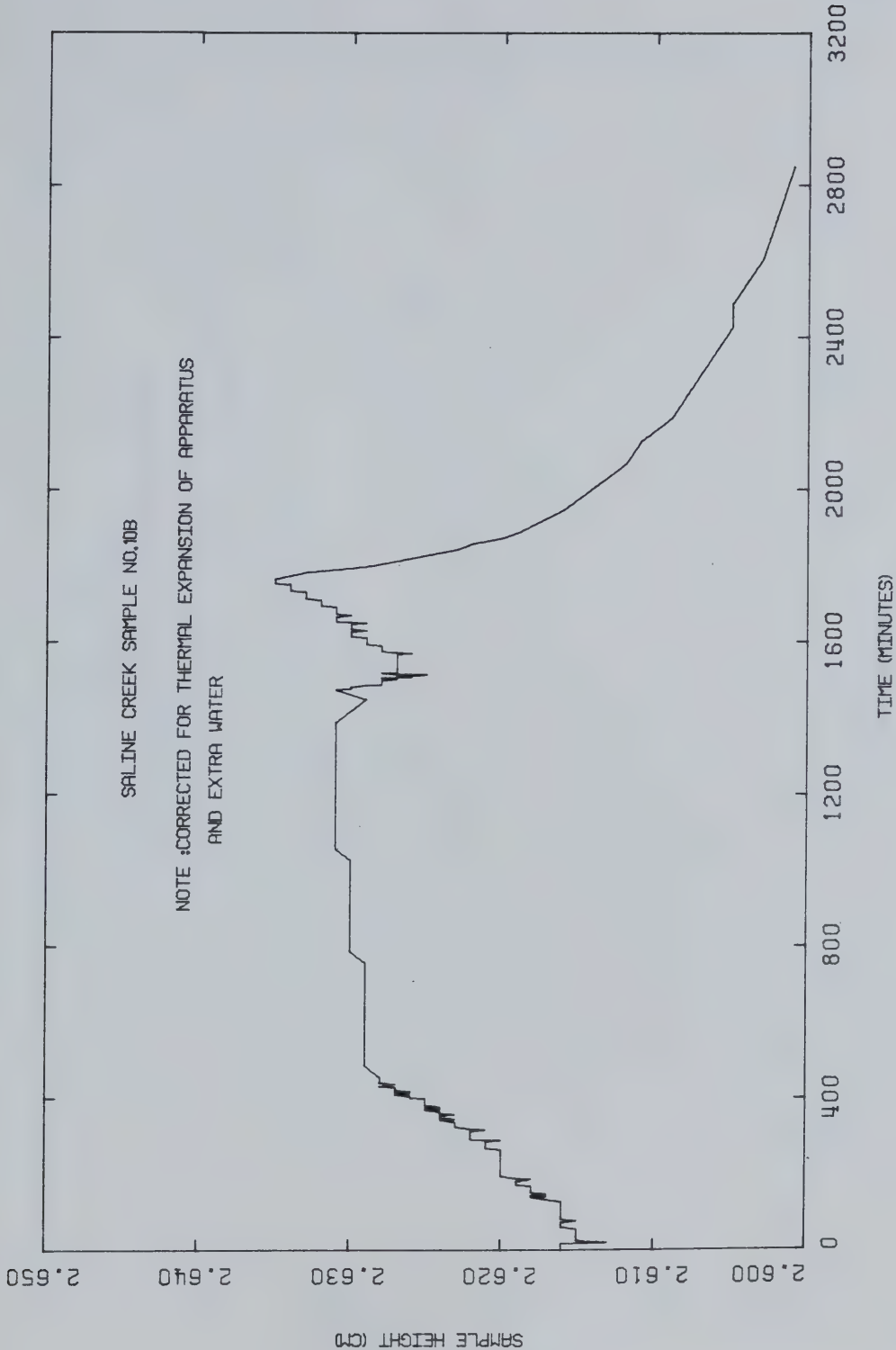


FIGURE B34 Sample Height Versus Time: Test COST7



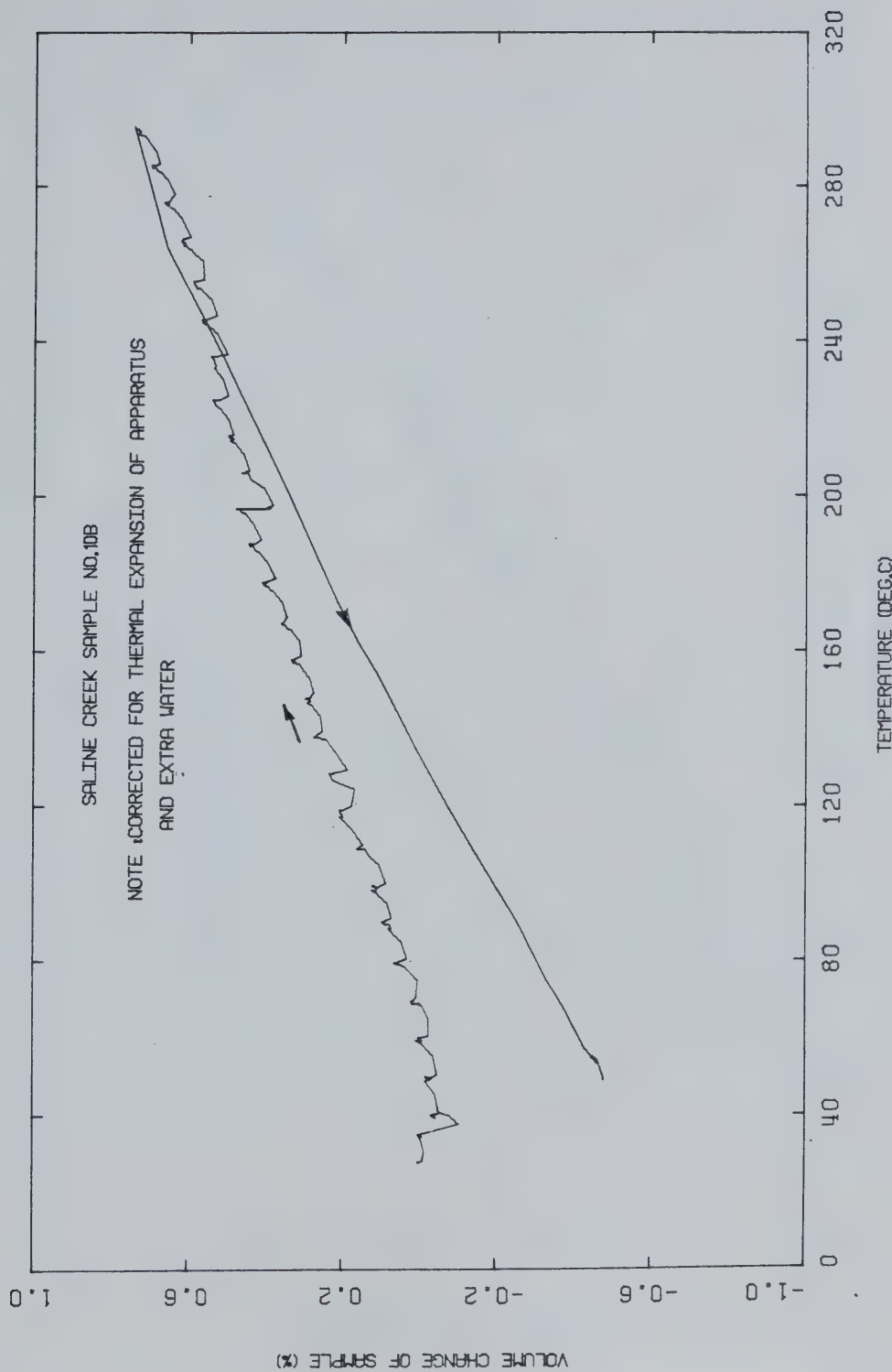


FIGURE B35 Drained Thermal Expansion: Test C057



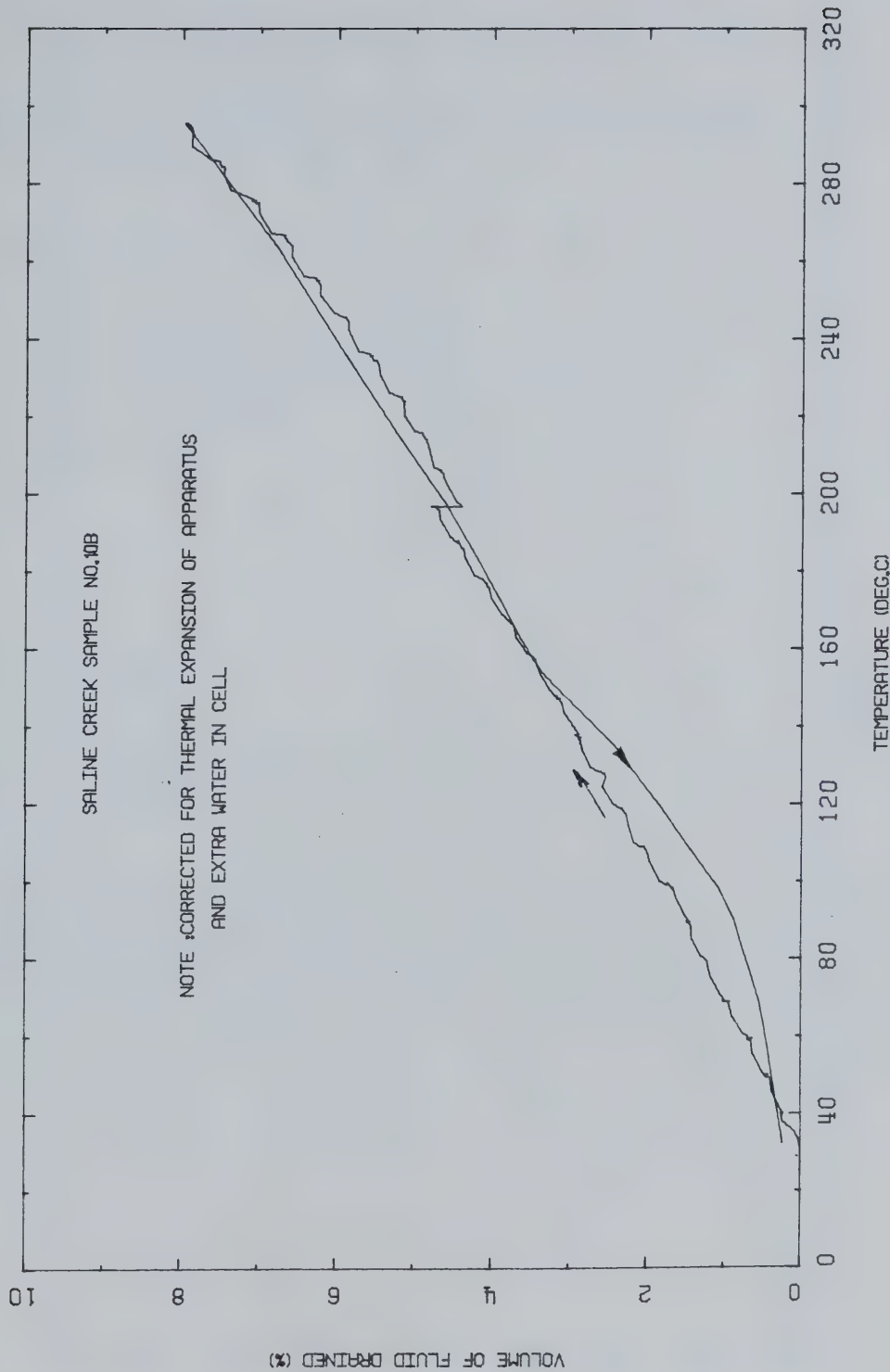


FIGURE B36 Volume of Pore Fluid Drained During Heating: Test C057



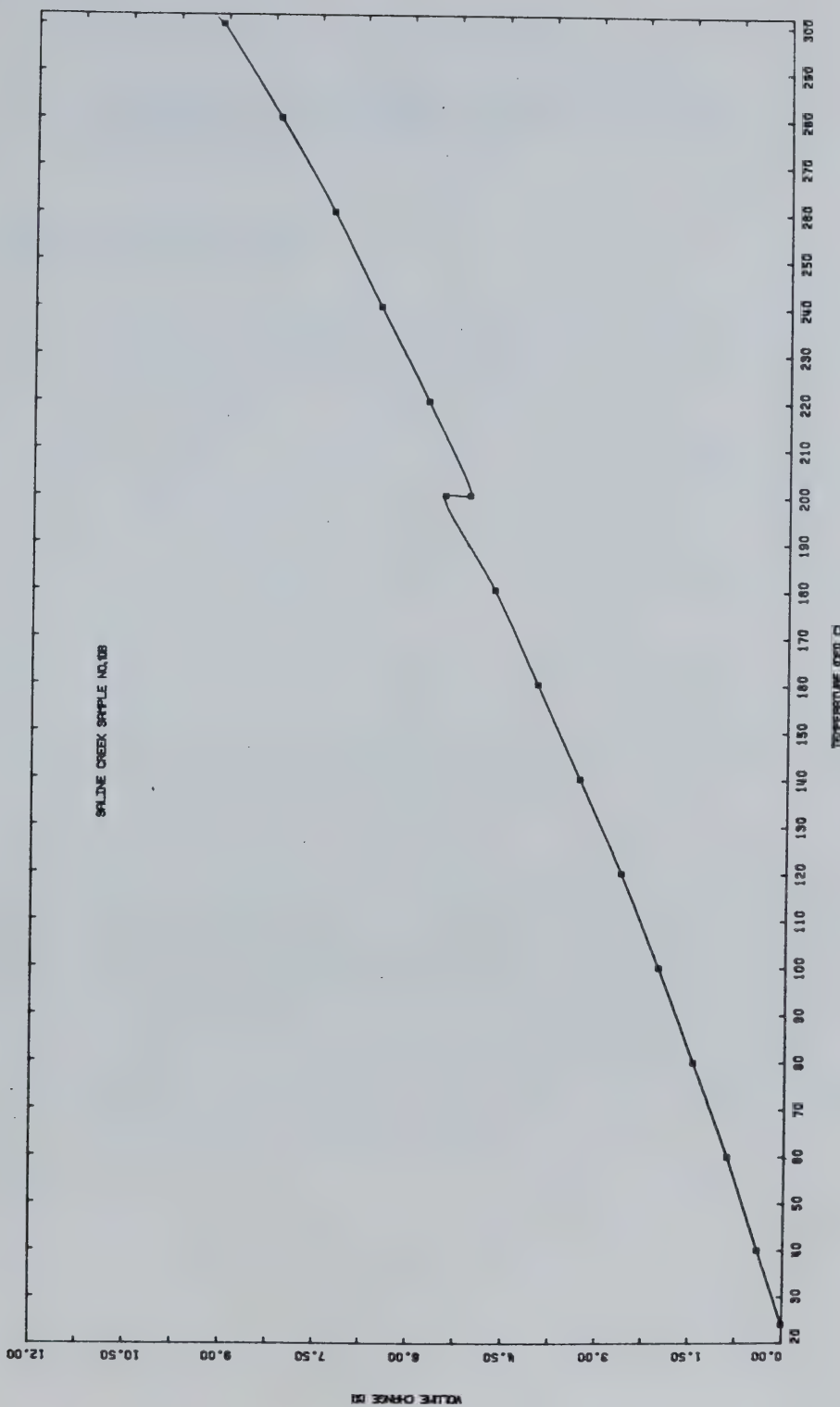


FIGURE B37 Equivalent Undrained Thermal Expansion:  
Test C037



## TEST COS8

Undrained Thermal Expansion at Nominal  
Effective Confining Stress and Gas Exsolution Test  
for Saline Creek Sample No. 42 from 20 - 300°C

Procedural Details: COS8

1. Saline Creek Sample No. 42 was confined under a nominal pressure to prevent thermal expansion and fabric disturbance as it warmed to room temperature.
2. The sample was saturated under confining and back pressures of approximately 2000 kPa for a period exceeding 24 hours.
3. The vertical confining pressure and back pressure were initially reduced to 200 kPa. The back pressure was then shut in.
4. The cell temperature was raised in 5°C increments.
5. Confining and back pressures were increased only when required to prevent phase change/or gas exsolution of the pore fluids.
6. Each time significant volumetric expansion was observed which was believed to be due to phase change/gas exsolution, the cell temperature was immediately decreased to the previous incremental temperature level. The confining pressure was increased gradually during these mini cool-down phases to maintain near-constant back pressure and to re-establish the previous sample volume.



7. The confining and back pressures were then increased simultaneously prior to applying the next temperature increment.
8. The purpose of the above procedure was to attempt to define a pressure-temperature relationship corresponding to gas exsolution and/or phase change of the pore fluids.
9. The test was terminated at 300°C. Sample volume change was monitored during cool-down.



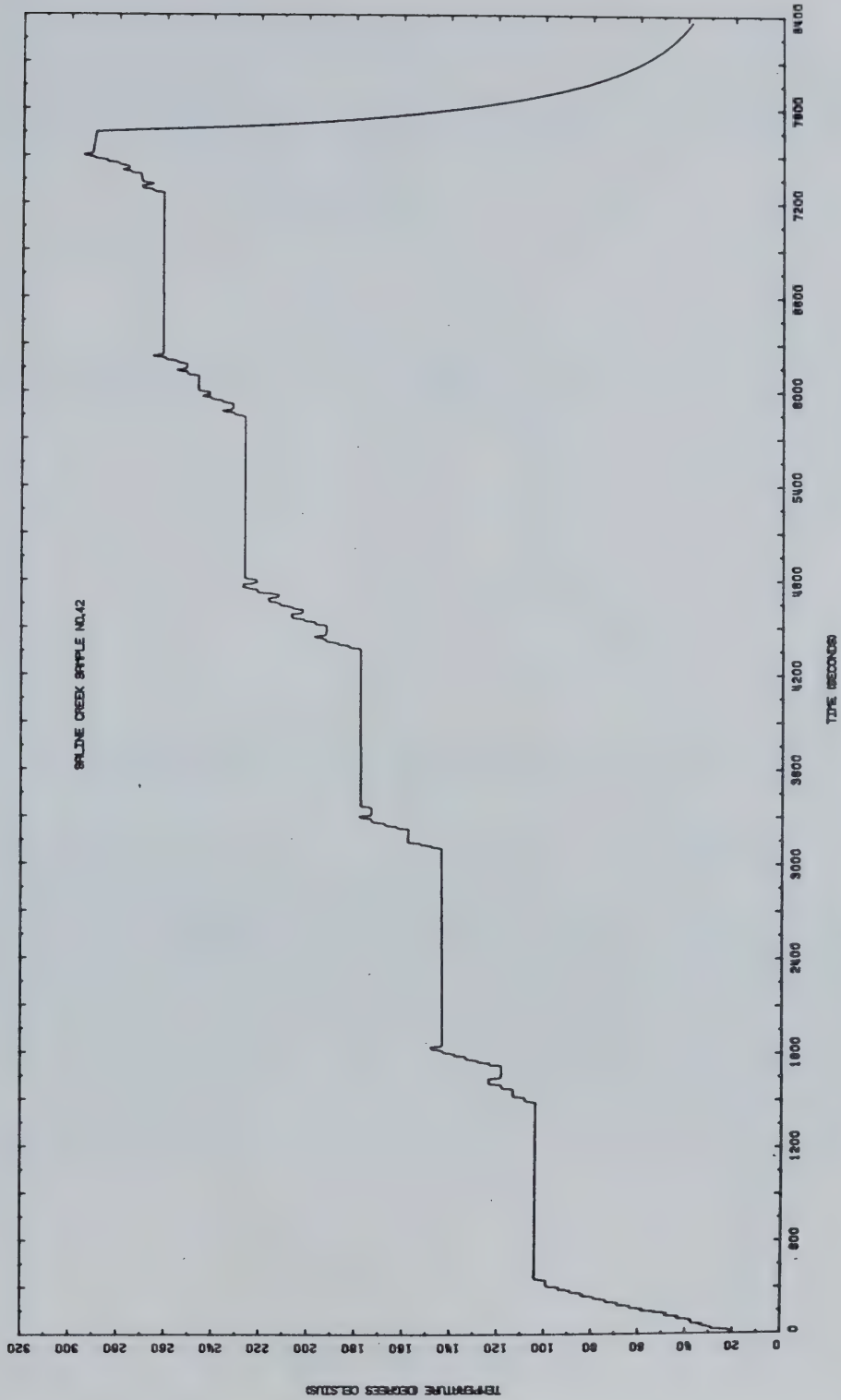


FIGURE B38 Temperature Versus Time: TEST C058





FIGURE B39 Back Pressure Versus Time: Test COS8



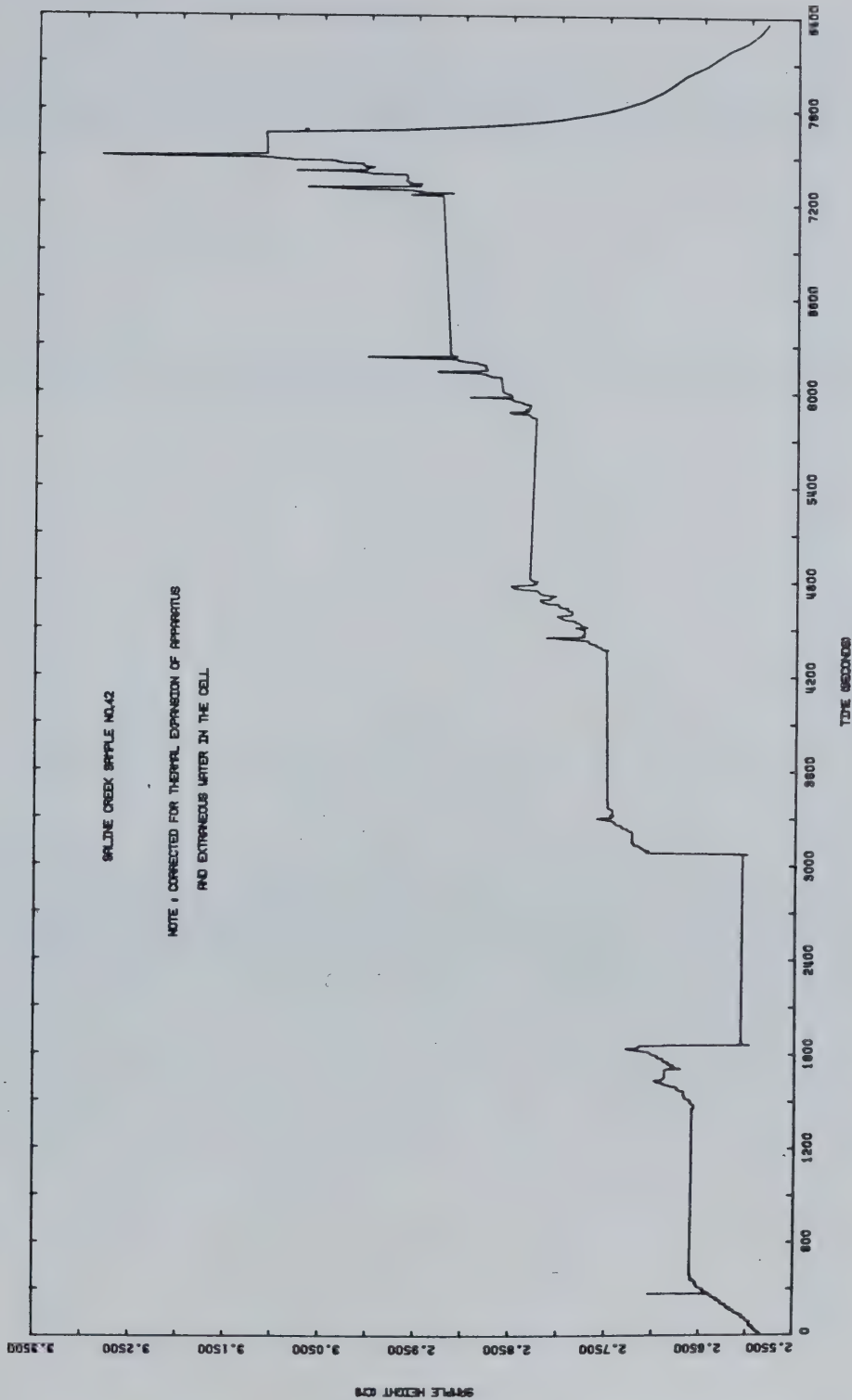


FIGURE B40 Sample Height Versus Time: Test COS8



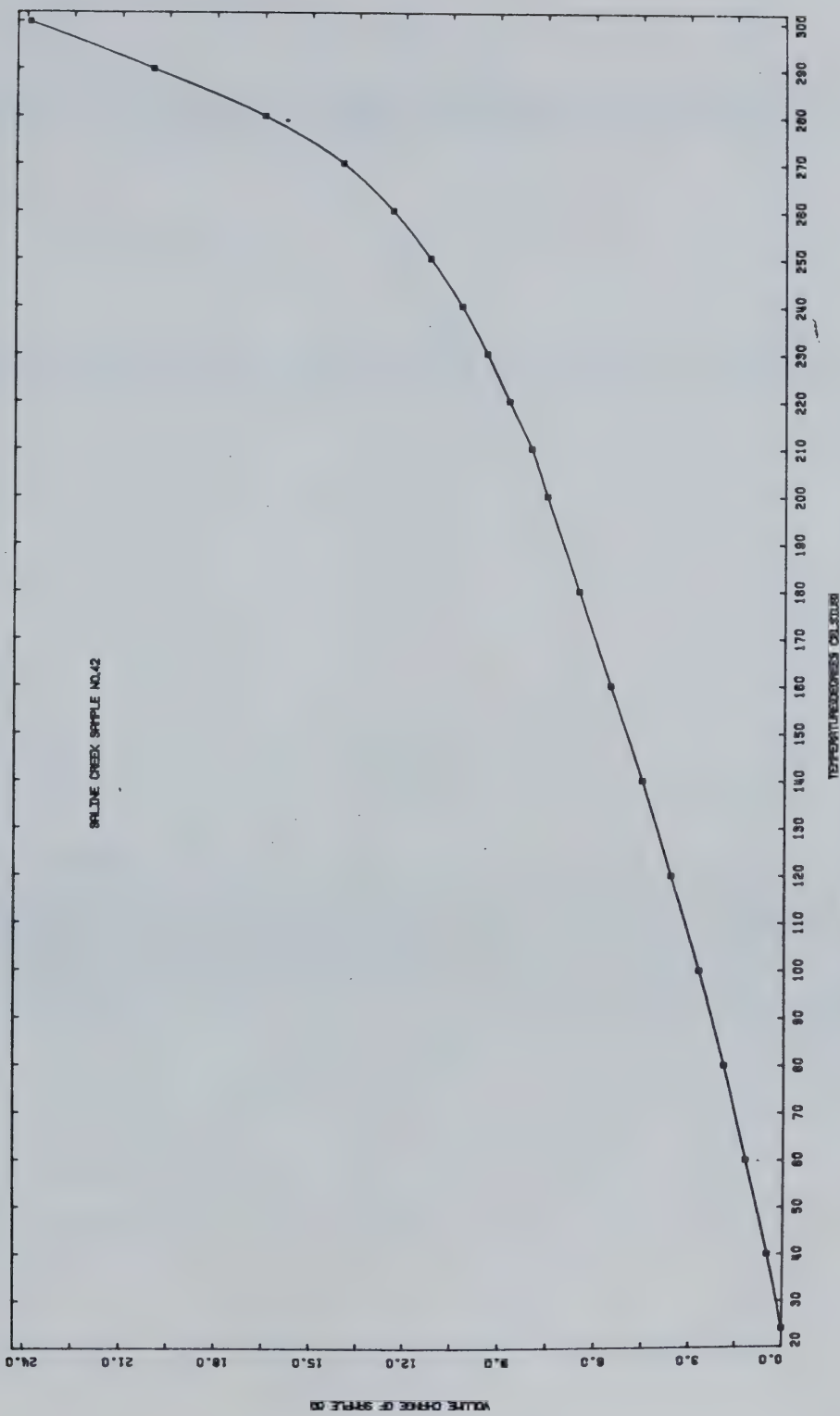


FIGURE B41 Undrained Volumetric Thermal Expansion:  
Test C058



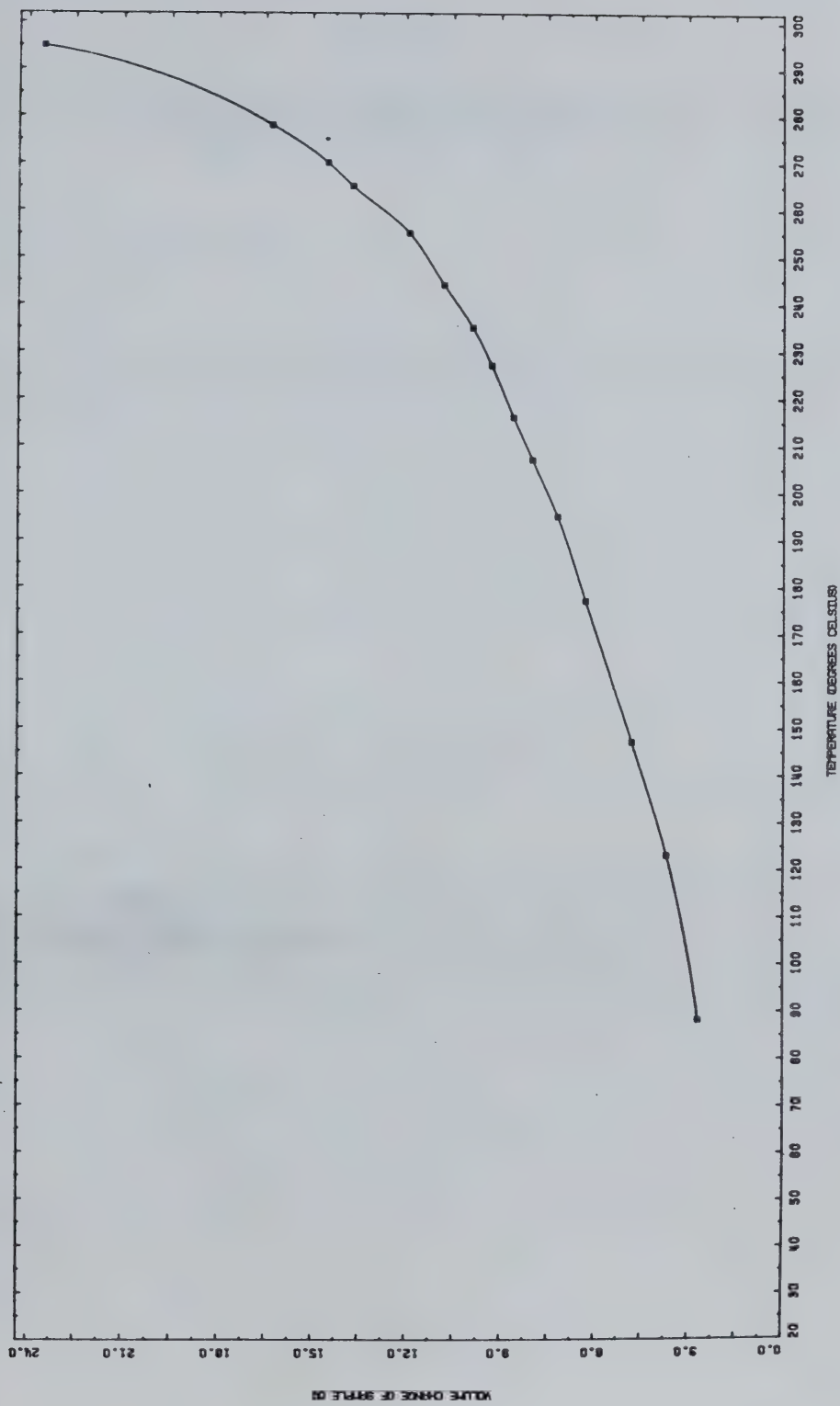


FIGURE B42 Undrained Thermal Expansion at Initiation  
of Gas Evolution: Test C088



## TEST COS9

Undrained Thermal Expansion of Saline  
Creek Sample No. 41 at 10 MPa  
Back Pressure from 20 - 300°C

Procedural Details: COS9

1. Sample no. 41 was warmed to room temperature under a nominal confining pressure of sufficient magnitude to prevent thermal expansion of the sample.
2. The sample was saturated for a period of 24 hours under confining and back pressures of 2000 kPa.
3. Confining pressure and back pressure were increased simultaneously, step-wise to 10,000 kPa. The back pressure line was shut in.
4. A room temperature compressibility test was performed over the effective stress range 2 - 18 MPa.
5. Cell temperatures were increased in 5°C to 10°C increments up to 300°C.
6. Sample height and undrained volumetric expansion were monitored continuously as heating proceeded.
7. The thermal expansion test was terminated at a temperature of 300°C. The gas exsolution pressure was checked at 300°C for comparison with Test COS8.
8. A compressibility test was performed at 300°C over the effective vertical stress range 4 - 18 MPa.
9. Sample volume was monitored during cool-down.



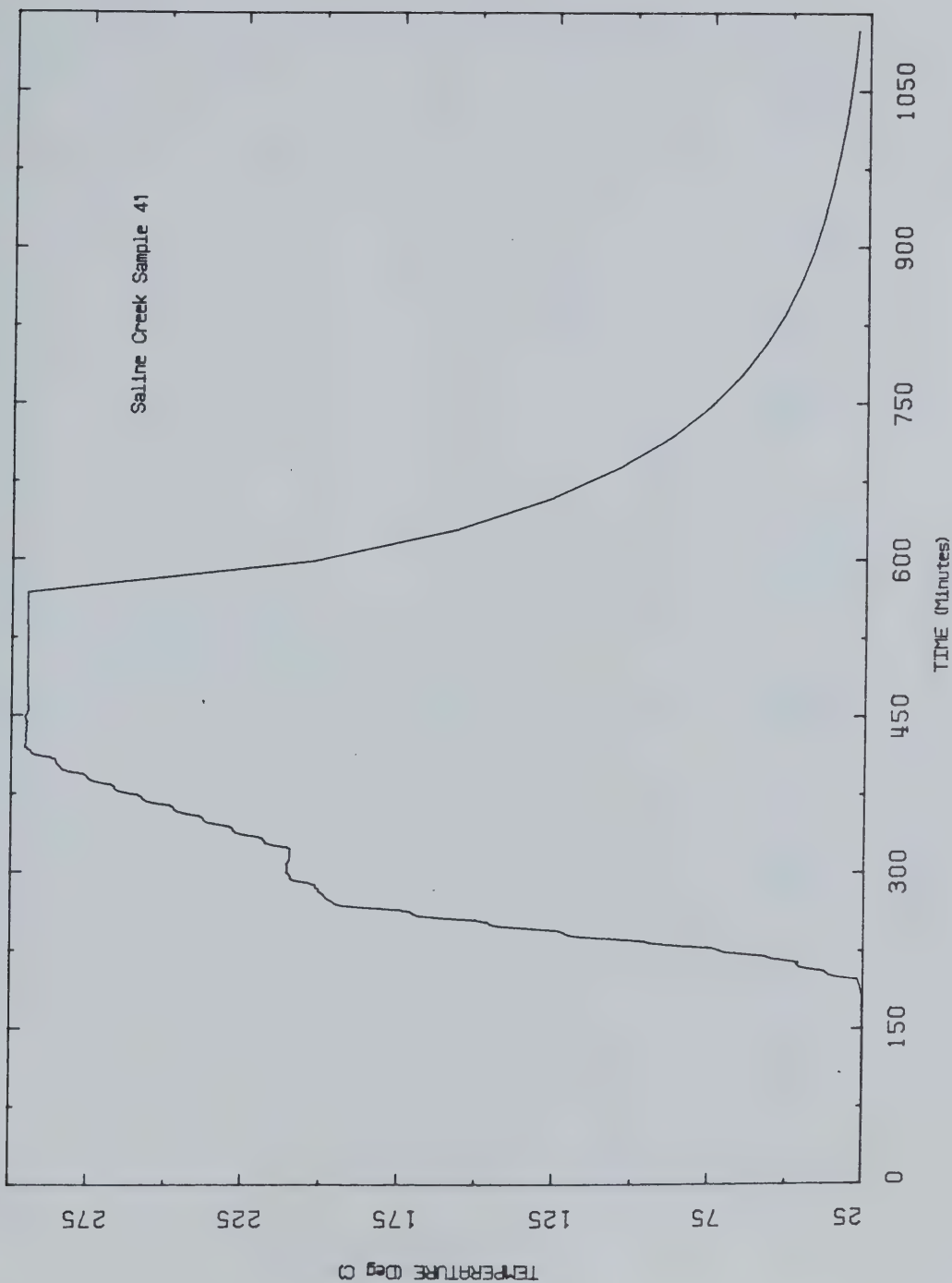


FIGURE B43 Temperature Versus Time: Test COS9



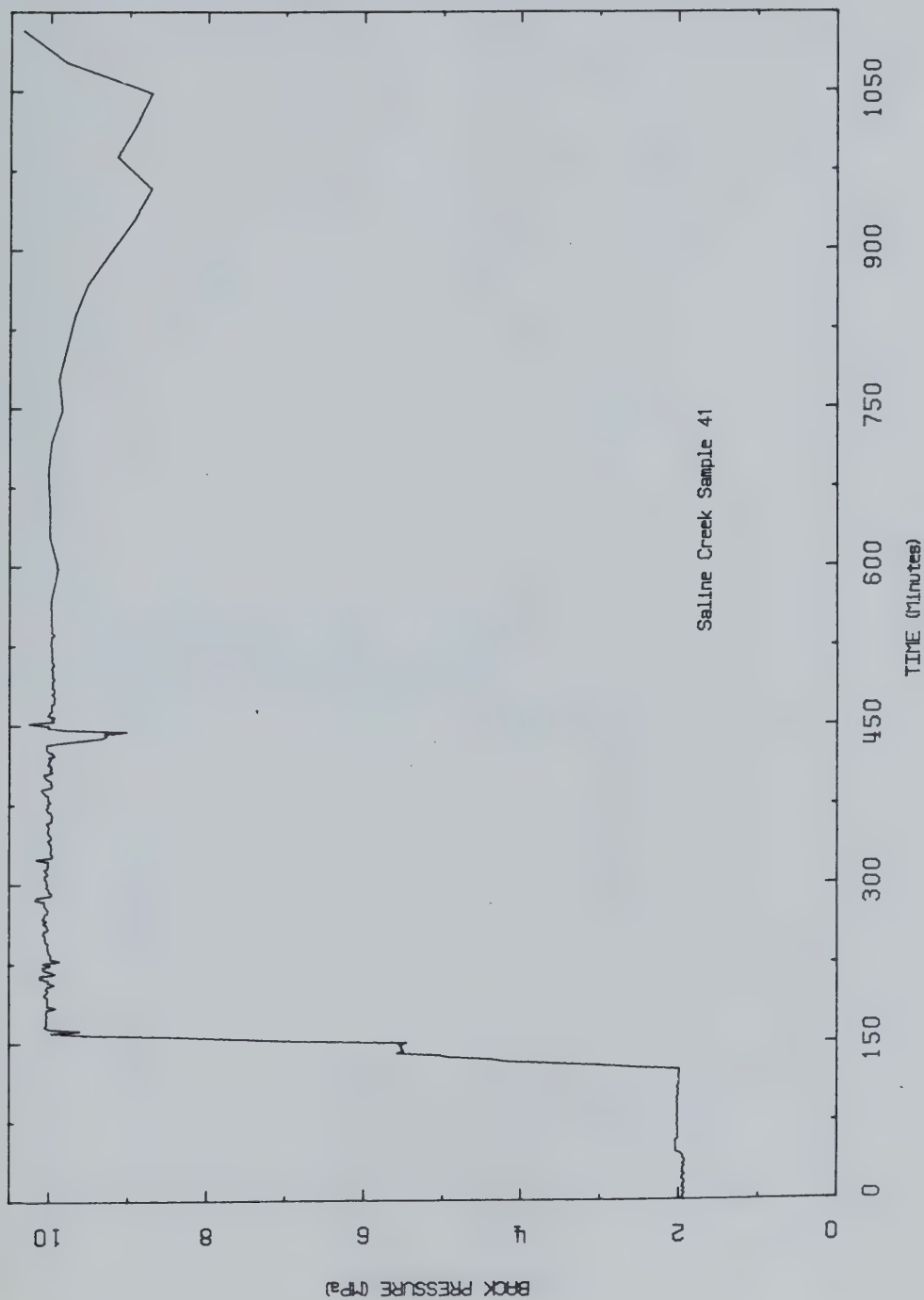


FIGURE B44 Back Pressure Versus Time: Test C059



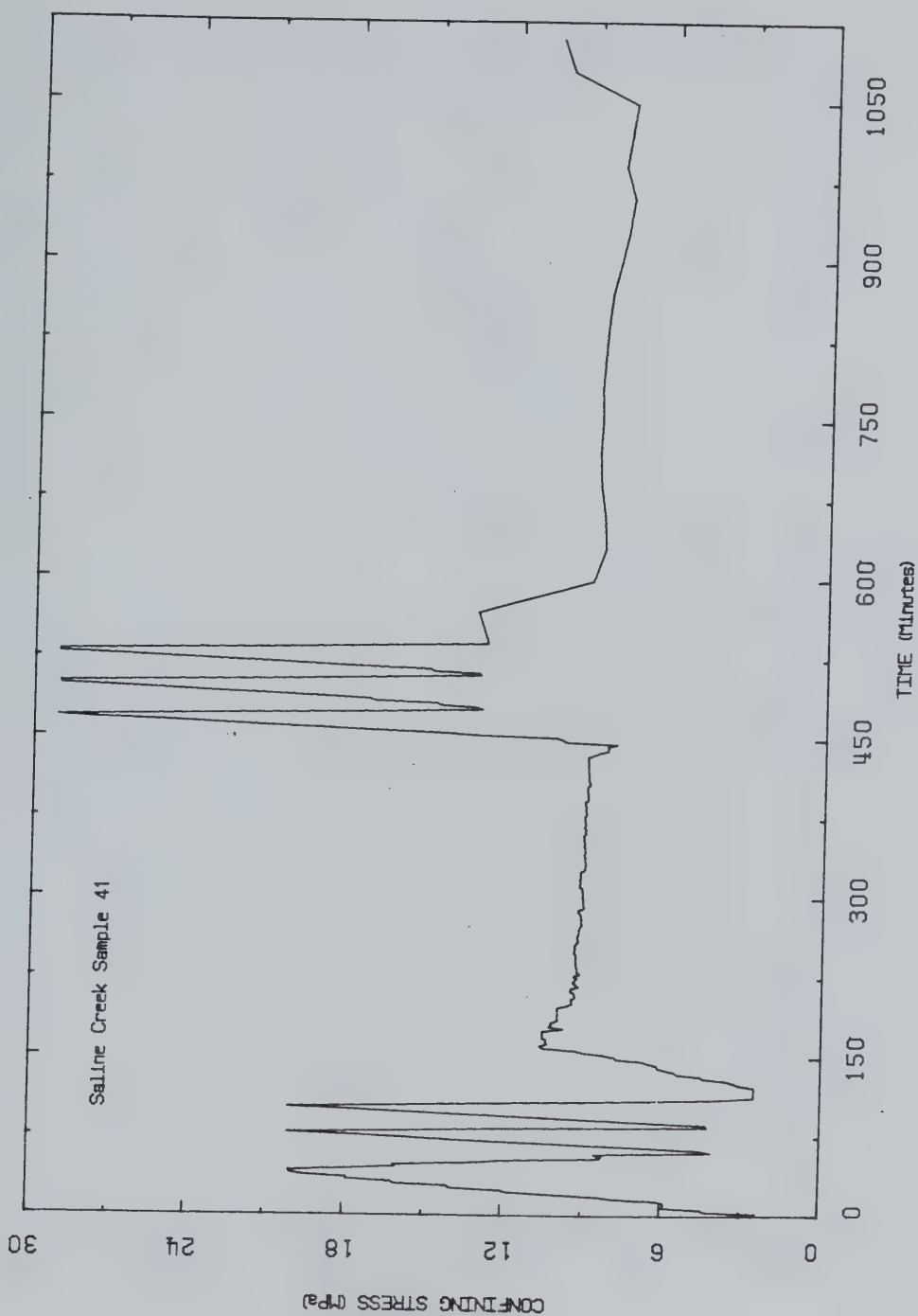


FIGURE B45 Confining Stress Versus Time: Test cos9



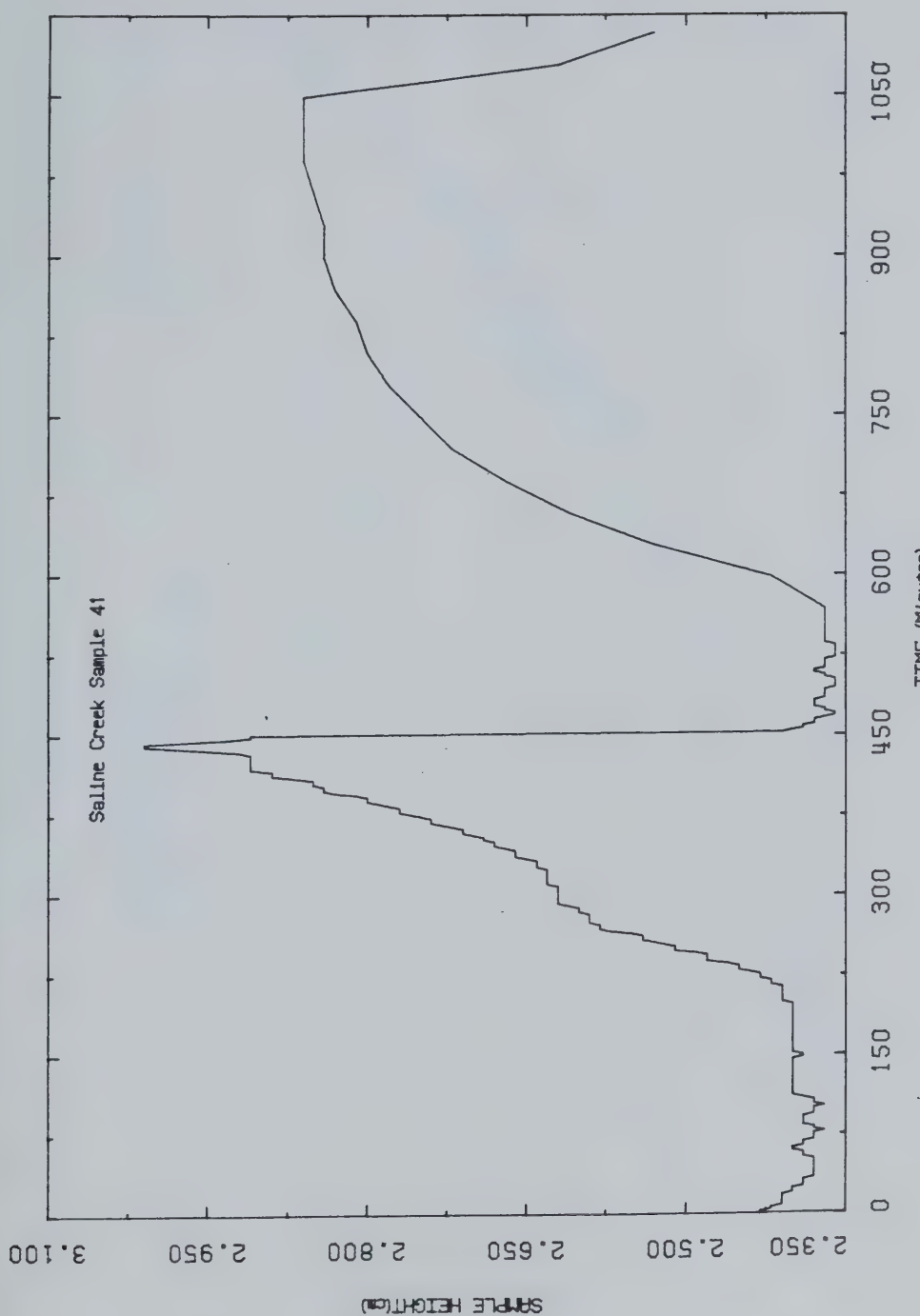


FIGURE B46 Sample Height Versus Time: Test C039



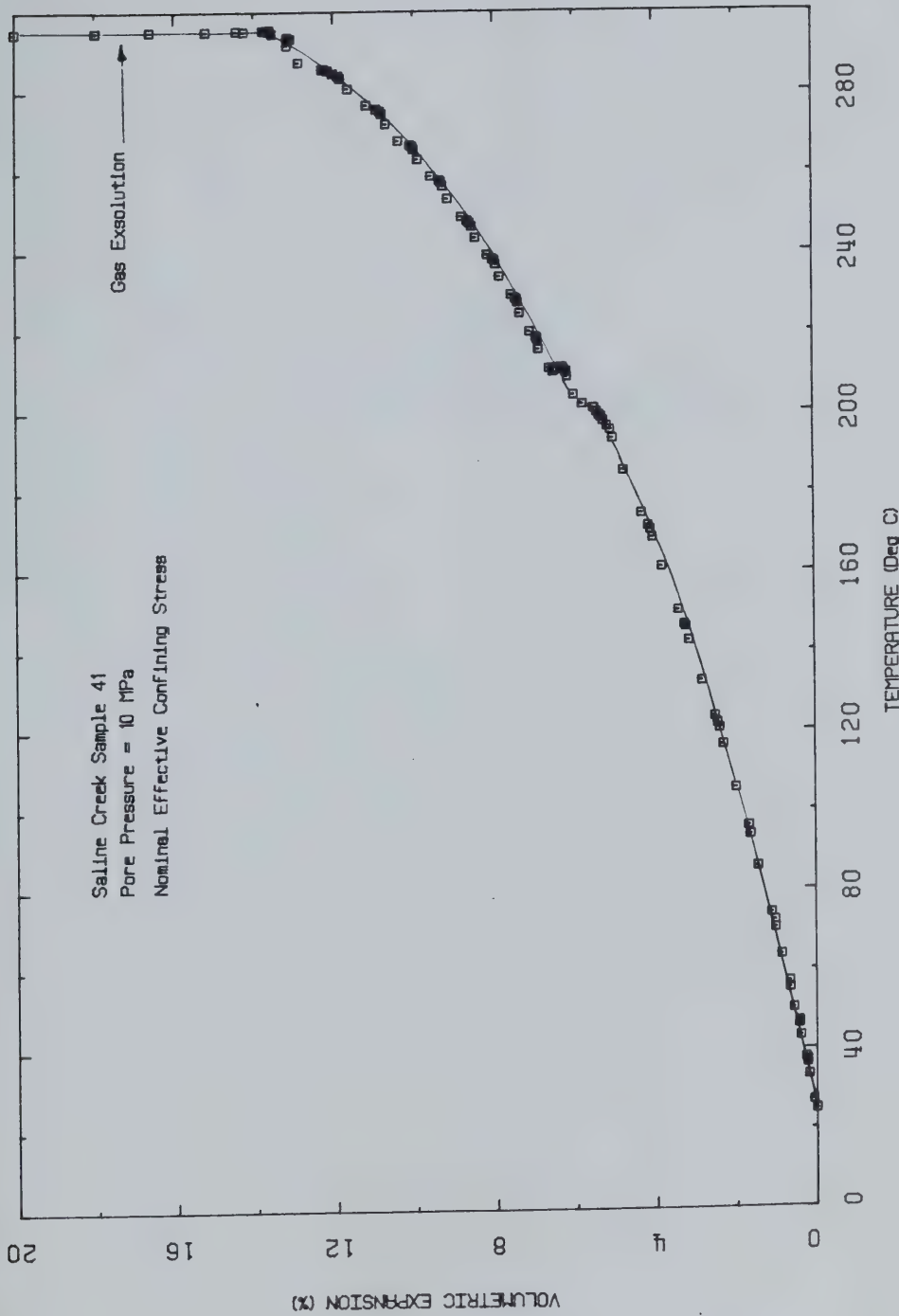


FIGURE B47 Undrained Volumetric Thermal Expansion:  
Test C059



APPENDIX C  
ONE DIMENSIONAL COMPRESSION TESTS



TABLE C-1  
DRAINED ONE DIMENSIONAL COMPRESSION TESTS

Test	Temperature (°C)	Sample No.	Initial Bulk Density (Mg/m <sup>3</sup> )	Initial Porosity	Range of Vertical Effective Stress (MPa)
CPERM 5	20	31A	2.04	0.37	0.5 - 5.0
CPERM 7	22	44	2.06	0.35	2.0 - 18.0
COS 9	22	41	2.07	0.35	2.0 - 18.0
CPERM 4	22	36	2.03	0.37	0.5 - 4.0
CPERM 4	100	36	2.03	0.36	4.0 - 26.0
CPERM 7	150	44	2.06	0.34	2.0 - 18.0
CPERM 5	200	31A	2.05	0.35	4.0 - 19.5
CPERM 6	250	31B	2.04	0.35	4.0 - 19.0
COS 9	300	41	2.00	0.34	4.0 - 18.0



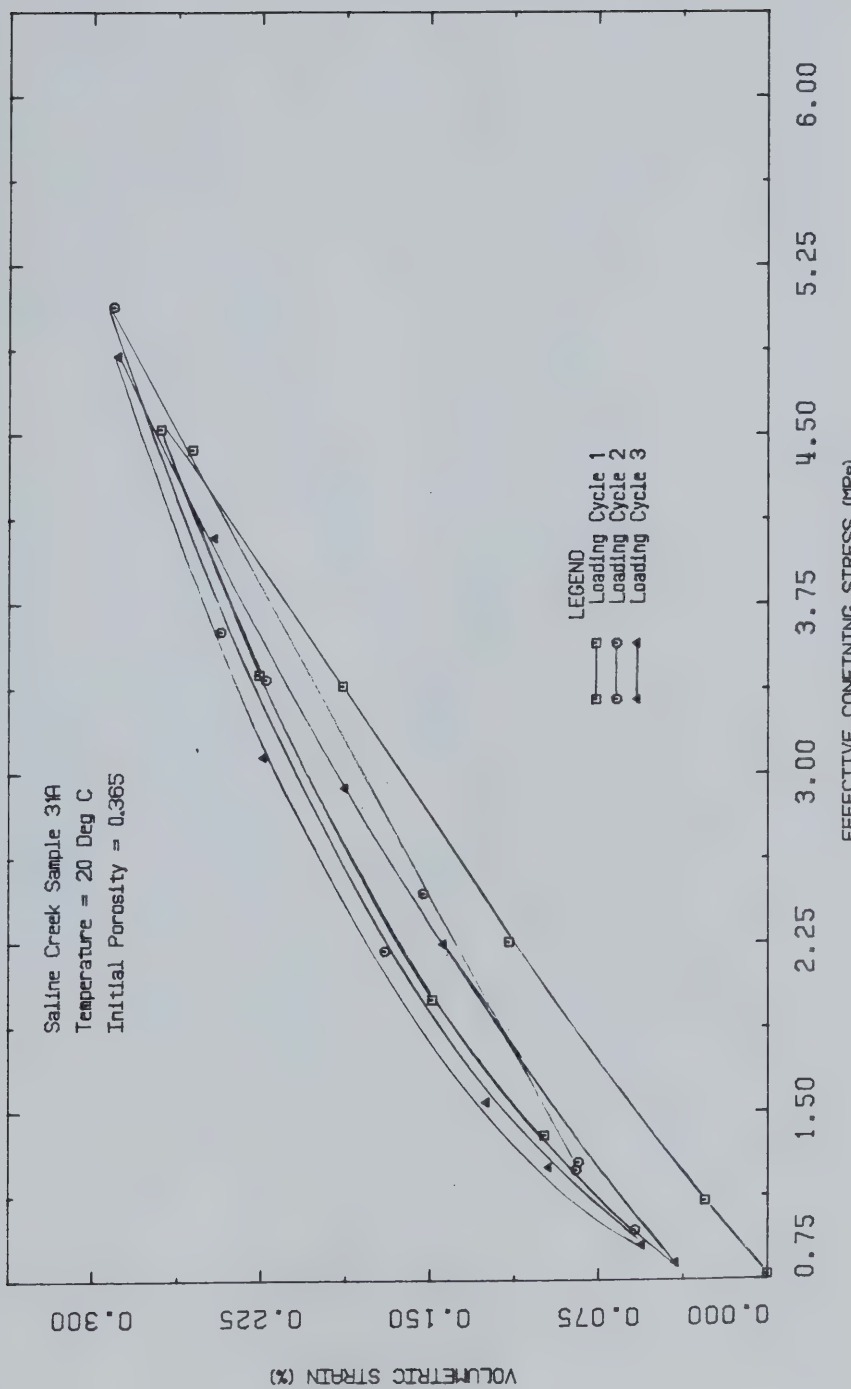


FIGURE C1 One Dimensional Compression at 20°C:  
Test CPERM5



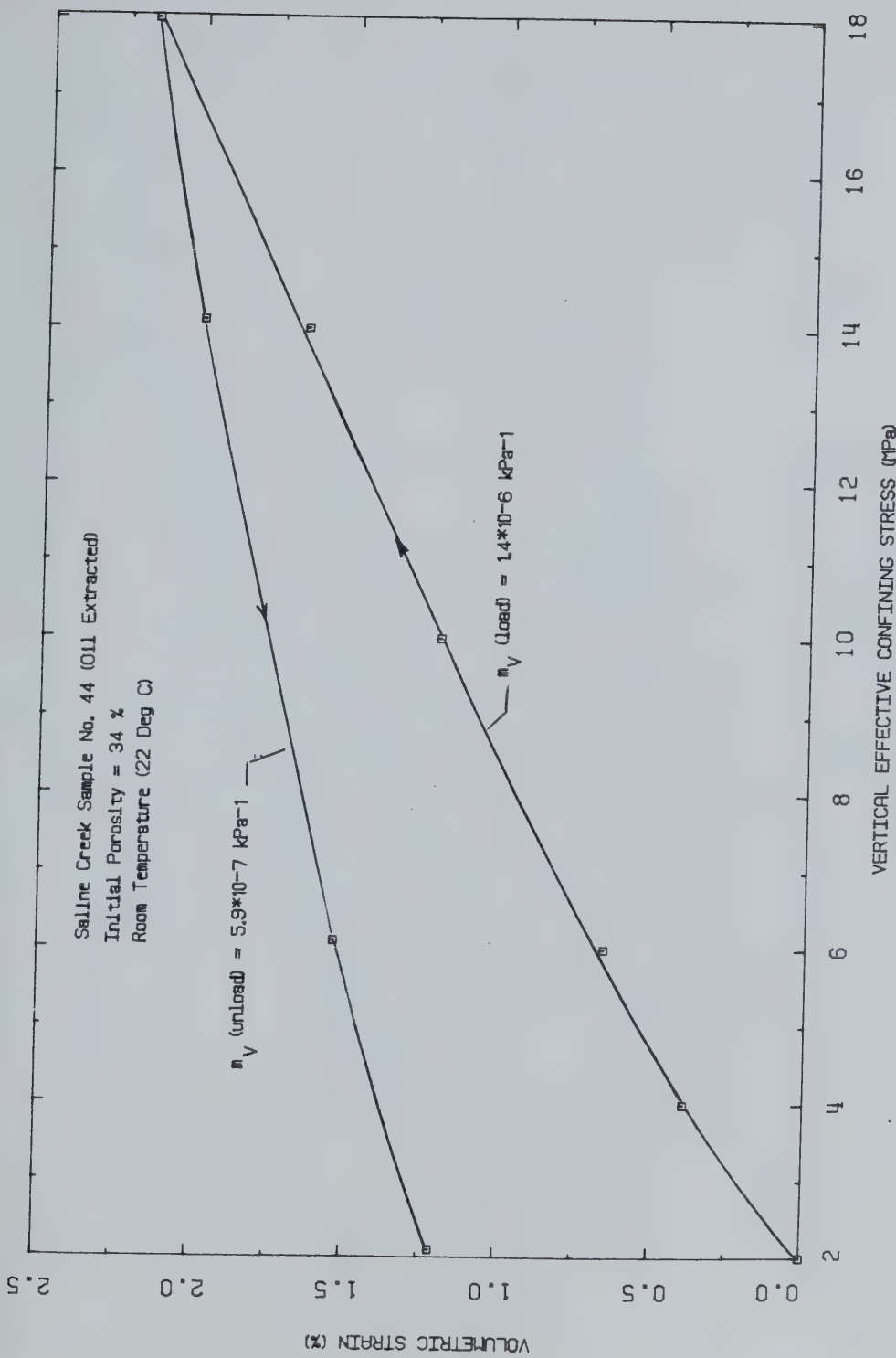


FIGURE C2 One Dimensional Compression at 22°C:  
Test CPERM7



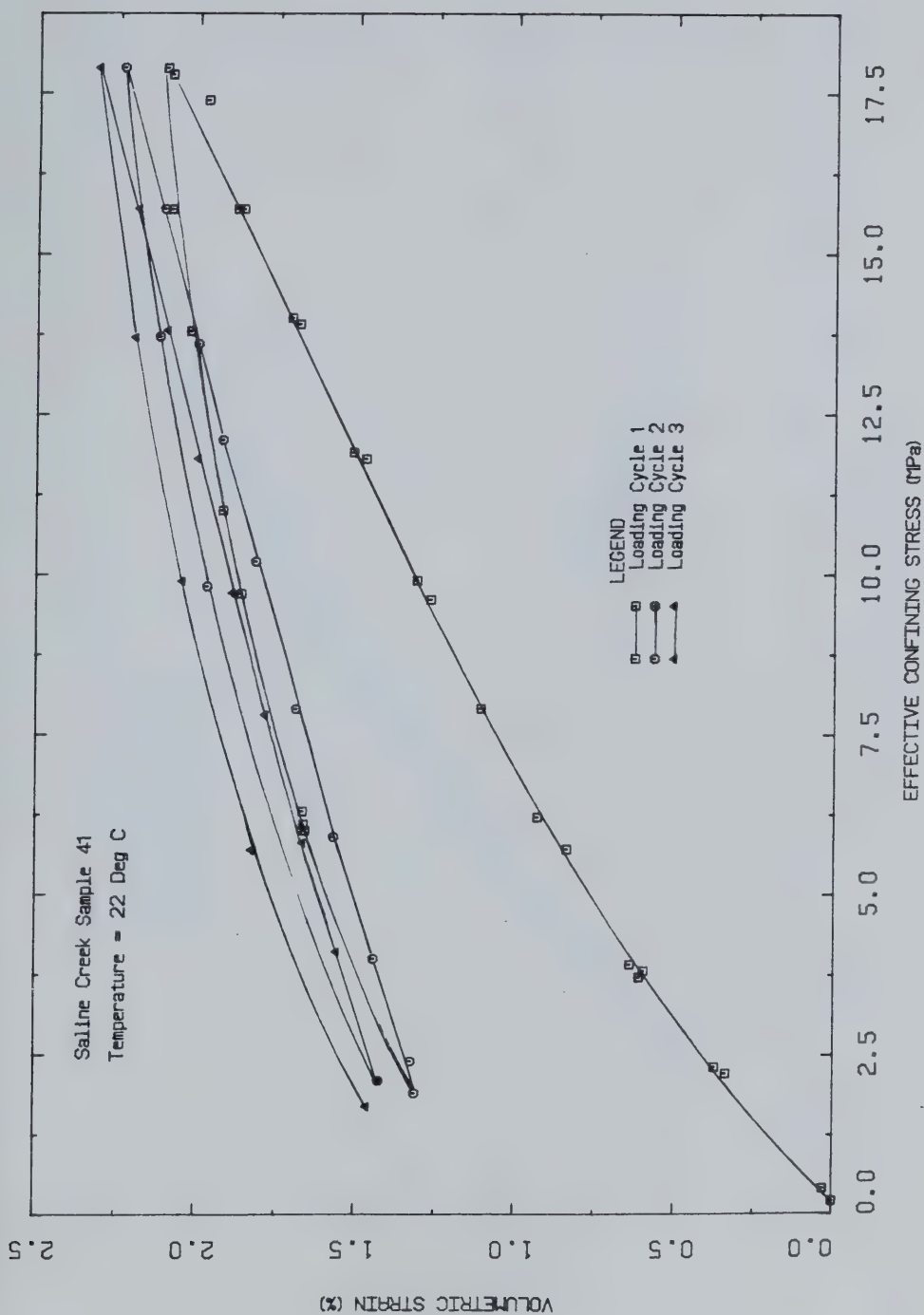


FIGURE C3 One Dimensional Compression at 22°C:  
Test C059



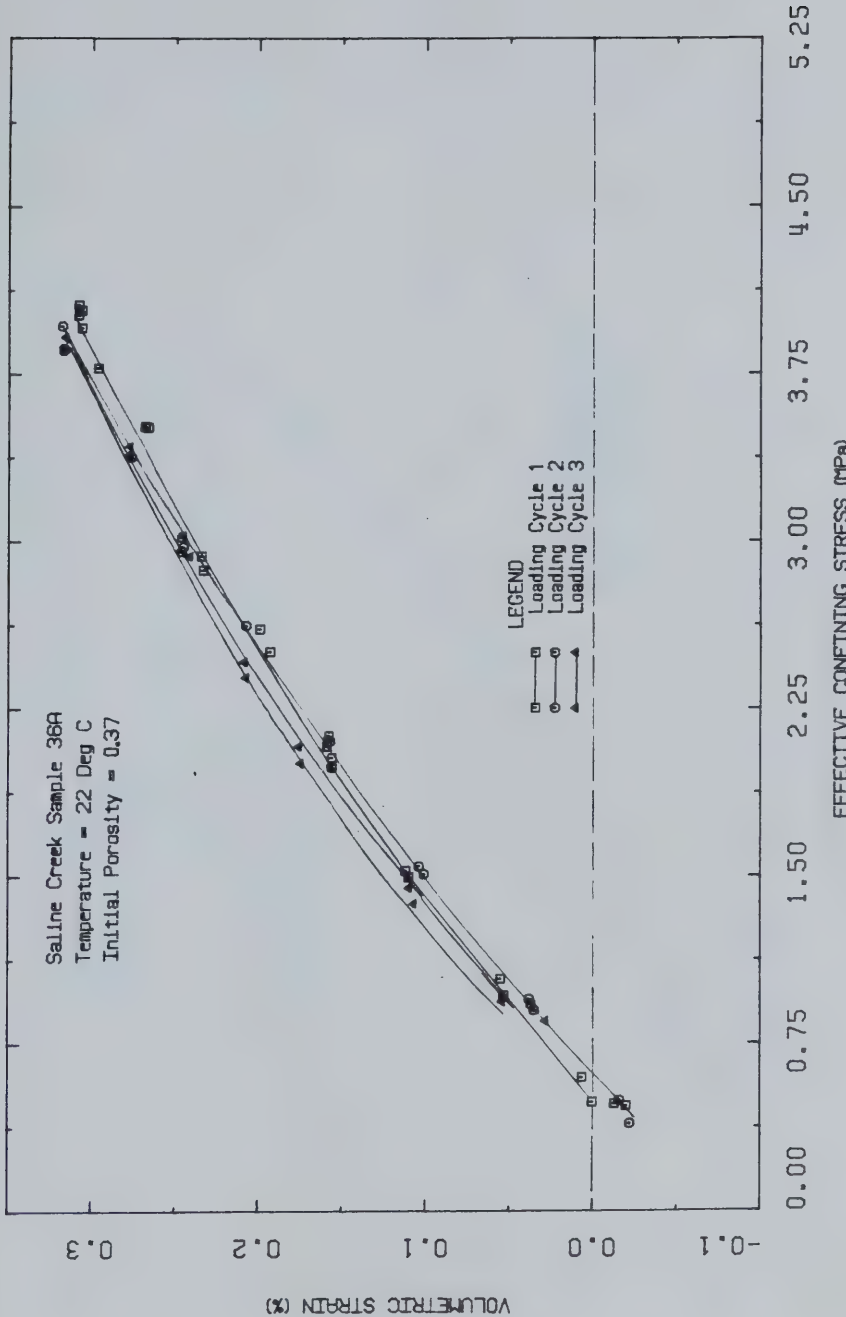


FIGURE C4 One Dimensional Compression at 22°C:  
Test CPERMA



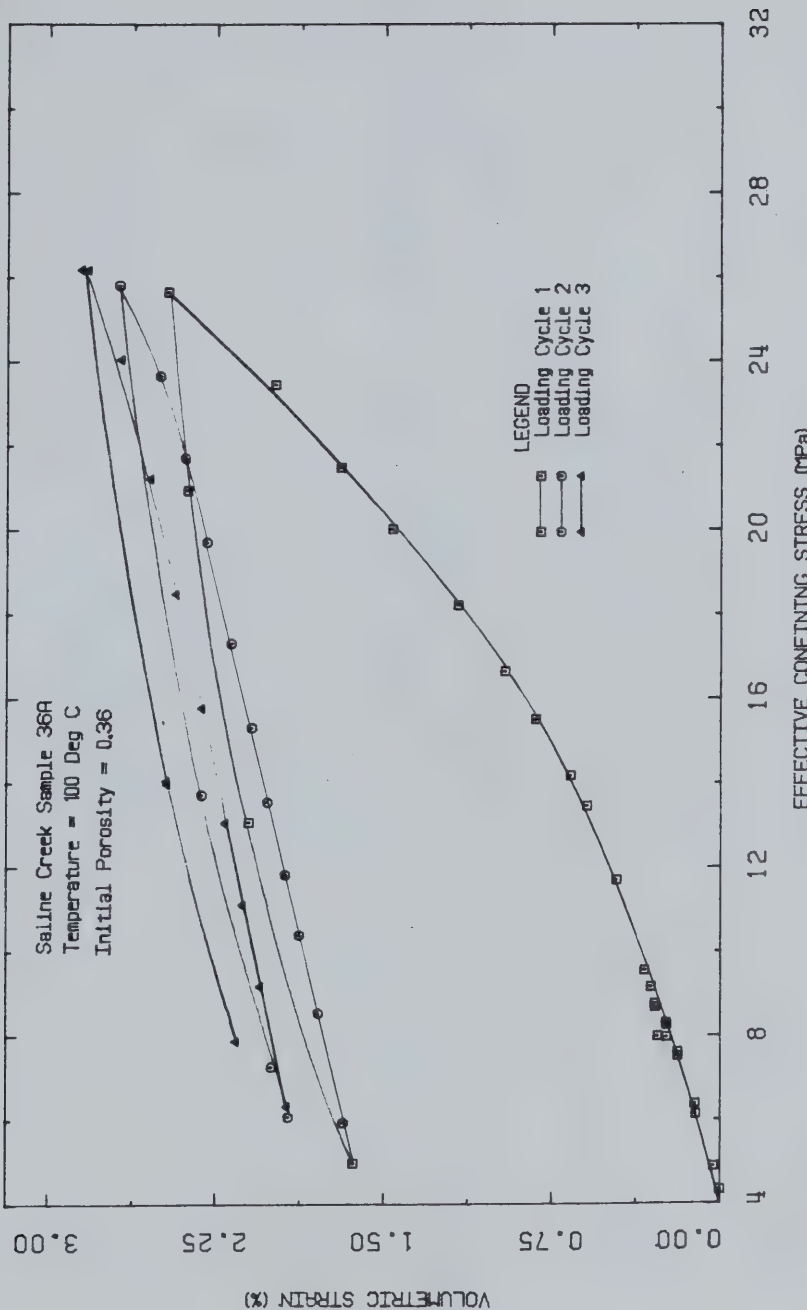


FIGURE C5. One Dimensional Compression at 100°C:  
Test CPERM4



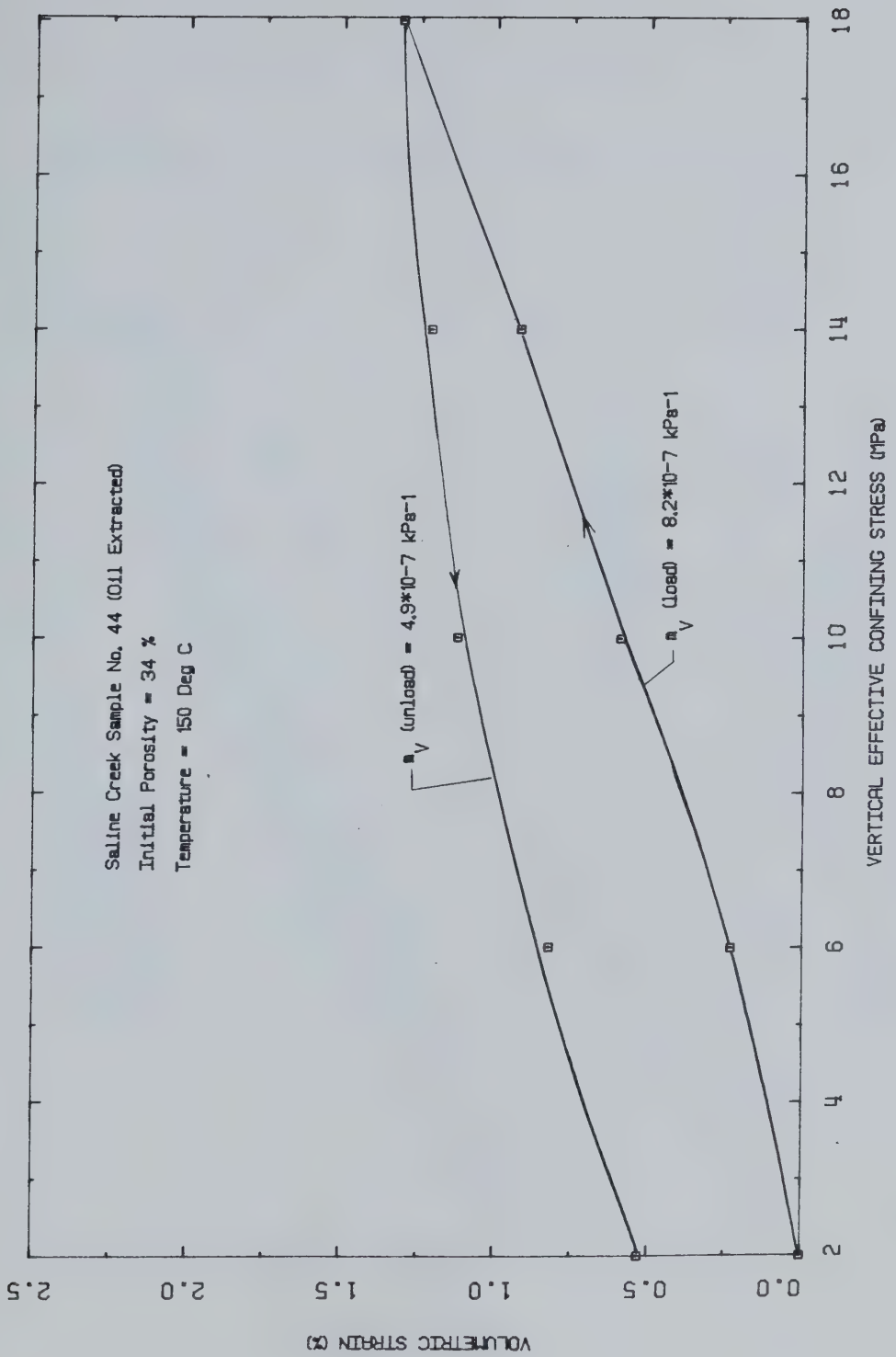


FIGURE C6 One Dimensional Compression at 150°C:  
Test C6 PERM7



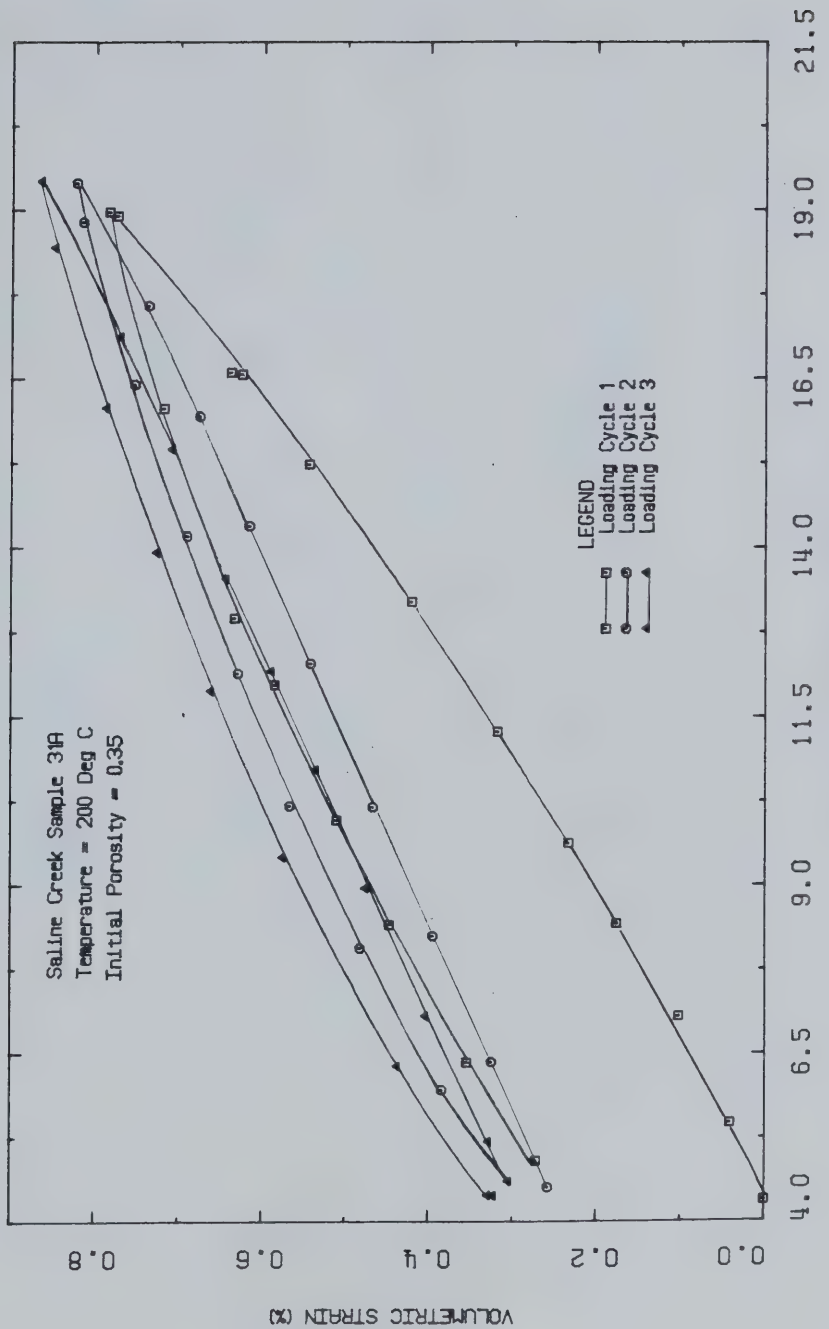


FIGURE C7 One Dimensional Compression at 200°C:  
Test CPERM5



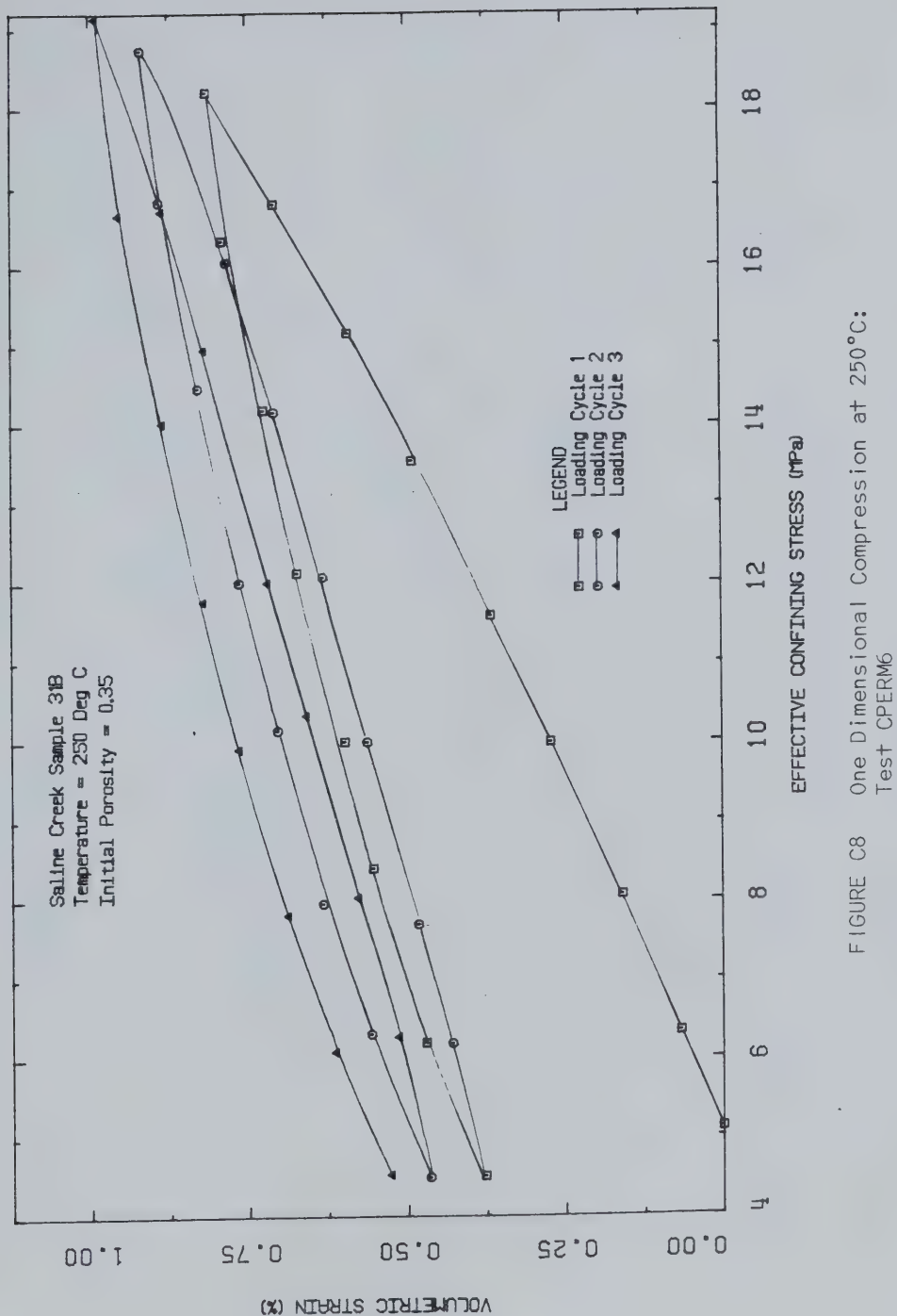


FIGURE C8 One Dimensional Compression at 250°C:  
Test CPERM6



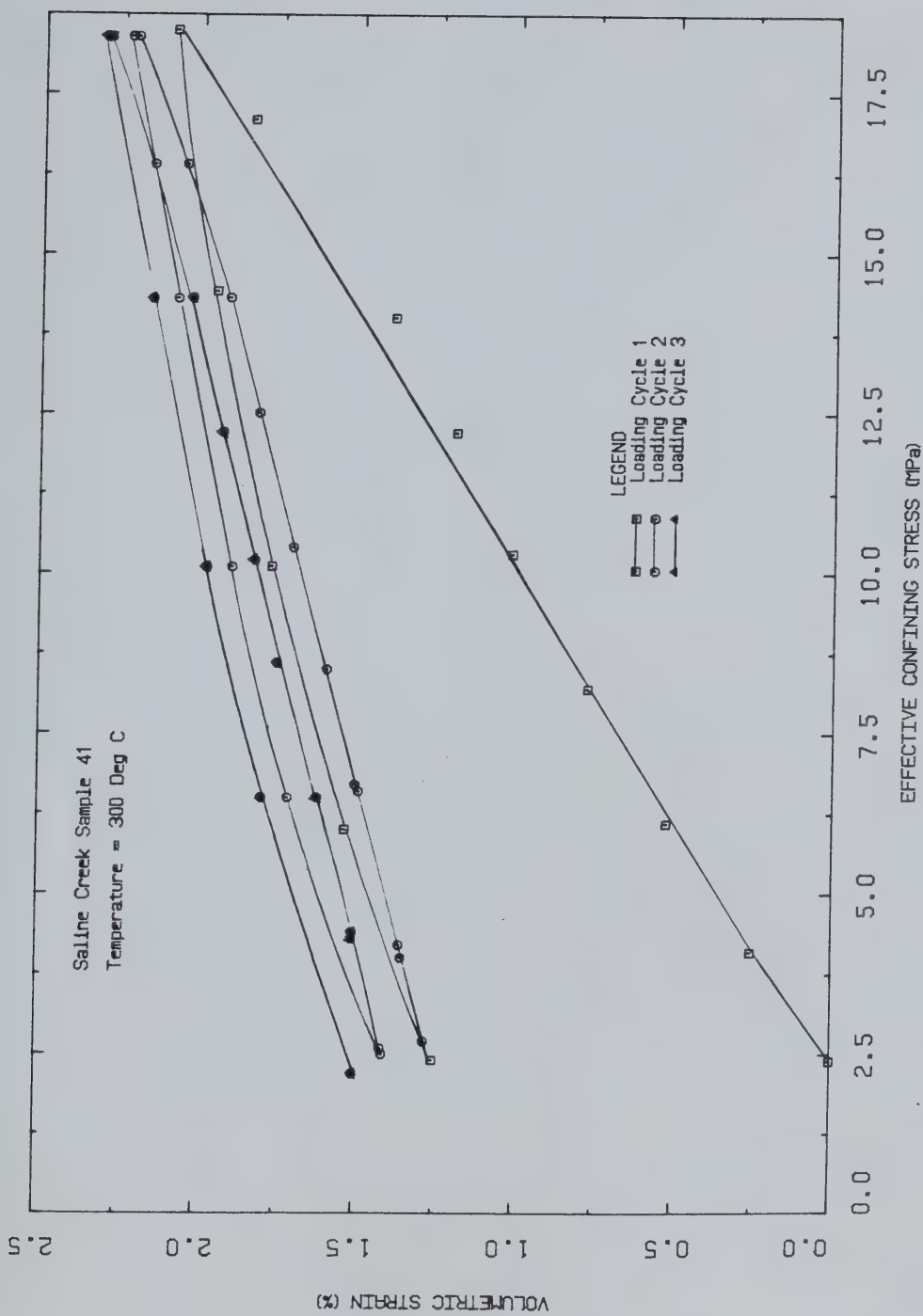


FIGURE C9

One Dimensional Compression at 300°C:  
Test C059



APPENDIX D  
PERMEABILITY TESTS



TABLE D-1  
SUMMARY OF PERMEABILITY TESTS

Test	Sample No.	Temperature Range (°C)	Effective Confining Stress (MPa)	Test Description
CPERM 1	10C	20	4 :	Inaccurate Differential Pressure Measurement.
CPERM 2	10D	50	2 - 4	Inaccurate Differential Pressure Measurement.
CPERM 3	M1	20	2 - 4	Absolute Permeability of remoulded oil free McMurray Formation Sand.
CPERM 4	36A	20 - 100	2 - 4	Permeability of undisturbed Saline Creek oil sand at room temperature and 100°C.
CPERM 5	31A	20 - 200	2 - 4	Permeability of undisturbed Saline Creek oil sand at room temperature and 200°C.
CPERM 6	31B	20 - 250	2 - 4	Permeability of undisturbed Saline Creek oil sand at room temperature and 250°C.
CPERM 7	44	20 - 150	2 - 18	Absolute permeability of undisturbed oil free Saline Creek oil sand at 20°C and 150°C over a range of effective confining stresses from 2 - 18 MPa.
CPERM 8	16	20 - 150	3	Permeability of undisturbed Saline Creek oil sand at 20°C and 150°C.
CPERM 9	36B	20 - 150	3	Permeability of remoulded Saline Creek oil sand at room temperature and 150°C.



## TEST CPERM 1

Room Temperature Permeability Test on Saline Creek  
Sample No. 10C Under 4 MPa Effective Confining Stress

TEST CPERM 1: SAMPLE DATASample No. 10C

$$H = 4.877 \text{ cm}$$

$$\text{Dia.} = 7.620 \text{ cm}$$

$$\text{c/s Area} = 45.604 \text{ cm}^2$$

$$V = 222.41 \text{ ml} \quad \text{DENSITY:} = 2.046 \text{ Mg/m}^3$$

$$\text{Mass} = 455.0 \text{ g}$$

$$W = 2.5 \% \text{ of } M_S \quad M_S = 374.8 \text{ g}$$

$$B = 18.9\% \text{ of } M_S \quad V_S = 141.45 \text{ ml}$$

$$V_V = 80.96 \text{ ml}$$

Initial Porosity

$$n = 0.364$$

$$S_W = 11.6\%$$

$$S_B = 87.5\%$$

$$S_G = 0.9\%$$

Note: Differential pressure across the sample could not be measured with sufficient accuracy to determine permeability using twin 34 MPa pressure transducers as illustrated in Figure D2.



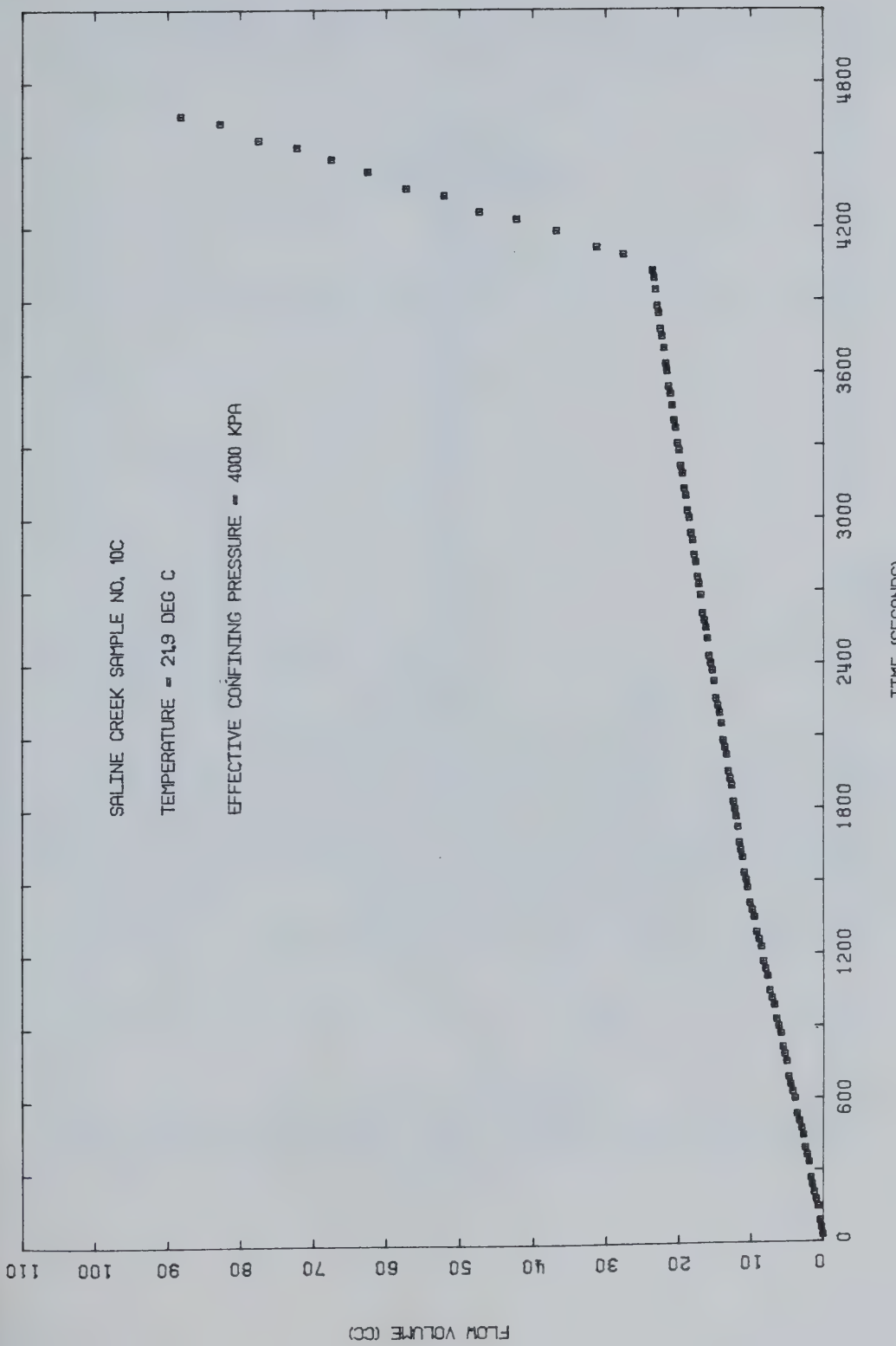


FIGURE D1 Flow Rate: Test CPERM1 (20 °C)



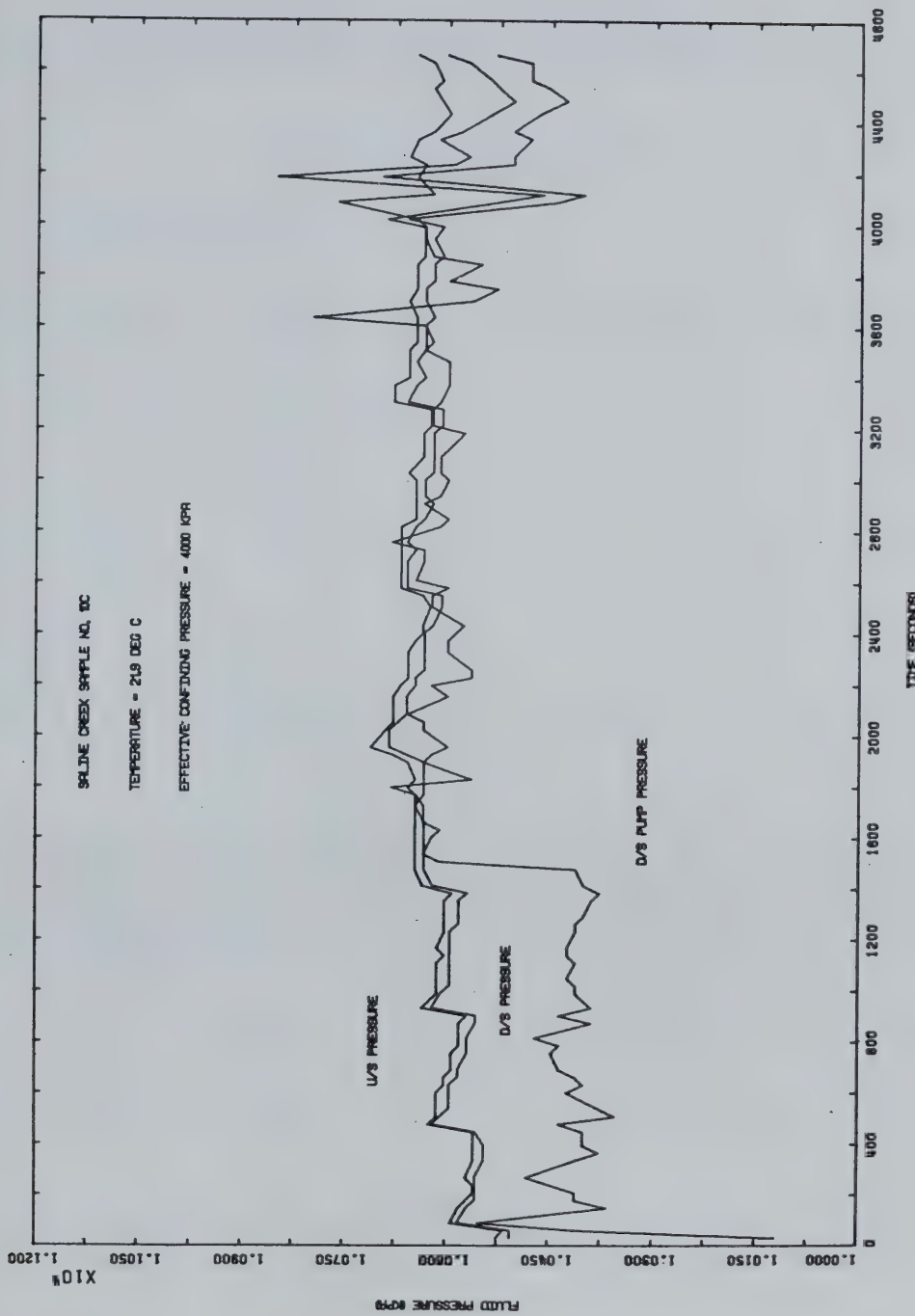


FIGURE D2 Pressure Variation With Time: Test CPERM1



## TEST CPERM 2

Permeability Test on Saline Creek Sample No. 10 C  
at 48°C and 4MPa Effective Confining Stress

TEST CPERM 2: SAMPLE DATAPretest Sample No. 10C

H = 4.877 cm  
Dia. = 7.620 cm  
c/s Area = 45.604 cm<sup>2</sup>  
V = 222.41 ml  
Mass = 455.25 g  
Density = 2.047 Mg/m<sup>3</sup>

w = 2.7 % of M<sub>S</sub>  
B = 18.9% of M<sub>S</sub>  
M " = 374.8 g  
V = 141.45 ml  
V = 80.96 ml

Initial Porosity

n = 0.364  
S<sub>W</sub> = 12.5%  
S<sub>B</sub> = 87.5%

Note: Differential pressure across the sample could not be measured with sufficient accuracy to determine permeability using twin 34 MPa pressure transducers as illustrated in Figure D4.



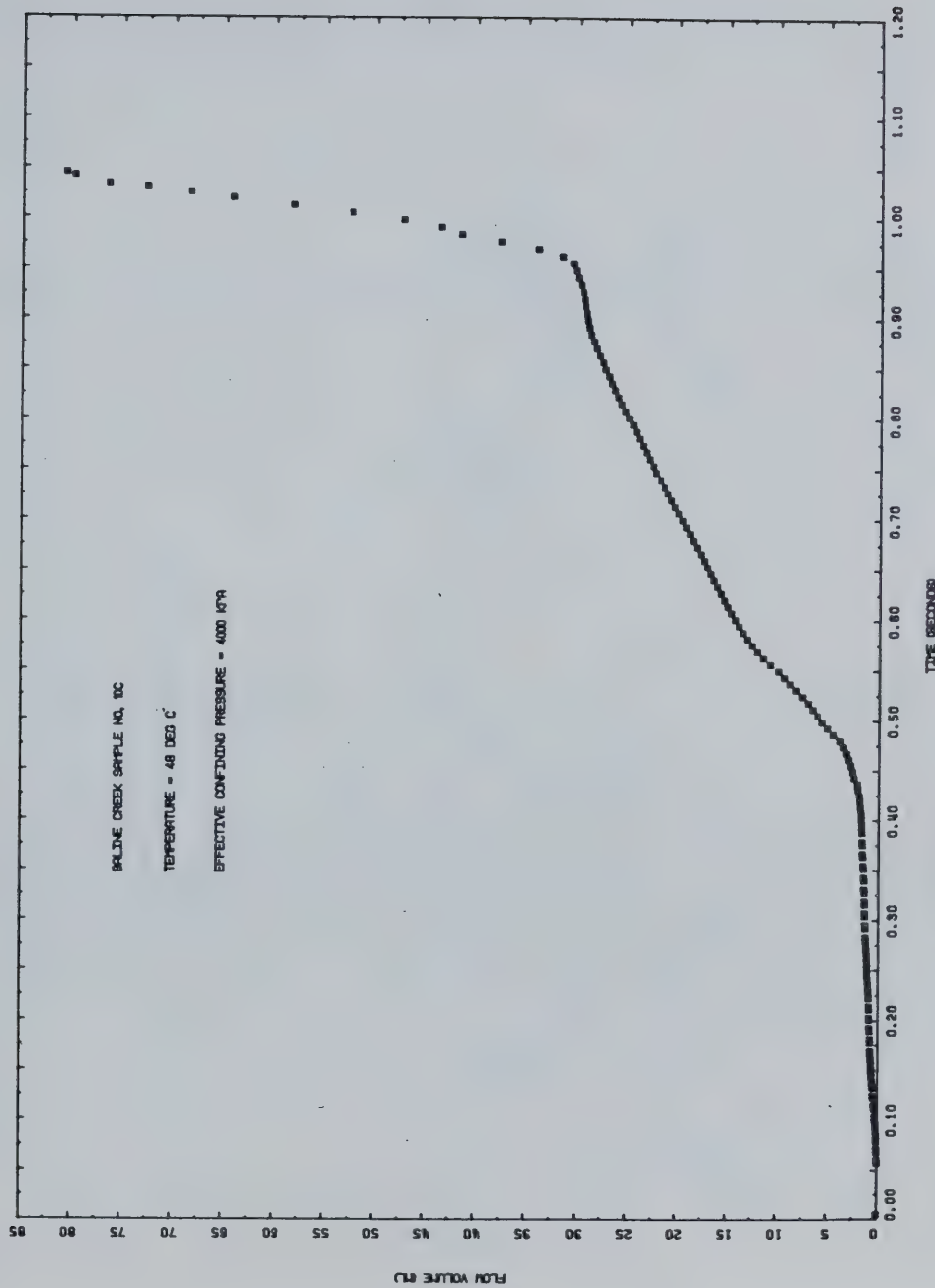


FIGURE D3 Flow Rate: Test CPERM2 (48°C)



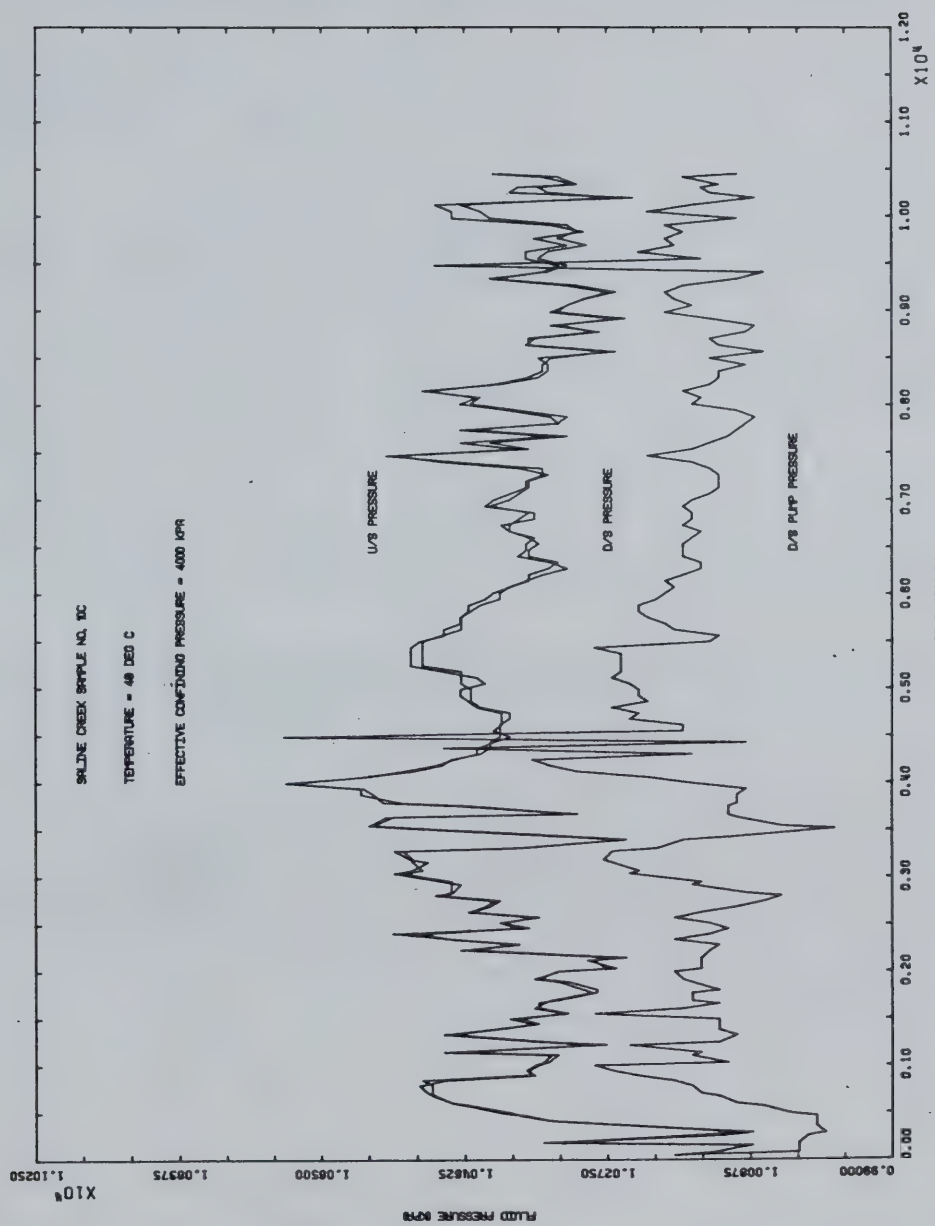


FIGURE D4 Pressure Variation With Time: Test CPERM2



TEST CPERM 3

Room Temperature Permeability of Remoulded Oil Free McMurray Sand Sample M1 at 2, 3 and 4 MPa Effective Confining Stresses

Procedural Details: Test CPERM 3

1. A sample of oil free McMurray Formation sand obtained from an outcrop along the High Hill River 40 km east of Fort McMurray in a remoulded state was compacted in 5 layers in the consolidometer cell.
2. The system and sample were back saturated under 2 MPa pore pressure for 24 hours and at .6 MPa confining stress.
3. Flow rate (i.e. volume change with time) and pressure drop across the sample were monitored simultaneously at room temperature and under effective confining stresses of 2, 3 and 4 MPa.
4. Pressure difference was measured at flow rates ranging up to 10 ml/minute at each effective confining stress level.



TEST CPERM 3: SAMPLE DATA

Remoulded "Oil-Free" McMurray Formation Sand Sample

Sample: Diameter:  $\emptyset = 7.610$  cmHeight:  $H = 5.920$  cmArea:  $A = 45.480$  cm<sup>2</sup>Volume:  $V = 269.24$  cm<sup>3</sup>Dry Mass:  $M = 448.8$  gDry Density:  $= \frac{448.8}{269.24} 1.670$  Mg/m<sup>3</sup>Void Ratio:  $= 0.587$ Porosity:  $= 0.370$ Water Saturated Bulk Density:  $= 2.040$  Mg/m<sup>3</sup>



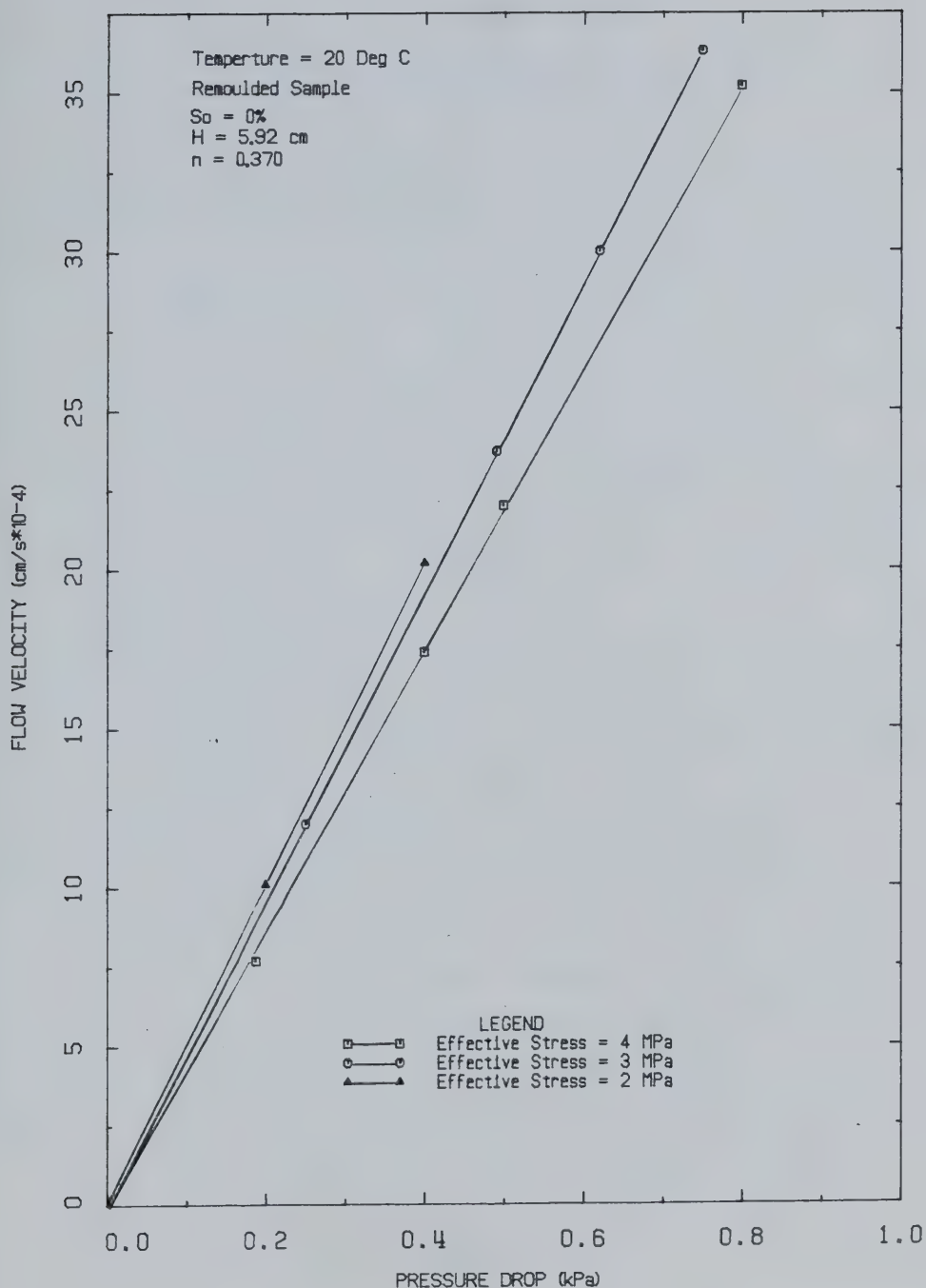


FIGURE D5 Flow Velocity Vs. Pressure Difference:  
Test CPERM3



## TEST CPERM 4

Permeability Tests on Saline Creek Oil Sand  
Sample No. 36A at 22°C and 100°C

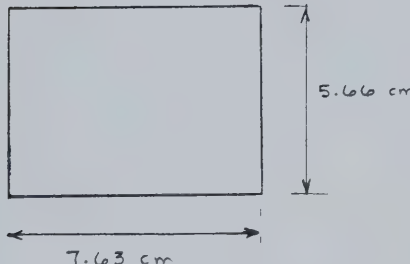
Procedural Details: Test CPERM 4

1. Sample 36A was mounted in the consolidometer under frozen conditions.
2. The sample was thawed and back saturated for 24 hours under 2 MPa back pressure and 6 MPa confining stress.
3. Compressibility of the sample was measured at room temperature (22°C) over a range of effective stress from 0.5 - 4.0 MPa. The compressibility test included three cycles of loading and unloading.
4. A room temperature permeability test was performed by circulating water through the sample at flow rates varying up to about 4 ml/minute. Effective confining stress was maintained constant at 3 MPa.
5. Back pressure and confining stress were increased simultaneously in increments to 10 MPa and 13 MPa respectively.
6. The system and sample were heated slowly up to 100°C. Drained thermal expansion and the volume of fluid expelled from the sample during heating were measured.
7. A permeability test was conducted at 100°C in which 100°C water was circulated through the sample. Bitumen was flushed from the sample reducing the bitumen saturation from 81 percent to 73 percent.



8. Compressibility was measured at 100°C for a range of effective confining stresses from 4 - 26 MPa. The test included 3 cycles of loading and unloading.
9. The sample was cooled down to room temperature and a room temperature permeability test was performed at the residual oil saturation of 73% and for flow rates varying up to about 5 ml/minute.



TEST CPERM 4: SAMPLE DATAOriginal Sample No. 36A at 22°C

$$\text{Total Mass} = 526.1 \text{ g}$$

$$\text{Total Volume} = 258.54 \text{ cm}^3$$

$$\text{Mass Sand} = \frac{526.1}{1+w+B} = 436.24$$

$$w = 2.8\%$$

$$B = 17.8\%$$

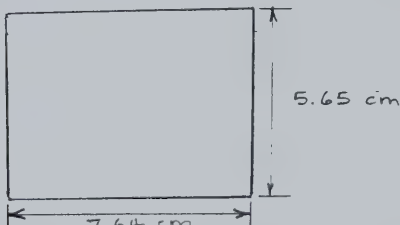
$$\text{Mass Bitumen} = 77.65 \text{ g}$$

$$\text{Volume Sand} = \frac{436.24}{2.65} = 164.62 \text{ cc}$$

$$\text{Volume Voids} = V_T - V_S = 93.92 \text{ cc} = 36\%$$

$$V_B = \frac{77.65}{1.027} = 75.61 \text{ cc} \quad S_B = 80.5\%$$

$$V_W = 18.31 \text{ cc} \quad S_W = 19.5\%$$

Sample No. 36A After 100°C Permeability Test

$$\begin{aligned} V_T &= 259.00 \\ V_S &= 165.00 \\ V_V &= 94.0 \text{ cc} \\ \text{Mass Bitumen} &= 67.2 \text{ g} \\ &= 15.4\% \end{aligned}$$

DISTRIBUTION OF WATER AND BITUMEN:

Top	$V_B = 62.8$	$S_B = 66.8\%$
	$V_W = 31.2$	$S_W = 33.2\%$
Middle	$V_B = 68.5$	$S_B = 72.9\%$
	$V_W = 25.5$	$S_W = 27.1\%$
Bottom	$V_B = 70.2$	$S_B = 74.7\%$
	$V_W = 23.8$	$S_W = 25.3\%$

AVERAGE SATURATIONS:

$$\begin{aligned} V_B &= 67.0 \text{ cc} \\ S_B &= 71.3\% \\ V_W &= 27.0 \text{ cc} \\ S_B &= 28.7\% \end{aligned}$$



SALINE CREEK SAMPLE NO.36

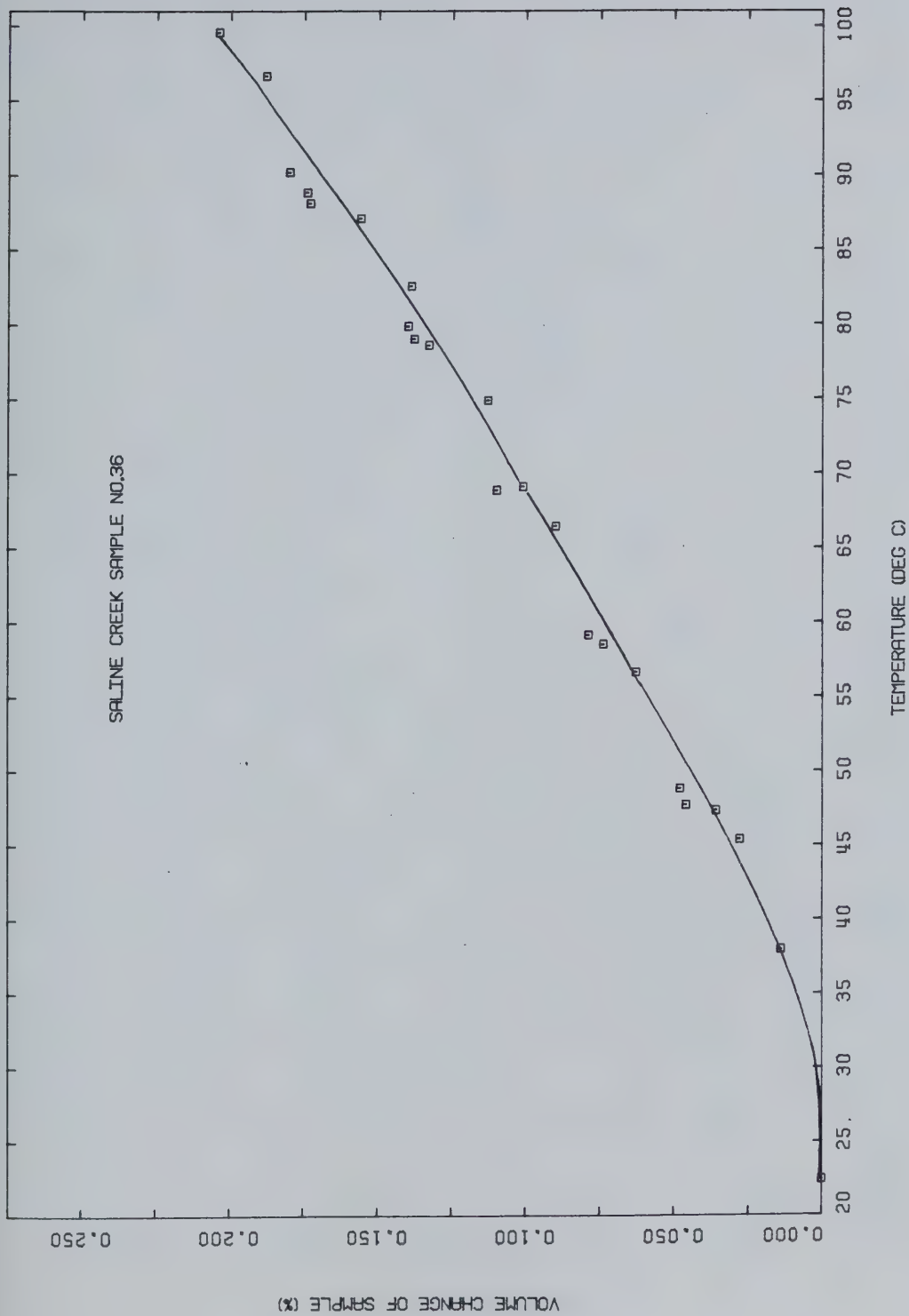


FIGURE D6 Drained Thermal Expansion: Test OPERM4



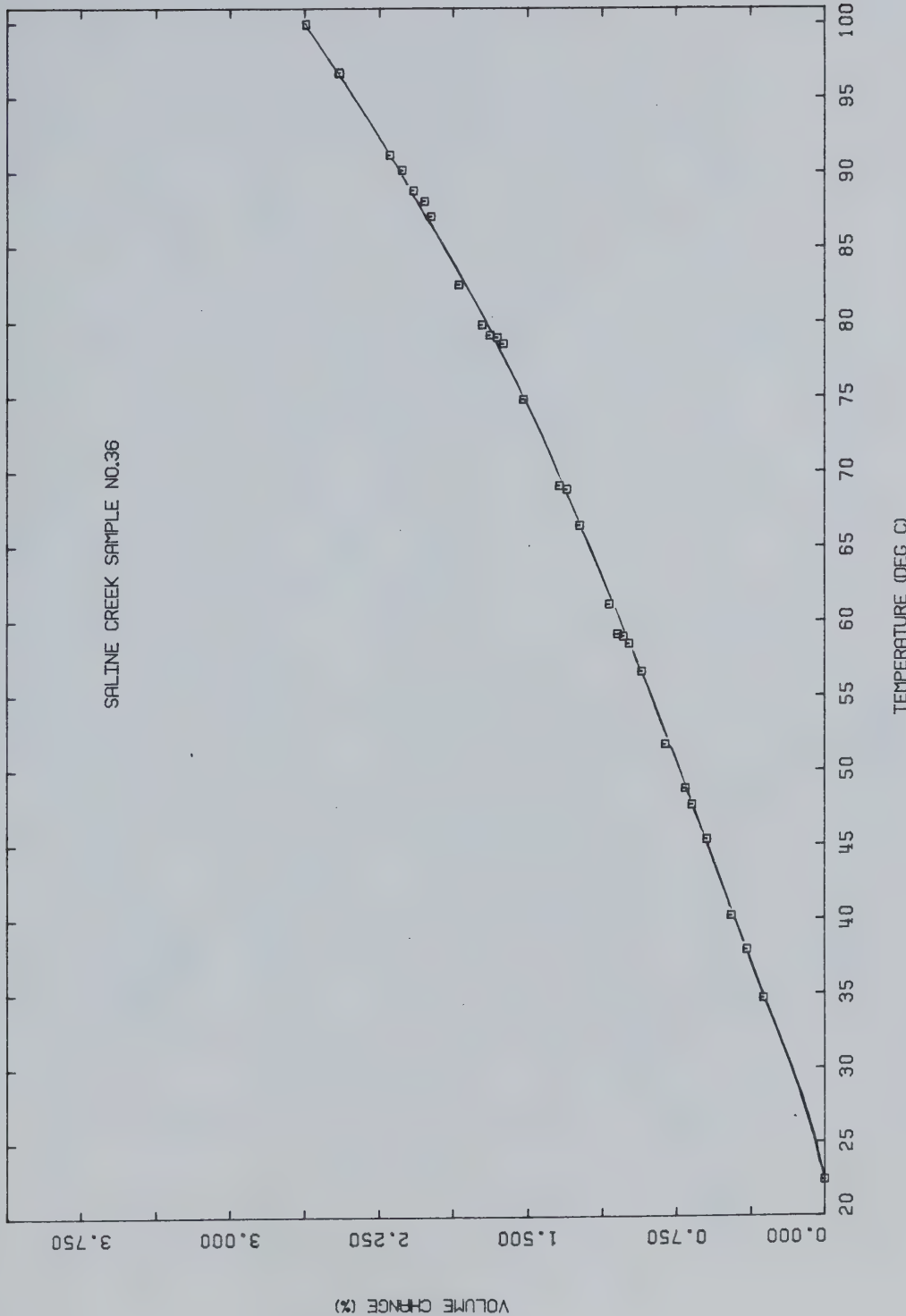


FIGURE D7 Undrained Thermal Expansion: Test CPERM4



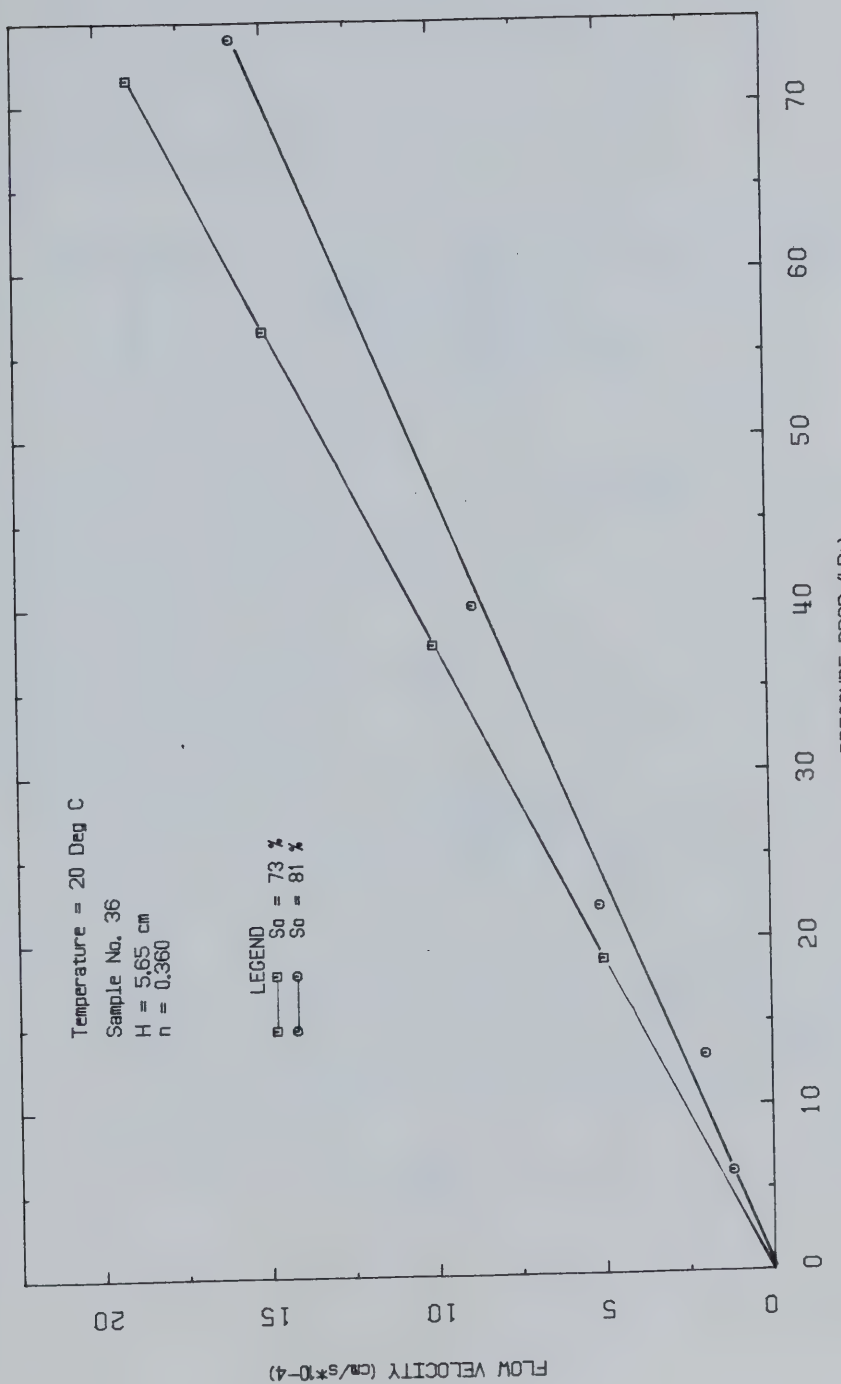


FIGURE D8 Flow Velocity Vs. Pressure Difference:  
Test CPERM4



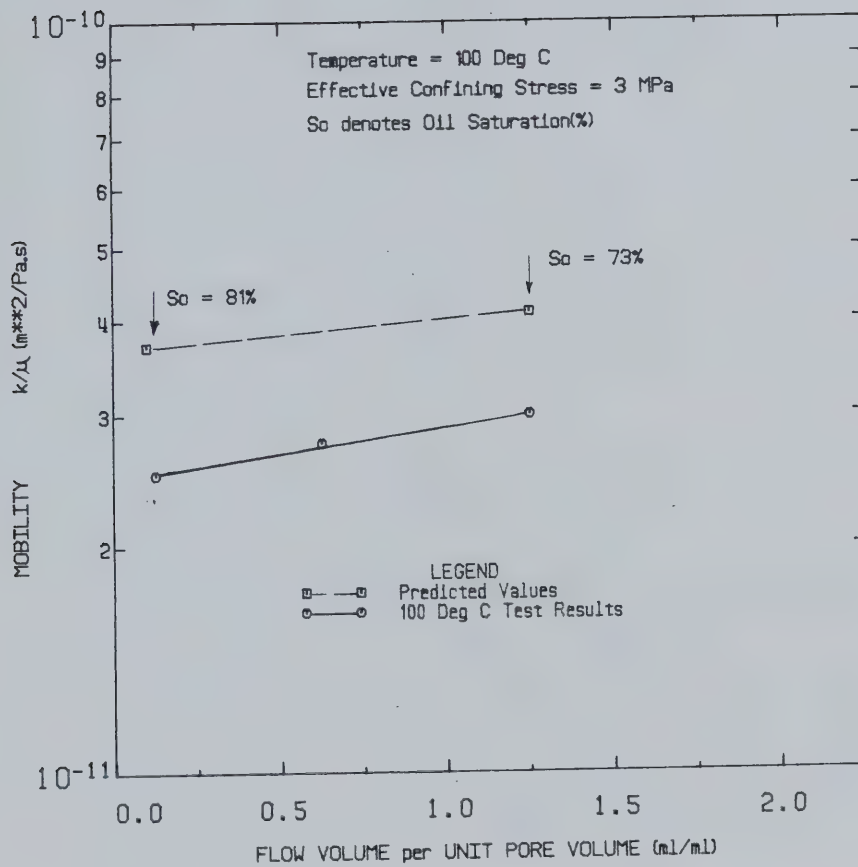


FIGURE D9 Fluid Mobility Vs. Normalized Flow Volume:  
Test CPERM4



## TEST CPERM 5

Permeability Tests on Saline Creek Sample No. 31A  
at 20°C and 200°CProcedural Details: Test CPERM 5

1. Saline Creek Sample No. 31A was thawed and back saturated for 24 hours under 2 MPa back pressure and 6 MPa confining stress.
2. Cyclic room temperature compressibility was measured over a range of effective stress from 0.5 - 5.0 MPa.
3. Room temperature permeability was measured by circulating water through the sample at flow rates varying up to 2.5 ml/minute. Effective confining stress was maintained constant at 3 MPa.
4. The back pressure and confining pressure were increased simultaneously in increments to 10 MPa and 14 MPa, respectively.
5. The apparatus and sample were heated to 200°C. Drained thermal expansion of the sample was monitored.
6. A permeability test was performed at 20°C by circulating heated water and measuring pressure drop across the sample. Bitumen was flushed from the sample reducing the bitumen saturation from 86% to 51%. Effective confining stress was maintained at 3 MPa.



7. Cyclic compressibility was measured at 200°C over the effective stress range 4 - 19.5 MPa.
8. Room temperature permeability as measured at the residual bitumen saturation of 51% for flow rates up to about 7.5 ml/minute.

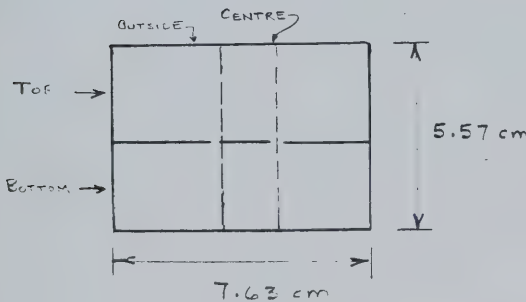


TEST CPERM 5: SAMPLE DATAOriginal Sample No. 31A at 22°C:

Dia.:  $\varnothing = 7.633 \text{ cm}$   
 Area:  $A = 45.756 \text{ cm}^2$   
 Height:  $H = 5.570 \text{ cm}$   
 Volume:  $V = 254.86 \text{ cm}^3$   
 Mass:  $M = 521.3 \text{ g}$

$$\begin{aligned}
 w &= 3\% & B &= 18.75\% & W_S &= \frac{521.3}{1+w+B} = 428.17 \text{ g} \\
 &= 12.85 \text{ g} & &= 80.28 \text{ g} \\
 V_S &= \frac{W_S}{2.65} = 61.57 \text{ cm}^3 & & & & \\
 V_V &= 254.86 - V_S = 93.29 \text{ cm}^3 & & & & = 36\%
 \end{aligned}$$

Initial Fluid Saturations:  $S_W = 13.8\%$   $S_O = 86.2\%$

After Permeability Test at 200°CDistribution of Pore Fluids:

Top Centre:	$w = 9.8\%$
	$B = 9.1\%$
	$S_O = 48.4\%$
	$S_W = 51.6\%$
Bottom Centre:	$w = 9.3\%$
	$B = 10.6\%$
	$S_O = 53.4\%$
	$S_W = 46.6\%$
Top Outside:	$w = 9.9\%$
	$B = 10.1\%$
	$S_O = 50.6\%$
	$S_W = 49.4\%$
Bottom Outside:	$w = 9.3\%$
	$B = 10.6\%$
	$S_O = 53.3\%$
	$S_W = 46.7\%$

Final Fluid Saturations:

Average Top Half:	$S_O = 49.5\%$	$S_W = 50.5\%$
Average Bottom Half:	$S_O = 53.4\%$	$S_W = 46.6\%$
Average For Sample:	$S_O = 51.4\%$	$S_W = 48.6\%$



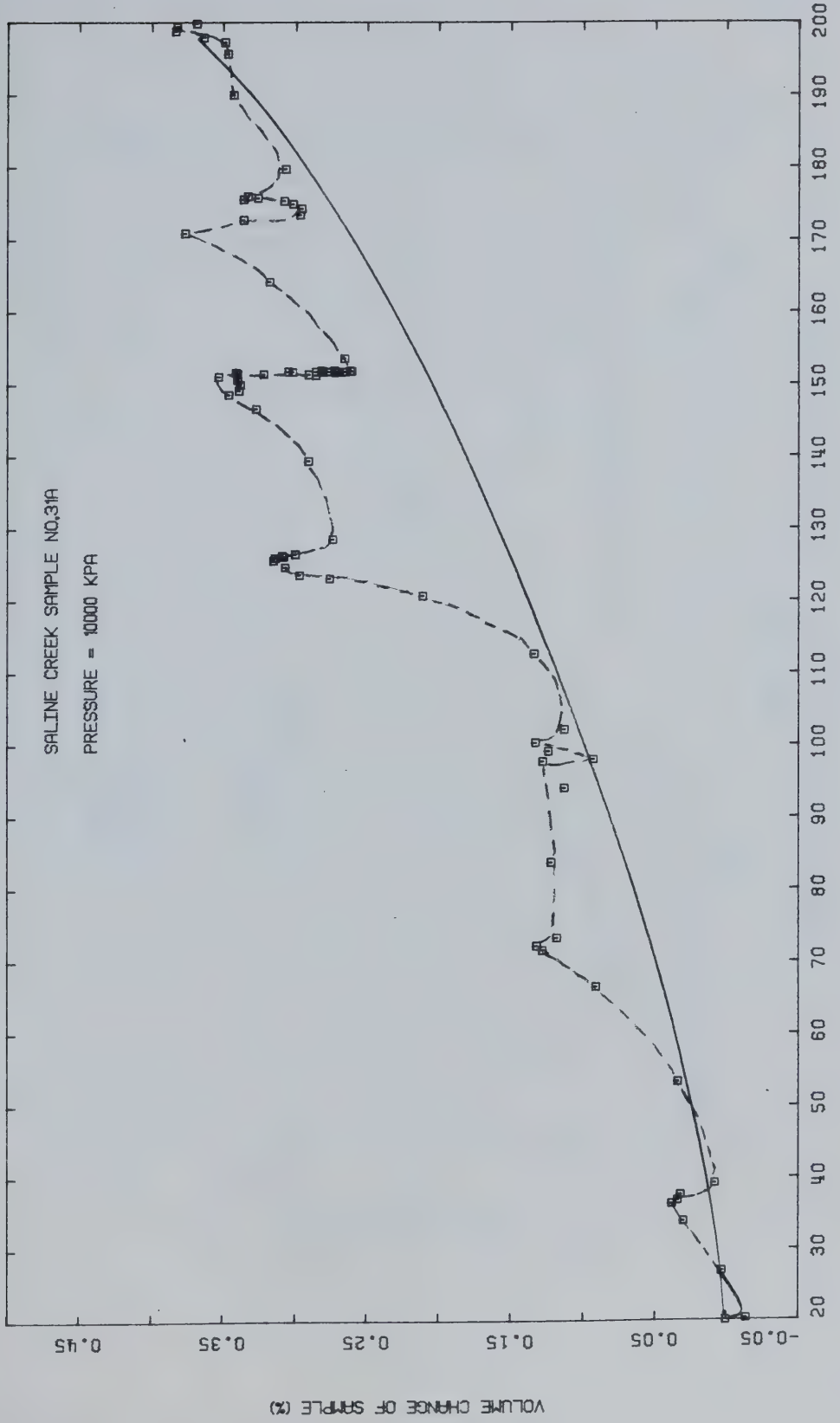
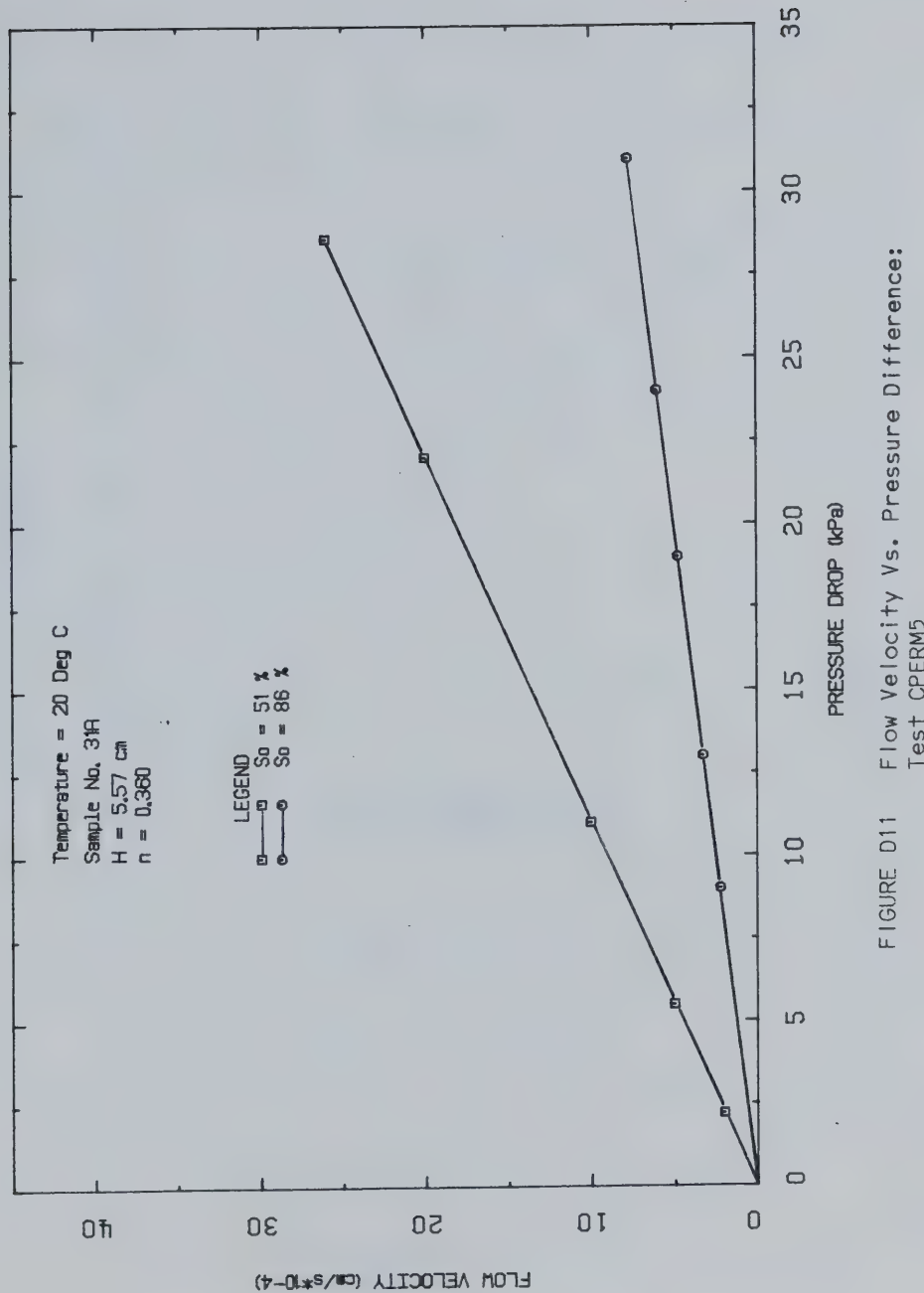


FIGURE D10 Drained Thermal Expansion: Test CPERM5







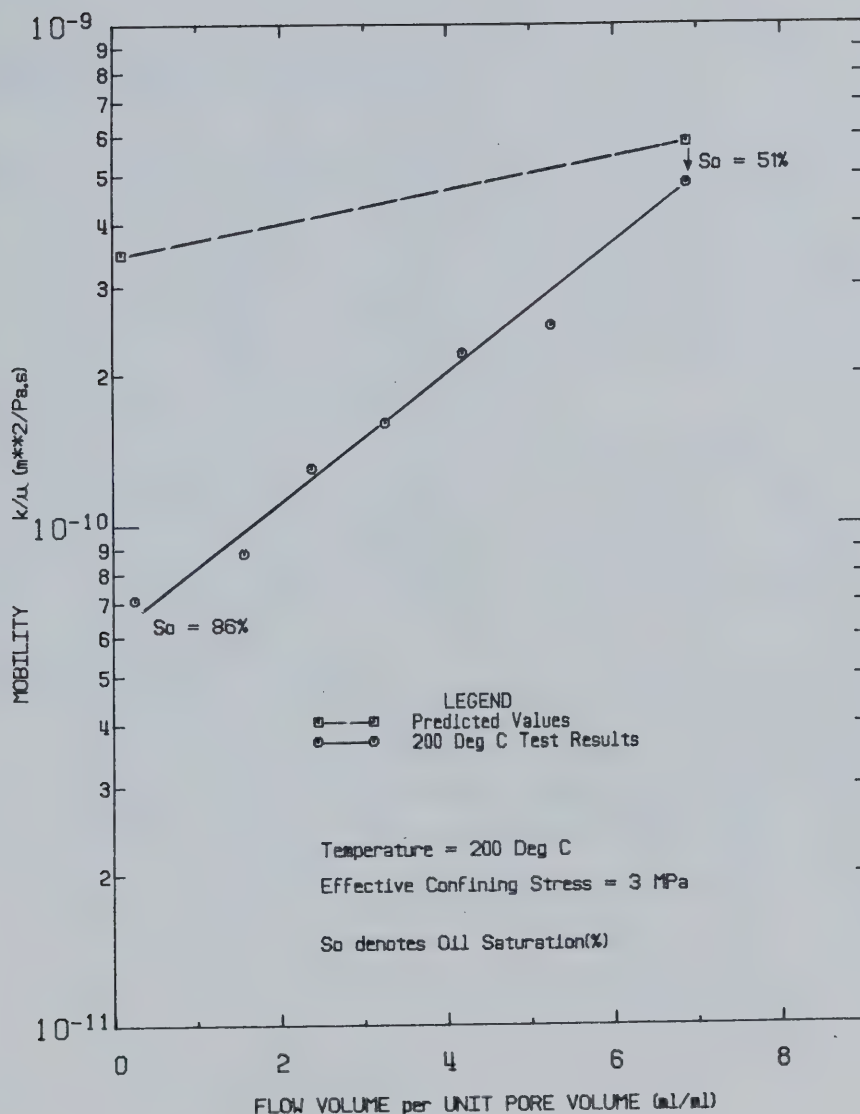


FIGURE D12 Fluid Mobility Vs. Normalized Flow Volume:  
Test CPERM5



## TEST CPERM 6

Permeability of Saline Creek Oil Sand Sample No. 31B  
at Room Temperature and 250°CProcedural Details: Test CPERM 6

1. Sample No. 31B was thawed and back saturated for 24 hours under 2 MPa back pressure and 6 MPa confining stress.
2. Room temperature permeability was measured by circulating water through the sample and measuring pressure difference at flow rates up to about 4 ml/minute. Effective confining stress was maintained at 3 MPa.
3. Back pressure and confining stress were increased simultaneously in increments up to 10 MPa and 13 MPa.
4. The apparatus and sample were heated to 250°C. Drained thermal expansion of the sample was monitored during heating.
5. A permeability test was performed at 250°C by circulating heated water and monitoring pressure drop across the sample. Bitumen was flushed from the sample pore space reducing the bitumen saturation from 81% to 38%.
6. Cyclic compressibility was measured at 250°C over a range of effective stresses from 4 - 19 MPa.
7. The sample was cooled down to room temperature and a permeability test performed at the residual bitumen saturation of 38 percent.



TEST CPERM 6: SAMPLE DATAOriginal Sample No. 31B at 20°C:

Dia.:  $\varnothing = 7.633 \text{ cm}$   
 Area:  $A = 45.756 \text{ cm}^2$   
 Height:  $H = 5.540 \text{ cm}$   
 Volume:  $V = 253.488 \text{ cm}^3$   
 Mass:  $M = 515.40 \text{ g}$

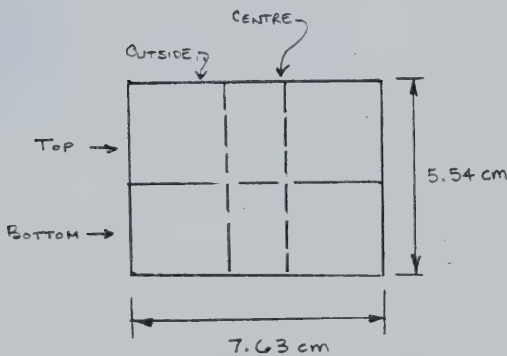
$$w = 4\% \quad B = 16.1$$

$$W_S = \frac{515.4}{1+W+B} = 429.14 \text{ g}$$

$$V_S = \frac{W_S}{2.65} = 161.94 \text{ ml}$$

$$V_V = V - V_S = 91.55 \text{ ml}$$

$$S_W = 19\% \quad S_O = 81\%$$

After 250°C Permeability TestDistribution of Pore Fluids:

Top Centre:	$w = 12.72\%$
	$B = 5.27\%$
	$S_O = 29.3\%$
	$S_W = 70.7\%$
Bottom Centre:	$w = 12.86\%$
	$B = 7.64\%$
	$S_O = 37.3\%$
	$S_W = 62.7\%$
Top Outside:	$w = 11.65\%$
	$B = 6.24\%$
	$S_O = 34.9\%$
	$S_W = 65.1\%$
Bottom Outside:	$w = 10.74\%$
	$B = 7.93\%$
	$S_O = 42.5\%$
	$S_W = 57.5\%$

Final Fluid Saturations:

Average for Sample  
 after 250°C test:      Wet Mass = 450.87      Dry Mass = 380.18  
 $w = 44.0 \text{ ml}$        $B = 26.69 \text{ ml}$   
 $= 11.57\%$        $= 7.02\%$   
 $S_W = 62.2\%$        $S_O = 37.8\%$



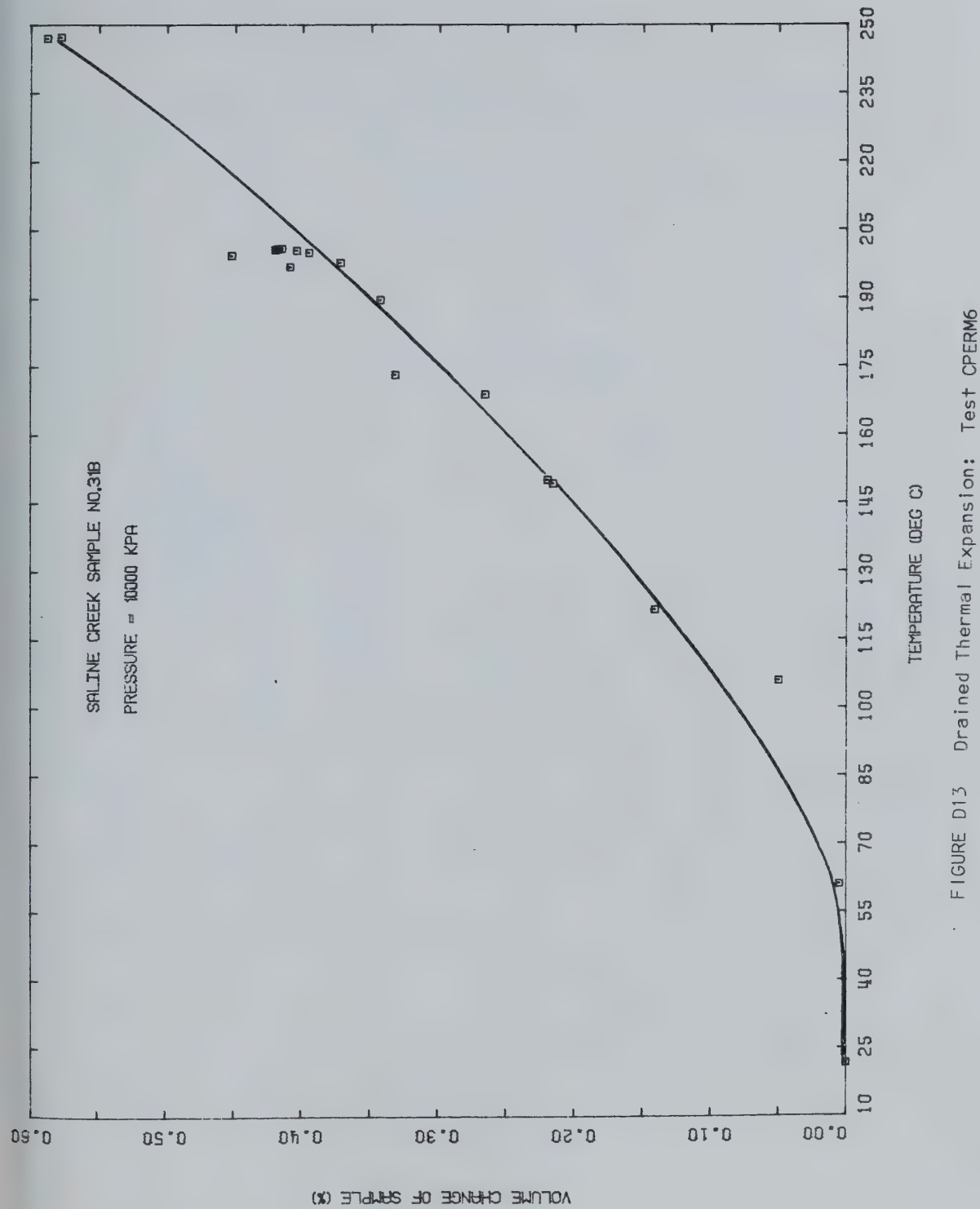


FIGURE D13 Drained Thermal Expansion: Test CPERM6



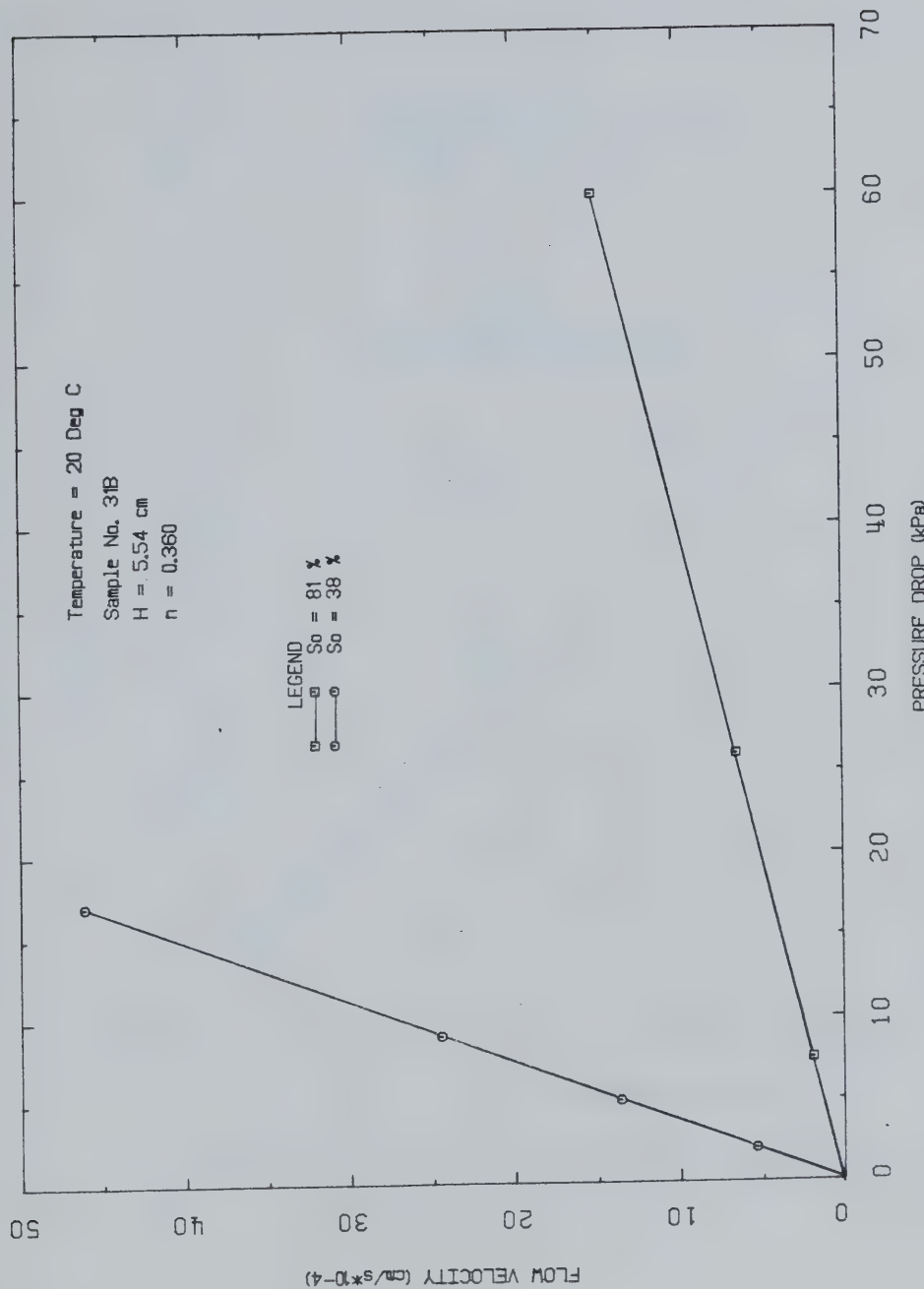


FIGURE D14 Flow Velocity Vs. Pressure Difference:  
Test CPERM6



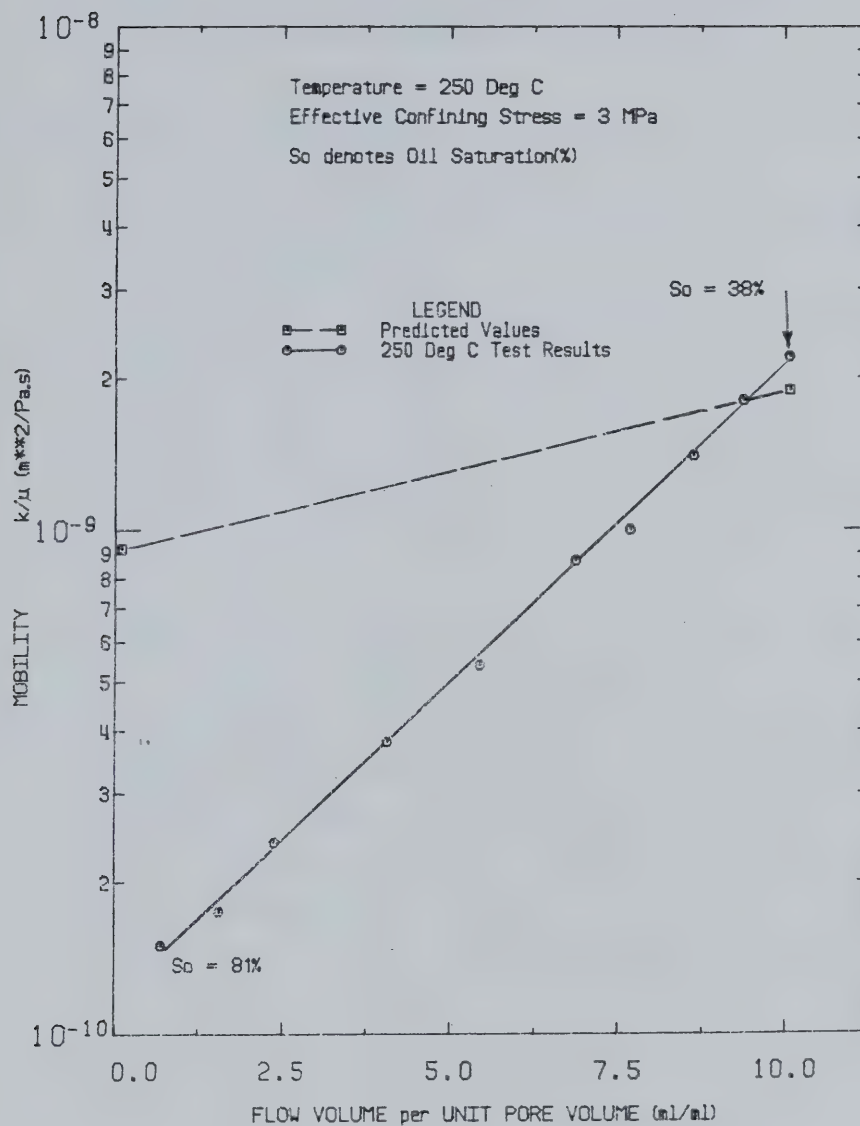


FIGURE D15 Fluid Mobility Vs. Normalized Flow Volume:  
Test CPERM6



## TEST CPERM 7

Absolute Permeability of Saline Creek Oil Sand  
Sample No. 44 (at 20°C and 150°C) and over a Range  
of Effective Stress from 2 to 18 MPa

Procedural Details: Test CPERM 7

1. Sample No. 44 was mounted and allowed to thaw under 2 MPa effective confining stress.
2. Bitumen was extracted from the pore space of the sample by alternate soaking and flushing; 3600 ml of benzene was circulated through the sample over a 10 day period to completely remove all the bitumen. Residual benzene was removed by flushing with 200 ml of acetone and finally with 500 ml of water.
3. The sample was back saturated for 24 hours under 10 MPa back pressure and 12 MPa confining stress.
4. Absolute permeability was measured at room temperature by circulating water through the sample at flow rates up to 10 ml/minute and measuring the pressure drop across the sample. Absolute permeability was measured at effective confining stresses of 2, 3, 4, 6, 10, 14 and 18 MPa. Compressibility of the sample was also measured as the effective stress was varied.
5. The system and sample were heated slowly to 150°C. Drained thermal expansion and the volume of pore fluid expelled from the sample were monitored during heating.



6. Absolute permeability was measured at 150°C by circulating heated water at flow rates up to 9 ml/minute and measuring pressure drop across the sample. Permeability was measured at effective confining stresses of 2, 6, 10, 14, 18, 14, 10 and 2 MPa. Compressibility of the sample was also measured as the effective confining stress was varied.



TEST CPERM 7: SAMPLE DATAOriginal Sample No. 44 at 20°C:

Height: H = 5.120 cm  
 Dia.: Ø = 7.600 cm  
 Area: A = 45.36 cm<sup>2</sup>  
 Volume: V = 232.27 cm<sup>3</sup>  
 Mass: M = 470 g

$$M_S = 390.4 \text{ g} \quad V_S = 147.3 \text{ ml}$$

Initial Water Content: w = 3.0%  
 Initial Bitumen Content: B = 17.1%

Initial Bulk Density: = 2.024  
 Initial Dry Density: = 1.681  
 Initial Void Ratio: = 0.577  
 Initial Porosity: = 0.366

Bitumen extraction by alternate "Soak and Flush" Process; 3600 ml of benzene (i.e. 45 pore volume circulated over a period of 10 days).

After 150°C Permeability Test:

Height: H = 5.012 cm  
 Dia.: Ø = 7.600  
 Volume: V = 227.5 ml  
 Mass: M = 470.6      Density = 2.069

$$w = 22.5\% \quad B = 0.00\%$$

Porosity: n = 0.353  
 Void Ratio: e = 0.544  
 So: = 0%



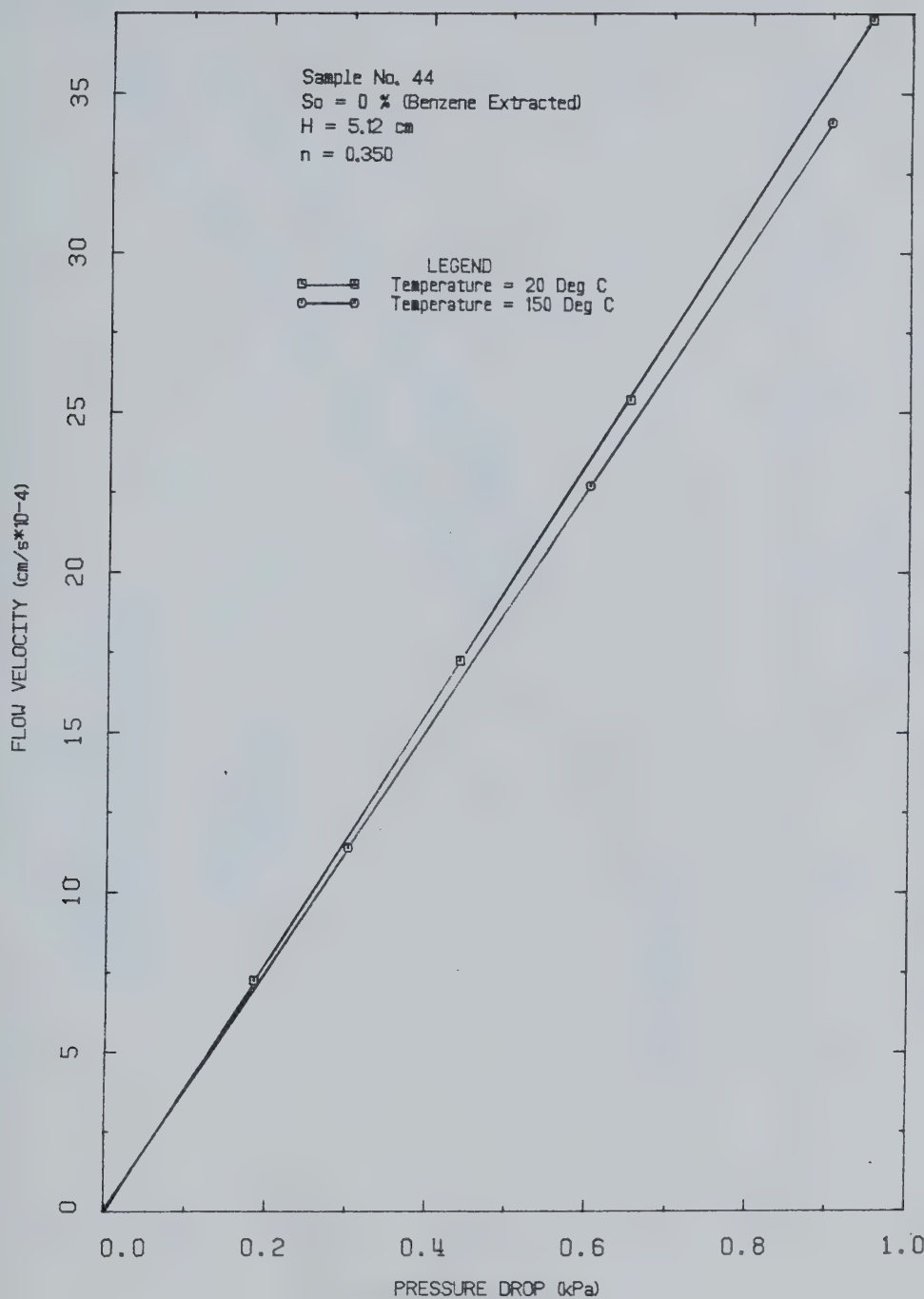


FIGURE D16 Flow Velocity Vs. Pressure Difference:  
Test CPERM7



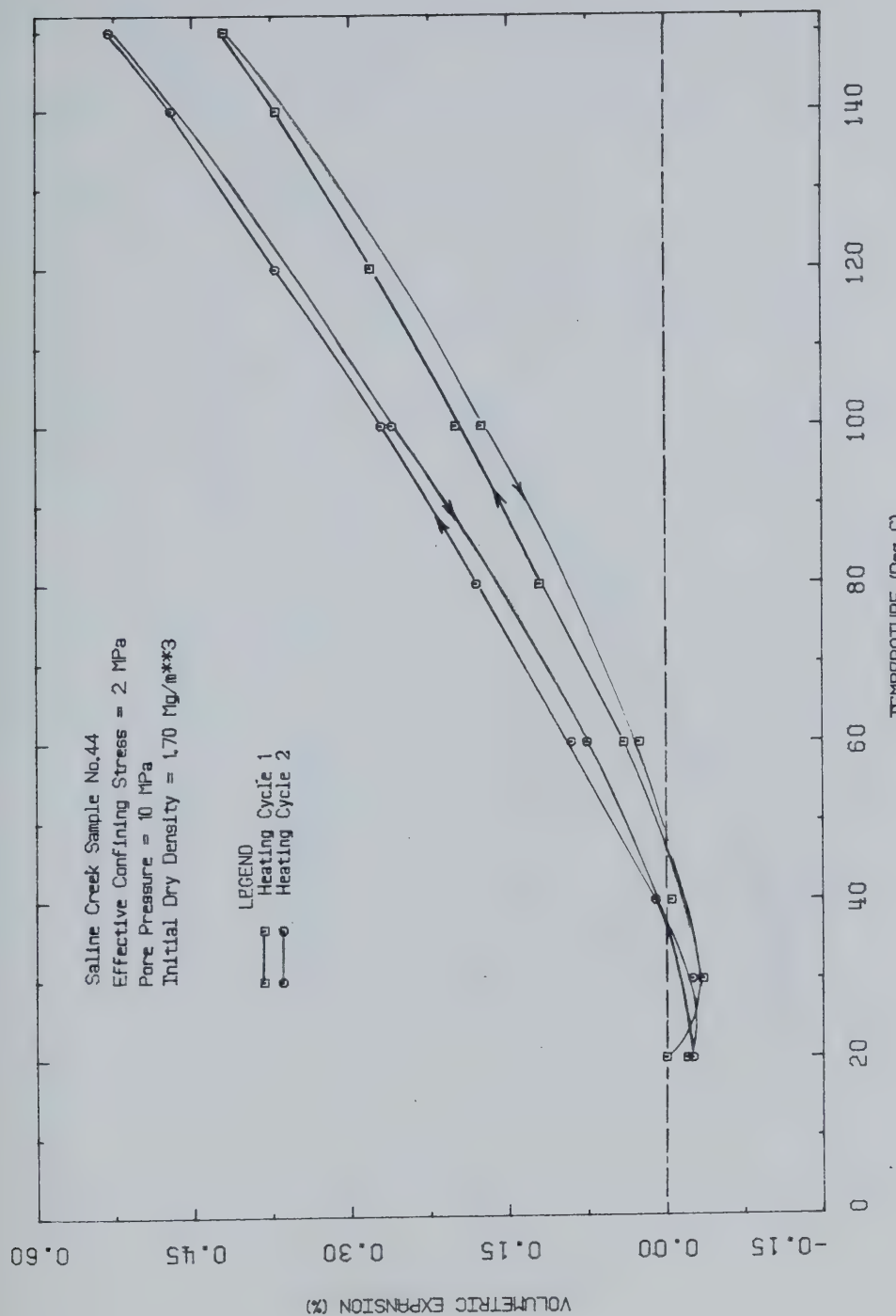


FIGURE D17 Drained Thermal Expansion: Test CPERM7



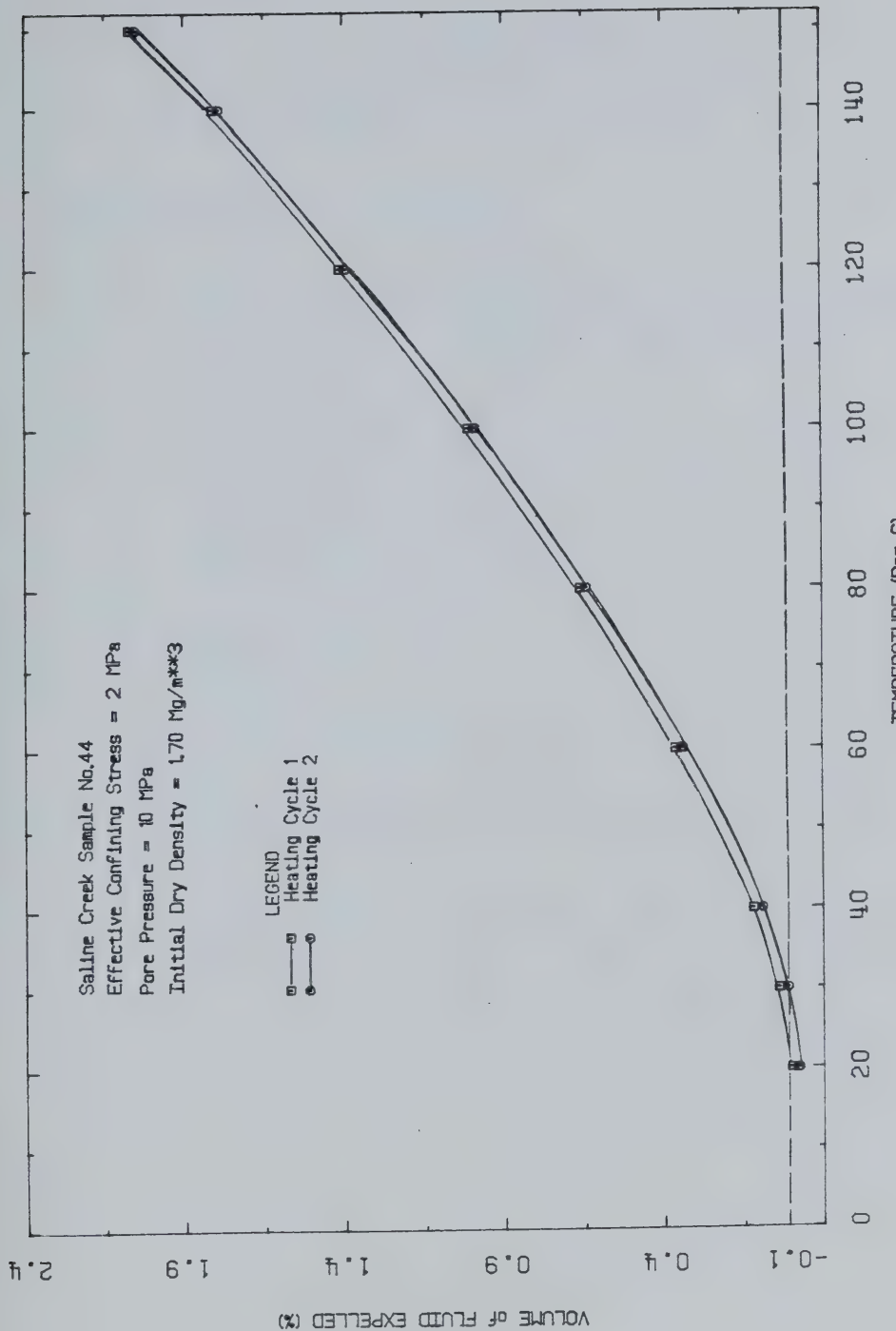


FIGURE D18 Volume of Fluid Drained During Heating:  
Test CPERM7



## TEST CPERM 8

Permeability of Saline Creek Oil Sand  
Sample No. 16 at 20°C and 150°CProcedural Details: Test CPERM 8

1. Sample No. 16 was allowed to thaw and then back saturated for 24 hours under 10 MPa back pressure and 13 MPa confining stress.
2. A room temperature permeability test was performed at flow rates varying up to 4 ml/minute. Effective confining stress was maintained constant at 3 MPa.
3. The system and sample were then heated slowly to 150°C. Drained thermal expansion of the sample was monitored during heating.
4. A permeability test was performed at 150°C by circulating heated water through the sample. Bitumen was flushed from the sample reducing the bitumen saturation from 88% to 52%.
5. The sample was then cooled down to room temperature and a room temperature permeability test was performed at the residual bitumen saturation of 52 percent.

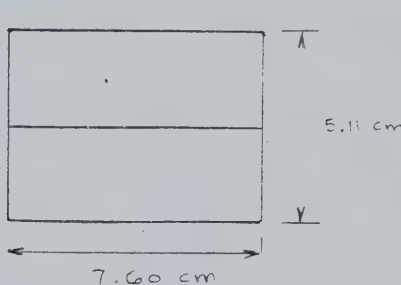


TEST CPERM 8: SAMPLE DATAOriginal Sample No. 16:

Dia.:  $\emptyset = 7.600 \text{ cm}$   
 c/s Area:  $A = 45.36 \text{ cm}^2$   
 Height:  $H = 5.121 \text{ cm}$   
 Volume:  $V = 232.31 \text{ cm}^3$   
 Mass:  $M = 478 \text{ g}$  Density:  $= 2.058$

$w = 2.2\%$   $B = 16.7\%$

$M_S = 402$   
 $V_S = 151.71 \text{ cm}^3$   
 $V_V = V - V_S = 80.60 \text{ cm}^3$   
 $= 0.347$   
 $S_W = 11.6\%$   $S_o = 88.4\%$

After 150°C Permeability Test

Top:  $w = 9.43\%$   
 $B = 8.70\%$   
 $S_o = 49.0\%$   
 $S_W = 51.0\%$

Bottom:  $w = 8.70\%$   
 $B = 10.21\%$   
 $S_o = 55.0\%$   
 $S_W = 46.0\%$

Average Fluid Saturations for Sample:

$S_o = 52.0\%$   
 $S_W = 48.0\%$



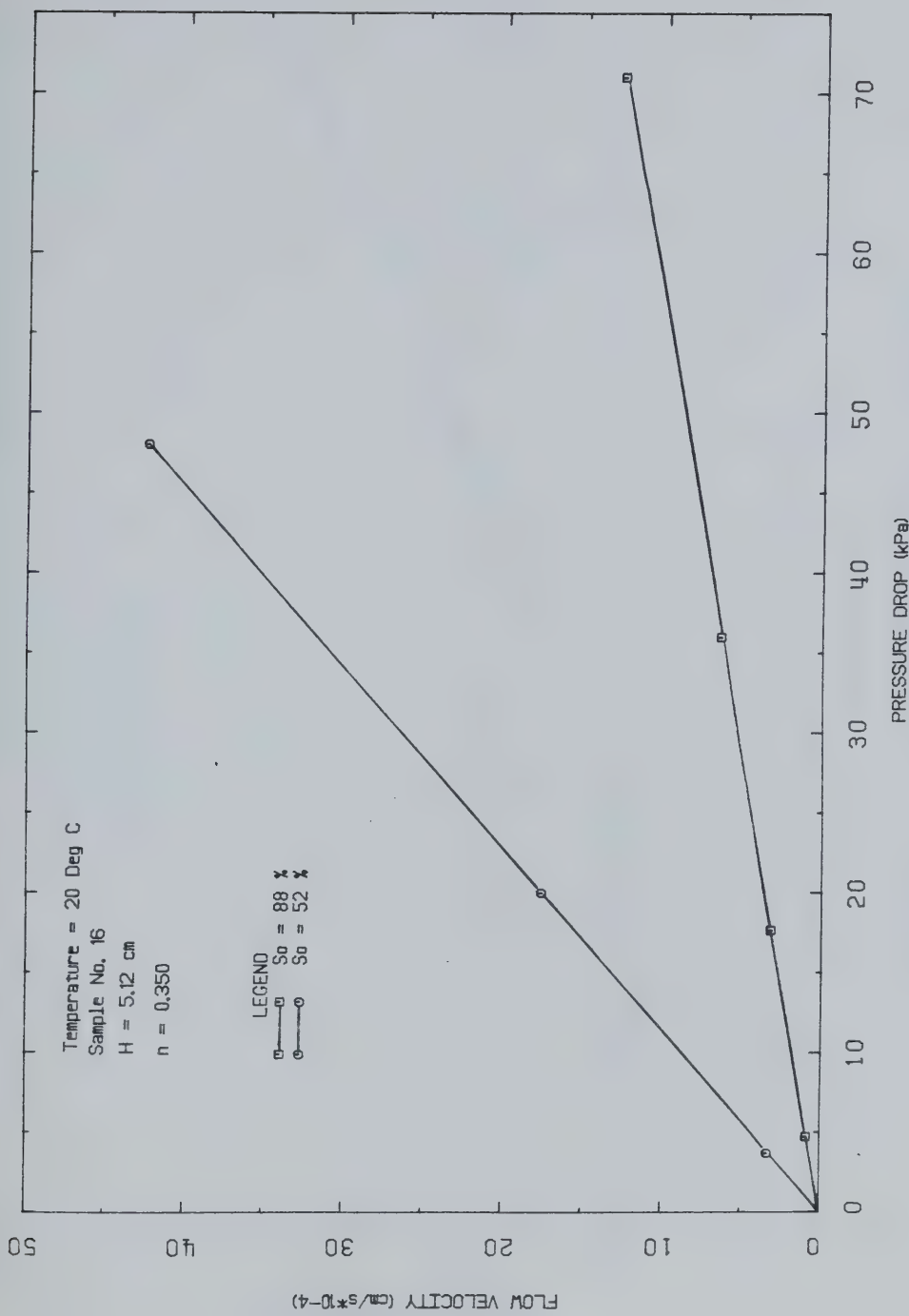
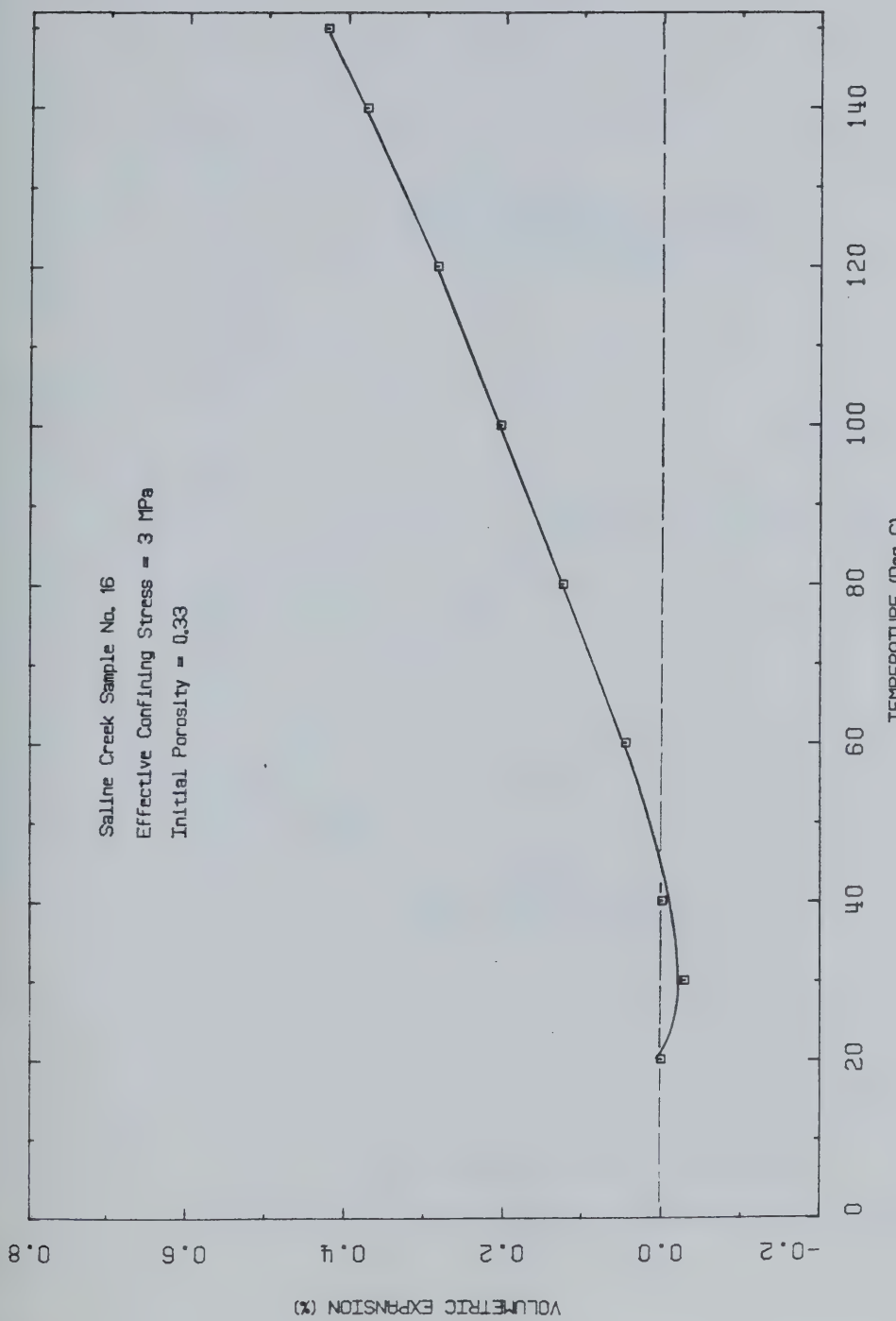


FIGURE D19 Flow Velocity Vs. Pressure Difference:  
Test CPERM8







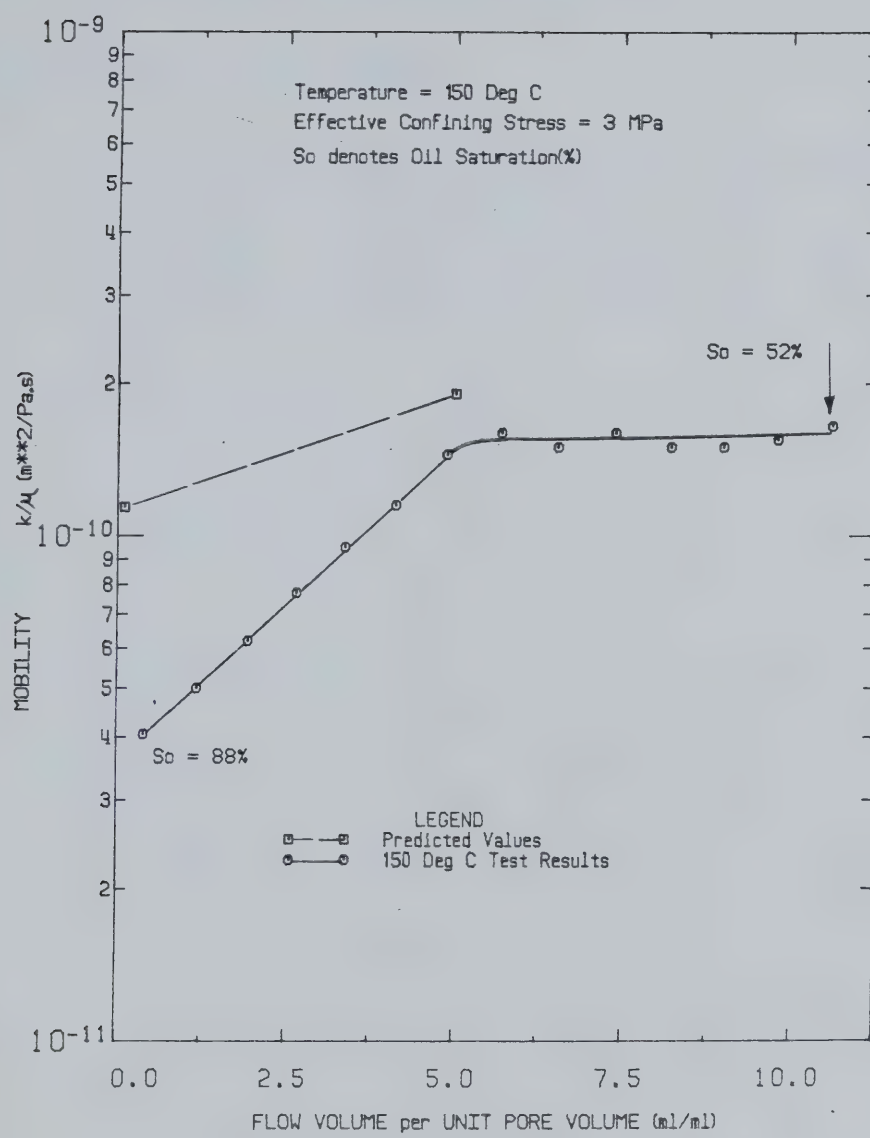


FIGURE D21 Fluid Mobility Vs. Normalized Flow Volume:  
Test CPERM8



## TEST CPERM 9

Permeability of Remoulded Saline Creek  
Sample No. 36B at 20°C and 150°CProcedural Details: Test CPERM 9

1. Saline Creek oil sample No. 36B was thawed, then remoulded by kneading. The sample was compacted in 5 layers in the consolidometer cell using a modified Proctor drop hammer. Compactive effort consisted of at least 30 hammer blows per layer.
2. The sample was further compacted by quick loading it under an effective confining stress of 10 MPa.
3. The sample was then back saturated for 24 hours with an applied back pressure of 10 MPa and a confining stress of 13 MPa.
4. Room temperature effective permeability to water was measured by circulating water through the sample at varying flow rates up to 4 ml/minute and measuring differential pressure difference across the sample and flow rate.
5. The apparatus and sample were slowly heated to 150°C under 10 MPa back pressure and 13 MPa confining stress. Drained thermal expansion was monitored during heating.
6. A permeability test was performed at 150°C by circulating heated water through the sample. Bitumen was flushed from the sample reducing the bitumen saturation from 80% to a residual value of 52% of the sample pore volume. Pressure drop and flow rate were monitored during the test.



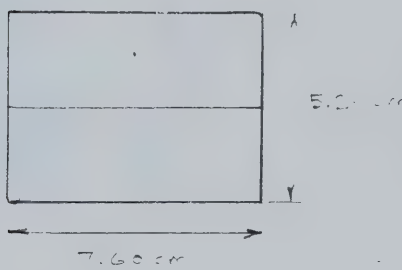
7. The apparatus and sample were cooled down to room temperature. Room temperature water permeability was measured at a residual oil saturation of 52%.



TEST CPERM 9: SAMPLE DATAOriginal Remoulded and Recompacted Sample No. 36B:

Dia.:  $\varnothing = 7.600 \text{ cm}$   
 c/s Area:  $A = 45.36 \text{ cm}^2$   
 Height:  $H = 5.22 \text{ cm}$   
 Volume:  $V = 236.8 \text{ ml}$   
 Mass:  $M = 478 \text{ g}$  Density:  $= 2.019$

$w = 4.9\%$   
 $B = 18.5\%$   
 $M_S = 387.5 \text{ g}$   
 $V_S = 146.2 \text{ ml}$   
 $V_V = V - V_S = 90.6 \text{ ml}$   
 $n = 0.383$   
 $S_W = 20.9\%$   
 $S_O = 79.1\%$

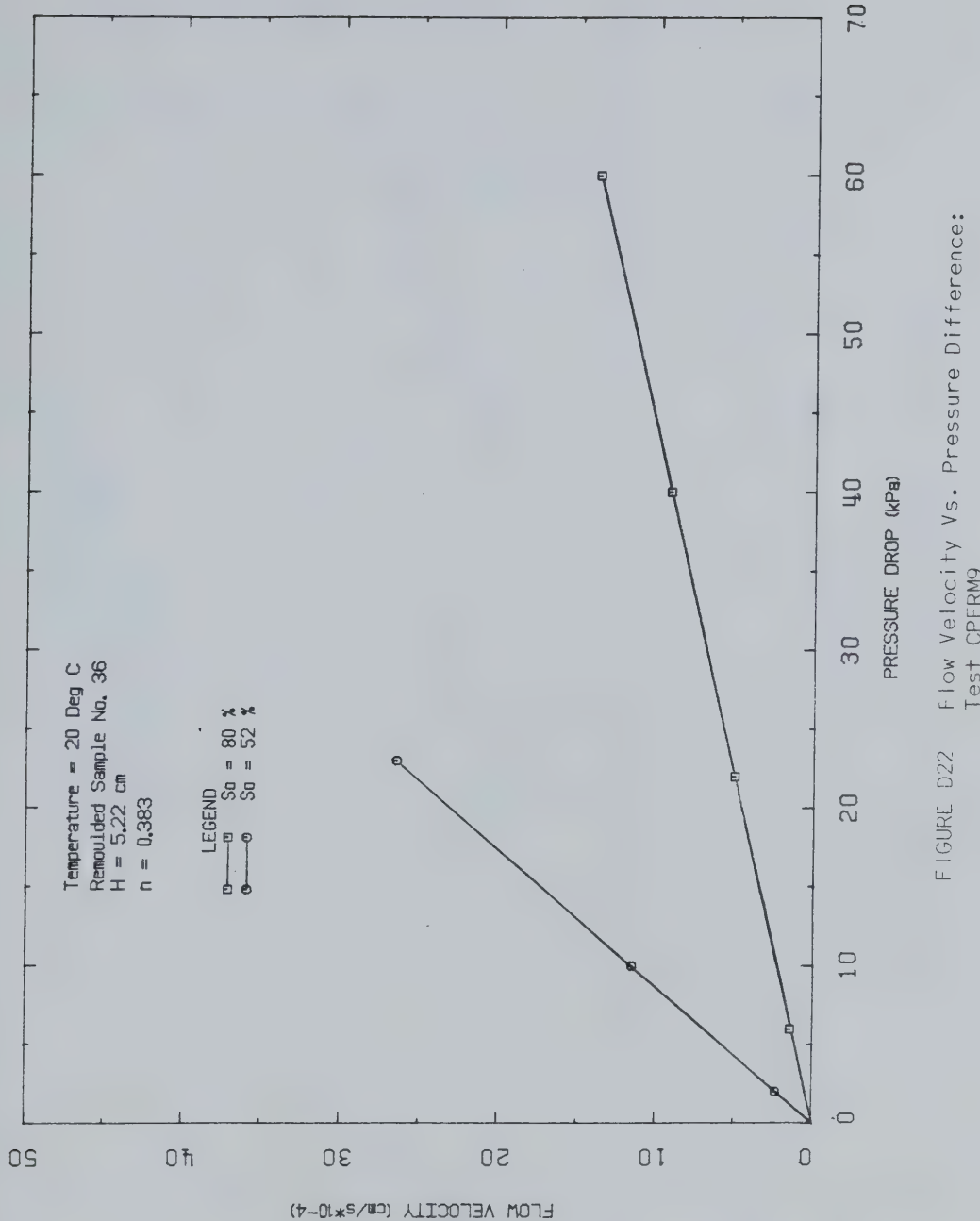
After 150°C Permeability Test

Top:  $w = 11.9\%$   
 $B = 12.0\%$   
 $S_O = 51.1\%$   
 $S_W = 48.9\%$

Bottom:  $w = 11.5\%$   
 $B = 12.3\%$   
 $S_O = 52.7\%$   
 $S_W = 47.3\%$

Average Fluid Saturations For Sample:  $S_O = 51.9\%$   
 $S_W = 48.1\%$







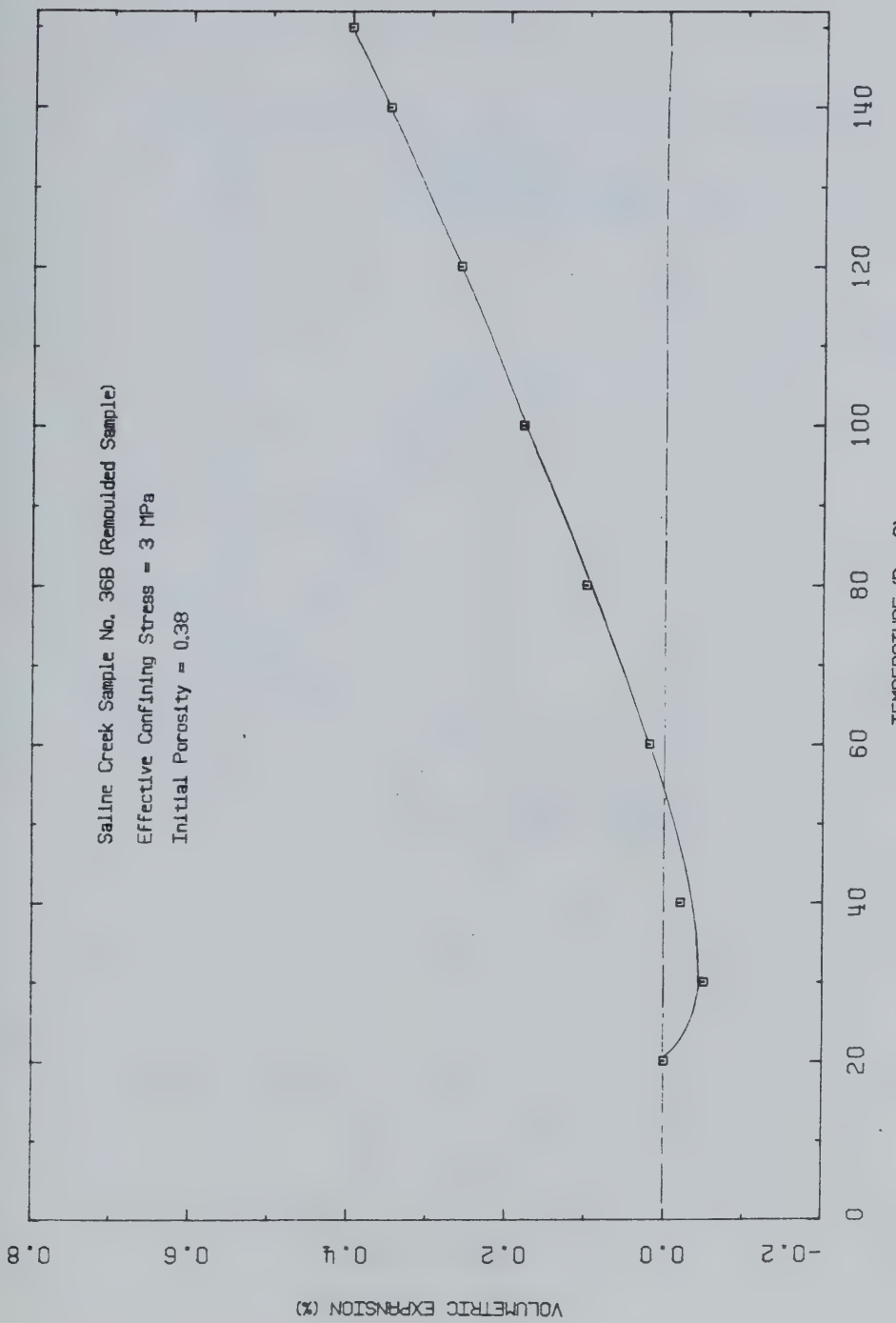


FIGURE D23 Drained Thermal Expansion: Test CTERM9



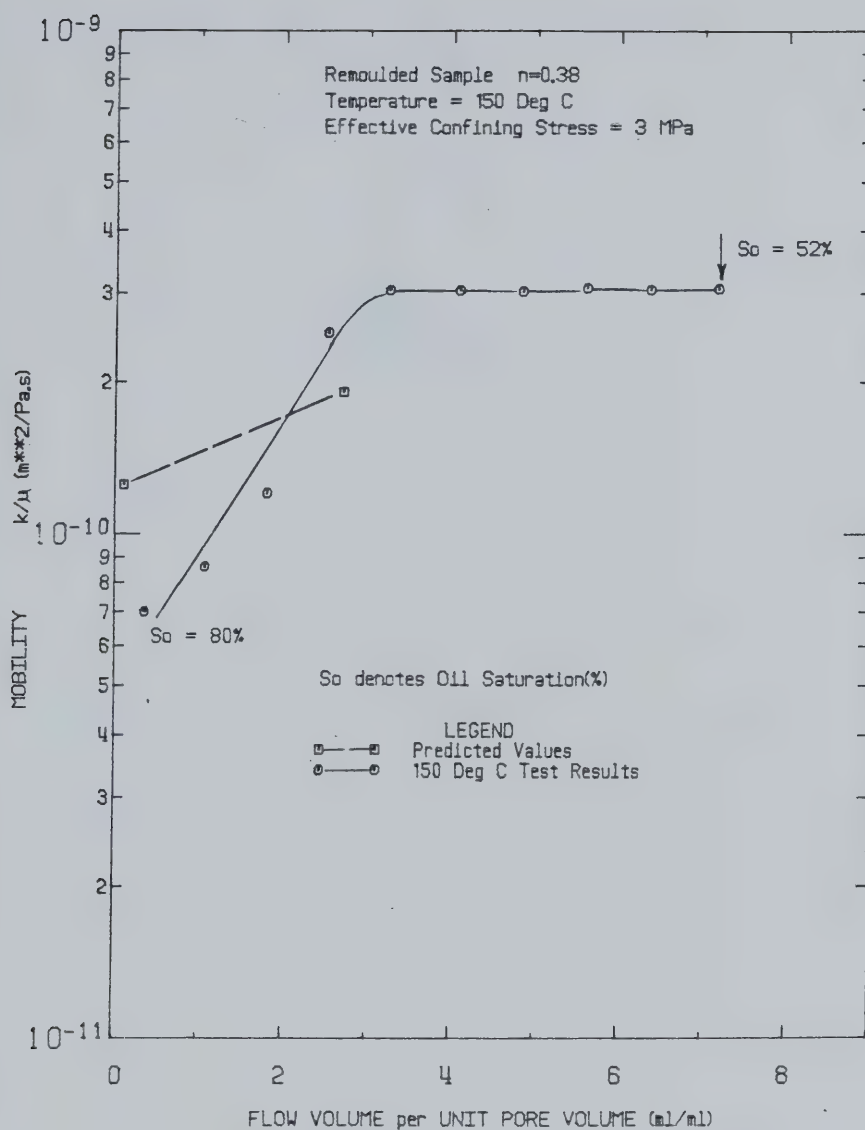


FIGURE D24 Fluid Mobility Vs. Normalized Flow Volume:  
 Test CPERM9



APPENDIX E  
TRIAXIAL TESTS



TABLE E-1  
Summary of Triaxial Tests

Test No.	Temperature (°C)	Effective Confining Stress (MPa)	Test Description
TOS 1	20	4 - 26	Isotropic Compression
TOS 2	20	4	Passive Compression
TOS 3	20	4 - 0.87	$J_1 \cong$ Constant
TOS 4	20	8	Passive Compression
TOS 5	20	8	Passive Compression
TOS 6	125	4 - 0.6	$J_1 \cong$ Constant
TOS 7	125	4	Passive Compression
TOS 8	220	12 - 20	Isotropic Compression
TOS 9	240	4 - 0	Membrane Meltdown
TOS 10	200	4 4 - 0.25	Undrained Heating with Constant and Undrained Passive Compression
TOS 11	100	4 - 0.25	Anisotropic Consolidation and Undrained Heating to Failure
TOS 12	200	4 - 17 4	Isotropic Compression and Passive Compression
TOS 13	240	4	Membrane Meltdown
TOS 14	20	2, 4, 8	Multistage Passive Compression of Remoulded Oil Sand
TOS 15	200	4 - 17 4	Isotropic Compression and Passive Compression of Cold Lake Oil Sand
TOS 16	200	4	Membrane Meltdown
TOS 17	200	8	Passive Compression
TOS 18	200	4 - 0.6	$J_1 \cong$ Constant
TOS 19	125	4 - 17 4	Isotropic Compression and Passive Compression
TOS 20	20	0	Unconfined Compression of Case Hardened Sample



## TEST TOS 1

Isotropic Compression of Saline Creek Oil Sand Sample  
No. 25 at 20°C: Drained and Undrained Isotropic CompressibilityProcedural Details: Test TOS 1

1. Saline Creek sample No. 25 was thawed, then back saturated for 24 hours at an applied back pressure of 2 MPa and isotropic confining stress of 6 MPa.
2. Back pressure drainage valves were closed and a B-test was performed to check the degree of saturation of the sample. Volumetric strains determined from internal strain gauge measurements were used to determine isotropic compressibility over a range of confining stress from 6 - 26 MPa.
3. Back pressure drainage valves were opened and a drained isotropic compression test was performed. Four cycles of compression and unloading were applied over a range of isotropic effective stress from 4 - 26 MPa. Volumetric strain determined from internal strain gauge device measurements (i.e. vertical and lateral deformations) was compared with volumetric strain determined using the volume change device. Volumetric strains varied by approximately  $\pm 1.6 \times 10^{-4}$  per MPa; internal strain measurements being rather more erratic. It was found that this rather substantial error resulted from inaccurate lateral (horizontal) deformation measurements.



The stiff lateral strain gauge clamp was found to distort lateral deformation of cohesionless oil sand samples.

4. A drained triaxial compression test was performed. The lateral strain gauge clamp, however, impeded lateral deformation and caused tensile stresses to develop in the orthogonal plane as vertical deformation proceeded. The sample was weakened and yielded prematurely. Effective lateral confining stress was maintained constant at 4 MPa and back pressure was maintained constant at 2 MPa during loading. Vertical effective stress was increased to a constant rate of 80 kPa/minute.



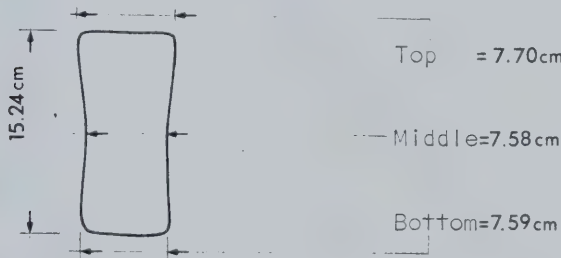
TEST TOS 1: SAMPLE DATAPretest Saline Creek Sample No. 25:

Dia.:	$\emptyset = 7.604$ cm	$w = 0.30$
Height:	$H = 15.316$	$B = 0.152$
Area:	$A = 45.412$ $\text{cm}^2$	
Volume:	$V = 695.54$	$V_S = 463.5$ ml
Mass:	$M = 1452$ g	$V_V = 232.0$ ml
$M_S$ :	$= 1228$ g	Dry Density = $1.766$ $\text{Mg/m}^3$

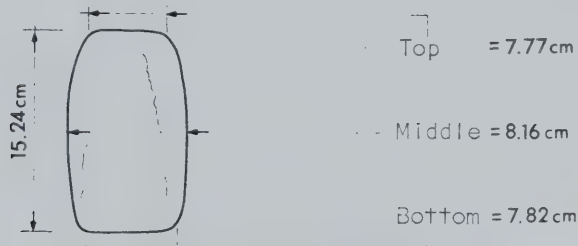
Density:	= $2.088$ $\text{Mg/m}^3$
Porosity:	= $0.333$
Void Ratio:	= $0.49914$ g

Failed Sample No. 25 After Test TOS 1

Diameter in plane parallel to lateral strain gauge clamp:



Diameter in plane perpendicular to lateral strain gauge clamp:





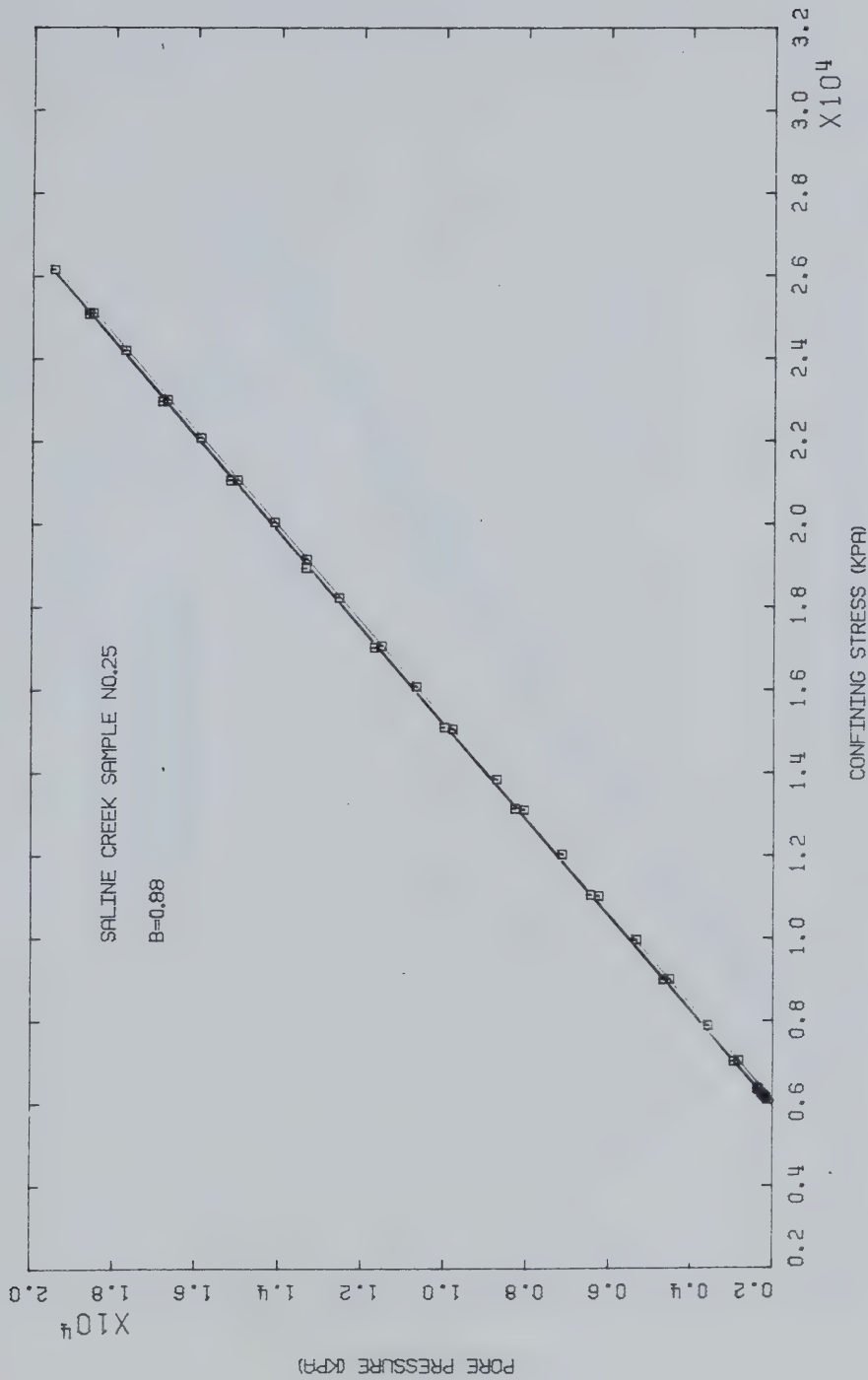


FIGURE E1.1 Triaxial Test TOS1: B Test



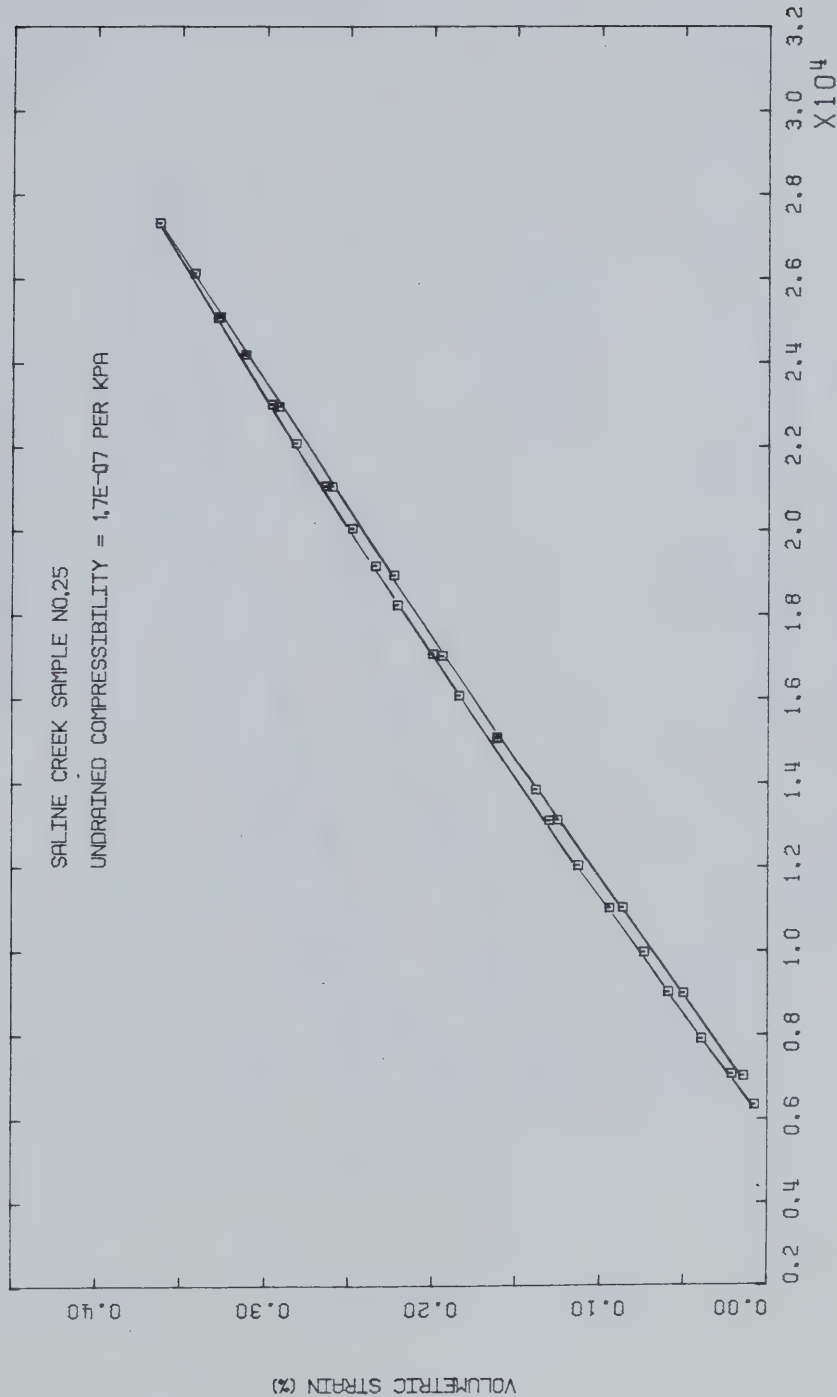


FIGURE E1.2      Triaxial Test TOS1:      Undrained  
Compressibility



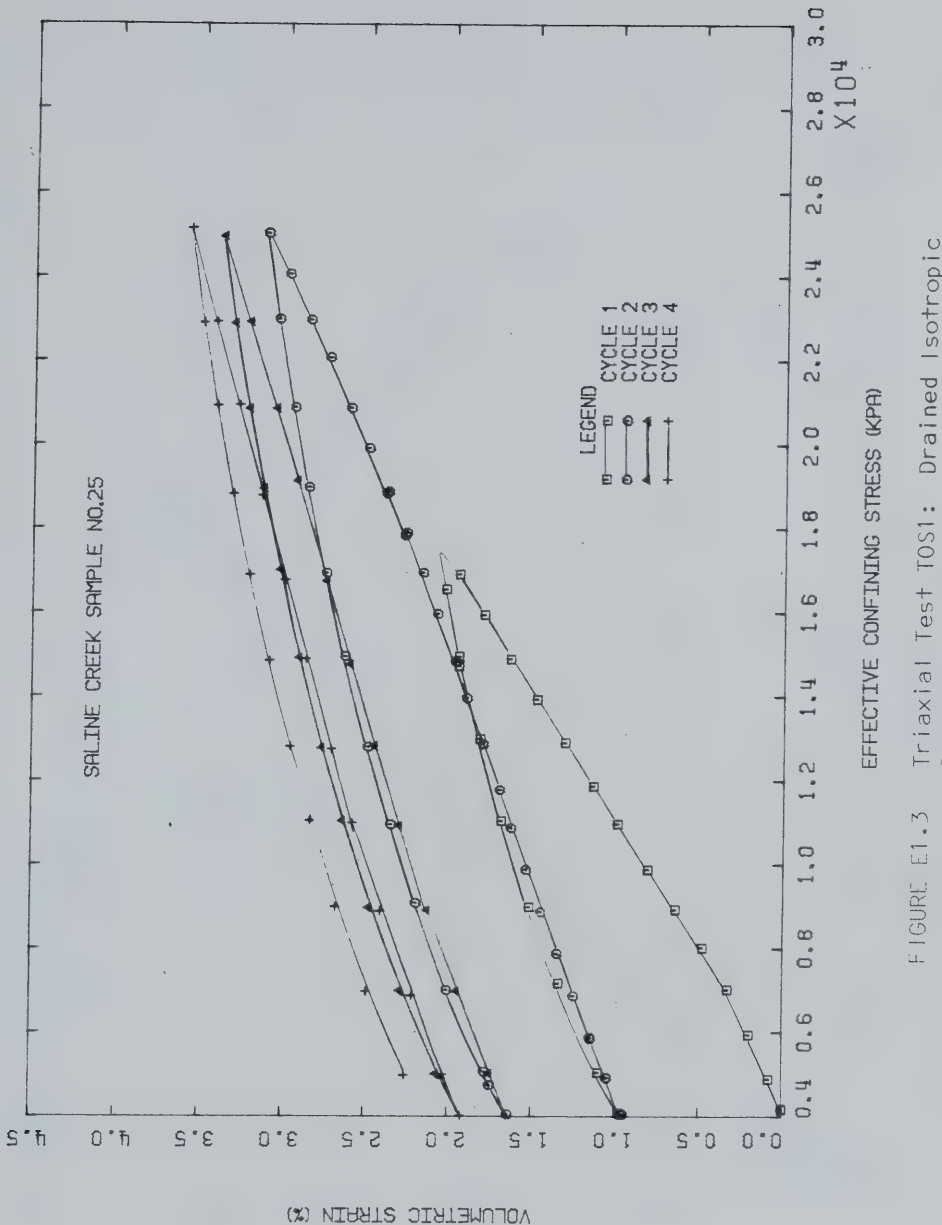
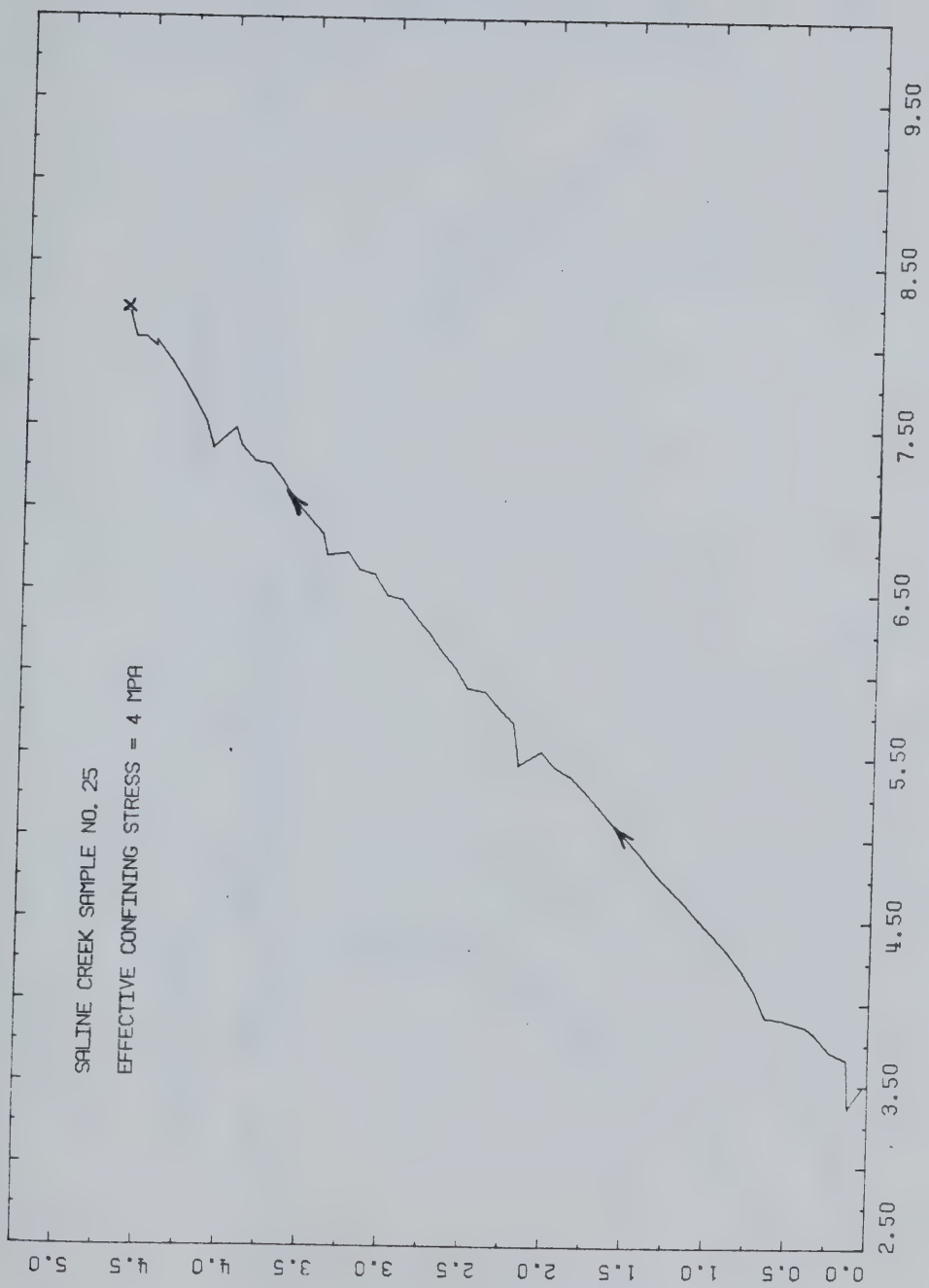


FIGURE E1.3 Triaxial Test T01: Drained Isotropic Compressibility





$$P = (S_1+S_3)/2 \text{ (MPa)}$$



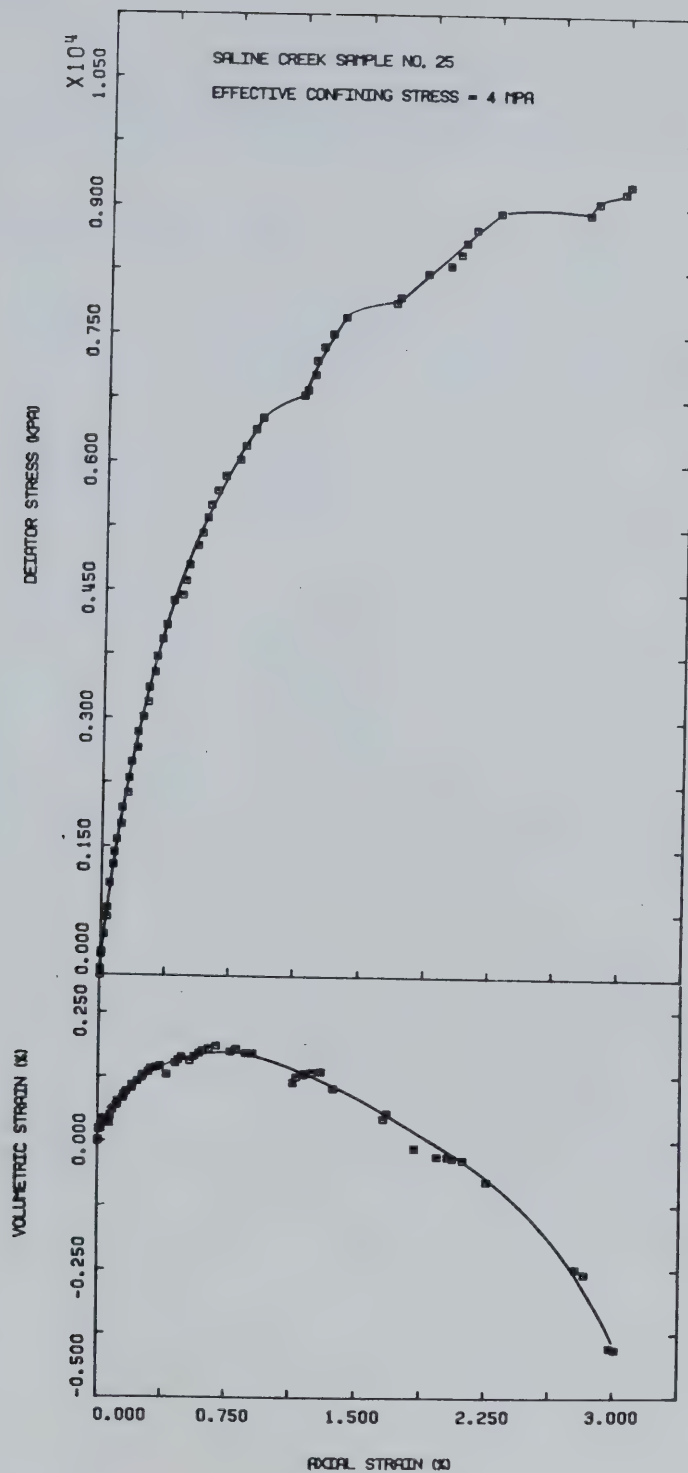


FIGURE E1.5 Triaxial Test T01: Deviator Stress Vs. Strain



## TEST TOS 2

Drained Triaxial Compression of Saline Creek Sample No. 33  
at 4 MPa Effective Confining Stress and at 20°C

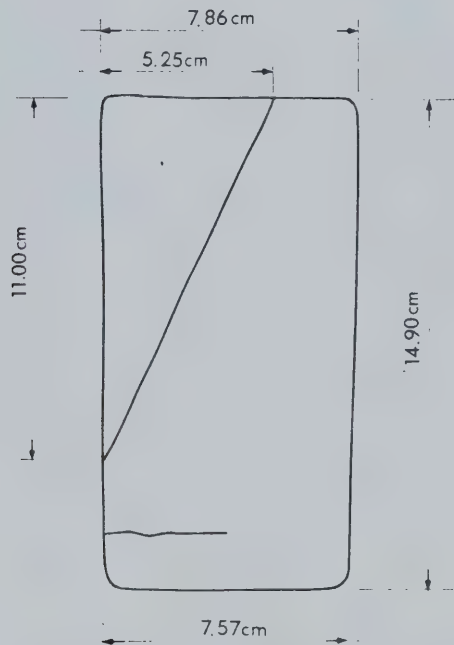
Procedural Details: Test TOS 2

1. Sample No. 33 was thawed and back saturated for 24 hours under 2 MPa back pressure and 6 MPa isotropic confining stress.
2. A B-test was performed to ensure that gases in the system had dissolved in the liquid phase (i.e. complete saturation).
3. A drained triaxial compression test was performed at room temperature (20°C) maintaining the effective lateral confining stress constant at 4 MPa and the back pressure constant at 2 MPa while vertical effective stress was increased at a near constant rate of 80 kPa per minute. Vertical (axial) and volumetric deformations were monitored during loading.



TEST TOS 2: SAMPLE DATAPretest Saline Creek Sample No. 33:

Dia.:  $\emptyset = 7.600$  cm       $w = 0.025$   
Height:  $H = 15.240$  cm       $B = 0.163$   
Area:  $A = 45.365$  cm $^2$   
Volume:  $V = 691.36$  ml       $V_S = 456.2$  ml  
Mass:  $M = 1436$  g       $V_V = 235.16$  ml  
 $M_S = 1209$  g      Dry Density =  $1.748$  Mg/m $^3$   
Density:      =  $2.077$  Mg/m $^3$   
Porosity:      =  $0.340$   
Void Ratio:      =  $0.515$  g

Failed Sample No. 33 After Test TOS 2



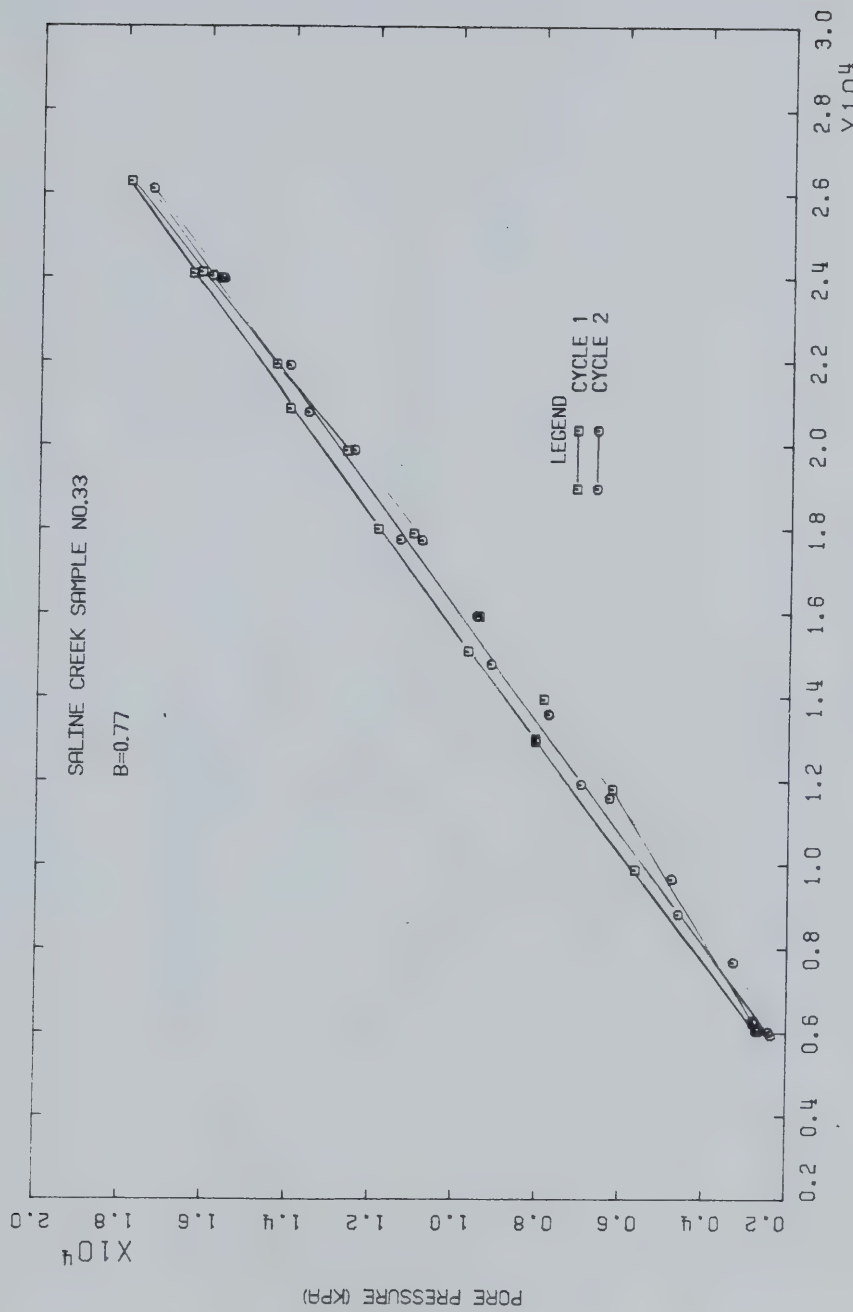
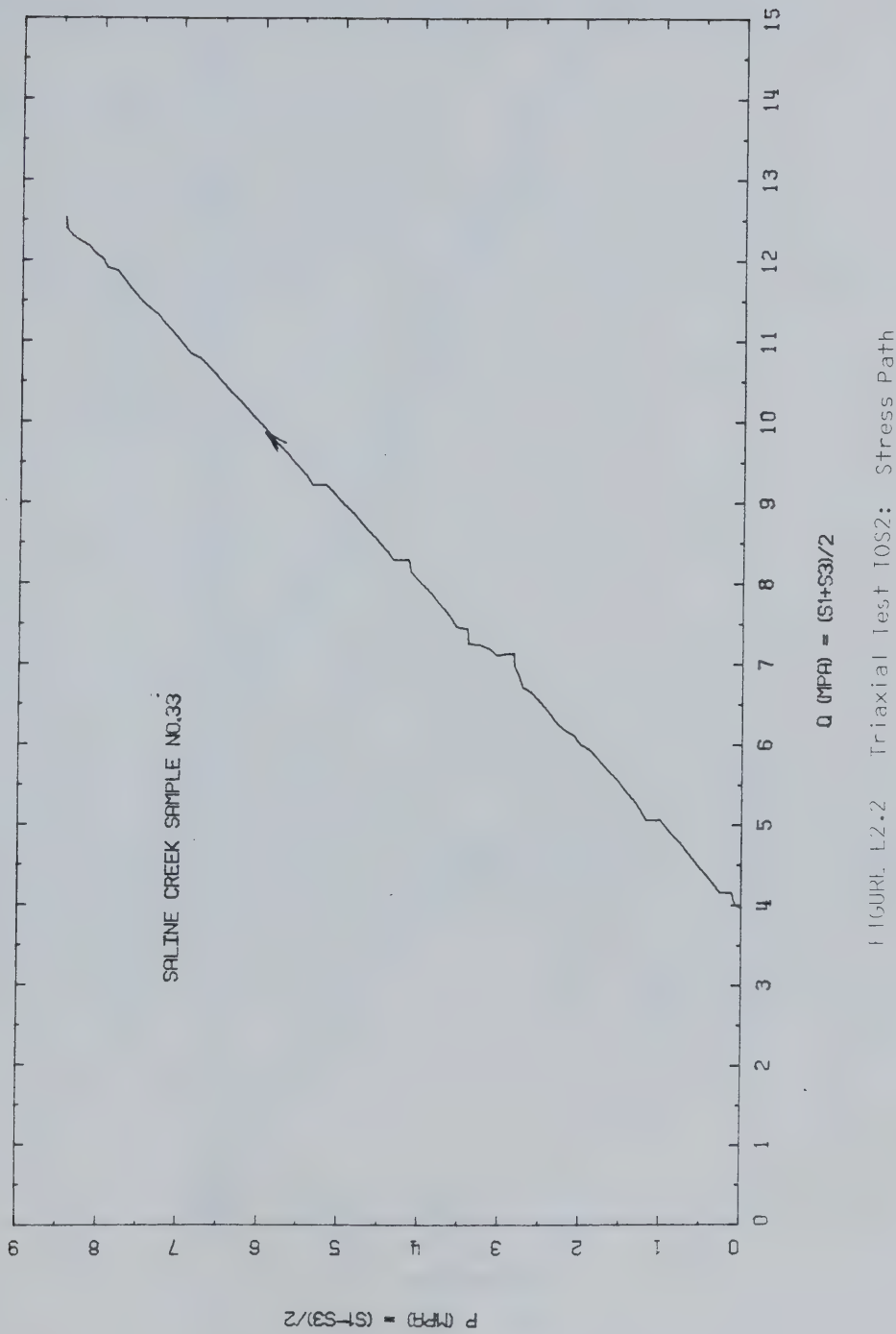


FIGURE E2.1 Triaxial Test TOS2: B Test







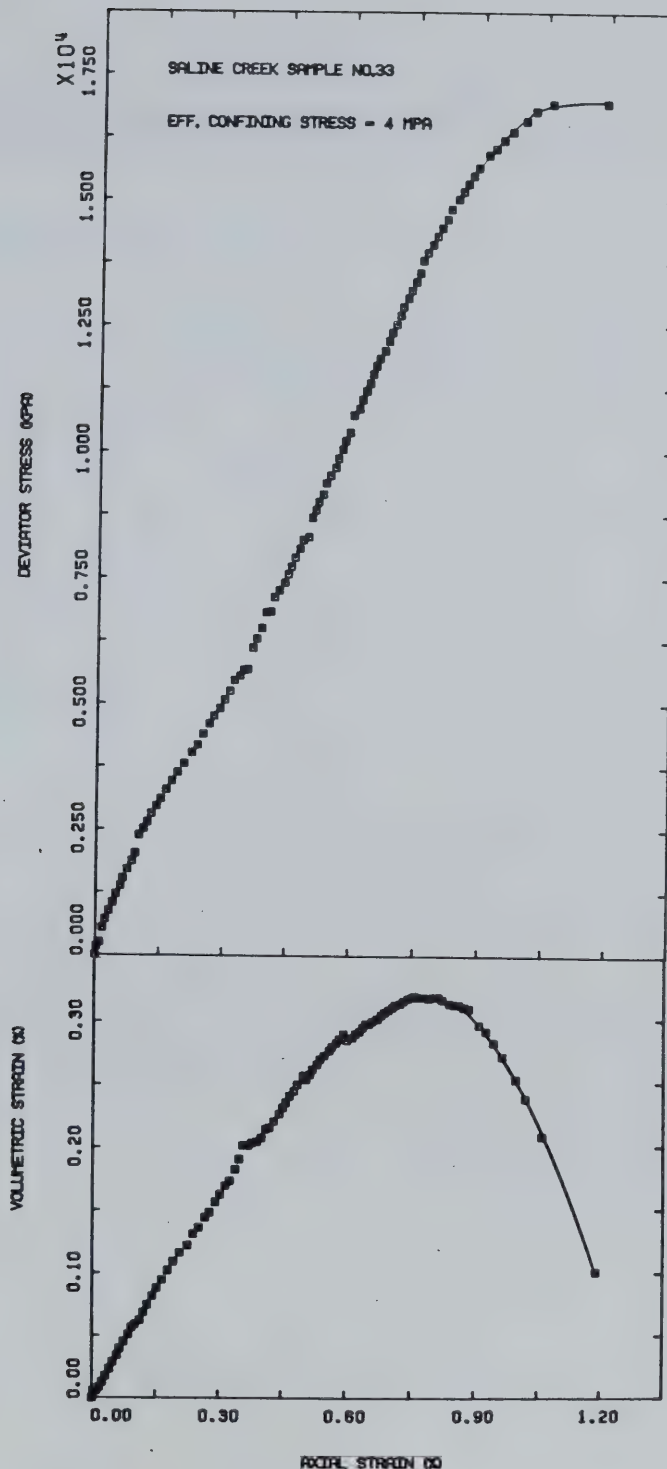


FIGURE E2.3 Triaxial Test TOS2: Deviator Stress Vs. Strain



## TEST TOS 3

Drained Triaxial Compression of Saline Creek Sample No. 43  
at 20°C Following Stress Path "F" (J1 Constant)

Procedural Details: Test TOS 3

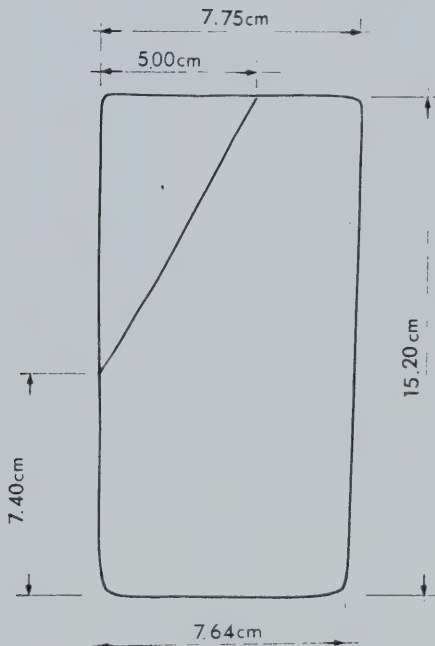
1. Saline Creek sample No. 43 was thawed and back saturated for 24 hours under 2 MPa back pressure and 6 MPa isotropic confining stress.
2. A B-test was performed over a range of confining stresses from 6 - 27 MPa to evaluate the degree of saturation of the pore fluid phase.
3. A drained triaxial compression test was performed following stress path "F", i.e. close to a J1 constant path:
  - a) Vertical stress was maintained constant at 6 MPa throughout the test.
  - b) Lateral confining stress was decreased in 250 kPa increments from 6 MPa to 1 MPa. Back pressure was decreased simultaneously in 50 - 75 kPa increments from 2 MPa to 870 kPa.
  - c) Vertical (axial) deformation and volume change were monitored during loading.



TEST TOS 3: SAMPLE DATAPretest Saline Creek Sample No. 43:

Dia.:  $\varnothing = 7.600$  cm      w = 0.030  
Height: H = 15.408 cm      B = 0.180  
Area: A = 45.365 cm<sup>2</sup>  
Volume: V = 698.98 ml      V<sub>S</sub> = 453.86 ml  
Mass: M = 1455 g      V<sub>V</sub> = 245.12 ml  
M<sub>S</sub>: = 1203 g      Dry Density = 1.721 Mg/m<sup>3</sup>

Density: = 2.082 Mg/m<sup>3</sup>  
Porosity: = 0.351  
Void Ratio: = 0.541 g

Failed Sample No. 43 After Test TOS 3



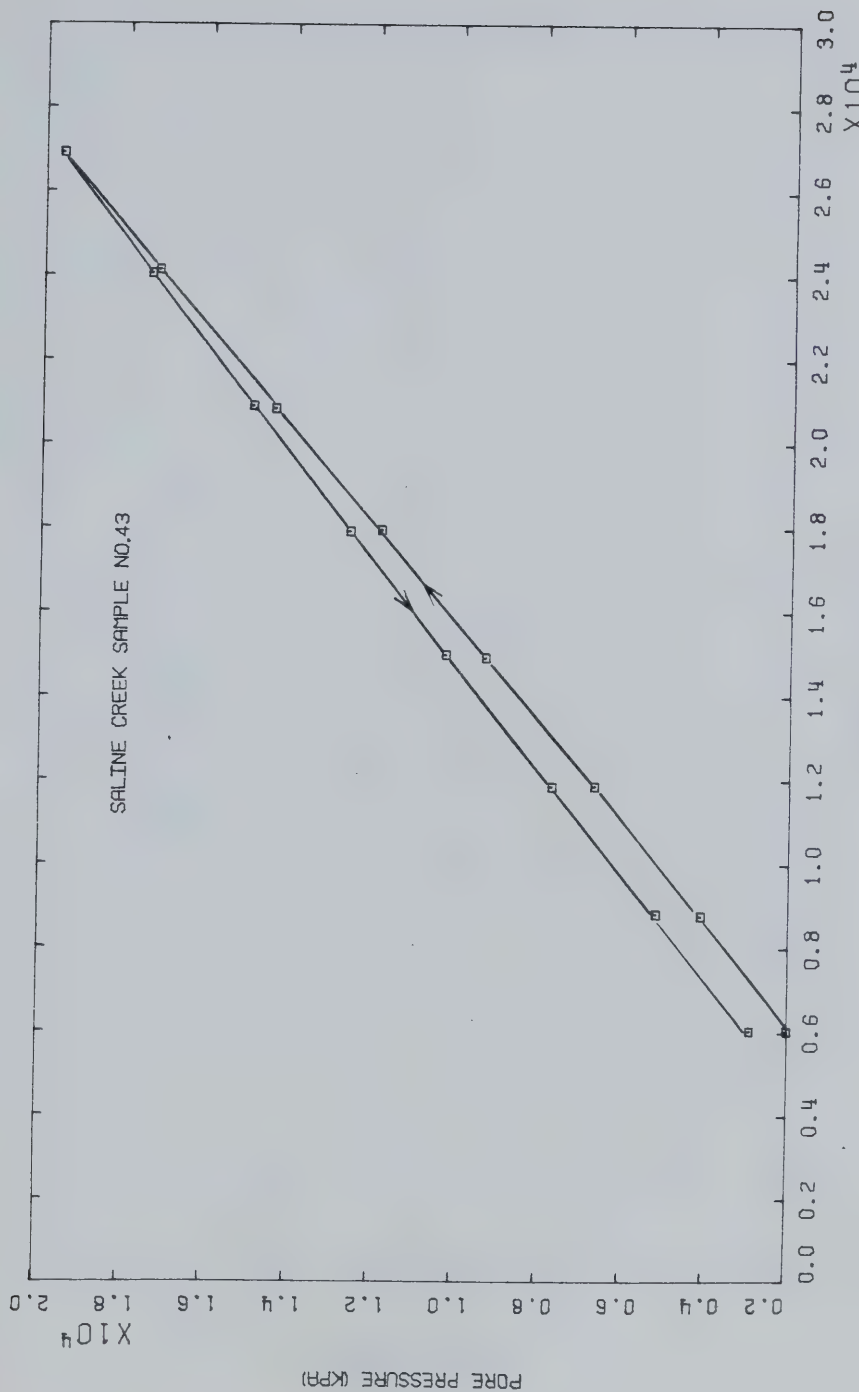
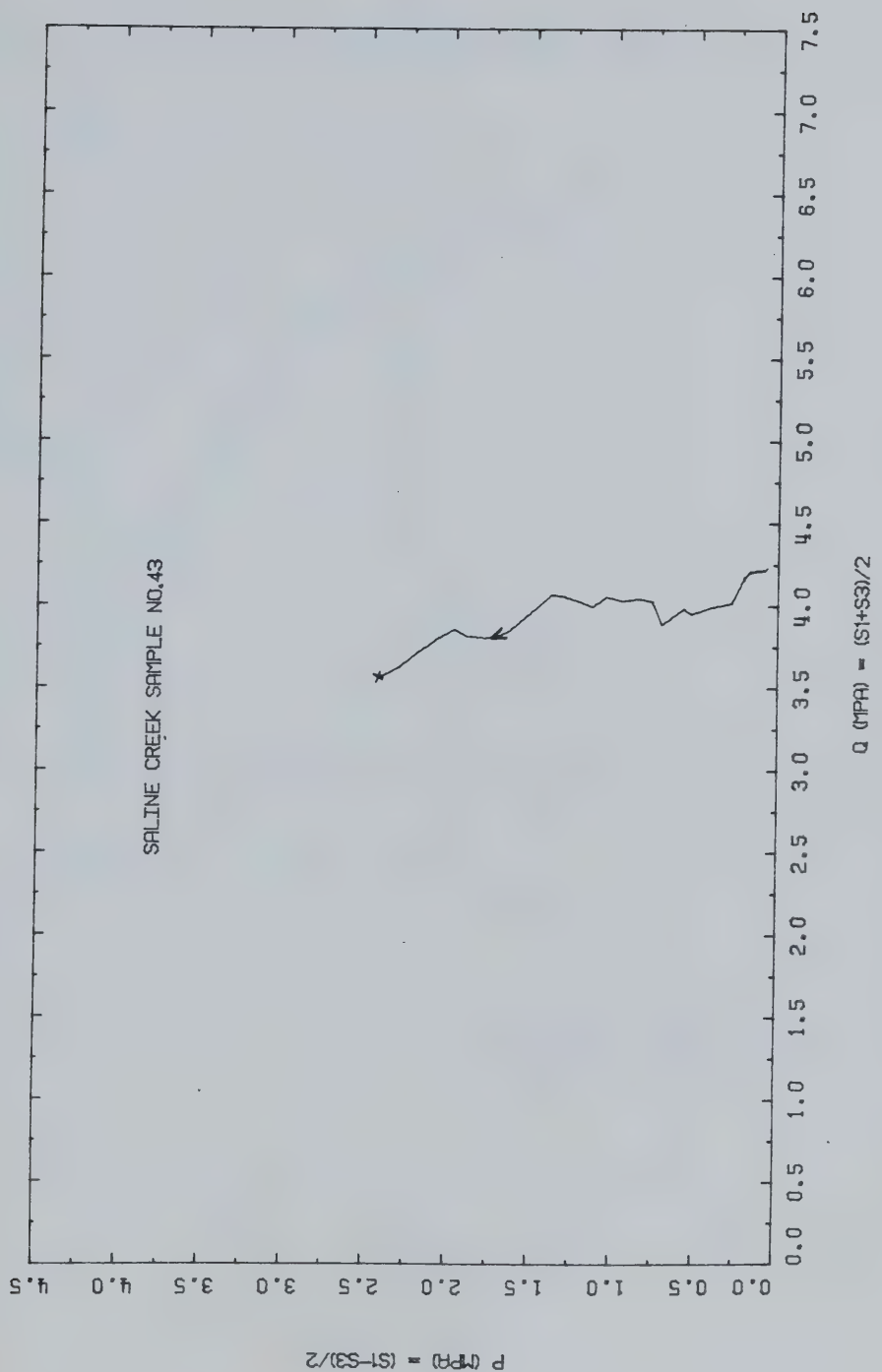


FIGURE E3.1 Triaxial Test Toss: B Test







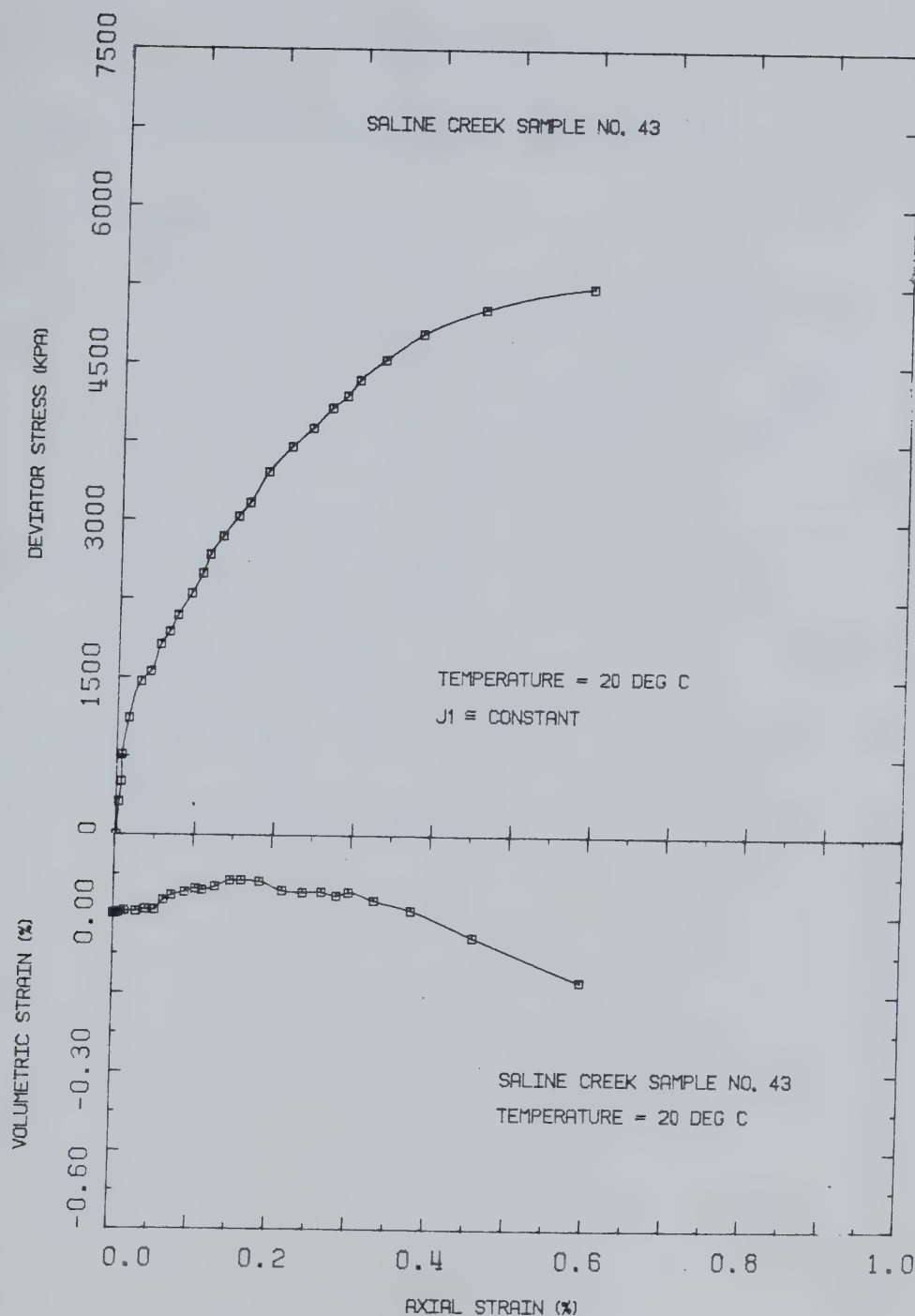


FIGURE E3.3 Triaxial Test TOS3: Deviator Stress Vs. Strain



## TEST TOS 4

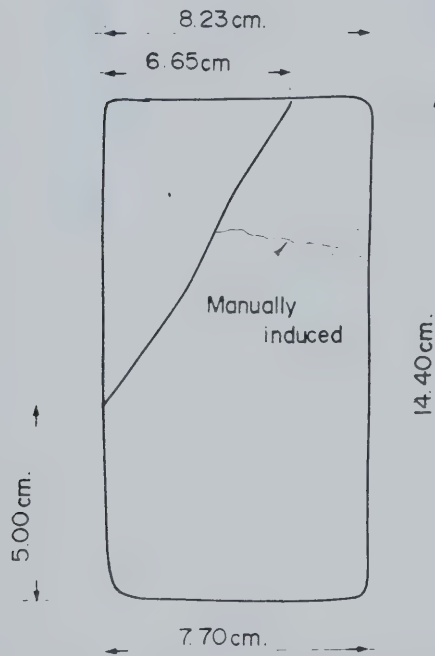
Drained Triaxial Compression of Saline Creek Sample No. 44  
at 20°C and 8 MPa Effective Confining StressProcedural Details: Test TOS 4

1. Sample 44 was thawed and back saturated for 24 hours under 2 MPa back pressure and 6 MPa isotropic confining stress.
2. A B-Test was performed to evaluate degree of saturation.
3. Isotropic confining stress was increased to 10 MPa and the sample was allowed to consolidate.
4. A drained triaxial compression test was performed increasing vertical stress with the lateral stress maintained constant at 10 MPa and back pressure constant at 2 MPa. The average loading rate was 85 kPa/minute.
5. The sample was slightly disturbed (i.e. initial porosity of 0.37) and failed along what appeared to have been a pre-formed plane of weakness.



TEST TOS 4: SAMPLE DATAPretest Saline Creek Sample No. 44:

Dia.:  $\emptyset = 7.590$  cm      w = 0.032  
Height: H = 15.100 cm      B = 0.171  
Area: A = 45.245 cm<sup>2</sup>  
Volume: V = 683.20 ml      V<sub>S</sub> = 431.4 ml  
Mass: M = 1375 g      V<sub>V</sub> = 251.6 ml  
M<sub>S</sub>: = 1143 g      Dry Density = 1.673 Mg/m<sup>3</sup>  
Density: = 2.013 Mg/m<sup>3</sup>  
Porosity: = 0.369  
Void Ratio: = 0.585 g

Failed Sample No. 44 After Test TOS 4



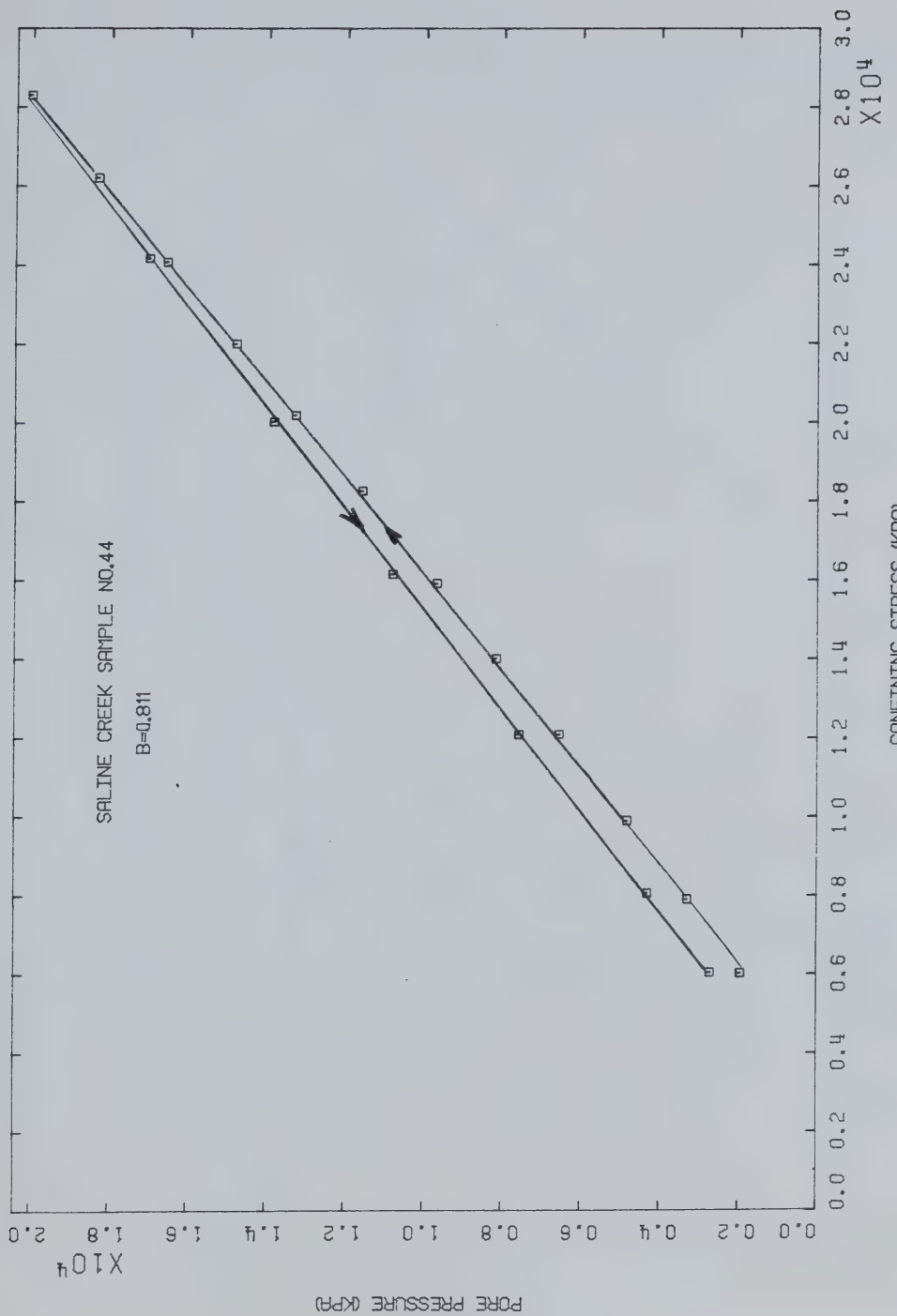


FIGURE E4.1 Triaxial Test TOS4: B Test



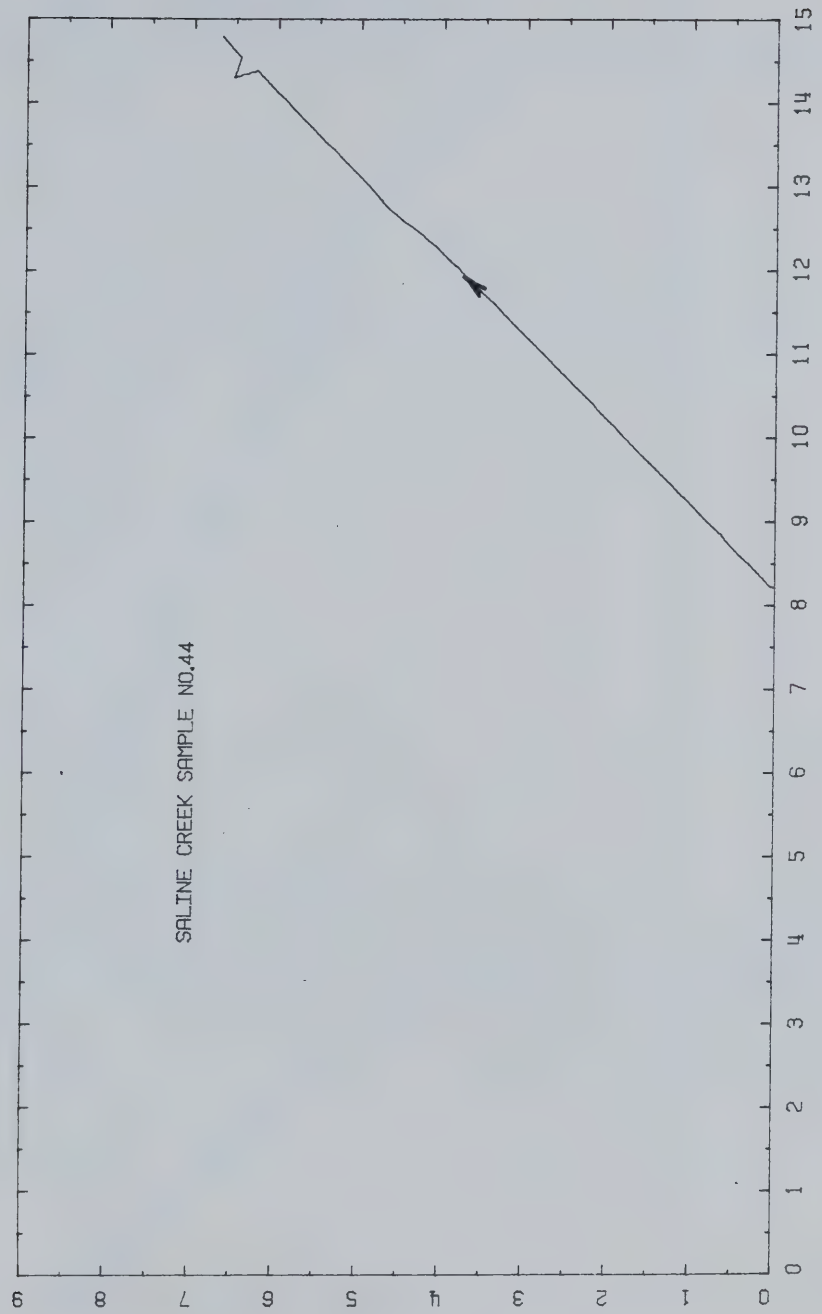


FIGURE E4.2 Triaxial Test TOS4: Stress Path



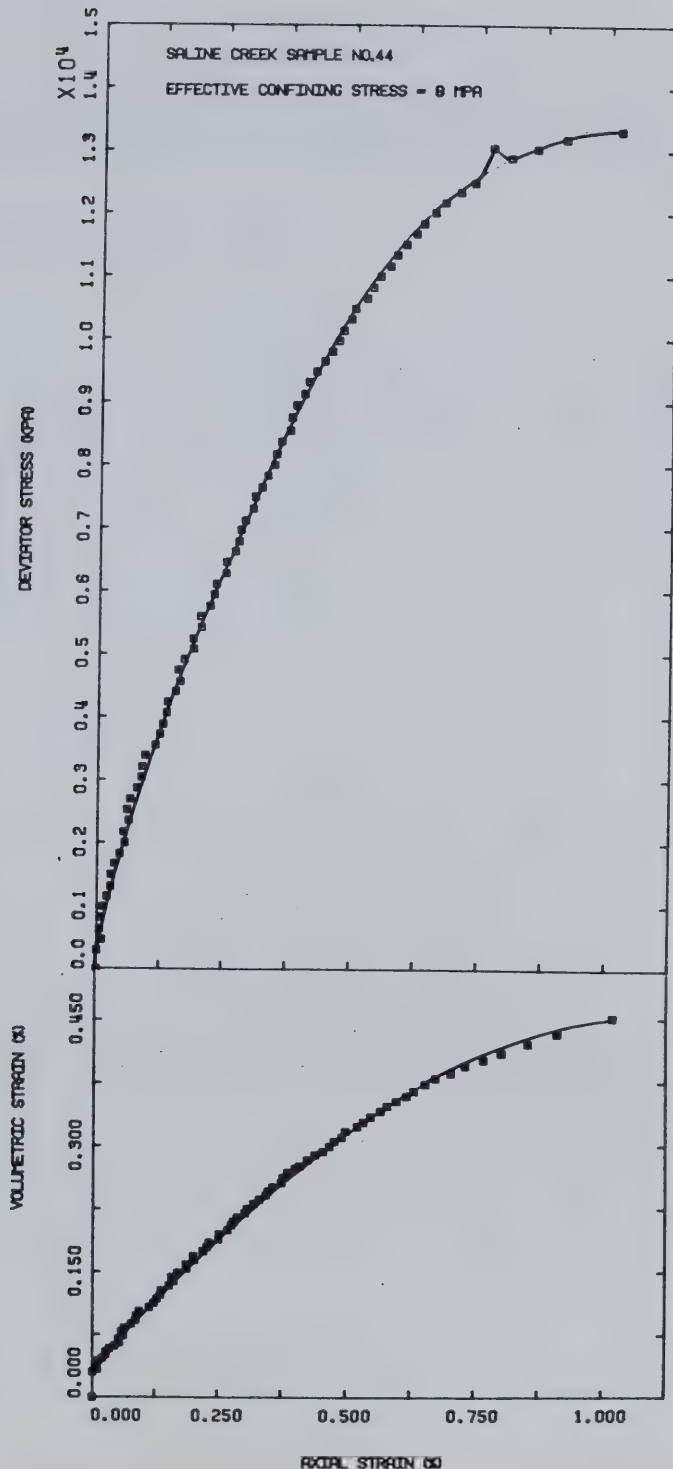


FIGURE E4.3 Triaxial Test TOS4: Deviator Stress Vs. Strain



TEST TOS 5

Drained Triaxial Compression of Saline Creek Sample No. 17  
at 20°C and 8 MPa Effective Confining Stress

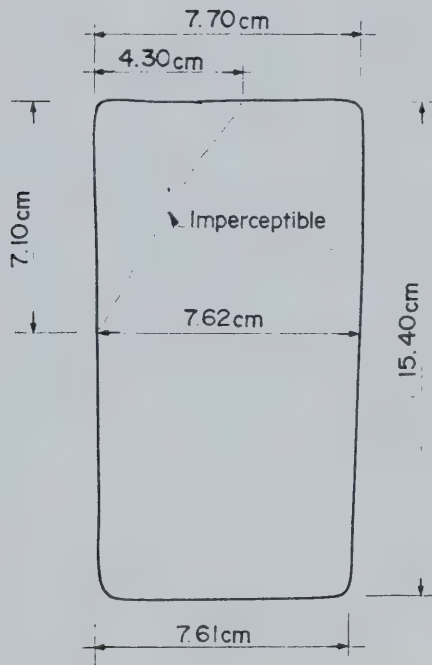
Procedural Details: Test TOS 5

1. Sample 17 was thawed and back saturated for 24 hours under 2 MPa back pressure and 10 MPa isotropic confining stress.
2. A drained triaxial compression test was performed with back pressure maintained constant at 2 MPa, lateral confining stress maintained constant at 10 MPa and temperature at 20°C. Vertical stress was increased at an average rate of 70 kPa per minute.

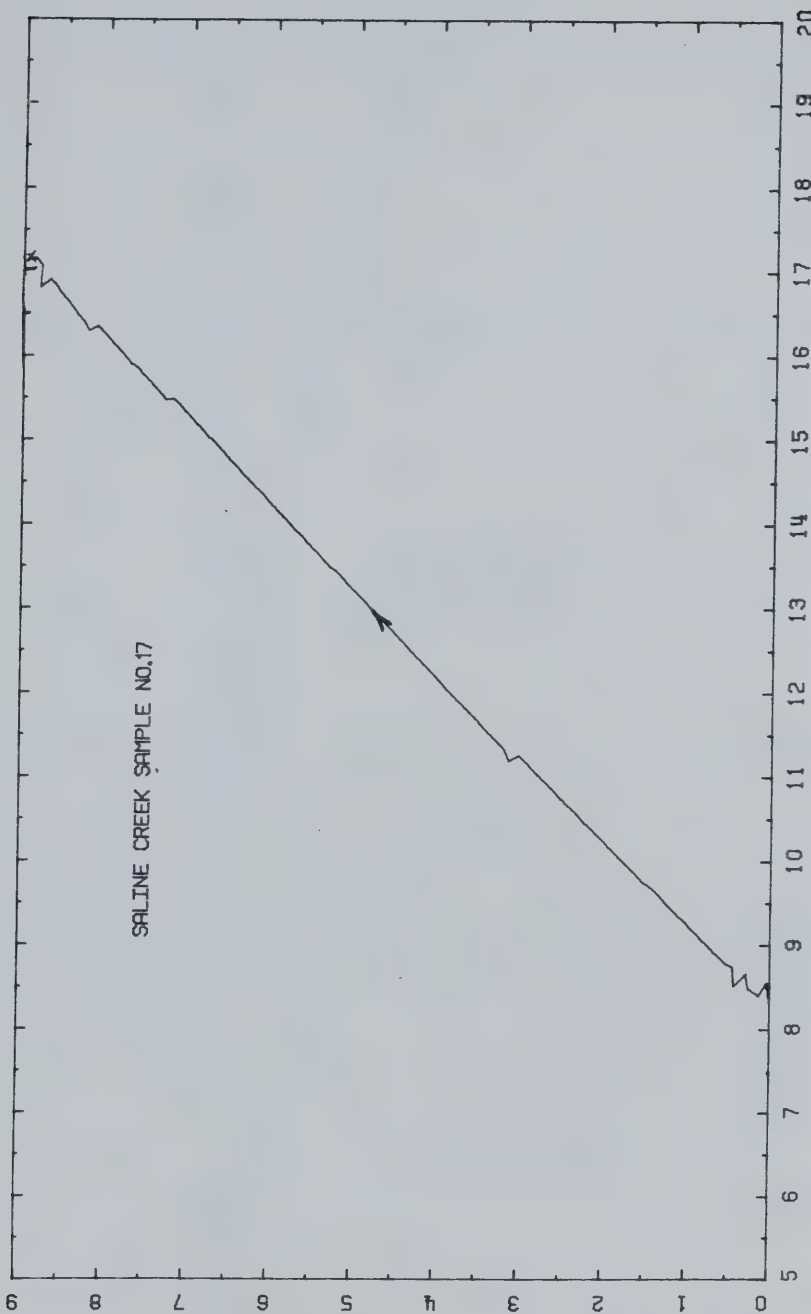


TEST TOS 5: SAMPLE DATAPretest Saline Creek Sample No. 17:

Dia.:  $\varnothing = 7.590$  cm      w = 0.035  
Height: H = 15.300 cm      B = 0.168  
Area: A = 45.245 cm<sup>2</sup>  
Volume: V = 692.25 ml      V<sub>S</sub> = 445.2 ml  
Mass: M = 1419 g      V<sub>V</sub> = 247.0 ml  
M<sub>S</sub>: = 1179.7 g      Dry Density = 1.704 Mg/m<sup>3</sup>  
Density: = 2.050 Mg/m<sup>3</sup>  
Porosity: = 0.357  
Void Ratio: = 0.555 g

Failed Sample No. 17 After Test TOS 5





$$P \text{ (MPa)} = (S_1 + S_3)/2$$

FIGURE E5.1 Triaxial Test TOS5: Stress Path

$$Q \text{ (MPa)} = (S_1 + S_3)/2$$



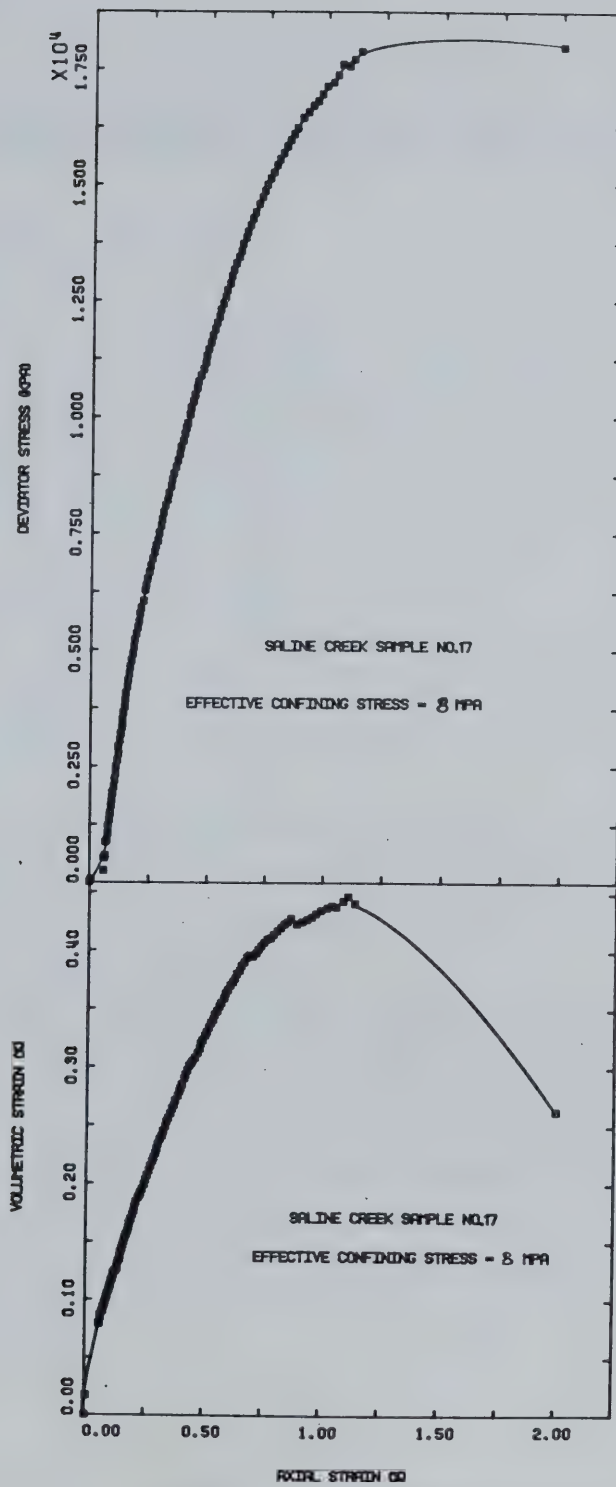


FIGURE E5.2 Triaxial Test T05: Deviator Stress Vs. Strain



## TEST TOS 6

Drained Triaxial Compression of Saline Creek Sample No. 16  
at 125°C Following Stress Path "F" (J1 Constant)

Procedural Details: Test TOS 6

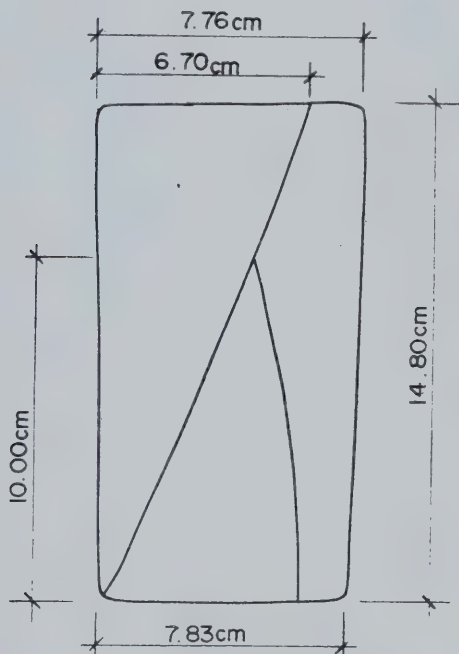
1. Sample 16 was thawed and back saturated under 10 MPa back pressure and 14 MPa isotropic confining stress.
2. Heating of the apparatus and sample was started prior to complete thawing of the sample. The system was heated to 125°C; the volume of pore fluid expelled from the sample was monitored during heat.
3. Back pressure and isotropic confining stress were simultaneously increased to 12 MPa and 16 MPa respectively. The sample was allowed to consolidate overnight (i.e. for 17 hours).
4. A drained triaxial compression test was performed following stress path "F", i.e. J1 approximately constant:
  - a) vertical stress was maintained constant at 16.3 MPa throughout the test.
  - b) lateral confining stress was decreased in 250 kPa increments from 16 MPa to 10.4 MPa. Back pressure was decreased simultaneously in 50 - 75 kPa increments from 12 MPa to 650 kPa. The average deviatoric loading rate was 35 kPa per minute.
  - c) vertical and volumetric deformations were monitored during the test.



TEST TOS 6: SAMPLE DATAPretest Saline Creek Sample No. 16:

Dia.:	$\varnothing = 7.600$ cm	$w = 0.022$
Height:	$H = 15.107$ cm	$B = 0.167$
Area:	$A = 45.365$ cm <sup>2</sup>	
Volume:	$V = 685.33$ ml	$V_s = 461.2$ ml
Mass:	$M = 1453$ g	$V_v = 224.1$ ml
$M_s$ :	$= 1222$ g	Dry Density = $1.783$ Mg/m <sup>3</sup>

Density:	$= 2.120$ Mg/m <sup>3</sup>
Porosity:	$= 0.327$
Void Ratio:	$= 0.486$ g

Failed Sample No. 16 After Test TOS 6



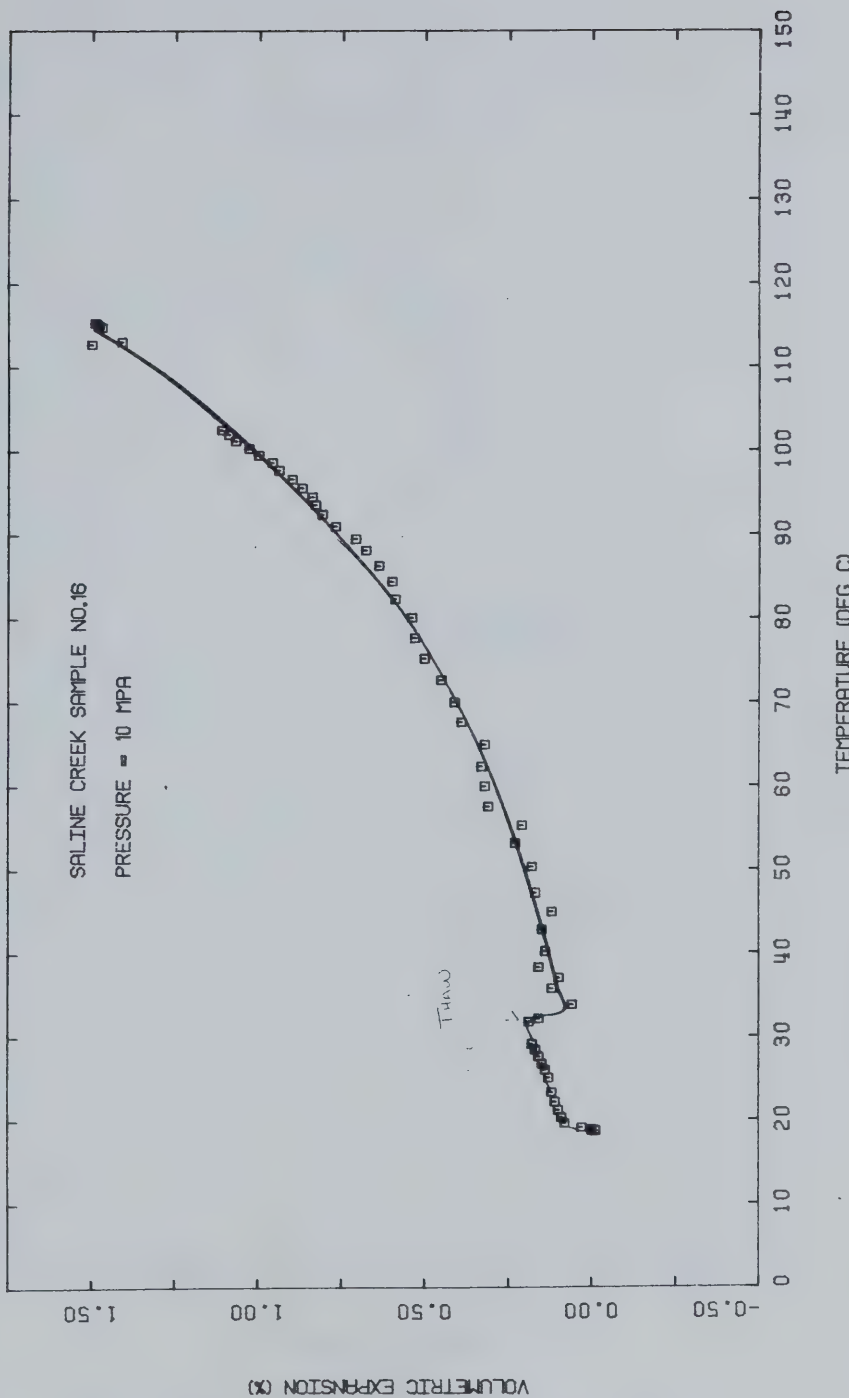


FIGURE E6.1 Triaxial Test T056: Drained Thermal Expansion



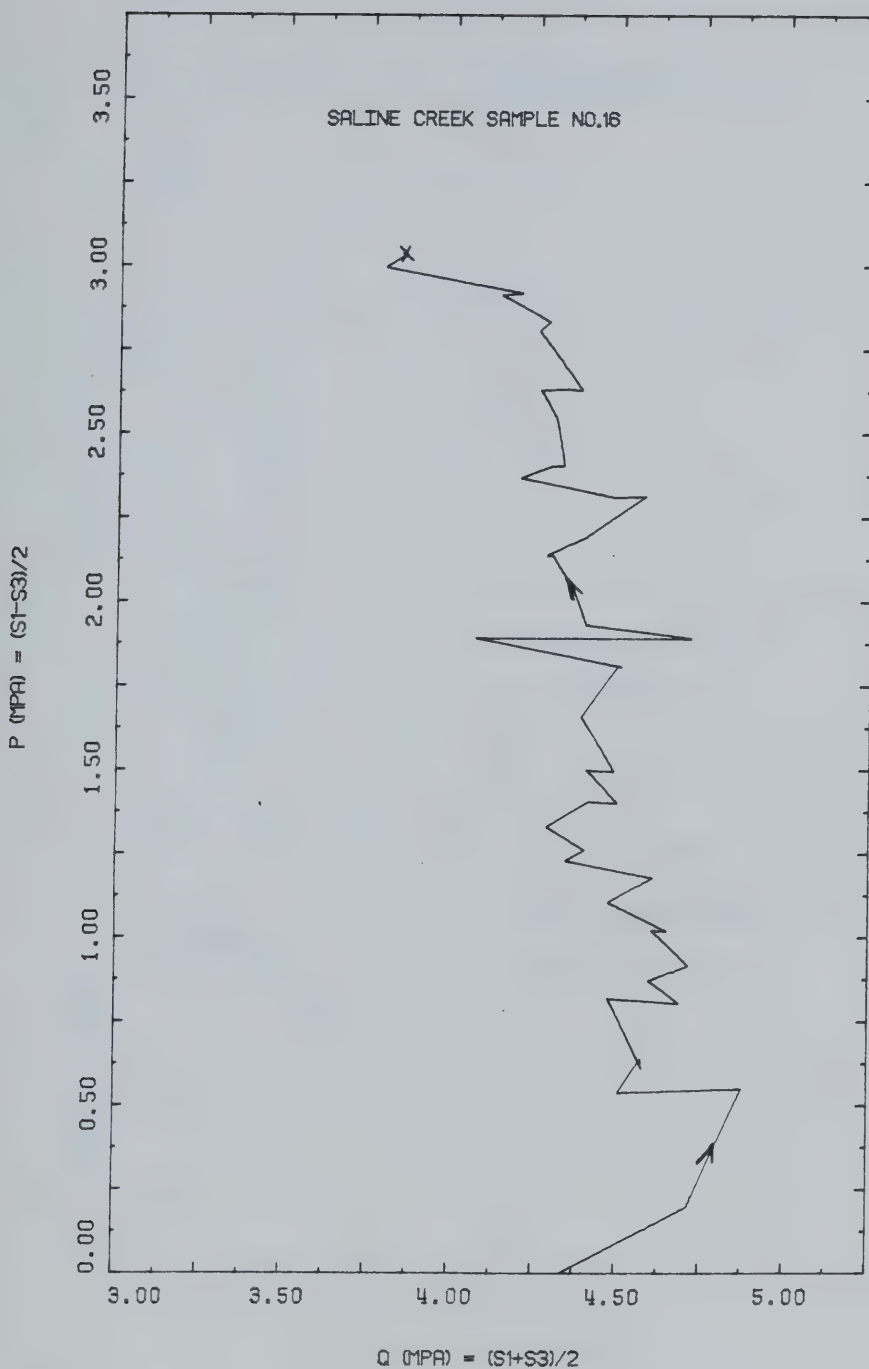


FIGURE E6.2 Triaxial Test TOS6: Stress Path



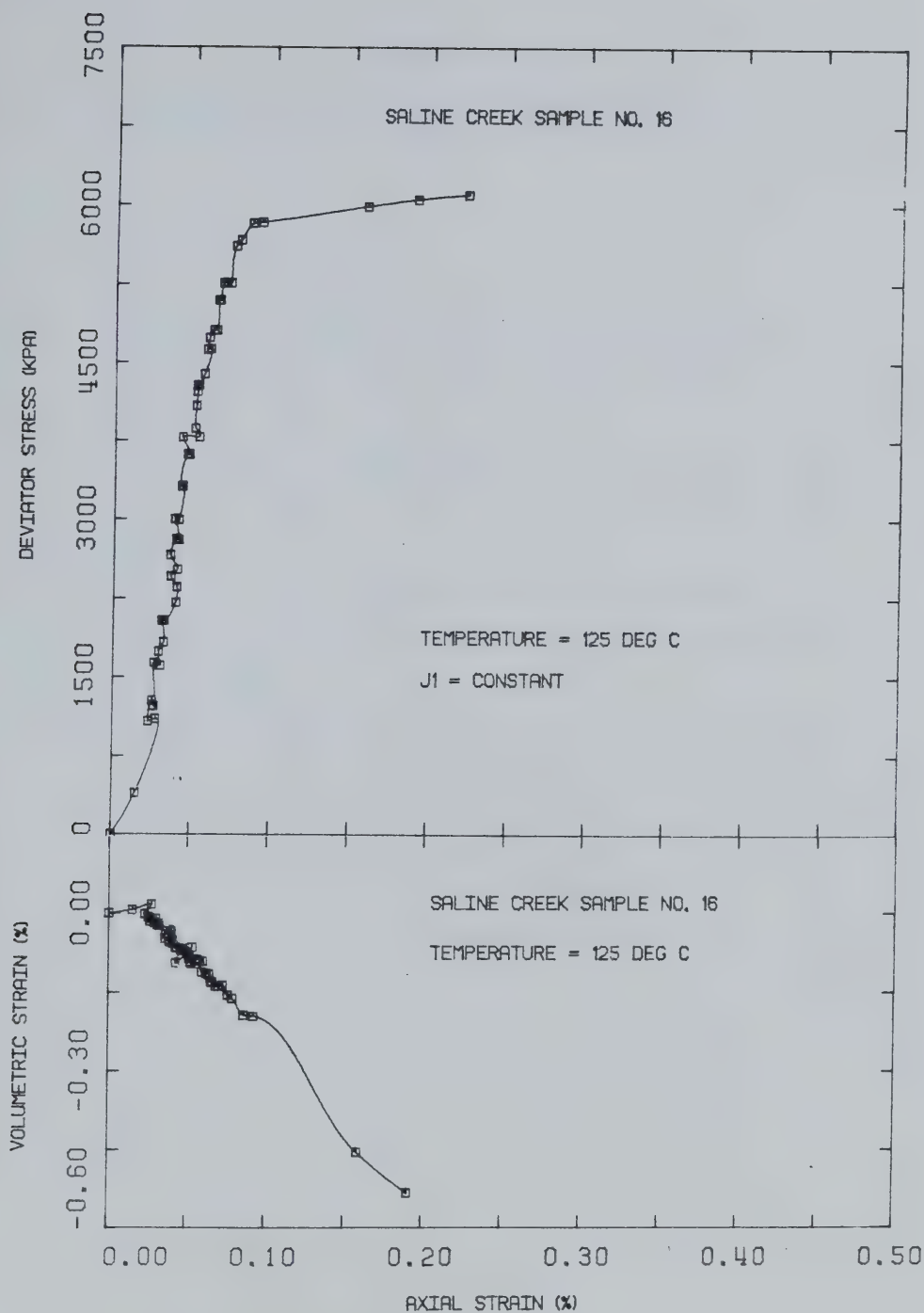


FIGURE E6.3 Triaxial Test TOS6: Deviator Stress Vs. Strain



## TEST TOS 7

Drained Triaxial Compression of Saline Creek Sample No. 45  
at 125°C and 4 MPa Effective Confining Stress

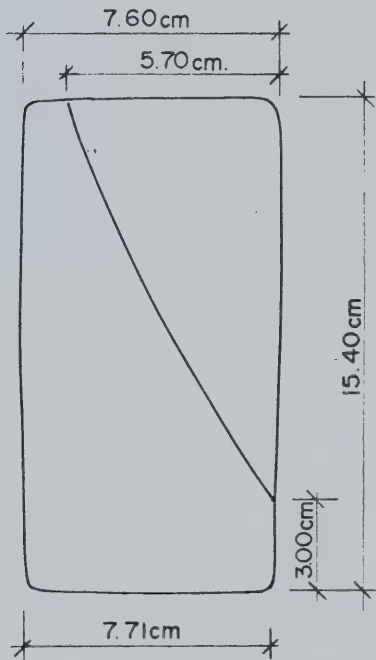
Procedural Details: Test TOS 7

1. Sample 45 was thawed and back saturated for 24 hours under 10 MPa back pressure and 14 MPa isotropic effective confining stress.
2. The apparatus and sample were heated to 125°C; the volume of pore fluid expelled from the sample was monitored during heating.
3. A drained triaxial compression test was performed:
  - a) vertical stress was increased at an average rate of 70 kPa/minute;
  - b) lateral confining stress was maintained constant at 14 MPa and the back pressure was held constant at 10 MPa;
  - c) vertical deformation and volume change were monitored during deviatoric passive compression.



TEST TOS 7: SAMPLE DATAPretest Saline Creek Sample No. 45:

Dia.:  $\emptyset = 7.610$  cm       $w = 0.022$   
Height:  $H = 15.430$  cm       $B = 0.160$   
Area:  $A = 45.484$   $\text{cm}^2$   
Volume:  $V = 701.82$  ml       $V_S = 453.3$  ml  
Mass:  $M = 1420$  g       $V_V = 248.5$  ml  
 $M_S = 1201$  g      Dry Density =  $1.712 \text{ Mg/m}^3$   
Density: =  $2.023 \text{ Mg/m}^3$   
Porosity: = 0.354  
Void Ratio: = 0.548 g

Failed Sample No. 45 After Test TOS 7



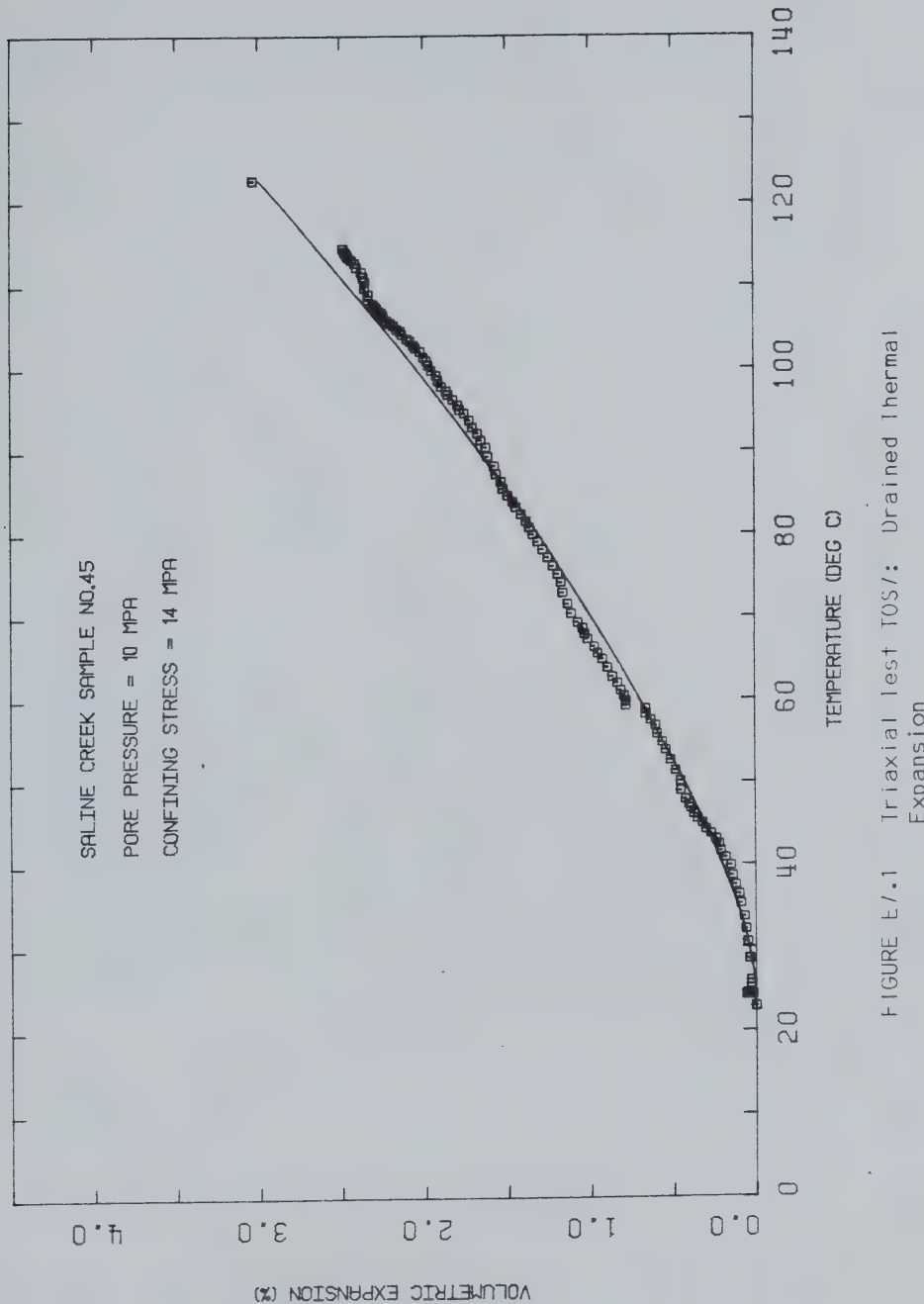


FIGURE E-1      Triaxial Test TOS/: Drained Thermal Expansion



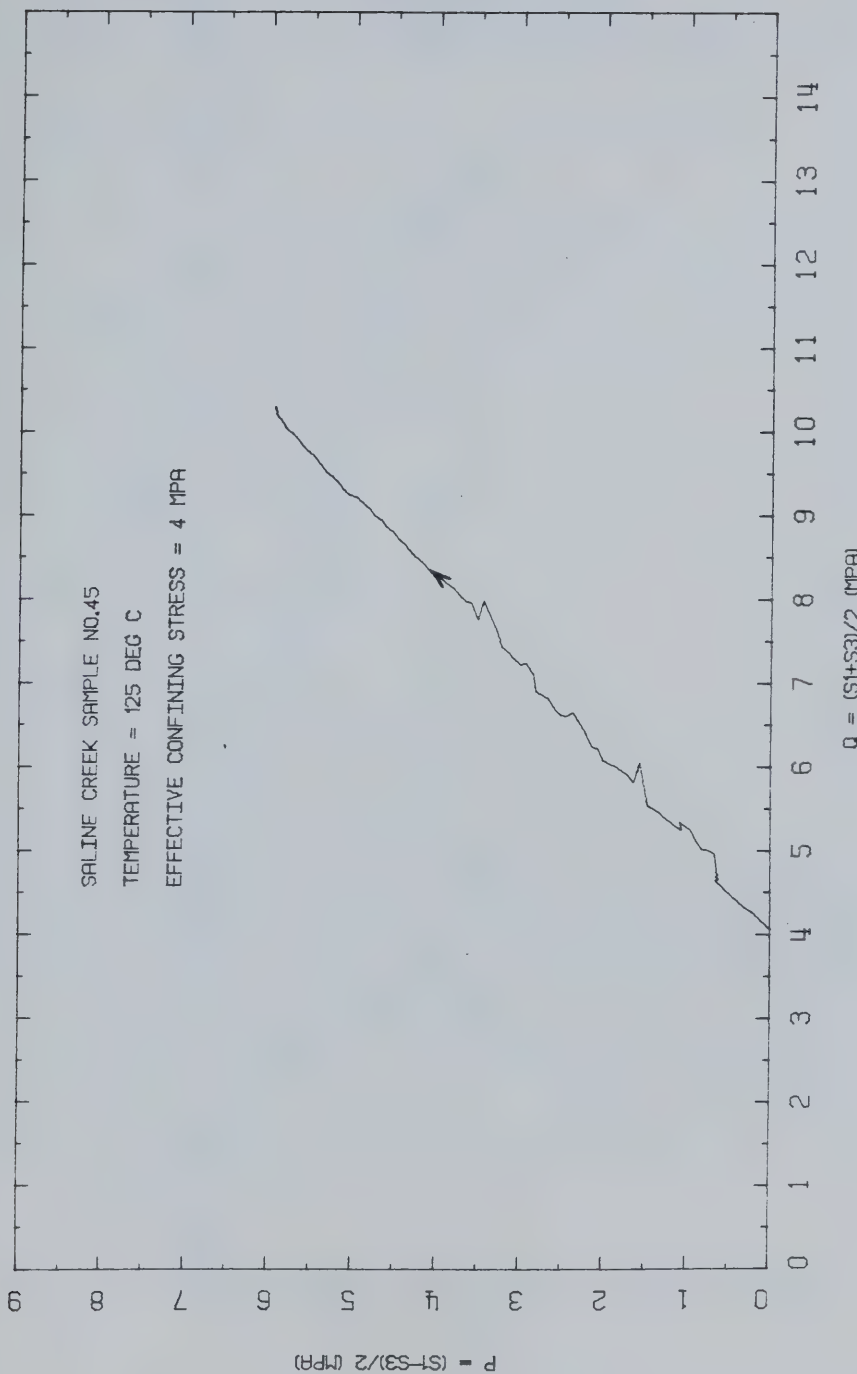


FIGURE E7.2 Triaxial Test TOS7: Stress Path



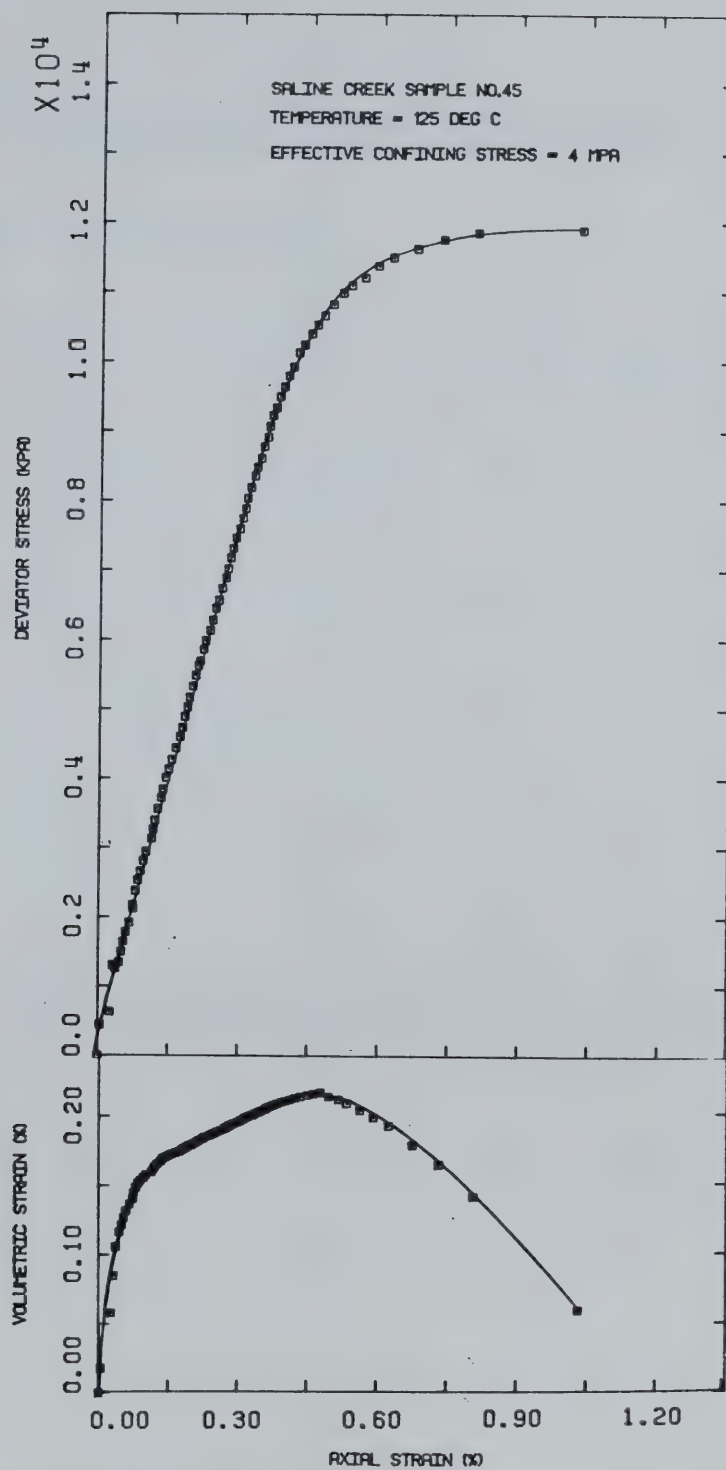


FIGURE E7.3 Triaxial Test TOS7: Deviator Stress Vs. Strain



## TEST TOS 8

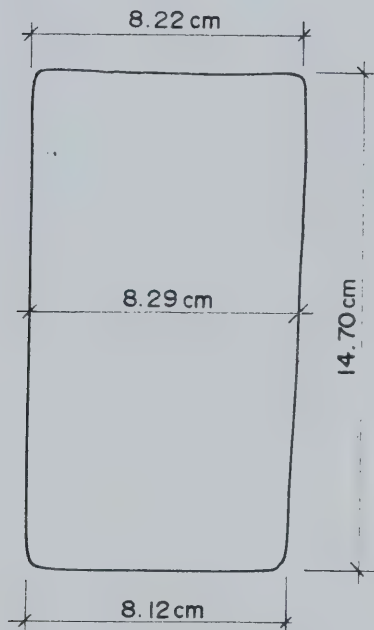
Undrained and Drained Isotropic Compression of Saline Creek  
Sample No. 28 at 220°C - O-Ring Seal FailureProcedural Details: Test TOS 8

1. Sample 28 was thawed and back saturated for 21 hours under 10 MPa back pressure and 12 MPa effective confining stress.
2. The sample was heated to 220°C under drained conditions. Drained thermal expansion and the volume of pore fluid expelled from the sample were measured during heating up to 200°C. However, lateral deformation measurements on the sample are not considered reliable due to stiffness of the strain gauge clamp. A small amount of leakage of cell fluid past the O-ring seal at the base of the triaxial cell was noticed at this stage. Heating was discontinued.
3. A B-test was performed over a range of isotropic confining stress from 12 - 20.5 MPa. Volumetric strain was determined during undrained loading from internal vertical and lateral strain gauge measurements giving undrained compressibility. Again however, lateral deformation measurements were not reliable.
4. A drained isotropic compression test was started. However, severe leakage of cell fluid started during the first loading cycle. The test was discontinued.



TEST TOS 8: SAMPLE DATAPretest Saline Creek Sample No. 28:

Dia.:  $\varnothing$  = 7.433 cm      w = 0.025  
Height: H = 15.293 cm      B = 0.170  
Area: A = 45.393 cm<sup>2</sup>  
Volume: V = 663.61 ml      V<sub>S</sub> = 428.8 ml  
Mass: M = 1358 g      V<sub>V</sub> = 234.8 ml  
M<sub>S</sub> = 1136 g      Dry Density = 1.712 Mg/m<sup>3</sup>  
Density: = 2.046 Mg/m<sup>3</sup>  
Porosity: = 0.354  
Void Ratio: = 0.548 g

Failed Sample No. 28 After Test TOS 8



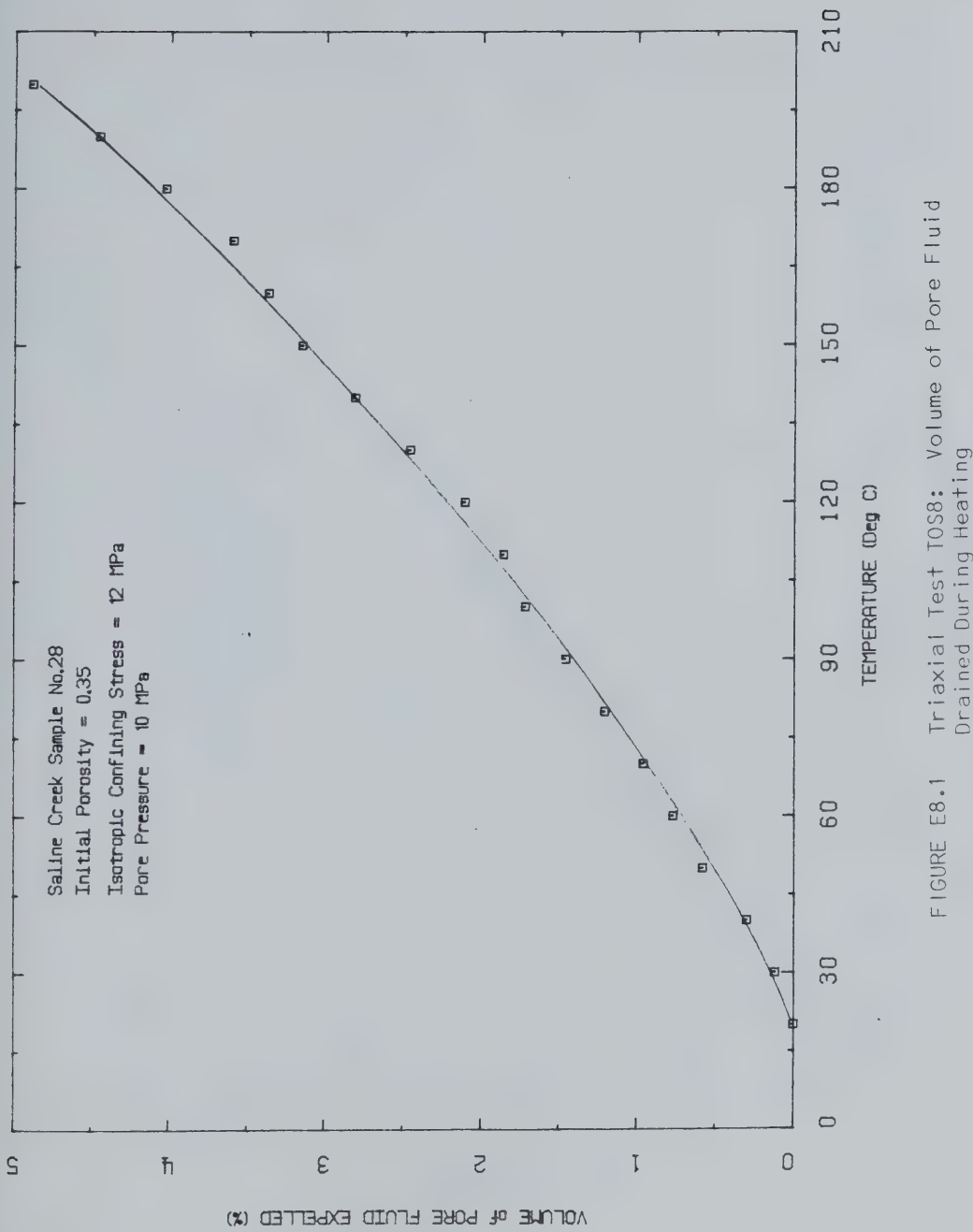


FIGURE E8.1 Triaxial Test TOS8: Volume of Pore Fluid Drained During Heating



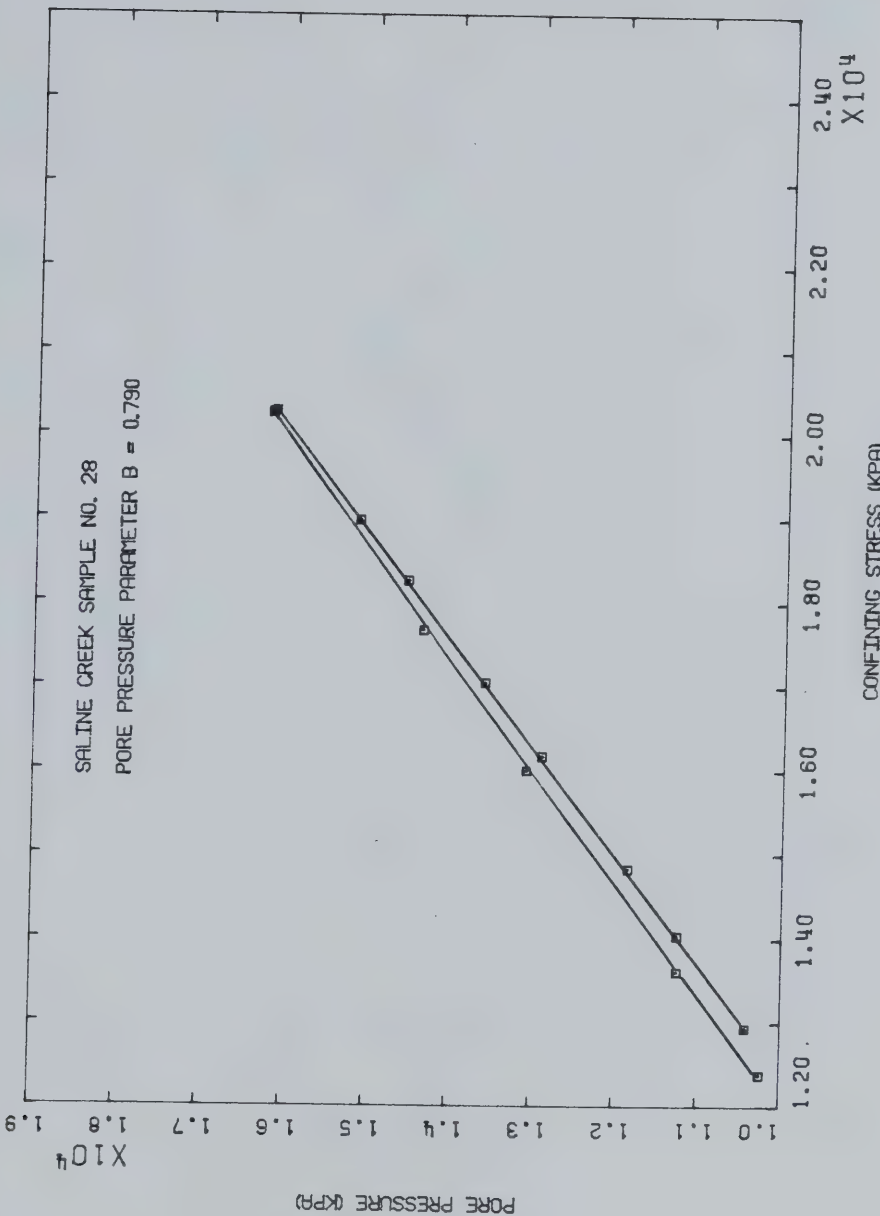
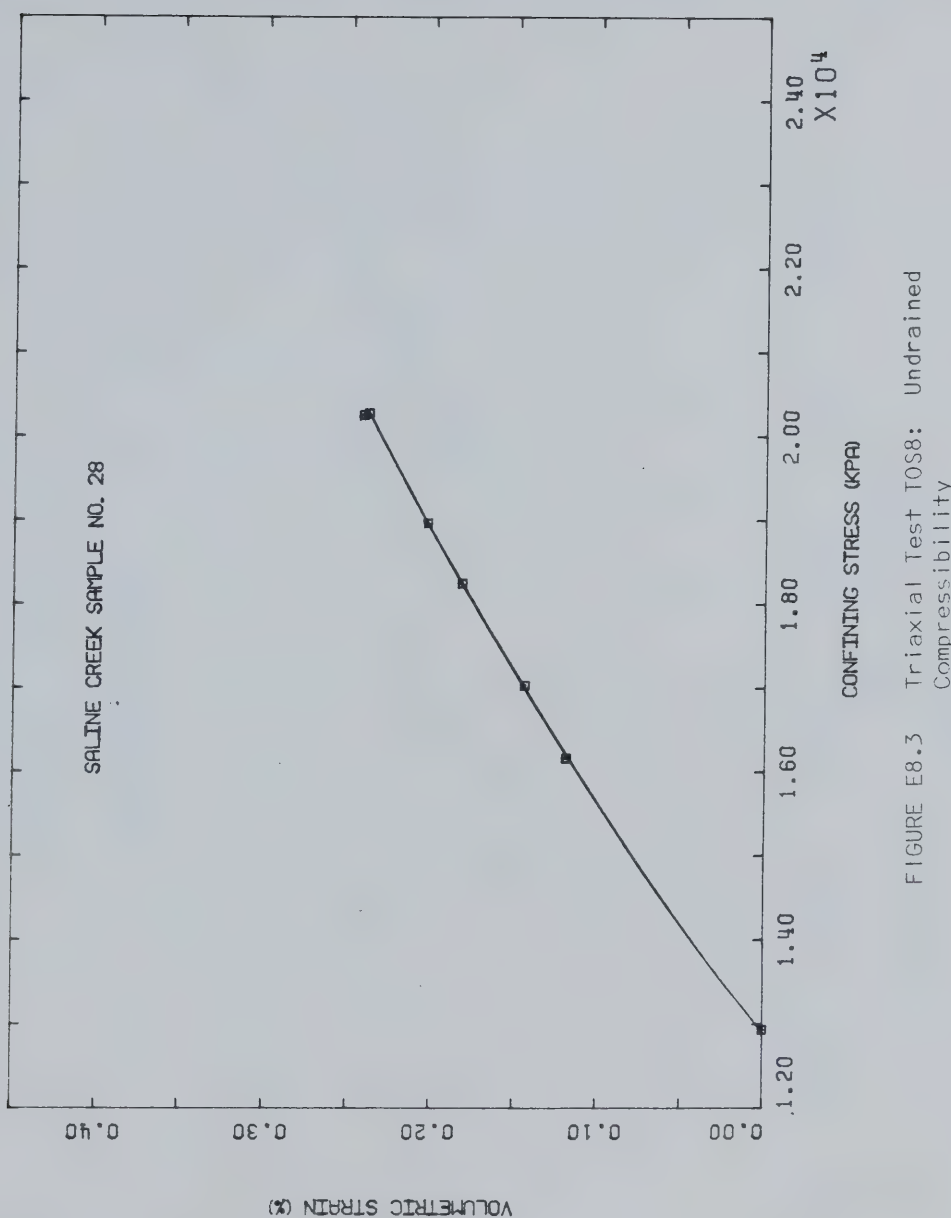


FIGURE E-8.2 Triaxial Test TOS8: B Test







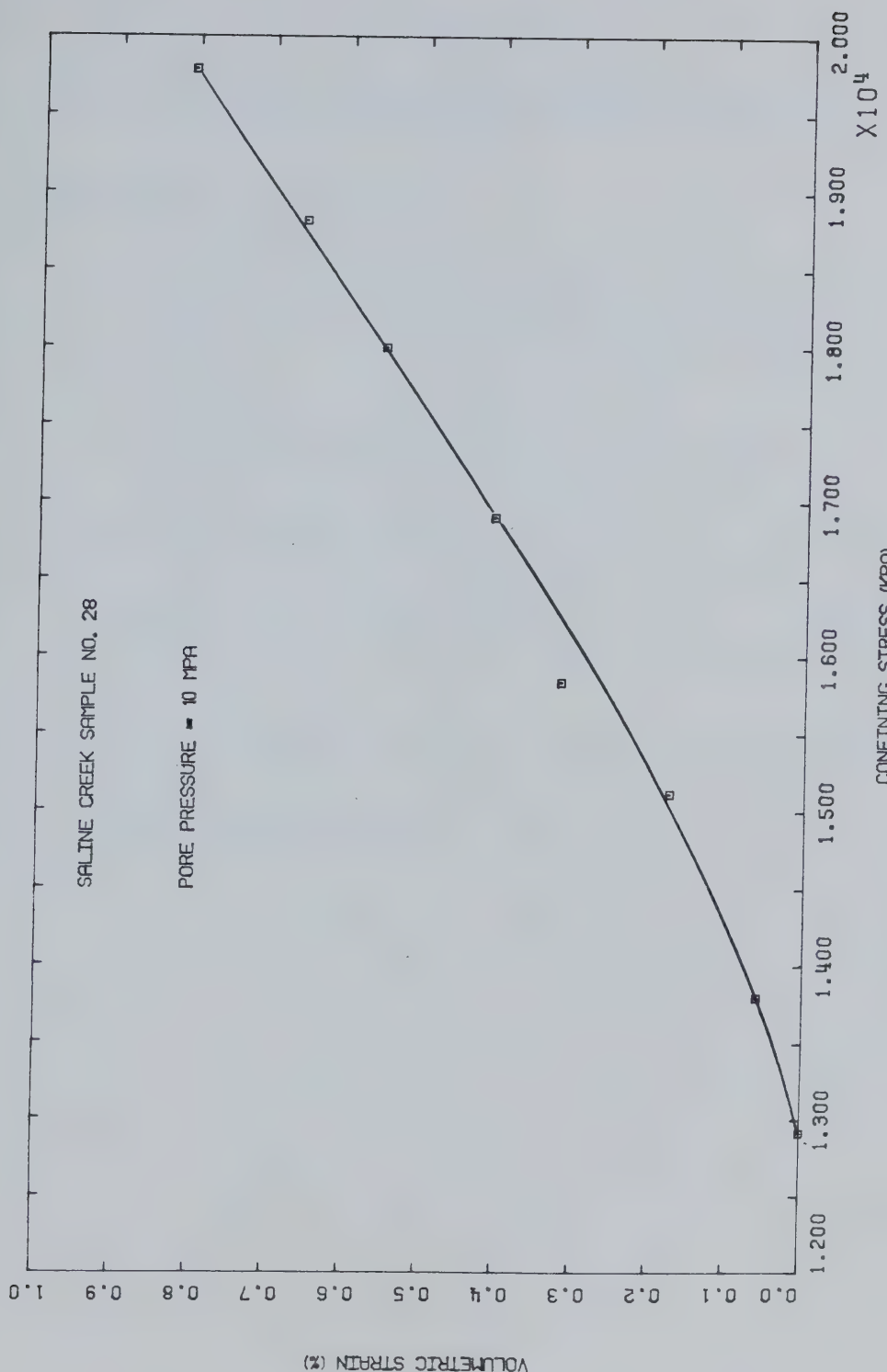


FIGURE L8.4 Triaxial Test TSS8: Drained Isotropic Compressibility



## TEST TOS 9

Triaxial Test: Thermal Expansion of Saline Creek Sample  
No. 27 to 235°C Followed by Membrane Failure

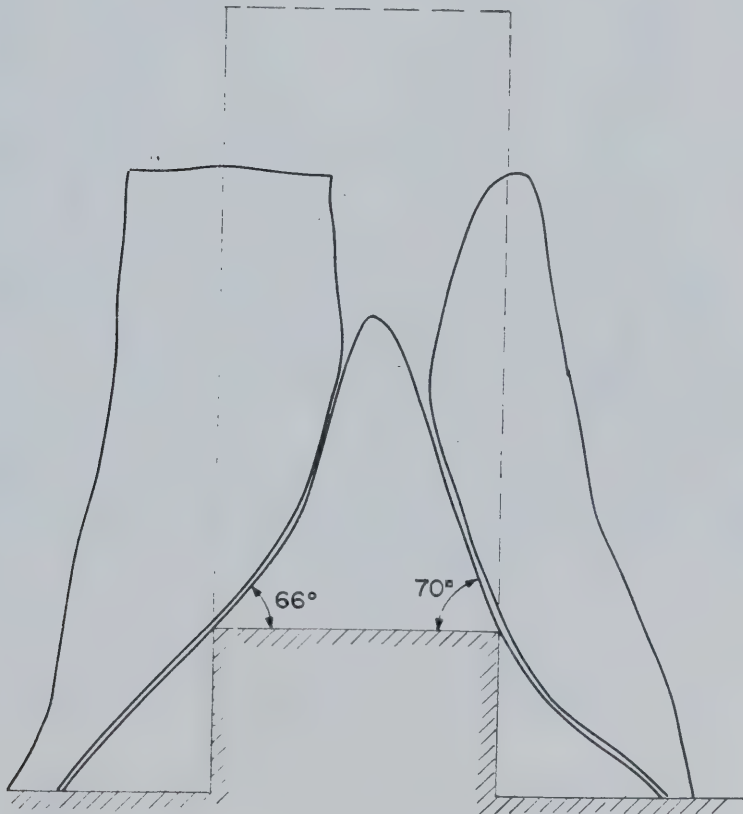
Procedural Details: Test TOS 9

1. Sample 27 was thawed and back saturated for 24 hours under 10 MPa back pressure and 14 MPa isotropic confining stress.
2. The apparatus and sample were heated under drained conditions (i.e. constant back pressure) to 240°C. The silicone rubber triaxial membrane depolymerized during the night resulting in back pressure/confining pressure communication. Heated silicone oil cell fluid was injected through the sample under a differential pressure which was initially 4 MPa.  
The metal bellows interface in the volume change device was damaged.
3. The test was terminated.



TEST TOS 9: SAMPLE DATAPretest Saline Creek Sample No. 27:

Dia.:  $\varnothing = 7.610$  cm       $w = 0.012$   
Height:  $H = 15.110$  cm       $B = 0.171$   
Area:  $A = 45.484$   $\text{cm}^2$   
Volume:  $V = 687.26$  ml       $V_S = 455.8$  ml  
Mass:  $M = 1429$  g       $V_V = 231.5$  ml  
 $M_S = 1208$  g      Dry Density =  $1.757$   $\text{Mg/m}^3$   
Density:      =  $2.079$   $\text{Mg/m}^3$   
Porosity:      =  $0.337$   
Void Ratio:      =  $0.508$  g

Sample 27 After Test TOS 9 Meltdown



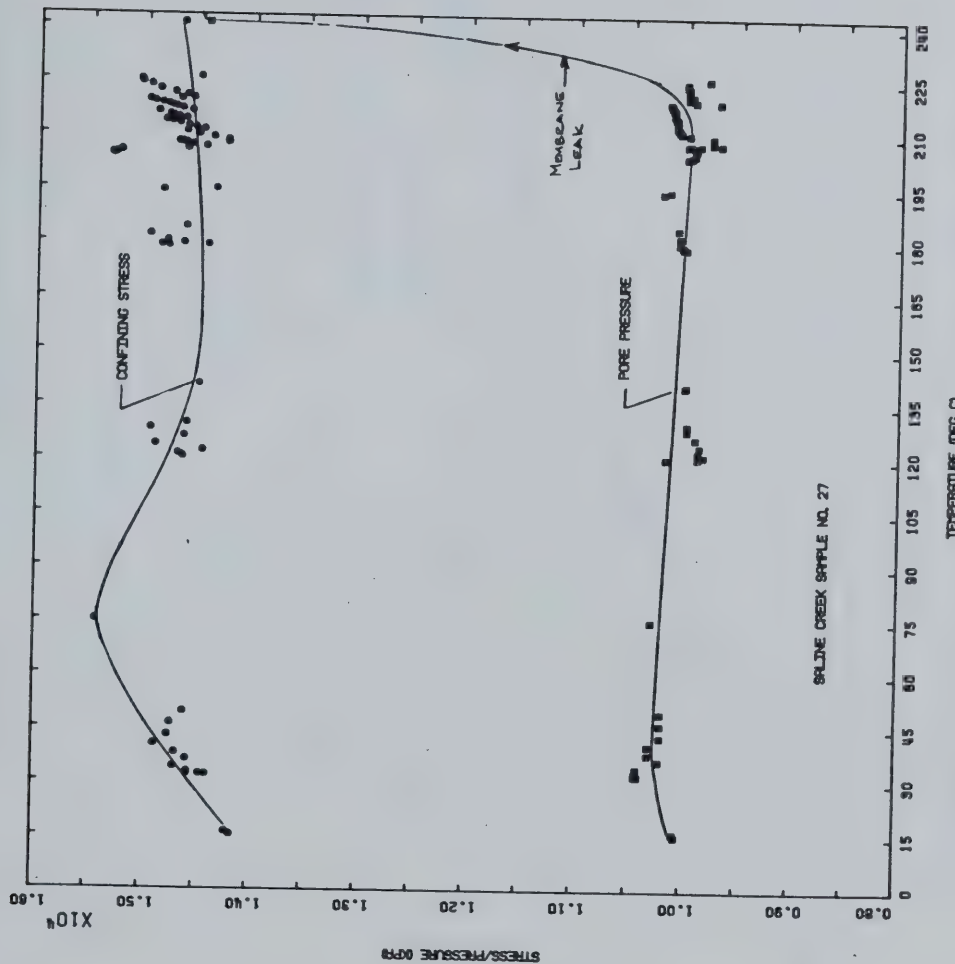


FIGURE E9.1 Triaxial Test T09: Confining Stress/Pore Pressure Vs. Temperature



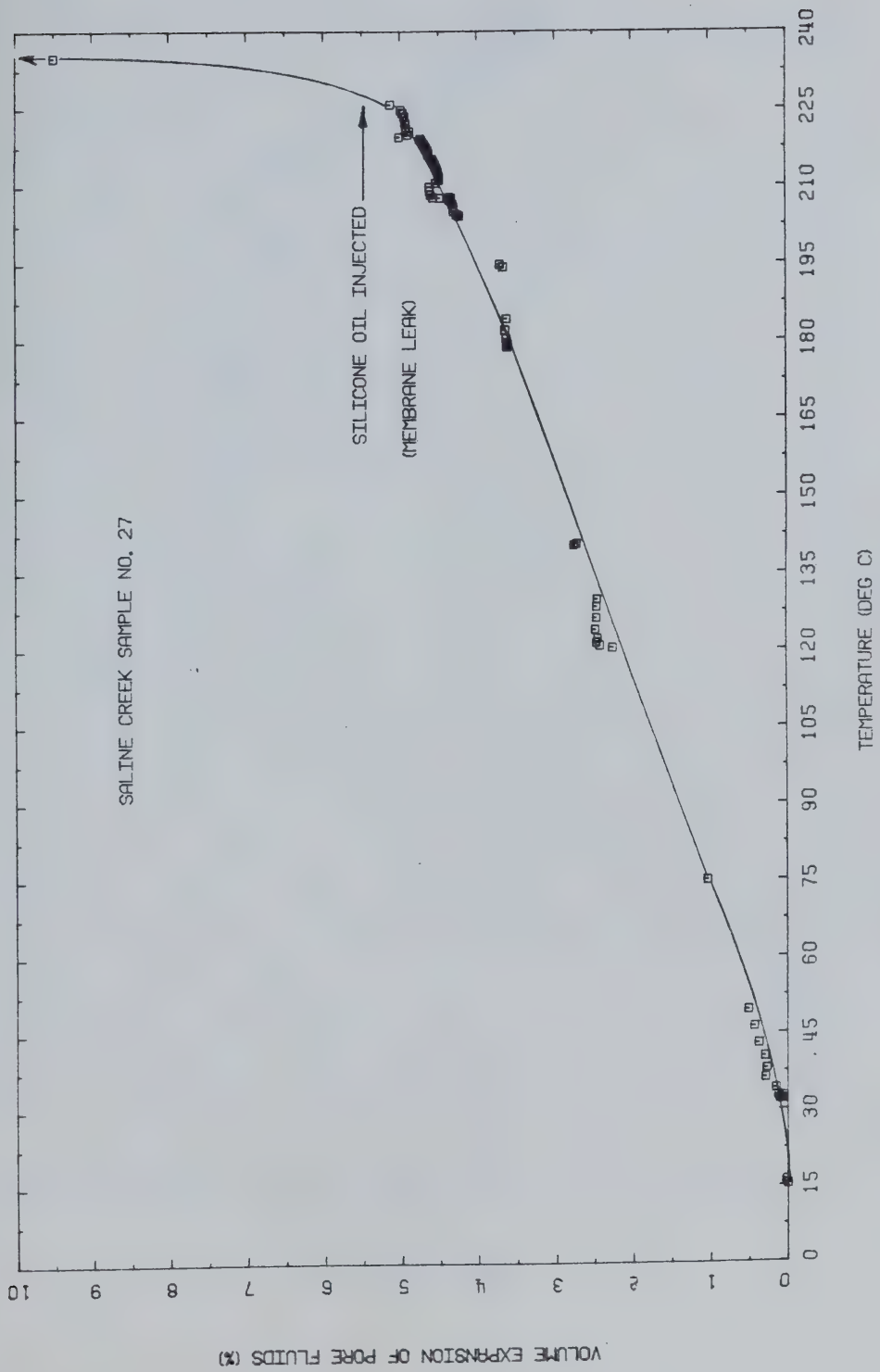


FIGURE E9.2 Triaxial Test TOS9: Thermal Expansion of Pore Fluids



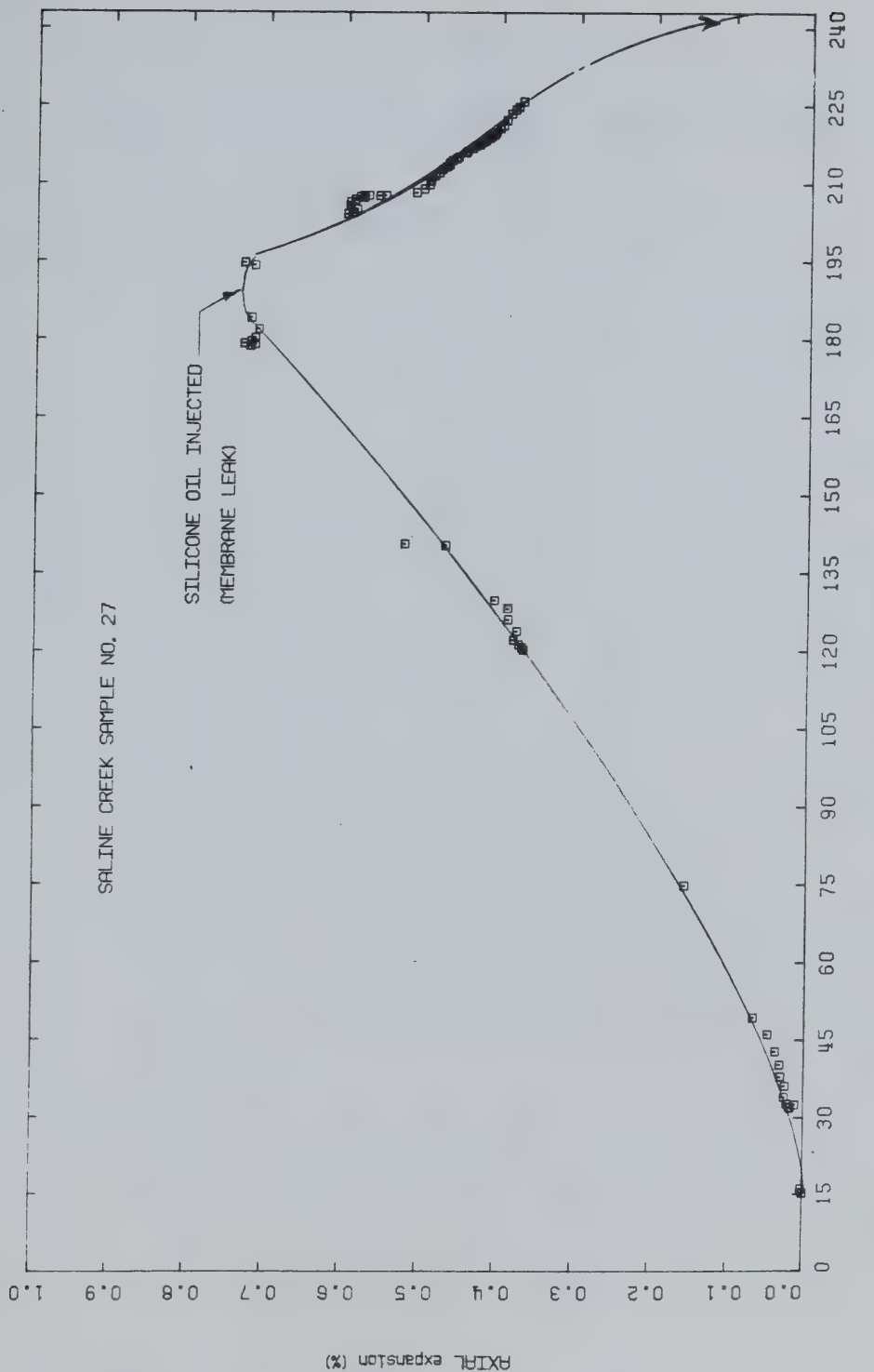


FIGURE E9.3 Triaxial Test TOS9: Vertical Thermal Expansion



## TEST TOS 10

## Pore Pressure Response to Undrained Heating and Undrained Triaxial Compression of Saline Creek Sample No. 20 at 200°C

Procedural Details: Test TOS 10

1. Sample 20 was thawed and back saturated for 21 hours under 10 MPa back pressure and 14 MPa isotropic confining stress.
2. Back pressure and isotropic confining stress were reduced simultaneously to 2 MPa and 6 MPa, respectively.
3. A B-test was performed over a range of confining stresses from 6 to 14 MPa to evaluate degree of saturation.
4. The back pressure and isotropic confining stress were set at 2 MPa and 6 MPa, respectively. Back pressure drainage valves were closed.
5. The apparatus and sample were heated slowly. Pore pressure response to undrained heating was monitored and confining stress was adjusted in an effort to maintain isotropic effective confining stress constant at about 4 MPa. The pressure limits of the apparatus were approached after a 25°C to 30°C temperature increase. Undrained heating was conducted in 8 heating cycles from 17.5°C to 200°C as shown in Table E2.
6. At the end of each heating cycle, the back pressure drainage valves were opened; back pressure and isotropic confining stress were reduced simultaneously to about 2-3



MPa respectively, always maintaining 4 MPa effective confining stress in the sample. Volume change (i.e. the volume of pore fluid expelled from the sample) was measured each time the drainage valves were opened.

7. Drainage valves were then reclosed and the next heating cycle started.
8. After undrained heating cycle No. 8 was completed, the back pressure was adjusted to 10 MPa and the isotropic confining stress was simultaneously adjusted to 14 MPa.
9. Back pressure drainage valves were closed. Vertical compression stress was increased at an average rate of 70 kPa per minute with lateral confining stress maintained constant and the temperature at 200°C.  
Pore pressure and vertical deformation were monitored during the undrained triaxial compression test.



TABLE E-2

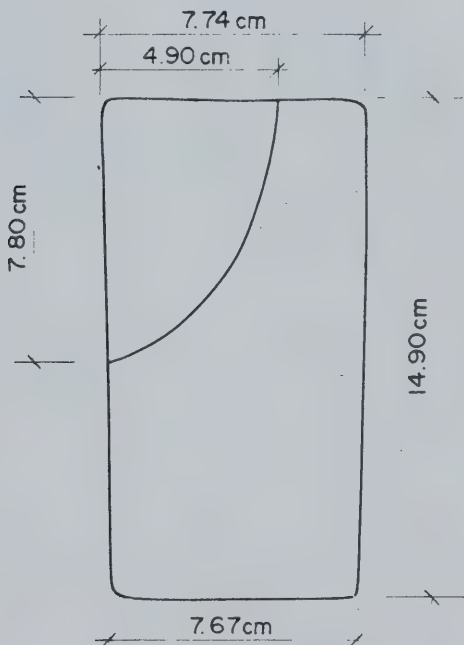
Test TOS 10: Summary of Undrained Heating Cycles

Heating Cycle	Temperature Range	$\Delta T$ (°C)	$\Delta u$ (kPa)	$B = \frac{\Delta u}{\Delta T}$ (kPa/°C)	Average Effective Confining Stress (kPa)	$F = B \frac{1}{\overline{b_3}}$ (°C <sup>-1</sup> )
1	25 - 44	19	18760	980	3630	0.270
2	50 - 64	14	12300	880	3800	0.232
3	70 - 85	15	12400	825	3900	0.212
4	90 - 106	16	12600	790	3800	0.208
5	112 - 109	17	11900	700	3700	0.189
6	130 - 152	22	12900	590	4100	0.144
7	157 - 176	19	9500	500	4900	0.102
8	182 - 195	13	5900	450	4200	0.107



TEST TOS 10: SAMPLE DATAPretest Saline Creek Sample No. 20:

Dia.:  $\emptyset = 7.610$  cm      w = 0.026  
Height: H = 15.170 cm      B = 0.178  
Area: A = 45.484 cm<sup>2</sup>  
Volume: V = 690.00 ml      V<sub>S</sub> = 449.0 ml  
Mass: M = 1432 g      V<sub>V</sub> = 241.5 ml  
M<sub>S</sub>: = 1190 g      Dry Density = 1.724 Mg/m<sup>3</sup>  
Density: = 2.076 Mg/m<sup>3</sup>  
Porosity: = 0.349  
Void Ratio: = 0.536 g

Sample 27 After Test TOS 10



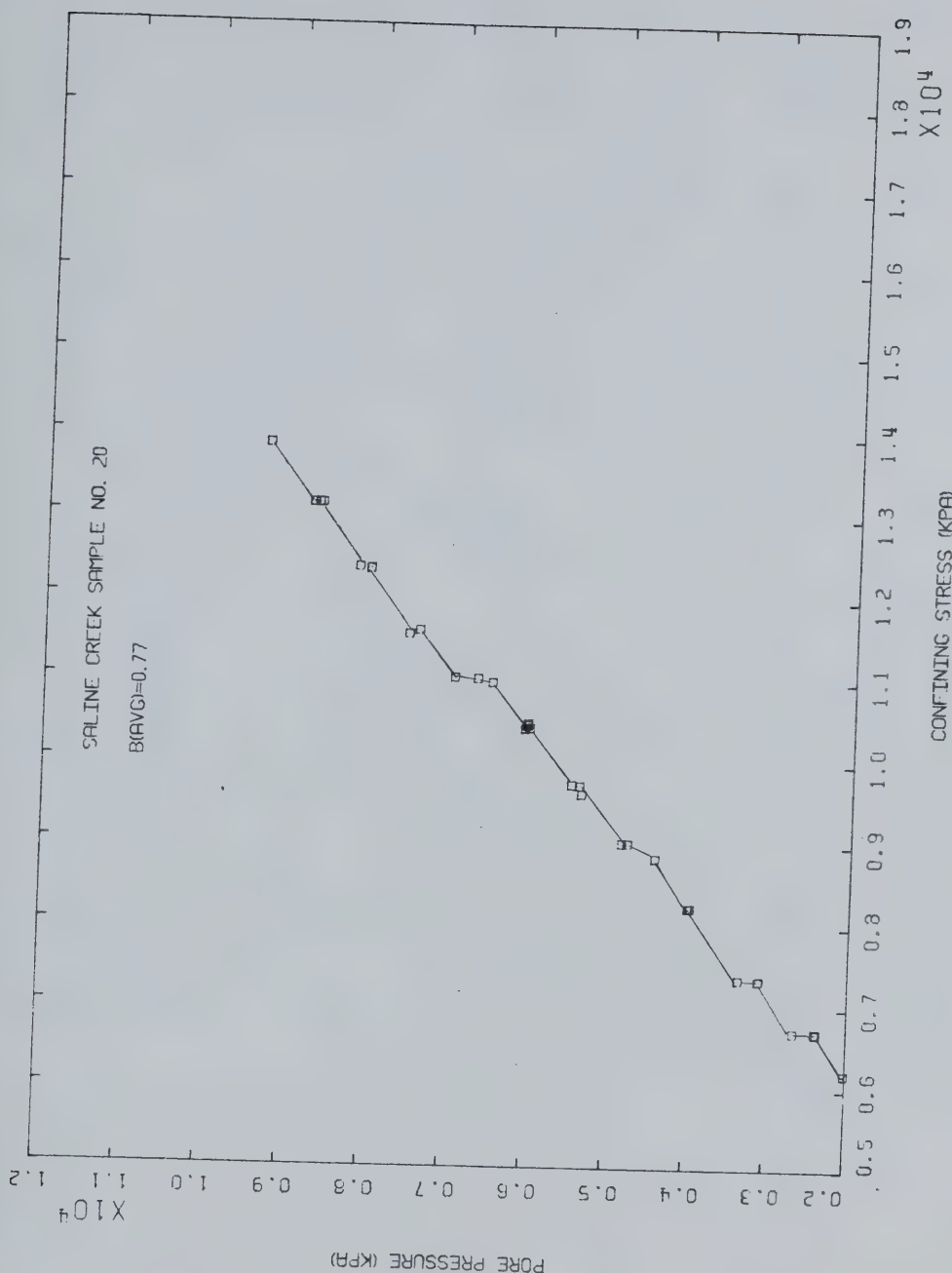


FIGURE E10.1 Triaxial Test TOS10: Modified B Test



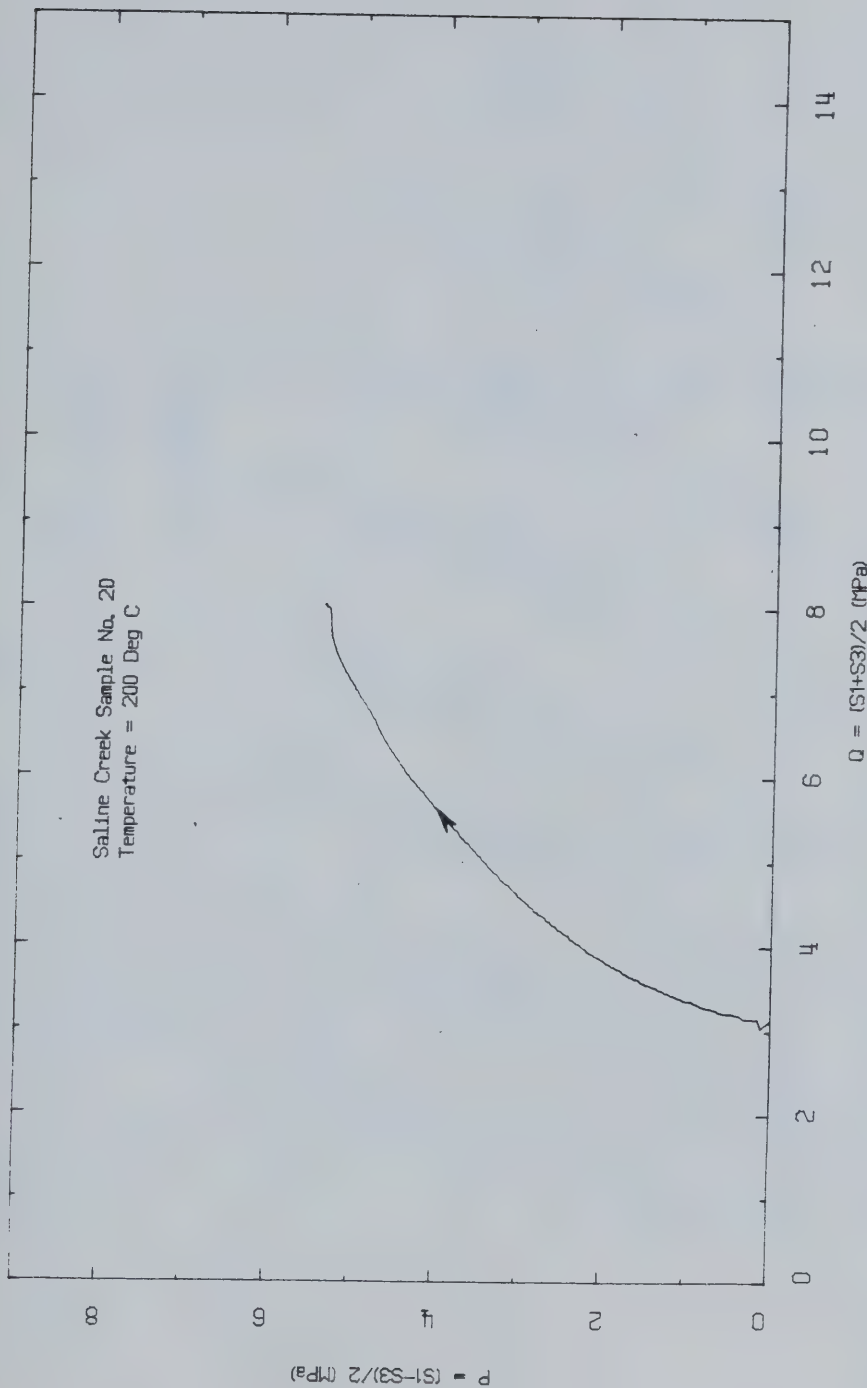


FIGURE E10.2 Triaxial Test TOS10: Effective Stress Path



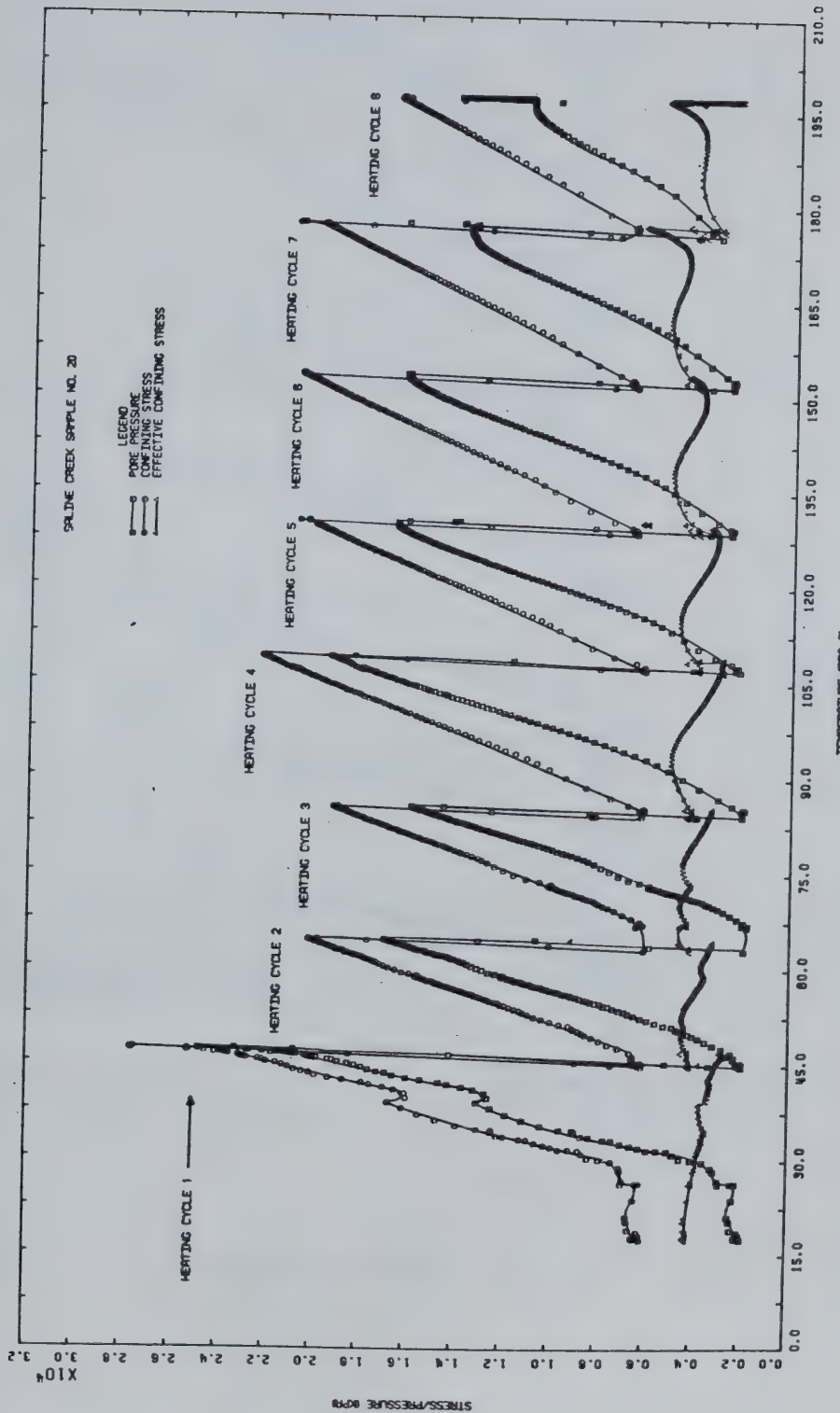


FIGURE E10.3 Triaxial Test TOS10: Pore Pressure and Confining Stress Changes With Temperature



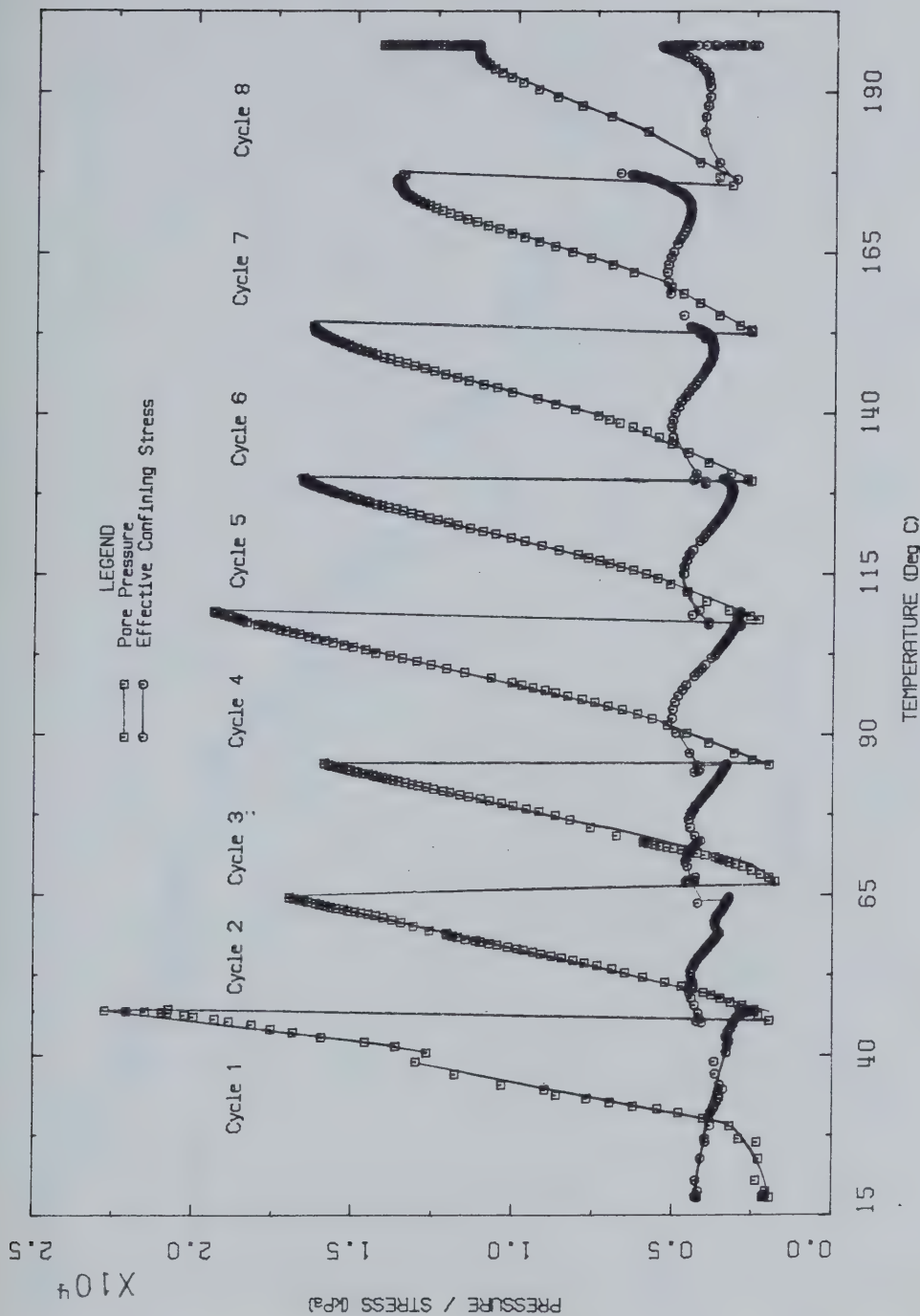


FIGURE E10.4 Triaxial Test T010: Pore Pressure Response to Undrained Heating



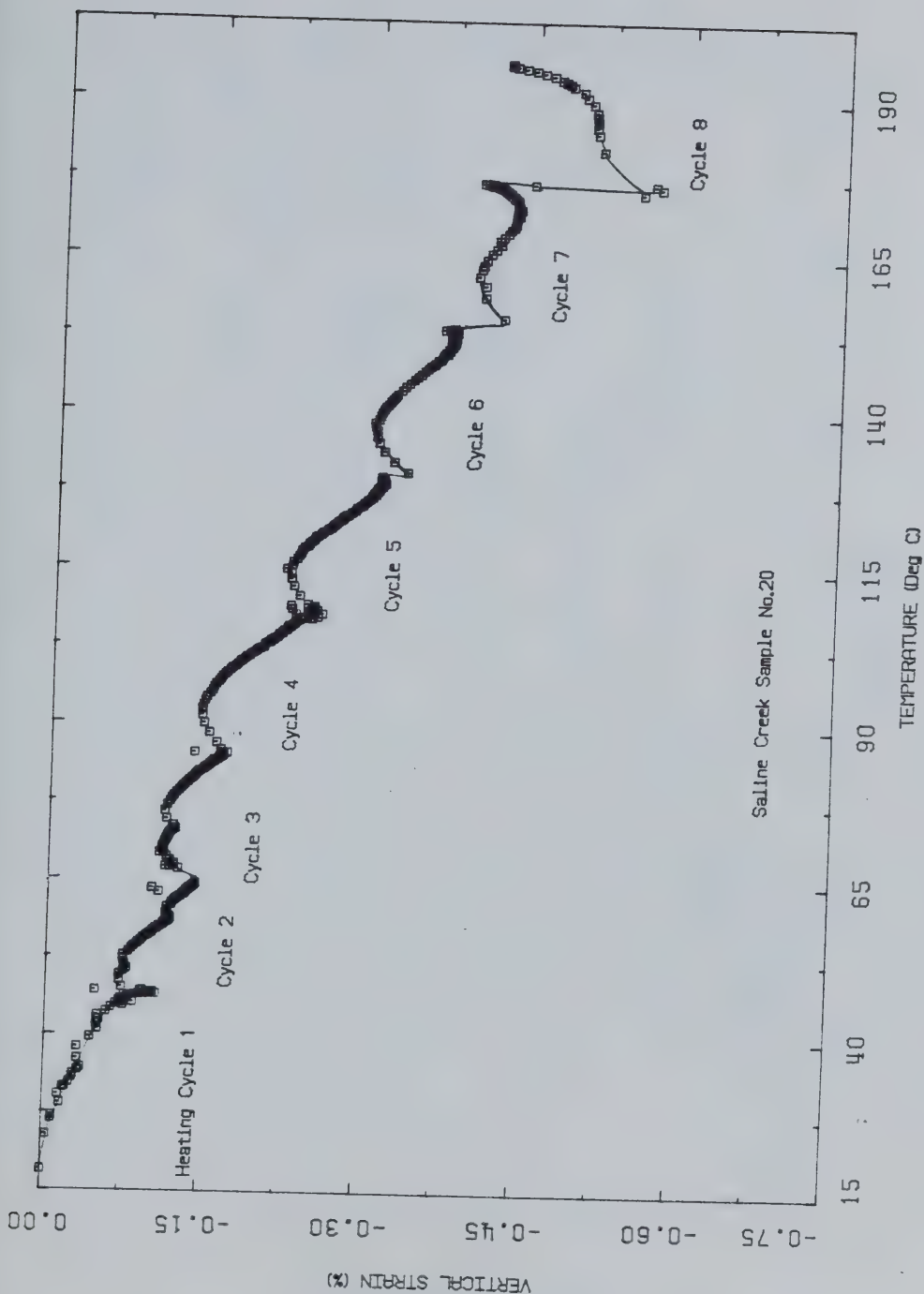


FIGURE E10.5 Triaxial Test TOS10: Vertical Strain During Heating



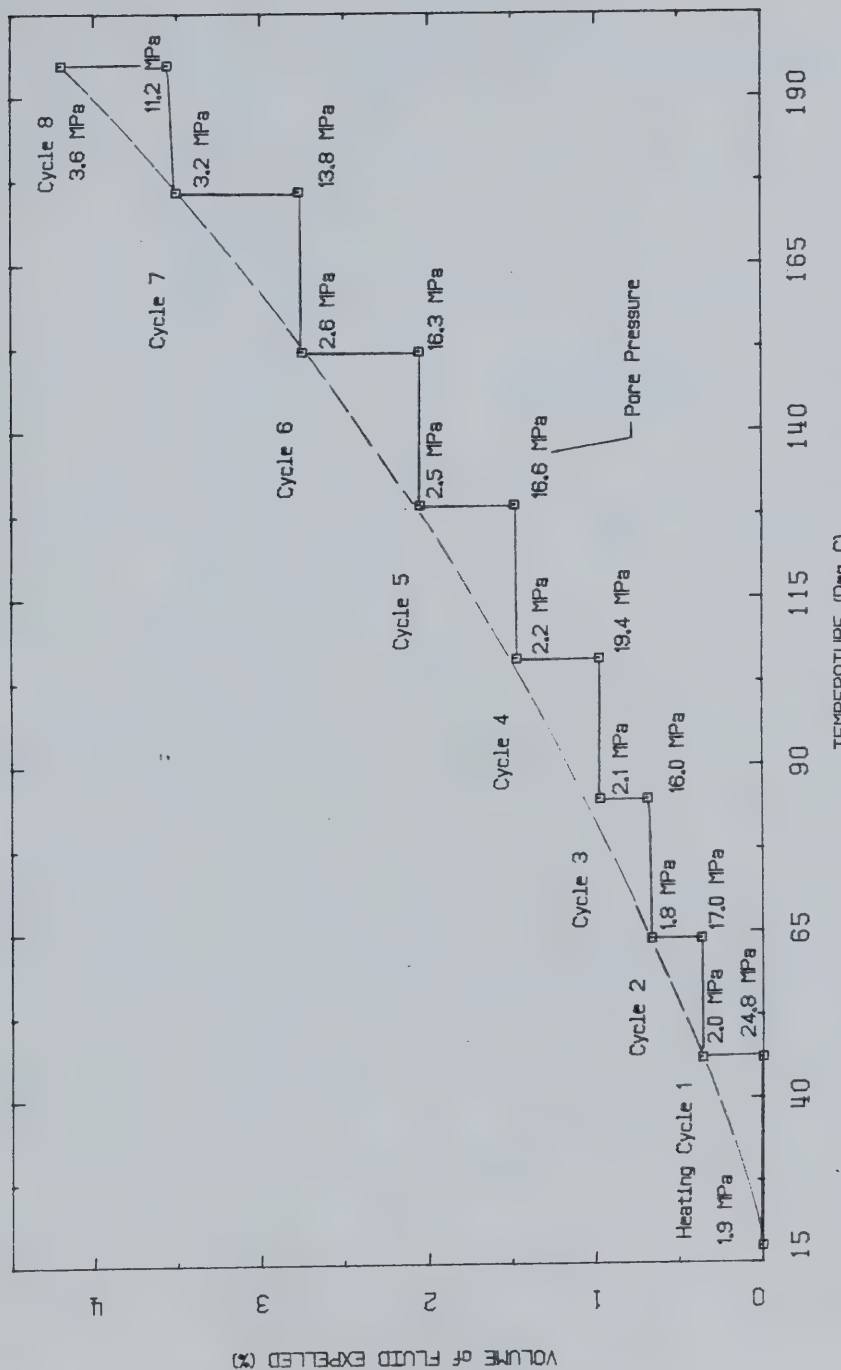


FIGURE E10.6 Triaxial Test T0510: Volume of Fluid Expelled During Heating



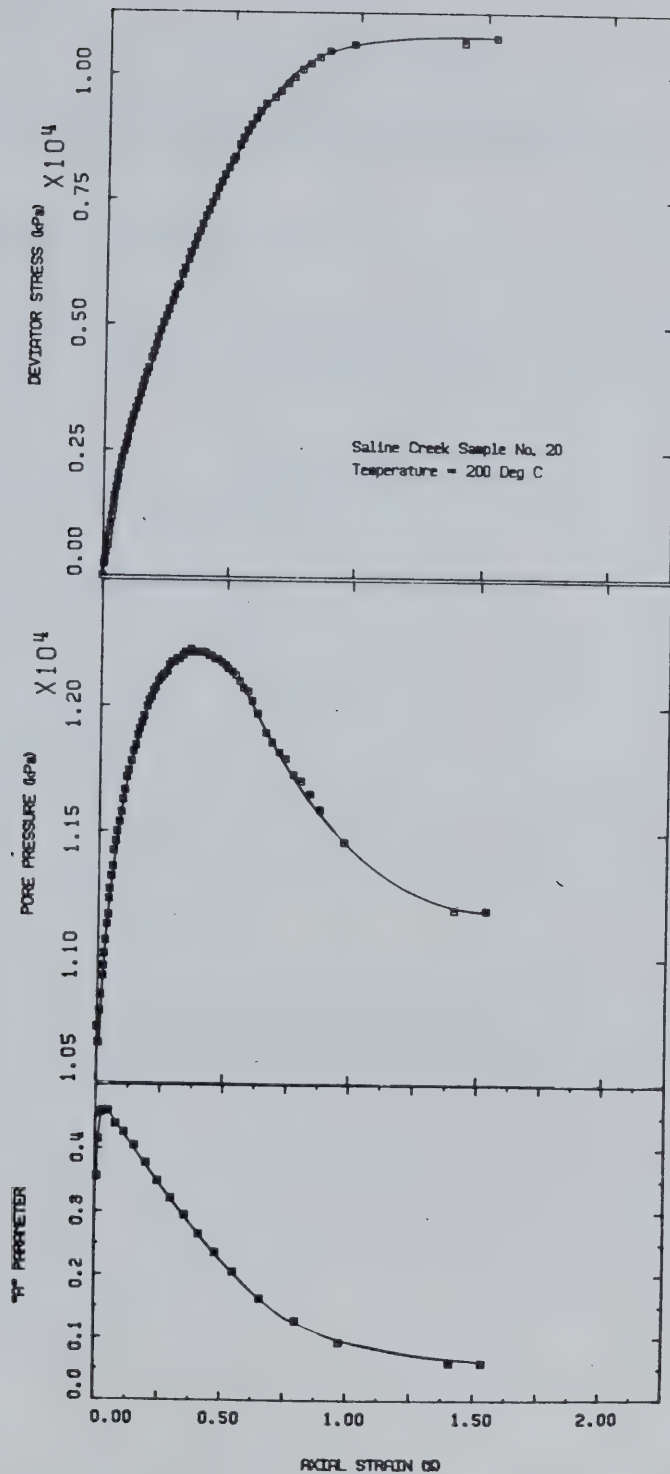


FIGURE E10.7 Triaxial Test TOS10: Deviator Stress and Undrained Pore Pressure Changes With Vertical Strain



## TEST TOS 11

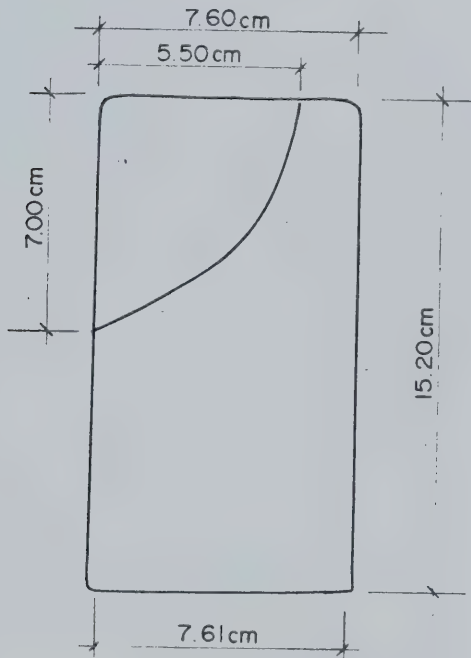
Anisotropic Consolidation and Undrained Heating  
to Failure of Saline Creek Oil Sand Sample No. 22Procedural Details: Test TOS 11

1. Sample 22 was thawed and back saturated for 22 hours under 10 MPa back pressure and 14 MPa isotropic confining stress.
2. Back pressure and confining stress were simultaneously reduced to 4 MPa and 8 MPa respectively.
3. A B-test was performed to evaluate degree of saturation over the range of confining stress 8 - 14.5 MPa.
4. Back pressure and isotropic confining stress were adjusted to 10 MPa and 14 MPa simultaneously.
5. Vertical compression stress was increased to 16 MPa. The sample was allowed to consolidate for approximately one hour under the ratio of horizontal to vertical effective stresses of 0.67.
6. Back pressure drainage valves were then closed. The apparatus and sample were heated slowly maintaining the vertical stress constant at 16 MPa and the horizontal stress constant at 14 MPa.  
Pore pressure and vertical (axial) strain were monitored during heating.
7. Heating was continued until shear failure (yielding) was observed at 101°C.



TEST TOS 11: SAMPLE DATAPretest Saline Creek Sample No. 22:

Dia.:  $\varnothing = 7.570 \text{ cm}$        $w = 0.025$   
Height:  $H = 15.300 \text{ cm}$        $B = 0.185$   
Area:  $A = 45.007 \text{ cm}^2$   
Volume:  $V = 688.60 \text{ ml}$        $V_S = 443.3 \text{ ml}$   
Mass:  $M = 1421 \text{ g}$        $V_V = 245.3 \text{ ml}$   
 $M_S = 1175 \text{ g}$       Dry Density =  $1.706 \text{ Mg/m}^3$   
Density:       $= 2.064 \text{ Mg/m}^3$   
Porosity:       $= 0.356$   
Void Ratio:       $= 0.553 \text{ g}$

Sample 22 After Test TOS 11



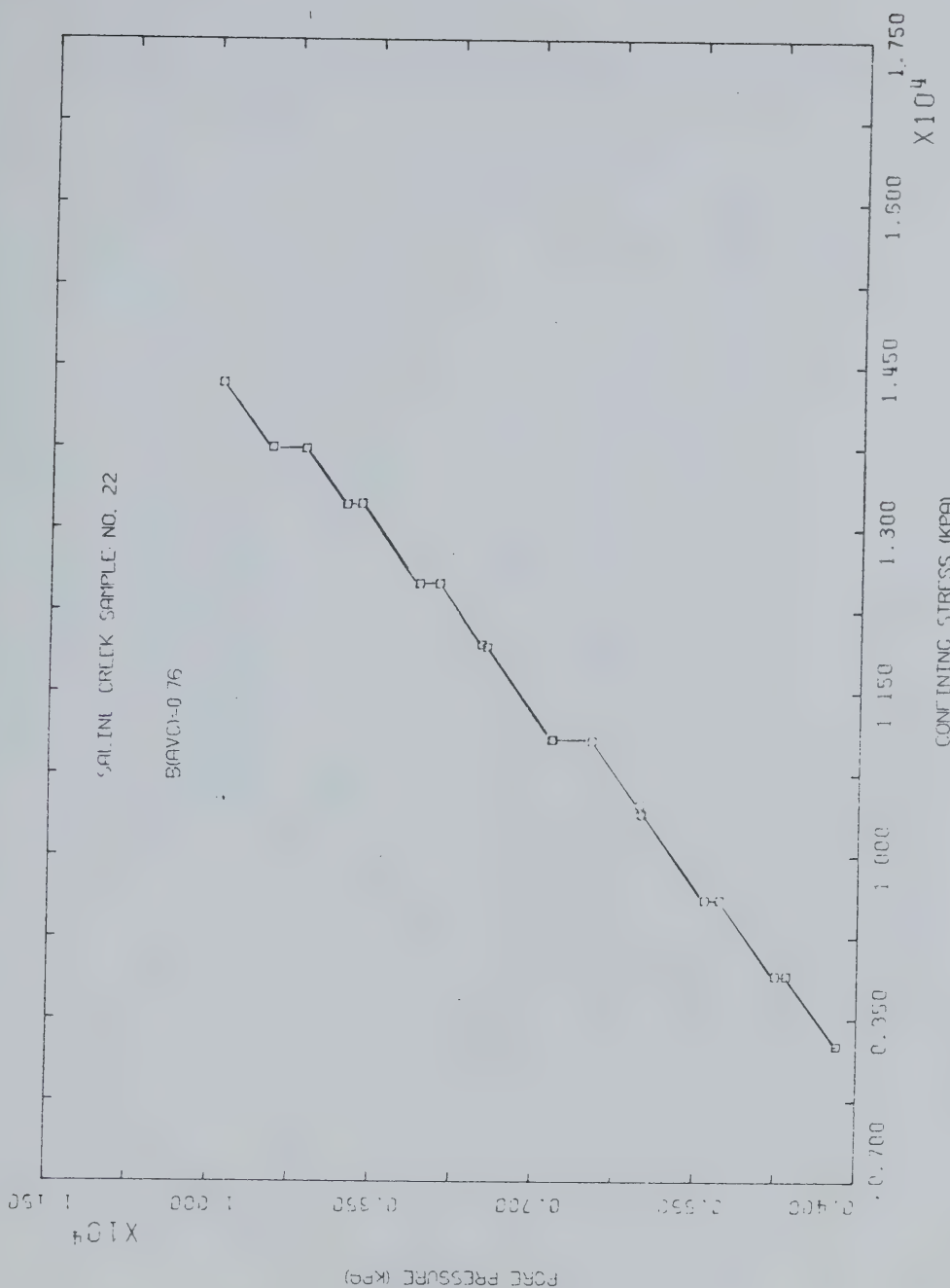


FIGURE E11.1 Triaxial Test TOS11: Modified B Test



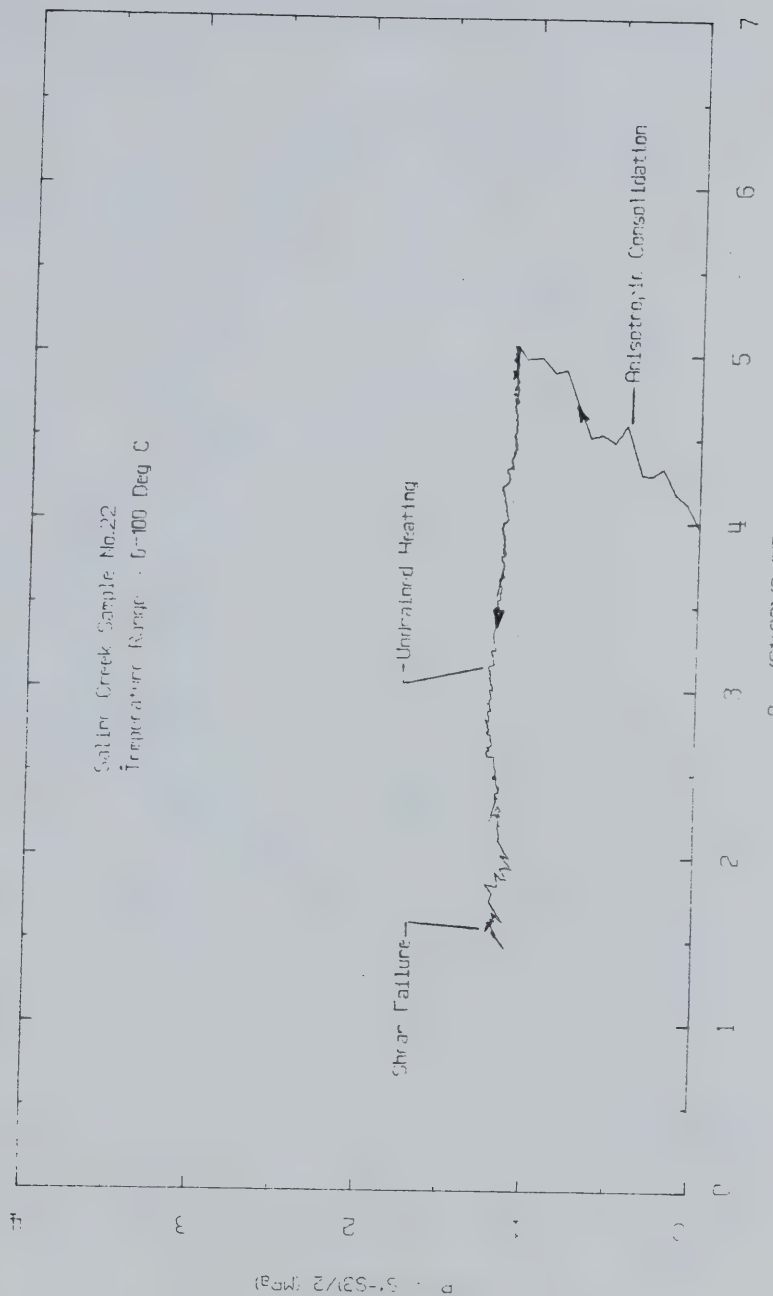


FIGURE F11.2 Triaxial Test TOS11: Stress Path



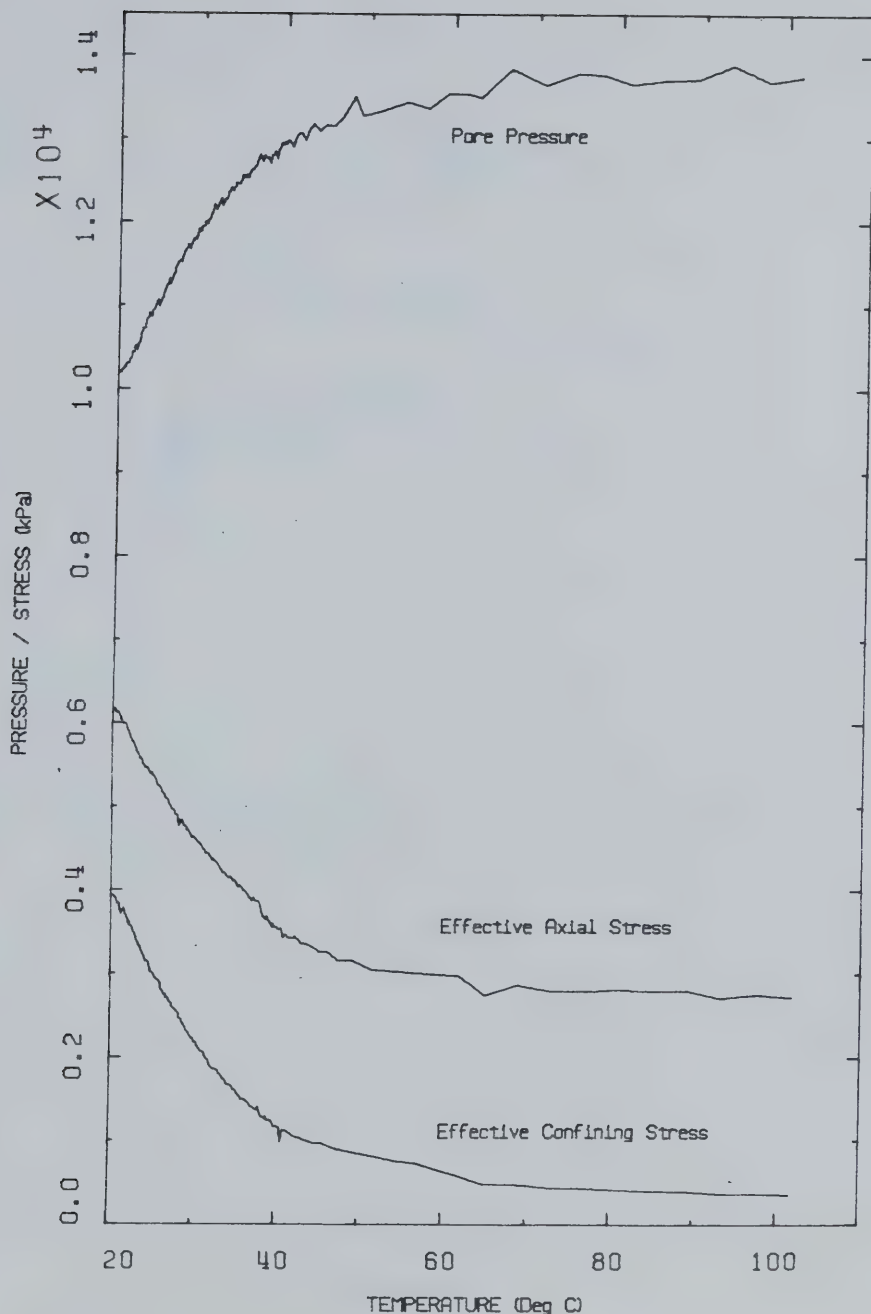


FIGURE E11.3 Triaxial Test TOS11: Pore Pressure and Effective Stress Changes During Undrained Heating



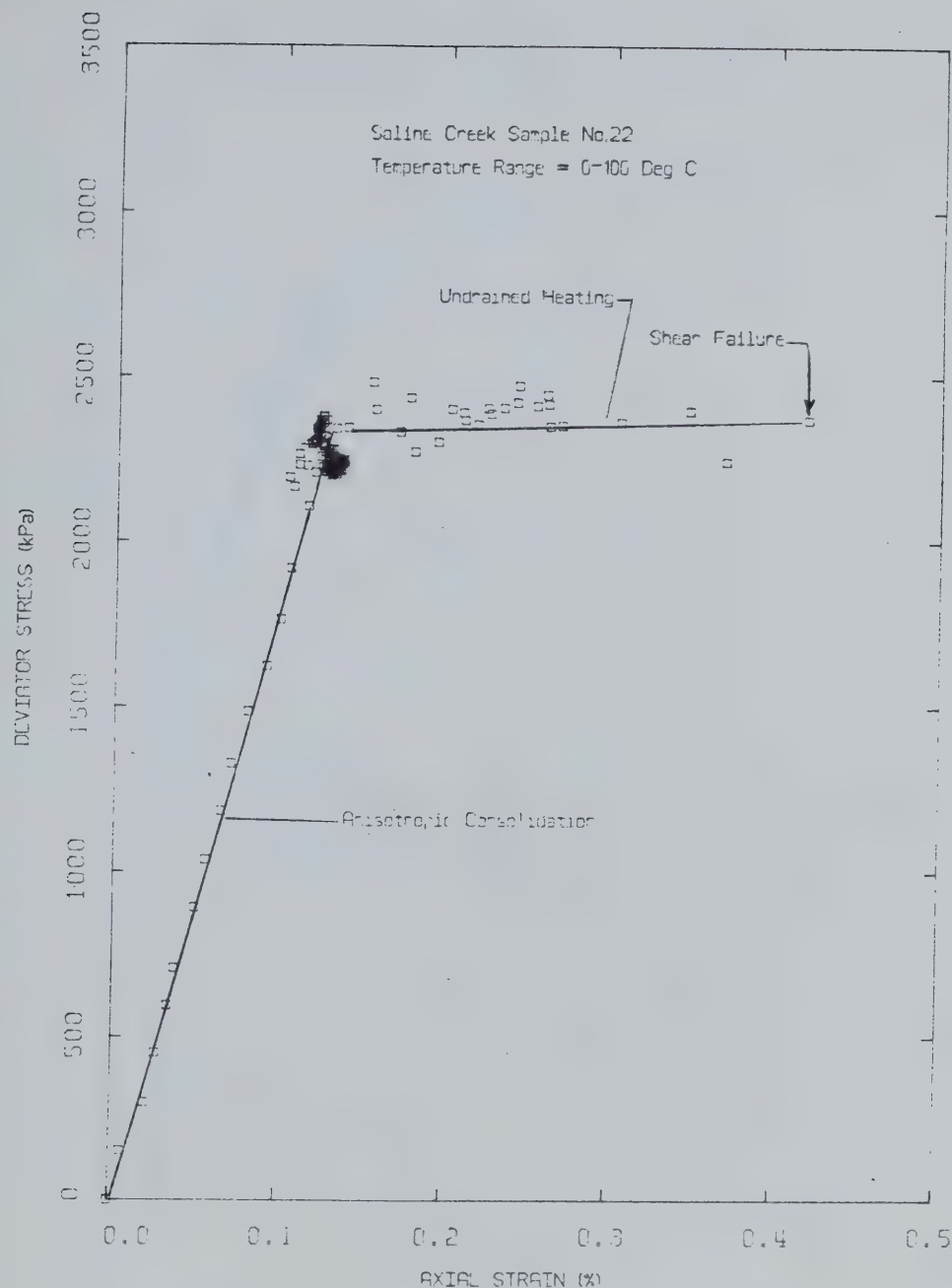


FIGURE E11.4 Triaxial Test TOS11: Deviator Stress Vs. Axial Strain



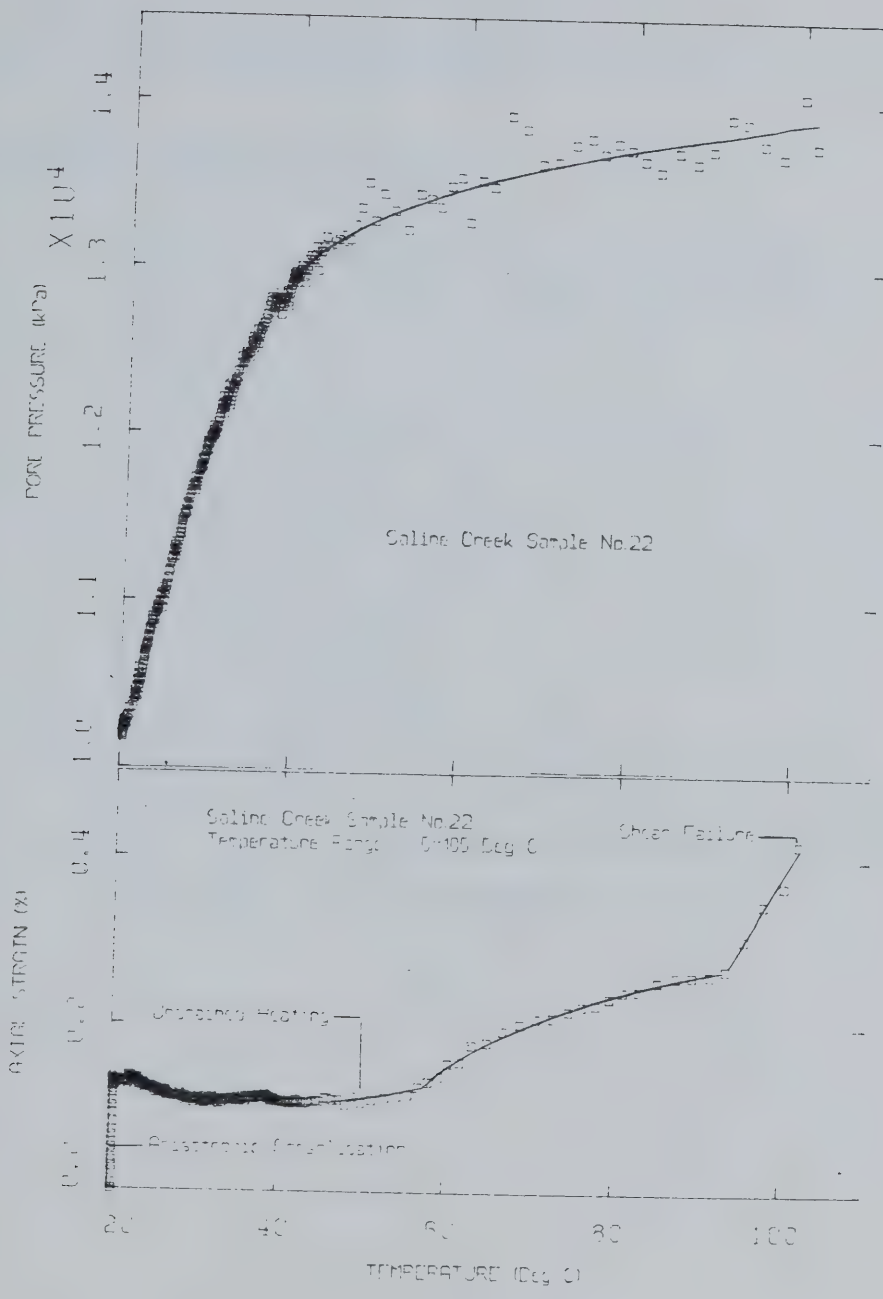


FIGURE E11.5 Triaxial Test TOS11: Pore Pressure Changes and Axial Strain During Undrained Heating



## TEST TOS 12

Drained Isotropic Compression and Passive Triaxial Compression  
of Saline Creek Sample No. 29 at 200°C

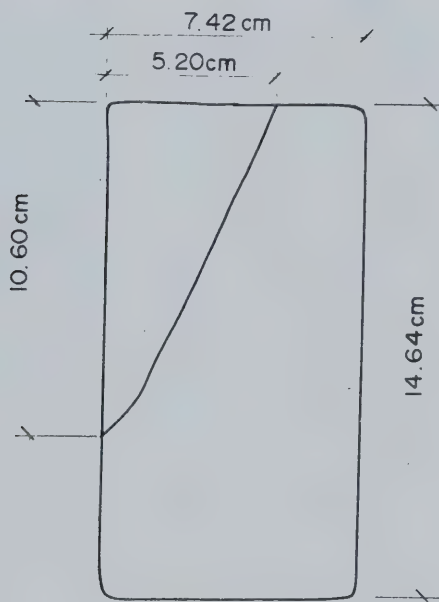
Procedural Details: Test TOS 12

1. Sample 29 was thawed and back saturated for 22 hours under 10 MPa back pressure and 14 MPa isotropic confining stress.
2. The apparatus and sample were heated drained to 200°C and temperature allowed to stabilize for 16 hours. Vertical (axial) expansion was monitored during heating, however the volume change device was isolated during heating because of doubt about the durability of the triaxial membrane.
3. An isotropic compression test was performed over the effective stress range 4 - 17 MPa.
4. A drained passive triaxial compression test was also performed by increasing vertical stress at an average rate of 70 kPa/minute. Vertical deformation and volume change were monitored during the compression tests.



TEST TOS 12: SAMPLE DATAPretest Saline Creek Sample No. 29:

Dia.:  $\emptyset = 7.510$  cm      w = 0.010  
Height: H = 14.837 cm      B = 0.188  
Area: A = 44.297 cm<sup>2</sup>  
Volume: V = 657.23 ml      V<sub>S</sub> = 443.1 ml  
Mass: M = 1375 g      V<sub>V</sub> = 224.1 ml  
Mass Solids = 1148 g      Dry Density = 1.746 Mg/m<sup>3</sup>  
Density: = 2.092 Mg/m<sup>3</sup>  
Porosity: = 0.341  
Void Ratio: = 0.517 g

Sample 29 After Test TOS 11



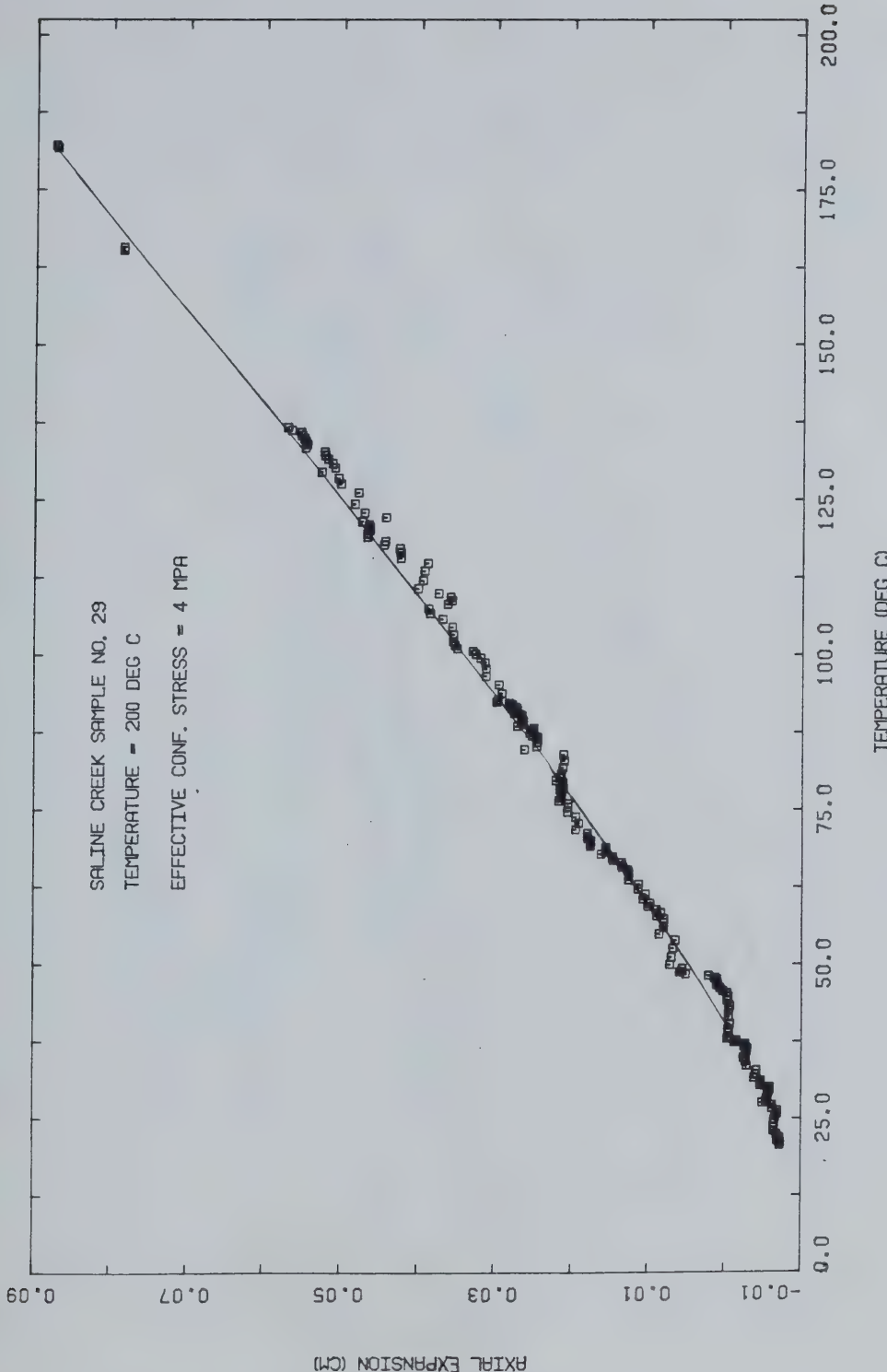


FIGURE E12.1 Triaxial Test TOS12: Axial Thermal Expansion



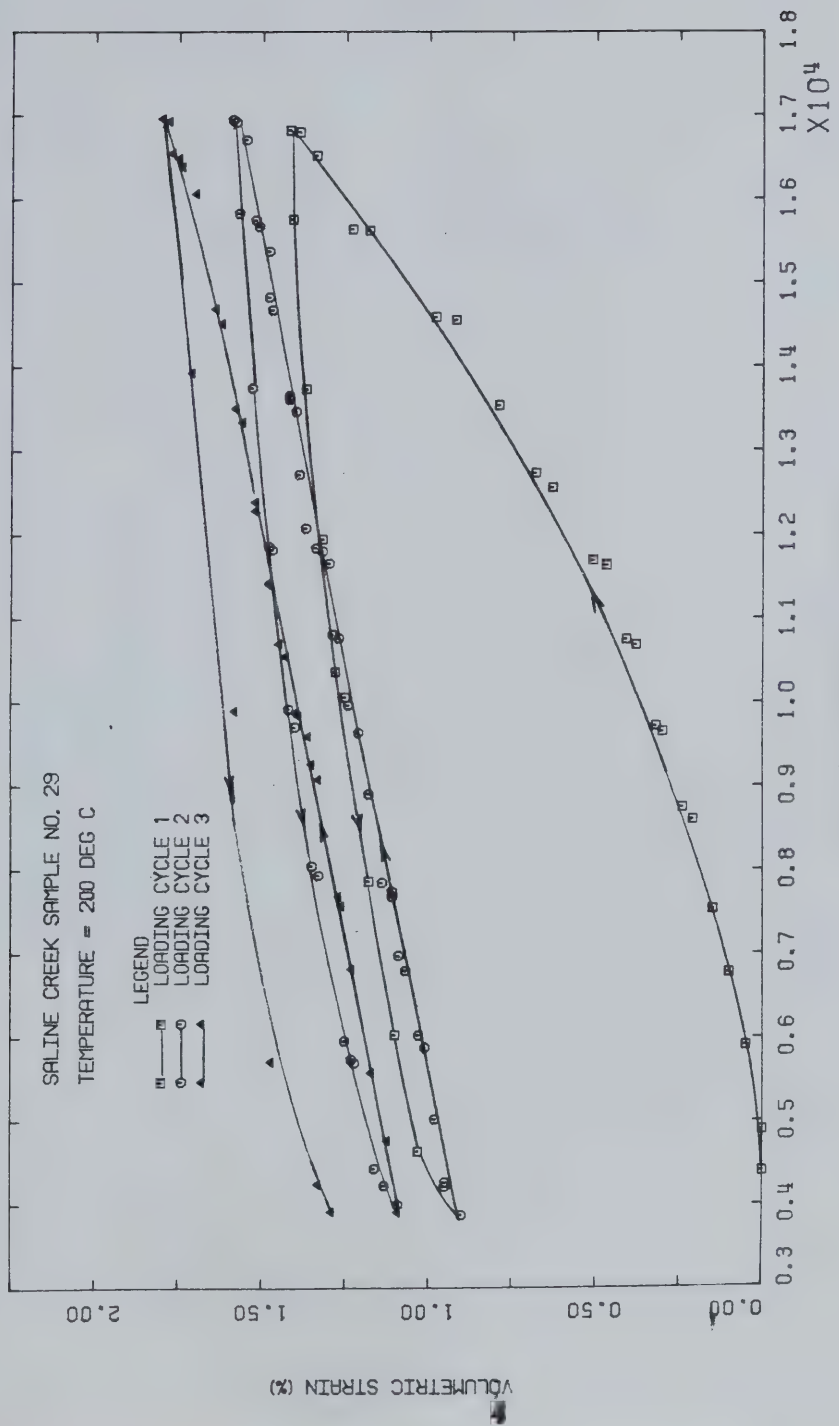


FIGURE E12.2 Triaxial Test TOS12: Drained Isotropic Compression



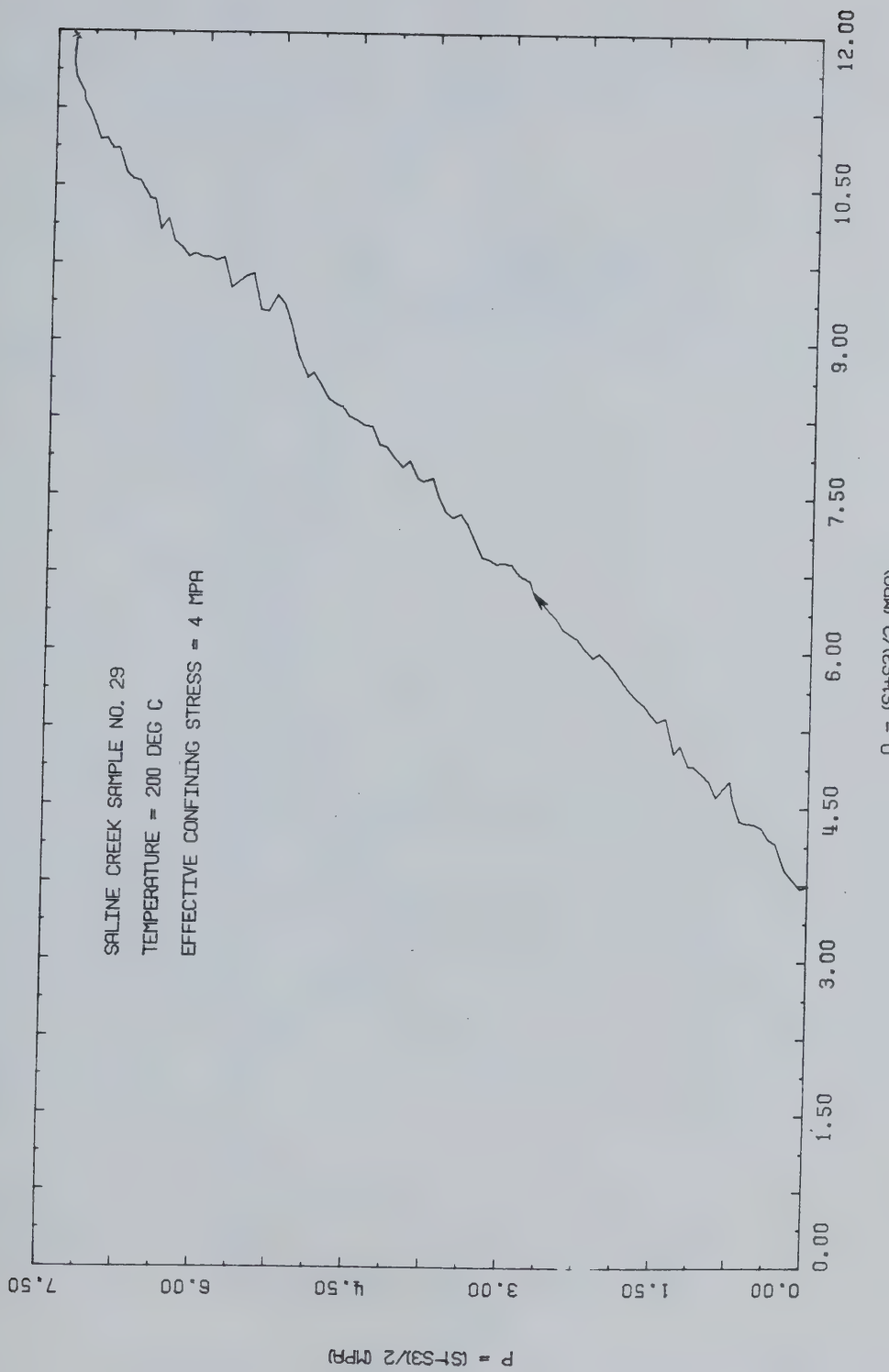


FIGURE E12.3 Triaxial Test TOS12: Stress Path



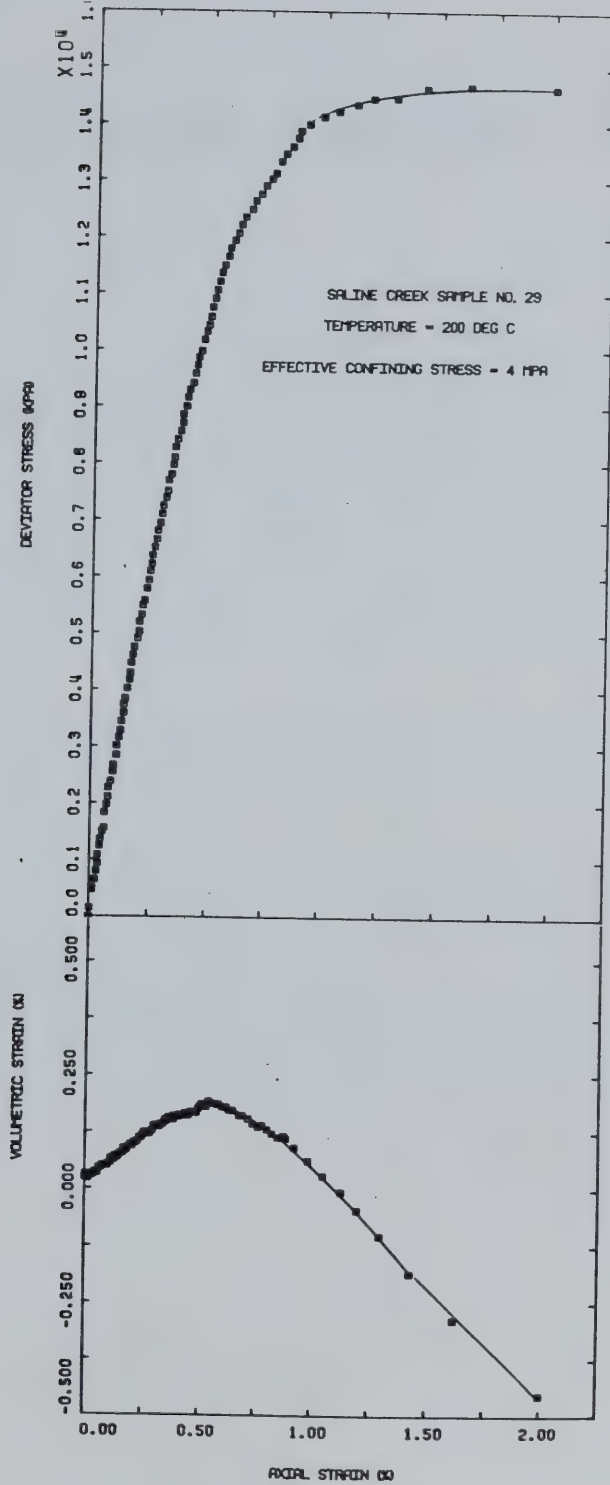


FIGURE E12.4 Triaxial Test TOS12: Deviator Stress Vs. Strain



## TEST TOS 13

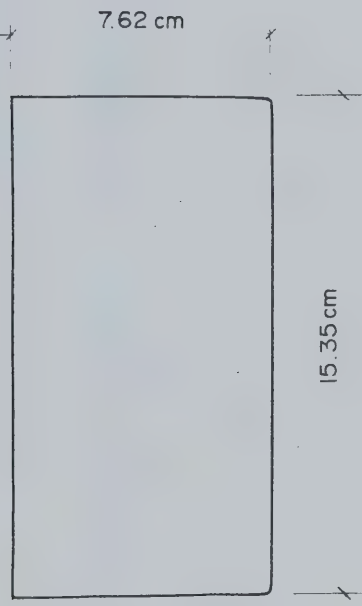
Thermal Expansion of Saline Creek Sample No. 26 -  
Membrane Meltdown at 240°CProcedural Details: Test TOS 13

1. A fluorosilicone compound (Dow Corning RTV730) was applied as recommended by the manufacturer as a protective coating 3 mm thick over the surface of a silicone rubber membrane. It was anticipated that the fluorosilicone would inhibit chemical reaction between the silicone oil cell fluid and the silicone rubber membrane resulting in swelling and depolymerization of the rubber at temperatures above 200°C.
2. Saline Creek Sample 26 was thawed and back saturated under 10 MPa back pressure and 14 MPa isotropic confining stress.
3. The apparatus and sample were heated drained to 240°C at which temperature membrane meltdown occurred. The test was terminated.
4. Vertical (axial) expansion and volume change (i.e. volume of fluid expelled) were monitored during heating.



TEST TOS 13: SAMPLE DATAPretest Saline Creek Sample No. 26:

Dia.:  $\emptyset$  = 7.620 cm      w = 0.036  
Height: H = 15.300 cm      B = 0.132  
Area: A = 45.604 cm<sup>2</sup>  
Volume: V = 697.74 ml      V<sub>S</sub> = 468.9 ml  
Mass: M = 1451 g      V<sub>V</sub> = 228.8 ml  
Mass Solids = 1243 g      Dry Density = 1.781 Mg/m<sup>3</sup>  
Density: = 2.080 Mg/m<sup>3</sup>  
Porosity: = 0.328  
Void Ratio: = 0.488 g

Sample 26 After Test TOS 13

No Visible Deformation



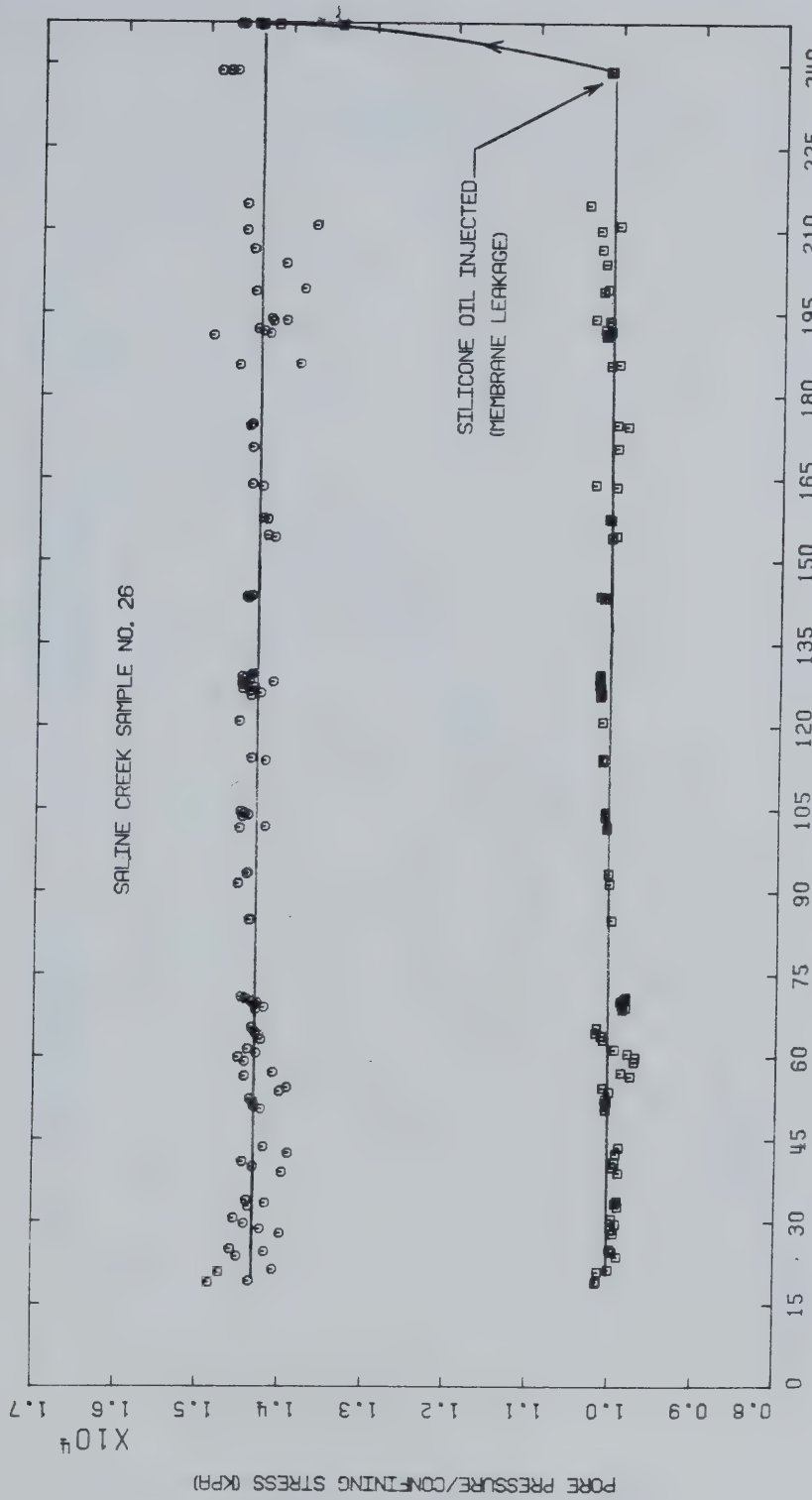


FIGURE 13.1 Triaxial Test TOS13: Pore Pressure and Confining Stress Vs. Temperature



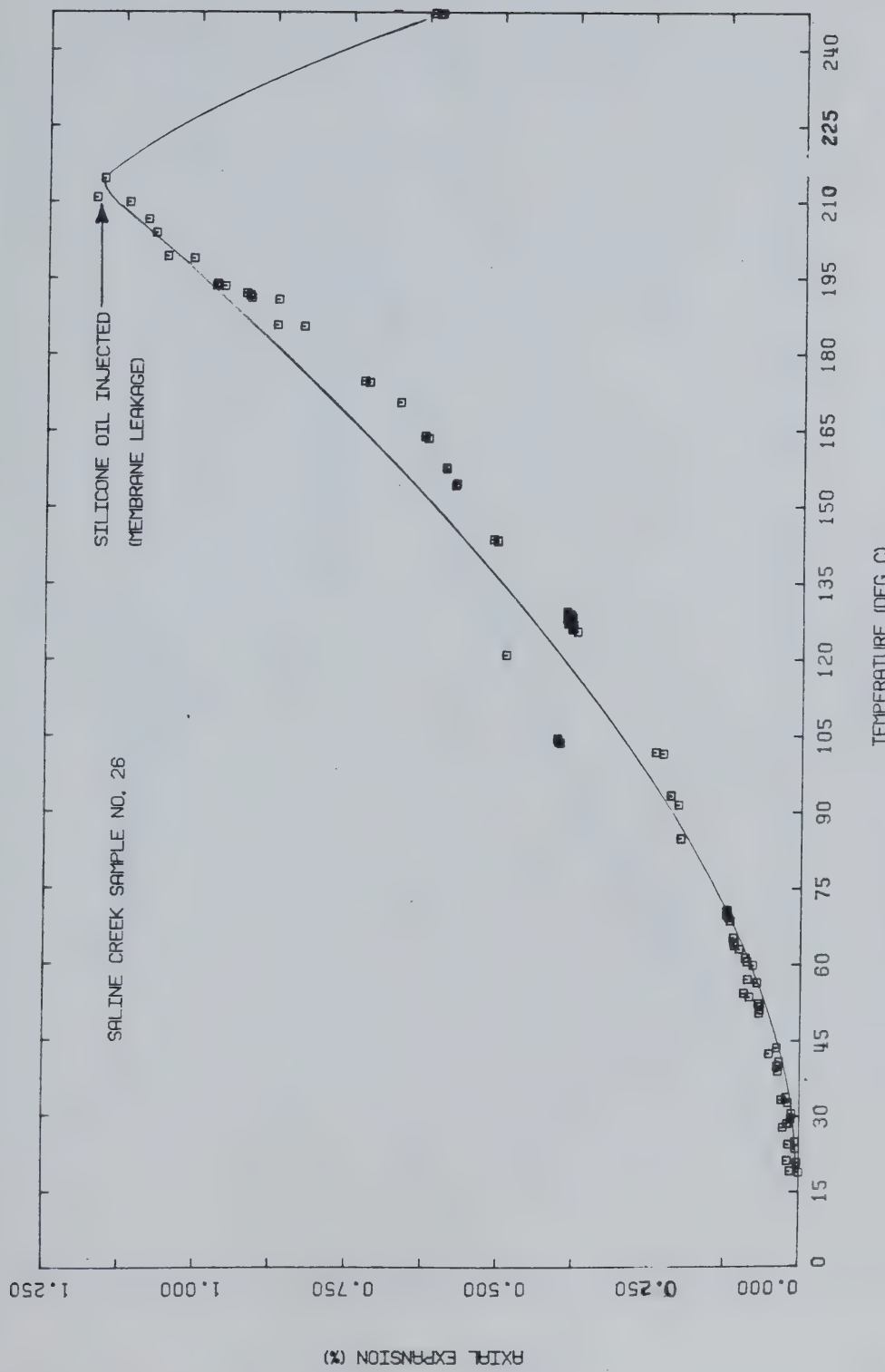


FIGURE E13.2 Triaxial Test T013: Axial Thermal Expansion



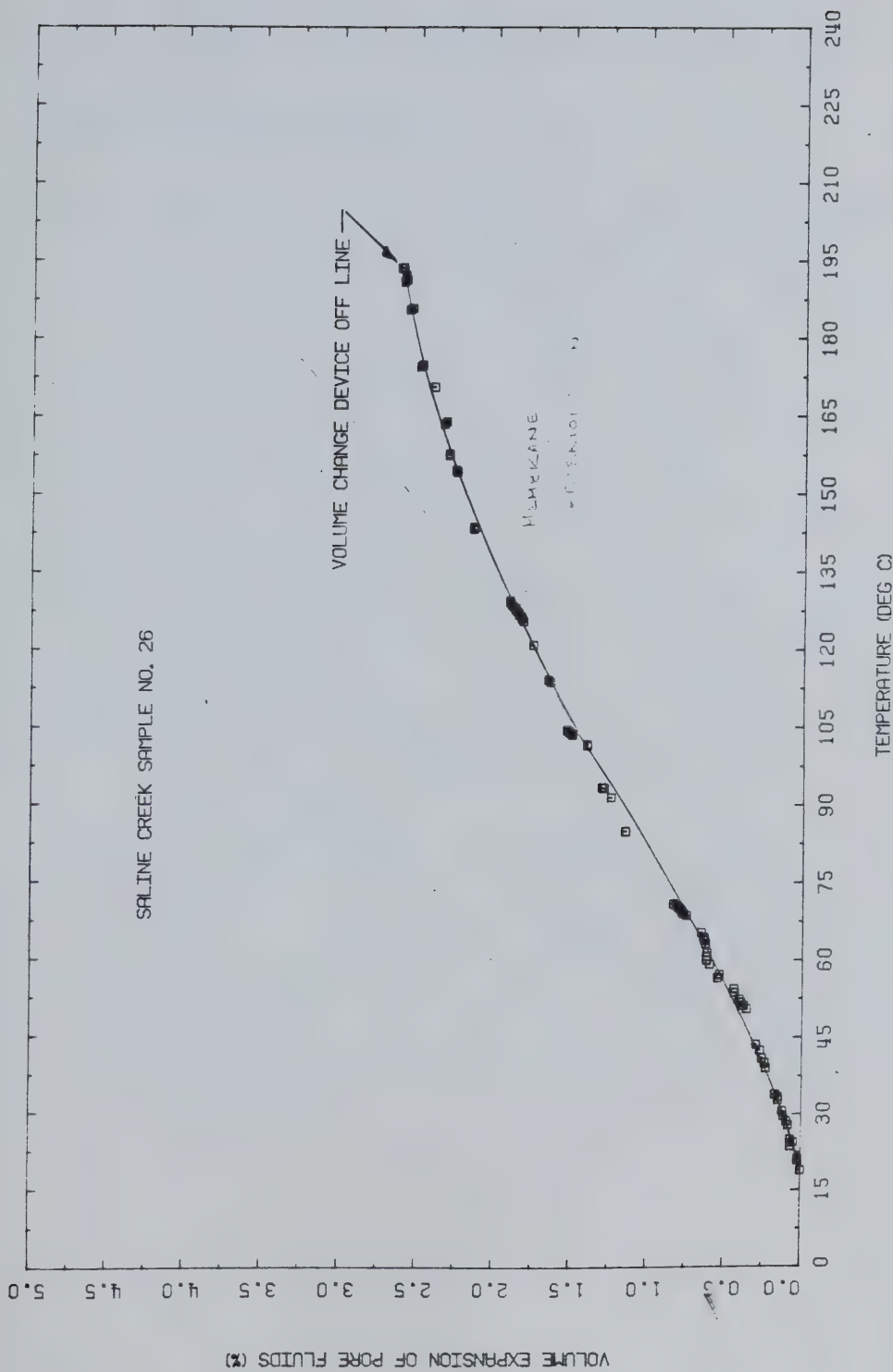


FIGURE E13.3 Triaxial Test TOS13: Volume of Pore Fluid Expelled During Heating



## TEST TOS 14

## Multistage Triaxial Compression of Remoulded Saline Creek Oil Sand: Combined Samples 5, 7, and 8

Procedural Details: Test TOS 14

1. Pieces of Saline Creek samples 5, 7, and 8 were permitted to thaw, then remoulded and mixed by kneading. The remoulded material was then placed in layers inside a steel split-ring cylindrical mould 7.58 cm in diameter. The material was compacted in 5 layers, each approximately 3 cm thick, using 30 blows per layer of a Modified Proctor compaction drop hammer. The compacted sample and mould were then placed in a freezer at -20°C for 48 hours.
2. The remoulded frozen oil sand sample was removed from the split-ring mould and mounted in the triaxial cell using procedures similar to those for undisturbed samples.
3. The sample was thawed and back saturated for 20 hours under a back pressure of 2 MPa and under 4 MPa isotropic confining stress.
4. A three stage, drained passive compression test was performed at room temperature with the back pressure maintained constant at 2 MPa. Vertical compressive stress was increased at an average rate of 55 kPa/minute. Three peak deviatoric stress levels were defined corresponding to effective confining stresses of 2 MPa, 4 MPa and 8 MPa.



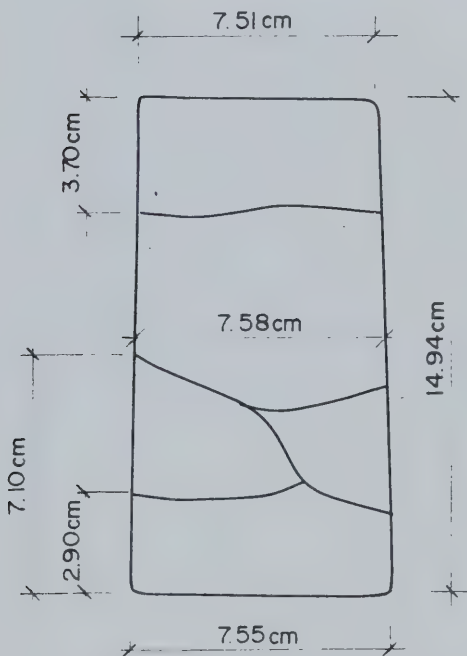
5. After the triaxial compression test, the apparatus and sample were heated to test the durability of the rubber membrane, formed from a silicone elastomer (Dow Corning Sylgard 170). This rubber cures by an addition reaction when components A and B are mixed. The manufacturer had recommended this product as an alternate to silicone rubber. The membrane decomposed between 100°C and 120°C.



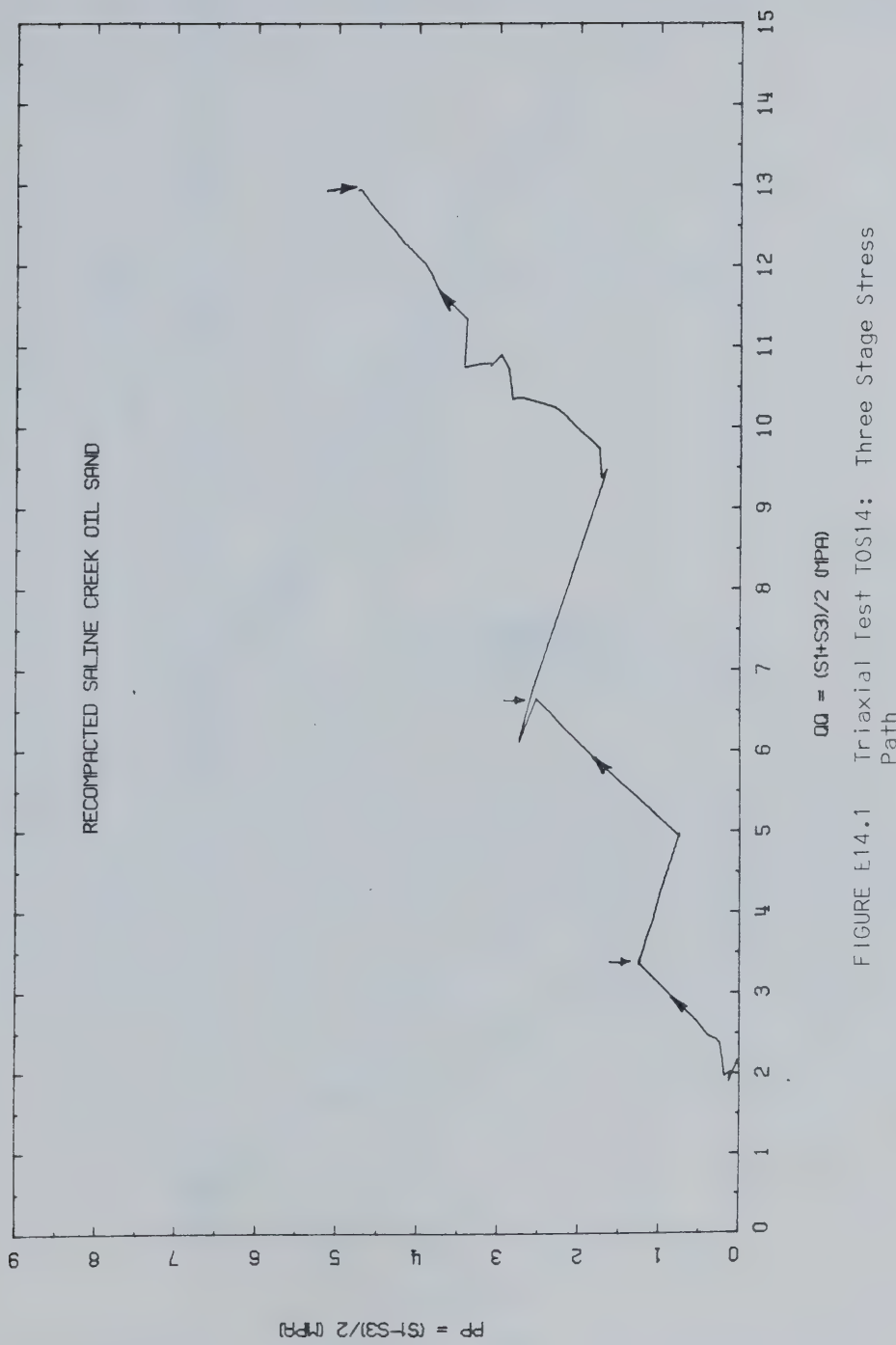
TEST TOS 14: SAMPLE DATA

Pretest Remoulded and Compacted Oil Sand Sample From Saline Creek  
Samples 5, 7 and 8:

Dia.:  $\emptyset = 7.576 \text{ cm}$        $w = 0.017$   
 Height:  $H = 15.238 \text{ cm}$        $B = 0.187$   
 Area:  $A = 45.079 \text{ cm}^2$   
 Volume:  $V = 686.91 \text{ ml}$        $V_S = 398.3 \text{ ml}$   
 Mass:  $M = 1270 \text{ g}$        $V_V = 288.6 \text{ ml}$   
 Mass Solids = 1055 g      Dry Density =  $1.537 \text{ Mg/m}^3$   
 Density: =  $1.850 \text{ Mg/m}^3$   
 Porosity: = 0.418  
 Void Ratio: = 0.718 g

Remoulded Sample After Test TOS 14







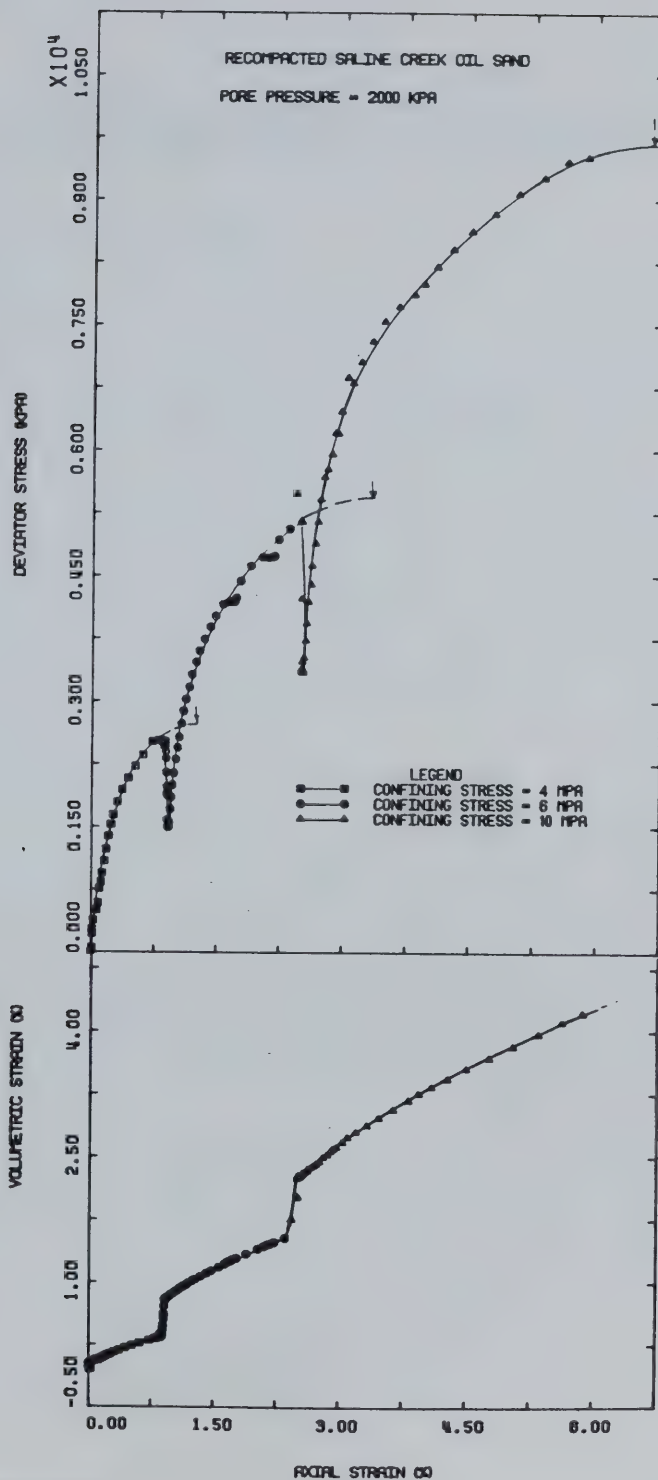


FIGURE E14.2 Triaxial Test TOS14: Deviator Stress Vs. Strain



## TEST TOS 15

Isotropic Compression and Passive Triaxial Compression  
of Cold Lake Oil Sand Sample 12B at 200°CProcedural Details: Test TOS 15

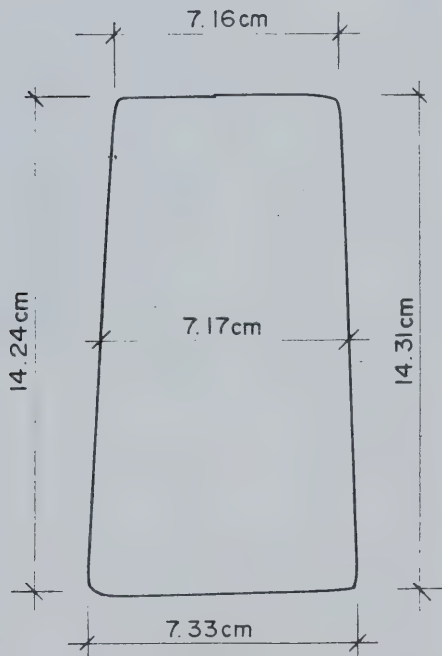
Note: Cold Lake oil sand sample 12B was a frozen core sample taken from the Clearwater Formation (depth 400 m) at Esso's Leming pilot project at Cold Lake in 1978.

1. Sample 12B was thawed and back saturated for 22 hours at 10 MPa back pressure and 14 MPa isotropic confining stress.
2. The apparatus and sample were heated to 200°C drained, i.e. at 10 MPa constant back pressure. Volume change (i.e. volume of pore fluid expelled) was monitored during heating.
3. The temperature was allowed to stabilize for 16 hours, then the sample was subjected to three cycles of isotropic compression over the effective stress range 4 - 17 MPa.
4. A drained triaxial passive compression test was performed by increasing vertical compressive stress at an average rate of 75 kPa/minute while maintaining the back pressure and horizontal confining stress constant at 10 MPa and 14 MPa respectively.
5. Pore pressure response to undrained heating was determined above 200°C. This was carried out, in part, to test the durability of a silicone rubber membrane coated with 4 to 5 mm of fluorosilicone (Dow Corning RTV730) rubber compound. The membrane depolymerized and began to leak at about 235°C. The test was terminated at 245°C.



TEST TOS 15: SAMPLE DATAPretest Cold Lake Oil Sand Sample 12B:

Dia.:  $\emptyset = 7.500$  cm       $w = 0.056$   
Height:  $H = 15.000$  cm       $B = 0.146$   
Area:  $A = 44.179$   $\text{cm}^2$   
Volume:  $V = 662.68$  ml       $V_S = 408.8$  ml  
Mass:  $M = 1302$  g       $V_V = 253.9$  ml  
Mass Solids = 1083 g      Dry Density = 1.635  $\text{Mg/m}^3$   
Density:      = 1.965  $\text{Mg/m}^3$   
Porosity:      = 0.383  
Void Ratio:      = 0.621 g

Cold Lake Sample 12B After Test TOS 15



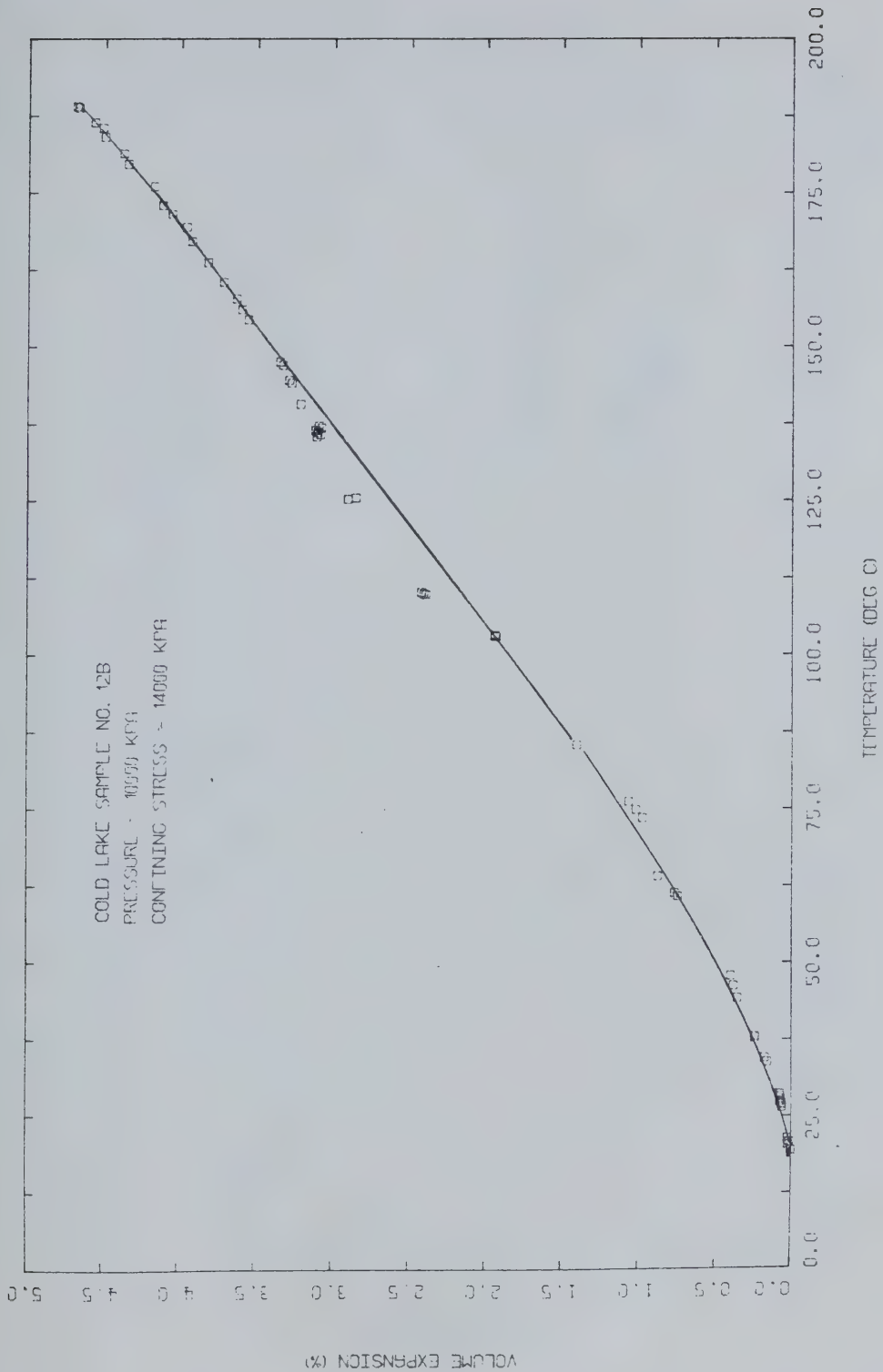


FIGURE E15.1 Triaxial Test TOS15: Volume of Pore Fluid Expelled During Heating



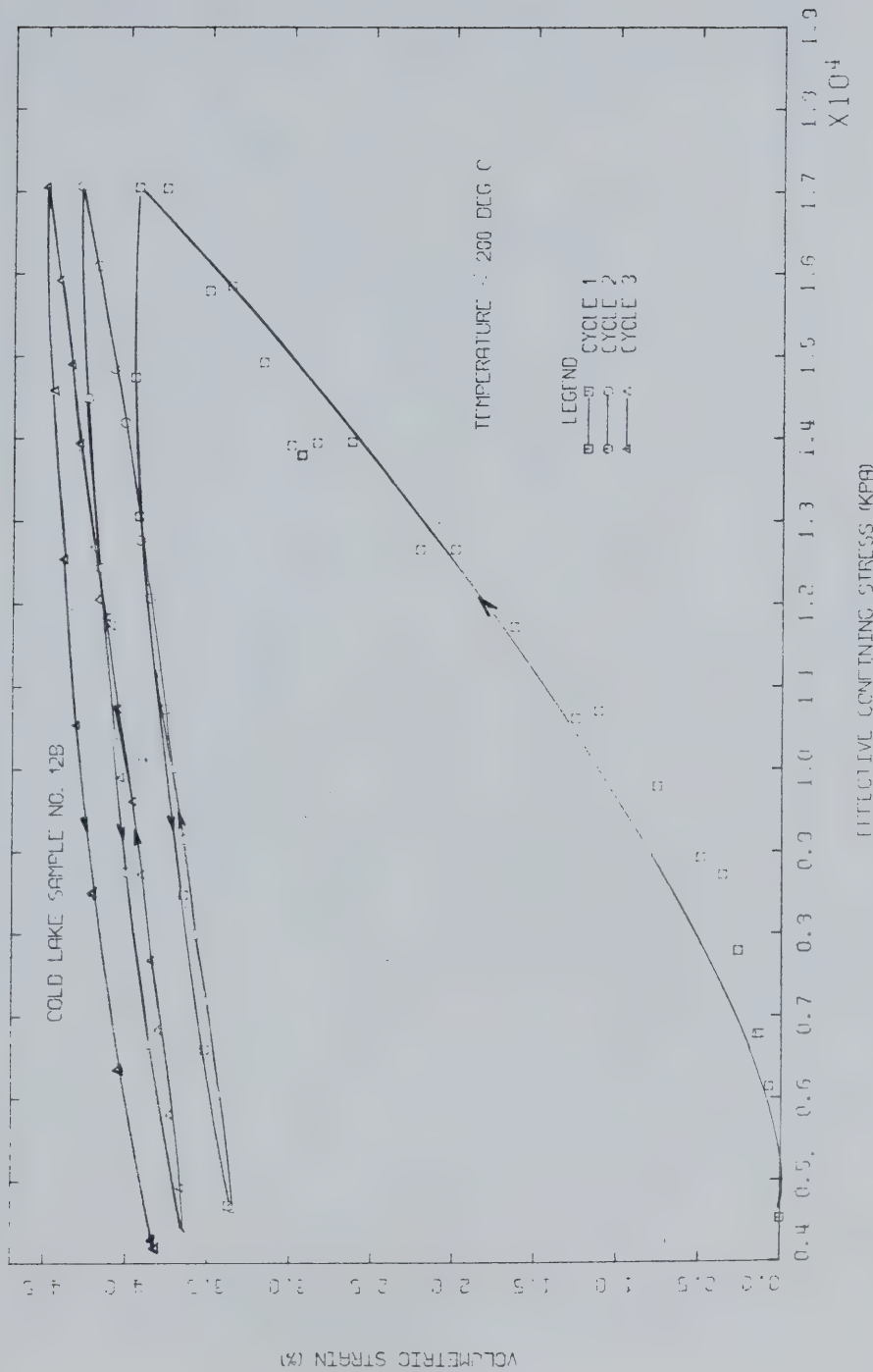


FIGURE E15.2 Triaxial Test TOS15: Drained Isotropic Compression



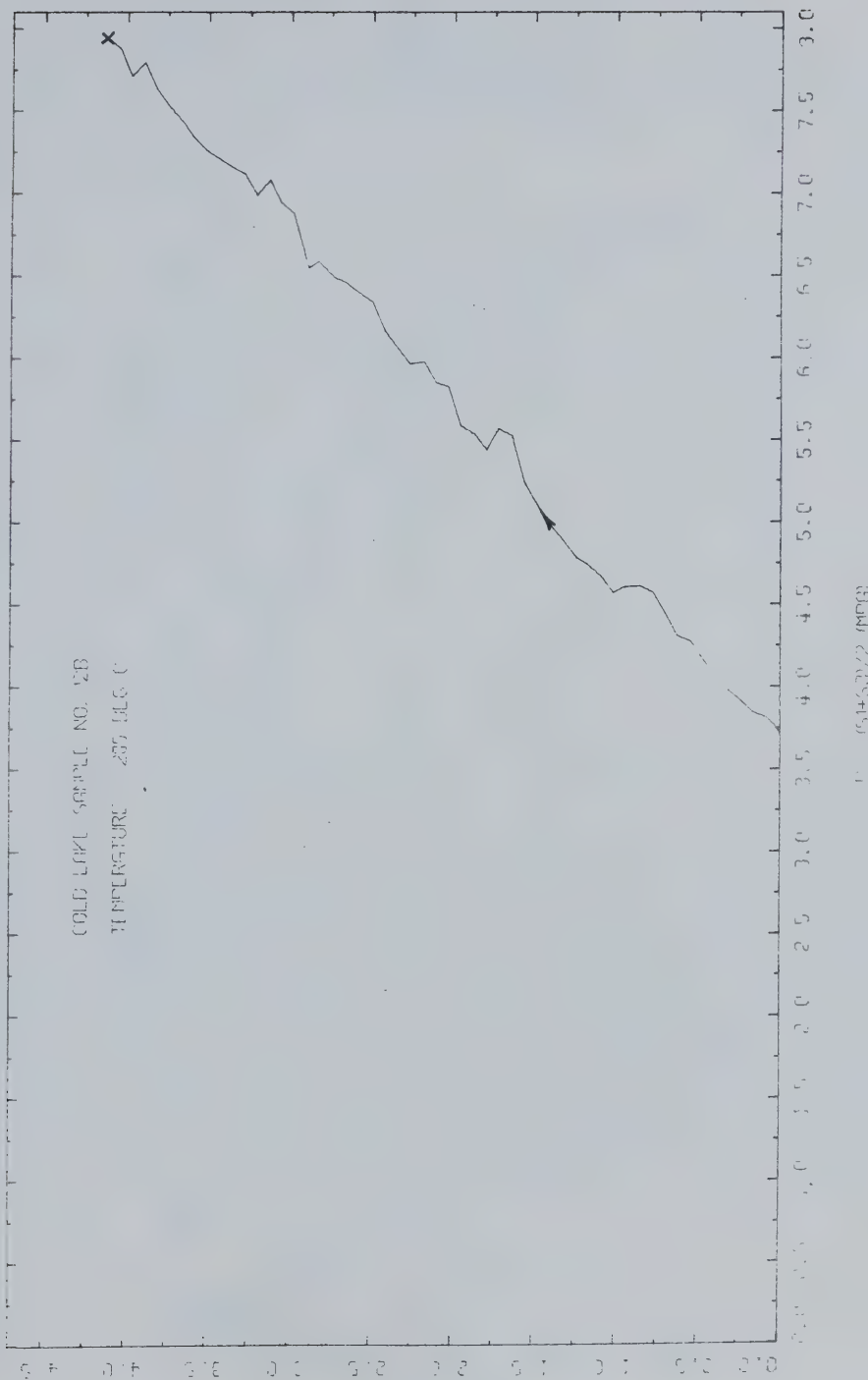


FIGURE E15.3 Triaxial Test TOS15: Stress Path



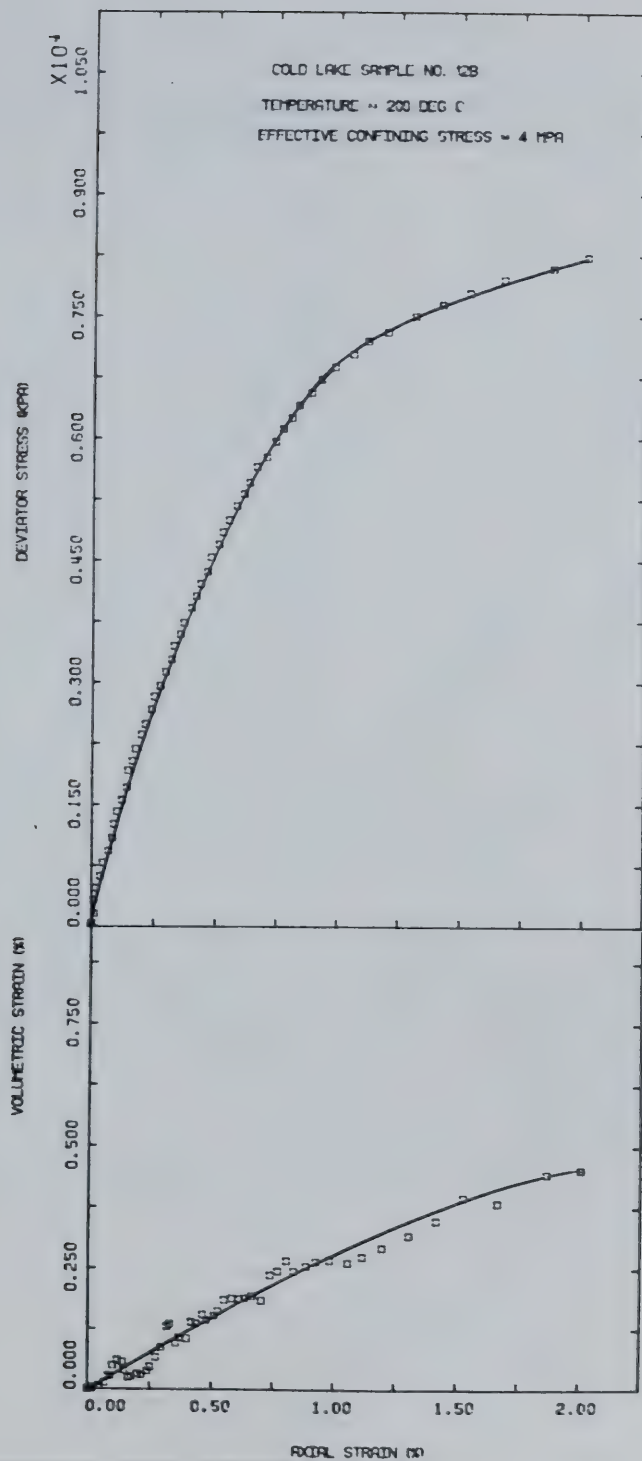


FIGURE E15.4 Triaxial Test TOS15: Deviator Stress Vs. Strain



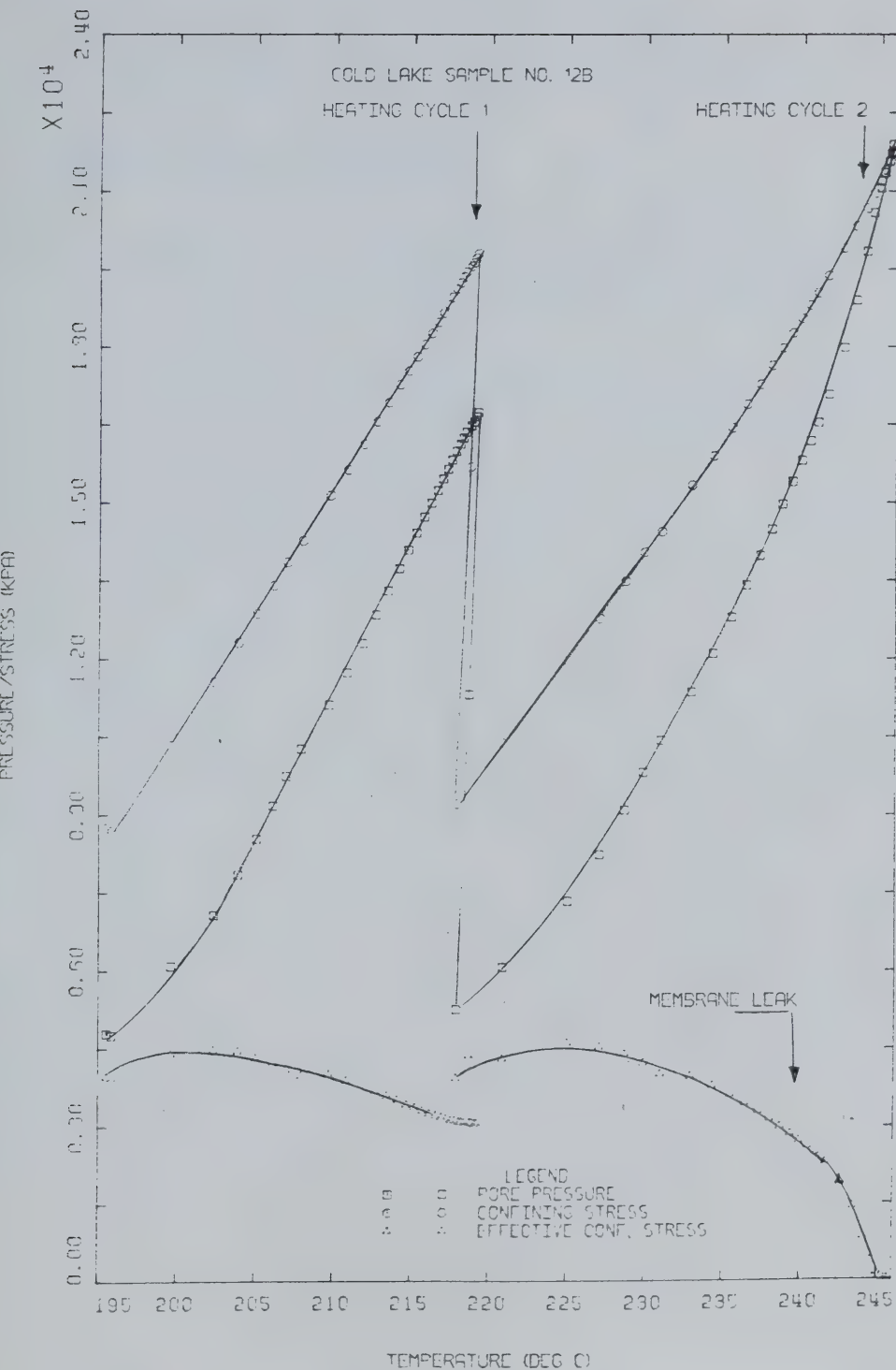


FIGURE E15.5 Triaxial Test T0S15: Pore Pressure Response to Undrained Heating



## TEST TOS 16

## Thermal Expansion of Saline Creek Oil Sand Sample No. 13

Procedural Details: Test TOS 16

1. Sample 13 was thawed and back saturated for 21 hours under 10 MPa back pressure and 14 MPa isotropic confining stress.
2. The apparatus and sample were heated drained, to 190°C at which point a leak developed in the rubber membrane. The test was terminated at this point.  
Vertical (axial) deformation and volume of fluid expelled from the sample were monitored during heating.



TEST TOS 16: SAMPLE DATAPretest Saline Creek Sample 13:

Dia.:  $\varnothing$  = 7.603 cm      w = 0.020  
Height: H = 15.235 cm      B = 0.190  
Area: A = 45.400 cm<sup>2</sup>  
Volume: V = 691.68 ml      V<sub>S</sub> = 442.9 ml  
Mass: M = 1420 g      V<sub>V</sub> = 248.8 ml  
Mass Solids = 1174 g      Dry Density = 1.697 Mg/m<sup>3</sup>

Density: = 2.053 Mg/m<sup>3</sup>  
Porosity: = 0.358  
Void Ratio: = 0.558 g



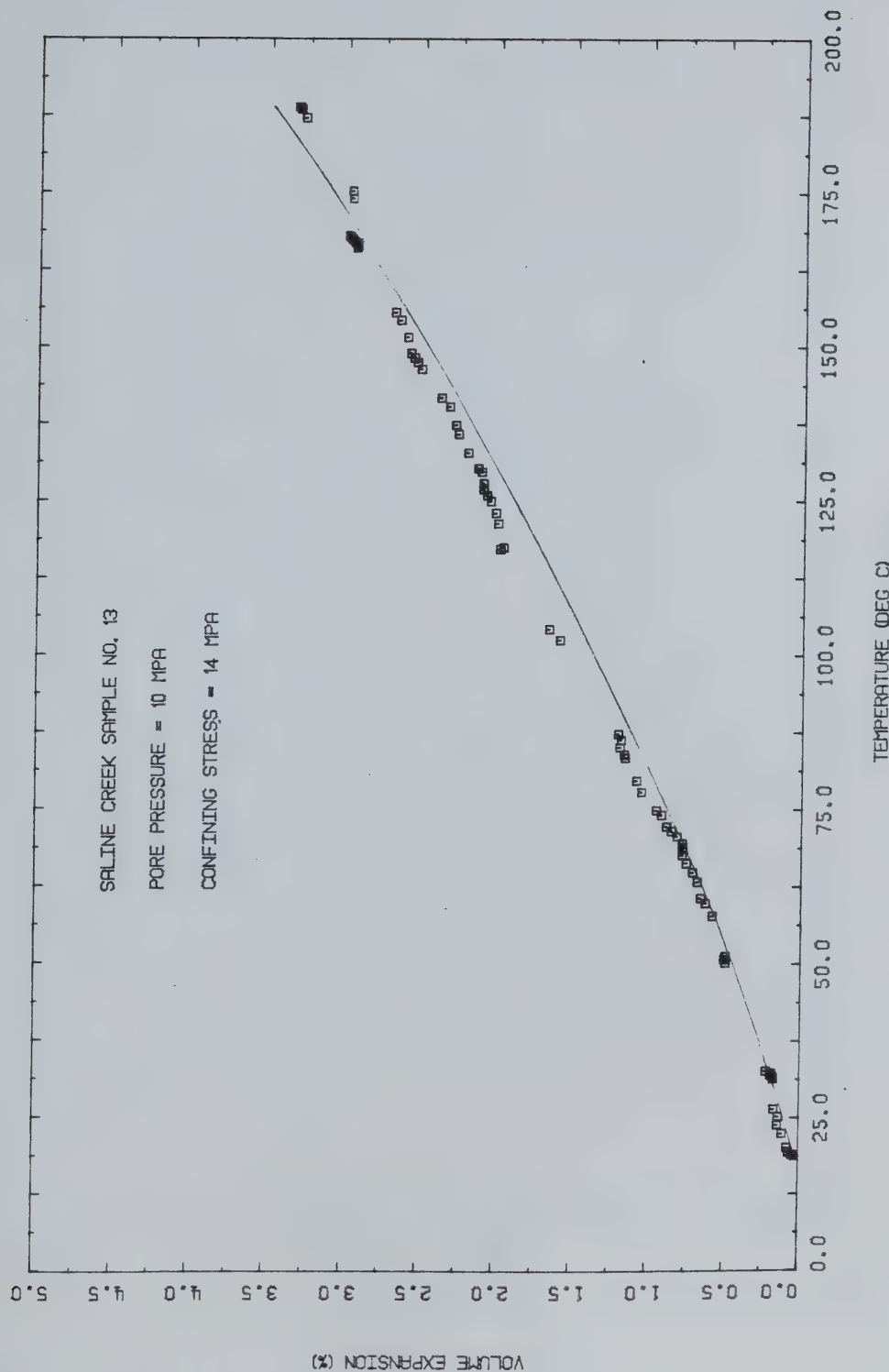


FIGURE E16.1 Triaxial Test TOS16: Volume of Pore Fluid Drained During Heating



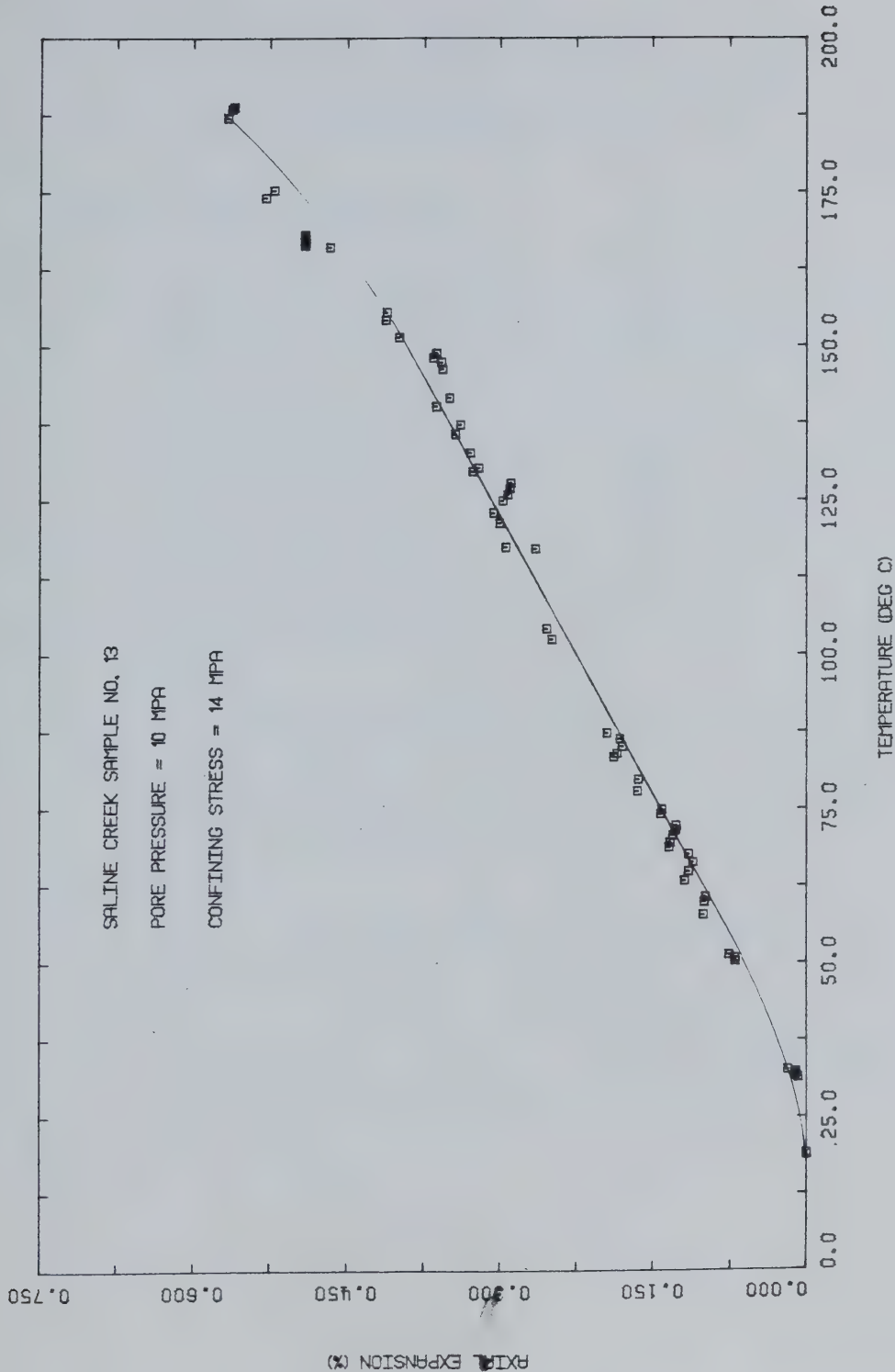


FIGURE E16.2 Triaxial Test TOS16: Vertical Thermal Expansion



## TEST TOS 17

Drained Triaxial Passive Compression of Saline Creek  
Oil Sand Sample No. 23 at 200°C

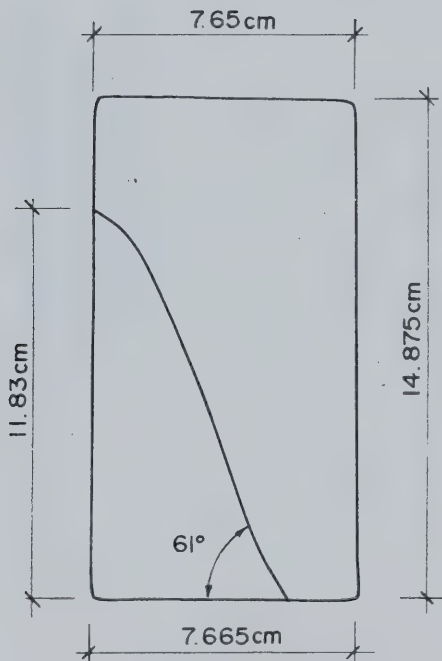
Procedural Details: Test TOS 17

1. Sample 23 was thawed and back saturated for 18 hours under 10 MPa back pressure and 18 MPa isotropic confining stress.
2. The apparatus and sample were heated under drained conditions to 200°C. The volume of pore fluid expelled from the sample was monitored up to 180°C, however the volume change device was isolated overnight. The temperature was allowed to stabilize for 15 hours at 200°C.
3. A drained triaxial compression test was performed at 200°C. Vertical compressive stress was increased at an average rate of 65 kPa/minute while back pressure and confining stress were maintained constant at 10 MPa and 18 MPa respectively. Vertical (axial) deformation and volume change were monitored during triaxial compression.
4. A very small membrane leak developed near the peak deviatoric stress. The rate of leakage was measured and volume change readings corrected accordingly.



TEST TOS 17: SAMPLE DATAPretest Saline Creek Sample No. 23:

Dia.:  $\emptyset = 7.650$  cm       $w = 0.020$   
Height:  $H = 15.042$  cm       $B = 0.190$   
Area:  $A = 45.963 \text{ cm}^2$   
Volume:  $V = 691.38 \text{ ml}$        $V_S = 442.9 \text{ ml}$   
Mass:  $M = 1420 \text{ g}$        $V_V = 248.5 \text{ ml}$   
Mass Solids = 1174 g      Dry Density =  $1.698 \text{ Mg/m}^3$   
Density: =  $2.054 \text{ Mg/m}^3$   
Porosity: = 0.359  
Void Ratio: = 0.560 g

Sample 23 After Test TOS 17



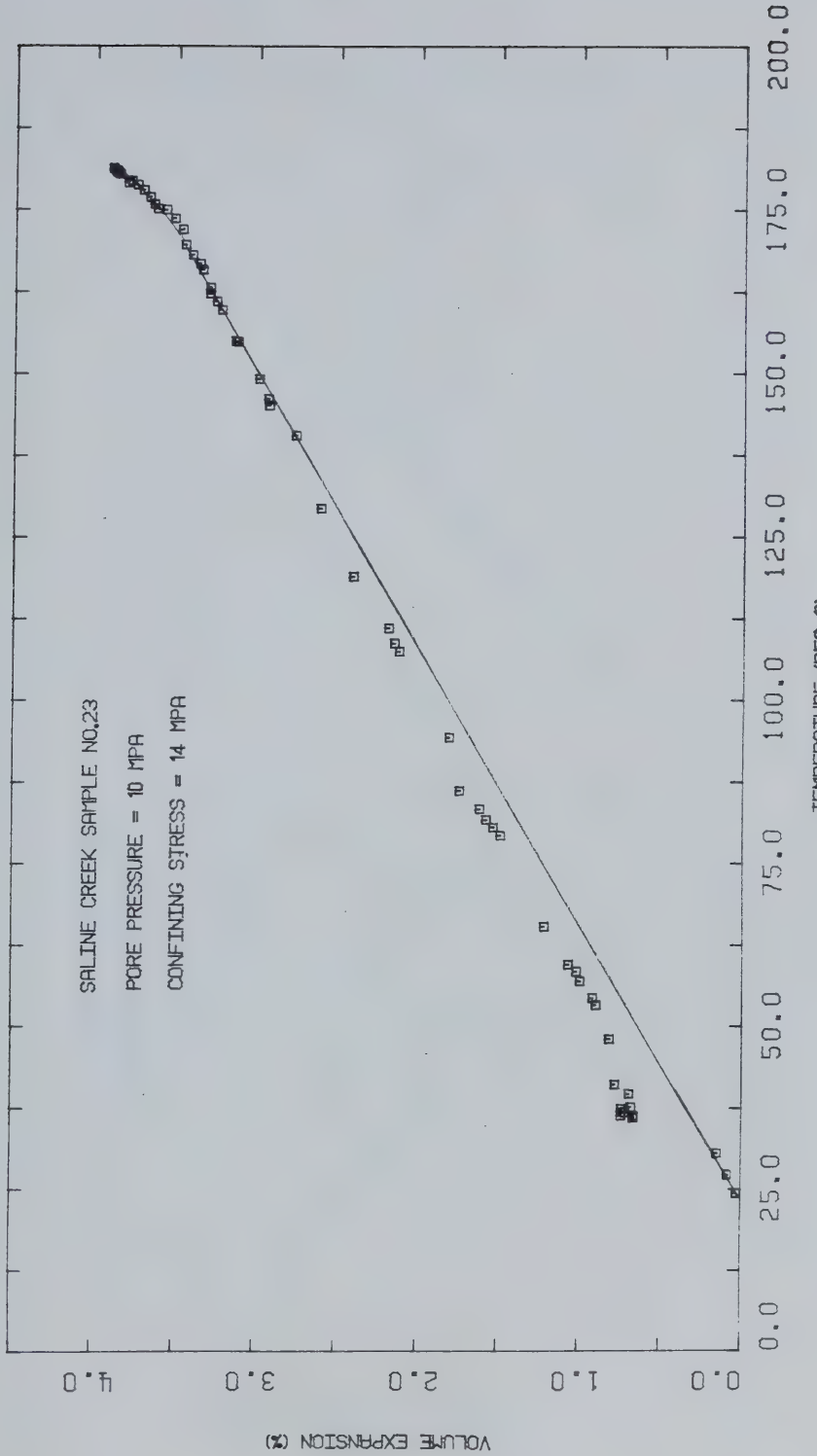


FIGURE E17.1 · Triaxial Test TOS17: Volume of Pore Fluid Drained During Heating



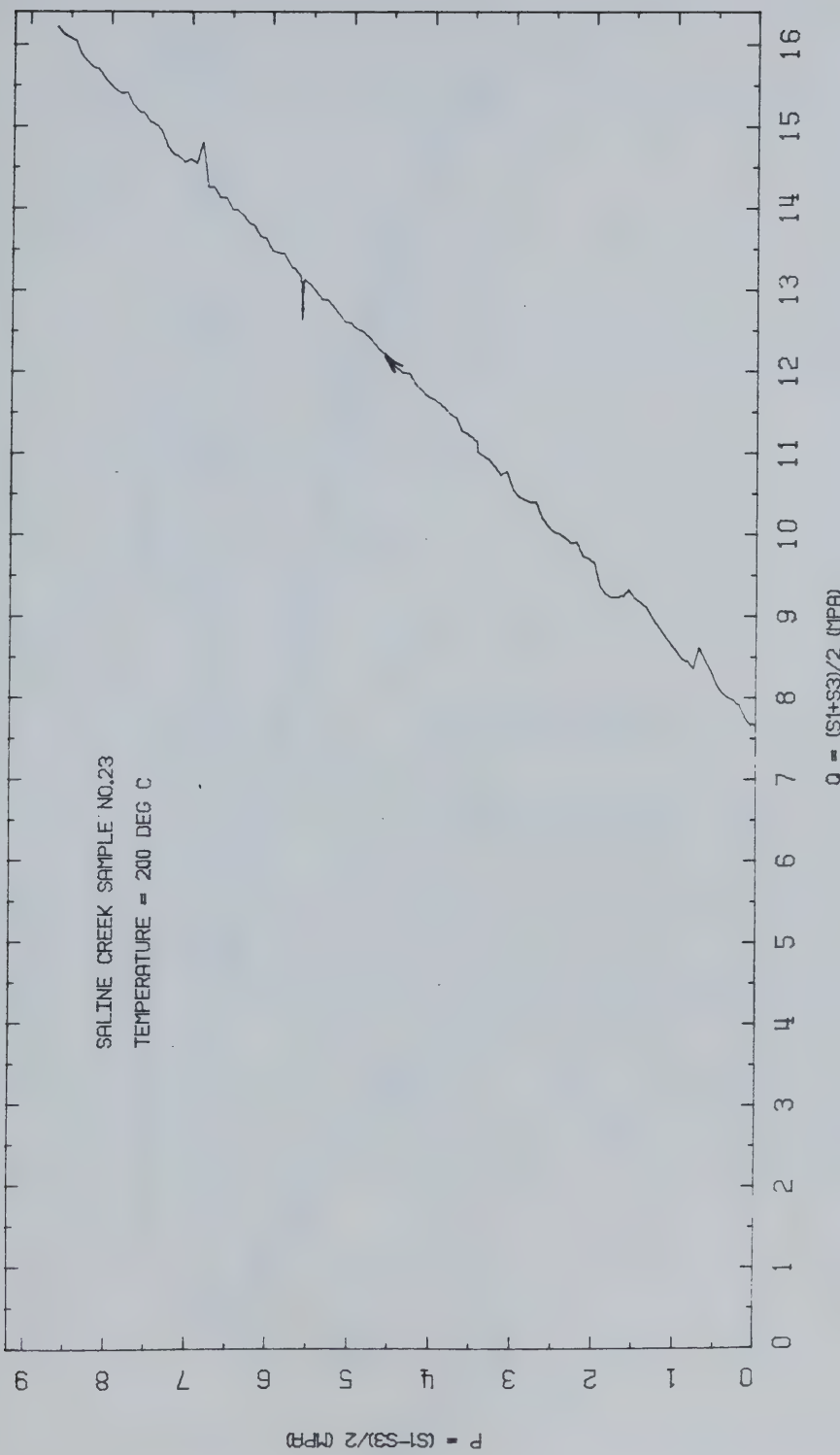


FIGURE E17.2 Triaxial Test TOS17: Stress Path



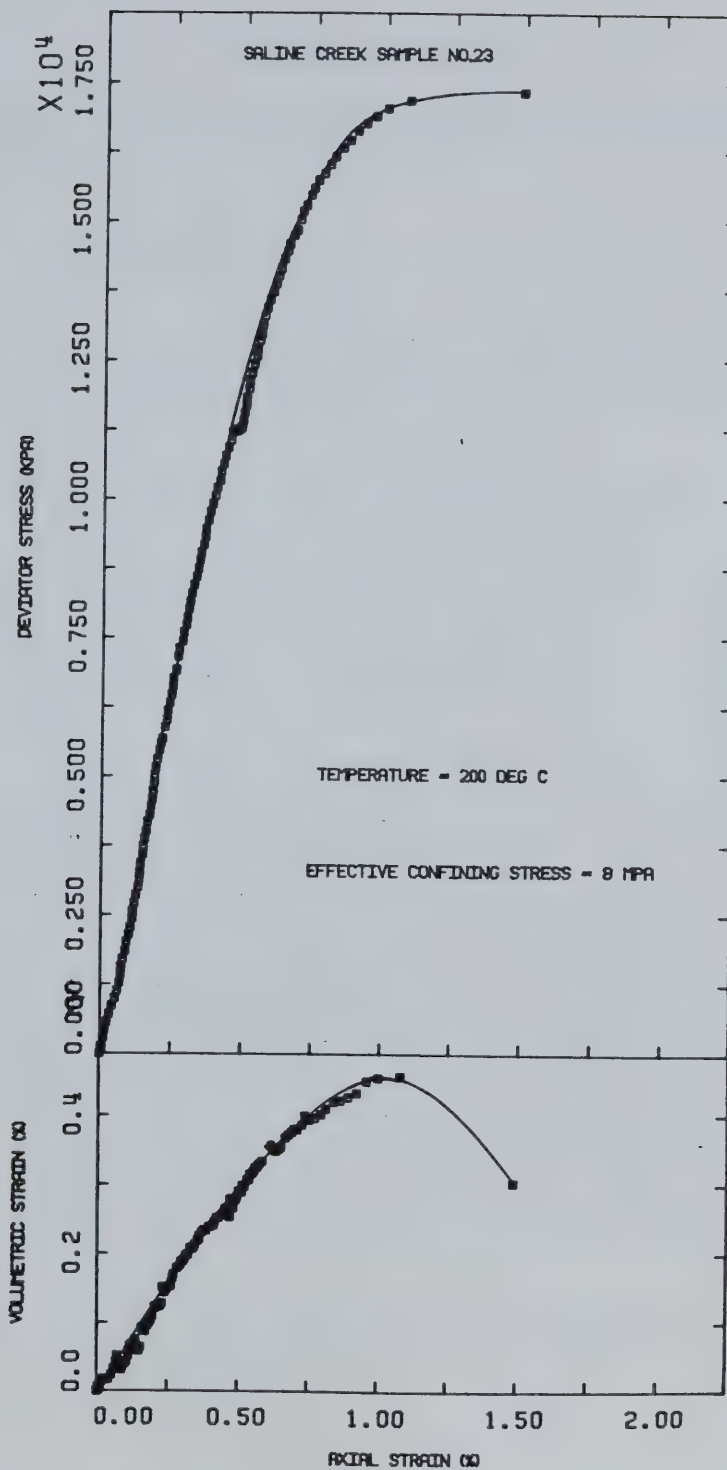


FIGURE E17.3 Triaxial Test TOS17: Deviator Stress Vs. Strain



## TEST TOS 18

Drained Triaxial Compression of Saline Creek Oil Sand  
Sample No. 24 at 200°C Following Stress Path "F" (J1 Constant)

Procedural Details: Test TOS 18

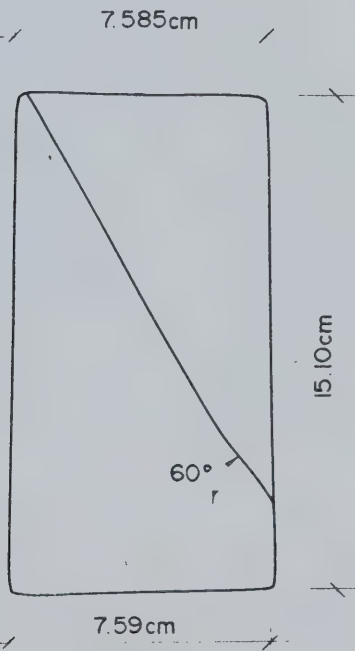
1. Sample 24 was thawed and back saturated for 19 hours under 10 MPa back pressure and 14 MPa isotropic confining stress.
2. The apparatus and sample were heated under drained conditions to 200°C. Volume of expelled pore fluid was monitored up to 180°C; however, the volume change device was isolated overnight in case of membrane failure. The temperature was allowed to stabilize overnight (i.e. for 16 hours).
3. A drained triaxial compression test was performed following stress path "F" as follows:
  - a) Back pressure and isotropic confining stress were increased simultaneously to 12 MPa and 16 MPa respectively.
  - b) Vertical stress was maintained constant at 16 MPa during the test.
  - c) Horizontal confining stress (i.e. cell pressure) was decreased in 250 kPa increments from 16 MPa to 10 MPa. Back pressure was decreased simultaneously from 12 MPa to 9.1 MPa.
  - d) Vertical deformation and volume change were monitored during the test.



TEST TOS 18: SAMPLE DATAPretest Saline Creek Sample No. 24:

Dia.:  $\emptyset = 7.590 \text{ cm}$        $w = 0.035$   
Height:  $H = 15.143 \text{ cm}$        $B = 0.145$   
Area:  $A = 45.245 \text{ cm}^2$   
Volume:  $V = 685.15 \text{ ml}$        $V_S = 455.7 \text{ ml}$   
Mass:  $M = 1425 \text{ g}$        $V_V = 229.4 \text{ ml}$   
Mass Solids = 1208 g      Dry Density =  $1.763 \text{ Mg/m}^3$

Density:       $= 2.080 \text{ Mg/m}^3$   
Porosity:       $= 0.334$   
Void Ratio:       $= 0.502 \text{ g}$

Sample 24 After Test TOS 18



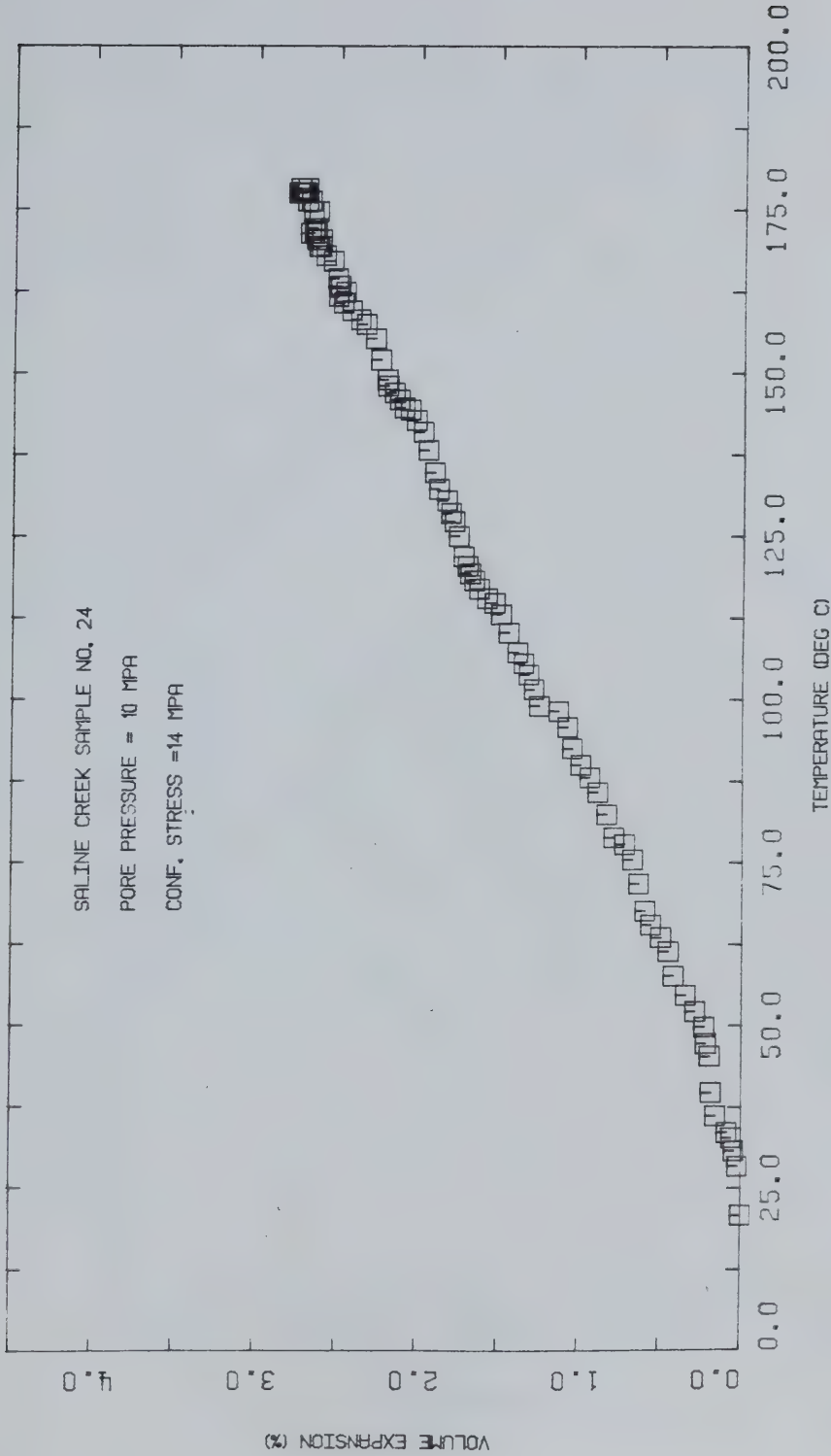


FIGURE E18.1 Triaxial Test TOS18: Volume of Pore Fluid Expelled During Heating



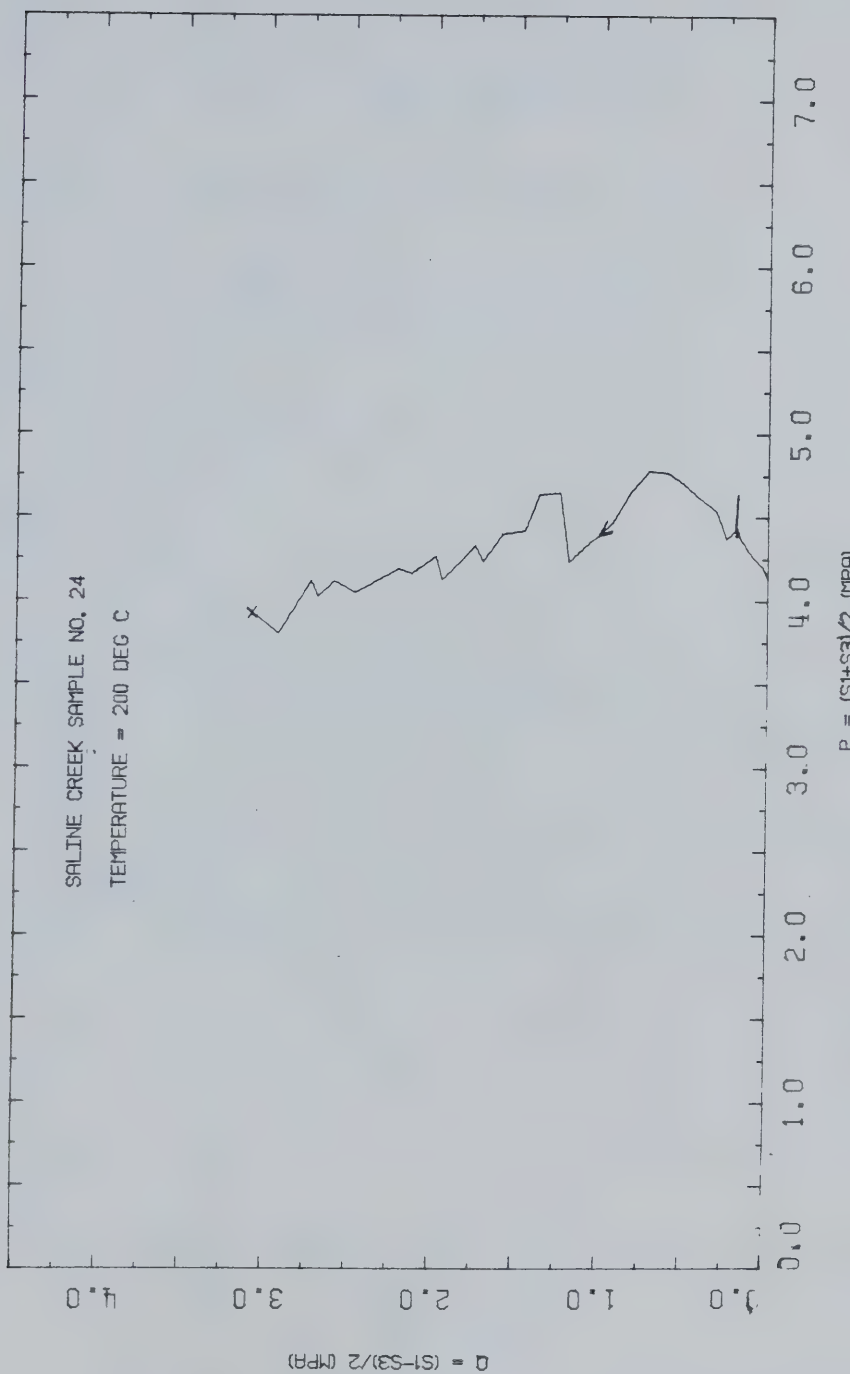


FIGURE I.18.2 Triaxial Test TOS18: Stress Path



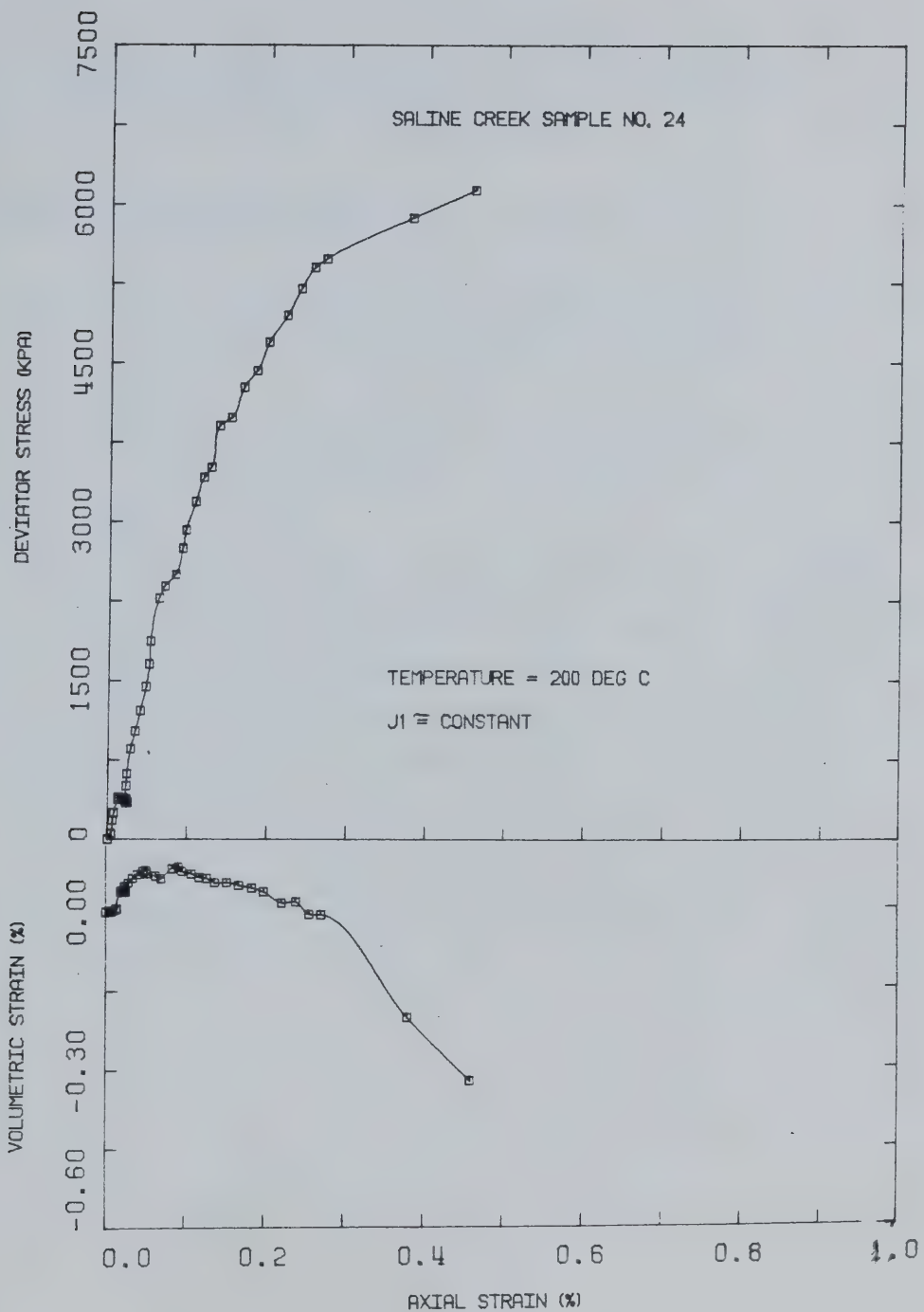


FIGURE E18.3 Triaxial Test TOS18: Deviator Stress Vs. Strain



## TEST TOS 19

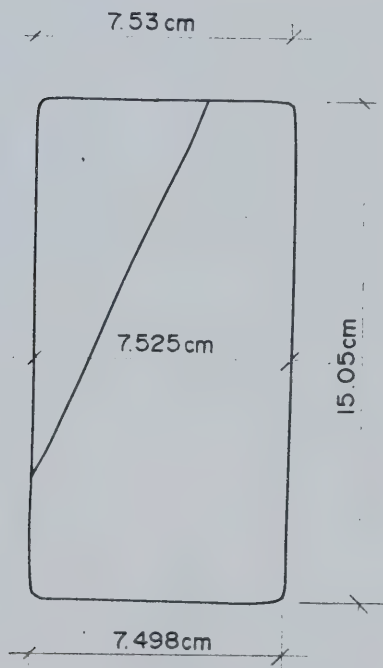
Drained Triaxial Isotropic and Passive Compression of  
Saline Creek Oil Sand Sample No. 19 at 125°C and 4 MPa  
Effective Confining StressProcedural Details: Test TOS 19

1. Sample 19 was thawed and back saturated for 23 hours under 10 MPa back pressure and 14 MPa isotropic confining stress.
2. The apparatus and sample were heated drained to 125°C. Volume of expelled pore fluid was monitored during heating.
3. Three cycles of drained isotropic compression and unloading were applied over the effective stress range 4 - 17 MPa. Back pressure was maintained constant at 10 MPa.
4. A drained triaxial passive compression test was performed. Vertical compressive stress was increased while horizontal confining stress and back pressure were maintained constant at 14 MPa and 10 MPa respectively. Vertical (axial) deformation and volume change were monitored during the test.



TEST TOS 19: SAMPLE DATAPretest Saline Creek Sample No. 19:

Dia.:  $\emptyset = 7.500$  cm      w = 0.021  
Height: H = 15.055 cm      B = 0.162  
Area: A = 44.179  $\text{cm}^2$   
Volume: V = 665.11 ml       $V_s = 442.1$  ml  
Mass: M = 1385 g       $V_v = 223.0$  ml  
Mass Solids = 1172 g      Dry Density = 1.762  $\text{Mg/m}^3$   
Density: = 2.084  $\text{Mg/m}^3$   
Porosity: = 0.334  
Void Ratio: = 0.502 g

Sample 19 After Test TOS 19



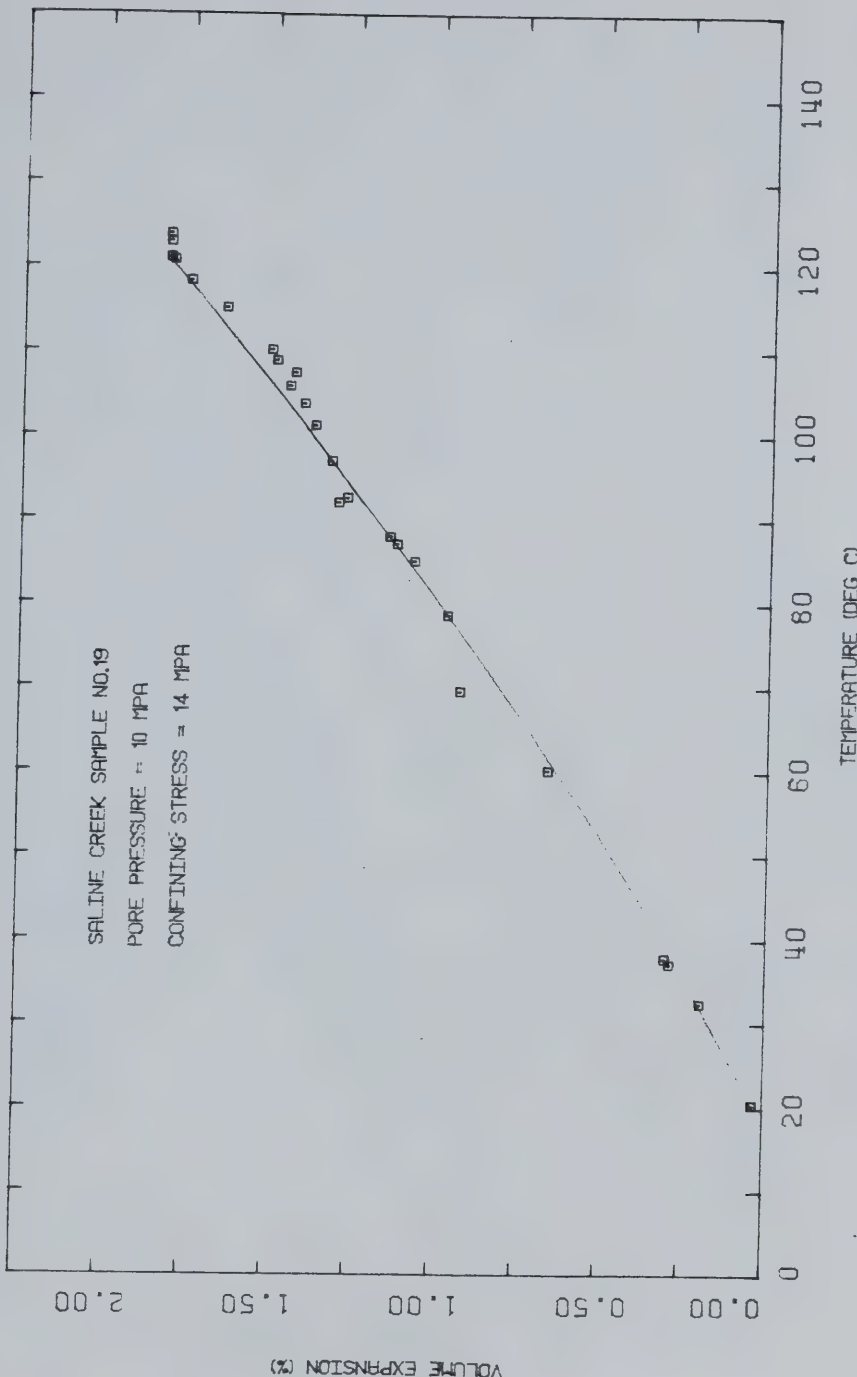


FIGURE E19.1 Triaxial Test TOS19: Volume of Pore Fluid Expelled During Heating



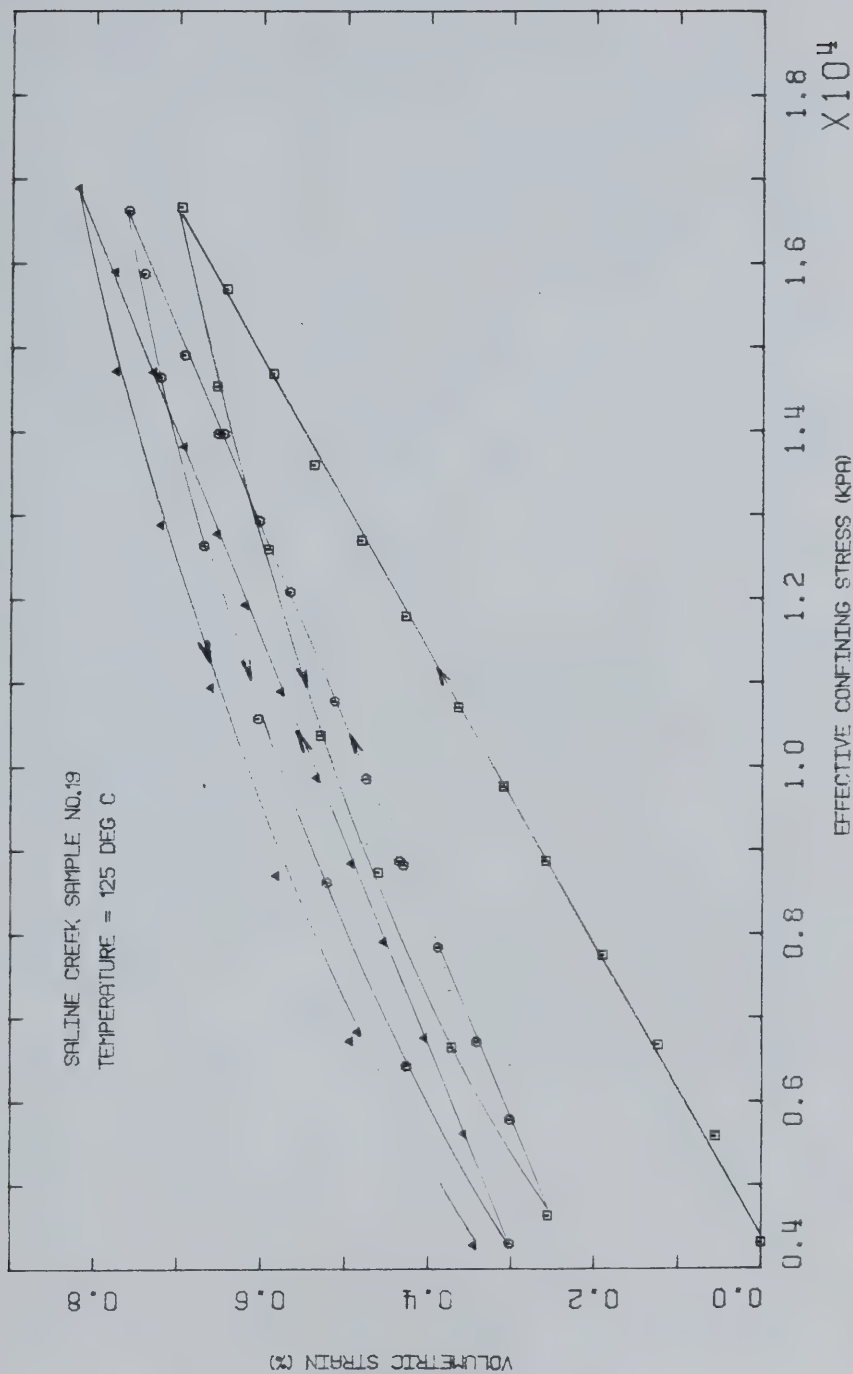


FIGURE E19.2 Triaxial Test TOS19: Drained Isotropic Compression



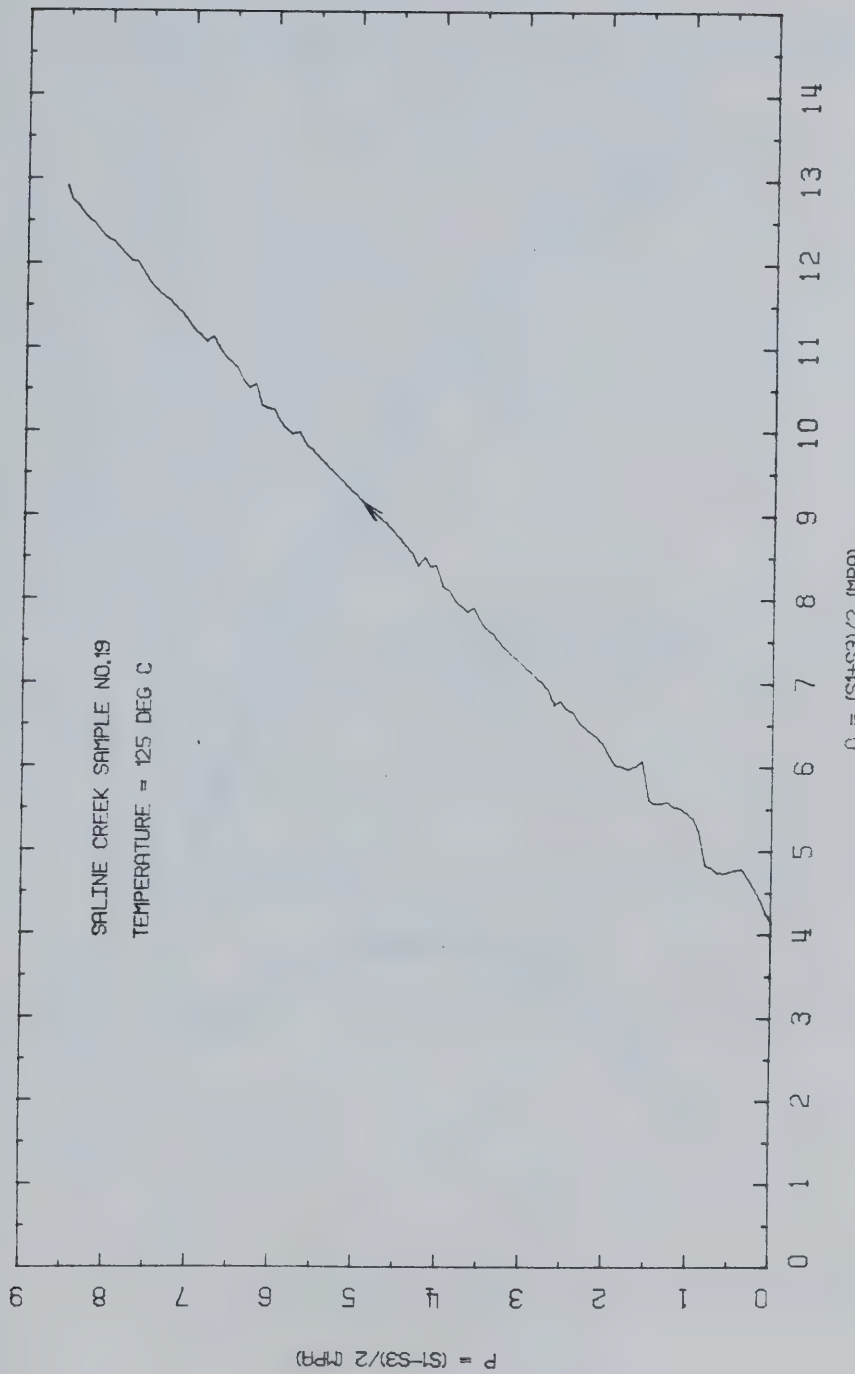


FIGURE E19.3 Triaxial Test TOS19: Stress Path



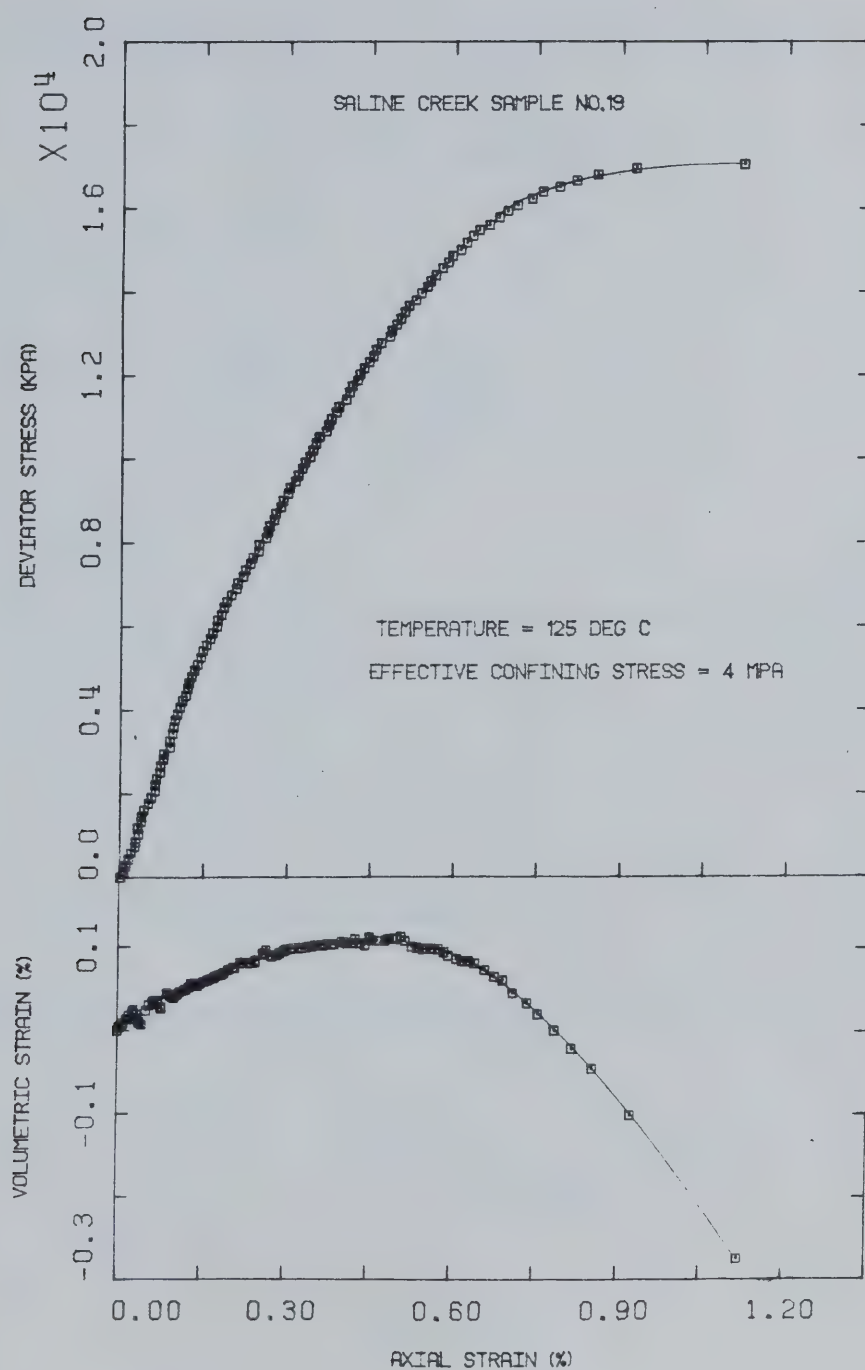


FIGURE E19.4 Triaxial Test TOS19: Deviator Stress Vs. Strain



TEST TOS 20

### Unconfined Compression of Case Hardened Saline Creek Oil Sand Sample No. 2 Following Unsaturated Heating at 150°C

TEST TOS 20: SAMPLE DATA

Saline Creek Sample No. 20:

Before Heating:      Height:      =      15.13 cm  
                                    Diameter:      =      7.54 cm  
                                    Mass:      =      1332 g  
                                    Bulk Density:      =      1.972 Mg/m<sup>3</sup>

### Heating Procedure:

1. Sample confined under 15 kPa stress and vented radially and vertically to atmospheric pressure.
2. Heating cycles:
  - a) 4 hours at 65°C
  - b) 24 hours at 105°C
  - c) 88 hours at 150°C
  - d) 36 hour cooldown at 20°C

#### Sample Dimensions After Heating and Cooldown:



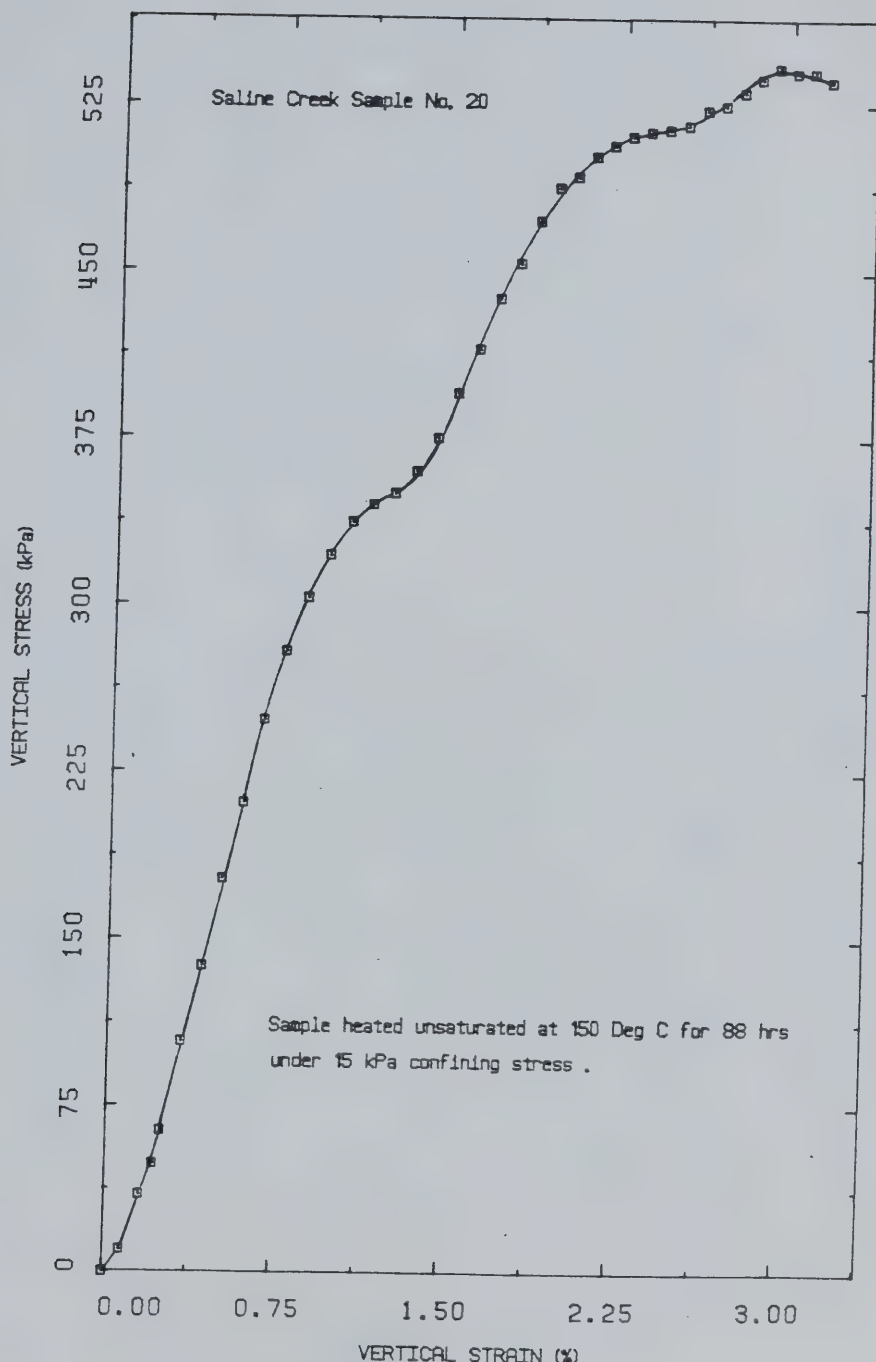
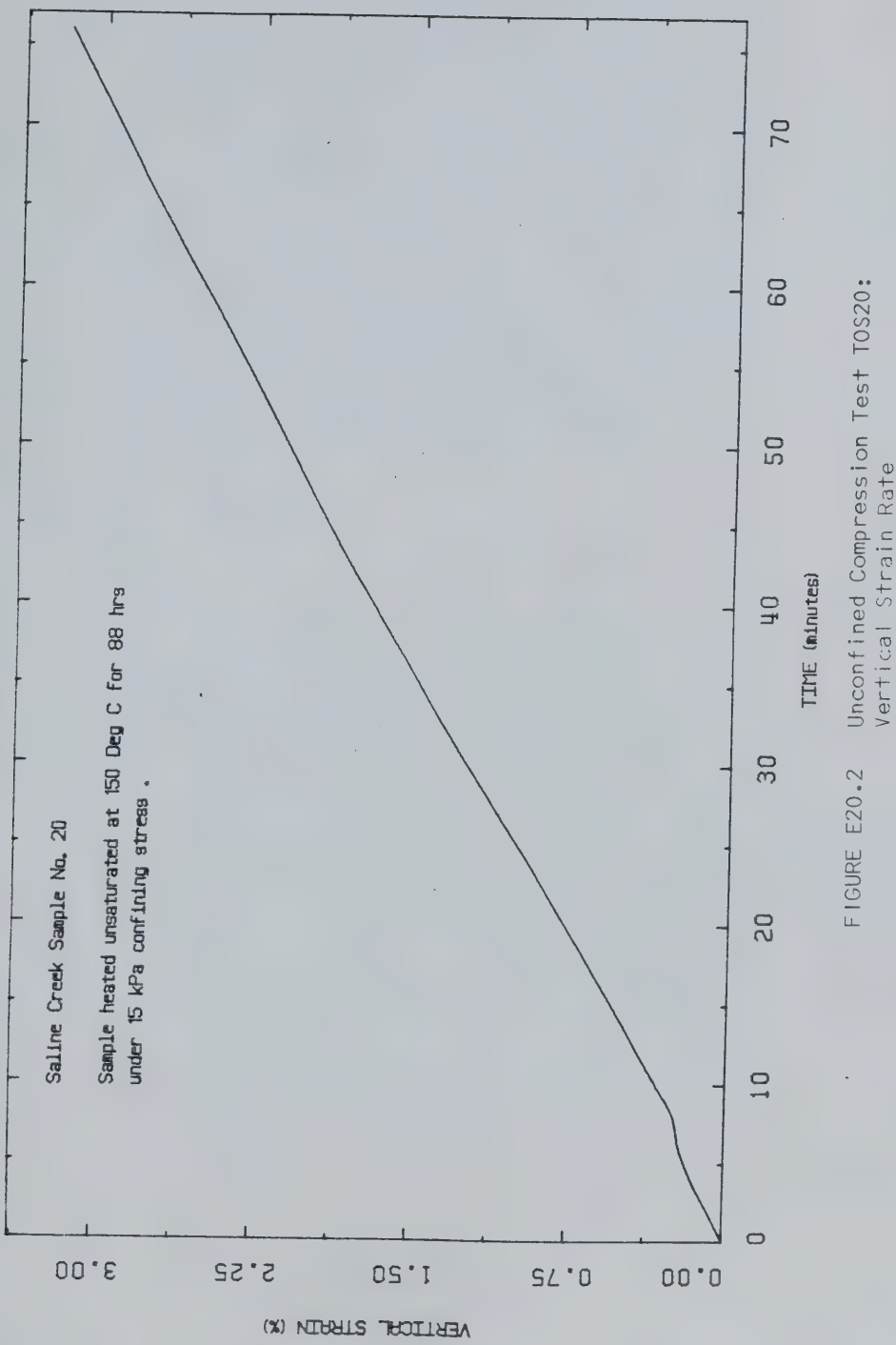


FIGURE E20.1 Unconfined Compression Test TOS20:  
Vertical Stress Vs. Strain

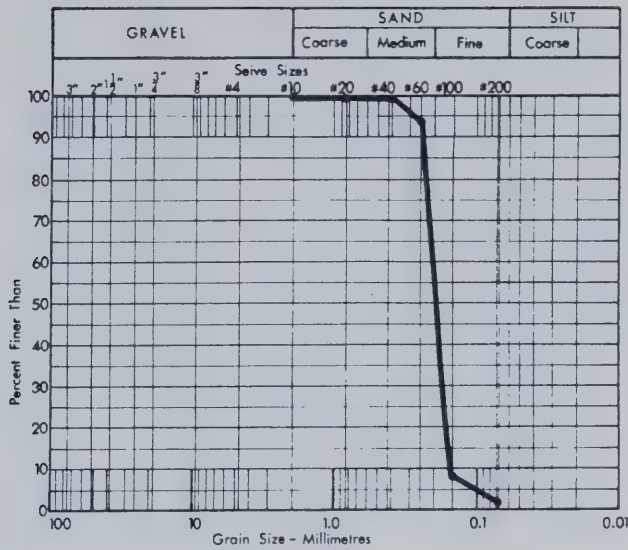




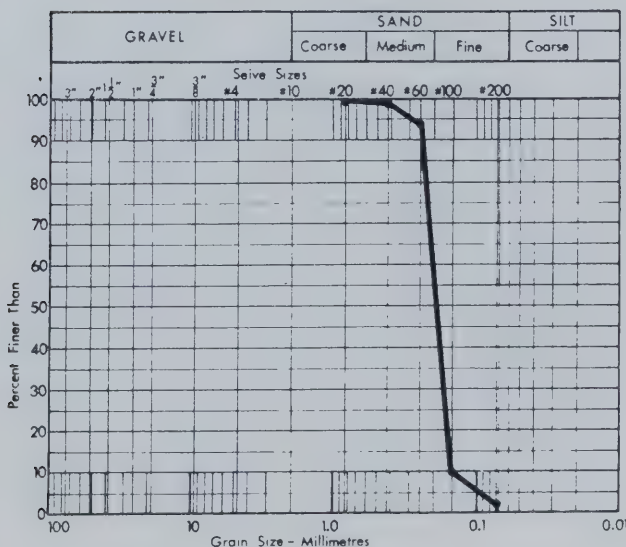


APPENDIX F  
GRAIN SIZE ANALYSES





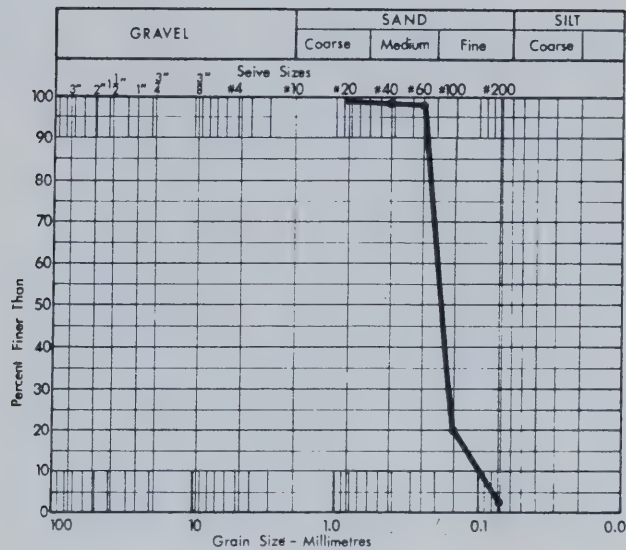
Before



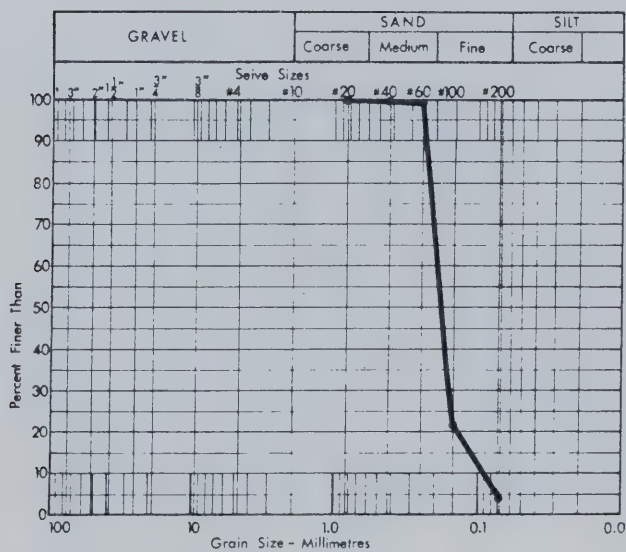
After

FIGURE F1      Sample #41  
Test COS 9





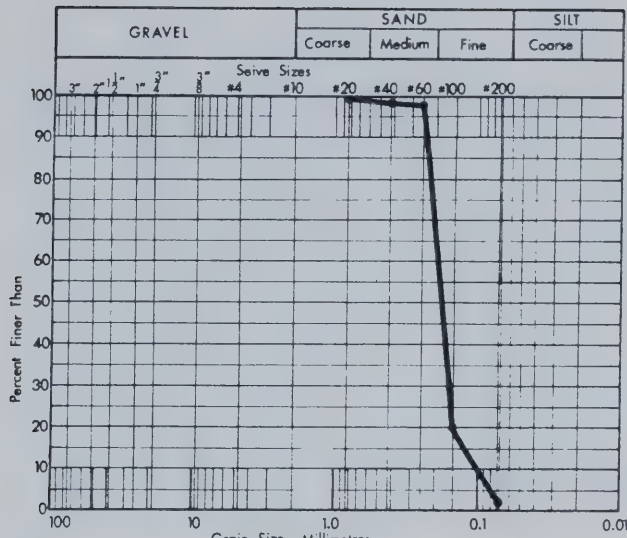
## Before



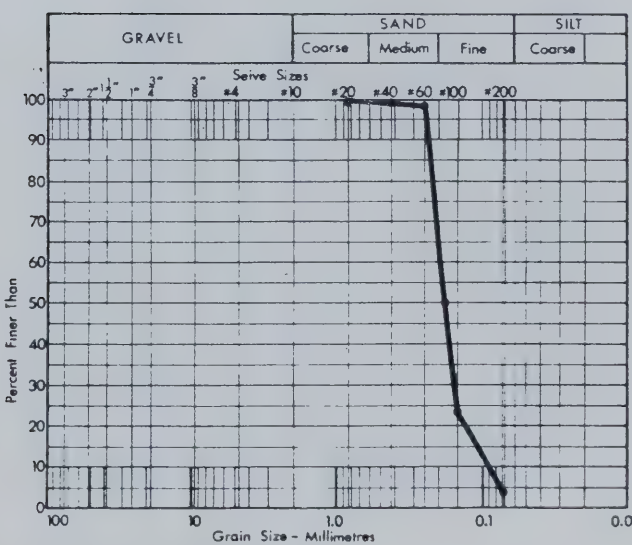
After ( Top )

FIGURE F2 Sample #36A  
Test CPERM 4





## Before

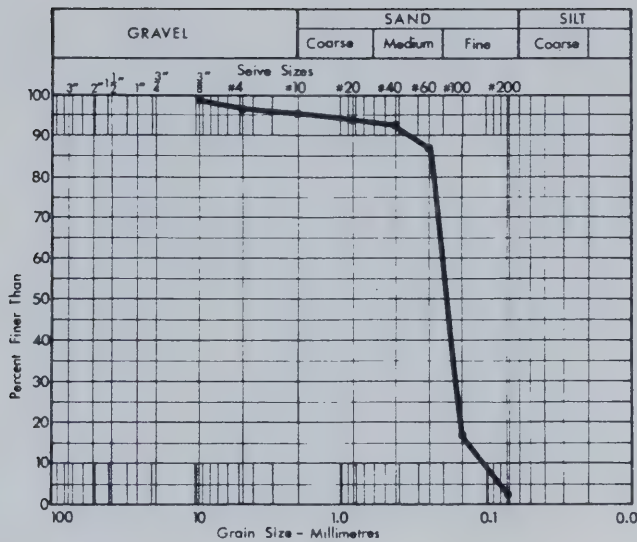


After ( Bottom )

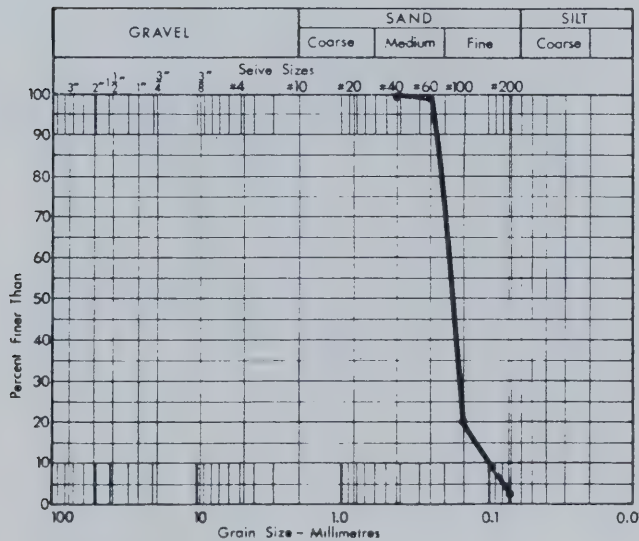
$$\begin{aligned}D_{10} &= 0.1 \text{ mm} \\D_{60} &= 0.2 \text{ mm} \\C_v &= 2.0\end{aligned}$$

FIGURE F3 Sample 36A  
Test CPERM 4





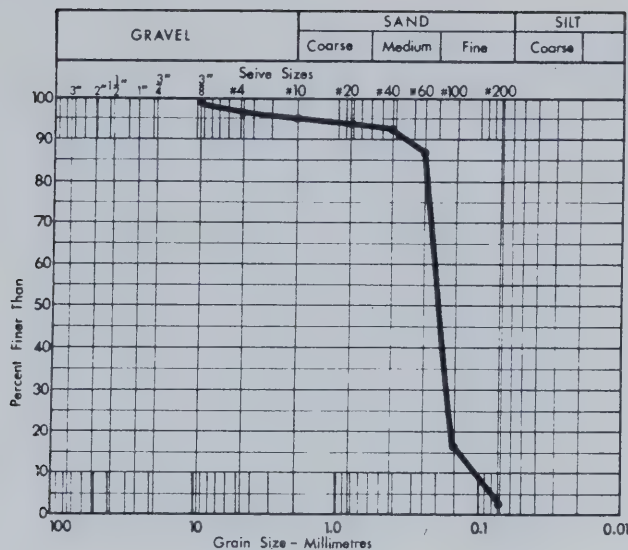
Before



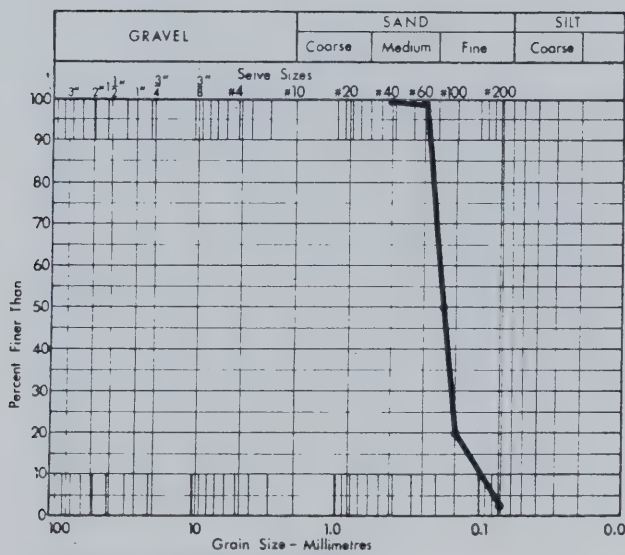
After (Top)

FIGURE F4      Sample #31A  
Test CPERM 5





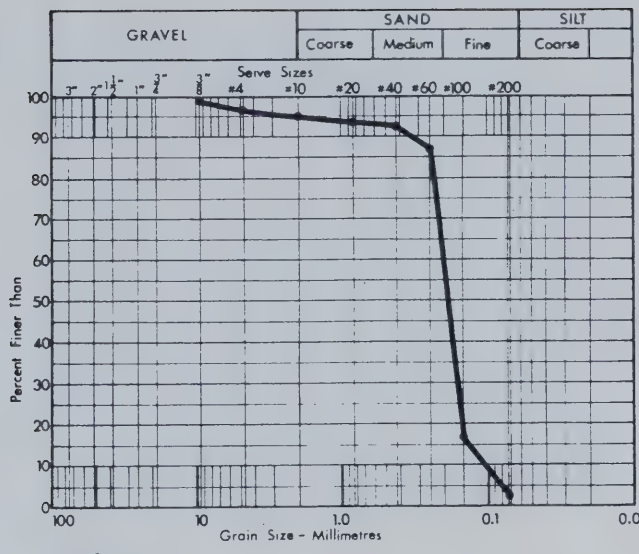
Before



After (Bottom Outside)

FIGURE F5      Sample #31A  
Test CPERM 5



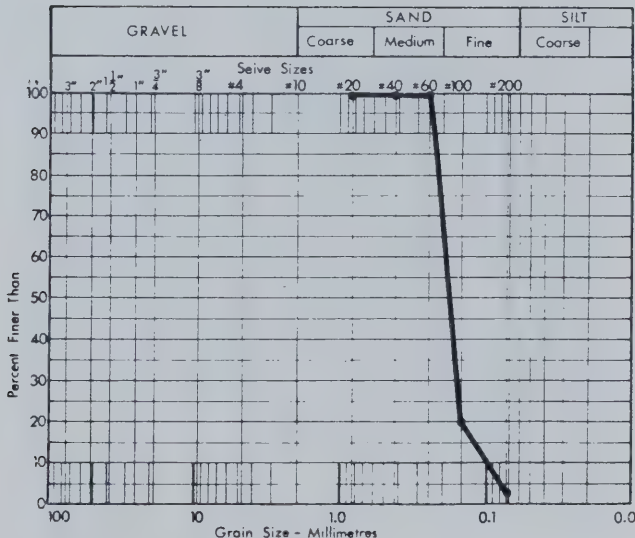


**Before**

$$D_{10} = 0.11 \text{ mm}$$

$$D_{60} = 0.22 \text{ mm}$$

$$C_u = 2.0$$



**After ( Bottom Centre )**

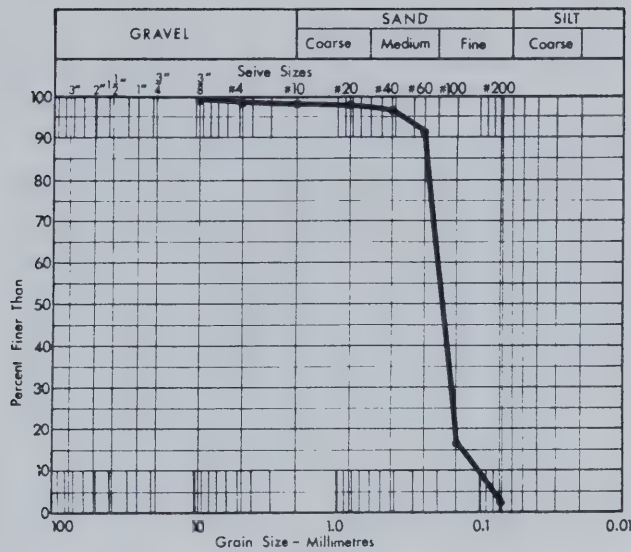
$$D_{10} = 0.1 \text{ mm}$$

$$D_{60} = 0.2 \text{ mm}$$

$$C_u = 2.0$$

FIGURE F6   Sample #31A  
Test CPERM 5



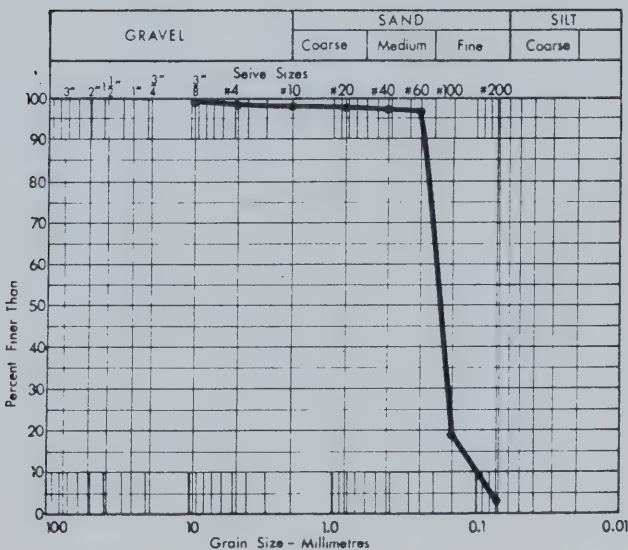


Before

$$D_{10} = 0.11\text{mm}$$

$$D_{60} = 0.21\text{mm}$$

$$C_u = 0.19$$



After

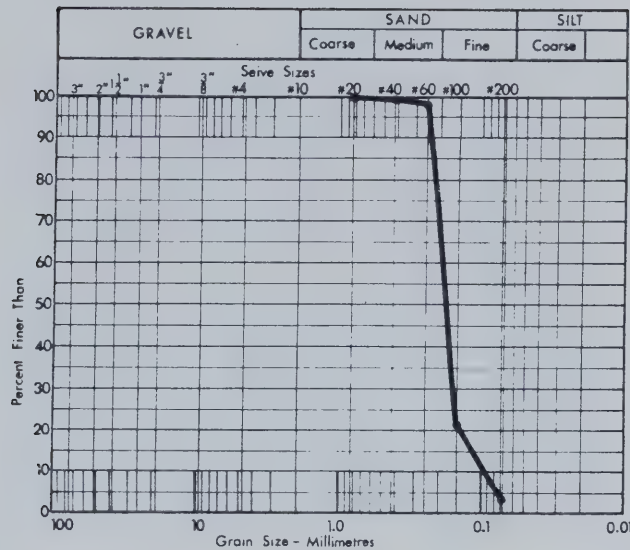
$$D_{10} = 0.1\text{mm}$$

$$D_{60} = 0.2\text{mm}$$

$$C_u = 2.0$$

FIGURE F7      Sample #31B  
Test CPERM 6



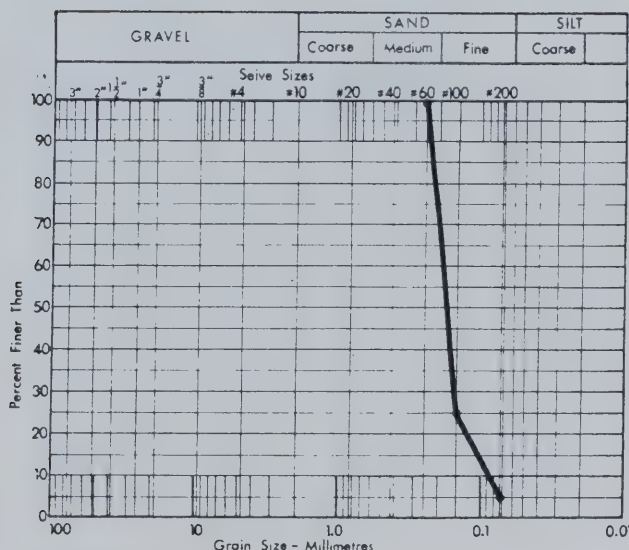


Before

$$D_{10} = 0.1 \text{ mm}$$

$$D_{60} = 0.2 \text{ mm}$$

$$C_u = 2.0$$



After

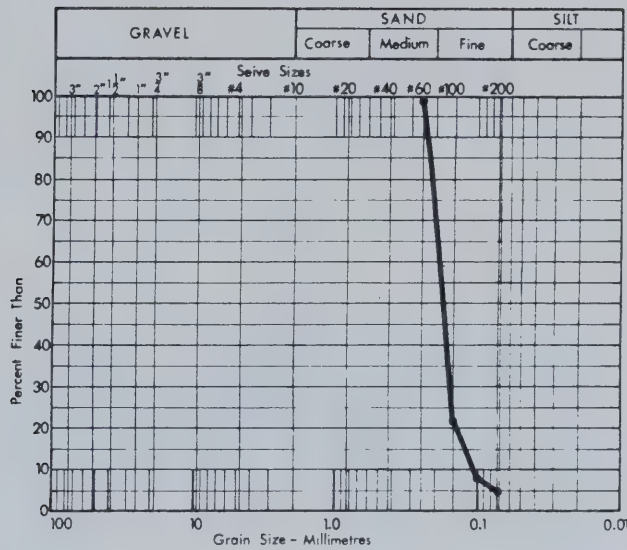
$$D_{10} = 0.09 \text{ mm}$$

$$D_{60} = 0.2 \text{ mm}$$

$$C_u = 2.2$$

FIGURE F8      Sample #36B  
Test CPERM 9



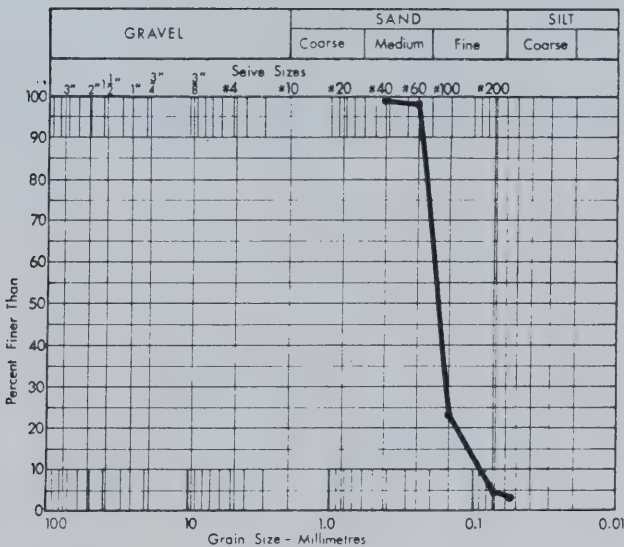


Before

$$D_{10} = 0.11 \text{ mm}$$

$$D_{60} = 0.2 \text{ mm}$$

$$C_u = 1.8$$



After

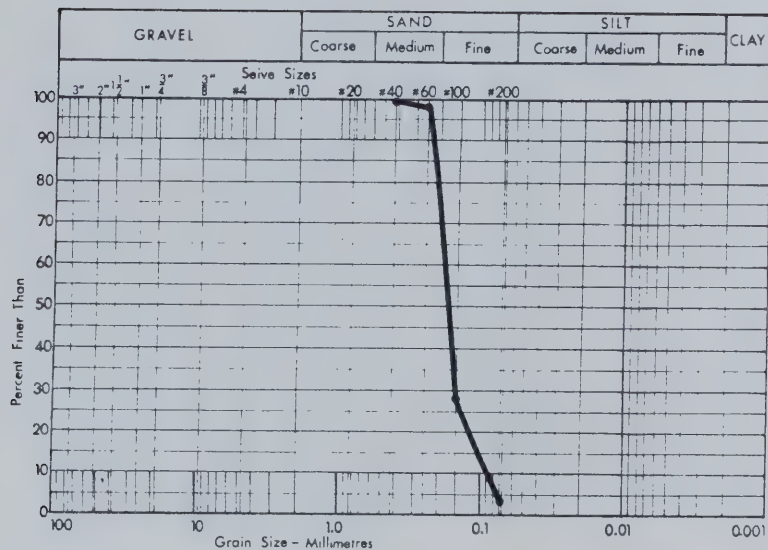
$$D_{10} = 0.085 \text{ mm}$$

$$D_{60} = 0.19 \text{ mm}$$

$$C_u = 2.2$$

FIGURE F9 Sample #25  
Test TOS 1

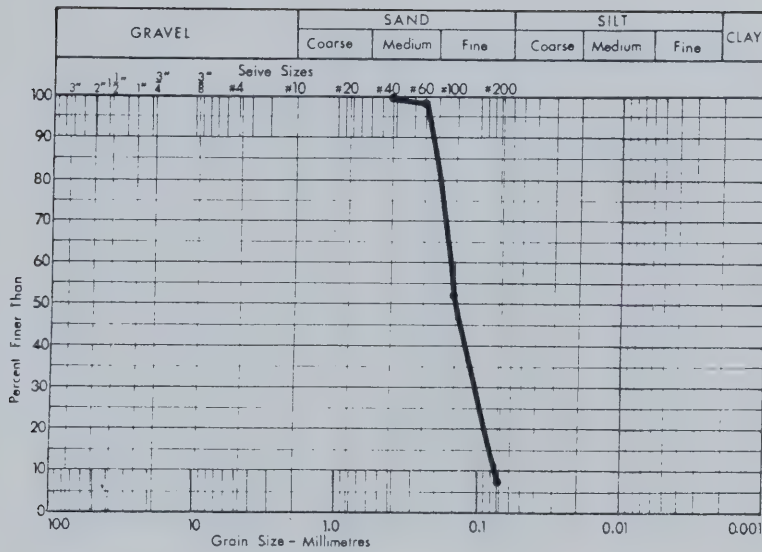




Before

FIGURE F10 Sample #33  
Test TOS 2

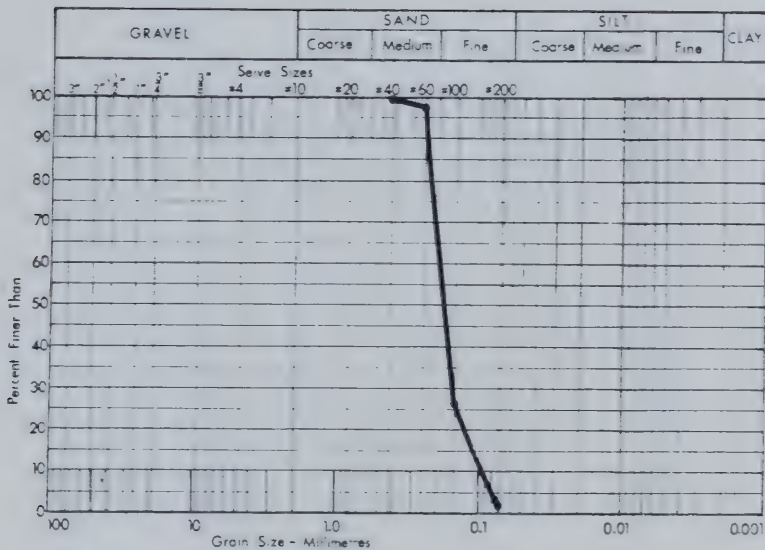




$$D_{10} = 0.078\text{mm}$$
$$D_{60} = 0.18\text{mm}$$
$$C_u = 2.3$$

FIGURE F11 Sample #43  
Test TOS 3

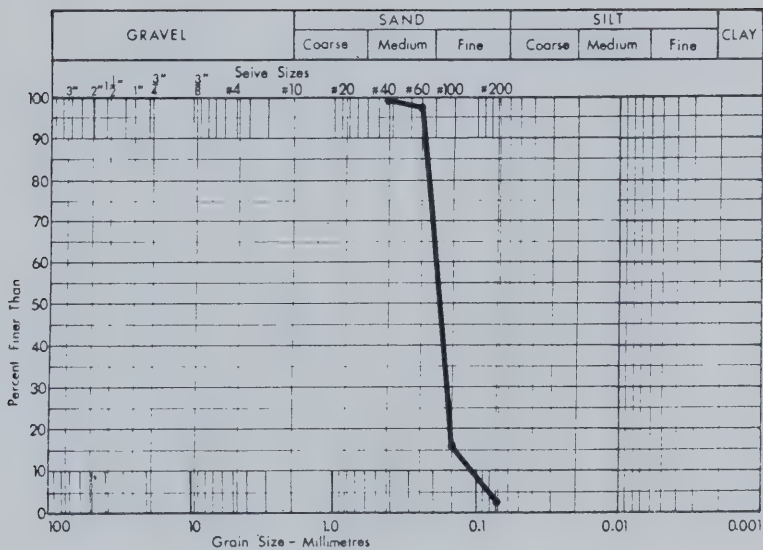




Before

FIGURE F12 Sample #44  
Test TOS 4

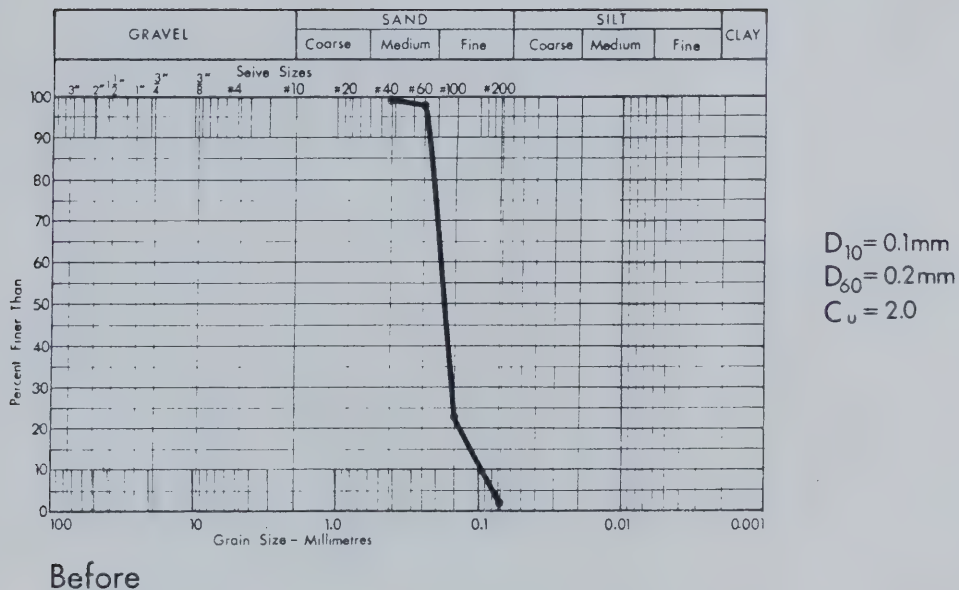




Before

FIGURE F13 Sample #17  
Test TOS 5

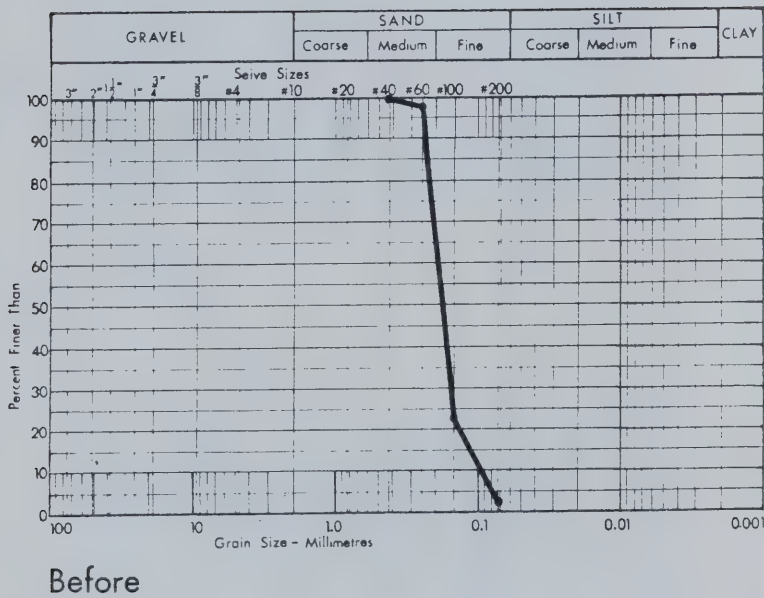




Before

FIGURE F14 Sample #16  
 Test TOS 6



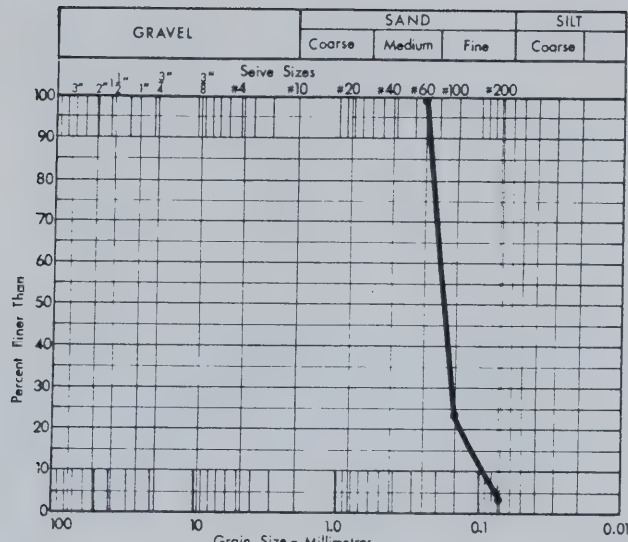


Before

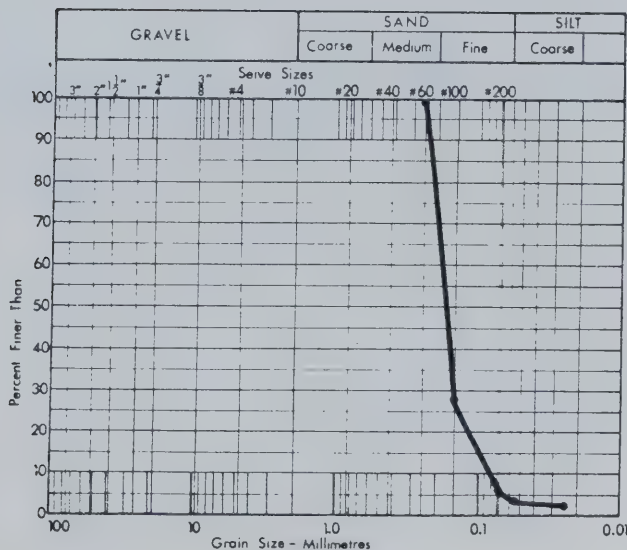
$$D_{10} = 0.1 \text{ mm}$$
$$D_{60} = 0.2 \text{ mm}$$
$$C_u = 2.0$$

FIGURE F15 Sample #45  
Test TOS 7





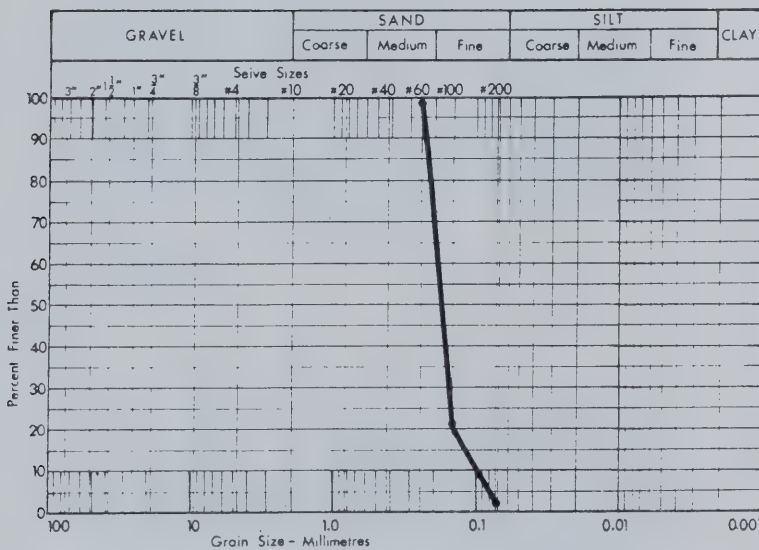
Before



After

FIGURE F16 Sample #20  
Test TOS 10

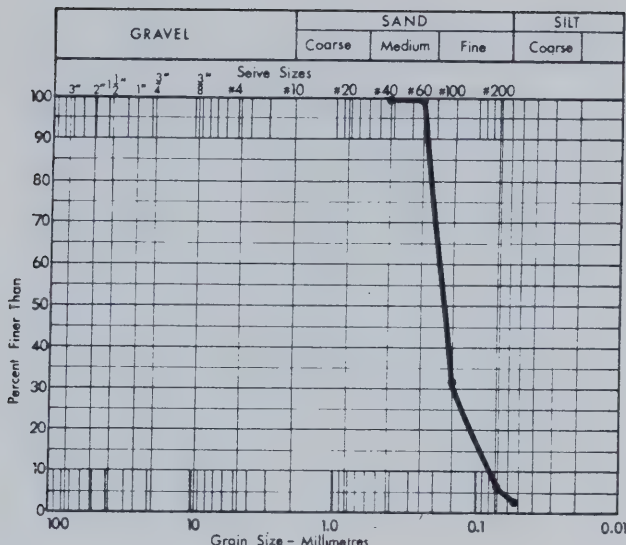




Before

FIGURE F17 Sample #22  
Test TOS 11



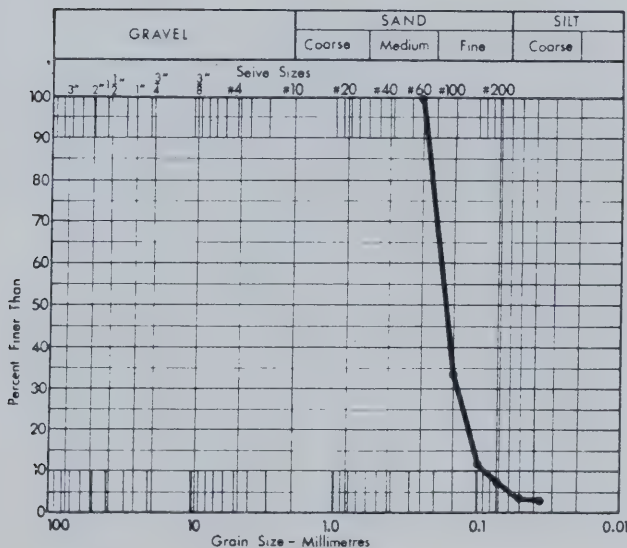


Before

$$D_{10} = 0.08\text{mm}$$

$$D_{60} = 0.19\text{mm}$$

$$C_u = 2.4$$



After

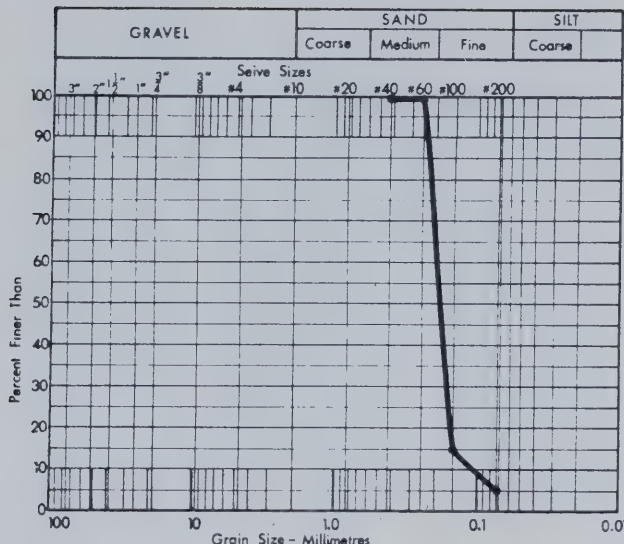
$$D_{10} = 0.09\text{mm}$$

$$D_{60} = 0.18\text{mm}$$

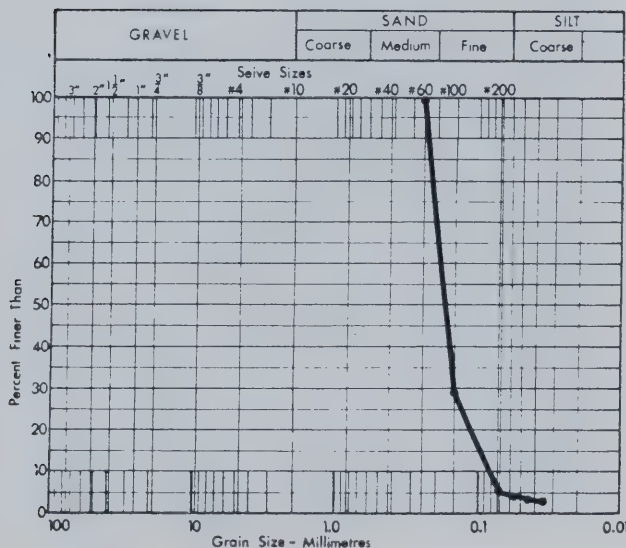
$$C_u = 2.0$$

FIGURE F18 Sample #29  
Test TOS 12





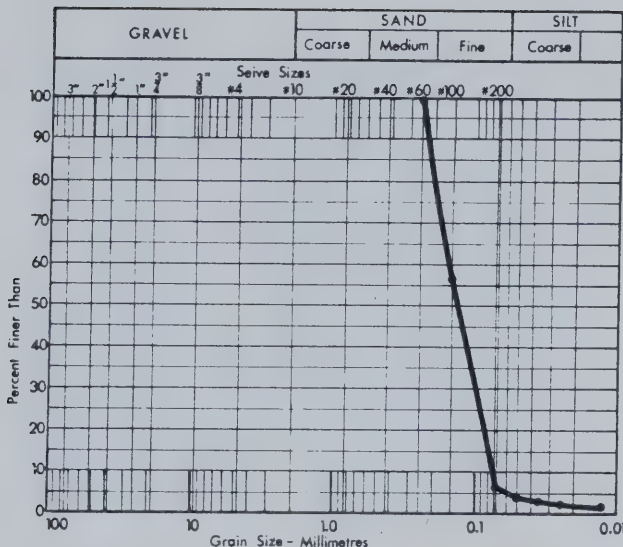
## Before



After

FIGURE F19 Sample #5, 7, 8  
Test TOS 14



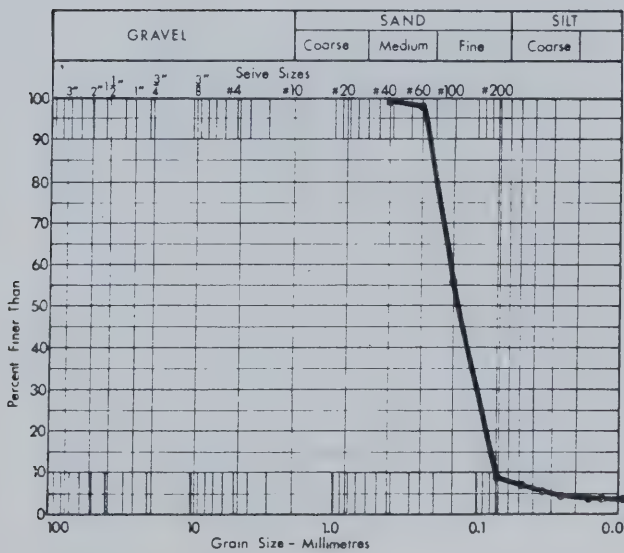


Before

$$D_{10} = 0.08 \text{ mm}$$

$$D_{60} = 0.17 \text{ mm}$$

$$C_u = 2.1$$



After

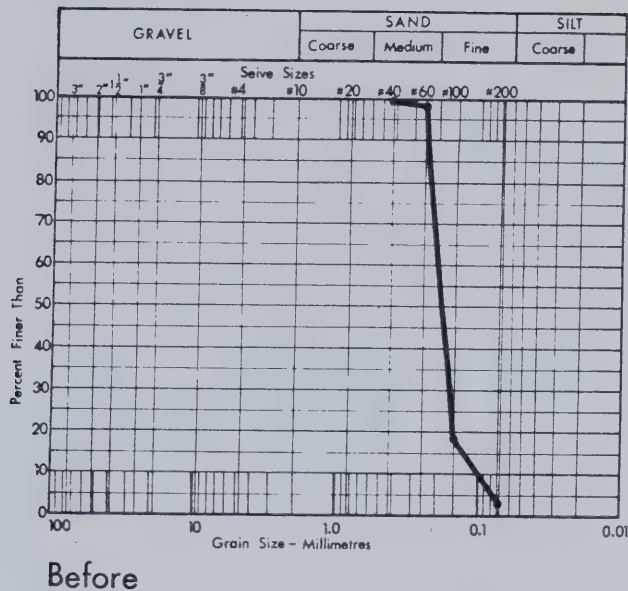
$$D_{10} = 0.07 \text{ mm}$$

$$D_{60} = 0.17 \text{ mm}$$

$$C_u = 2.4$$

FIGURE F20 Sample #23  
Test TOS 17

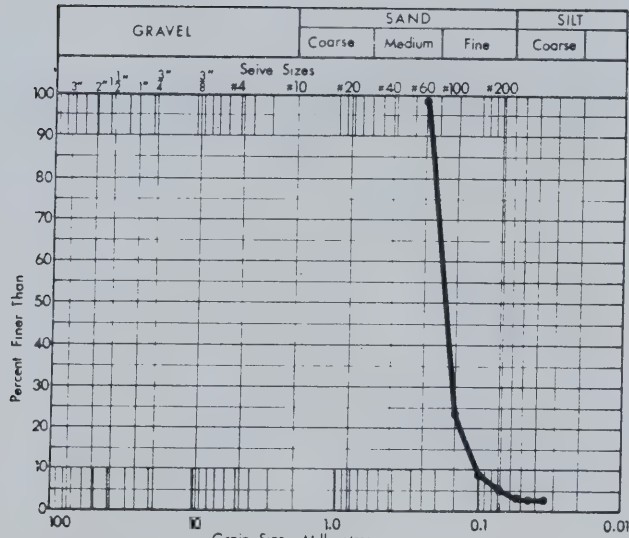




$$D_{10} = 0.1 \text{ mm}$$

$$D_{60} = 0.2 \text{ mm}$$

$$C_u = 2.0$$



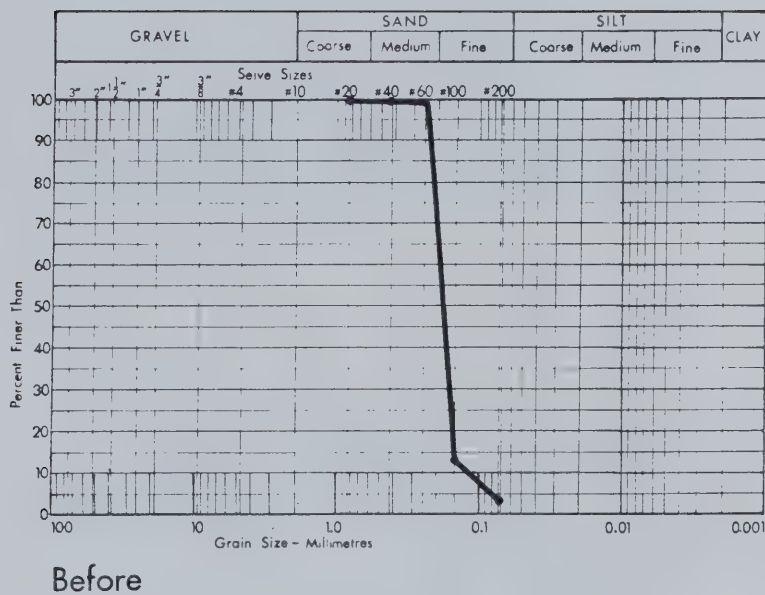
$$D_{10} = 0.1 \text{ mm}$$

$$D_{60} = 0.2 \text{ mm}$$

$$C_u = 2.0$$

FIGURE F21 Sample #24  
Test TOS 18





$$D_{10} = 0.12 \text{ mm}$$

$$D_{60} = 0.2 \text{ mm}$$

$$C_u = 1.7$$

FIGURE F22 Sample #19  
Test TOS 19



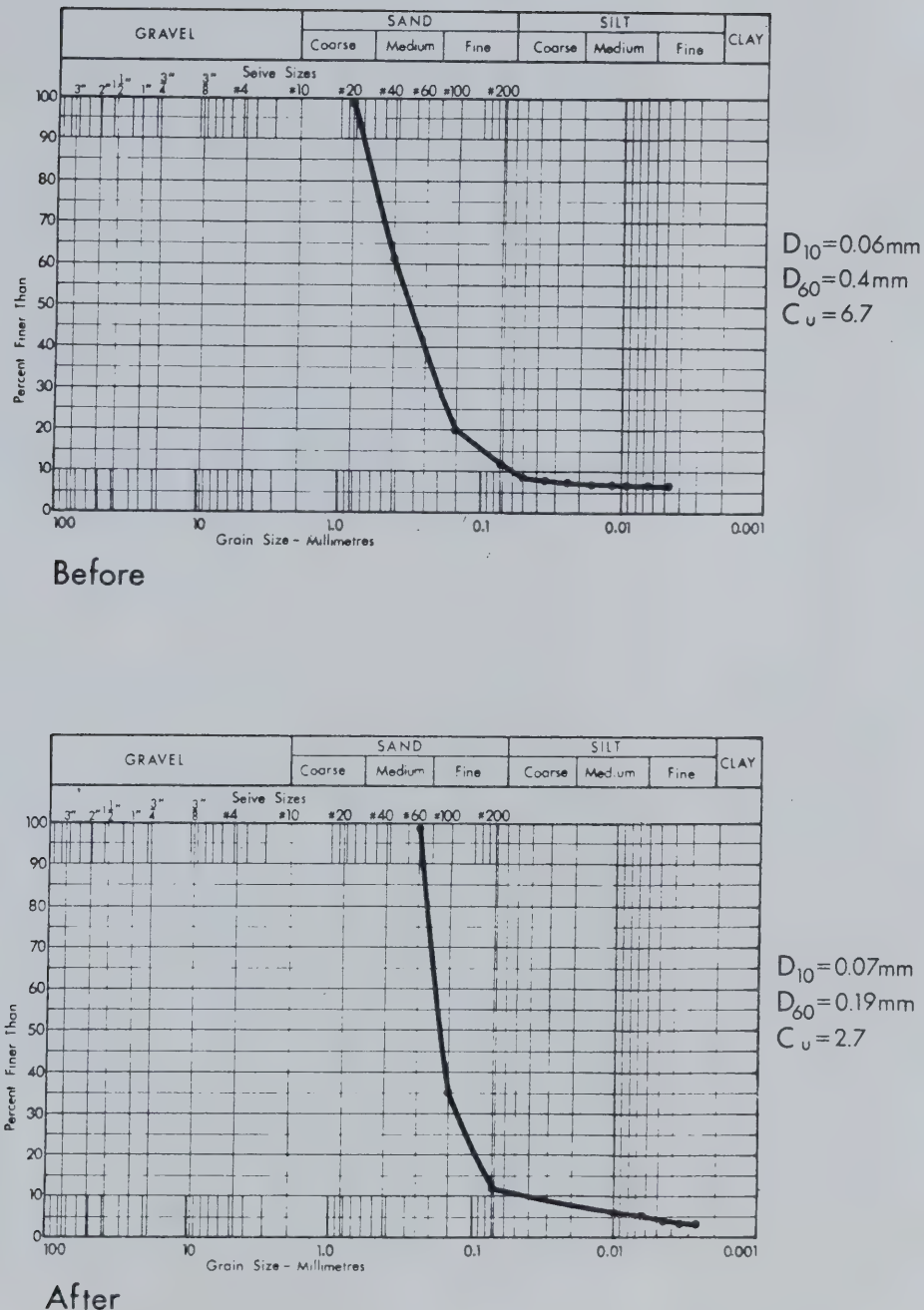


FIGURE F23 Sample #12B  
Test TOS 15



APPENDIX G

SCANNING ELECTRON MICROPHOTOGRAPHS OF VARIOUS OIL SANDS  
BEFORE AND AFTER HEATING EXPERIMENTS



NOTES:

1. Scanning electron microphotographs of Athabasca and Cold Lake oil sand specimens presented in Appendix G were studied and photographed using a Cambridge Stereoscan electron microscope.
2. Mineral grain fabric and texture of seventeen oil sand specimens are included. Specimen preparation and study methods are described in section 3.9.2 of Volume I.
3. Mineralogic and textural alterations resulting from elevated pressures and temperatures were detected, however, these were relatively minor. Grain crushing is believed to contribute to loss of grain interlocking and reduced angle of shearing resistance.



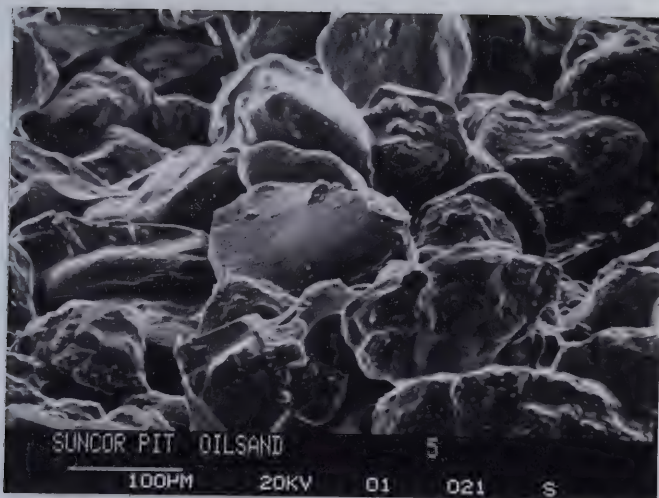


PLATE G-1 Oven-dried McMurray Formation oil sand from the Suncor minesite.



PLATE G-2 Crystal overgrowth in McMurray Formation oil sand from the Suncor minesite.



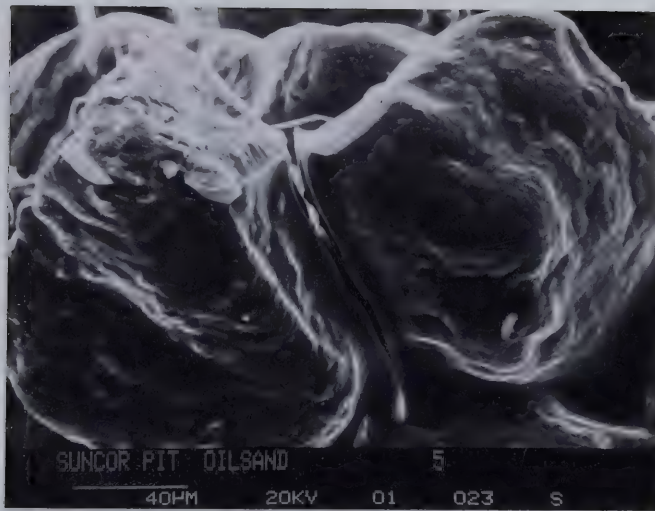


PLATE G-3 Tension crack in "case-hardened" Athabasca bitumen between two sand grains (in oven-dried oil sand).



PLATE G-4 "Case-hardening" of bitumen due to unsaturated heating of Athabasca oil sand.



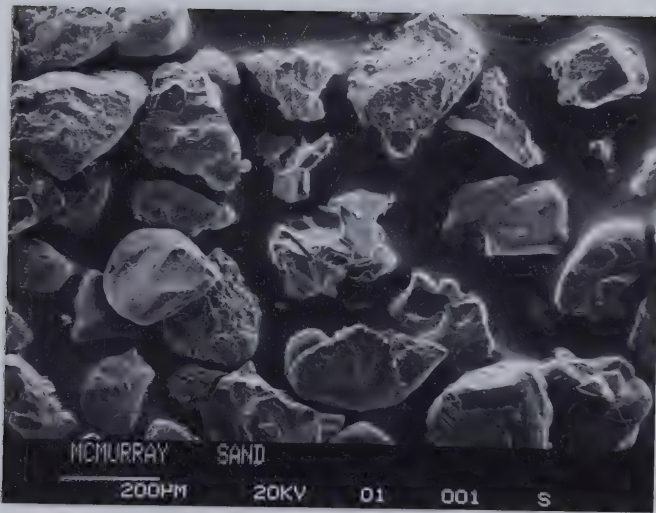


PLATE G-5 Oil-free McMurray Formation sand grains (loosely packed).



PLATE G-6 Oil-free McMurray Formation sand grains.



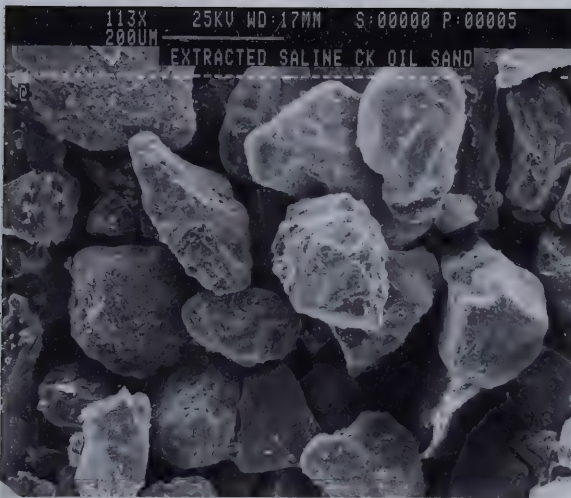


PLATE G-7 Oil-free Saline Creek sand grains (closely packed).



PLATE G-8 Intact oil-rich Saline Creek oil sand fabric.





PLATE G-9 Bitumen-coated Saline Creek sand grains.



PLATE G-10 Rugose pore channel in Saline Creek oil sand.



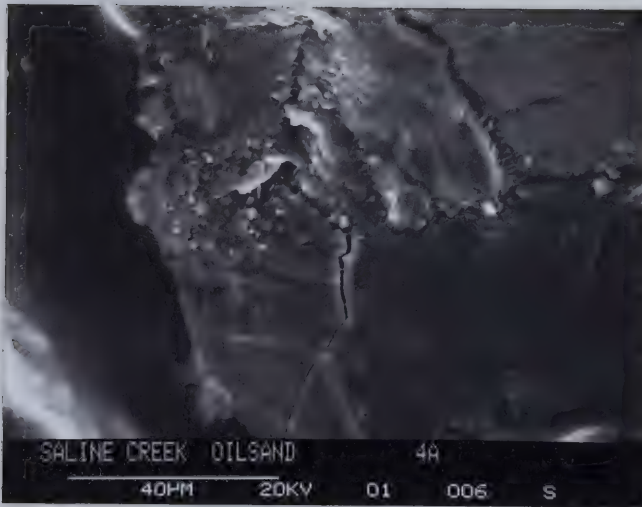


PLATE G-11 Crystal overgrowth features in  
Saline Creek oil sand.



PLATE G-12 Saline Creek oil sand fabric  
following 100°C permeability test  
in which 10 percent of the bitumen  
was removed.



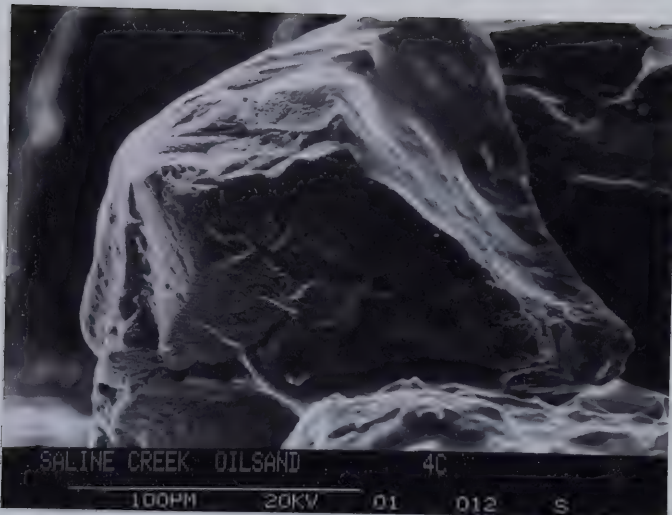


PLATE G-13 Saline Creek sand grain after 100°C permeability experiment.



PLATE G-14 Saline Creek oil sand fabric after 100°C permeability experiment.





PLATE G-15 Bitumen-coated Saline Creek sand grains after 100°C permeability experiment.



PLATE G-16 Saline Creek oil sand fabric following a 250°C permeability experiment.



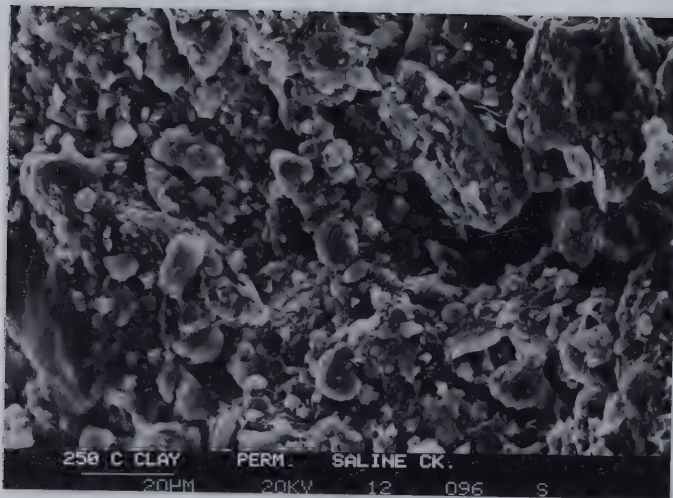


PLATE G-17 Clay particles in Saline Creek oil sand after a 250°C permeability experiment.

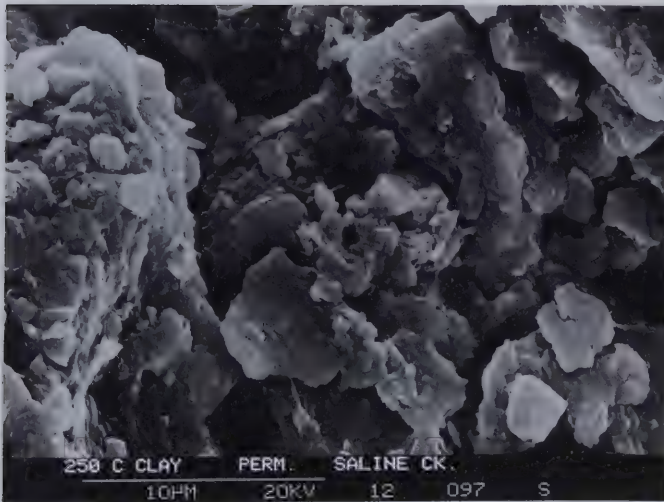


PLATE G-18 Clay particles in Saline Creek oil sand fabric (note the platy shape of the clay particles).





PLATE G-19 Saline Creek oil sand fabric after compression under 6 MPa confining stress and 300°C.



PLATE G-20 Bitumen-coated Saline Creek sand grains following 300°C compression test.



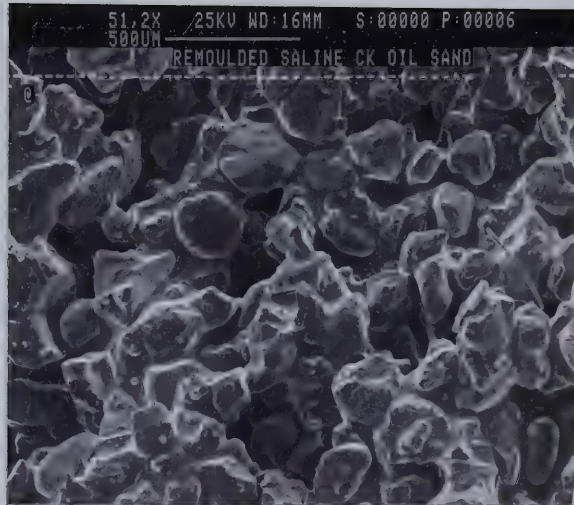


PLATE G-21 Remoulded Saline Creek oil sand fabric (note the clusters of "oil-bonded" grains).



PLATE G-22 Saline Creek oil sand fabric after triaxial compression under 8 MPa effective confining stress at 200°C.





PLATE G-23 Saline Creek oil sand fabric along the principal shear plane following triaxial compression at 200°C.

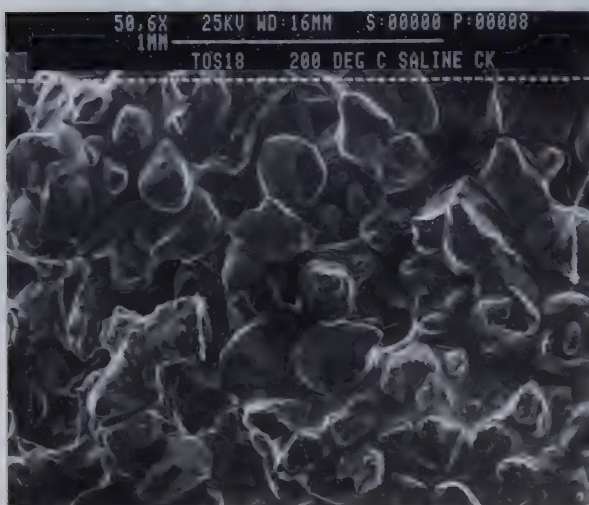


PLATE G-24 Saline Creek oil sand fabric after triaxial compression at 200°C (J1 constant stress path).



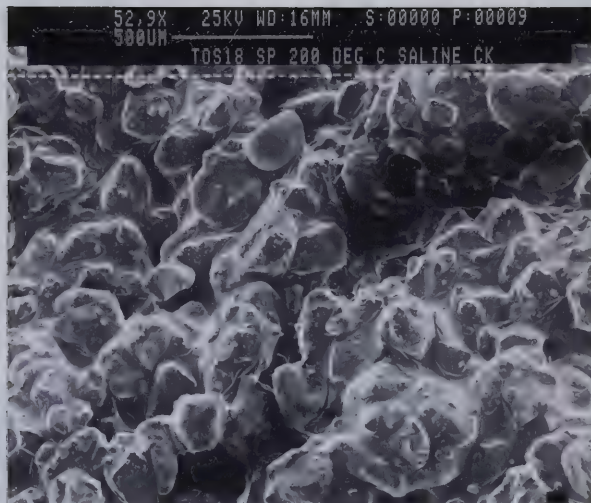


PLATE G-25 Saline Creek oil sand-shear plane fabric after 200°C triaxial compression test.



PLATE G-26 Fabric of oil-rich Saline Creek oil sand after 125°C triaxial compression test.



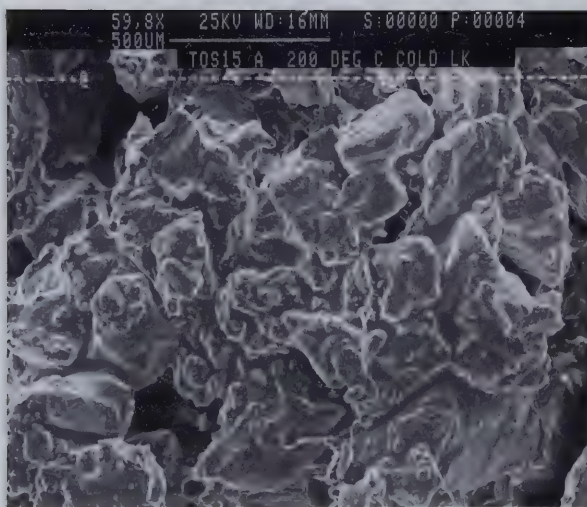


PLATE G-27 Cold Lake oil sand fabric after triaxial compression under 4 MPa effective confining stress at 200°C.



APPENDIX H  
X-RAY DIFFRACTION ANALYSES



## APPENDIX H

LEGEND FOR SYMBOLS  
ON X-RAY DIFFRACTION TRACES

**Q** - Quartz

**F** - Feldspar

**P** - Pyrite ( $\text{FeS}_2$ )

**B** - Brookite ( $\text{TiO}_2$ )

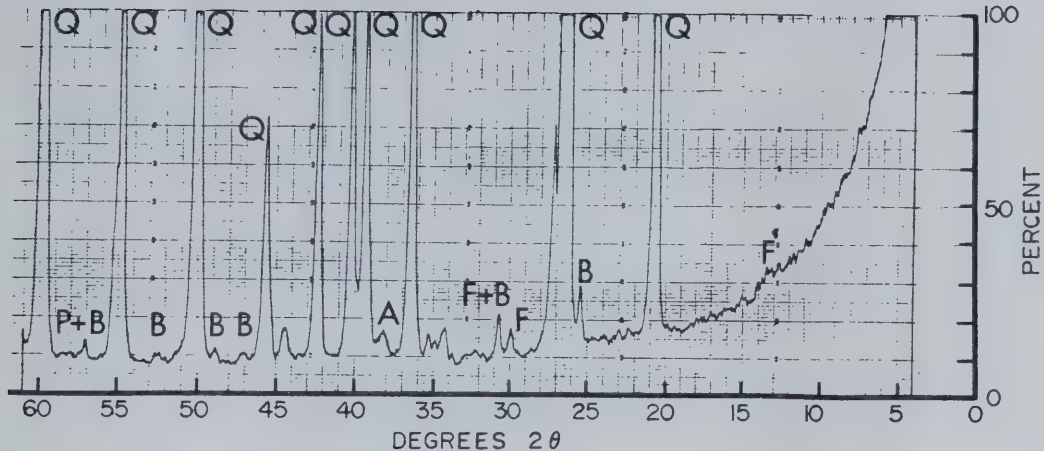
**A** - Alumunium sample holder

**K** - Kaolinite

**I** - Illite

**M** - Montmorillonite

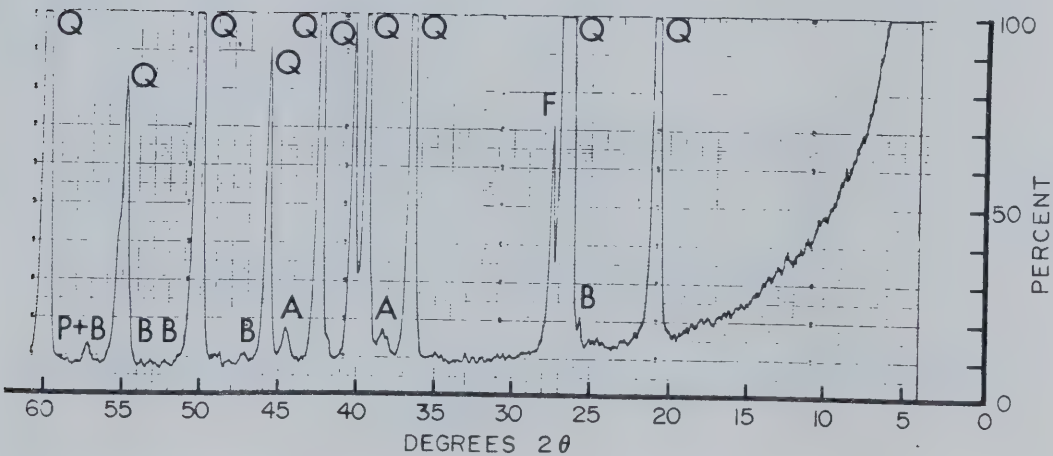




**SAMPLE #20**

**TEST TOS 10** (BEFORE)

FIGURE H1

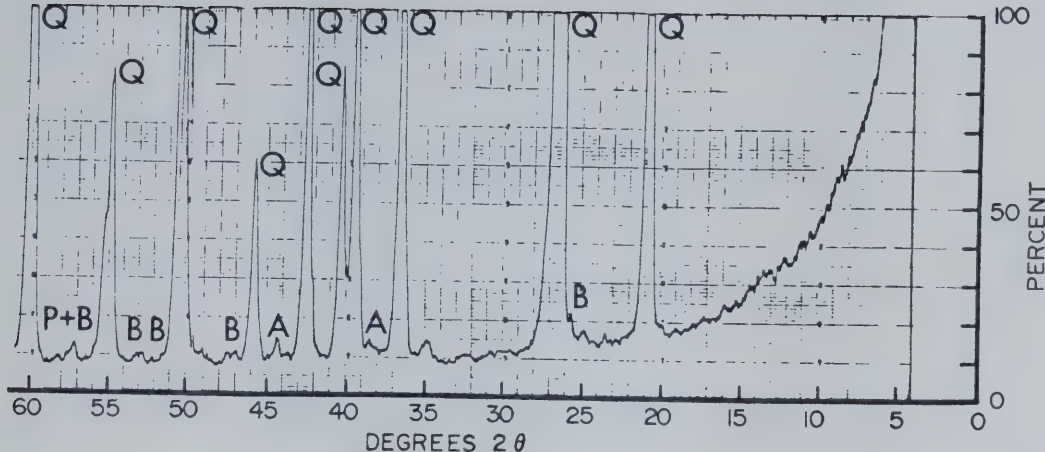


**SAMPLE #20**

**TEST TOS 10** (AFTER)

FIGURE H2

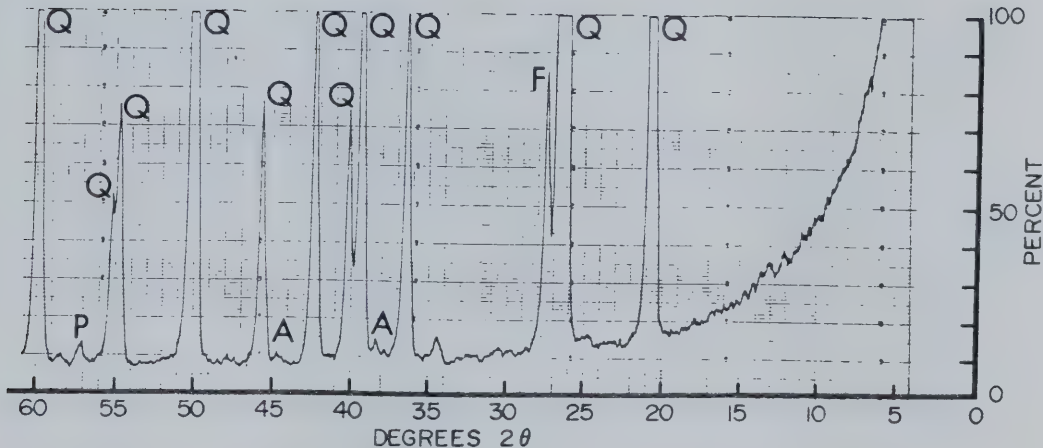




**SAMPLE #31**

**TEST CPERM 5 & CPERM 6 (BEFORE)**

FIGURE H3

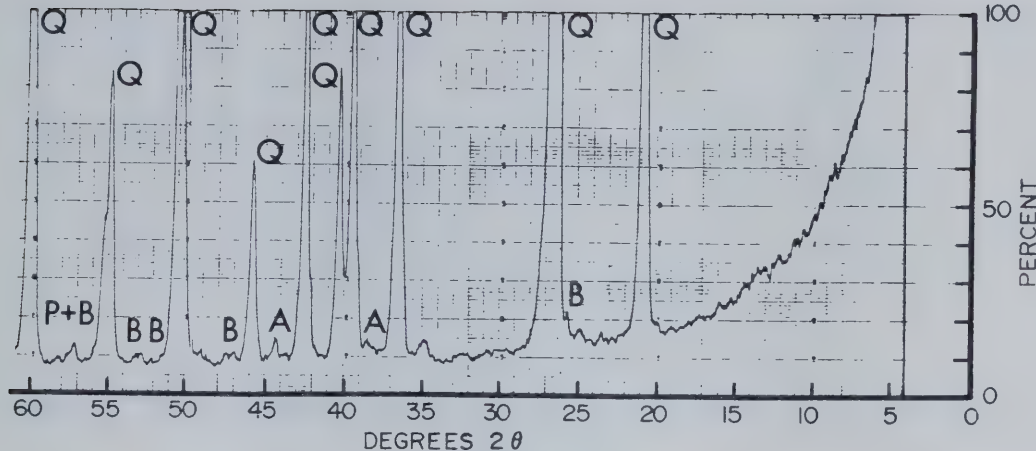


**SAMPLE #31A**

**TEST CPERM 5 (AFTER)**

FIGURE H4

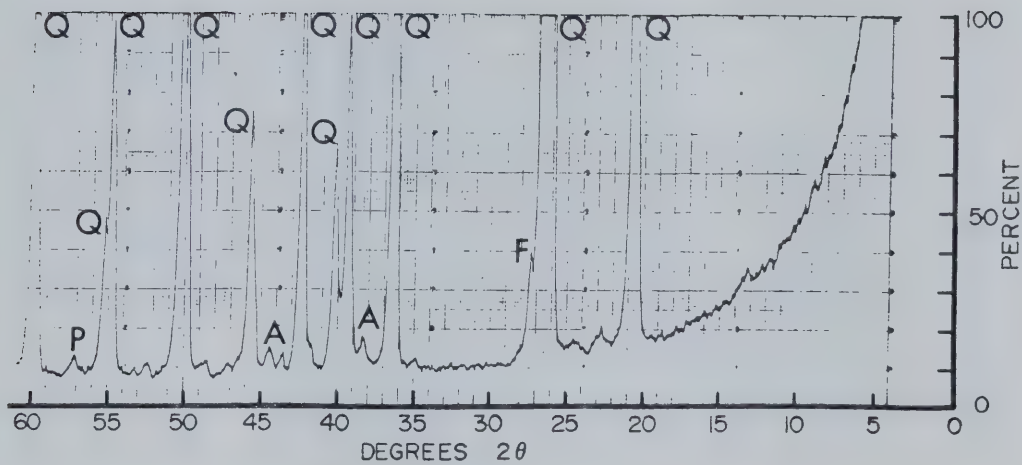




**SAMPLE #31**

## TEST CPERM 5 & CPERM 6 (BEFORE)

FIGURE H3

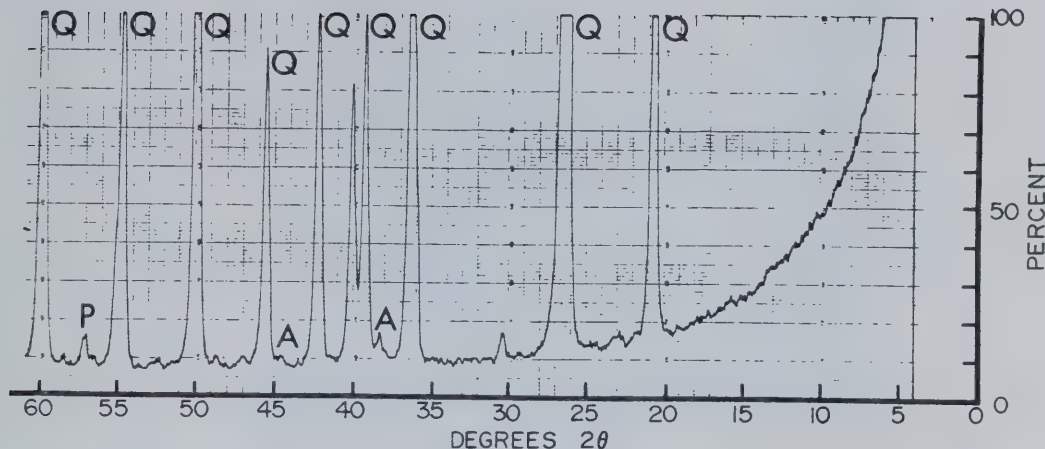


**SAMPLE #31B**

## TEST CPERM 6 (AFTER)

FIGURE H5

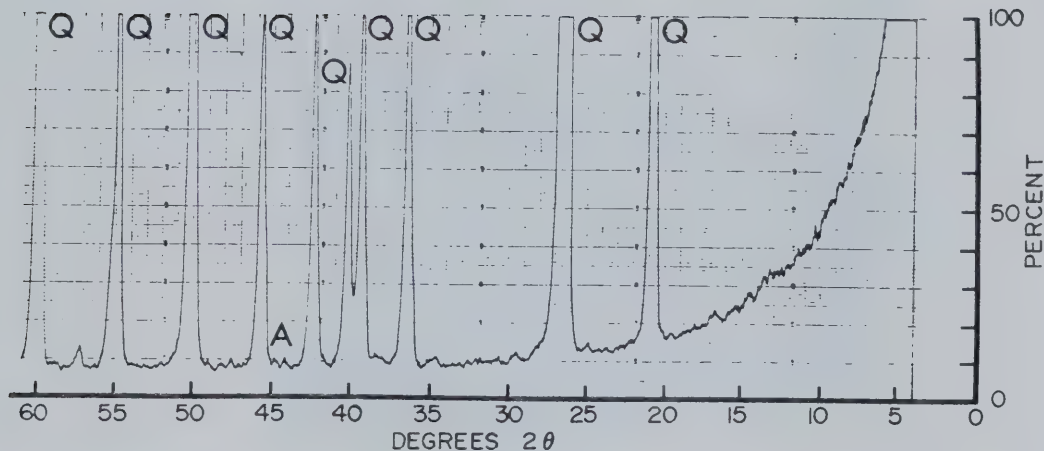




**SAMPLE #41**

**TEST COS 9 (BEFORE)**

FIGURE H6

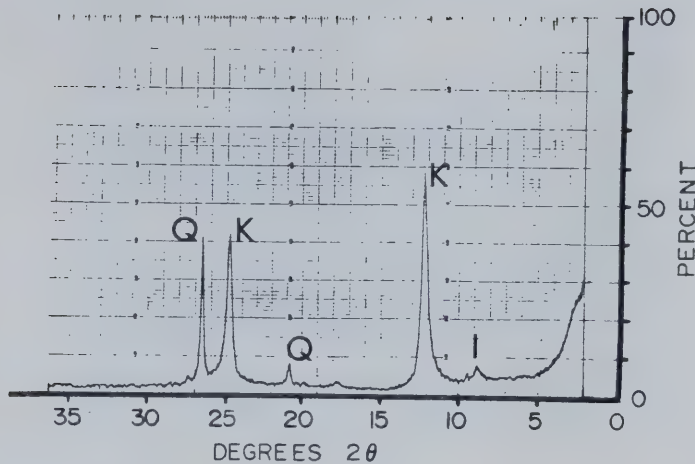


**SAMPLE #41**

**TEST COS 9 (AFTER)**

FIGURE H7

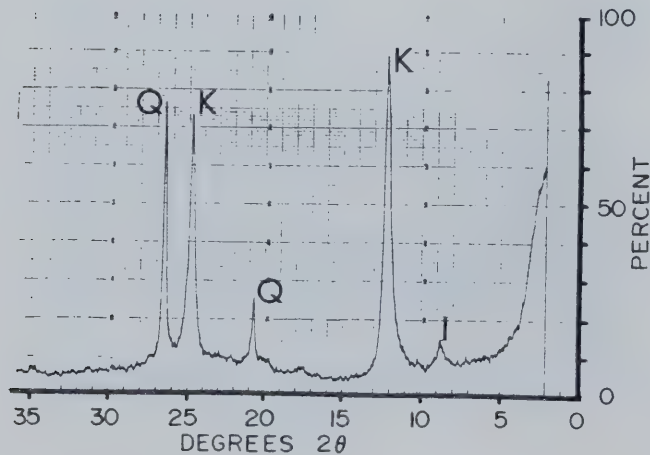




**SAMPLE #20** (fines  $< 2\mu\text{m}$ )

**TEST TOS 10** (BEFORE)

FIGURE H8

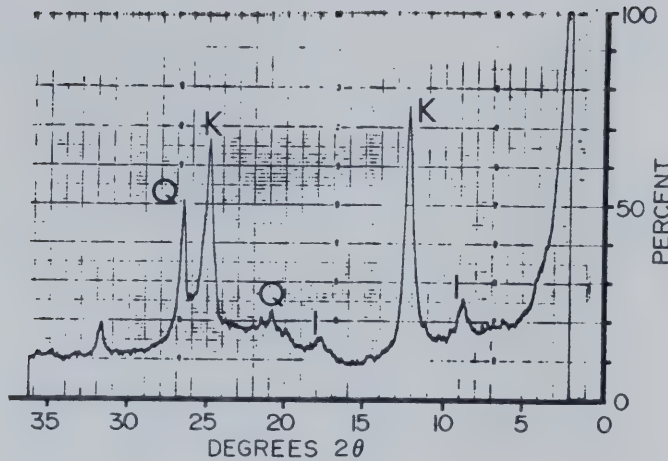


**SAMPLE #20** (fines  $< 2\mu\text{m}$ )

**TEST TOS 10** (AFTER)

FIGURE H9

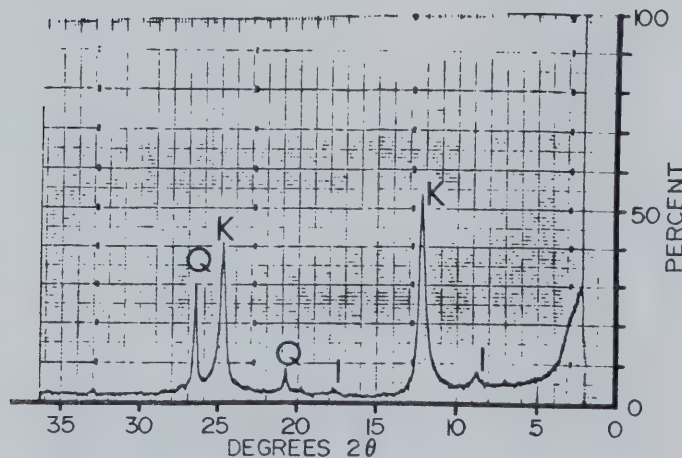




**SAMPLE #31** (fines  $< 2 \mu\text{m}$ )

**TEST CPERM 5 & CPERM 6 (BEFORE)**

FIGURE H10

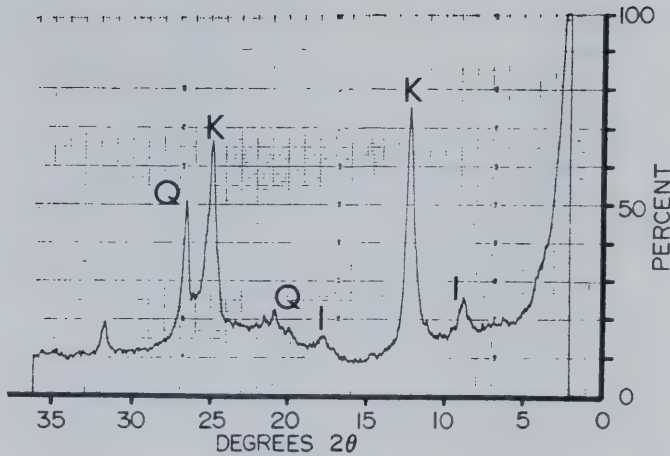


**SAMPLE #31A** (fines  $< 2 \mu\text{m}$ )

**TEST CPERM 5 (AFTER)**

FIGURE H11

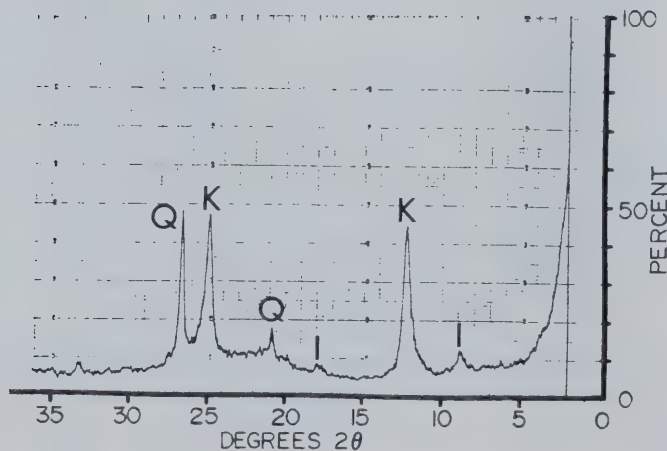




**SAMPLE #31** (fines  $< 2 \mu\text{m}$ )

**TEST CPERM 5 & CPERM 6 (BEFORE)**

FIGURE H10

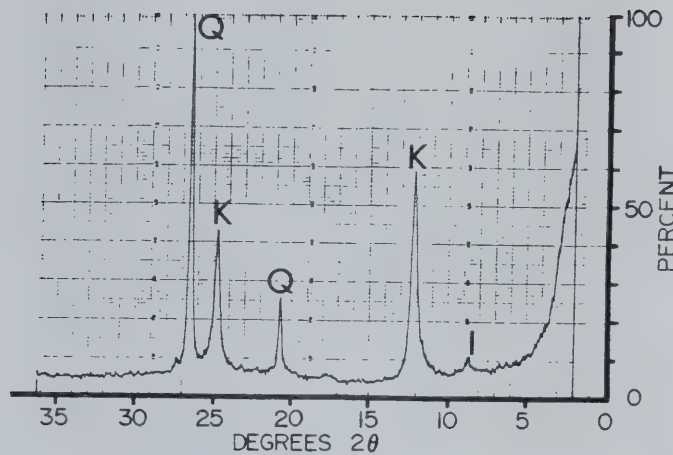


**SAMPLE #31** (fines  $< 2 \mu\text{m}$ )

**TEST CPERM 6 (AFTER)**

FIGURE H12

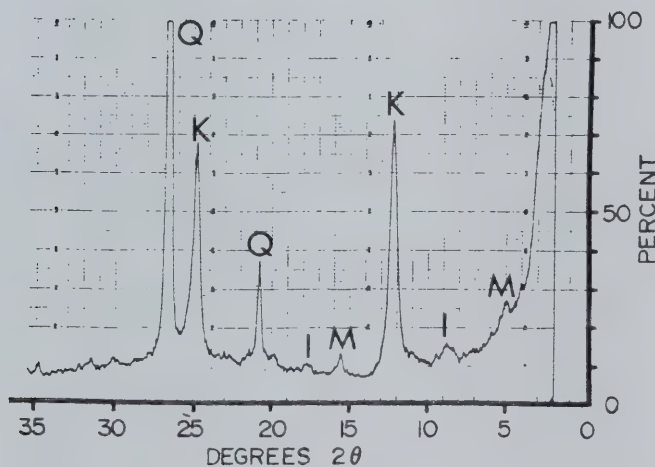




**SAMPLE #41** (fines  $< 2\mu\text{m}$ )

**TEST COS 9** (BEFORE)

FIGURE H13



**SAMPLE #41** (fines  $< 2\mu\text{m}$ )

**TEST COS 9** (AFTER)

FIGURE H14



APPENDIX I

VISCOSITY OF ATHABASCA BITUMEN AFTER UNSATURATED HEATING

Plate viscometer tests performed in accordance with  
ASTM D3570-77 Procedure B



TABLE I-1: PLATE VISCOMETER TEST RESULTS FOR AN ATHABASCA BITUMEN SAMPLE  
HEATED AT 135°C AND 1 ATMOSPHERE FOR 24 HOURS

Plate Area (cm <sup>2</sup> )	Film Thickness (μm)	Plate Disp. per Chart Div. (cm)	Chart Speed (cm/sec)	Chart Disp. Divs. (#)	Chart Disp. (cm)	Load (Grams)	Shearing Stress (Pascals)	Rate of Shear (sec <sup>-1</sup> )	Viscosity (Pa.s)
6.0	19.4	5 x 10 <sup>-4</sup>	2.82 x 10 <sup>-2</sup>	36.0	2.54	200	3.27 x 10 <sup>3</sup>	10.30 x 10 <sup>-2</sup>	0.3 x 10 <sup>5</sup>
6.0	19.4	5 x 10 <sup>-4</sup>	2.82 x 10 <sup>-2</sup>	29.0	1.27	250	4.09 x 10 <sup>3</sup>	16.60 x 10 <sup>-2</sup>	0.2 x 10 <sup>5</sup>
6.0	19.4	5 x 10 <sup>-4</sup>	2.82 x 10 <sup>-2</sup>	59.0	1.90	300	4.90 x 10 <sup>3</sup>	22.57 x 10 <sup>-2</sup>	0.2 x 10 <sup>5</sup>
6.0	19.4	5 x 10 <sup>-4</sup>	2.82 x 10 <sup>-2</sup>	52.0	1.27	350	5.72 x 10 <sup>3</sup>	29.76 x 10 <sup>-2</sup>	0.2 x 10 <sup>5</sup>
6.0	19.4	5 x 10 <sup>-4</sup>	2.82 x 10 <sup>-2</sup>	34.0	0.64	400	6.54 x 10 <sup>3</sup>	38.60 x 10 <sup>-2</sup>	0.2 x 10 <sup>5</sup>
6.0	19.4	5 x 10 <sup>-4</sup>	2.82 x 10 <sup>-2</sup>	42.0	0.64	450	7.36 x 10 <sup>3</sup>	47.68 x 10 <sup>-2</sup>	0.1 x 10 <sup>5</sup>



TABLE I-2: PLATE VISCOMETER TEST RESULTS FOR AN ATHABASCA BITUMEN SAMPLE  
REHEATED AT 150°C FOR 24 HOURS (AT 1 ATMOSPHERE)

Plate Area (cm <sup>2</sup> )	Film Thickness (μm)	Plate Disp. per Chart Div. (cm)	Chart Speed (cm/sec)	Chart Divs. (#)	Chart Disp. (cm)	Load (Grams)	Shearing Stress (Pascals)	Rate of Shear (sec <sup>-1</sup> )	Viscosity (Pa.s)
6.0	31.4	5 × 10 <sup>-4</sup>	2.82 × 10 <sup>-2</sup>	27.0	2.54	300	4.90 × 10 <sup>3</sup>	4.77 × 10 <sup>-2</sup>	1.0 × 10 <sup>5</sup>
6.0	31.4	5 × 10 <sup>-4</sup>	2.82 × 10 <sup>-2</sup>	33.0	1.90	400	6.54 × 10 <sup>3</sup>	7.80 × 10 <sup>-2</sup>	0.8 × 10 <sup>5</sup>
6.0	31.4	5 × 10 <sup>-4</sup>	2.82 × 10 <sup>-2</sup>	58.0	2.54	500	8.18 × 10 <sup>3</sup>	10.25 × 10 <sup>-2</sup>	0.8 × 10 <sup>5</sup>
6.0	31.4	5 × 10 <sup>-4</sup>	2.82 × 10 <sup>-2</sup>	79.0	2.54	600	9.81 × 10 <sup>3</sup>	13.97 × 10 <sup>-2</sup>	0.7 × 10 <sup>5</sup>
6.0	31.4	5 × 10 <sup>-4</sup>	2.82 × 10 <sup>-2</sup>	76.0	1.90	700	11.45 × 10 <sup>3</sup>	17.96 × 10 <sup>-2</sup>	0.6 × 10 <sup>5</sup>
6.0	31.4	5 × 10 <sup>-4</sup>	2.82 × 10 <sup>-2</sup>	60.0	1.27	800	13.08 × 10 <sup>3</sup>	21.21 × 10 <sup>-2</sup>	0.6 × 10 <sup>5</sup>
6.0	31.4	5 × 10 <sup>-4</sup>	2.82 × 10 <sup>-2</sup>	77.0	1.27	900	14.72 × 10 <sup>3</sup>	27.22 × 10 <sup>-2</sup>	0.5 × 10 <sup>5</sup>
6.0	31.4	5 × 10 <sup>-4</sup>	2.82 × 10 <sup>-2</sup>	44.0	0.64	1000	16.35 × 10 <sup>3</sup>	30.87 × 10 <sup>-2</sup>	0.5 × 10 <sup>5</sup>



TABLE I-3: PLATE VISCOMETER TEST RESULTS FOR AN ATHABASCA BITUMEN SAMPLE  
REHEATED AT 175°C FOR 24 HOURS (AT 1 ATMOSPHERE)

Plate Area (cm <sup>2</sup> )	Film Thickness (μm)	Plate Disp. per Chart Div. (cm)	Chart Speed (cm/sec)	Chart Disp. Divs. (#)	Chart Disp. (cm)	Load (Grams)	Shearing Stress (Pascals)	Rate of Shear (sec <sup>-1</sup> )	Viscosity (Pd.S.)
6.0	37.1	5 × 10 <sup>-4</sup>	2.82 × 10 <sup>-2</sup>	24.0	1.51	500	8.18 × 10 <sup>5</sup>	1.18 × 10 <sup>-2</sup>	6.9 × 10 <sup>5</sup>
6.0	37.1	5 × 10 <sup>-4</sup>	2.82 × 10 <sup>-2</sup>	27.0	4.44	700	11.45 × 10 <sup>5</sup>	2.27 × 10 <sup>-2</sup>	5.0 × 10 <sup>5</sup>
6.0	37.1	5 × 10 <sup>-4</sup>	2.82 × 10 <sup>-2</sup>	49.0	5.70	900	14.72 × 10 <sup>5</sup>	5.21 × 10 <sup>-2</sup>	4.6 × 10 <sup>5</sup>
6.0	37.1	5 × 10 <sup>-4</sup>	2.82 × 10 <sup>-2</sup>	81.0	6.52	1100	17.99 × 10 <sup>5</sup>	4.71 × 10 <sup>-2</sup>	3.8 × 10 <sup>5</sup>
6.0	37.1	5 × 10 <sup>-4</sup>	2.82 × 10 <sup>-2</sup>	80.0	4.42	1300	21.25 × 10 <sup>5</sup>	6.75 × 10 <sup>-2</sup>	3.1 × 10 <sup>5</sup>
6.0	37.1	5 × 10 <sup>-4</sup>	2.82 × 10 <sup>-2</sup>	85.0	5.16	1650	26.98 × 10 <sup>5</sup>	10.06 × 10 <sup>-2</sup>	2.7 × 10 <sup>5</sup>



APPENDIX J

COMPUTER CODES FOR ONE DIMENSIONAL HEAT CONSOLIDATION ANALYSES



## LIST OF PARAMETERS

NN:	No. of Nodes
M:	No. of Time Steps
Z:	Height above base (m)
DZ:	Mesh spacing (m)
ZD:	Dimensionless Height Ratio
T:	Temperature (°C)
DT:	Temperature Increase (°C)
DTI:	Incremental Temperature Increase (°C)
DTA:	Average Temperature Increase for element (°C)
DTAI:	Average Incremental Temperature Increase (°C)
P:	Pore Fluid Pressure (kPa)
U:	Excess pore pressure (kPa)
BT:	Pore Pressure Parameter relating pore pressure with temperature
DU:	Pore pressure increase due to heating (kPa)
UDR:	Pore pressure dissipated (kPa)
SVO:	Initial Total Confining Stress (kPa)
SVEO:	Initial Effective Vertical Stress (kPa)
DELT:	Time Increment
ALPHAT:	Thermal Diffusivity (m <sup>2</sup> /unit time)
CV:	Coefficient of 1-D Consolidation (m <sup>2</sup> /unit time)
MV:	1-D Coefficient of volume compressibility (kPa <sup>-1</sup> )
ALPHAS:	Coefficient of Thermal Expansion of solid particles (°C <sup>-1</sup> )
ALPHAF:	Coefficient of Thermal Expansion of solid pore fluids (°C <sup>-1</sup> )
ALPHDR:	Drained Coefficient of Thermal Expansion of oil sand (°C <sup>-1</sup> )
BETAS:	Compressibility of solid particles (kPa <sup>-1</sup> )
BETAF:	Compressibility of pore fluids (kPa <sup>-1</sup> )
POR:	Porosity
GAMF:	Density of pore fluid (kN/m <sup>3</sup> )
GAMS:	Density of solid particles (kN/m <sup>3</sup> )
GAM:	Density of oil sand (kN/m <sup>3</sup> )
DM:	Total stress change due to density change (kPa)
HCR:	Dimensionless Heat Consolidation Ratio = (cv/ )
RM:	Fluid Mobility Ratio =
ALP:	Partially Drained Coefficient of Thermal Expansion (°C <sup>-1</sup> )
DETA:	Dimensionless distance
DTAU:	Dimensionless time
RT:	Ratio of dimensionless time to dimensionless distance
OMEGA:	Weighting parameter
NPE:	Peclet Number



PROGRAM HC



```

$list hc on *print*
1      C*****
2      C*
3      C*          PROGRAM HC
4      C*
5      C*  One dimensional heat consolidation of a deeply buried
6      C*  oil sand layer subjected to rapid , non-transient heating.
7      C*  Mathematical solution of pore pressure dissipation with
8      C*  time using the solution presented by Taylor(1948).
9      C*  Taylor's solution was derived by the Separation of
10     C*  Variables technique ; pore pressure isochrones are
11     C*  characterized as sine wave functions .
12     C*
13     C*****
14     C
15     C  Dimension Array Parameters
16     C
17     C  DIMENSION ZD(32),TD(15),TV(15),DHT(10)
18     C  DIMENSION U(32,15),DZ(32,15),HT(32,15)
19     C
20     C  Constant Parameters & Initial Conditions
21     C
22     M=12
23     N=31
24     SVEO=6000.
25     H=15.
26     ALPHDR=3.6E-05
27     MV=5.0E-07
28     DO 3 K=1,1
29     KK=K-1
30     DT=200
31     CV=1.08*(10**((DT/200)))
32     BT=1/(0.0016667+(DT/SVEO))
33     UO=BT*DT
34     HO=2*H*(1+MV*UO+ALPHDR*DT)
35     DHO=100*((MV*UO)+(ALPHDR*DT))
36     C
37     C  Consolidation
38     C
39     DO 2 J=1,M
40     DO 1 I=1,N
41     II=I-1
42     JJ=J-1
43     ZD(I)=II/(2*H)
44     TD(J)=J*30
45     TV(J)=CV*TD(J)/(H**2)
46     F=3.14159/2
47     U(I,J)=2*UO*(SIN(2*F*ZD(I))*EXP(-TV(J)*(F**2)))/F
48     HT(1,J)=0.
49     IF (I.EQ.1) GO TO 1
50     DZ(I,J)=(1+MV*U(I,J)+ALPHDR*DT)
51     HT(I,J)=HT(II,J)+DZ(I,J)
52     1  CONTINUE
53     DHT(J)=100*(ALPHDR*DT)
54     2  CONTINUE
55     C
56     C  Printout
57     C
58     WRITE(6,100) DT,UO

```



```
59      100  FORMAT(//,'DT =' ,F5.1,/, 'U0=' ,F10.2,//)
60      DO 10 J=1,M
61      WRITE(6,101)(U(I,J),ZD(I),I=1,N)
62      101  FORMAT(G10.4,' ,',F10.3,' ,')
63      10  CONTINUE
64      WRITE(6,102) HO,DHO
65      102  FORMAT(//,'HO=' ,F12.5,/, 'DHO=' ,G10.3,//)
66      WRITE(6,103) (TD(J),HT(N,J),DHT(J),J=1,M)
67      103  FORMAT(F10.2,' ,',G10.4,' ,',G10.5,' ,')
68      3  CONTINUE
69      STOP
70      END
```

End of file

\$copy \*1 \*print\*



PROGRAM HCD



\$LIST hcd ON \*PRINT\*

```

1      C*****
2      C*
3      C*          ****
4      C*          * PROGRAM HCD *
5      C*          ****
6      C*      Semi Implicit Finite Difference Solution for
7      C*      One Dimensional HEAT CONSOLIDATION of Oil Sand
8      C*      Coupled with Transient Heating by Thermal Diffusion.
9      C*
10     C*
11     C*      Properties of the oil sand vary with temperature,
12     C*      pressure,& effective stress . Variable parameters
13     C*      include fluid mobility,porosity,bulk density,fluid
14     C*      & solid densities , pore pressure response to
15     C*      undrained heating & coefficient of consolidation .
16     C*
17     C*      ASSUMPTIONS :
18     C*
19     C*      1.Oil Saturation is assumed to be constant during
20     C*      gravity drainage .
21     C*      2.Total vertical stress varies with density of the
22     C*      heated materials .
23     C*      3.One-way drainage is assumed ; the top boundary of
24     C*      the oil sand layer is a no-flow boundary.
25     C*      4.The top boundary of the oil sand layer is assumed
26     C*      to inhibit heat flow .
27     C*      5.Properties of Saline Creek oil sand are used in
28     C*      the analysis .
29     C*
30     C*      CODED by J.G.Agar , July 1983
31     C*      All rights reserved by the author
32     C*
33     C*****
34     C
35     C      ****
36     C      * MAIN PROGRAM *
37     C      ****
38     C
39     C
40     C      Dimension Array Parameters
41     C
42     C      NN=32
43     C      M=1441
44     C      M1=721
45     C      M2=361
46     C      M3=92
47     C      M4=181
48     C      M5=61
49     C      M6=11
50     C      M7=11
51     C      N=NN-1
52     C      MM=M-1
53     C      NI=NN-2
54     C      REAL *4 MV
55     C      COMMON /BLK1/ NN,M,N,MM,NI,DELT,ALPHAT,SVEO
56     C      COMMON /BLK2/ DZ(35,3000),T(35,3000)
57     C      COMMON /BLK3/ Z(35,3000),ZD(35,3000)
58     C      COMMON /BLK4/ UDR(35,3000),U(35,3000)

```



```

119      GAMS=26.5/(1+ALPHAS*DT(I,J)+BETAS*U(I,JI))
120      GAM(I,J)=POR*GAMF+((1-POR)*GAMS)
121      DGAM=GAM(I,J)-21.0
122      DM(I,J)=DGAM*DZ(I,JI)
123      BT(I,J)=1/((1/BT(I,1))+(DT(I,J)/(AF*(SVEO-U(I,JI))))))
124      DU(I,J)=BT(I,J)*DT(I,J)
125      CV(I,J)=CV(I,1)*(10**((DT(I,J)/200)))
126      25  CONTINUE
127      CALL CONSOL(J,JJ,JI)
128      DO 20 I=2,N
129      JJ=J+1
130      JI=J-1
131      IJ=I+1
132      II=I-1
133      DZ(I,J)=DZ(I,1)*(1+(MV*U(I,J))+ALPHDR*DT(I,J))
134      Z(I,J)=Z(II,J)+DZ(I,J)
135      T(I,J)=T(I,1)+DT(I,J)
136      P(I,J)=P(I,1)+U(I,J)
137      20  CONTINUE
138      30  CONTINUE
139      C
140      C Dimensionless Parameters
141      C
142      DO 50 J=2,M
143      DO 40 I=2,N
143.5      DH(I,J)=100*(Z(I,J)-Z(I,1))/Z(I,1)
143.51     IF(DT(I,J).LT..001) GO TO 41
143.58     ALP(I,J)=((MV*U(I,J))+(ALPHDR*DT(I,J)))/DT(I,J)
143.65     GO TO 42
143.72     41  ALP(I,J)=ALPHDR
144     42  ZD(I,J)=Z(I,J)/Z(N,J)
145     40  HCR(I,J)=(CV(I,J)/ALPHAT)/1000
146     40  CONTINUE
147     50  CONTINUE
148      C
149      C Printout
150      C
151      C PRINT 95
152      C95  FORMAT(' Depth Temperature Pressure Time ',//)
153      C  WRITE(6,96) (Z(I,M7),T(I,M7),P(I,M7),M7,I=1,N)
154      C96  FORMAT(F7.4,2F11.3,I6)
155      C  WRITE(6,97) (Z(I,M5),T(I,M5),P(I,M5),M5,I=1,N)
156      C97  FORMAT(F7.4,2F11.3,I6)
157      C  WRITE(6,98) (Z(I,M2),T(I,M2),P(I,M2),M2,I=1,N)
158      C98  FORMAT(F7.4,2F11.3,I6)
159      C  WRITE(6,99) (Z(I,M),T(I,M),P(I,M),M,I=1,N)
160      C99  FORMAT(F7.4,2F11.3,I6)
161      C
162      PRINT 100
163      100 FORMAT(//2X,' Temperature vs. Depth & Time' )
164      WRITE(6,101)(DT(I,M7),ZD(I,M7),I=1,N)
165      101 FORMAT(G10.3,' ',G10.3,' ')
166      C  WRITE(6,102)(DT(I,M6),ZD(I,M6),I=1,N)
167      C102 FORMAT(1X,G10.3,' ',G10.3,' ')
168      WRITE(6,103)(DT(I,M5),ZD(I,M5),I=1,N)
169      103 FORMAT(G10.3,' ',G10.3,' ')
170      WRITE(6,104)(DT(I,M4),ZD(I,M4),I=1,N)
171      104 FORMAT(1X,G10.3,' ',G10.3,' ')
172      C  WRITE(6,121)(DT(I,M3),ZD(I,M3),I=1,N)
173      C121 FORMAT(G10.3,' ',G10.3,' ')

```



```

174      WRITE(6,122)(DT(I,M2),ZD(I,M2),I=1,N)
175      122  FORMAT(1X,G10.3,',',G10.3,',')
176      WRITE(6,123)(DT(I,M1),ZD(I,M1),I=1,N)
177      123  FORMAT(G10.3,',',G10.3,',')
178      WRITE(6,124)(DT(I,M),ZD(I,M),I=1,N)
179      124  FORMAT(1X,G10.3,',',G10.3,',')
180      C
181      PRINT 105
182      105  FORMAT(//2X,' Pore Pressure vs. Depth & Time' )
183      WRITE(6,106)(U(I,M7),ZD(I,M7),I=1,N)
184      106  FORMAT(G10.3,',',G10.3,',')
185      C    WRITE(6,107)(U(I,M6),ZD(I,M6),I=1,N)
186      C107  FORMAT(1X,G10.3,',',G10.3,',')
187      WRITE(6,108)(U(I,M5),ZD(I,M5),I=1,N)
188      108  FORMAT(G10.3,',',G10.3,',')
189      WRITE(6,109)(U(I,M4),ZD(I,M4),I=1,N)
190      109  FORMAT(1X,G10.3,',',G10.3,',')
191      C    WRITE(6,126)(U(I,M3),ZD(I,M3),I=1,N)
192      C126  FORMAT(G10.3,',',G10.3,',')
193      WRITE(6,127)(U(I,M2),ZD(I,M2),I=1,N)
194      127  FORMAT(1X,G10.3,',',G10.3,',')
195      WRITE(6,128)(U(I,M1),ZD(I,M1),I=1,N)
196      128  FORMAT(G10.3,',',G10.3,',')
197      WRITE(6,129)(U(I,M),ZD(I,M),I=1,N)
198      129  FORMAT(1X,G10.3,',',G10.3,',')
199      C
200      PRINT 115
201      115  FORMAT(//2X,' Thermal Expansion Coeff. vs. Depth&Time' )
202      WRITE(6,116)(ALP(I,M7),ZD(I,M7),I=1,N)
203      116  FORMAT(G10.3,',',G10.3,',')
204      C    WRITE(6,117)(ALP(I,M6),ZD(I,M6),I=1,N)
205      C117  FORMAT(1X,G10.3,',',G10.3,',')
206      WRITE(6,118)(ALP(I,M5),ZD(I,M5),I=1,N)
207      118  FORMAT(G10.3,',',G10.3,',')
208      WRITE(6,119)(ALP(I,M4),ZD(I,M4),I=1,N)
209      119  FORMAT(1X,G10.3,',',G10.3,',')
210      C    WRITE(6,130)(ALP(I,M3),ZD(I,M3),I=1,N)
211      C130  FORMAT(G10.3,',',G10.3,',')
212      WRITE(6,131)(ALP(I,M2),ZD(I,M2),I=1,N)
213      131  FORMAT(1X,G10.3,',',G10.3,',')
214      WRITE(6,132)(ALP(I,M1),ZD(I,M1),I=1,N)
215      132  FORMAT(G10.3,',',G10.3,',')
216      WRITE(6,133)(ALP(I,M),ZD(I,M),I=1,N)
217      133  FORMAT(1X,G10.3,',',G10.3,',')
218      C
218.3    PRINT 135
218.6    135  FORMAT(//2X,' Vertical Expansion vs. Time' )
219      WRITE(6,120) DH(N,M7),DH(N,M5),DH(N,M4),DH(N,M2),
220      &DH(N,M1),DH(N,M)
221      120  FORMAT(3G12.6,/,3G12.6,/)
222      C
223      STOP
224      END
225      C
226      C
227      C
228      ****
229      C
230      C          SUBROUTINE TEMPD
231      C          Determines temperature distribution with time in

```



```

232      C      oil sand due to 1-D thermal diffusion . The semi
233      C      implicit formulation yields a tridiagonal matrix
234      C      at each time step which is solved using
235      C      THOMAS'S ALGORITHM .
236      C
237      C*****
238      C
239      C      SUBROUTINE TEMPD(J,JJ,JI)
240      C
241      COMMON /BLK1/ NN,M,N,MM,NI,DELT,ALPHAT,SVEO
242      COMMON /BLK2/ DZ(35,3000),T(35,3000)
243      COMMON /BLK5/ DT(35,3000),DTI(35,3000)
244      COMMON /BLK6/ DTA(35,3000),DTAI(35,3000)
245      COMMON /BLK10/ A(35),B(35),C(35)
246      COMMON /BLK11/ W(35),G(35)
247      C
248      DO 1 I=2,N
249      II=I-1
250      IJ=I+1
251      A(I)=- (ALPHAT*DELT)/(DZ(I,JI)**2)
252      B(I)=1+(2*ALPHAT*DELT)/(DZ(I,JI)**2)
253      C(I)=A(I)
254      IF (I.GT.2) GO TO 2
255      W(2)=C(2)/B(2)
256      G(2)=(DT(2,JI)-A(2)*DT(1,JI))/B(2)
257      GO TO 1
258      2 IF (I.EQ.N) GO TO 3
259      W(I)=C(I)/(B(I)-A(I)*W(I))
260      G(I)=(DT(I,JI)-A(I)*G(I))/(B(I)-A(I)*W(I))
261      GO TO 1
262      3 G(N)=(DT(N,JI)-(2*A(N)*G(N)))/(B(N)-(2*A(N)*W(N)))
263      DT(N,J)=G(N)
264      1 CONTINUE
265      NII=N-2
266      DO 4 I=1,NII
267      IB=N-I
268      IBJ=IB+1
269      DT(IB,J)=G(IB)-W(IB)*DT(IBJ,J)
270      4 CONTINUE
271      DO 5 I=2,N
272      II=I-1
273      DTI(I,J)=DT(I,J)-DT(I,JI)
274      DTA(I,J)=(DT(I,J)+DT(II,J))/2
275      DTAI(I,J)=(DTI(I,J)+DTI(II,J))/2
276      5 CONTINUE
277      RETURN
278      END
279      C
280      C
281      C*****
282      C
283      C      SUBROUTINE CONSOL
284      C      Determines pore pressure dissipation with time
285      C      in oil sand due to 1-D consolidation following each
286      C      transient heating increment . The semi-implicit
287      C      formulation yields a tridiagonal matrix at each
288      C      time step which is solved using THOMAS'S ALGORITHM .
289      C
290      C*****
291      C

```



```

292      SUBROUTINE CONSOL(J,JJ,JI)
293
294      COMMON /BLK1/ NN,M,N,MM,NI,DELT,ALPHAT,SVEO
295      COMMON /BLK2/ DZ(35,3000),T(35,3000)
296      COMMON /BLK4/ UDR(35,3000),U(35,3000)
297      COMMON /BLK5/ DT(35,3000),DTI(35,3000)
298      COMMON /BLK6/ DTA(35,3000),DTAI(35,3000)
299      COMMON /BLK8/ CV(35,3000),DM(35,3000)
300      COMMON /BLK9/ BT(35,3000),DU(35,3000)
301      COMMON /BLK12/ AA(35),BB(35),CC(35)
302      COMMON /BLK13/ WW(35),GG(35),DGAM(35,3000)
303      COMMON /BLK14/ DH(35,3000)
304
305      C
306      DO 1 I=2,N
307      II=I-1
308      IJ=I+1
309      IF (I.GT.2) GO TO 2
310      AA(2)=-(CV(2,J)*DELT)/(DZ(I,1))
311      BB(2)=1+(2*CV(2,J)*DELT/(DZ(I,1)))
312      CC(2)=AA(2)
313      WW(2)=CC(2)/BB(2)
314      GG(2)=(U(2,JI)-AA(2)*U(1,JI))/BB(2)
315      GO TO 1
316      2  CVAVG=(CV(I,J)+CV(II,J))/2
317      AA(I)=- (CVAVG*DELT)/(DZ(I,JI)**2)
318      BB(I)=1+(2*CVAVG*DELT/(DZ(I,JI)**2))
319      CC(I)=AA(I)
320      IF (I.EQ.N) GO TO 3
321      WW(I)=CC(I)/(BB(I)-AA(I)*WW(II))
322      GG(I)=(U(I,JI)-AA(I)*GG(II))/(BB(I)-AA(I)*WW(II))
323      GO TO 1
324      3  GG(N)=(U(N,JI)-(2*AA(N)*GG(NI)))/(BB(N)-(2*AA(N)*WW(NI))
325      UDR(N,J)=GG(N)
326      1  CONTINUE
327      NII=N-2
328      DO 4 I=1,NII
329      IB=N-I
330      IBJ=IB+1
331      4  UDR(IB,J)=GG(IB)-WW(IB)*UDR(IBJ,J)
332      CONTINUE
333      DO 5 I=2,N
334      5  U(I,J)=DU(I,J)+UDR(I,J)+DM(I,J)
335      CONTINUE
336      RETURN
      END
End of file
$COPY *1 *PRINT*

```



PROGRAM HCCD



\$LIST hccd ON \*PRINT\*

```

1  C*****
2  C*
3  C*          ****
4  C*          * PROGRAM HCCD *
5  C*          ****
6  C*          Semi Implicit Finite Difference Solution for
7  C*          One Dimensional HEAT CONSOLIDATION of Oil Sand
8  C*          Coupled with Transient Heating by both Thermal
9  C*          CONVECTION & DIFFUSION.
10 C*
11 C*
12 C*
13 C*          Properties of the oil sand vary with temperature,
14 C*          pressure,& effective stress . Variable parameters
15 C*          include fluid mobility,porosity,bulk density,fluid
16 C*          & solid densities,pore pressure response to undrained
17 C*          heating & coefficient of consolidation .
18 C*
19 C*          ASSUMPTIONS :
20 C*
21 C*          1.Oil Saturation is assumed to be constant during
22 C*          gravity drainage .
23 C*          2.Total vertical stress varies only with density
24 C*          changes of the heated material .
25 C*          3.One-way drainage is assumed ; the top boundary of
26 C*          the oil sand layer is a no-flow boundary.
27 C*          4.The top boundary of the oil sand layer is assumed
28 C*          to be a barrier to heat flow .
29 C*          5.Properties of Saline Creek oil sand are used in
30 C*          the analysis .
31 C*
32 C*          CODED by J.G.Agar , July 1983
33 C*          All rights reserved by the author
34 C*
35 C*****
36 C
37 C          ****
38 C          * MAIN PROGRAM *
39 C          ****
40 C
41 C
42 C          Dimension Array Parameters
43 C
44 C          NN=32
45 C          M=1441
46 C          M1=541
47 C          M2=721
48 C          M3=361
49 C          M4=181
50 C          M5=61
51 C          M6=11
52 C          M7=6
53 C          N=NN-1
54 C          MM=M-1
55 C          NI=NN-2
56 C          REAL *4 MV
57 C          COMMON /BLK1/ NN,M,N,MM,NI,DELT,ALPHAT,SVEO
58 C          COMMON /BLK2/ DZ(35,3000),T(35,3000)

```



```
59      COMMON /BLK3/ Z(35,3000),ZD(35,3000)
60      COMMON /BLK4/ UDR(35,3000),U(35,3000)
61      COMMON /BLK5/ DT(35,3000),DTI(35,3000)
62      COMMON /BLK6/ DTA(35,3000),DTAI(35,3000)
63      COMMON /BLK7/ P(35,3000)
64      COMMON /BLK8/ CV(35,3000),DM(35,3000)
65      COMMON /BLK9/ BT(35,3000),DU(35,3000)
66      COMMON /BLK10/ A(35),B(35),C(35)
67      COMMON /BLK11/ W(100),G(100),RM(35,3000)
68      COMMON /BLK12/ AA(35),BB(35),CC(35)
69      COMMON /BLK13/ WW(100),GG(100),GAM(35,3000)
70      COMMON /BLK14/ DH(35,3000)
71      C
72      C      Initial Conditions
73      C
74      SVO=9000.
75      SVEO=6000.
76      DO 10 I=2,NN
77      II=I-1
78      DT(I,1)=0
79      DTA(I,1)=0
80      T(I,1)=5.0
81      P(I,1)=3150.-(10*II)
82      DZ(I,1)=1.0
83      Z(I,1)=II*DZ(I,1)
84      U(I,1)=0.
85      CV(I,1)=1.08
86      RM(I,1)=5.4E-07
87      BT(I,1)=SVEO/10.
88      10      CONTINUE
89      C
90      C      Boundary Conditions
91      C
92      DO 11 J=1,M
93      Z(1,J)=0.
94      T(1,J)=205.
95      DT(1,J)=200.
96      U(1,J)=1.
97      P(1,J)=3150.
98      CV(1,J)=10.8
99      RM(1,J)=5.4E-06
100     11      CONTINUE
101     C
102     C      Constants
103     C
104     AF=1.00
105     DELT=1.0
106     MV=5.0E-07
107     ALPHDR=3.6E-05
108     ALPHAT=6.0E-05
109     ALPHAF=5.2E-04
110     BETAS=5.0E-09
111     ALPHAS=4.3E-05
112     C
113     C      Heat Consolidation Calculation
114     C
115     DO 30 J=2,M
116     JJ=J+1
117     JI=J-1
118     CALL TEMPC(J,JJ,JI)
```



```

119      DO 25 I=2,N
120      BETAF=4.0E-07*(10**((DTA(I,J)/200)))
121      POR=0.33*(1+MV*U(I,JI)-(ALPHDR-ALPHAS)*DTA(I,J))
122      GAMF=9.85/(1+ALPHAF*DTA(I,J)-BETAF*U(I,J))
123      GAMS=26.5/(1+ALPHAS*DTA(I,J)+BETAS*U(I,J))
124      GAM(I,J)=POR*GAMF+((1-POR)*GAMS)
125      DGAM=GAM(I,J)-21.0
126      DM(I,J)=DGAM*DZ(I,JI)
127      BT(I,J)=1/((1/BT(I,1))+(DTAI(I,J)/(AF*(SVEO-U(I,JI))))) )
128      DU(I,J)=BT(I,J)*DTAI(I,J)
129      CV(I,J)=CV(I,1)*(10**((DTA(I,J)/200)))
130      RM(I,J)=CV(I,J)*MV
131      25  CONTINUE
132      CALL CONSOL(J,JJ,JI)
133      DO 20 I=2,N
134      JJ=J+1
135      JI=J-1
136      IJ=I+1
137      II=I-1
138      DZ(I,J)=DZ(I,1)*(1+(MV*U(I,J))+ALPHDR*DTA(I,J))
139      Z(I,J)=Z(II,J)+DZ(I,J)
140      T(I,J)=T(I,1)+DT(I,J)
141      P(I,J)=P(I,1)+U(I,J)
142      20  CONTINUE
143      30  CONTINUE
144      C
145      C Dimensionless Parameters
146      C
147      DO 50 J=2,M
148      DO 40 I=1,N
148.5    DH(I,J)=100*(Z(N,J)-30)/30
149      ZD(I,J)=Z(I,J)/Z(N,J)
150      40  CONTINUE
151      50  CONTINUE
152      C
153      C Printout
154      C
155      C PRINT 95
156      C95   FORMAT(' Depth Temperature Pressure Time ',//)
157      C     WRITE(6,96) (Z(I,M7),T(I,M7),P(I,M7),M7,I=1,N)
158      C96   FORMAT(F7.4,2F11.3,I6)
159      C     WRITE(6,97) (Z(I,M5),T(I,M5),P(I,M5),M5,I=1,N)
160      C97   FORMAT(F7.4,2F11.3,I6)
161      C     WRITE(6,98) (Z(I,M3),T(I,M3),P(I,M3),M3,I=1,N)
162      C98   FORMAT(F7.4,2F11.3,I6)
163      C     WRITE(6,99) (Z(I,M),T(I,M),P(I,M),M,I=1,N)
164      C99   FORMAT(F7.4,2F11.3,I6)
165      C
166      C PRINT 100
167      100  FORMAT(//2X,' Temperature vs. Depth & Time')
168      C     WRITE(6,101)(DT(I,M7),ZD(I,M7),I=1,N)
169      101  FORMAT(G10.3,' ','G10.3',' ')
170      C     WRITE(6,102)(DT(I,M6),ZD(I,M6),I=1,N)
171      C102  FORMAT(1X,G10.3,' ','G10.3',' ')
172      C     WRITE(6,103)(DT(I,M5),ZD(I,M5),I=1,N)
173      103  FORMAT(G10.3,' ','G10.3',' ')
174      C     WRITE(6,104)(DT(I,M4),ZD(I,M4),I=1,N)
175      104  FORMAT(1X,G10.3,' ','G10.3',' ')
176      C     WRITE(6,121)(DT(I,M3),ZD(I,M3),I=1,N)
177      121  FORMAT(G10.3,' ','G10.3',' ')

```



```

178      WRITE(6,122)(DT(I,M2),ZD(I,M2),I=1,N)
179      122  FORMAT(1X,G10.3,' ',G10.3,' ')
180      C    WRITE(6,123)(DT(I,M1),ZD(I,M1),I=1,N)
181      C123  FORMAT(G10.3,' ',G10.3,' ')
182      124  WRITE(6,124)(DT(I,M),ZD(I,M),I=1,N)
183      124  FORMAT(1X,G10.3,' ',G10.3,' ')
184      C
185      PRINT 105
186      105  FORMAT(//2X,' Pore Pressure vs. Depth & Time' )
187      WRITE(6,106)(U(I,M7),ZD(I,M7),I=1,N)
188      106  FORMAT(G10.3,' ',G10.3,' ')
189      C    WRITE(6,107)(U(I,M6),ZD(I,M6),I=1,N)
190      C107  FORMAT(1X,G10.3,' ',G10.3,' ')
191      108  WRITE(6,108)(U(I,M5),ZD(I,M5),I=1,N)
192      108  FORMAT(G10.3,' ',G10.3,' ')
193      109  WRITE(6,109)(U(I,M4),ZD(I,M4),I=1,N)
194      109  FORMAT(1X,G10.3,' ',G10.3,' ')
195      126  WRITE(6,126)(U(I,M3),ZD(I,M3),I=1,N)
196      126  FORMAT(G10.3,' ',G10.3,' ')
197      127  WRITE(6,127)(U(I,M2),ZD(I,M2),I=1,N)
198      127  FORMAT(1X,G10.3,' ',G10.3,' ')
199      C    WRITE(6,128)(U(I,M1),ZD(I,M1),I=1,N)
200      C128  FORMAT(G10.3,' ',G10.3,' ')
201      129  WRITE(6,129)(U(I,M),ZD(I,M),I=1,N)
202      129  FORMAT(1X,G10.3,' ',G10.3,' ')
203      C
204      C
205      WRITE(6,120) DH(N,M7),DH(N,M5),DH(N,M4),
206      &DH(N,M3),DH(N,M2),DH(N,M)
207      120  FORMAT(3G12.6./,3G12.6./)
208      C
209      STOP
210      END
211      C
212      C
213      C
214      ****
215      C
216      C          SUBROUTINE TEMPC
217      C          Determines temperature distribution with time in
218      C          oil sand due to 1-D thermal convection & diffusion .
219      C          The "TRUNCATION CANCELLATION PROCEDURE" (Laumbach,
220      C          1975) was used to formulate the semi-implicit
221      C          difference equations . Forward difference expressions
222      C          are used to approximate time derivatives & central
223      C          differences are used for spatial derivatives. Flow
224      C          velocity is described by Darcy's Law . A central
225      C          difference expression is used to approximate the
226      C          the velocity which varies nonlinearly in space &
227      C          time . Triadiagonal matrices are inverted & solved
228      C          by Thomas's Algorithm.
229      C
230      ****
231      C
232      C          SUBROUTINE TEMPC(J,JJ,JI)
233      C
234      COMMON /BLK1/ NN,M,N,MM,NI,DELT,ALPHAT,SVEO
235      COMMON /BLK2/ DZ(35,3000),T(35,3000)
236      COMMON /BLK3/ Z(35,3000),ZD(35,3000)
237      COMMON /BLK5/ DT(35,3000),DTI(35,3000)

```



```

238 COMMON /BLK6/ DTA(35,3000),DTAI(35,3000)
239 COMMON /BLK10/ A(35),B(35),C(35)
240 COMMON /BLK11/ W(100),G(100),RM(35,3000)
241 COMMON /BLK4/ UDR(35,3000),U(35,3000)
242 DOUBLE PRECISION NPE(35),DTAU(35),DETA(35)
243 DOUBLE PRECISION RT(35),OMEGA(35),V(35)
244 DIMENSION A1(35),B1(35),C1(35),DD(35)
245
246 C
247 U(1,1)=5715.
248 DO 1 I=2,N
249   II=I-1
250   IJ=I+1
251   RMAV=(RM(IJ,JI)+RM(I,JI)+RM(II,JI))/3
252   V(I)=RMAV*((U(IJ,JI)-U(II,JI))/(2*DZ(I,JI)))
253   IF(V(I).EQ.0) V(I)=-1.0*RMAV/DZ(I,JI)
254   IF(V(I).LT.-1.0) V(I)=-1.0
255   IF(V(I).GT.1.0) V(I)=1.0
256   DETA(I)=DZ(I,JI)/30
257   DTAU(I)=(V(I)*DELT)/30
258   RT(I)=V(I)*DELT/DZ(I,JI)
259   OMEGA(I)=(0.3333)+((RT(I)**2)/6)
260   IF(OMEGA(I).GT.0.5) OMEGA(I)=0.5
261   NPE(I)=(V(I)*30)/(ALPHAT/6)
262   A(I)=((OMEGA(I)/(2*DTAU(I)))-(1/(2*NPE(I)*(DETA(I)**2)))
263   &-(1/(4*DETA(I)))))
264   B(I)=((1-OMEGA(I))/DTAU(I))+(1/(NPE(I)*DETA(I)**2))
265   C(I)=(OMEGA(I)/(2*DTAU(I))-(1/(2*NPE(I)*DETA(I)**2))
266   &+(1/(4*DETA(I)))))
267   A1(I)=((OMEGA(I)/(2*DTAU(I)))+(1/(2*NPE(I)*(DETA(I)**2))
268   &+(1/(4*DETA(I)))))
269   B1(I)=((1-OMEGA(I))/DTAU(I))-(1/(NPE(I)*DETA(I)**2))
270   C1(I)=(OMEGA(I)/(2*DTAU(I))+(1/(2*NPE(I)*DETA(I)**2))
271   &-(1/(4*DETA(I)))))
272   IF (I.GT.2) GO TO 2
273   DD(2)=A1(2)*DT(1,JI)+B1(2)*DT(2,JI)+C1(2)*DT(3,JI)
274   W(2)=C(2)/B(2)
275   G(2)=(DD(2)-A(2)*DT(1,JI))/B(2)
276   GO TO 1
277 2  IF (I.EQ.N) GO TO 3
278   DD(I)=A1(I)*DT(II,JI)+B1(I)*DT(I,JI)+C1(I)*DT(IJ,JI)
279   W(I)=C(I)/(B(I)-A(I)*W(II))
280   G(I)=(DD(I)-A(I)*G(II))/(B(I)-A(I)*W(II))
281   GO TO 1
282 3  DD(N)=((A1(N)+C1(N))*DT(NI,JI))+(B1(N)*DT(N,JI))
283   G(N)=(DD(N)-((A(N)+C(N))*G(NI)))/(B(N)-((A(N)+C(N))*W(N
284   DT(N,J)=G(N)
285   1  CONTINUE
286   NII=N-2
287   DO 4 I=1,NII
288     IB=N-I
289     IBJ=IB+1
290     DT(IB,J)=G(IB)-W(IB)*DT(IBJ,J)
291   4  CONTINUE
292   DO 5 I=2,N
293     II=I-1
294     IF(DT(I,J).LT.0) DT(I,J)=-DT(I,J)
295     IF(DT(I,J).GT.200) DT(I,J)=200.
296     DTI(I,J)=DT(I,J)-DT(I,JI)
297     DTA(I,J)=(DT(I,J)+DT(II,J))/2
298     DTAI(I,J)=(DTI(I,J)+DTI(II,J))/2

```



```

298      5      CONTINUE
299      RETURN
300      END
301      C
302      C
303      C*****
304      C
305      C          SUBROUTINE CONSOL
306      C      Determines pore pressure dissipation with time
307      C      in oil sand due to 1-D consolidation following each
308      C      transient heating increment. The semi-implicit
309      C      formulation yields a tridiagonal matrix at each
310      C      time step which is inverted & solved using
311      C      "THOMAS'S ALGORITHM".
312      C
313      C*****
314      C
315      C          SUBROUTINE CONSOL(J,JJ,JI)
316      C
317      COMMON /BLK1/ NN,M,N,MM,NI,DELT,ALPHAT,SVEO
318      COMMON /BLK2/ DZ(35,3000),T(35,3000)
319      COMMON /BLK4/ UDR(35,3000),U(35,3000)
320      COMMON /BLK5/ DT(35,3000),DTI(35,3000)
321      COMMON /BLK6/ DTA(35,3000),DTAI(35,3000)
322      COMMON /BLK8/ CV(35,3000),DM(35,3000)
323      COMMON /BLK9/ BT(35,3000),DU(35,3000)
324      COMMON /BLK12/ AA(35),BB(35),CC(35)
325      COMMON /BLK13/ WW(100),GG(100),DGAM(35,3000)
326      COMMON /BLK14/ DH(35,3000)
327      C
328      U(1,1)=0.
329      DO 1 I=2,N
330      II=I-1
331      IJ=I+1
332      IF (I.GT.2) GO TO 2
333      AA(2)=-(CV(2,J)*DELT)/1.0
334      BB(2)=1+(2*CV(2,J)*DELT/1.0)
335      CC(2)=AA(2)
336      WW(2)=CC(2)/BB(2)
337      GG(2)=(U(2,JI)-AA(2)*U(1,JI))/BB(2)
338      GO TO 1
339      2      CVAVG=(CV(I,J)+CV(II,J))/2
340      AA(I)=-(CVAVG*DELT)/(DZ(I,JI)**2)
341      BB(I)=1+(2*CVAVG*DELT/(DZ(I,JI)**2))
342      CC(I)=AA(I)
343      IF (I.EQ.N) GO TO 3
344      WW(I)=CC(I)/(BB(I)-AA(I)*WW(II))
345      GG(I)=(U(I,JI)-AA(I)*GG(II))/(BB(I)-AA(I)*WW(II))
346      GO TO 1
347      3      GG(N)=(U(N,JI)-(2*AA(N)*GG(NI)))/(BB(N)-(2*AA(N)*WW(NI)))
348      UDR(N,J)=GG(N)
349      1      CONTINUE
350      NII=N-2
351      DO 4 I=1,NII
352      IB=N-I
353      IBJ=IB+1
354      UDR(IB,J)=GG(IB)-WW(IB)*UDR(IBJ,J)
355      4      CONTINUE
356      DO 5 I=2,N
357      U(I,J)=DU(I,J)+UDR(I,J)+DM(I,J)

```



```
358      IF(U(I,J).LT.0) U(I,J)=-U(I,J)
359      5      CONTINUE
360      RETURN
361      END
```

End of file

\$COPY \*1 \*PRINT\*



PROGRAM HCDR



\$LIST hcdr ON \*PRINT\*

```

1  ****
2  C*
3  C*          ****
4  C*          * PROGRAM HCDR *
5  C*          ****
6  C*      Semi Implicit Finite Difference Solution for
7  C*      One Dimensional HEAT CONSOLIDATION of Oil Sand
8  C*      Coupled with Transient Heating by Thermal Diffusion
8.5 C*      in Radial Coordinates .
9  C*
10 C*
11 C*      Properties of the oil sand vary with temperature,
12 C*      pressure,& effective stress . Variable parameters
13 C*      include fluid mobility,porosity,bulk density,fluid
14 C*      & solid densities , pore pressure response to
15 C*      undrained heating & coefficient of consolidation .
16 C*
17 C*      ASSUMPTIONS :
18 C*
19 C*      1.Oil Saturation is assumed to be constant during
20 C*      gravity drainage .
21 C*      2.Total stress variation with density of the heated
22 C*      material is not considered .
23 C*      3.One-way radial drainage is assumed ;
25 C*      4.The lateral boundaries are constant pressure/temp-
26 C*      erature boundaries .
27 C*      5.Properties of Saline Creek oil sand are used in
28 C*      the analysis .
29 C*
30 C*      . CODED by J.G.Agar , July 1983
31 C*      All rights reserved by the author
32 C*
33 ****
34 C*
35 C          ****
36 C          * MAIN PROGRAM *
37 C          ****
38 C*
39 C*
40 C      Dimension Array Parameters
41 C*
42 C      NN=32
43 C      M=1441
44 C      M1=541
45 C      M2=721
46 C      M3=361
47 C      M4=181
48 C      M5=61
49 C      M6=11
50 C      M7=6
51 C      N=NN-1
52 C      MM=M-1
53 C      NI=NN-2
54 C      REAL *4 MV
55 COMMON /BLK1/ NN,M,N,MM,NI,DELT,ALPHAT,SVEO
56 COMMON /BLK2/ DR(35,3000),T(35,3000)
57 COMMON /BLK3/ R(35,3000),RD(35,3000)
58 COMMON /BLK4/ UDR(35,3000),U(35,3000)

```



```
59      COMMON /BLK5/ DT(35,3000),DTI(35,3000)
60      COMMON /BLK6/ DTA(35,3000),DTAI(35,3000)
61      COMMON /BLK7/ P(35,3000),HCR(35,3000)
62      COMMON /BLK8/ CV(35,3000),DM(35,3000)
63      COMMON /BLK9/ BT(35,3000),DU(35,3000)
64      COMMON /BLK10/ A(35),B(35),C(35)
65      COMMON /BLK11/ W(35),G(35)
66      COMMON /BLK12/ AA(35),BB(35),CC(35)
67      COMMON /BLK13/ WW(35),GG(35),GAM(35,3000)
67.3    COMMON /BLK14/ ALP(35,3000)
69      C
70      C      Initial Conditions
71      C
71.3    SVO=9000.
71.6    SVEO=6000.
73      DO 10 I=2,NN
74      II=I-1
75      DT(I,1)=0
76      DTA(I,1)=0
77      T(I,1)=5.0
78      P(I,1)=3000.
79      DR(I,1)=2.0
80      R(I,1)=II*DR(I,1)
81      U(I,1)=0.
82      CV(I,1)=1.08
83      BT(I,1)=SVEO/10.
84      10  CONTINUE
85      C
86      C      Boundary Conditions
87      C
88      DO 11 J=1,M
89      R(1,J)=0.
90.1    RD(1,J)=0.
90      T(1,J)=205.
91      DT(1,J)=200.
92      U(1,J)=0.
93      P(1,J)=3000.
94      CV(1,J)=10.8
95      11  CONTINUE
96      C
97      C      Constants
98      C
99      AF=1.00
101     DELT=5.0
102     MV=5.0E-07
103     ALPHDR=3.6E-05
104     ALPHAT=6.0E-05
105     ALPHAF=5.2E-04
106     BETAS=5.0E-09
107     ALPHAS=4.3E-05
108     C
109     C      Heat Consolidation Calculation
110     C
111     DO 30 J=2,M
112     JJ=J+1
113     JI=J-1
114     CALL TEMPD(J,JJ,JI)
115     DO 25 I=2,N
116     BETAF=4.0E-07*(10**((DT(I,J)/200)))
117     POR=0.33*(1+MV*U(I,JI)-(ALPHDR-ALPHAS)*DT(I,J))
```



```

118      GAMF=9.85/(1+ALPHAF*DT(I,J)-BETAF*U(I,J))
119      GAMS=26.5/(1+ALPHAS*DT(I,J)+BETAS*U(I,J))
120      GAM(I,J)=POR*GAMF+((1-POR)*GAMS)
121      DGAM=GAM(I,J)-21.0
122      DM(I,J)=DGAM*1.0
123      BT(I,J)=1/((1/BT(I,1))+(DT(I,J)/(AF*(SVEO-U(I,JI)))))
124      DU(I,J)=BT(I,J)*DT(I,J)
125      CV(I,J)=CV(I,1)*(10**((DT(I,J)/200)))
126      25  CONTINUE
127      CALL CONSOL(J,JJ,JI)
128      DO 20 I=2,N
129      JJ=J+1
130      JI=J-1
131      IJ=I+1
132      II=I-1
133      DR(I,J)=DR(I,1)*(1+(MV*U(I,J))+ALPHDR*DT(I,J))
134      R(I,J)=R(II,J)+DR(I,J)
135      T(I,J)=T(I,1)+DT(I,J)
136      P(I,J)=P(I,1)+U(I,J)
137      20  CONTINUE
138      30  CONTINUE
139      C
140      C Dimensionless Parameters
141      C
142      DO 50 J=2,M
143      DO 40 I=2,N
143.05  IF(DT(I,J).LE.0.001)GO TO 41
143.1    ALP(I,J)=((MV*U(I,J))+(ALPHDR*DT(I,J)))/DT(I,J)
143.2    GO TO 42
143.3    41  ALP(I,J)=ALPHDR
144      42  RD(I,J)=R(I,J)/R(N,J)
145      HCR(I,J)=(CV(I,J)/ALPHAT)/1000
146      40  CONTINUE
147      50  CONTINUE
148      C
149      C Printout
150      C
151      C
152      C95  PRINT 95
153      C    FORMAT(' Radius Temperature Pressure Time ',//)
154      C    WRITE(6,96) (R(I,M7),T(I,M7),P(I,M7),M7,I=1,N)
155      C    FORMAT(F7.4,2F11.3,I6)
156      C    WRITE(6,97) (R(I,M5),T(I,M5),P(I,M5),M5,I=1,N)
157      C    FORMAT(F7.4,2F11.3,I6)
158      C    WRITE(6,98) (R(I,M3),T(I,M3),P(I,M3),M3,I=1,N)
159      C    FORMAT(F7.4,2F11.3,I6)
160      C    WRITE(6,99) (R(I,M),T(I,M),P(I,M),M,I=1,N)
161      C    FORMAT(F7.4,2F11.3,I6)
162      C
163      C99  PRINT 100
164      C    FORMAT('//2X,' Temperature vs. Depth & Time')
165      C    WRITE(6,101)(RD(I,M7),DT(I,M7),I=1,N)
166      C    FORMAT(G10.3,' ','G10.3',' ')
167      C    WRITE(6,102)(RD(I,M6),DT(I,M6),I=1,N)
168      C    FORMAT(1X,G10.3,' ','G10.3',' ')
169      C    WRITE(6,103)(RD(I,M5),DT(I,M5),I=1,N)
170      C    FORMAT(G10.3,' ','G10.3',' ')
171      C    WRITE(6,104)(RD(I,M4),DT(I,M4),I=1,N)
172      C    FORMAT(1X,G10.3,' ','G10.3',' ')
173      C    WRITE(6,121)(RD(I,M3),DT(I,M3),I=1,N)
174      C    FORMAT(G10.3,' ','G10.3',' ')

```



```

174      WRITE(6,122)(RD(I,M2),DT(I,M2),I=1,N)
175      122  FORMAT(1X,G10.3,',',G10.3,',')
176      C     WRITE(6,123)(RD(I,M1),DT(I,M1),I=1,N)
177      C123  FORMAT(G10.3,',',G10.3,',')
178      124  WRITE(6,124)(RD(I,M),DT(I,M),I=1,N)
179      C     FORMAT(1X,G10.3,',',G10.3,',')
180
181      PRINT 105
182      105  FORMAT(//2X,'Pore Pressure vs. Depth & Time')
183      WRITE(6,106)(RD(I,M7),U(I,M7),I=1,N)
184      106  FORMAT(G10.3,',',G10.3,',')
185      C     WRITE(6,107)(RD(I,M6),U(I,M6),I=1,N)
186      C107  FORMAT(1X,G10.3,',',G10.3,',')
187      WRITE(6,108)(RD(I,M5),U(I,M5),I=1,N)
188      108  FORMAT(G10.3,',',G10.3,',')
189      WRITE(6,109)(RD(I,M4),U(I,M4),I=1,N)
190      109  FORMAT(1X,G10.3,',',G10.3,',')
191      WRITE(6,126)(RD(I,M3),U(I,M3),I=1,N)
192      126  FORMAT(G10.3,',',G10.3,',')
193      WRITE(6,127)(RD(I,M2),U(I,M2),I=1,N)
194      127  FORMAT(1X,G10.3,',',G10.3,',')
195      C     WRITE(6,128)(RD(I,M1),U(I,M1),I=1,N)
196      C128  FORMAT(G10.3,',',G10.3,',')
197      WRITE(6,129)(RD(I,M),U(I,M),I=1,N)
198      129  FORMAT(1X,G10.3,',',G10.3,',')
199      C
200      PRINT 115
201      115  FORMAT(//2X,'Thermal Expansion Coeff. vs. Depth & Time')
202      WRITE(6,116)(RD(I,M7),ALP(I,M7),I=1,N)
203      116  FORMAT(G10.3,',',G10.3,',')
204      C     WRITE(6,117)(RD(I,M6),ALP(I,M6),I=1,N)
205      C117  FORMAT(1X,G10.3,',',G10.3,',')
206      WRITE(6,118)(RD(I,M5),ALP(I,M5),I=1,N)
207      118  FORMAT(G10.3,',',G10.3,',')
208      WRITE(6,119)(RD(I,M4),ALP(I,M4),I=1,N)
209      119  FORMAT(1X,G10.3,',',G10.3,',')
210      WRITE(6,130)(RD(I,M3),ALP(I,M3),I=1,N)
211      130  FORMAT(G10.3,',',G10.3,',')
212      WRITE(6,131)(RD(I,M2),ALP(I,M2),I=1,N)
213      131  FORMAT(1X,G10.3,',',G10.3,',')
214      C     WRITE(6,132)(RD(I,M1),ALP(I,M1),I=1,N)
215      C132  FORMAT(G10.3,',',G10.3,',')
216      WRITE(6,133)(RD(I,M),ALP(I,M),I=1,N)
217      133  FORMAT(1X,G10.3,',',G10.3,',')
218      C
219      STOP
220      END
221
222      C
223      C
224      C
225      C*****
226      C
227      C
228      C*****
229      C
230      C          SUBROUTINE TEMPD
231      C          Determines temperature distribution with time in
232      C          oil sand due to 1-D thermal diffusion . The semi
233      C          implicit formulation yields a tridiagonal matrix
234      C          at each time step which is solved using
235      C          THOMAS'S ALGORITHM .
236      C
237      C*****

```



```

238      C
239      C      SUBROUTINE TEMPD(J,JJ,JI)
240      C
241      COMMON /BLK1/ NN,M,N,MM,NI,DELT,ALPHAT,SVEO
242      COMMON /BLK2/ DR(35,3000),T(35,3000)
242.5    COMMON /BLK3/ R(35,3000),RD(35,3000)
243      COMMON /BLK5/ DT(35,3000),DTI(35,3000)
244      COMMON /BLK6/ DTA(35,3000),DTAI(35,3000)
245      COMMON /BLK10/ A(35),B(35),C(35)
246      COMMON /BLK11/ W(35),G(35)
247      C
247.5    NII=N-2
248      DO 1 I=2,N
249      II=I-1
250      IJ=I+1
251      A(I)=(ALPHAT*DELT)*((1/(2*R(I,JI)*DR(I,JI)))-(1/(DR(I,JI)
251.1  &**2)))
252      B(I)=1+(2*ALPHAT*DELT)/(DR(I,JI)**2)
253      C(I)=(ALPHAT*DELT)*((-1/(2*R(I,JI)*DR(I,JI)))-(1/(DR(I,JI)
253.5  &**2)))
254      IF (I.GT.2) GO TO 2
255      W(2)=C(2)/B(2)
256      G(2)=(DT(2,JI)-A(2)*DT(1,JI))/B(2)
257      GO TO 1
258      2      IF (I.EQ.N) GO TO 3
259      W(I)=C(I)/(B(I)-A(I)*W(II))
260      G(I)=(DT(I,JI)-A(I)*G(II))/(B(I)-A(I)*W(II))
261      GO TO 1
262      3      G(N)=(DT(N,JI)-(2*A(N)*G(NI)))/(B(N)-(2*A(N)*W(NI)))
263      DT(N,J)=G(N)
264      1      CONTINUE
265      DO 4 I=1,NII
266      IB=N-I
267      IBJ=IB+1
268      DT(IB,J)=G(IB)-W(IB)*DT(IBJ,J)
269      4      CONTINUE
270      DO 5 I=2,N
271      II=I-1
272      DTI(I,J)=DT(I,J)-DT(I,JI)
273      DTA(I,J)=(DT(I,J)+DT(II,J))/2
274      DTAI(I,J)=(DTI(I,J)+DTI(II,J))/2
275      5      CONTINUE
276      RETURN
277      END
278
279      C
280      C
281      ****
282      C
283      C      SUBROUTINE CONSOL
284      C      Determines pore pressure dissipation with time
285      C      in oil sand due to 1-D consolidation following each
286      C      transient heating increment. The semi-implicit
287      C      formulation yields a tridiagonal matrix at each
288      C      time step which is solved using THOMAS'S ALGORITHM .
289      C
290      ****
291      C
292      C      SUBROUTINE CONSOL(J,JJ,JI)
293      C
294      COMMON /BLK1/ NN,M,N,MM,NI,DELT,ALPHAT,SVEO

```



```

295      COMMON /BLK2/ DR(35,3000),T(35,3000)
295.5    COMMON /BLK3/ R(35,3000),RD(35,3000)
296      COMMON /BLK4/ UDR(35,3000),U(35,3000)
297      COMMON /BLK5/ DT(35,3000),DTI(35,3000)
298      COMMON /BLK6/ DTA(35,3000),DTAI(35,3000)
299      COMMON /BLK8/ CV(35,3000),DM(35,3000)
300      COMMON /BLK9/ BT(35,3000),DU(35,3000)
301      COMMON /BLK12/ AA(35),BB(35),CC(35)
302      COMMON /BLK13/ WW(35),GG(35),DGAM(35,3000)
304      C
304.5    NII=N-2
305      DO 1 I=2,N
306      II=I-1
307      IJ=I+1
307.1    AA(I)=(CV(I,J)*DELT)*((1/(2*R(I,JI)*DR(I,JI)))
307.2    &-(1/(DR(I,JI)**2)))
307.3    BB(I)=1+(2*CV(I,J)*DELT/(DR(I,JI)**2))
307.4    CC(I)=(CV(I,J)*DELT)*(-(1/(2*R(I,JI)*DR(I,JI)))
307.5    &-(1/(DR(I,JI)**2)))
308      IF (I.GT.2) GO TO 2
312      WW(2)=CC(2)/BB(2)
313      GG(2)=(U(2,JI)-AA(2)*U(1,JI))/BB(2)
314      GO TO 1
319      2      IF (I.EQ.N) GO TO 3
320      WW(I)=CC(I)/(BB(I)-AA(I)*WW(II))
321      GG(I)=(U(I,JI)-AA(I)*GG(II))/(BB(I)-AA(I)*WW(II))
322      GO TO 1
323      3      GG(N)=(U(N,JI)-(2*AA(N)*GG(NI)))/(BB(N)-(2*AA(N)*WW(NI)))
324      UDR(N,J)=GG(N)
325      1      CONTINUE
327      DO 4 I=1,NII
328      IB=N-I
329      IBJ=IB+1
330      UDR(IB,J)=GG(IB)-WW(IB)*UDR(IBJ,J)
331      4      CONTINUE
332      DO 5 I=2,N
333      U(I,J)=DU(I,J)+UDR(I,J)+DM(I,J)
334      5      CONTINUE
335      RETURN
336      END

```

End of file

\$COPY \*1 \*PRINT\*



APPENDIX K

ONE DIMENSIONAL HEAT CONSOLIDATION OF OIL SAND:  
NUMERICAL SOLUTIONS



Influence of Temporal Discretization on Predicted  
Pore Pressures and Volumetric Strains



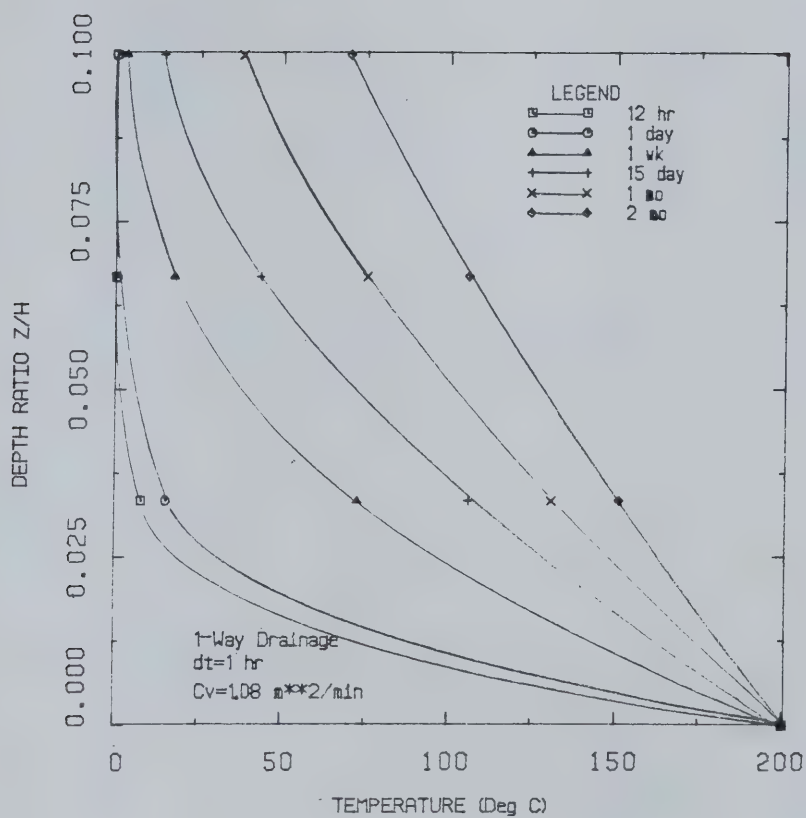


FIGURE K1.1 Transient Temperatures - One-Way Drainage (1 Hour Time Step)



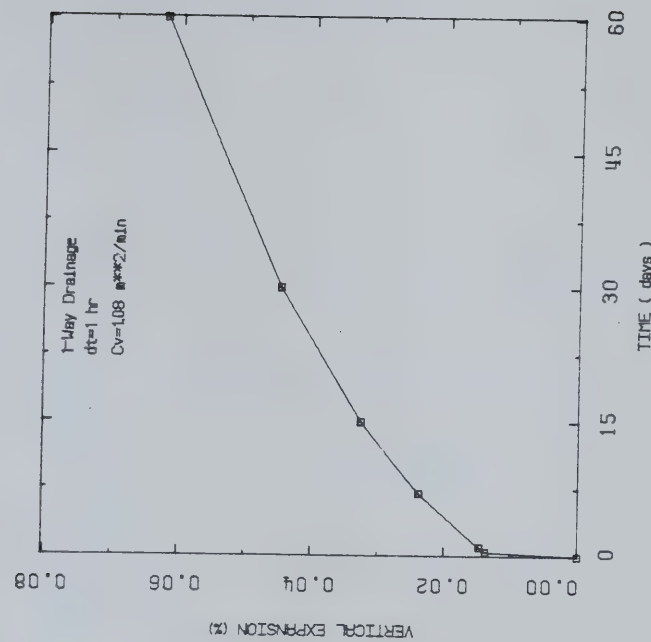


FIGURE K1.3 Transient Vertical Expansion - One-Way Drainage (1 Hour Time Step)

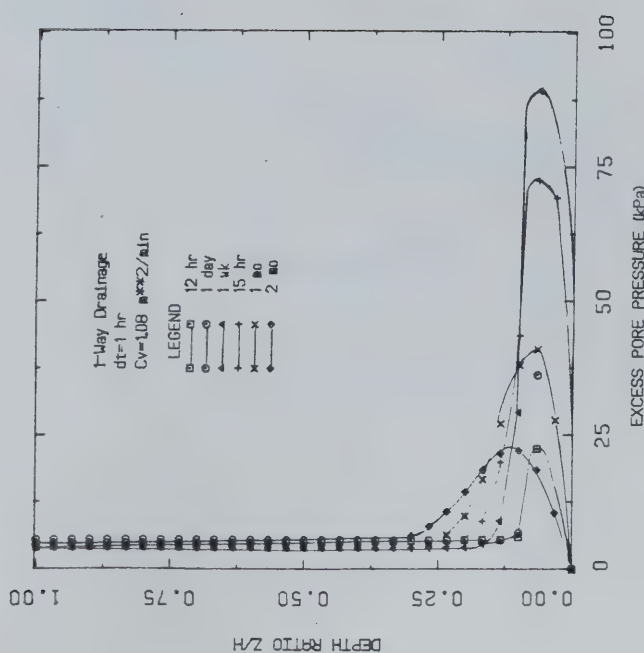


FIGURE K1.2 Transient Temperatures - One-Way Drainage (1 Hour Time Step)

FIGURE K1.1 Transient Vertical Expansion - One-Way Drainage (1 Hour Time Step)



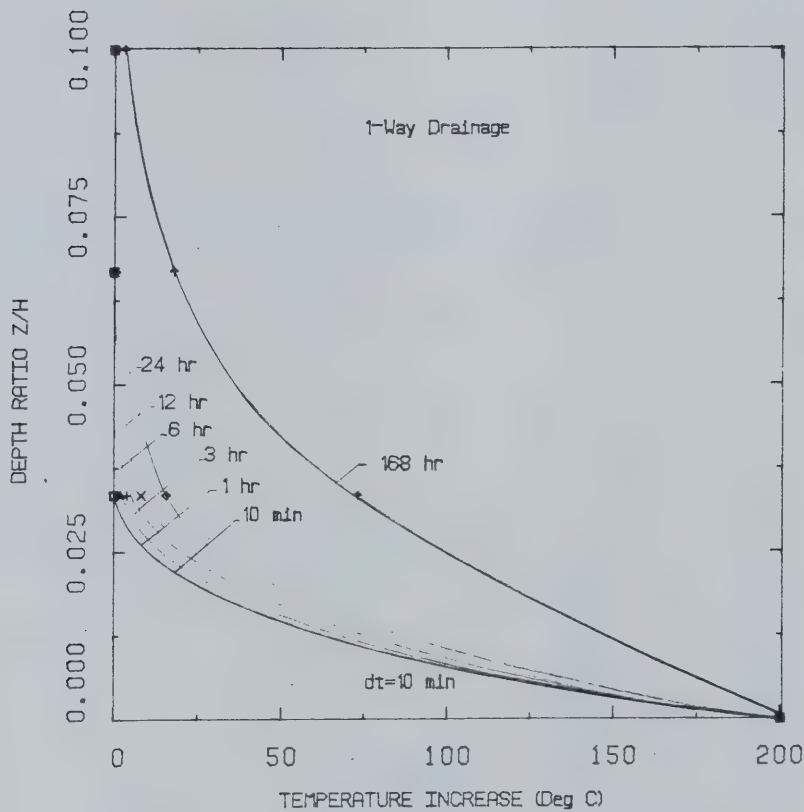


FIGURE K2.1 Transient Temperatures - One-Way  
Drainage (10 Minute Time Step)



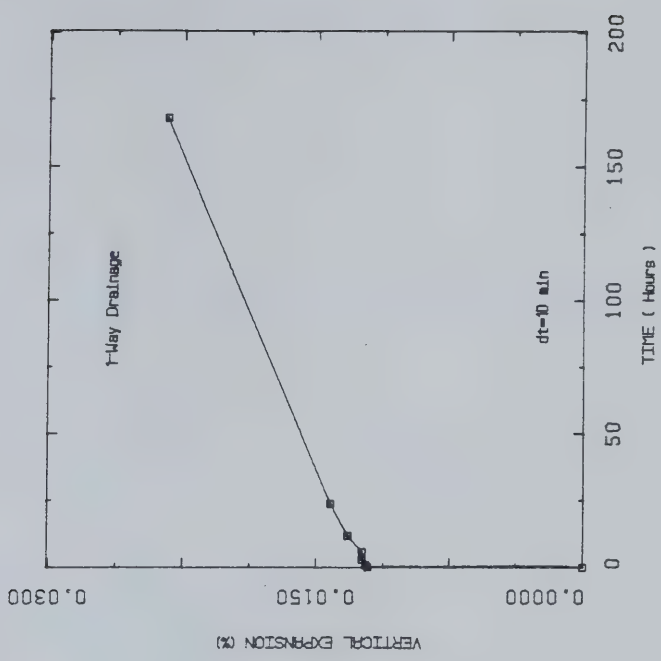


FIGURE K2.3 Transient Vertical Expansion - One-Way Drainage (10 Minute Time Step)

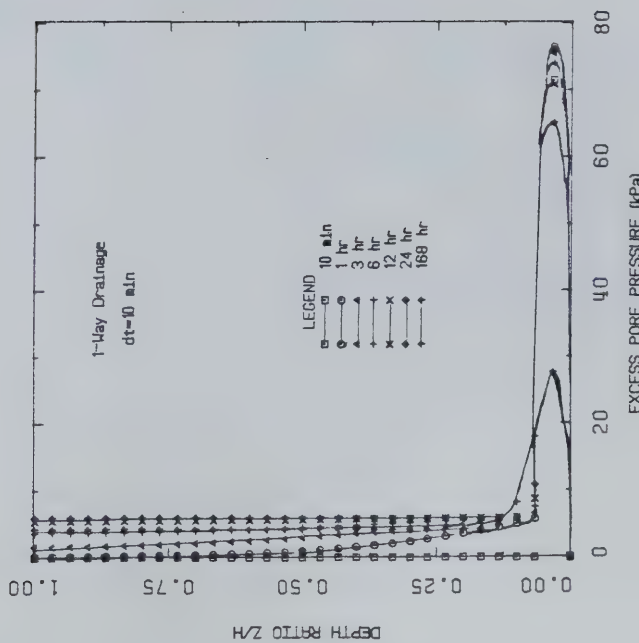


FIGURE K2.2 Transient Excess Pore Pressure - One-Way Drainage (10 Minute Time Step)



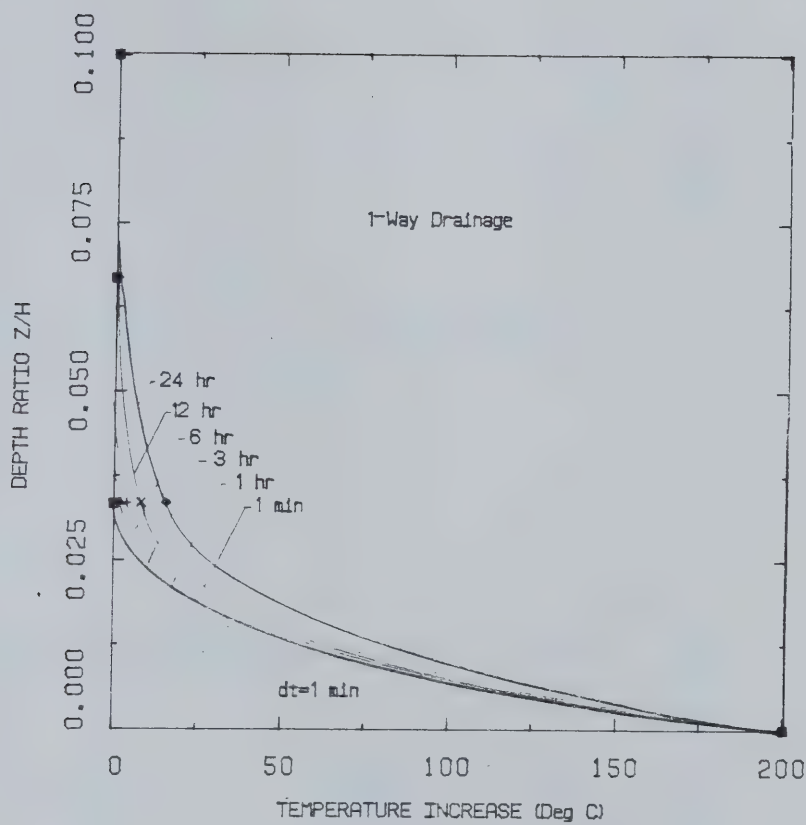


FIGURE K3.1 Transient Temperatures - One-Way Drainage (1 Minute Time Step)



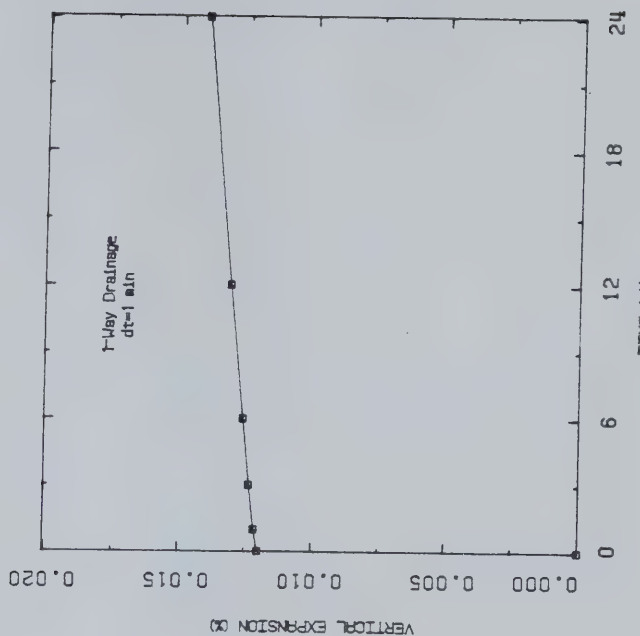


FIGURE K3.2 Transient Excess Pore Pressures—One-Way Drainage (1 Minute Time Step)

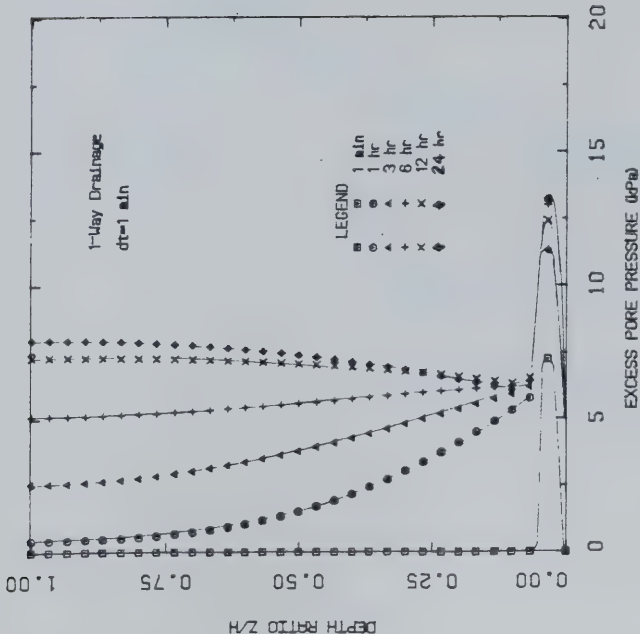


FIGURE K3.3



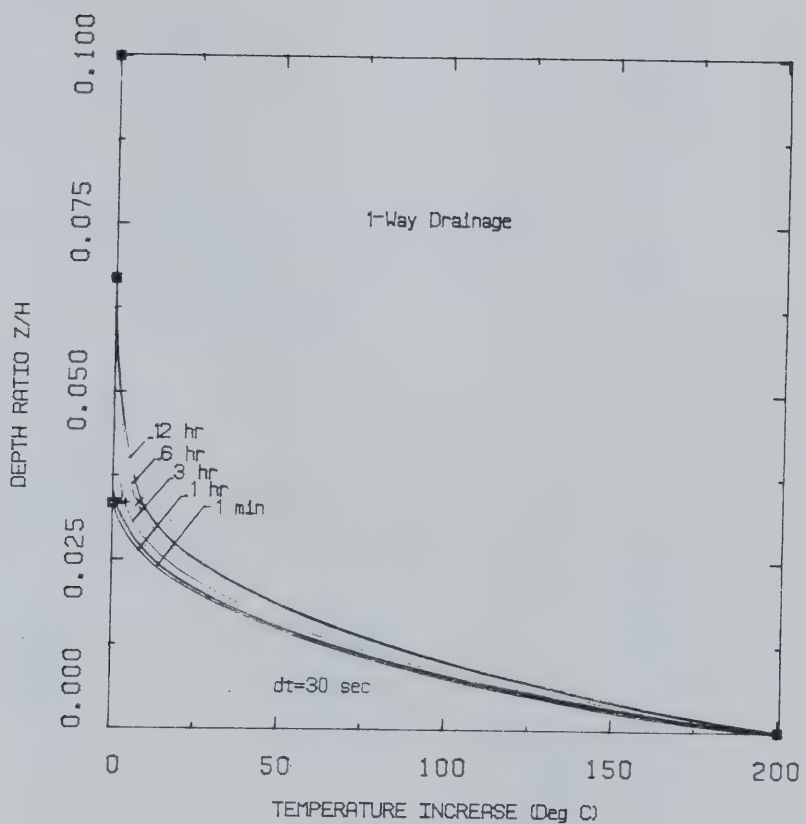


FIGURE K4.1 Transient Temperatures - One-Way Drainage (30 Second Time Step)



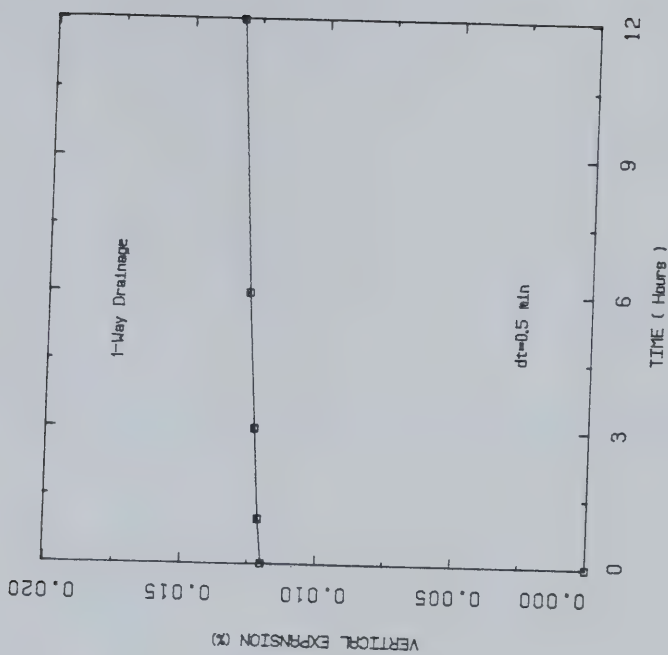


FIGURE K4.3  
Transient Vertical Expansion - One-Way Drainage (30 Second Time Step)

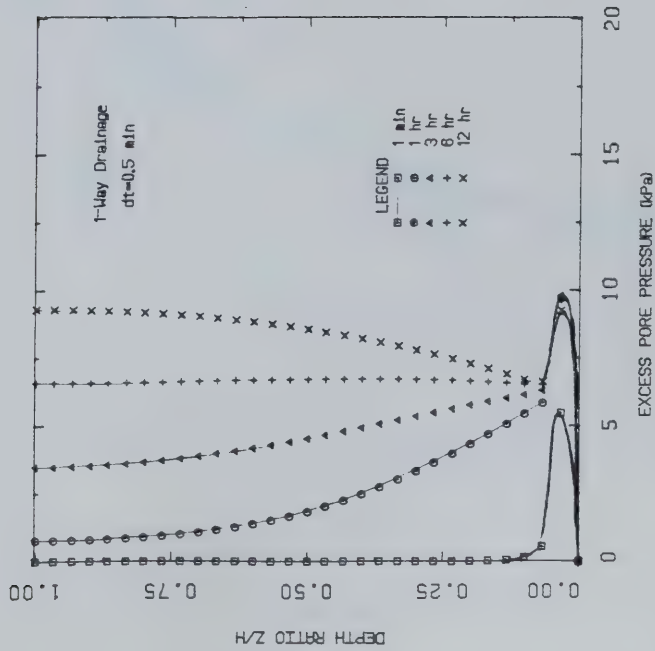


FIGURE K4.2  
Transient Excess Pore Pressures - One-Way Drainage (30 Second Time Step)

Transient Vertical Expansion - One-Way Drainage (30 Second Time Step)



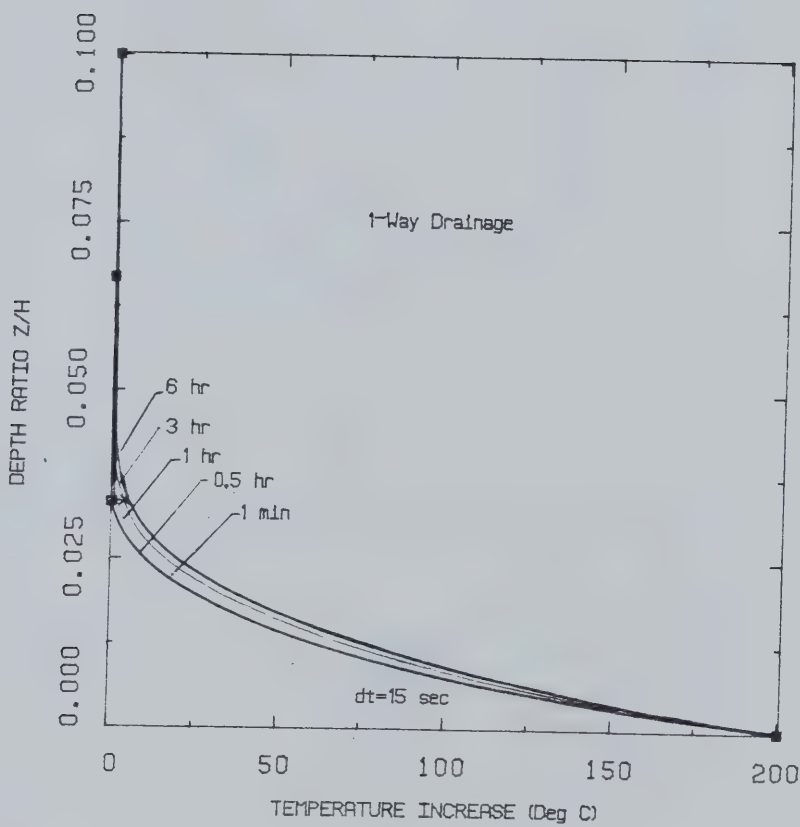


FIGURE K5.1 Transient Temperatures - One-Way  
Drainage (15 Second Time Step)



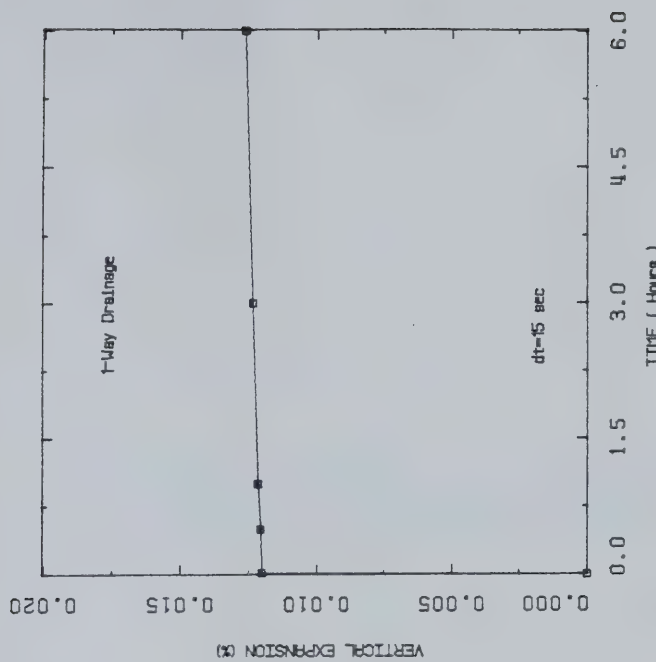


FIGURE K5.2 Transient Excess Pore Pressures - One-Way Drainage (15 Second Time Step)

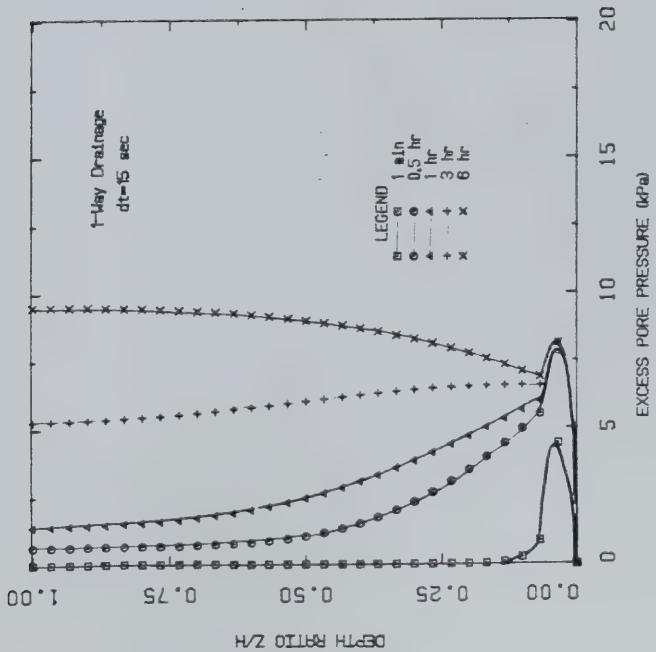


FIGURE K5.3 Transient Vertical Expansion - One-Way Drainage (15 Second Time Step)



Influence of Oil Sand Permeability on Predicted  
Pore Pressures and Volumetric Strains



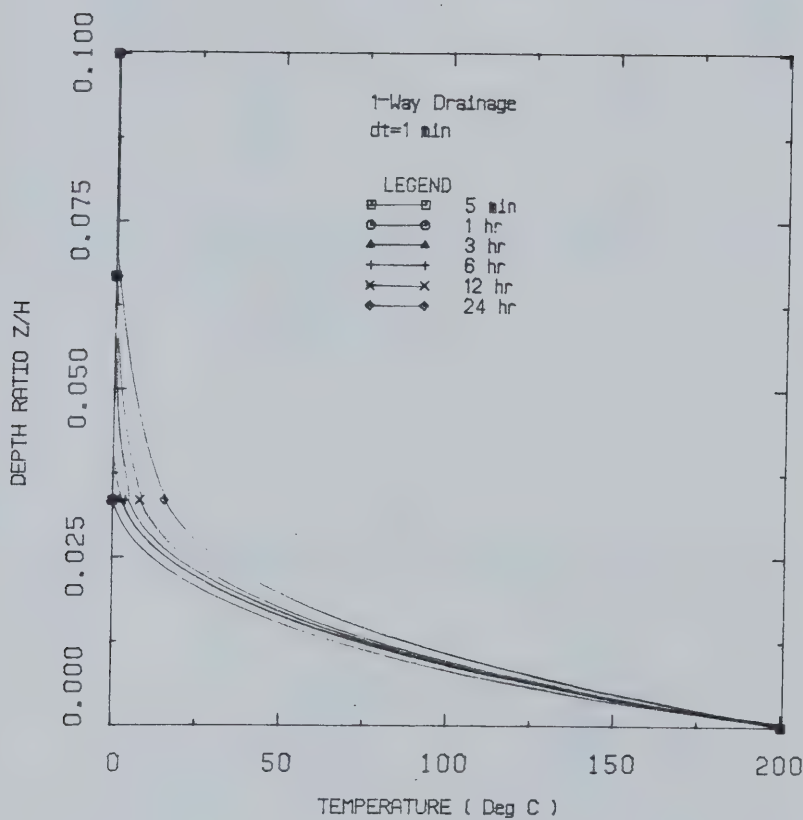


FIGURE K6 Transient Temperatures for One-Way Drainage (1 Minute Time Step)



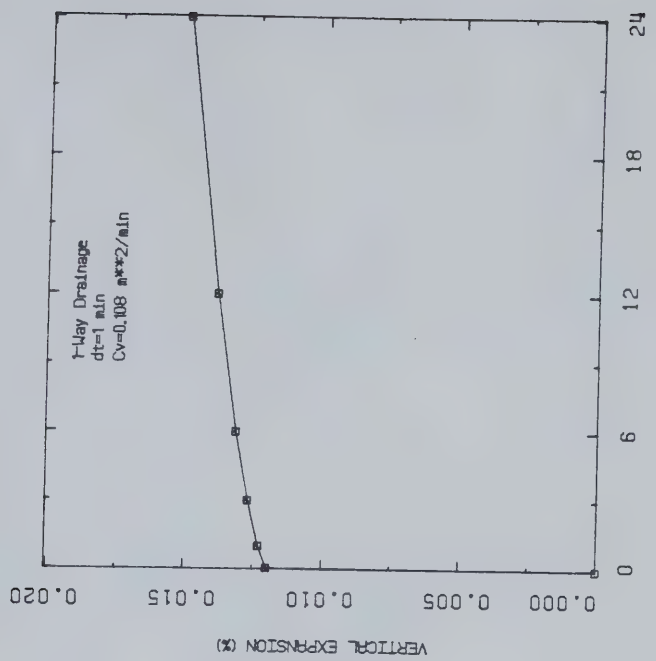


FIGURE K7.2 Transient Vertical Expansion  
 $(R_T = 1800)$

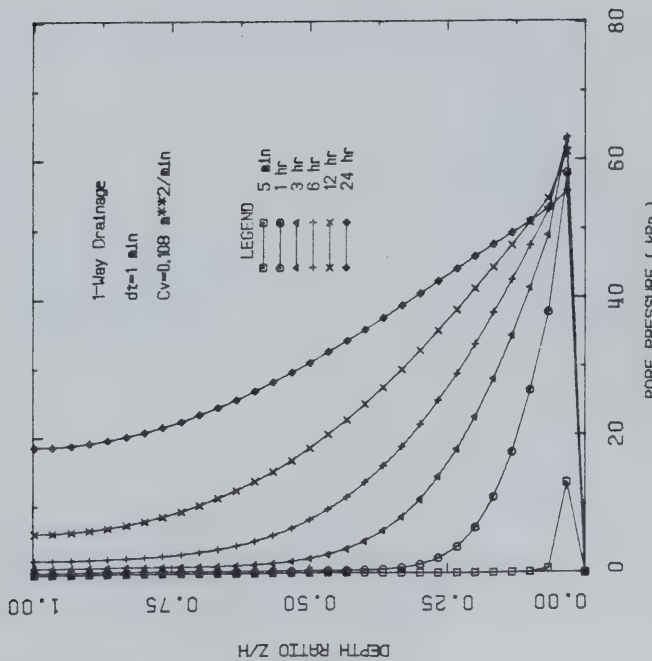


FIGURE K7.1 Transient Excess Pore Pressures  
 $(R_T = 1800)$



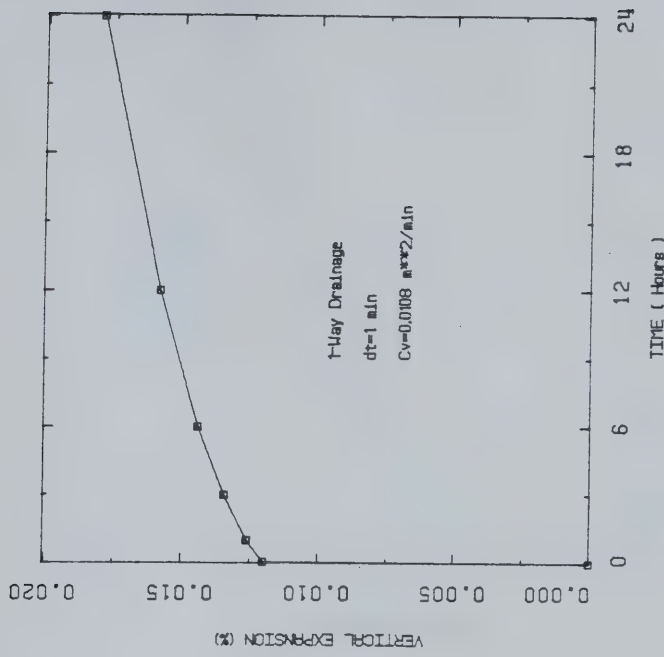


FIGURE K8.1 Transient Excess Pore Pressures  
( $R_T = 180$ )

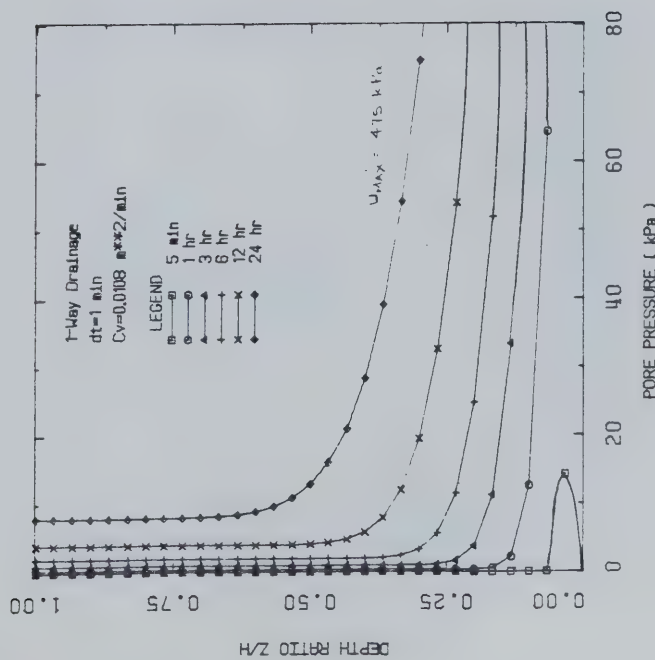


FIGURE K8.2 Transient Vertical Expansion  
( $R_T = 180$ )



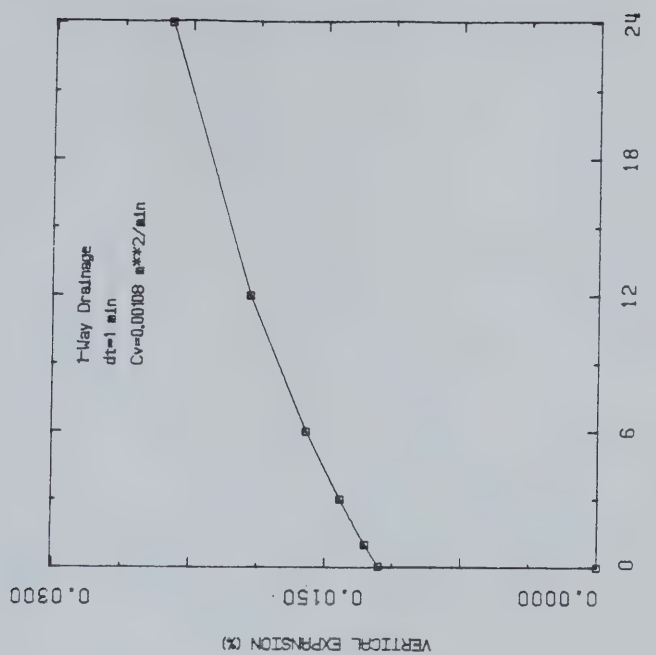
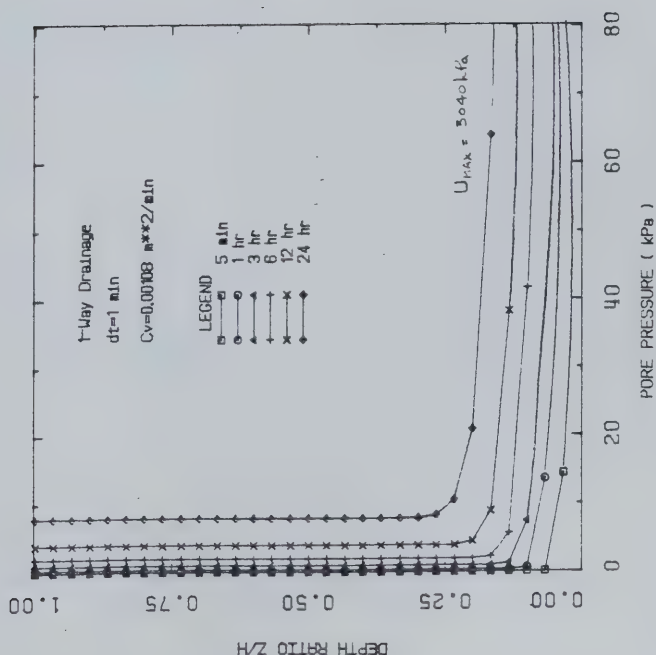


FIGURE K9.1 Transient Excess Pore Pressures  
( $R_T = 18$ )





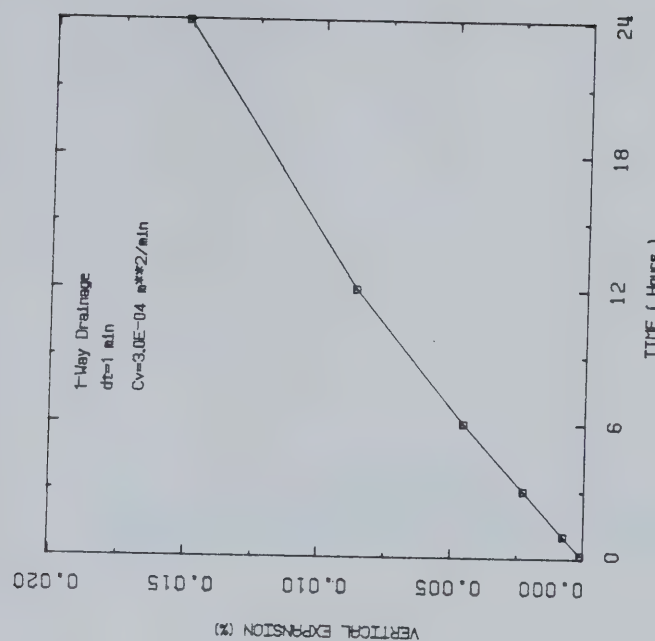


FIGURE K10.2 Transient Vertical Expansion  
 $(R_T = 5)$

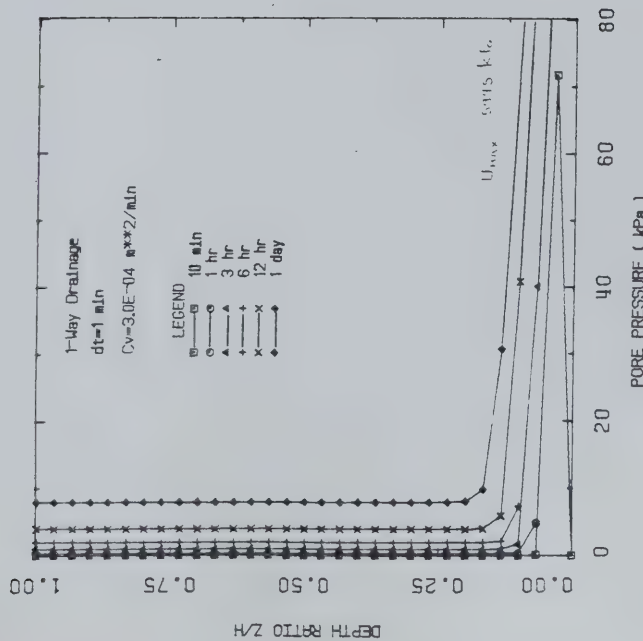


FIGURE K10.1 Transient Excess Pore Pressures  
 $(R_T = 5)$



APPENDIX L  
RESULTS OF THERMOELASTIC STRESS-STRAIN ANALYSES



Thermal Stress Changes and Deformations Adjacent  
to a Shaft In Oil Sand Assuming a Rigid Boundary  
Condition at the Production Zone



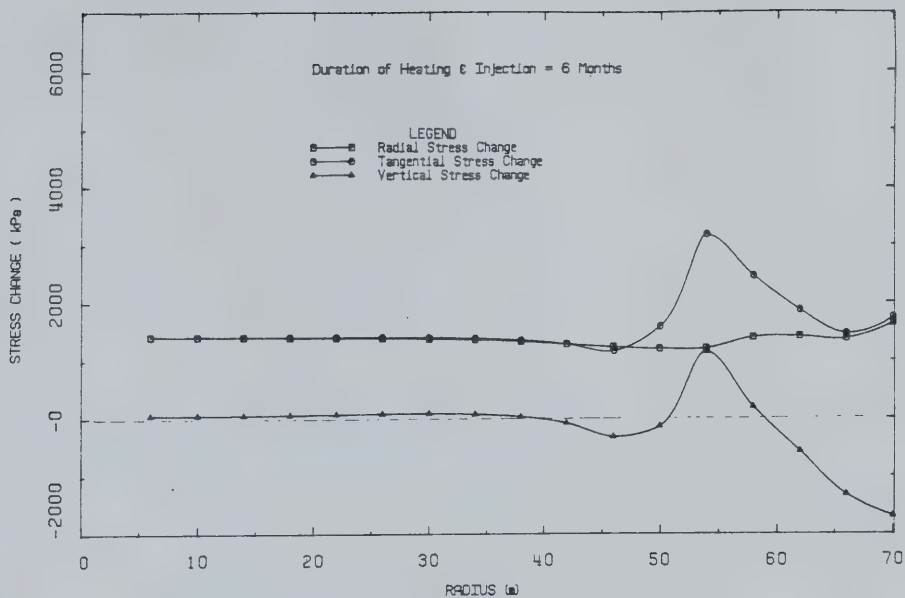


FIGURE L1.1 Stress Changes Around the Shaft After 6 Months of Steam Injection



FIGURE L1.2 Deformations Around the Shaft After 6 Months of Steam Injection

DISPLACEMENT SCALE 1:100



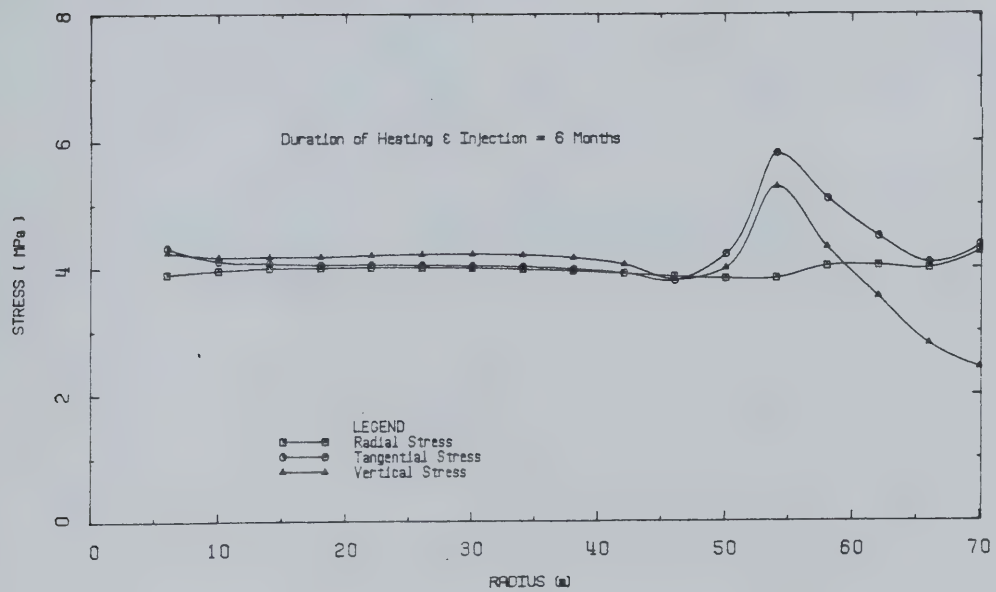


FIGURE L1.3 Effective Stresses Around the Shaft  
After 6 Months of Steam Injection



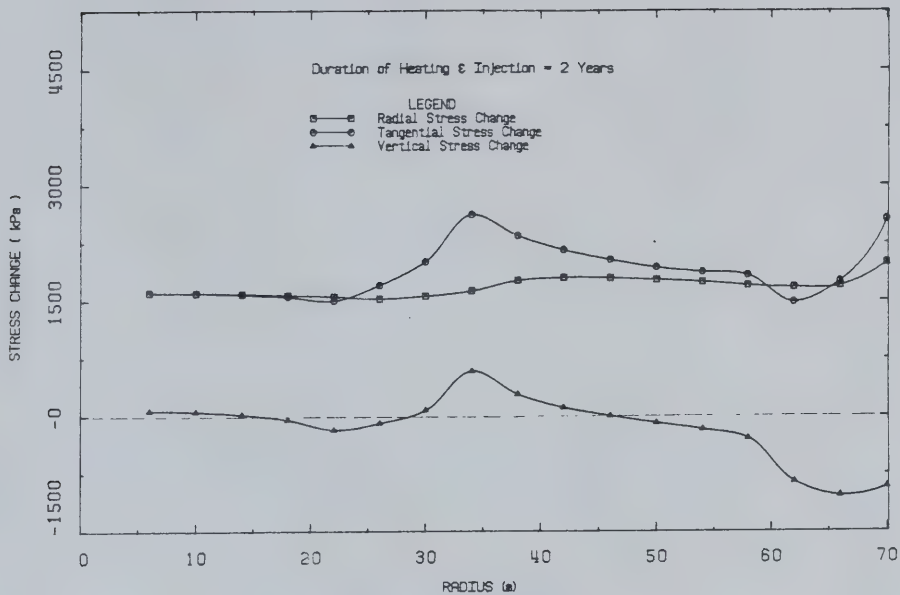


FIGURE L2.1 Stress Changes Around the Shaft After 2 Years of Steam Injection

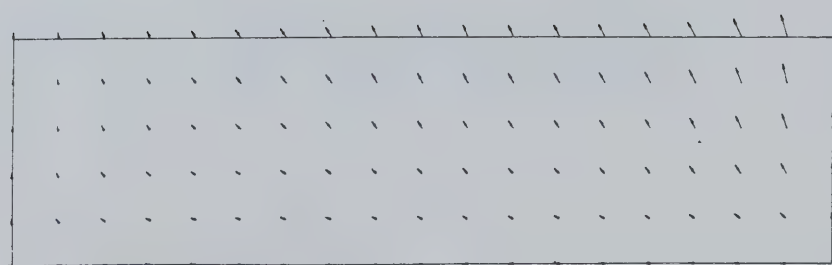


FIGURE L2.2 Deformations Around the Shaft After 2 Years of Steam Injection

DISPLACEMENT SCALE 1:100



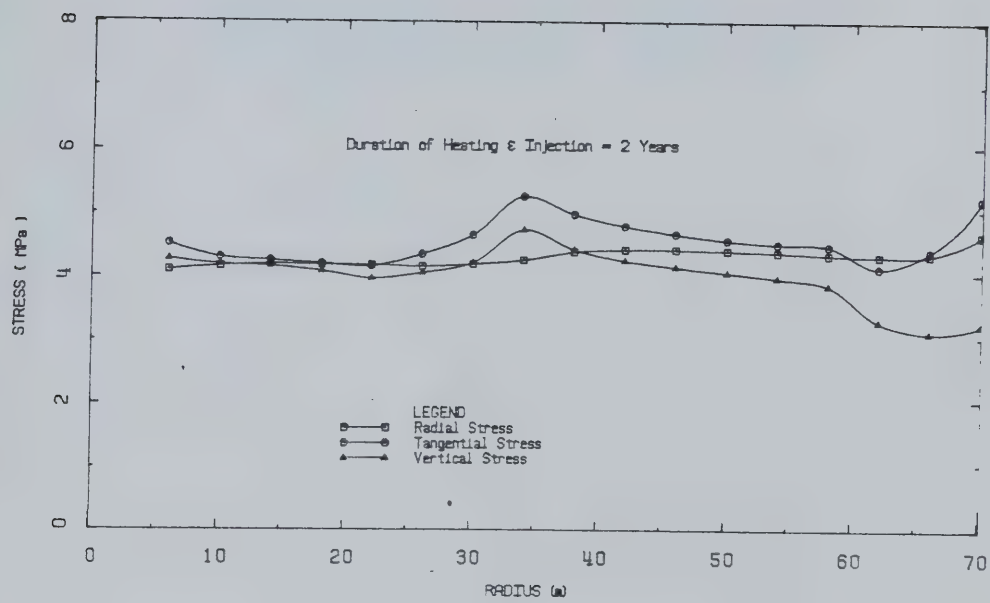


FIGURE L2.3 Effective Stresses Around the Shaft  
After 2 Years of Steam Injection



Stress Changes and Deformations Adjacent to a  
Shaft in Oil Sand Assuming a Constant Pressure  
Boundary Condition at the Production Zone



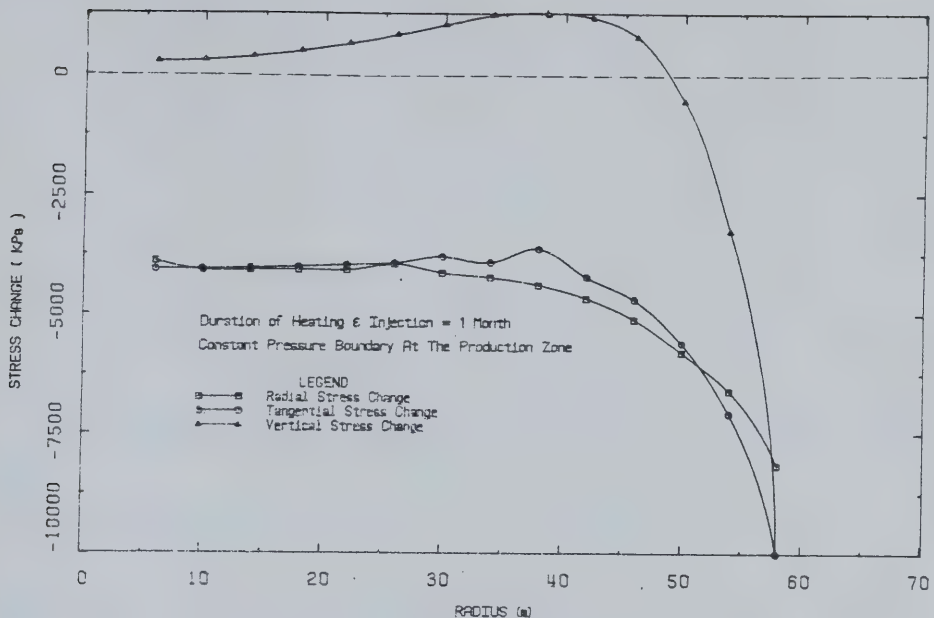


FIGURE L3.1 Stress Changes Around the Shaft After 1 Month of Steam Injection



FIGURE L3.2 Deformations Around the Shaft After 1 Month of Steam Injection

DISPLACEMENT SCALE 1:1000



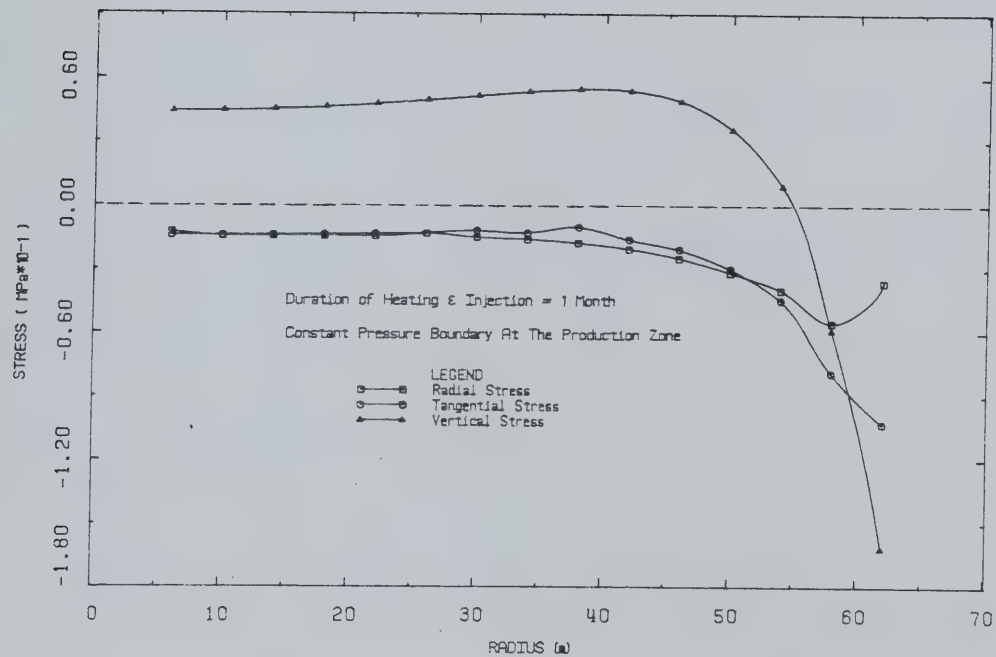


FIGURE L3.3 Effective Stresses Around the Shaft After 1 Month of Steam Injection



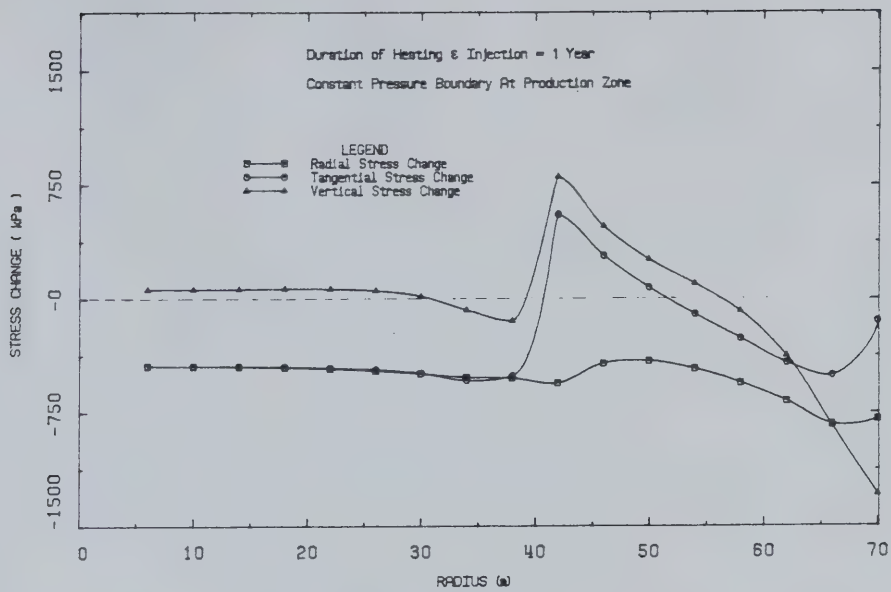


FIGURE L3.4 Stress Changes Around the Shaft After 1 Year of Steam Injection

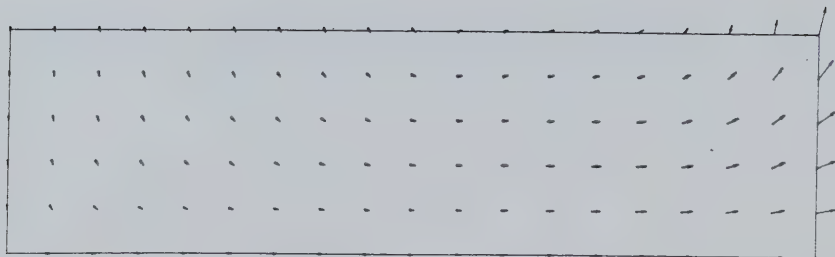


FIGURE L3.5 Deformations Around the Shaft After 1 Year of Steam Injection



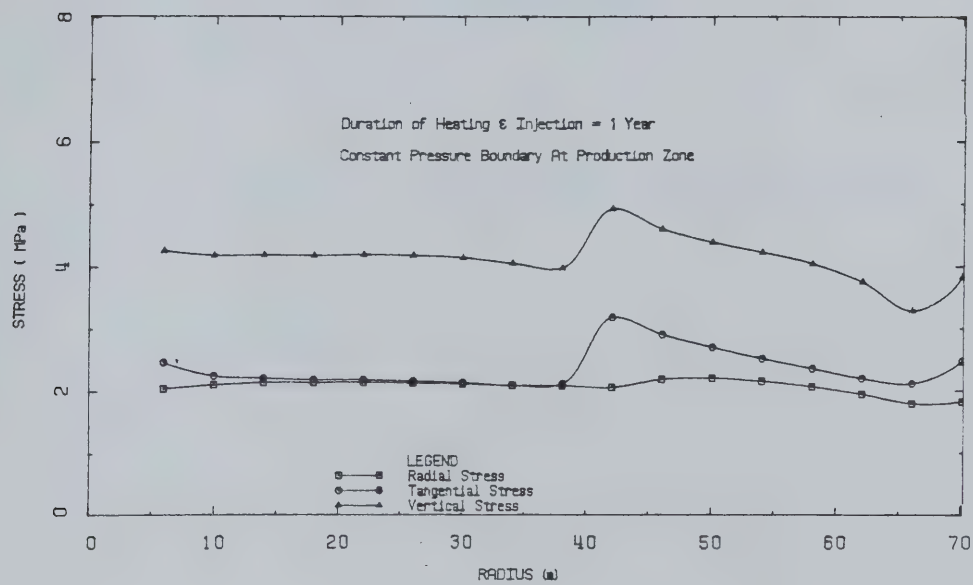


FIGURE L3.6 Effective Stresses Around the Shaft  
After 1 Year of Steam Injection



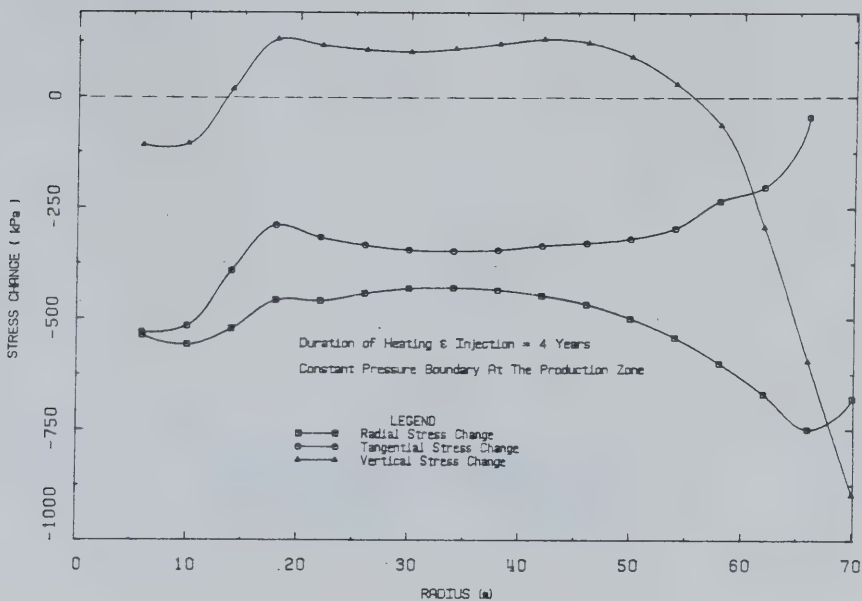


FIGURE L3.7 Stress Changes Around the Shaft After 4 Years of Steam Injection

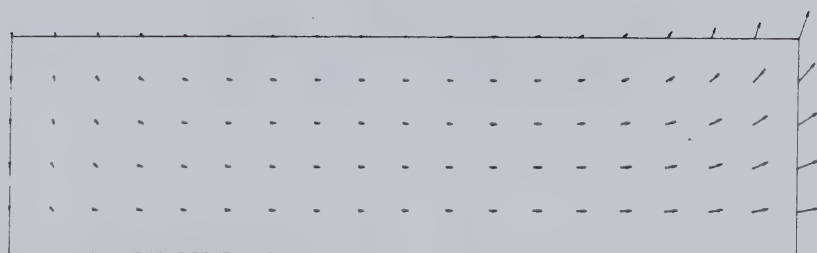


FIGURE L3.8 Deformations Around the Shaft After 4 Years of Steam Injection

DISPLACEMENT SCALE 1:100



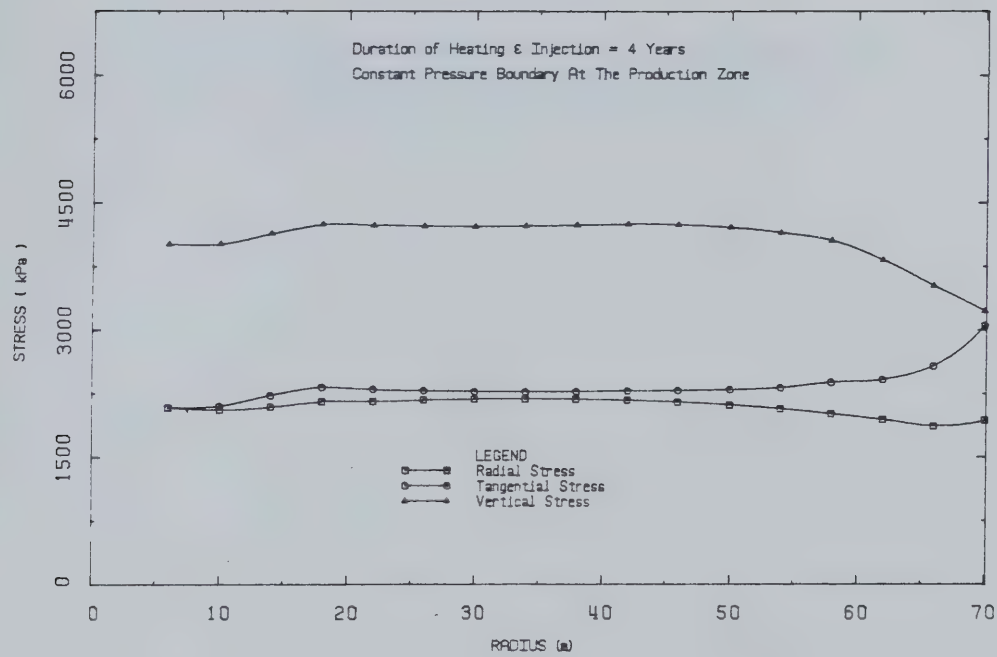


FIGURE L3.9 Effective Stresses Around the Shaft  
After 4 Years of Steam Injection



Thermal Stress Changes and Deformation Adjacent to a  
Shaft in Oil Sand Assuming a Compressible Boundary  
Condition at the Production Zone



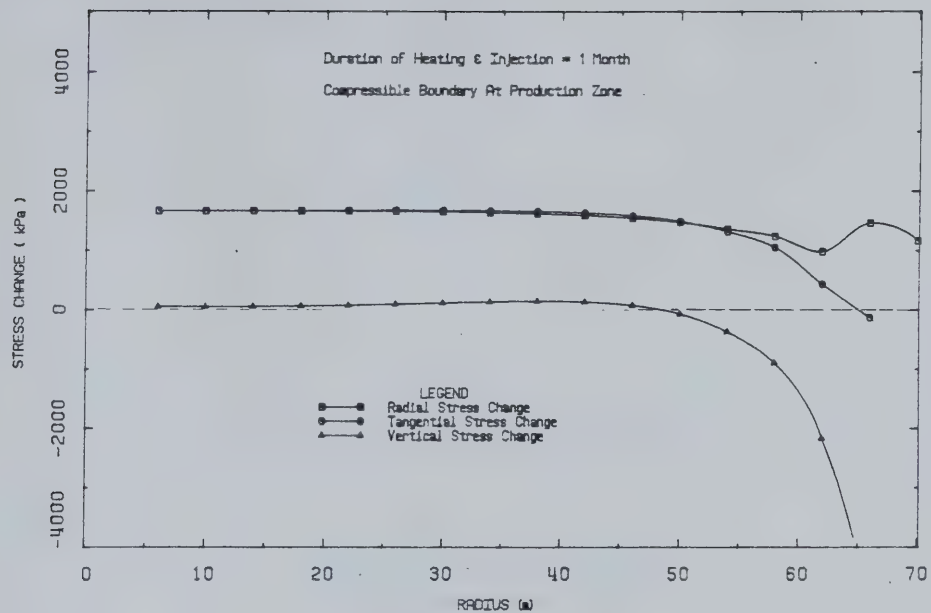


FIGURE L4.1 Stress Changes Around the Shaft After 1 Month of Steam Injection



FIGURE L4.2 Deformations Around the Shaft After 1 Month of Steam Injection



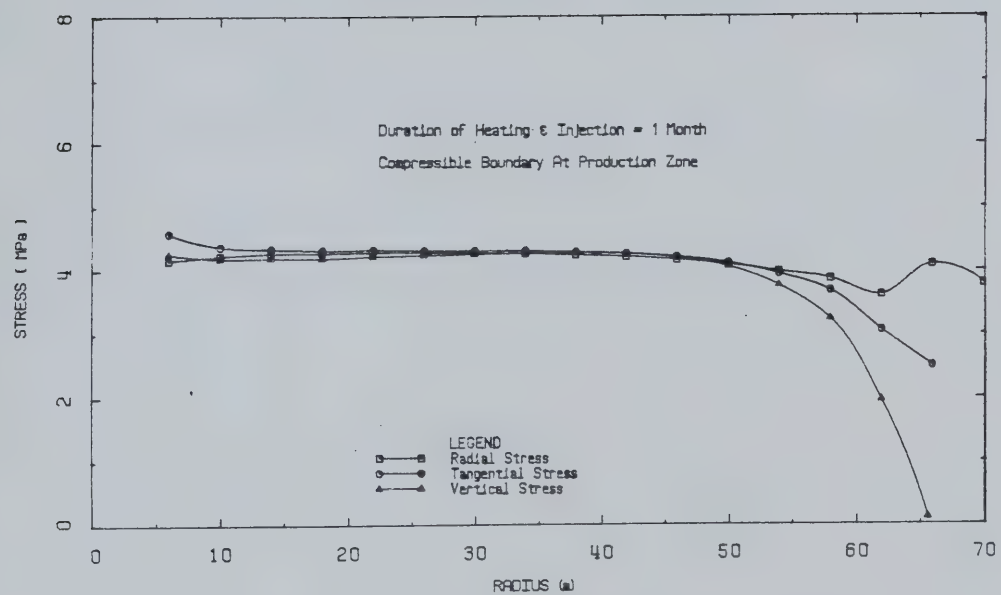


FIGURE L4.3 Effective Stresses Around the Shaft  
After 1 Month of Steam Injection



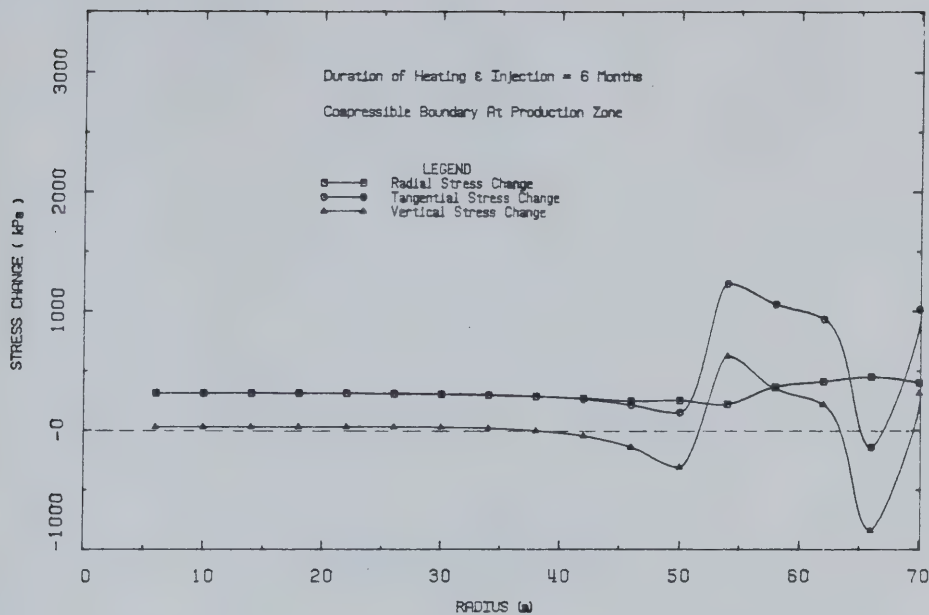


FIGURE L4.4 Stress Changes Around the Shaft After 6 Months of Steam Injection



FIGURE L4.5 Deformations Around the Shaft After 6 Months of Steam Injection

DISPLACEMENT SCALE 1:100



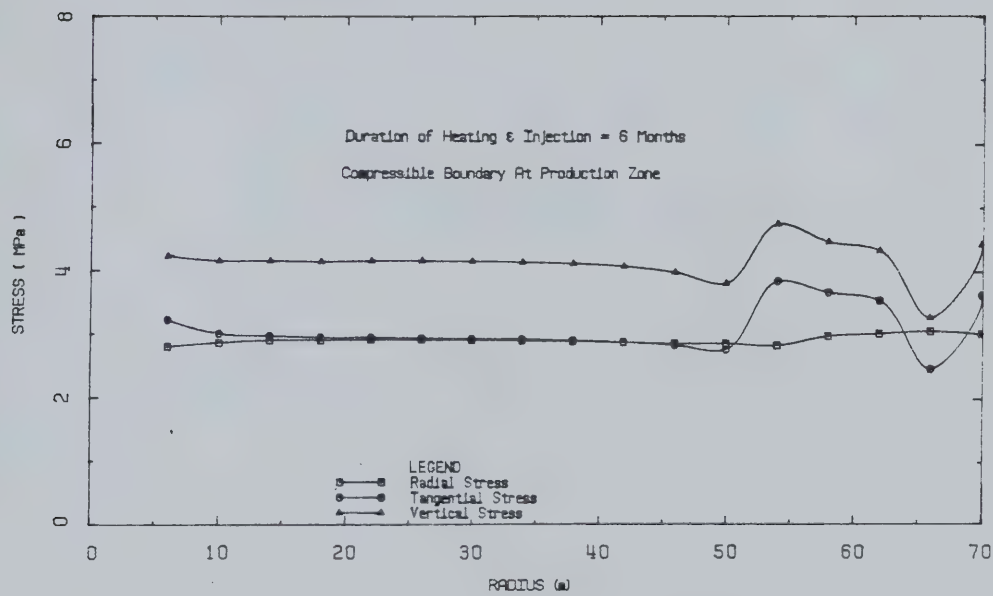


FIGURE L4.6 Effective Stresses Around the Shaft  
After 6 Months of Steam Injection



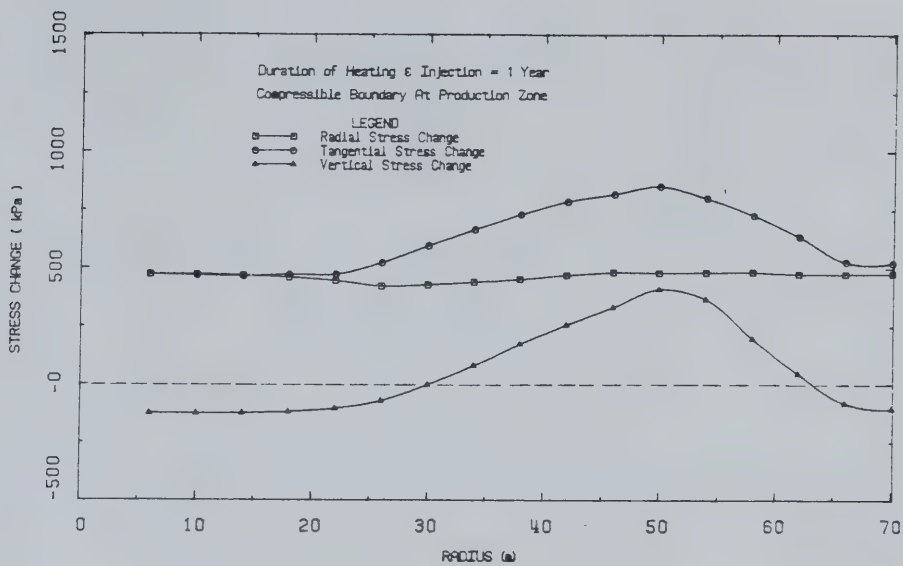


FIGURE L4.7 Stress Changes Around the Shaft After 1 Year of Steam Injection

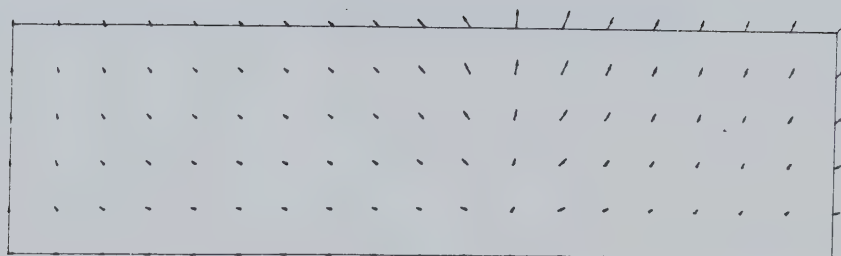


FIGURE L4.8 Deformations Around the Shaft After 1 Year of Steam Injection

DISPLACEMENT SCALE 1:100



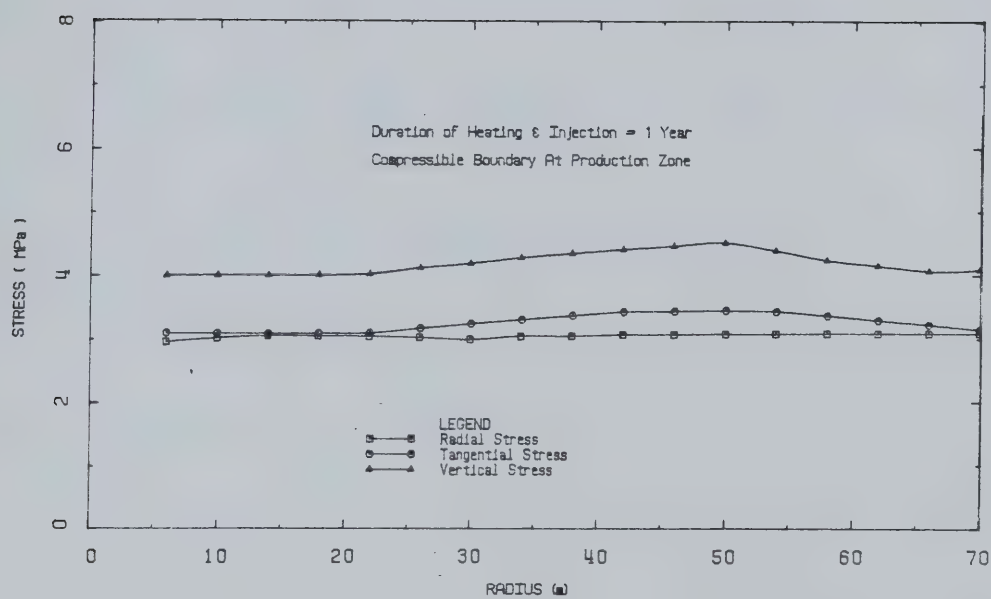


FIGURE L4.9 Effective Stresses Around the Shaft  
After 1 Year of Steam Injection



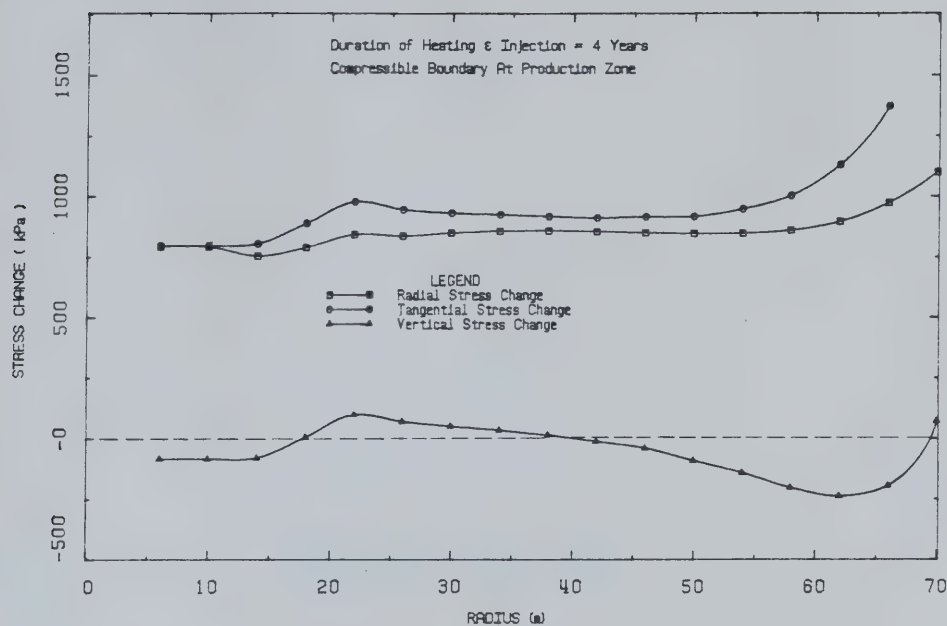


FIGURE L4.10 Stress Changes Around the Shaft After 4 Years of Steam Injection



FIGURE L4.11 Deformations Around the Shaft After 4 Years of Steam Injection



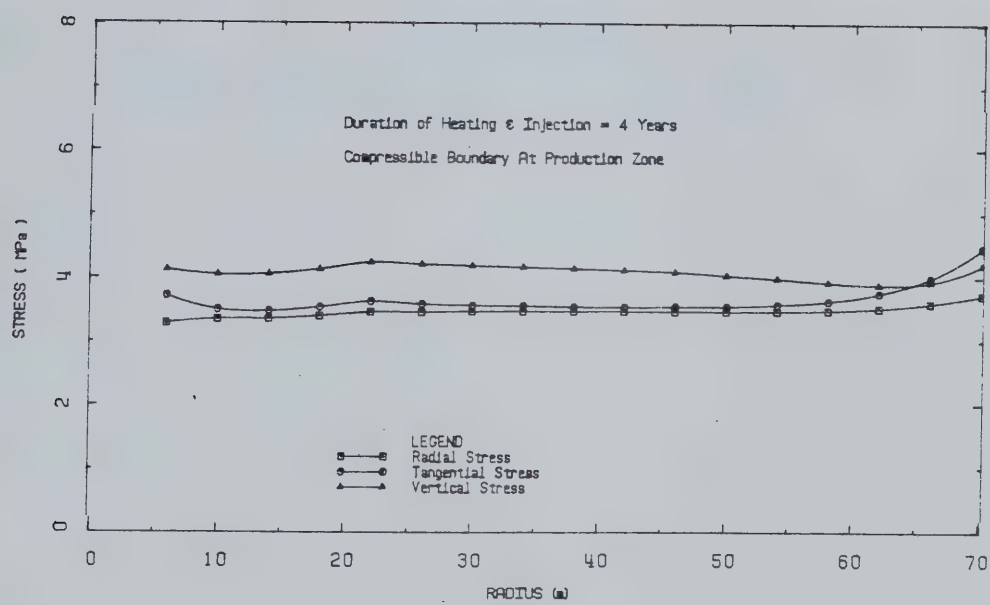


FIGURE L4.12 Effective Stresses Around the Shaft  
After 4 Years of Steam Injection



Drained Analyses

Thermal Stress Changes and Deformations Adjacent to a  
Shaft Assuming Drained Conditions



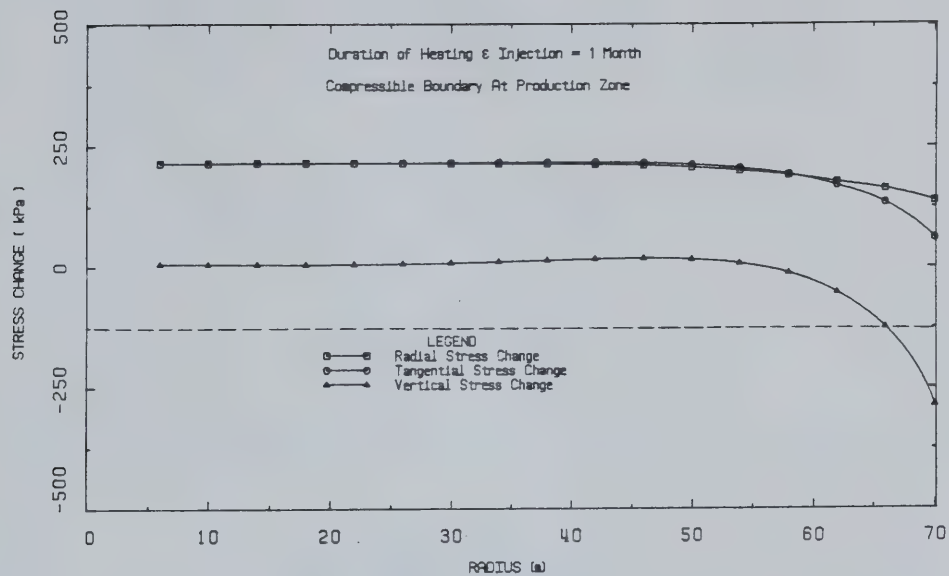


FIGURE L5.1 Stress Changes Around the Shaft After 1 Month of Drained Heating

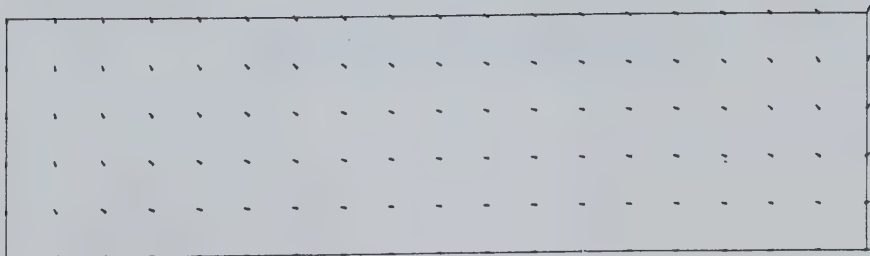


FIGURE L5.2 Deformations Around the Shaft After 1 Month of Drained Heating

DISPLACEMENT SCALE 1:100



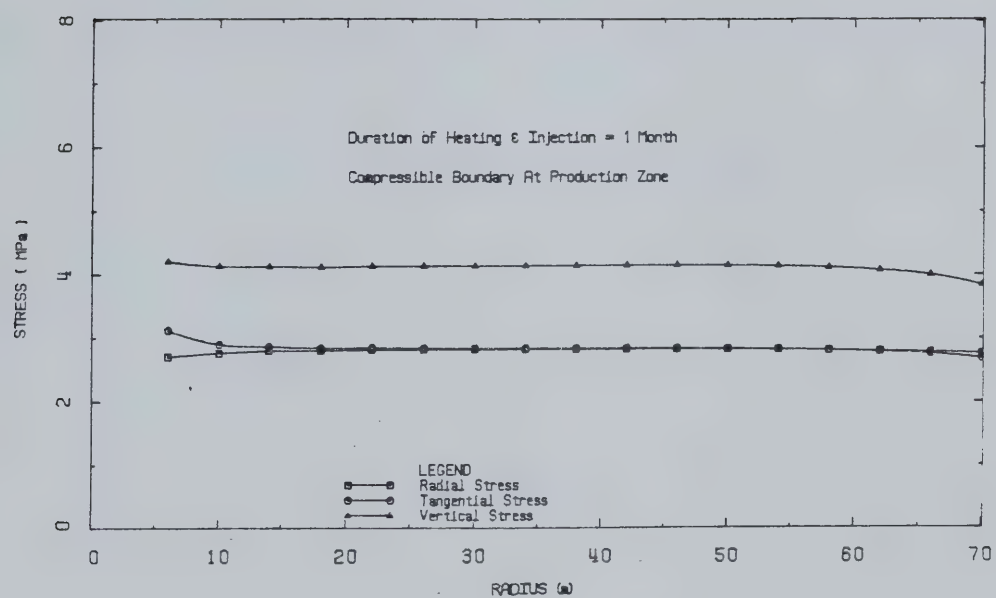


FIGURE L5.3 Effective Stresses Around the Shaft  
After 1 Month of Drained Heating



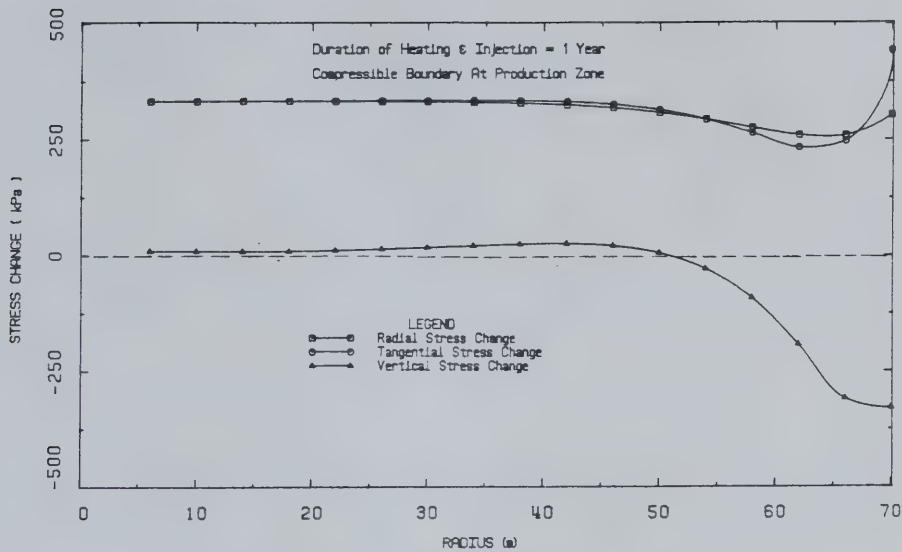


FIGURE L5.4 Stress Changes Around the Shaft After 1 Year of Drained Heating



FIGURE L5.5 Deformations Around the Shaft After 1 Year of Drained Heating



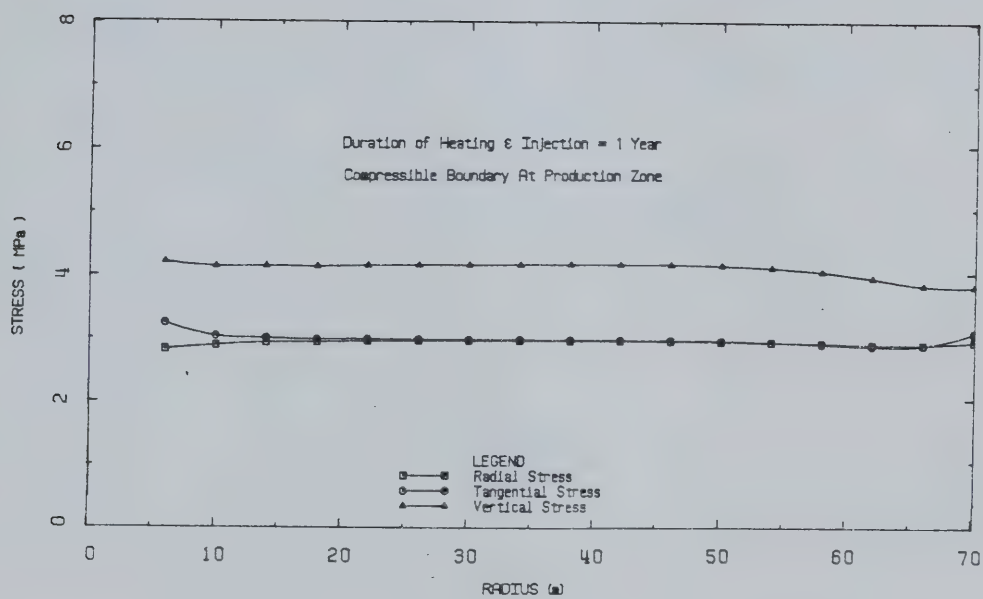


FIGURE L5.6 Effective Stresses Around the Shaft  
After 1 Year of Drained Heating



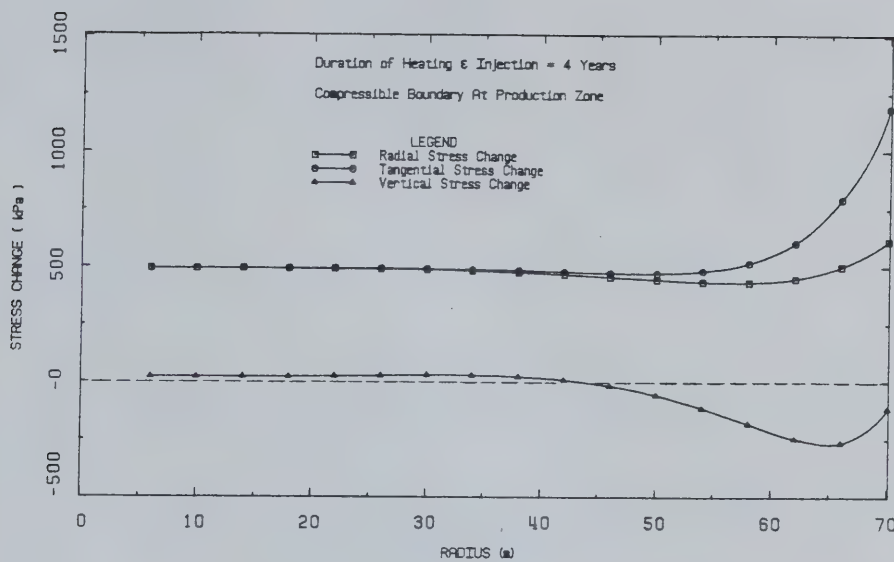


FIGURE L5.7 Stress Changes Around the Shaft After 4 Years of Drained Heating

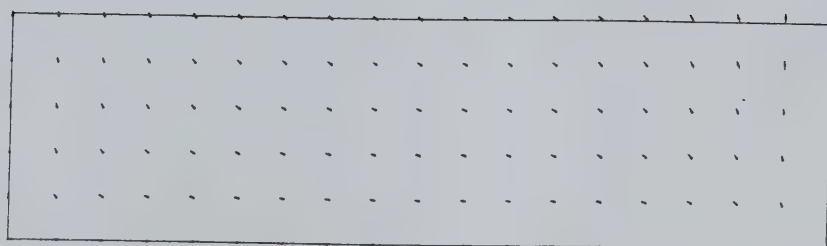


FIGURE L5.8 Deformations Around the Shaft After 4 Years of Drained Heating



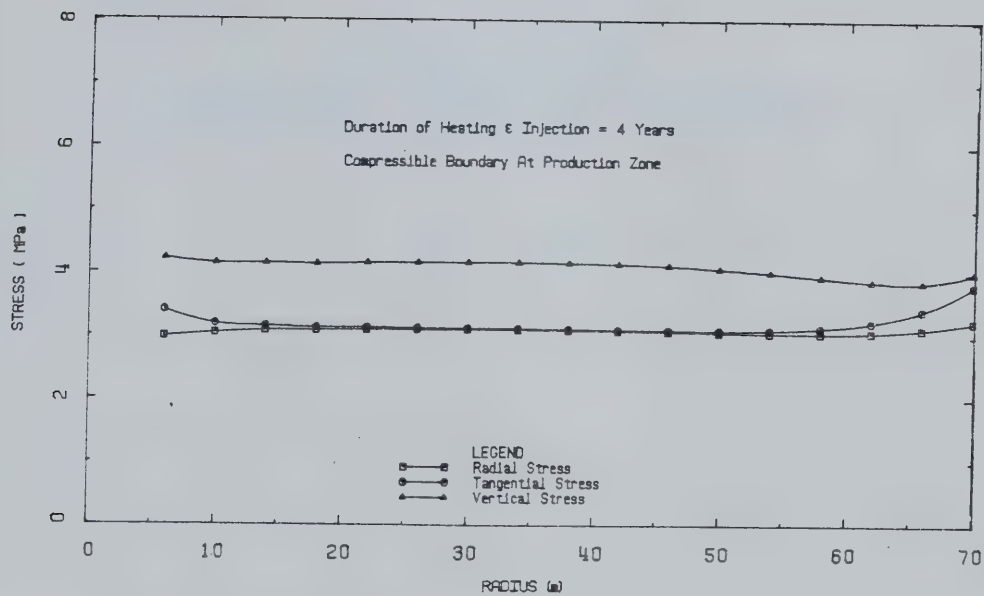


FIGURE L5.9 Effective Stresses Around the Shaft  
After 4 Years of Drained Heating



Undrained Analysis #1

Undrained Stress Changes and Deformations Using  
Constant Undrained Thermoelastic Coefficients



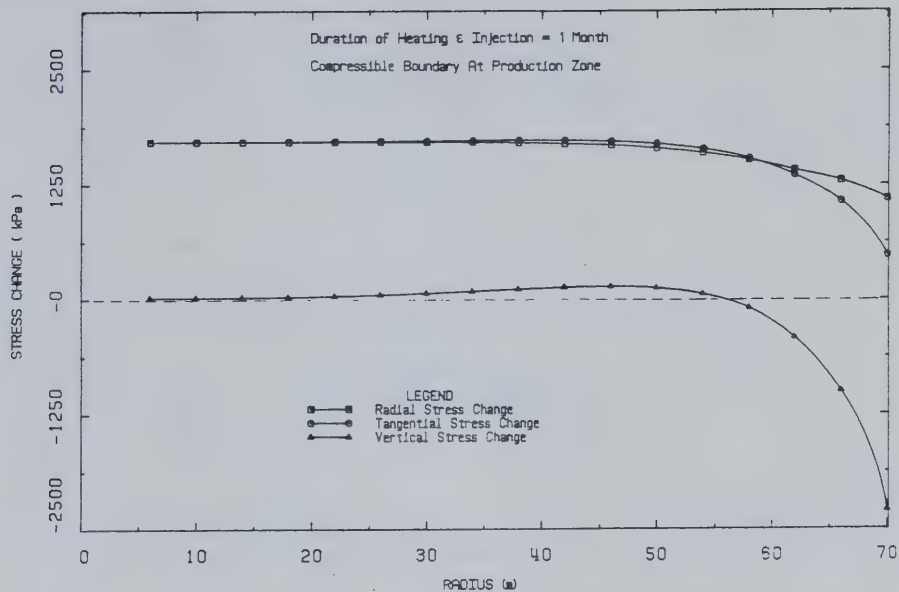


FIGURE L6.1 Stress Changes Around the Shaft After 1 Month of Undrained Heating (constant thermoelastic coefficients)



FIGURE L6.2 Deformations Around the Shaft After 1 Month of Undrained Heating (constant thermoelastic coefficients)

DISPLACEMENT SCALE 1:100



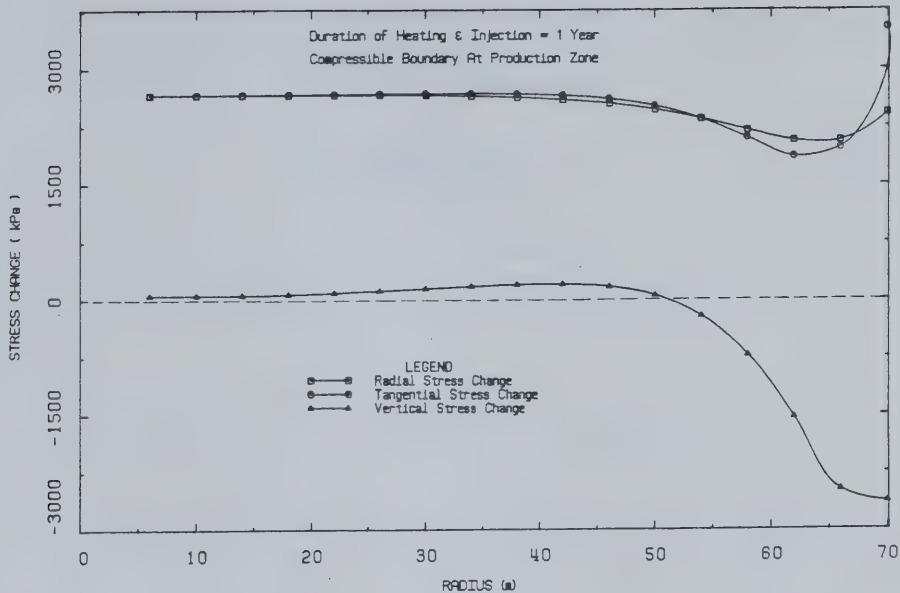


FIGURE L6.3 Stress Changes Around the Shaft After 1 Year of Undrained Heating (constant thermoelastic coefficients)



FIGURE L6.4 Deformations Around the Shaft After 1 Year of Undrained Heating (constant thermoelastic coefficients)

DISPLACEMENT SCALE 1:100



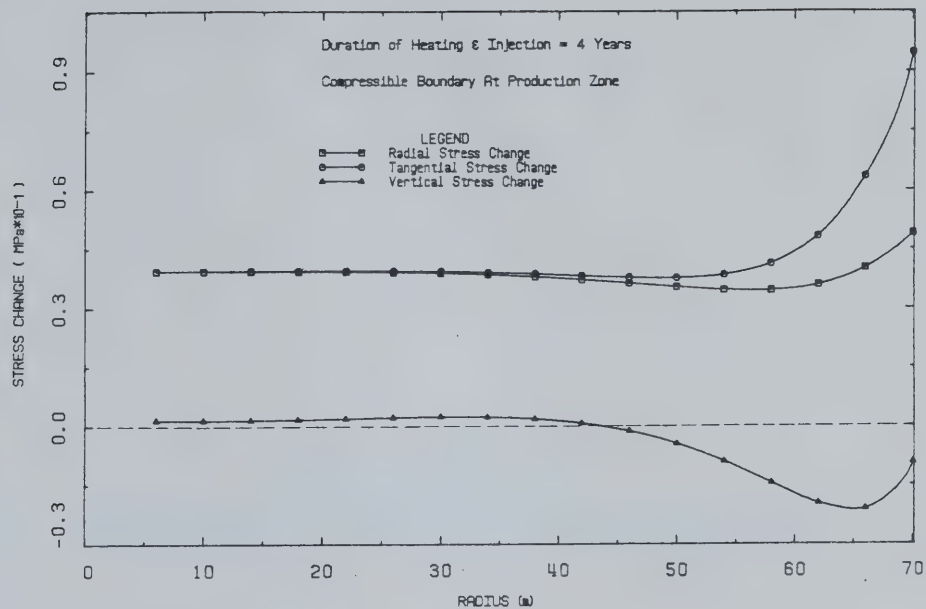


FIGURE L6.5 Stress Changes Around the Shaft After 4 Years of Undrained Heating (constant thermoelastic coefficients)

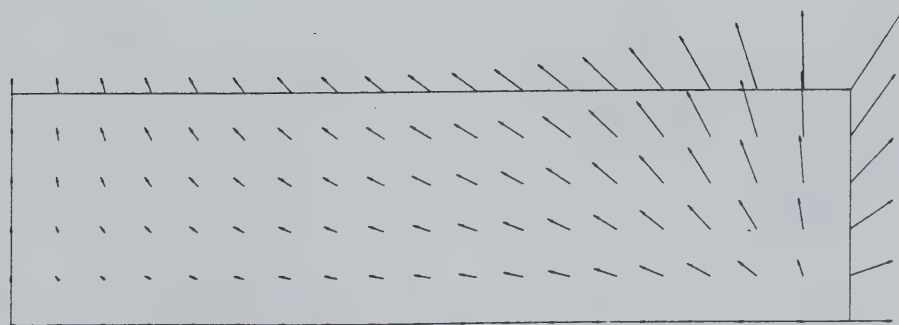


FIGURE L6.6 Deformations Around the Shaft After 4 Years of Undrained Heating (constant thermoleastic coefficients)

DISPLACEMENT SCALE 1:100



Undrained Analysis #2

Undrained Stress Changes and Deformations Determined  
Using Variable Thermoelastic Coefficients



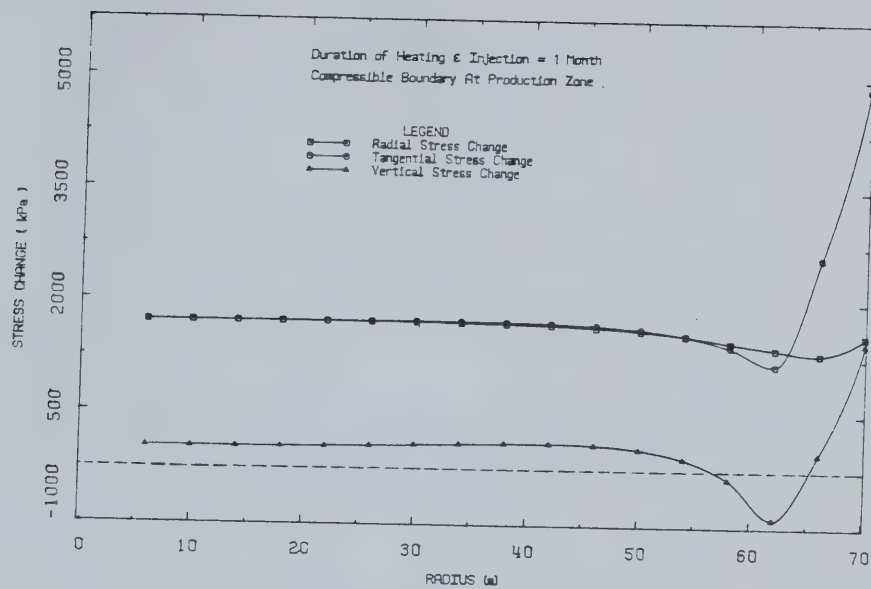


FIGURE L7.1 Stress Changes Around the Shaft After 1 Month of Transient Undrained Heating



FIGURE L7.2 Deformations Around the Shaft After 1 Month of Transient Undrained Heating



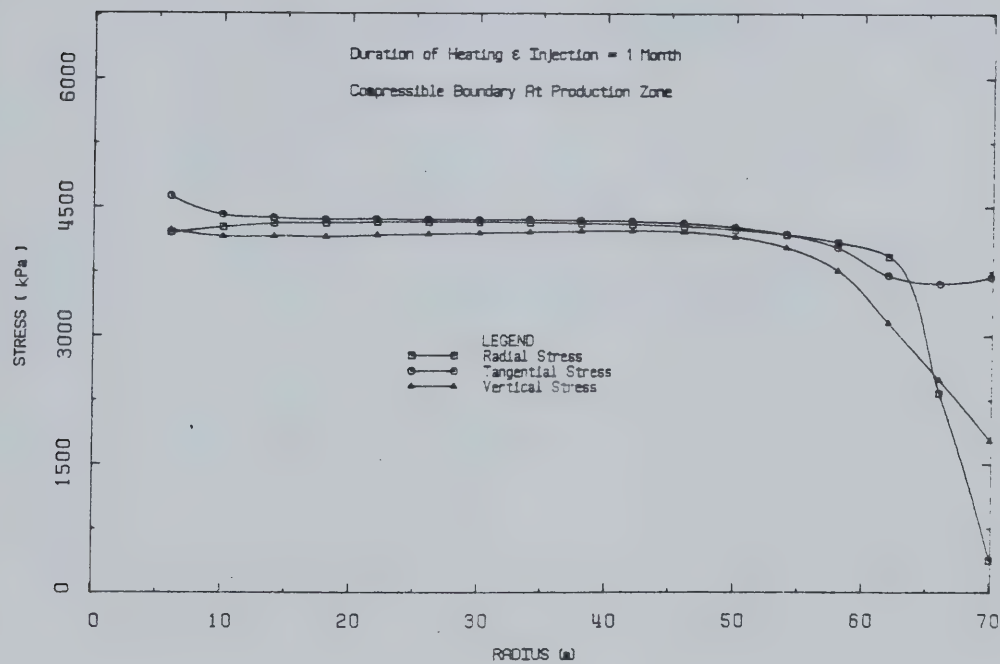


FIGURE L7.3 Effective Stresses Around the Shaft  
After 1 Month of Transient Undrained  
Heating



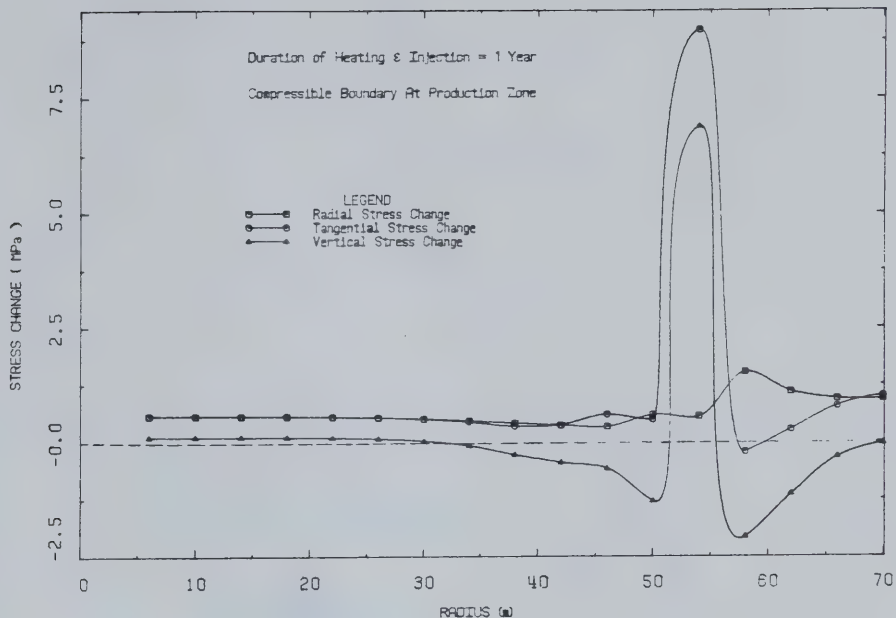


FIGURE L7.4 Stress Changes Around the Shaft After 1 Year of Transient Undrained Heating



FIGURE L7.5 Deformations Around the Shaft After 1 Year of Transient Undrained Heating

DISPLACEMENT SCALE 1:100



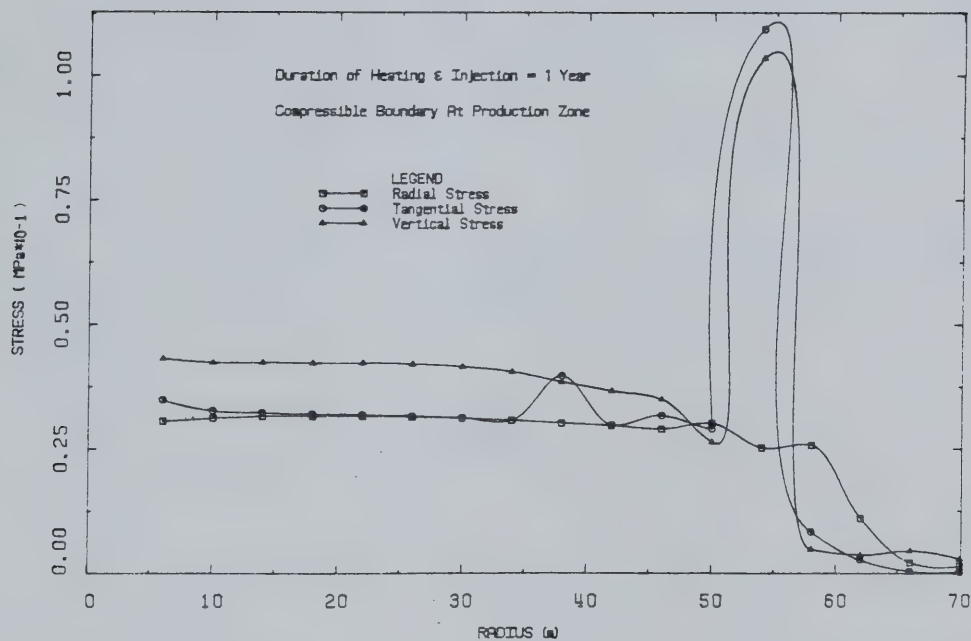


FIGURE L7.6 Effective Stress Around the Shaft  
After 1 Year of Transient Undrained  
Heating



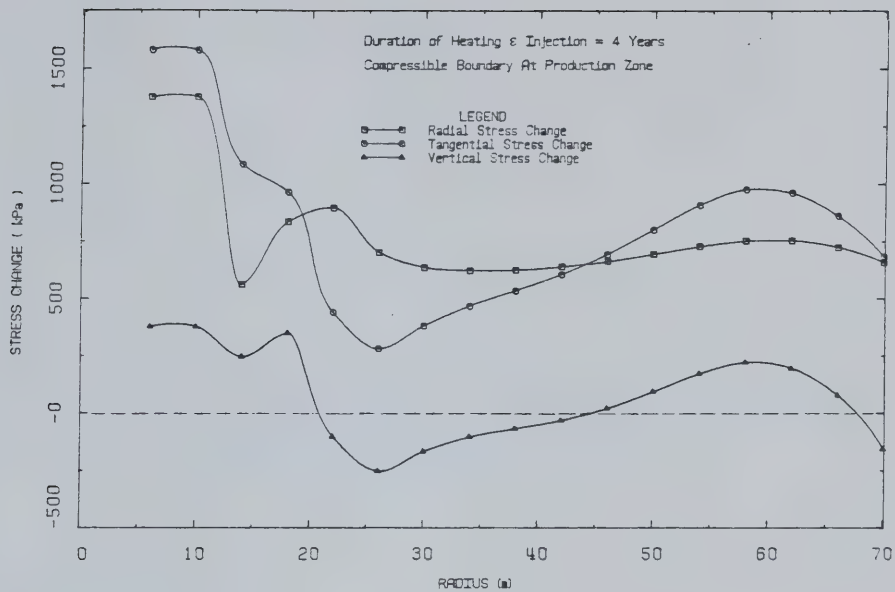


FIGURE L7.7 Stress Changes Around the Shaft After 4 Years of Transient Undrained Heating

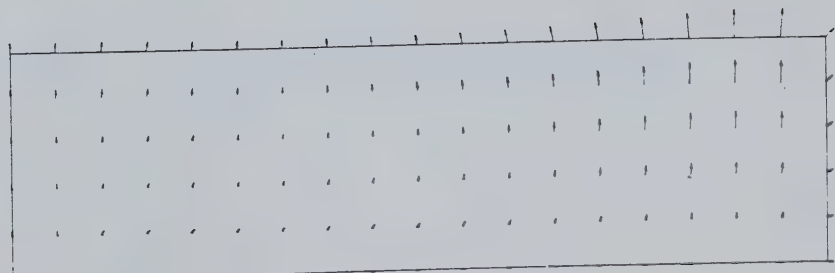


FIGURE L7.8 Deformations Around the Shaft After 4 Years of Transient Undrained Heating

DISPLACEMENT SCALE 1:100



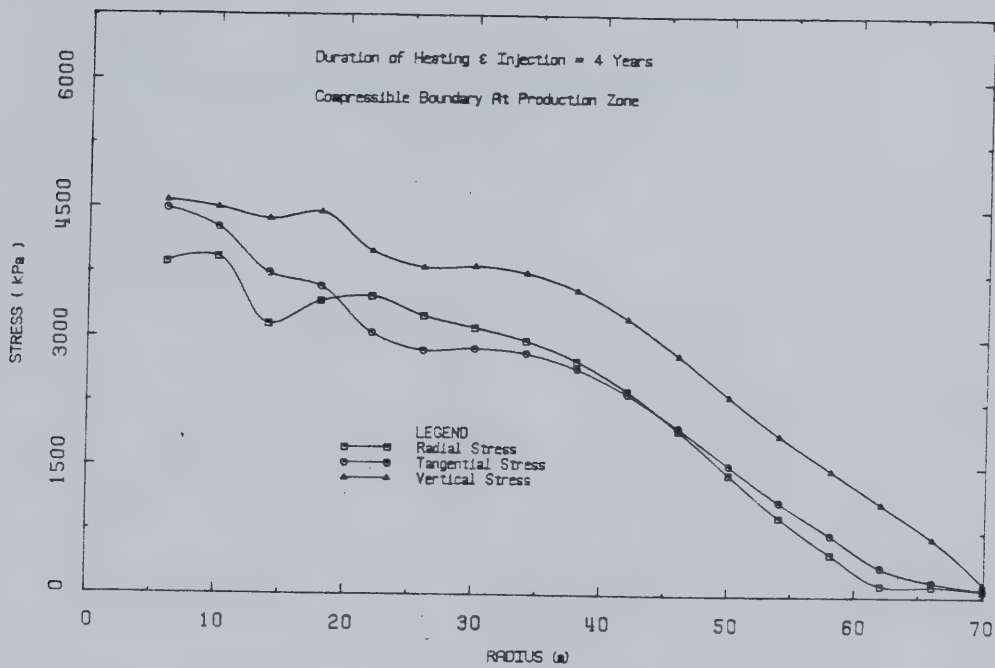


FIGURE L7.9 Effective Stresses Around the Shaft After 4 Years of Transient Undrained Heating



Thermal Stress Changes and Deformations Adjacent to a  
Shaft or Low Permeability Oil Sand



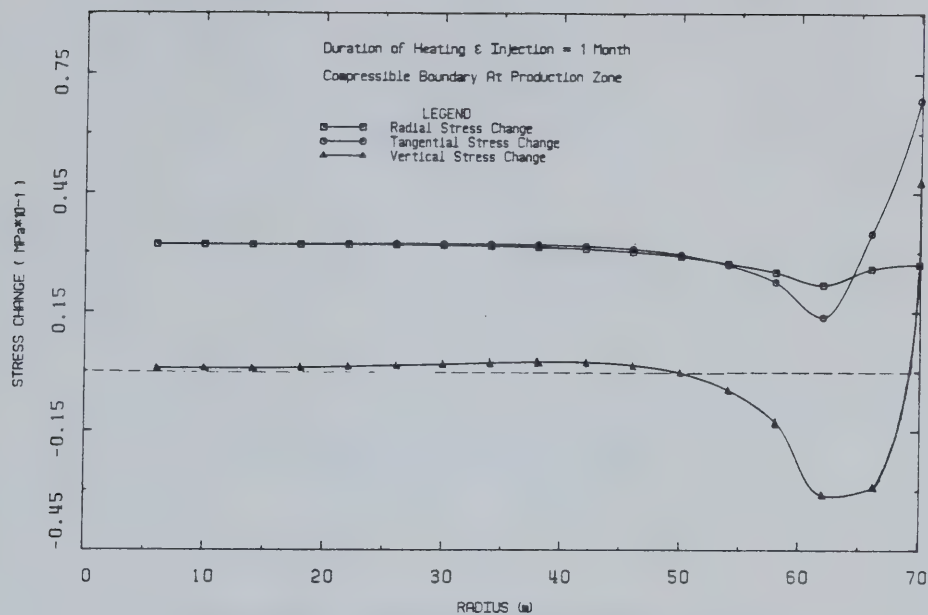


FIGURE L8.1 Stress Changes Around the Shaft After 1 Month of Steam Injection in Shale



FIGURE L8.2 Deformations Around the Shaft After 1 Month of Steam Injection in Shale

DISPLACEMENT SCALE 1:100



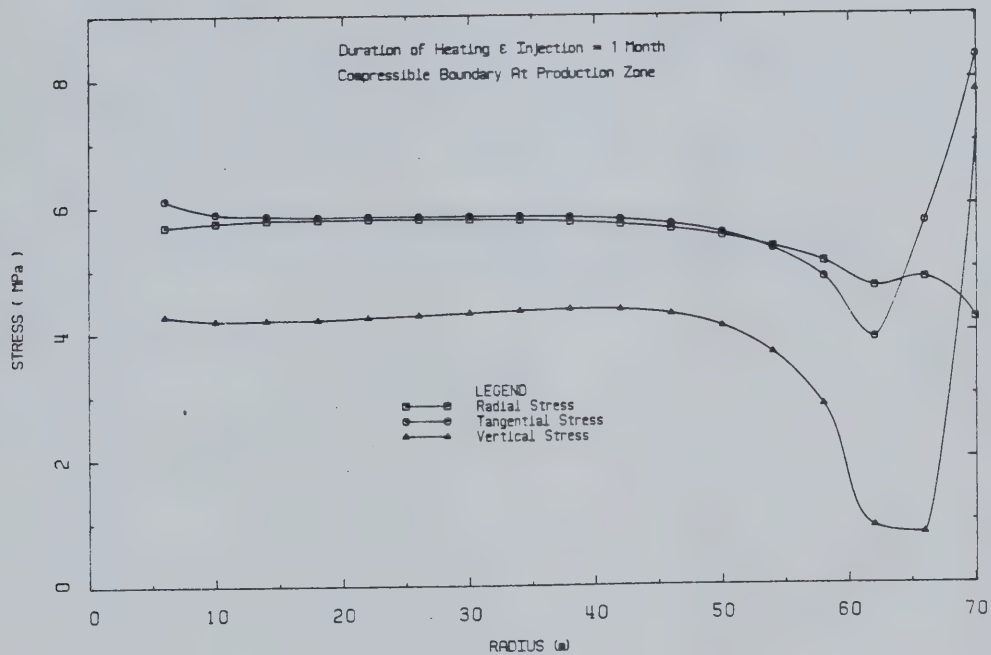


FIGURE L8.3 Effective Stresses Around the Shaft  
After 1 Month of Steam Injection in  
Shale



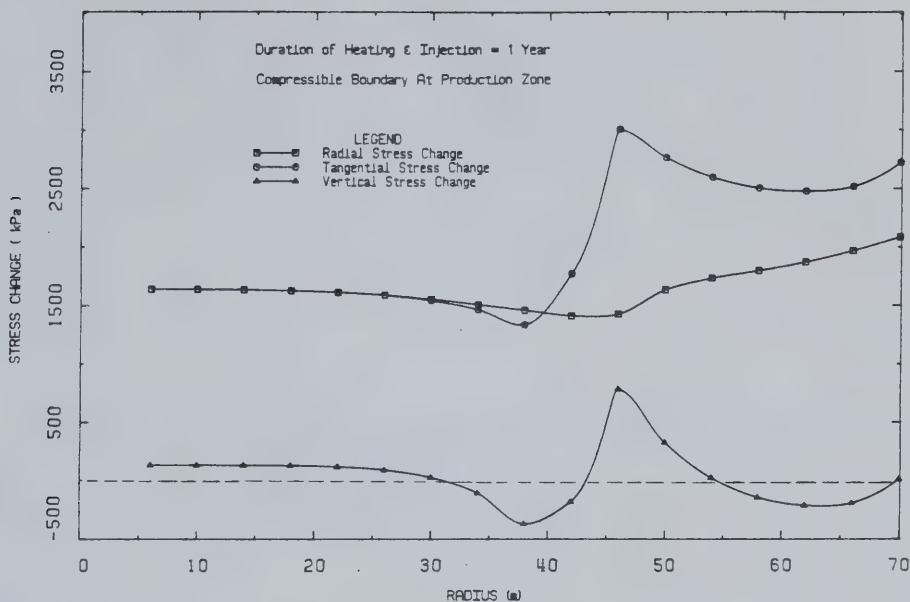


FIGURE L8.4 Stress Changes Around the Shaft After 1 Year of Steam Injection In Shale



FIGURE L8.5 Deformations Around the Shaft After 1 Year of Steam Injection In Shale

DISPLACEMENT SCALE 1:100



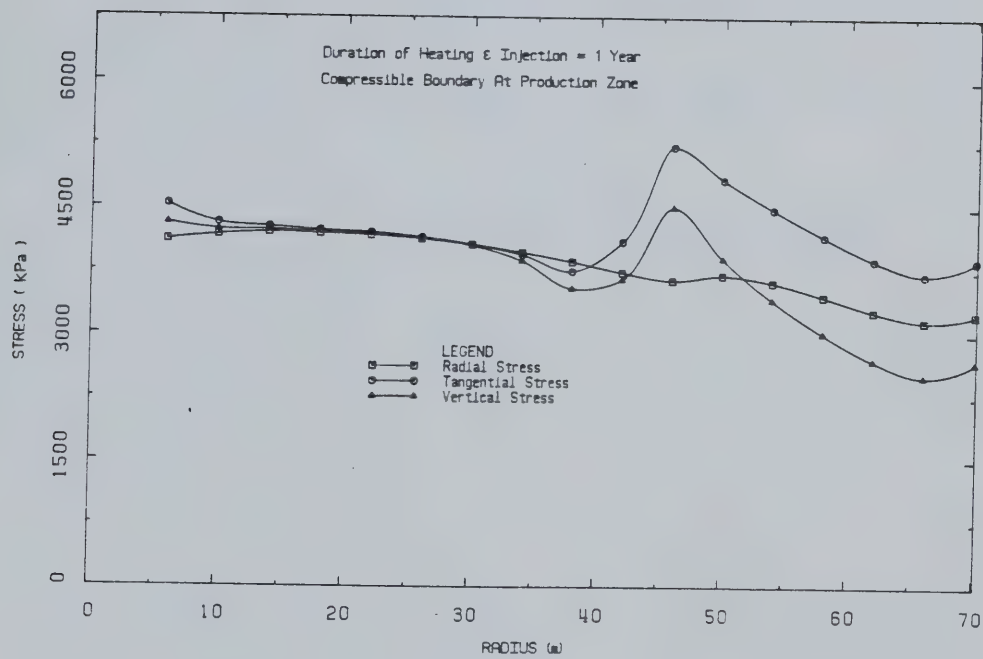


FIGURE L8.6 Effective Stresses Around the Shaft  
After 1 Year of Steam Injection in  
Shale



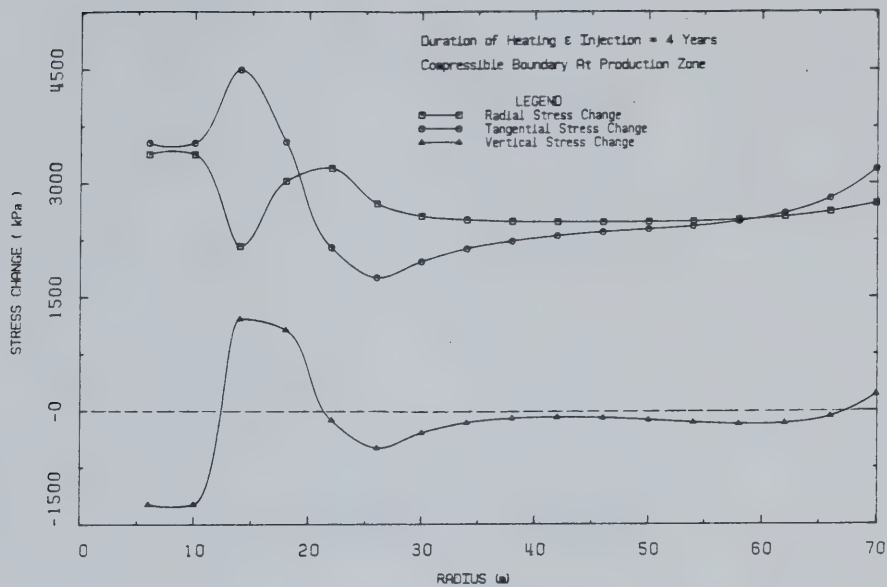


FIGURE L8.7 Stress Changes Around the Shaft After 4 Years of Steam Injection in Shale



FIGURE L8.8 Stress Changes Around the Shaft After 4 Years of Steam Injection in Shale



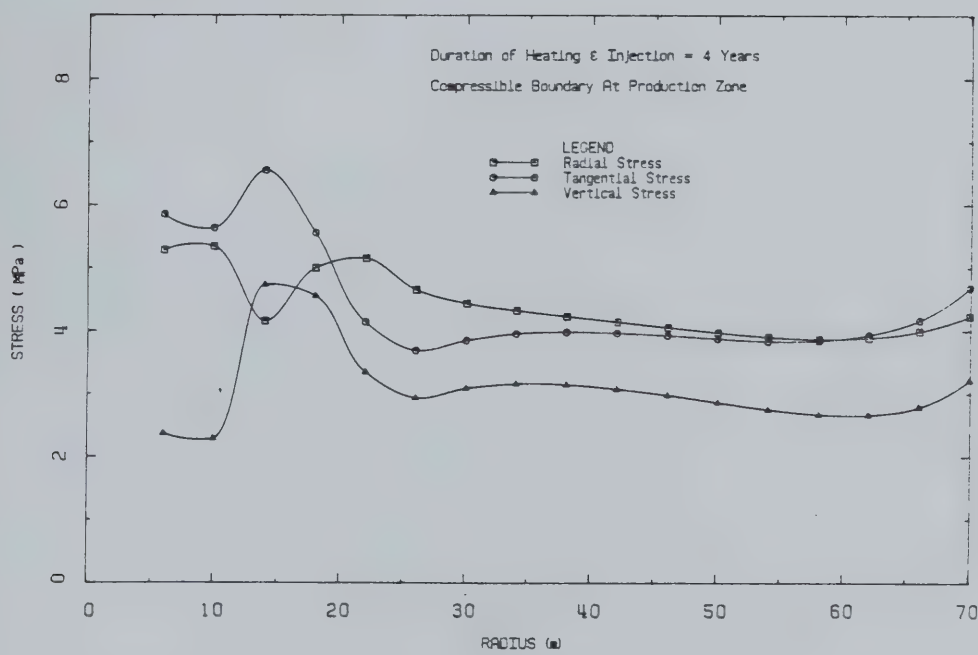


FIGURE L8.9 Stress Changes Around the Shaft After 4 Years of Steam Injection in Shale









**B30405**